UNIVERSITY OF OKLAHOMA

GRADUATE COLLEGE

U/PB DETRITAL ZIRCON PROVENANCE OF MID-PENNSYLVANIAN SEDIMENTS INTO THE ANADARKO BASIN: IMPLICATIONS FOR PALEOGEOGRAPHY AND SEQUENCE STRATIGRAPHY

A THESIS

SUBMITTED TO THE GRADUATE FACULTY

in partial fulfillment of the requirements for the

Degree of

MASTER OF SCIENCE

By

DALILA ARMANDA DE JESUS
Norman, Oklahoma
2021

U/PB DETRITAL ZIRCON PROVENANCE OF MID-PENNSYLVANIAN SEDIMENTS INTO THE ANADARKO BASIN: IMPLICATIONS FOR PALEOGEOGRAPHY AND SEQUENCE STRATIGRAPHY

A THESIS APPROVED FOR THE
SCHOOL OF GEOSCIENCES

BY THE COMMITTEE CONSISTING OF

Dr. Michael J. Soreghan, Chair

Dr. Gerilyn S. Soreghan

Dr. Matthew J. Pranter

ACKNOWLEDGEMENTS

I would like to dedicate this thesis to my Lord and Savior, Jesus Christ, to my mother, Ana de Jesus, to my sisters, Yuma, Zaida and Nawik, and to my nephews, Yukelson and Daniel Soares. The pursuit of furthering my education would not have been possible without their never-ending support and guidance. Above all, may the glory be to Jesus Christ, who worked within me and made all things possible.

I would first like to express my deepest appreciation and gratitude to my advisor, Dr. Michael Soreghan. Dr. Mike accepted me into his research group in 2019 when my former advisor, Dr. Roger Slatt, had become very ill and unfortunately passed away in 2020. Dr. Mike's knowledge, guidance and encouragement have molded and fostered not only my research capabilities but also my leadership skills. His extraordinary guidance and confidence in my abilities were incomparable. This research study wouldn't have been as fascinating and exciting without his presence and incredible advisement throughout the past two years. Similarly, I would like to acknowledge and thank my mentor and friend, Dr. Folarin Kolawole, whose unparalleled academic and research experiences, expertise and invaluable advice inspired and motivated me to continue this journey.

I would also like to extend a sincere appreciation to the late Dr. Roger Slatt. Dr. Slatt was an extraordinary person and advisor who led his research group with intelligence and enthusiasm. "A bad day in the field is better than a good day in the office" and "Load 'em up, move 'em up" are phrases that will forever remind me of the fantastic times I spent with Dr. Slatt and the Institute of Reservoir Characterization group. I also thank Dr. Gerilyn Soreghan and Dr. Matthew Pranter who served on my thesis committee and provided invaluable suggestions for the project. I am appreciative of your time, expertise, and insights regarding my thesis work.

I would also like to thank the following individuals and entities for their support: Luis Buatois and Gabriela Mangano for their helpful insights on the identification and classification of trace fossils; the amazing teams at the Oklahoma Petroleum Information Center (OPIC) and the Arizona LaserChron Center, for processing my samples and sharing their facilities and geological insights with me; the Geological Society of America, the American Association of Petroleum Geologists and the National Association of Black Geoscientists, for partially funding this research; the School of Geosciences for great resources and financial support through graduate research assistant scholarships; and my research group, for their willingness to lend their time and insights into this project (special thanks to Alicia Bonar and Jamie Bowie who supported me tirelessly).

Lastly, I would like to thank my mother, Ana de Jesus, and sister, Yuma Soares, for their unconditional love, support, and guidance since the beginning of my academic pursuit. Their multiple sacrificial acts of care and unprecedented hard work shaped me into being the woman I am today. Furthermore, I thank my best friend and sister, Nawik Saraiva, who has provided companionship as well as empathic advice and new perspectives on STEM and life. I am forever grateful to my family and friends for their endless love and support; a special thanks to Sulcivania Uonzo, Ibrahim Avelino, Kesia Silva, Kelson Gando, Delcio Teixeira, Pascoal Nkunzi, Daldic Jose, and Tara Putri.

TABLE OF CONTENTS

List of Figures

List of Tables

ABSTRACT

Late Paleozoic tectonism coupled with high-frequency climatic variations influenced sediment dispersal patterns across the midcontinent that resulted in frequent shifts of sediment sources to depocenters. Despite the numerous provenance studies conducted in Pennsylvanian strata of the midcontinent, fundamental questions remain unresolved regarding sediment transport into the Anadarko Basin and its spatio-temporal variation. The prolific Middle Pennsylvanian Red Fork Sandstone (Cherokee Group) of the Anadarko Basin, Oklahoma, provides an exceptional opportunity to address this issue. The Red Fork Sandstone is interpreted as a series of ribbon and sheet sandstones deposited in fluvial, deltaic, shelfal and deep-water environments during a time of rapid tectonic subsidence and substantial (in magnitude and frequency) glacioeustatic fluctuations. This study tests whether Middle Pennsylvanian sediment-routing systems into the Anadarko Basin varied spatially and on sequence-stratigraphic scales. Well-log correlation of three incised valley systems along the eastern margin of the Anadarko Basin was coupled with core analysis of three cores that represent each of the incised valley fills. Modal mineralogy of seven samples and 2011 concordant detrital zircon U-Pb ages from seven Red Fork Sandstone samples were collected from these three cores. Facies and facies-stacking interpretations were combined with sandstone compositions buttressed with the U/Pb detrital-zircon geochronology to assess the mineralogy, sequence stratigraphy, and provenance signatures of the units.

The facies within the cored intervals of the Red Fork Sandstone are inferred to represent tidal, marginal marine, marine and non-marine nvironments primarily and exhibit stacking patterns that suggest each of the cored intervals contain a major sequence boundary overlain by a lowstand systems tract. Two of the cored intervals (Cores 2 and 3) contain stacked facies that

represent transgressive and highstand system tracts, but differences in the facies expression of these tracts between the two cores suggest differences in environments and response to the relative sea level rise; the third core is incomplete (Core 1) and does not contain evidence of the transgressive or highstand systems tracts.

Differences in U-Pb ages of the detrital zircons indicate that sand provenance varied among the three cored intervals. Three major detrital zircon signatures characterize the sandstones in this study: Type 1, 2 and 3. Type 1, which corresponds to sandstones of sublith-litharenite composition, occurs within the lowstand system tracts of the northern and north-central Anadarko Shelf (Cores 1 and 2) and displays a prominent age cluster corresponding to the Neoproterozoic Northern Appalachian (560-740 Ma) basement terrane. Type 2, which corresponds to sandstones of quartzarenite compositions, occurs within the lowstand and highstand system tracts of the eastern Anadarko Shelf (Core 3) and is characterized by a high percentage of Grenvillian-age (900-1300 Ma) grains. Finally, Type 3, which is only found in the highstand system tract sands of Core 2, contains a more mixed source reflecting derivation from Grenvillian (900-1300 Ma) terranes and subordinate Yavapai-Mazatzal (1600-1800 Ma) and Granite Rhyolite (1300-1600 Ma) terranes.

Comparative assessment of published U-Pb detrital zircon ages from time equivalent sandstones and exposed basement rocks across the North American craton indicates that Type 1, lowstand sandstones (also considering their metamorphic lithics content) from the northern and north-central shelf reflect sourcing by a distal, transcontinental dispersal system that originated in the Northern Appalachians, either by exhumation of peri-Gondwanan basement rocks or by recycling of Neoproterozoic sedimentary cover. These sandstones are interpreted to reflect a southwestward transport of sediments across the midcontinent and into the Anadarko Shelf and

Basin during a time of sea level drawdown. Detrital zircon signatures from Type 2, low- and highstand, sandstones suggest both a major sourcing by a distal, extrabasinal fluvial system originating in the Central Appalachians, with a minor local midcontinent source, that likely had a sufficient sediment supply as to outpace relative sea level rise at least during initial rise. Type 3, highstand, sandstone zircon signatures suggest that within the area of the incised valleys along the northern shelf, the Neoproterozoic-rich sediment was not supplied, but likely trapped in fluvio-deltaic systems farther east as relative rise outpaced sediment supply and that the deposited sands were a mixture of reworking of the local sands and from the still active fluvio-deltaic system along the eastern Anadarko Shelf.

CHAPTER I

INTRODUCTION

The Late Paleozoic is marked by several significant disturbances to Earth's surface, and these dynamic interactions among tectonics and climate are recorded in the coeval sedimentary systems. Many of these changes occurred during the Pennsylvanian Period including the ongoing assemblage of the supercontinent Pangea and the ice volume changes in southern Gondwanaland (Fig.1; Parrish, 1993; Davydov et al., 2005; Montañez and Poulsen, 2013; Qie et al., 2019). The results of such impactful events include sea-level fluctuations caused by ice volume changes (Heckel, 1980, 1994), massive coal formation on low gradient continental margins (Parrish, 1993; DiMichelle et al., 2001; Davydov et al., 2005), and both plate boundary and within plate orogenic events that controlled regional and local sediment routing systems and depositional environments within evolving sedimentary basins of Laurentia (Fig. 2; Moore, 1979; Johnson, 2008; Kissock et al., 2018). In the southern midcontinent (United States), growing uplifts, which served as potential sediment sources (e.g., Appalachian Mountains, Ouachita Mountains, Amarillo-Wichita uplift, Ancestral Rocky Mountains, and others), the closing of the Ouachita seaway, and the evolution of the Anadarko Basin, posed primary controls on the regional and the stratigraphic character of the Pennsylvanian geology (Fig. 1; Moore, 1979; Johnson et al. 1989). These tectonic changes coupled with icehouse climatic variations resulted in frequent shifts of the major and minor sediment sources at different times and influenced sediment dispersal patterns through specific routing systems (Dickinson, 1983; Thomas et al., 2016; Kissock et al, 2018).

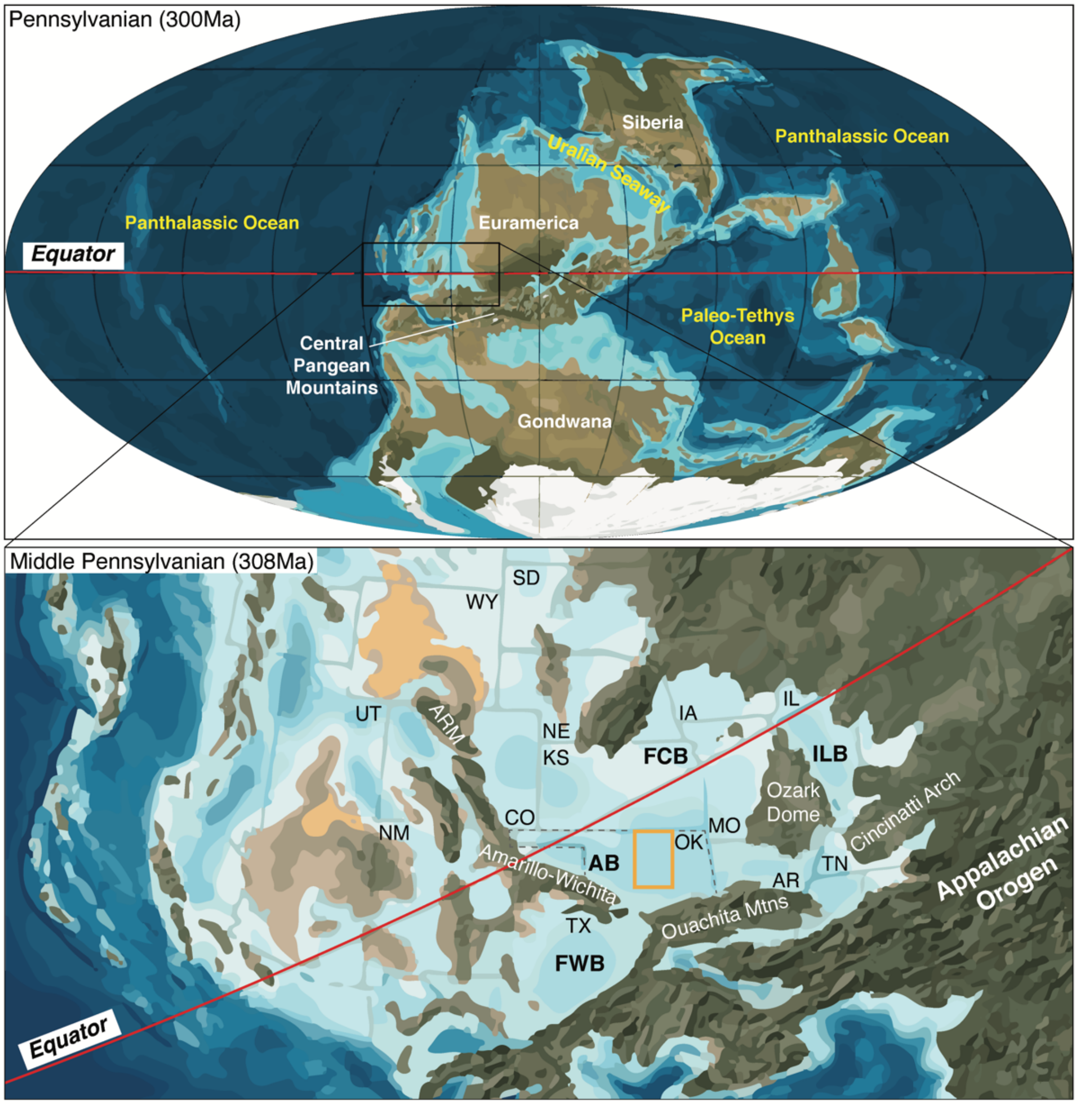

Figure 1. Global and regional paleogeographic map of the Pennsylvanian period showing the locations of the study area (box in lower panel) (top panel modified from Montañez and Poulsen, 2013 and Gibson, 2014; bottom panel modified from North American Key Time Slices ©2013 Colorado Plateau Geosystems Inc.). AB = Anadarko Basin; FCB = Forest City Basin; FWB = Fort Worth Basin; ILB = Illinois Basin; ARM = Ancestral Rocky Mountains.

Large-scale provenance studies on Mississippian and Pennsylvanian strata point to large continental-scale drainage systems carrying sediments from eastern-most sources, such as the Appalachians, to as far west as the Grand Canyon (Fig. 2; Archer and Greb, 1995; Chapman and Laskowski, 2019); however, fundamental questions remain unresolved on sediment transport across the southern midcontinent, especially given the potential impact of large-magnitude glacio-eustatic sea level changes that flooded larger regions of the midcontinent (Heckel, 1986, 1994). This study aims to specifically test whether Middle Pennsylvanian sediment-routing systems into the Anadarko Basin varied on sequence stratigraphic scales, thus providing insight into the controls of Pennsylvanian-age sedimentation patterns and sediment composition into the Anadarko Basin. A better understanding of the sediment dispersal patterns and sediment composition in the deep Anadarko Basin poses important implications for resolving sediment transport across the North American midcontinent as well as for assessing reservoir quality and sandstone connectivity relevant for hydrocarbon accumulations within the Pennsylvanian intervals of the basin.

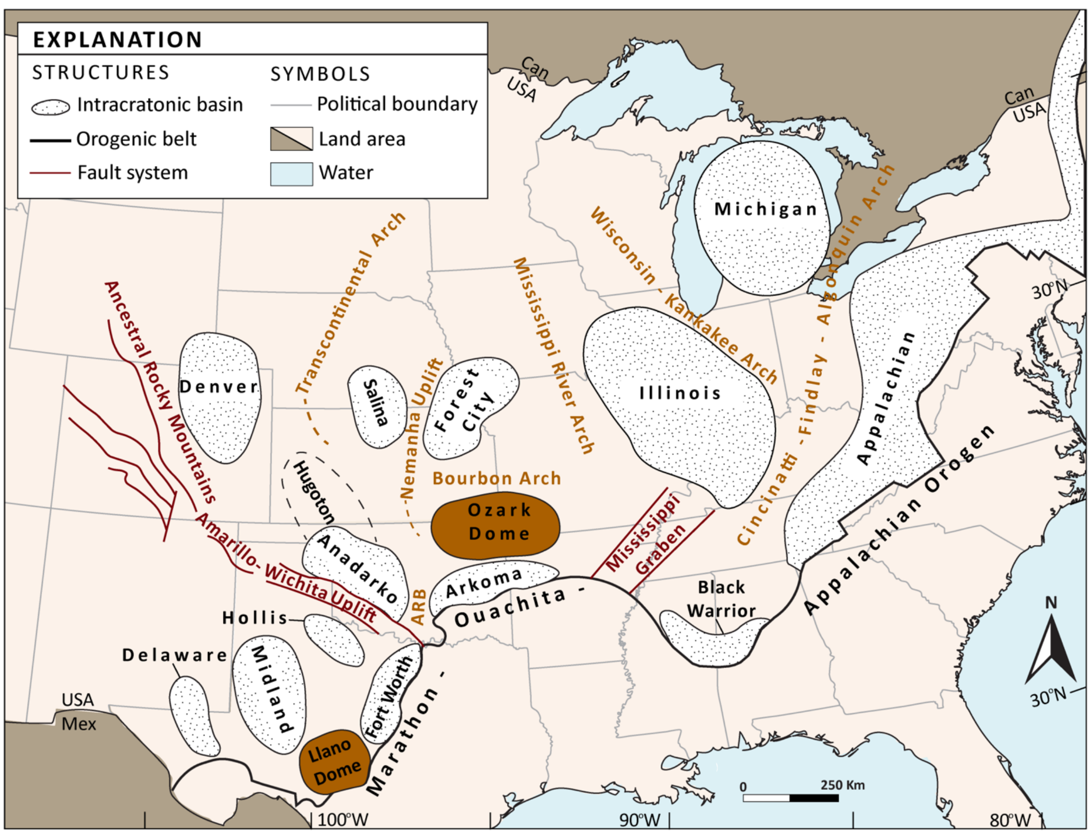

Figure 2. Middle Pennsylvanian paleogeographic map of North America (U.S. map from vecteezy.com; geology modified from McKee and Crosby, 1975; Thomas, 2011; Kissock et. al., 2018; Kushner, 2018 and sources therein). ARB = Arbuckle Mountains.

CHAPTER II
BACKGROUND

Global and Regional Paleogeography

Pennsylvanian paleogeography was controlled by Pangean assembly, which consisted of a convoluted collisional suturing of the northern Laurentia and the southern Gondwanan continents along the paleo equator (Fig. 1; Domeier and Torsvik, 2014). This rotational and complex collision resulted in the closing of ocean gateways, including the Iapetus Ocean, and in the orogenesis that created the Hercynian, Variscan and the Alleghenian Mountain chains, the latter beginning at the end of Mississippian and persisting until the end of the Pennsylvanian (Thomas, 1977; Hatcher, 1979). The Laurentia continent, which was generally positioned near the equator during the late Mississippian, drifted northward during the Mississippian-Pennsylvanian transition (Domeier and Torsvik, 2014). This event was followed by the closing of the Iapetus Ocean during the Mississippian-Pennsylvanian transition, which resulted in regional compression/deformation away from the plate boundary and is reflected in uplift of igneous basement associated with the Southern Oklahoma Aulacogen (SOA) and the subsidence of the Anadarko Basin (Fig. 2; Price, 2016). Tectonic features of the Pennsylvanian, formed as far-field stress responses from the Pangean assembly, controlled subsidence, sedimentation, and depositional patterns in similar intracratonic basins (e.g., Michigan, Williston, Illinois; Fig. 2, 3) of the midcontinent US (Moore, 1979; Klein and Hsui, 1987). A Pennsylvanian transcontinental river system is one mechanism suggested for the presence of sediment derived from basement assemblages of the Appalachians in the Michigan, Forest City, and Illinois Basins, and as far southwest as Grand Canyon, Arizona (Archer and Greb, 1995; Gleason et al., 2007; Gehrels et al., 2011; Thomas et al., 2016; Kissock et al., 2018). Paleochannel direction studies indicate a north, east, west, and southwest sediment transport route into the midcontinent during different times of the Late Paleozoic (Tate, 1985; Hentz, 1994; Andrews, 1997; Lambert, 2006; Kissock et.al., 2018).

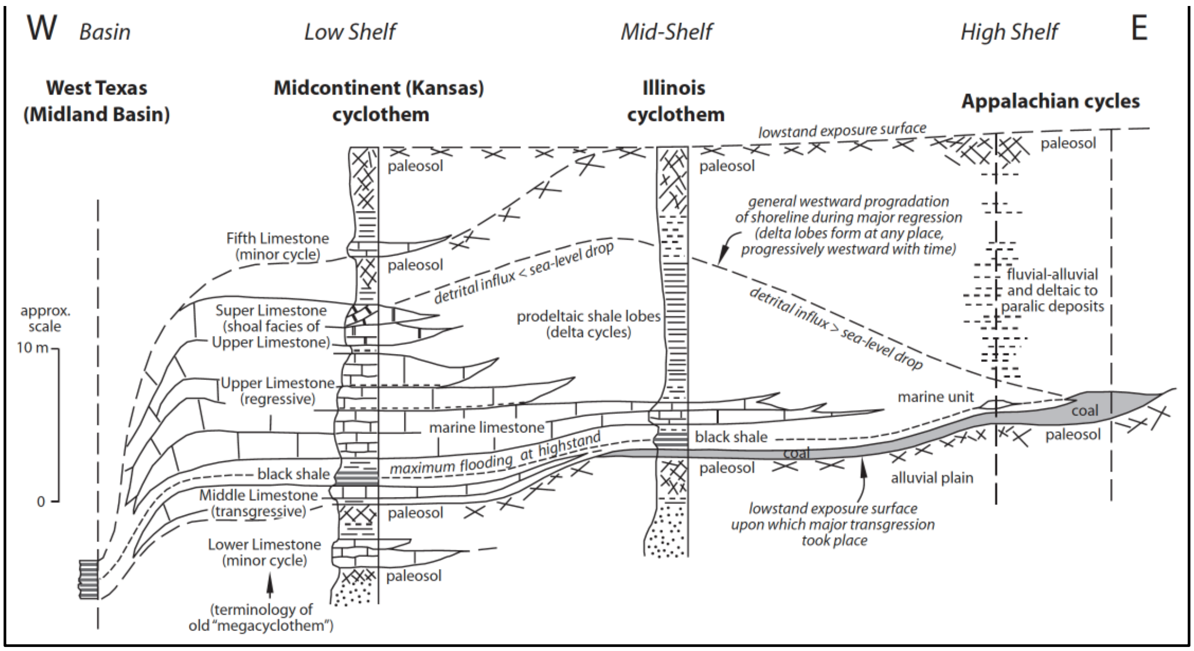

Figure 3. Style of major cyclothems from deep marine deposition in Midland Basin, west Texas, onto shelf through Kansas and Illinois, to Appalachian Basin (from Heckel, 2008).

In the southern midcontinent, the early Pennsylvanian was marked by an eustatic sea-level low, the initiation of the Amarillo-Wichita uplift, and rapid subsidence in the Anadarko Basin (Fig. 2; Moore, 1979; Kissock et al., 2018; Johnson, 2008). During the Middle Pennsylvanian, the Ouachita Mountains likely rose above sea level (Johnson, 2008), peat vegetation accumulated and ultimately formed the coal beds of the Arkoma Basin and northeastern Oklahoma, and continued subsidence coeval with fluvial-deltaic sedimentation occurred in the Anadarko Basin (Moore, 1979; Johnson, 2008). The late Pennsylvanian was marked by continued subsidence in the Anadarko Basin, deposition of black shales, and the Arbuckle orogeny, which caused thrusting in the Ardmore, Marietta, and a late-stage movement on structures bordering the Anadarko Basin (Heckel, 1980; Moore, 1979; Johnson, 1989, 2008; Turko, 2019).

Late Paleozoic Paleoclimate

The equatorial Pennsylvanian paleoclimate was marked by an everwet-seasonal climate phase in eastern Laurentia (the now central and eastern North America and Europe), and a relatively dry climate in the western portion (e.g., Colorado Plateau, New Mexico; Parrish, 1993; Soreghan, 1994). The climate transitioned to drier conditions in the late Pennsylvanian and by the Permian, was a seasonally arid climate driven by a mega-monsoonal circulation (Parrish, 1993; Soreghan, 1994; Qie et al., 2019). The prominent drivers of these extensive climatic changes are both the supercontinental reconfiguration and the glaciation/ice volume changes in southern Gondwanaland (Fig 1; Poulsen et al., 2007; Fielding et al., 2008; Montañez and Poulsen, 2013). These ice-volume changes controlled eustatic sea-level fluctuations (Heckel, 1986, 1994; Eriksson et al., 2019). These persistent glacioeustatic fluctuations and climatic changes in rainfall (Kutzbach et al., 2011) are recorded by extensive cyclothem deposits throughout low-gradient continental margins of North America composed of coal deposits, paleosols, incised valley fill (IVF) sandstones, and limestones (Fig. 3; Archer and Greb, 1995; Cecil et al., 2003; Heckel, 2008; Belt et al., 2011; Eriksson et al., 2019). Understanding the climatic conditions that persisted in the late Paleozoic midcontinent US is crucial to the accurate study of sediment provenance and composition since paleoclimate affects mineralogical composition, weathering rates, sediment transport and distribution, and ultimately fluvial pathways and stratigraphy (Archer and Greb, 1995; Hay, 1996; Kissock et al., 2018).

Geologic History of the Anadarko Basin

The Anadarko Basin occupies the northern flank of the late Proterozoic-early Paleozoic Southern Oklahoma Aulacogen (Fig. 1, 2; Perry, 1989). The basin center and its respective shelf (Anadarko Shelf) are bordered by the Nemaha uplift to the northeast, by the Ozark uplift and the Arkoma Basin to the east, and by the Amarillo-Wichita Mountains to the southwest (Figs. 2, 4). It preserves one of the thickest series of Paleozoic sedimentary packages in North America, consisting of ~12 km (40,000 ft) of strata, of which ~9 km is late Paleozoic (Fig. 5; Johnson et al., 1989; Perry, 1989).

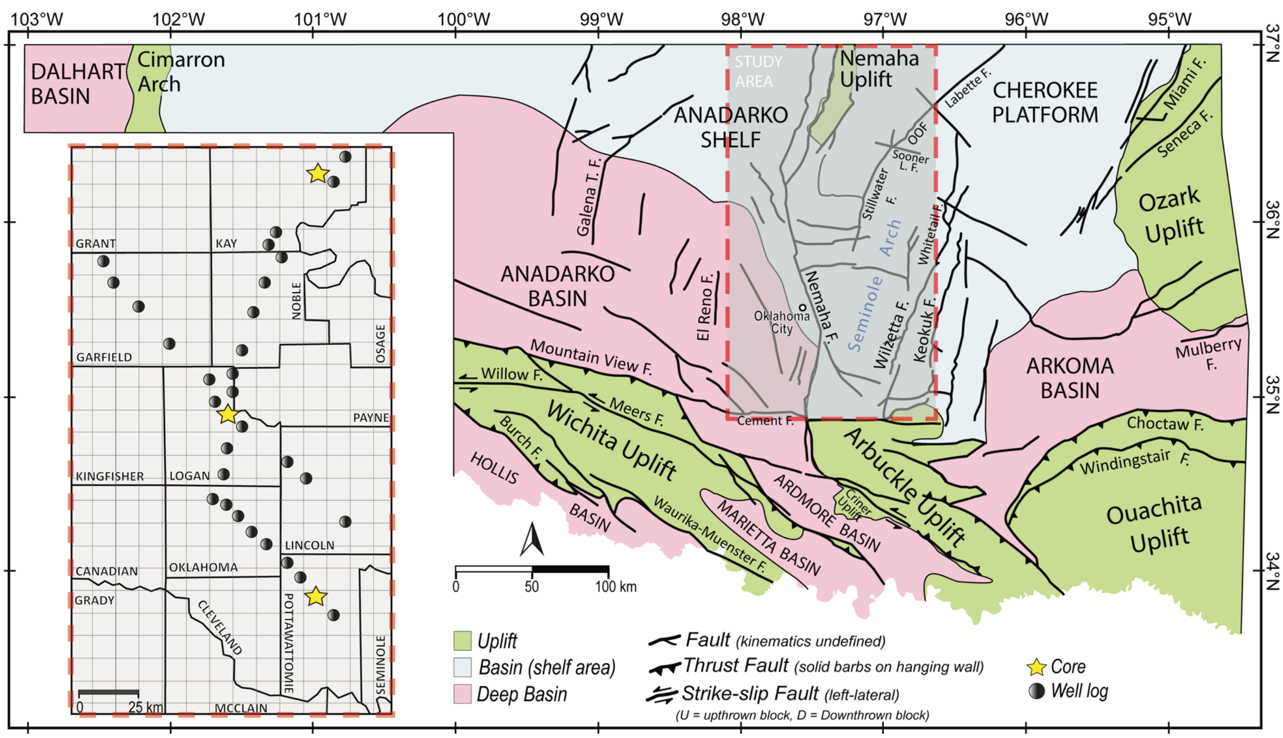

Figure 4. Oklahoma state map with major Pennsylvanian geologic provinces and structures, and sample locations (yellow stars and black dots) for this study (modified after Kolawole et al., 2020, and others therein).

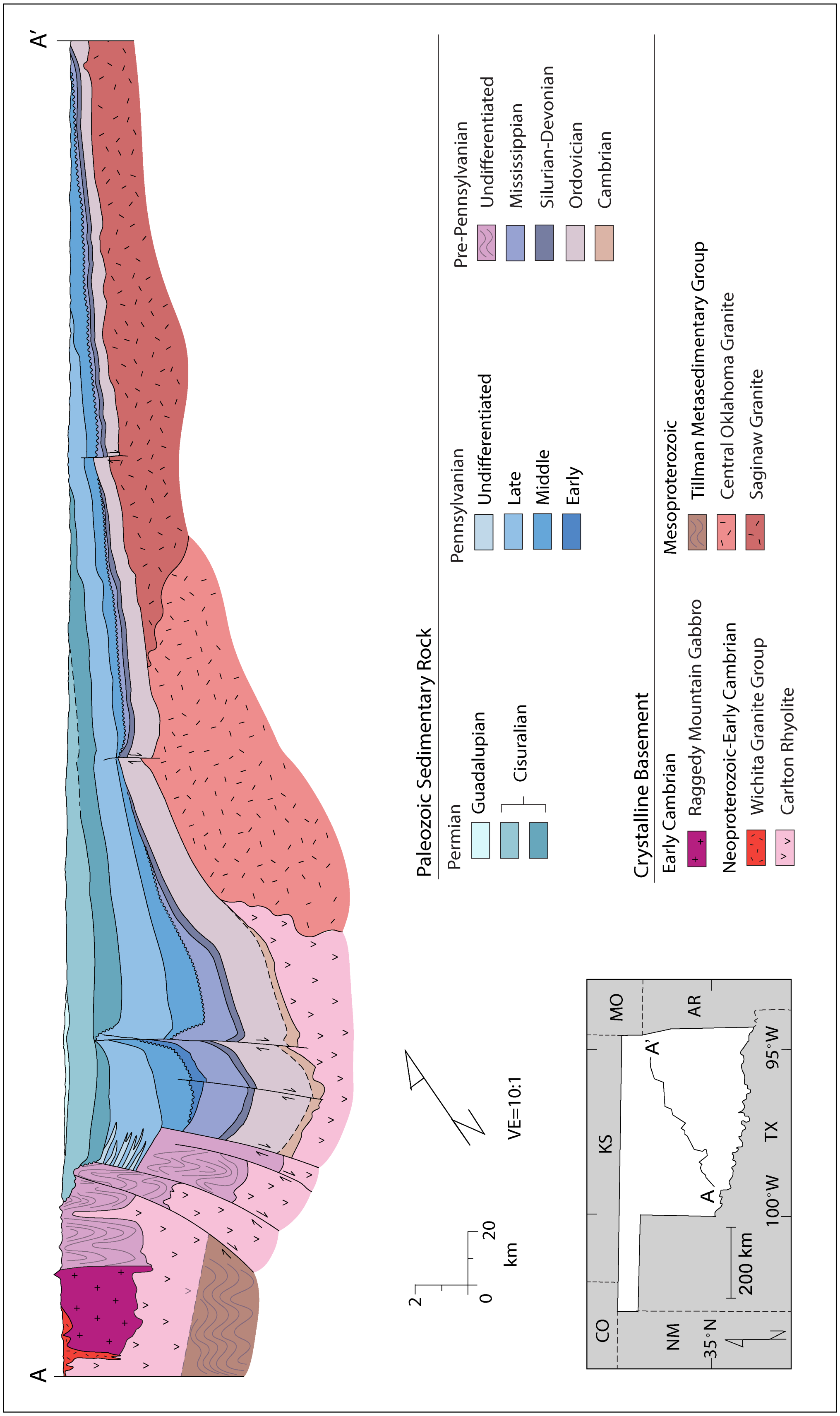
A
A'
2
0
20
km
VE=10:1
Paleozoic Sedimentary Rock
Permian
Guadalupian
Cisuralian
Pennsylvanian
Undifferentiated
Late
Middle
Early
Pre-Pennsylvanian
Undifferentiated
Mississippian
Silurian-Devonian
Ordovician
Cambrian
Crystalline Basement
Early Cambrian
Raggedy Mountain Gabbro
Neoproterozoic-Early Cambrian
Wichita Granite Group
Carlton Rhyolite
Mesoproterozoic
Tillman Metasedimentary Group
Central Oklahoma Granite
Saginaw Granite
CO
KS
MO
NM
AR
TX
35°N
100°W
95°W
200 km
N

Figure 5. General cross section of the Anadarko Basin from the deep basin (SW; A) to the shelf (NE; A'). Note the thickness of proximal Pennsylvanian strata relative to distal stratal packages (from Kushner, 2018, and others therein).

The basin is a major hydrocarbon-producing area within the North American craton, producing over 124 TCF and 5700 MMBO from Paleozoic systems as of 2011 (Mitchell, 2011). The history of the Oklahoma Basin (the earlier Anadarko Basin) is complex as the area experienced multiple periods of subsidence (Soreghan et al., 2012). The initial phase of subsidence was driven by rifting of the supercontinent Rodinia (early Paleozoic/Early Cambrian) and opening of the Iapetus Ocean (Powell et al., 1980; Soreghan et al., 2012; Price, 2016). The rifting, along what is called the Southern Oklahoma Aulacogen included a series of granitic and gabbroic intrusions and rhyolitic volcanic eruptions (Powell et al., 1980). The second subsidence phase was marked by Early Paleozoic thermal subsidence (Ham, 1973). Finally, most workers suggest that thrust-loading of the Amarillo-Wichita Uplift created coeval flexural subsidence -forming the Anadarko Basin -during the latest Mississippian and into the Pennsylvanian (Perry, 1989; Price, 2016). This compressional episode is thought related to the Ancestral Rocky Mountains (ARM) that formed during the late Mississippian-early Pennsylvanian (Fig. 2; Kluth and Coney, 1981; Soreghan et al., 2012). Occurrence of minor granitic inselbergs rising above Permian strata suggest continued subsidence and burial of both the Anadarko Basin and the Amarillo-Wichita uplift (Soreghan et al., 2012; Price, 2016).

Study Area and Study Interval

The area of this study is located along the eastern Anadarko Basin, on the Anadarko Shelf (Fig. 4). Specifically, the three cores used are in Kay, Logan and Pottawatomie Counties of Oklahoma (Table 1). Well cores were picked based on their location within the shelfal areas and where previous work had identified channelized systems within the Red Fork interval. The well-log data used to identify and correlate incised valleys are in northern and central Oklahoma, covering parts of Kay, Garfield, Noble, Logan, Lincoln, Oklahoma, and Pottawatomie Counties (Fig. 4).

The study interval is termed the Red Fork Sandstone and consists of fluvial and deltaic sandstones of Desmoinesian (Moscovian) age. The Red Fork has had a long history as a prominent oil and gas producer in the Anadarko Basin as it was one of the first producing reservoirs discovered in Oklahoma (Withrow, 1968; Houston and Kerr, 2008). The name Red Fork is the informal subsurface equivalent to the Taft Sandstone (upper Boggy Formation) at the surface, to the Chicken Farm Sandstone of Oklahoma County and the Earlsboro sand of Pottawatomie County in the subsurface (Jordan, 1957; Ye and Kerr, 2000). The formation's name was given by Hutchinson (1911) to describe a shallow producing sandstone in the Fork field, southwest Tulsa, Oklahoma (Jordan, 1957).

The Red Fork belongs to the Krebs Group (Cherokee Group) of the Middle Pennsylvanian (Desmoinesian) System (Figs. 6, 7). The Cherokee Group comprises rocks from the base of the Oswego Limestone to the base of the Desmoinesian Series. In the vicinity of Logan and Pottawatomie Counties, OK, the Cherokee Group is mainly unconformable upon Ordovician (Sylvan Shale) and Mississippian (Caney Shale, Mayes Limestone) rocks except in eastern portions of Pottawatomie County, where the Group conformably overlies rocks of Atokan age (lower Middle Pennsylvanian; Tate, 1985). The formation thickness is said to be controlled by the configuration of the Cherokee platform, the Nemaha fault zone and central Oklahoma uplift, and the Anadarko Basin (Andrews, 1997). The Red Fork interval is relatively uniform and thin (less than or equal to 100 ft) across much of central and northeastern OK;

however, the interval thickens greatly to the southwest (Fig. 5). Studies suggest that the uniform thickness in central and northeastern OK indicates low depositional gradient on the shelf and Cherokee platform and attenuation or erosion along the Nemaha uplift (Fig. 8, Tate, 1985; Andrews, 1997). The Red Fork Sandstone, along with other Cherokee sandstones, consists of interbedded sandstone, shale, thin limestone, and coal bounded at the top and bottom by transgressive limestone marker beds – the Pink and Inola limestones, respectively (Withrow, 1968; Frezon and Dixon, 1975; Tate, 1985; Puckette et al., 2000; Puckette and Al-Shaieb, 2002). The Red Fork is overall interpreted as fluvial, deltaic, shelfal and deeper-water environments during a time of both tectonic subsidence and glacioeustatic fluctuations in sea level (Ye and Kerr, 2000; Puckette et al., 2000; Puckette and Al-Shaieb, 2002).

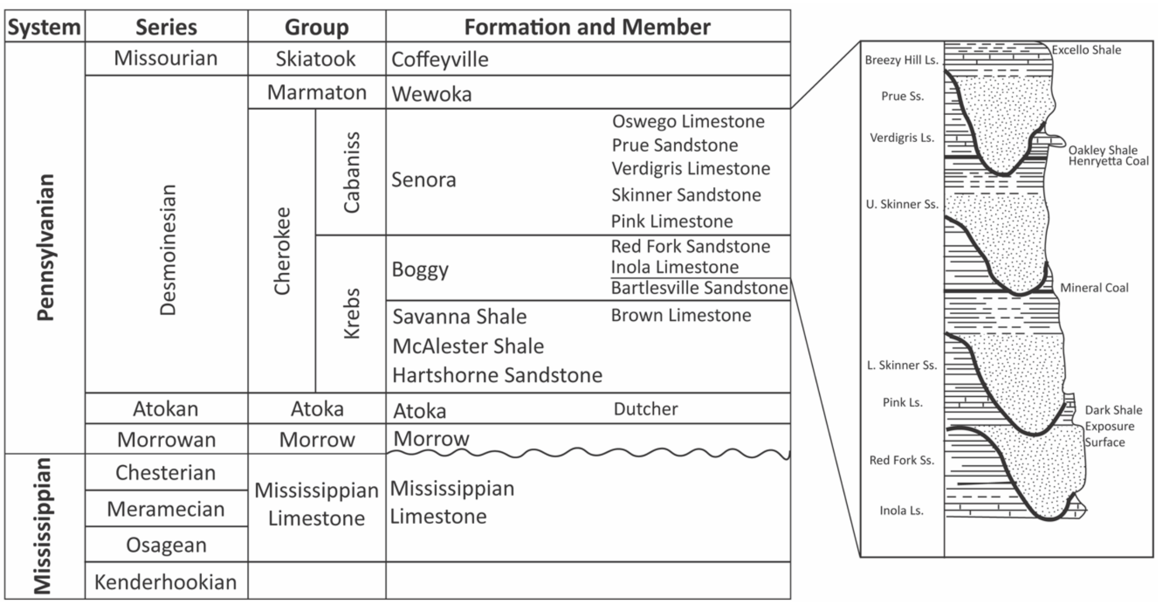

Figure 6. Stratigraphic nomenclature of the Late Paleozoic in Oklahoma (modified after Ye and Kerr, 2000; adapted from Puckette, 2003).

Previous studies reveal that the interval was a result of early Desmoinesian transgression (Inola Limestone deposition) interrupted by several regressions of deltaic advances across the shelf and into the Anadarko Basin (Visher et al., 1971; Andrews, 1997; Wallet et al., 2012). The

Red Fork overlies weathered Mississippian rocks in areas where the Inola limestone marker is absent (Glass, 1978). Previous work has classified the Red Fork as a 3rd order sequence, divided into at least three (3) upwardly coarsening parasequences (transgressive-regressive episodes), separated by thin regional limestones or shales (Frezon and Dixon, 1975; Puckette et al., 2003). Cyclic sequences in northern and northeastern Oklahoma contain coal beds that are absent elsewhere in Oklahoma (Frezon and Dixon, 1975). Source areas of the Red Fork have been proposed to the south, west, north, northeast, and east of Oklahoma and adjacent regions (Dogan, 1969; Moore, 1979; Andrews, 1997; Lambert, 2006; Johnson, 2018). Previous studies propose major sandstone trends oriented primarily north to south (Visher et al., 1971; Tate, 1985), but with trends also to the southwest just to the west of the Nemaha uplift in central OK (Andrews, 1997; Lambert, 2006; Fig. 9).

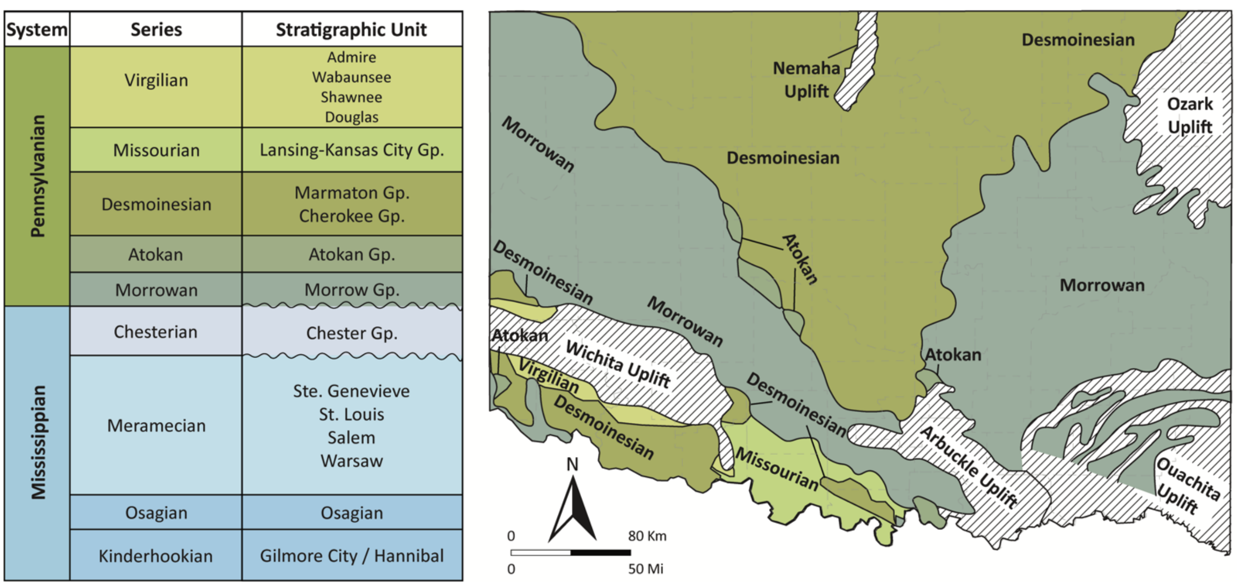

Figure 7. General stratigraphic column (left) and subsurface distribution of Pennsylvanian strata in Oklahoma (right) (modified from Frezon and Dixon, 1975; Wang and Bigdoli, 2019).

In central and northern Oklahoma, the Red Fork Sandstone accumulated in channels incised into shale (Puckette et al., 2003; Lambert, 2006). The Red Fork is further divided into

Lower, Middle, and Upper incised valley fill intervals, which resulted in a stratigraphically complex internal architecture (Peyton et al., 1998; Wallet et al., 2012; Davogustto et al., 2013). To date, five different stages of valley incision have been defined by previous authors (Withrow et al., 1968; Peyton et al., 1975, 1998; Warner, 2006; Lambert, 2006; Davogustto et al., 2013).

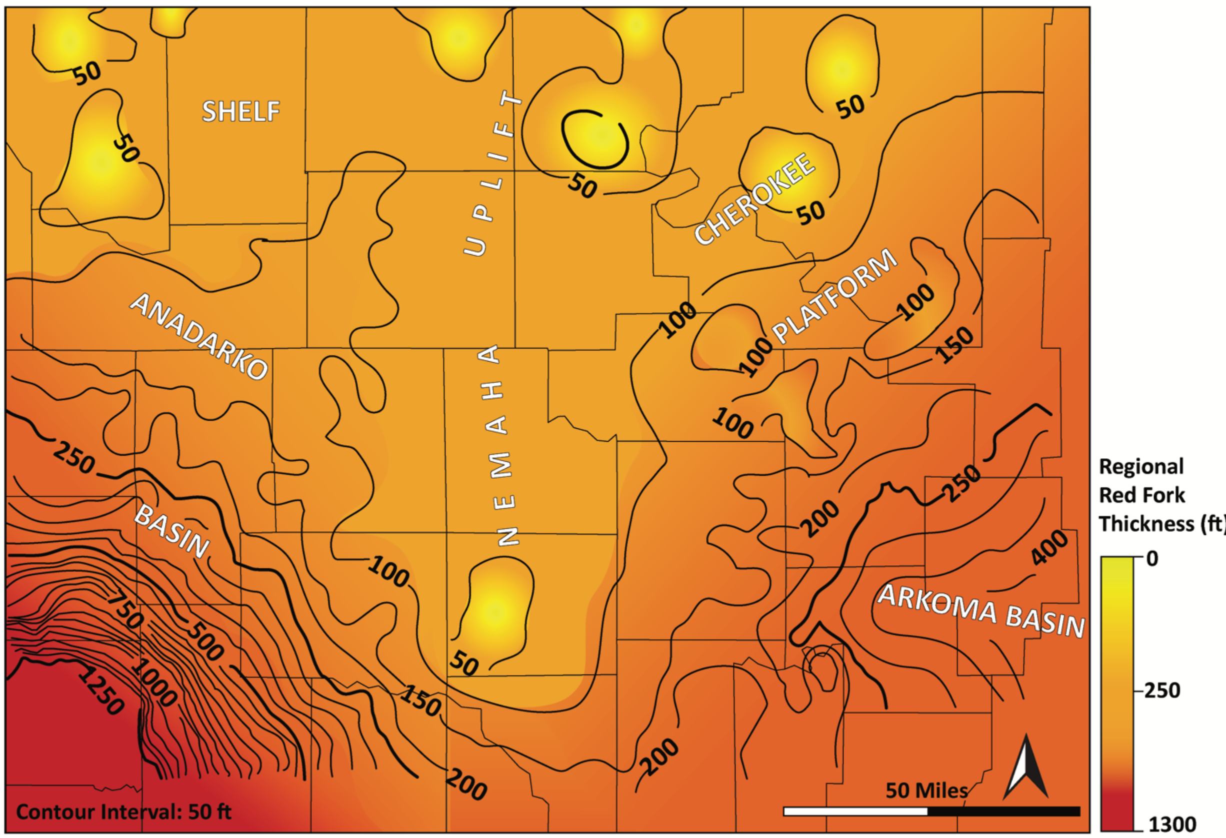

Figure 8. Generalized regional isopach map of the Red Fork Sandstone plus the Pink Limestone (from the top of the Pink Limestone to the top of the Inola Limestone), Oklahoma. Contour interval is 50 ft; white dots are well cores used in this study (modified from Andrews, 1997).

In general, Phase I is described as poorly correlative shale, siltstone and tight sandstone superposed on a basal "lag" deposit; it is defined as the earliest valley incision event (narrow, initial downcutting), and thus had been eroded in many places in the Anadarko Basin (Fig. 10A; Withrow, 1968; Peyton et al.,1998; Lambert, 2006). Phase II was deposited in a period of valley widening and maturation and is characterized by an upwardly fining succession (Fig. 10B). Phase III is described as thick, blocky, porous and re-worked sandstone that represents the last major incision, which occurred within a narrow steep walled system. The sandstone is overlain by low-resistivity marine shale deposited during a transgression that drowned the valley (Fig. 10C; Peyton et al., 1998; Lambert, 2006). Phase IV is characterized by interbedded sandstone and shale packages with a basal (or close to the base) coaly shale interval (Peyton et al., 1998). Nevertheless, Withrow (1968) and Suarez (2008) described the facies of this as lagoon/coal swamp or delta head deposits. Phase V was recognized by Peyton and others (1998) from seismic studies using spectral decomposition and coherency; stage V is represented by non-productive sandstone in a shale-filled valley (Fig. 10D).

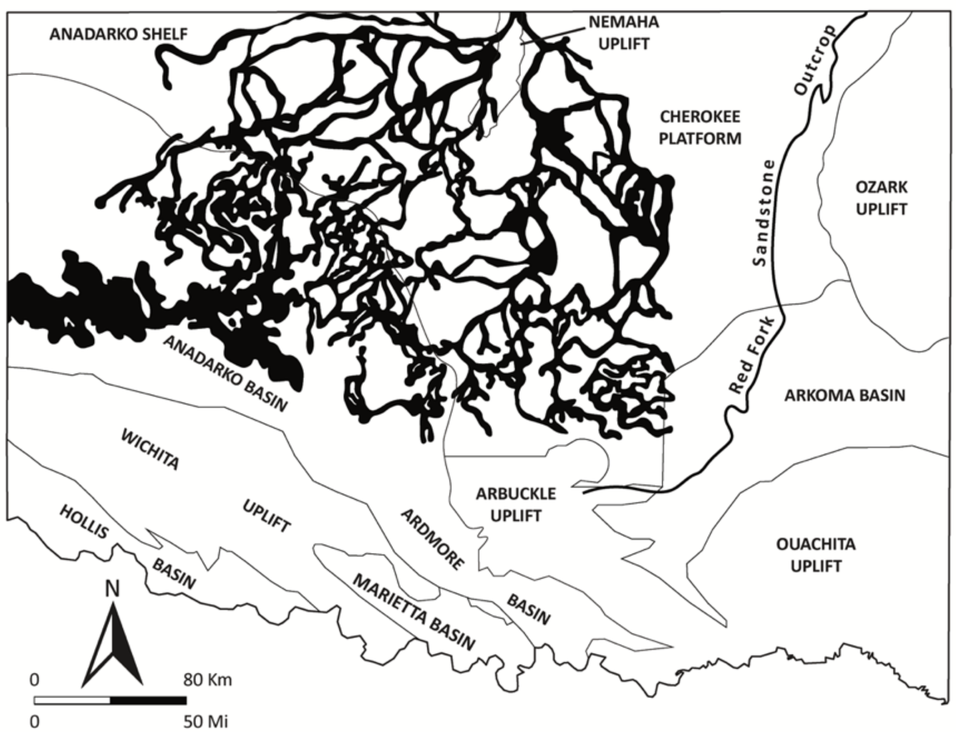

Figure 9. General distribution of major Red Fork sandstone bodies in Oklahoma (modified from Tate, 1985; Andrews, 1997; Lambert, 2006, and others therein).

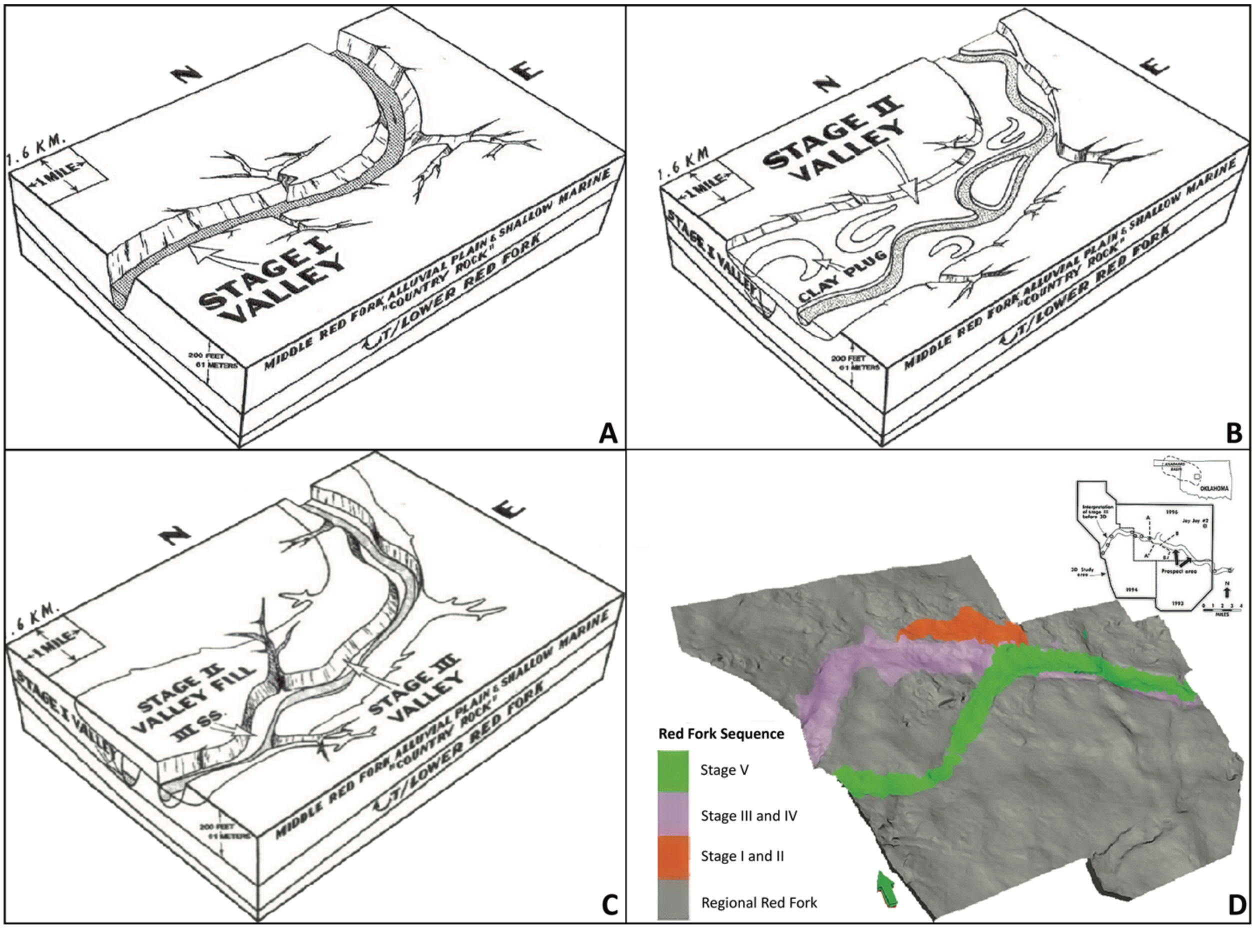

Figure 10. A-C: Bock diagram illustrating interpretation of incised valley formation **A)** Initial development of Stage I valley incision following regression at the end of middle Red Fork time; **B)** Stage II valley sequence marked by channel migration and erosion caused by valley broadening and fill with terrigenous sediment; **C)** Stage III rapid valley incision (lower base level) through poorly consolidated Stage II incised valley fill (Stage III sands were reworked from older Stage II sediments) (Modified from Lambert, 2006). **D)** Three-dimensional model of the Red Fork incised valley stages (Modified from Davogustto et al., 2013; after Peyton et al., 1998).

CHAPTER III

METHODS

This study aims to test whether Middle Pennsylvanian sediment-routing systems into the Anadarko Basin varied on different systems tracts of stratigraphic sequences thus providing insight into the controls of Pennsylvanian-age sedimentation patterns and sediment composition into the Anadarko Basin. I hypothesize that different source terranes provided sediment into the Anadarko Basin at different sequence's systems tracts during the Desmoinesian. There were four (4) components of methods utilized to test the research hypotheses of this study: well-log correlation and interpretation, well core descriptions, petrographic thin section analysis, and U/Pb detrital zircon analysis.

Well-Log Correlation and Core Description

Well-log interpretation and correlation techniques were applied to construct the stratigraphic framework for the Cherokee Group in the study area, display stratal geometries, and assess the presence of paleovalleys in the Anadarko Shelf during Middle Pennsylvanian time. Correlations were made using a total of 33 wells from Kay (4), Noble (4), Garfield (4), Logan (9), Oklahoma (5), Lincoln (3), and Pottawatomie (4) Counties (Appendix A). Recognition of marker beds was made possible by the work of previous authors on the Cherokee Group of Oklahoma (Withrow, 1968; Tate, 1985; Andrews, 1997). A total of eight (8) stratigraphic cross sections were constructed in the study area (Fig. 4) to document thickness, lateral continuity, and stratal geometries. However, only three cross sections from Kay, Logan and Pottawatomie Counties are discussed in the text. Correlations and interpretations were made from the base of the Verdigris Limestone to the top of the lower Pennsylvanian (or Mississippian or Devonian) packages (Figs. 6, 7, 11). Three well core intervals of the Red Fork Sandstone were described at the centimeter scale, delineating, lithology, grain size and texture, sedimentary structures, and the nature of contacts. The well cores are located in Kay, Logan and Pottawatomie Counties of Oklahoma (Fig. 4; Table 1) and display thicknesses of 40 ft (12 m), 120 ft (37 m) and 140 ft (43 m), respectively. Construction of a sequence stratigraphic framework for the Red Fork was performed after well log correlations and the characterization of lithofacies.

Petrographic Analysis

Thin section petrographic analysis was conducted to complement core descriptions for the three well-cores, and aid in the characterization of lithofacies and interpretation of the environments of deposition. In addition, point-counting of sandstones was employed to quantify mineral components and the percentage of each phase and ultimately interpret the provenance of the sandstones (Dickinson, 1970; Ingersoll et al., 1984). Point-counting analysis involved the classification of 300 sand-sized (>62.5 um) framework grains on a 1x1 mm grid, with 11 compositional categories from the Gazzi-Dickinson point-counting method (Table 2; Dickinson, 1970; Ingersoll et al., 1984). Ternary diagrams were used to plot the point count data and interpret provenance regions based on mineral composition.

Table 1. Cored intervals used in this study of the Desmoinesian Red Fork Sandstone.

Core ID	API	Operator	Well	Sec	TW	RG	Q	Lat	Long (-)	County	Top (ft)	Bottom (ft)	Study Interval (ft)
1	35071003210000	Gulf	Dora Goodson 1	24	28N	03E	NW NE NW	36.89673	96.93557	Kay	2862	3206	3160-3206
2	35083209270000	Universal	Flasch 1-2	02	17N	02W	NENW	35.98006	97.38132	Logan	5113	5707	5117-5237
3	35125210550000	Estoril	Farris 1-16	16	10N	03E	SWSW	35.334	96.99717	Pottawatomie	4780	4920	4780-4920

Note: The top and bottom depths reflect the entire cored interval; Sec = section; TW = township; RG = range; Q = quarter.

Detrital Zircon Geochronology

Detrital zircon geochronology is used to determine the crystalline or recycled source from which sandstones/sand were derived through weathering prior to their final deposition (Gehrels, 2014). U-Pb geochronology of zircon crystals was conducted by laser ablation-inductively coupled mass spectrometry (LA-ICPMS) at the Arizona LaserChron Center, using techniques from Gehrels et al (2008) and Gehrels and Pecha (2014). Between 1 and 2 kg of sandstone, from stratigraphically distinct units of each core in this study (Table 3), were slabbed by Oklahoma Petroleum Information Center (OPIC) technicians. At the University of Arizona, samples were crushed, and zircons were isolated using basic separation techniques (Gehrels et al., 2006; 2008). Mounts of extracted detrital zircon grains were compiled with calibration-standard zircon grains. Cathodoluminescence (CL) and Backscattered-Electron (BSE) imaging allowed for distinguishing zircon from monazite grains, as well as for avoiding spot areas with zoning, inclusions, and cracks. LA-ICPMS analysis was conducted using 20 µm spot size on 300 randomly selected grains. Normal and reverse concordance within samples was permitted to 20 and 5 percent, respectively.

Table 2. Summary of modal composition parameters used for point counting of sandstones in this study. Modified from Dickinson et al. (1983) and Ingersoll et al. (1984).

- Quartz (Q) = Qm+ Qp+ Chert
- Monocrystalline quartz (Qm)
- Polycrystalline quartz (Qp)
- Chert (C)
- Feldspar (F) = P + K
- Plagioclase (P)
- Potassium feldspar (K)

- Lithic fragments (L) = Ls + Lm + Lv
- Lithic sedimentary (Ls)
- Mudstone (Lsm)
- Sandstone (Lss)
- Lithic metamorphic (Lm)
- Lithic volcanic (Lv)
- Lt = Ls + Lm + Lv + Qp + C
Note: Grains of mica, opaques and other accessory minerals were also included in point count totals. Cement components were not counted in the 300-grain framework total.

Table 3. Information for detrital-zircon samples used in this study.

DZ Sample	Depth (ft)	Lithology	Formation	Location	Coordinates
DG-A	3177	Medium to fine-grained sandstone	Red Fork	Kay	36.89673; 96.93557
DG-B	3191.5	Fine-grained sandstone	Red Fork	Kay	36.89673; 96.93558
UF-A	5119.5	Fine-grained sandstone	Skinner?	Logan	35.9801715; 97.3820093
UF-B	5154.2	Fine to very fine-grained sandstone	Red Fork	Logan	35.9801715; 97.3820093
UF-C	5226	Very fine-grained and silty sandstone	Red Fork	Logan	35.9801715; 97.3820093
SF-A	4803	Fine-grained sandstone	Red Fork	Pottawatomie	35.334; 96.99717
SF-B	4897	Fine-grained sandstone	Red Fork	Pottawatomie	35.334; 96.99718

Note: Sample UF-B is from Kushner, 2018.

CHAPTER IV
STRATIGRAPHIC FRAMEWORK

Introduction

Figure 11 shows a typical well log of the Red Fork Sandstone from the study region, depicting sandstone zones and key marker beds used to establish the stratigraphic framework within the Cherokee Group. The Verdigris, Pink, Inola and Brown Limestones are the marker beds that divide the Cherokee Group. The Red Fork Sandstone is the interval between the base of the Pink Limestone and the top of the Inola Limestone. The Verdigris Limestone was selected as the stratigraphic datum due to its consistent presence throughout the region as well as its distinctive gamma-ray log signature. Thus, on the stratigraphic cross sections, correlations were made from the base of the Verdigris Limestone to the base of the Pennsylvanian (top of Mississippian or Devonian) packages. Correlation of the Pink and Inola Limestones was done using previous published studies and reports including those of Withrow (1968), Tate (1985), Andrews (1997), Puckette et al. (2003) and others. In general, the two limestone markers are approximately <10 ft thick in the study area, display low GR with sharp but non-abrupt contacts, display high resistivity, and are commonly found is association with "hot" shales (organic-carbon-rich shales). As noted above, eight (8) stratigraphic cross sections were constructed in the study area (Fig. 4) to illustrate thickness, lateral continuity, and stratal geometries; four, which contain the cored wells, are discussed below while the other cross sections are presented in Appendix A.

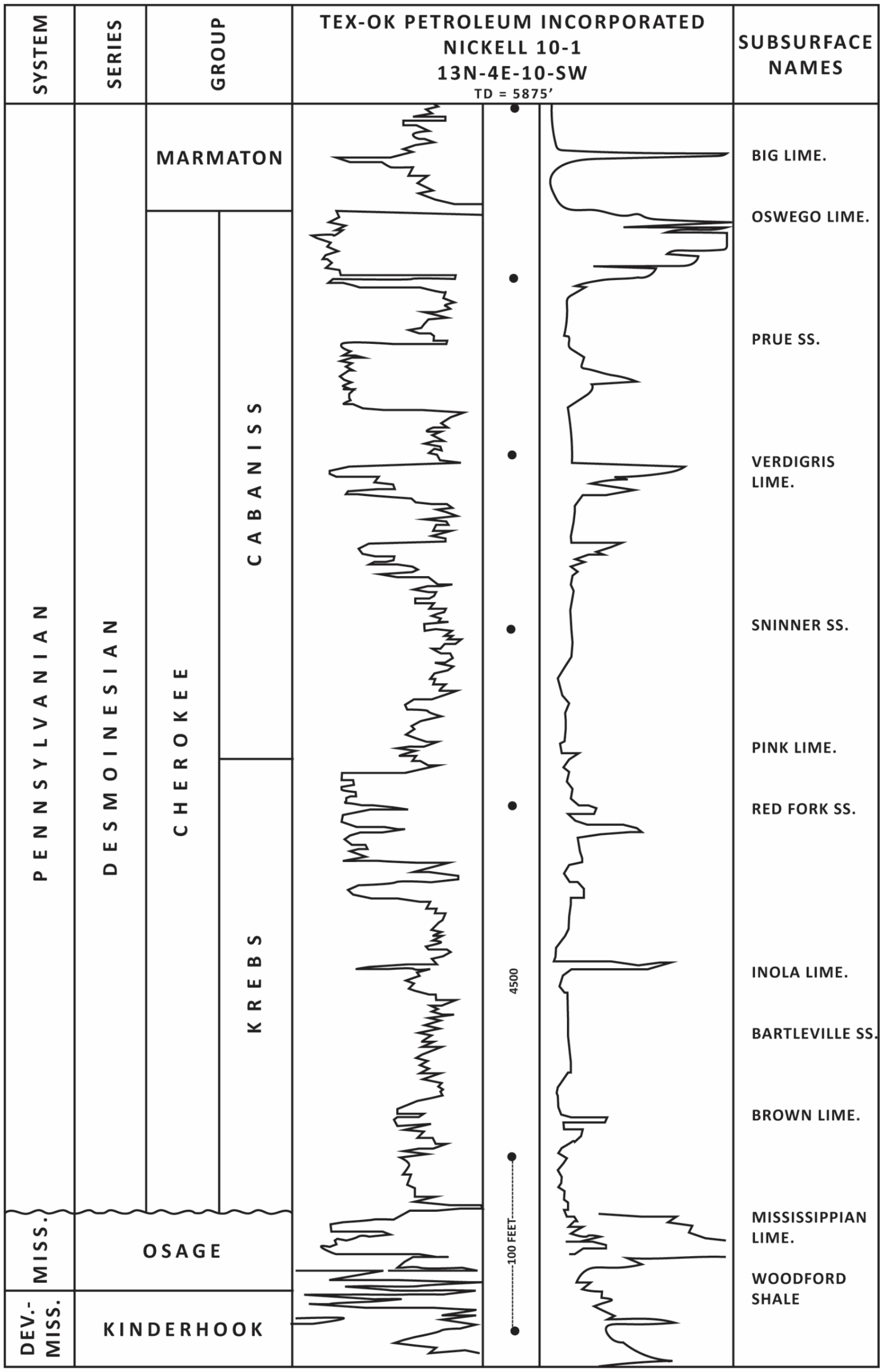

Figure 11. Type log of study area (left - Gamma-Ray log; right - Resistivity log). Interpretations were made using previous Red Fork investigations (Withrow, 1968; Tate, 1985; Puckette et al., 2003).

Kay County Cross Section

The Kay County cross section is a northeast-southwest section crossing the extreme northern portion of the study area from T.29N., R.4E. to T.25N., R.1E. (Fig. 12). The cross section is composed of four (4) wells. Well number 2 was chosen based on its proximity to the Kay County core (Core 1; Table 1 and Appendix 1), because no gamma-ray log for the cored well exists. The Red Fork Sandstone is well developed in wells 2 and 3, displaying a blocky well log pattern, characteristic upwardly fining succession that cuts underlying strata (abrupt basal contact), and vertical stacking of sand bodies, which are indicative of channel-fill (incised valley-fill) deposits. That suggestion is also supported by the absence of the Inola Limestone in well 3 and abrupt top of the Mississippian. The Inola Limestone was probably eroded prior to the deposition of the Red Fork in the areas of well 3. Thickness of the channel-fill deposits range from 30 ft to 45 ft and sand bodies are separated by thin, <5 ft to 10 ft, shale packages. Inferred non-channel deposits of the Red Fork Sandstone are illustrated in wells 1 and 4 as they display characteristic interbedded “ratty” sandstone/shale and gamma-ray “hugging” shale with no distinct upwardly fining- or coarsening trends, which are patterns suggestive of marginal marine to marine deposits (Andrews, 1997; Boucher, 2002).

A significant feature observed in this cross section is overall thickening and thinning of the Cherokee interval from the base of the Verdigris Limestone to the top of the Mississippian Limestone. The complete interval thins from 270 ft in well 1 to 230 ft in well 2 but thickens to 300 ft in well 3 and thins to 280 ft in well 4. On the other hand, the Red Fork interval thins from ~120 ft in wells 1 and 2 to ~100 ft in wells 3 and 4.

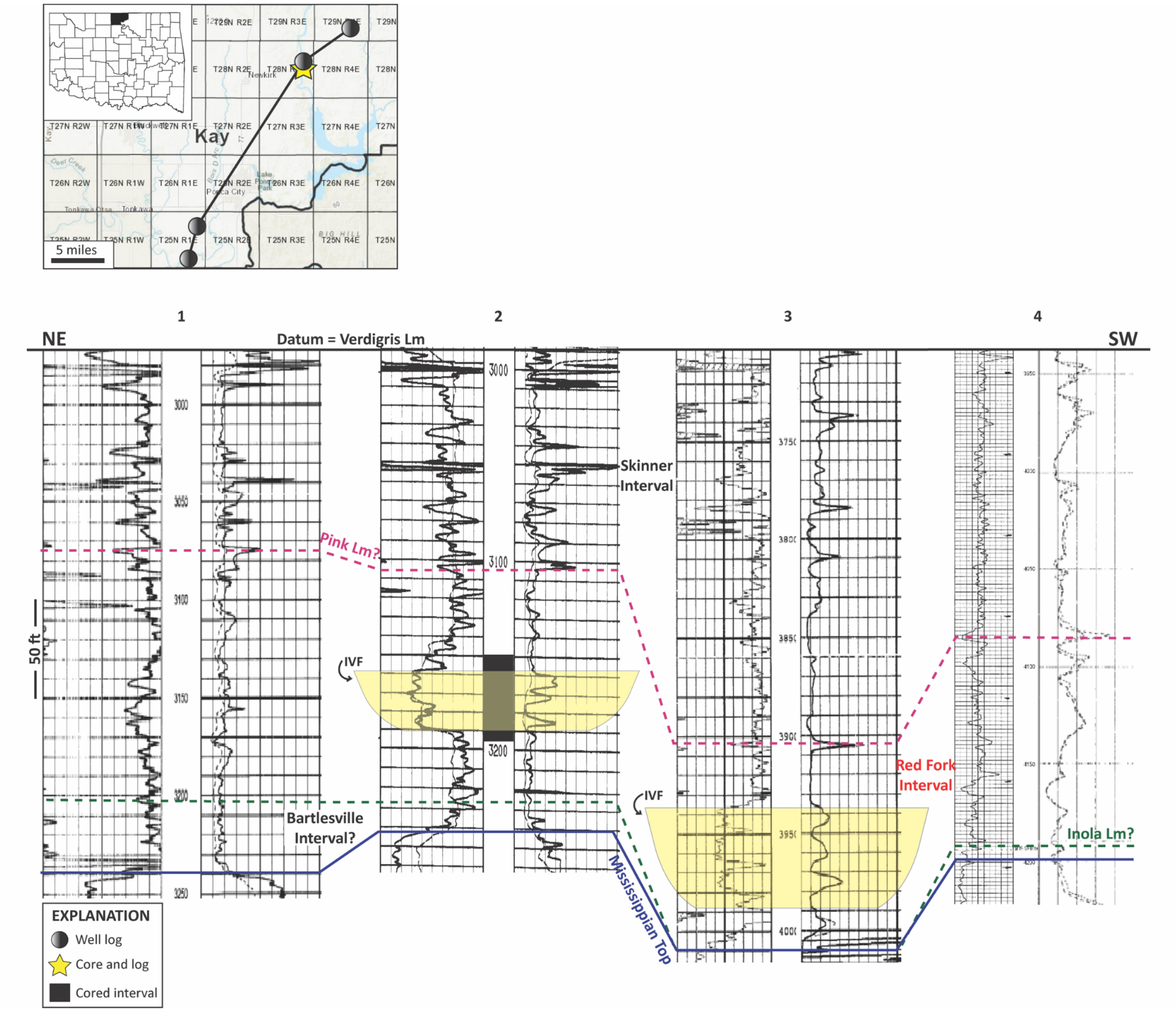

Figure 12. Northeast-southwest stratigraphic cross section of the middle and lower Cherokee Group in Kay County. The Verdigris Limestone is the stratigraphic datum. Yellow star = location of Core 1 (not used in the cross section). IVF = incised valley fill. The left and right logs are Gamma-Ray (GR) and Resistivity logs, respectively.

Logan County Cross Sections

The Logan County cross section trends northwest-southeast in the north-central portion of the study area from T.19N., R.3W. to T.17N., R.1W. (Fig. 13). The cross section comprises four (4) wells, including Core 2 (Table 1). The Red Fork Sandstone is better developed in wells

27, 28 (Core 2), and 29, displaying a blocky to bell shape, characteristic upwardly fining successsion that cuts underlying strata (abrupt basal contact), indicative of channel-fill (incised valley fill) deposits. This interpretation is also supported by the overall incision pattern displayed in the top of the Mississippian and the absence/erosion of the Inola Limestone in all wells, except for well 26.

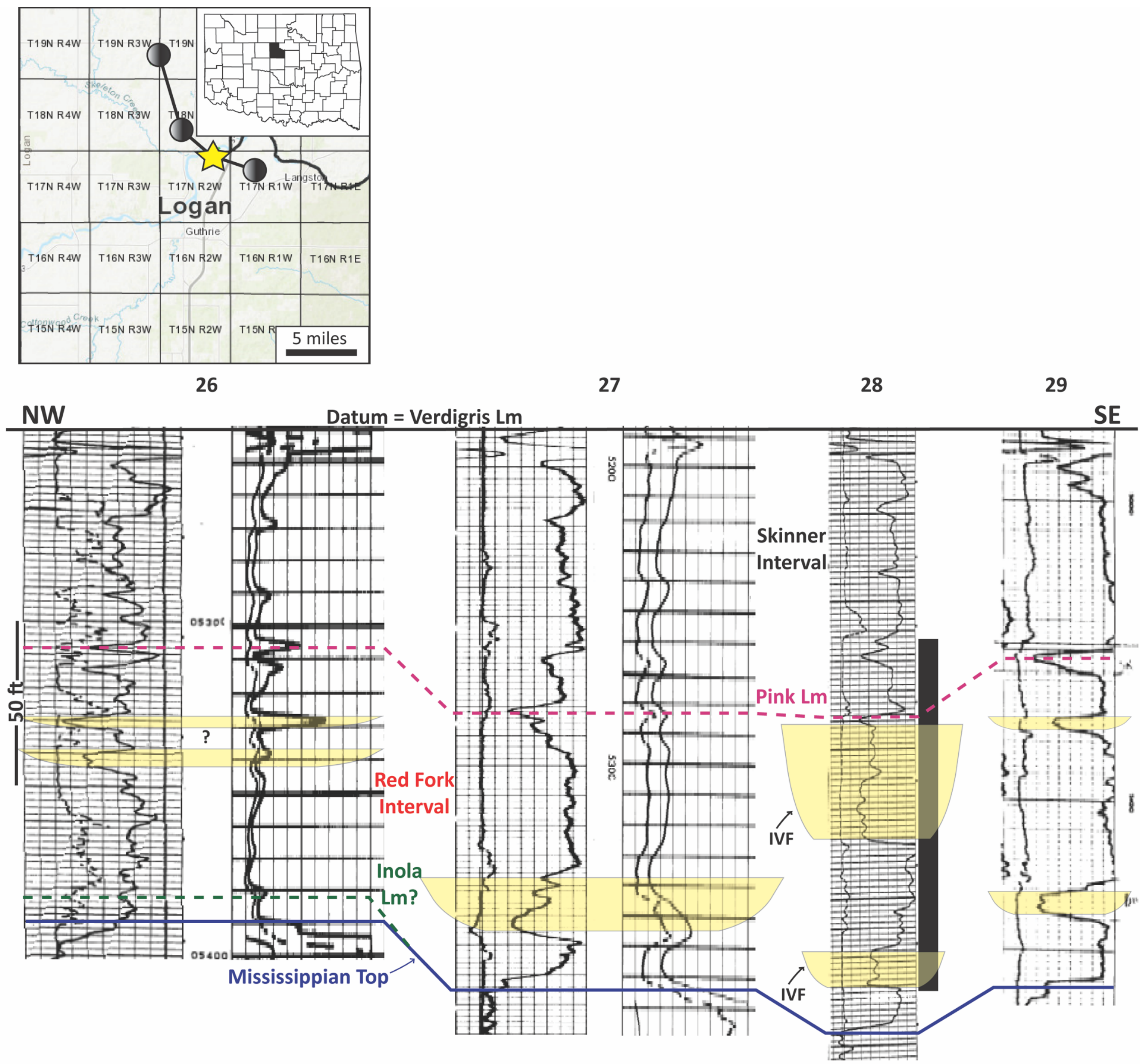

Figure 13. Northwest-southeast stratigraphic cross section of the middle and lower Cherokee Group in Logan County. The Verdigris Limestone is the stratigraphic datum. Yellow star = location of Core 2; IVF = incised valley fill. The left and right logs are Gamma-Ray (GR) and Resistivity logs, respectively. Wells 28 and 29 show GR logs only.

Thickness of the channel-fill deposits range from 10 ft to ~45 ft and sand bodies are separated by shale packages. Channel fills in wells 26 and 29 are likely amalgamated sand bodies and are much thinner (less than or equal to 5 ft ft) than in wells 27 (~25 ft) and 28 (~10 ft to ~45 ft). Non-channel deposits of the Red Fork Sandstone are inferred between channel-fill units. The overall Red Fork Sandstone interval thickness averages 110 ft in the area.

A second north-south cross section was constructed for Logan County, from T.19N., R.2W. to T.15N., R.2W. (Fig. 14) that consists of five (5) wells also centered on Core 2 (well 11 in this section). The Red Fork Sandstone is well developed in wells 10, 11 and 13. A significant feature observed in this cross section is the variable thickness trend of the Cherokee interval from the base of the Verdigris Limestone to top of the pre-Pennsylvanian strata. The interval thins from 180 ft in well 9 to 116 ft in well 13. On the other hand, the Red Fork interval thickens from ~50 ft (wells 9 and 10) to 120 ft (well 11) and thins to ~50 ft in wells 12 and 13.

Pottawatomie County Cross Section

The Pottawatomie County cross section is a northwest-southeast section crossing the south-central portion of the study area from T.11N., R.2E. to T.13N., R.3E. (Fig. 15). The cross section comprises four (4) wells. The Red Fork Sandstone is well developed in wells 19, 20 and 21 (Core 3; Table 1), displaying a blocky to bell-shaped well log pattern and characteristic upwardly fining upward succession that cuts underlying strata (abrupt basal contact), indicative of channel-fill deposits. The channel-fill deposits range from 55 to 60 ft in thickness and the sand bodies in wells 20 and 21 exhibit a stacking pattern separated by ~20 ft thick shale package. An overall thickening and thinning pattern of the Cherokee interval from the base of the Verdigris Limestone to top of the Mississippian Limestone was observed. The interval thins from 450 ft in well 19 to 370 ft in well 20 but thickens to 500 ft in well 21 and thins to 350 ft in well 22.

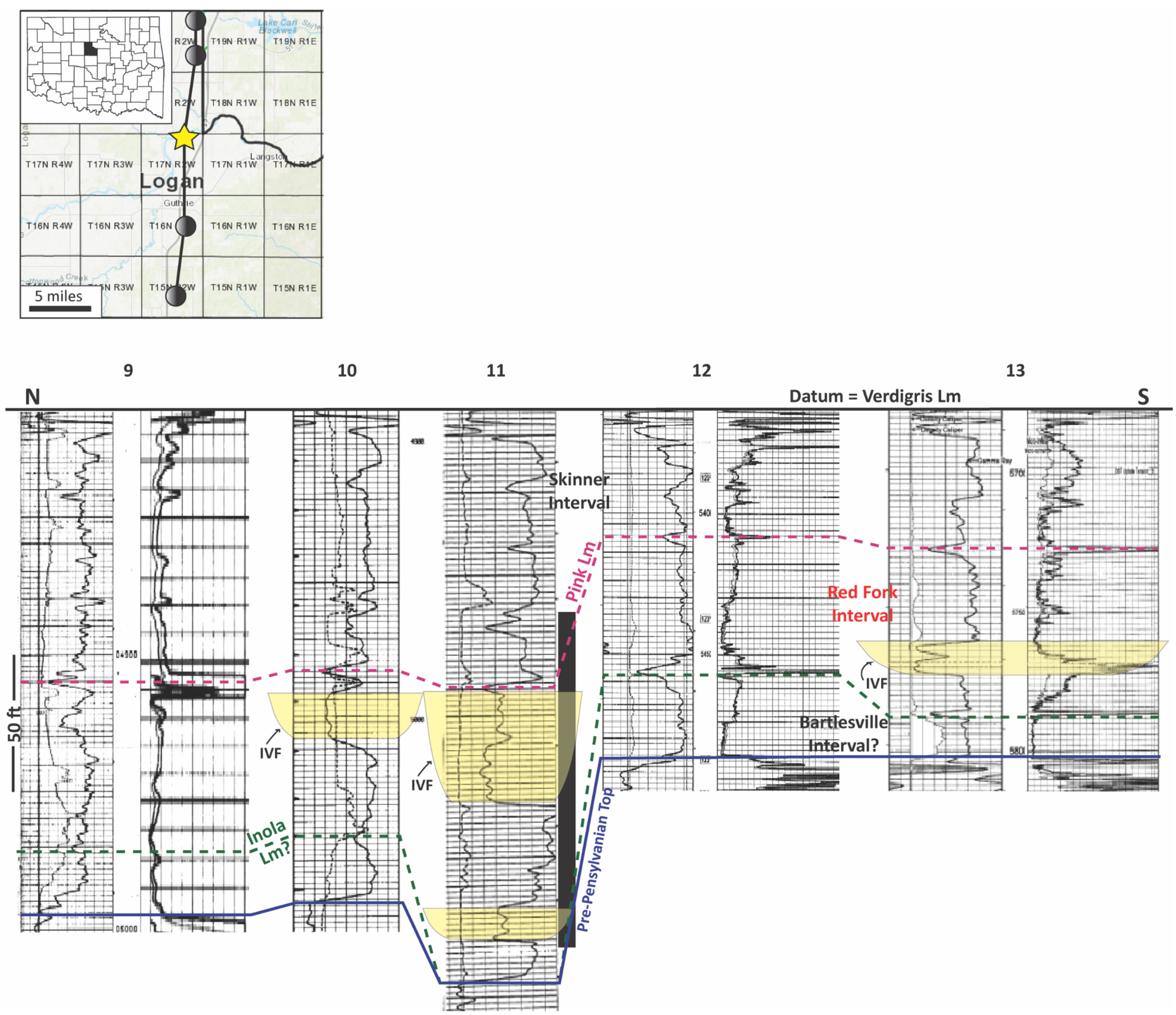

Figure 14. North-south stratigraphic cross section of the middle and lower Cherokee Group in Logan County. The Verdigris Limestone is the stratigraphic datum. Yellow star = location of Core 2; IVF = incised valley fill. The left and right logs are Gamma-Ray (GR) and Resistivity logs, respectively. Wells 10 and 11 show GR logs only.

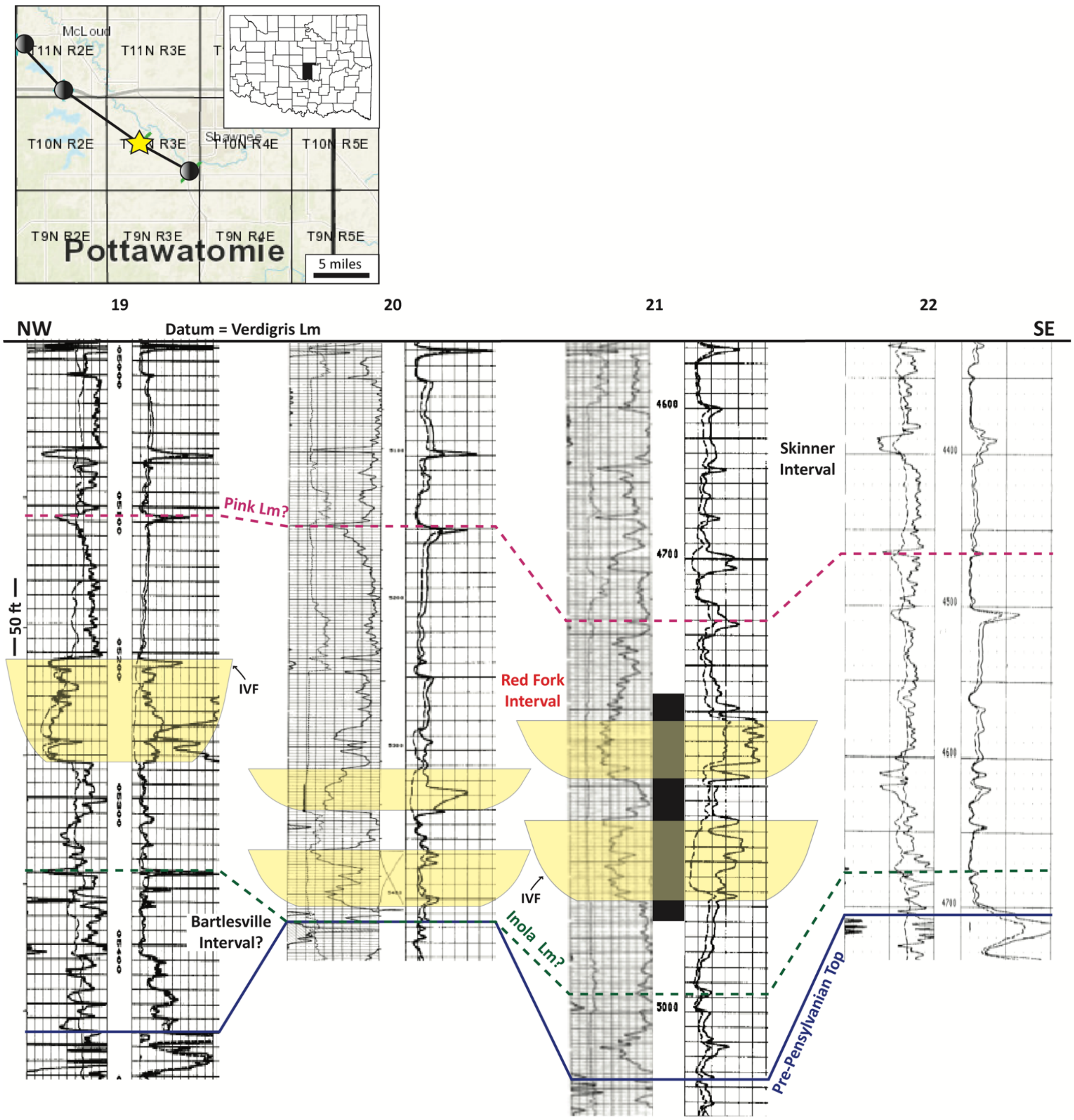

Figure 15. Northwest-southeast stratigraphic cross section of the middle and lower Cherokee Group in Pottawatomie County. The Verdigris Limestone is the stratigraphic datum. Yellow star = location of Core 3; IVF = incised valley fill. The left and right logs are Gamma-Ray (GR) and Resistivity logs, respectively.

Analysis of the Stratigraphic Cross Sections

From the analysis of the stratigraphic cross sections, the Red Fork interval is continuous throughout the study area; sand bodies of the Red Fork are discontinuous, however. The Cherokee Group as well as the Red Fork interval and the channel deposits within are all thicker in Pottawatomie County compared to Kay and Logan Counties. The Red Fork interval varies in thickness from 250 ft to 350 ft from Kay and Logan Counties to Pottawatomie County (Figs. 12-15). This increase in thickness to the south agrees with regional cross sections (Fig. 5) and is likely caused by regional and local variations in tectonic subsidence during Desmoinesian time (Granath, 1989; Perry, 1989; Johnson, 2008; Kushner, 2018; Turko and Mitra, 2021); additional variation in thickness relates to the presence of the inferred incised valleys. The underlying unit below the Red Fork varies from the Mississippian Limestone to the lower Paleozoic Bartlesville Sandstone.

The log signatures suggest the Red Fork sandstones are composed of both channel-fill and non-channel-fill deposits. Channel-fill deposits are indicated by blocky or bell-shaped log patterns with characteristic abrupt/sharp basal contacts and channel stacking. Sharp lateral contacts are assumed by abrupt basal contacts. Furthermore, these blocky sandstones tend to occur where evidence of incision into the lower units is present. Non-channelized deposits are suggested by interbedded "ratty" sandstone/shale and gamma-ray "hugging" shale patterns with general abrupt basal contacts and gradational upper contacts (evidenced by a serrated log pattern).

CHAPTER V

DEPOSITIONAL ENVIRONMENTS

Introduction

Several surface and subsurface studies have been conducted on the Cherokee Group in Oklahoma. In general, the Red Fork is interpreted to be of fluvial-deltaic origin (Brown, 1979; Andrews, 1997). Specifically, the Red Fork has been interpreted as lower deltaic plain (southern Noble County; Candler, 1977) with complex bifurcating and anastomosing patterns (east flank of the Nemaha ridge; Cole, 1969). Hudson (1969) concluded that the interval in south-central Kansas and north-central Oklahoma represents a large river and deltaic system. In northwestern Oklahoma, specifically Grant and Alfalfa counties, Withrow (1968) suggested that the main Red Fork depositional environment was a series of offshore bars due to the "en-echelon" pattern of sand bodies, gradational lateral contacts, and the overall paleogeography.

In central Oklahoma, including Payne, western Lincoln, southeastern Logan, and other adjacent counties, the Red Fork was interpreted as a complex of deltaic environments (Hawissa, 1965; Shulman, 1966; Dogan, 1969; Verish, 1979; Walker, 1979). In south-central Oklahoma, including Pottawatomie, Cleveland and McClain counties, the same interpretation has been made for the Red Fork (Pulling, 1979; Tate, 1985) except for the detail that the deltaic channels prograded along a coastal plain of low relief (Albano, 1975). The depositional model for the Krebs Group in Oklahoma has been constructed by several authors; however, in this study, four depositional systems have been recognized: tide-dominated estuaries and deltas, tidal flats, and marine environments. Detailed description and classification of each depositional system will be discussed in following sections of this chapter.

Facies Analysis

The description and classification of sedimentary units into lithologic facies and the characterization of stratigraphic packages were used to interpret depositional environments and to develop a sequence stratigraphic framework for the Red Fork Sandstone that will help tie sedimentary processes and depositional changes to changes in sediment composition (next section). In this study, 16 facies across the northern, central, and south-central Oklahoma, Anadarko Shelf, were characterized (Table 4) from the three cores. Lithofacies descriptions include lithology, color, composition, grain characteristics, bedding thickness and characteristics, sedimentary structures, trace and body fossils, post-depositional features, and overlying and underlying nature of contacts (Table 5). The lithofacies characterization was based exclusively on available cores and thus may not reflect attributes in other areas of the Anadarko Shelf. The lithofacies' descriptions are followed by the interpretation of the depositional settings and processes. Appendix B contains a page for each facies that summarizes it's features.

Table 4. Facies scheme of the Red Fork Sandstone in Kay, Logan and Pottawattamie Counties, Anadarko Shelf.

No.	Lithofacies	Depositional Process	Sedimentary Environment
1	Black, thinly laminated shales	Low energy sediment fallout; sediment reworking	Offshore marine; prodelta
2	Parallel laminated sandy mudstones	Sediment fallout and low energy tidal currents	Tidal channel

3	Black carbonaceous shales	Peat growth/accumulation without coalification	Supratidal flat / swamp
4	Gray sideritic shales	Low energy sediment fallout; sediment reworking	Marine
5	Mottled shales and sandstones	Pedogenesis of existing lithologies	Paleosol; interfluve
6	Shaly carbonates	High energy carbonate reworking; current reworking	Shallow / deep marine; transgressive lag
7	Skeletal wackstones to packstones	Low to high energy carbonate production; current reworking	Shallow marine (subtidal-intertidal); storm deposit
8	Burrowed and interbedded, sideritic sandstones and mudstones	Migration of subaqueous, bidirectional flow ripples, high-energy tidal currents; slackwater sediment fallout; bioturbation	Tidal channel; proximal delta front?
9	Heterolithic siltstones	Low energy tidal currents and slackwater fallout; bioturbation	Lower tidal flat or subtidal coastline
10	Heterolithic sandstones	High energy tidal currents; slackwater sediment fallout	Upper tidal flat, channel, or coastline (subtidal-intertidal)
11	Fine grained sandstone	Unidirectional tractive currents	Channel bar deposit
12	Medium to fine grained sandstones with mud drapes	Tidal currents, migration of subaqueous, bidirectional flow ripples, and slackwater sediment fallout	Tidal channel, subtidal, intertidal, or supratidal channels
13	Ripple laminated sandstone	Migration of subaqueous, unidirectional flow ripples	Tidal channel (upper unit)
14	Bioturbated sandy siltstones	Storm current sediment reworking; bioturbation	Marginal marine (intertidal-supratidal); storm deposits
15	Conglomerates	High energy, unidirectional tractive currents	Channel bar (basal lag)
16	Interlaminated and thinly interbedded sandstones and mudstones	Migration of subaqueous, bidirectional flow ripples and dunes, high-energy tidal currents; slackwater sediment fallout;	Distal delta front of tidal delta

Facies 1: Black, Thinly Laminated Shales

Description

Facies 1 consists of parallel laminated, silty, fissile, dark-gray, calcareous shale (Figs. 16-17). In Core 1, this facies occurs once at the core base and is composed of parallel laminated, fissile black shale and a bivalval/brachiopodal black shale interval (Fig. 16B; 3.6 ft/1.1 m). In Core 2, this facies presents itself as a parallel laminated, silty shale (Fig. 16A; 1 ft/0.3 m). Sedimentary structures include very thin (<1 mm) laminae (displayed by fissility) to thin (1-3 mm) continuous to discontinuous parallel silty and lenticular laminations. Very thin, silty, normally graded laminae were observed within the parallel laminated, silty shale of Core 2. The bivalve/brachiopod-rich shale contains plant material in the form of tiny "specks" or filaments and a 0.2 ft/0.06 m chaotic, less fissile, silty bed that displays bivalve and brachiopod fragments, oriented concave up and down, and > 2 cm long vertical burrows (Fig. 16B; filled with carbonate).

Trace fossils are relatively abundant throughout this facies' intervals. The trace fossils are present in the form of horizontal burrows, vertical, and concentric silt- and calcite-filled features. Some identified ichnofossils include *Planolites* and *Thalassinoides* (Fig. 16A). Body fossil constituents were observed in Cores 1 and 2 and include crinoid, brachiopod and bivalve fragments (very minor in Core 2; Figs. 16-17B). In thin section, the very thin to thin silty (quartz dominated) laminations are more apparent. The general mineralogy in the black shale facies includes abundant assorted angular to sub-rounded quartz, mica, clay, and minor carbonate cement and grains, and possible organic matter-filled voids. Facies 12 and 14 (the medium to fine-grained sandstones with mud drapes and the bioturbated sandy siltstones) overlie this facies and their contacts are sharp (Table 5).

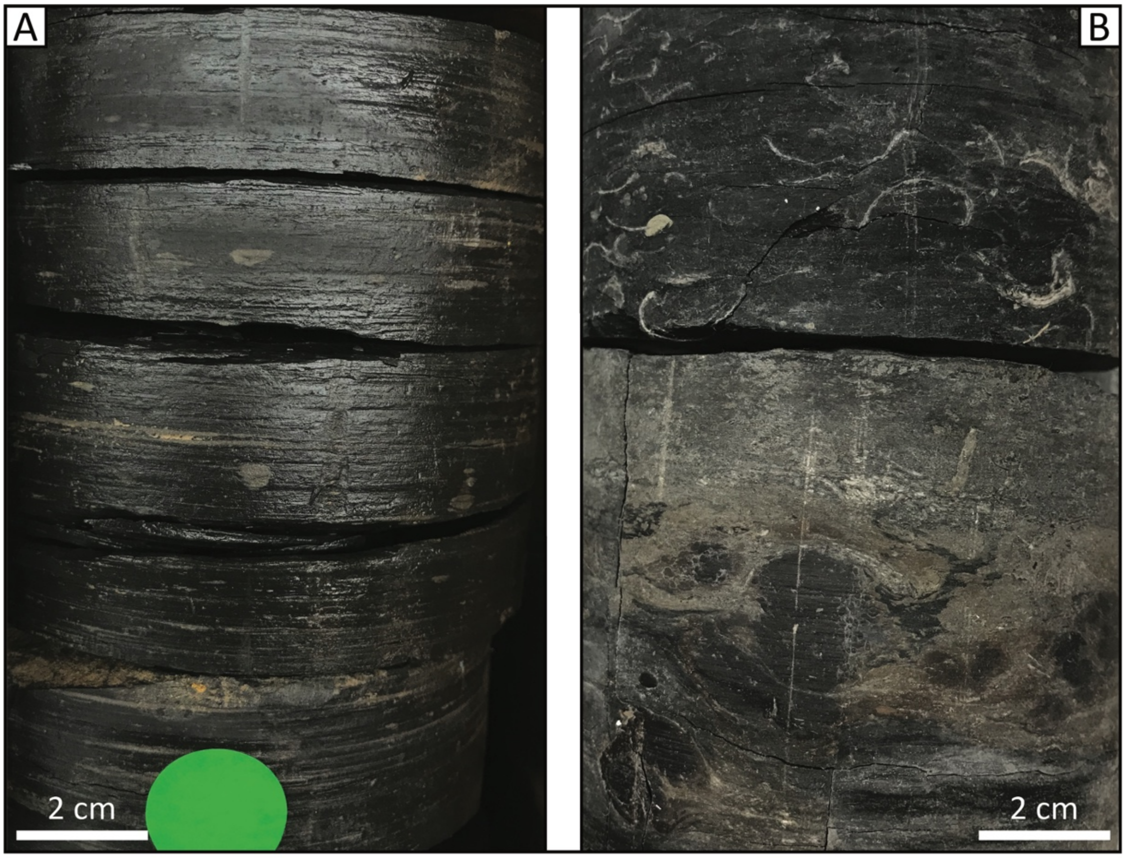

Figure 16. Core images of the black, thinly laminated shale facies. **A)** Dark gray laminated silty shale interval; note trace fossils and silty laminations. **B)** Brachipodal, dark gray shale interval; note large bivalve shells, large phosphatic (?) nodules within silty band below bivalval band.

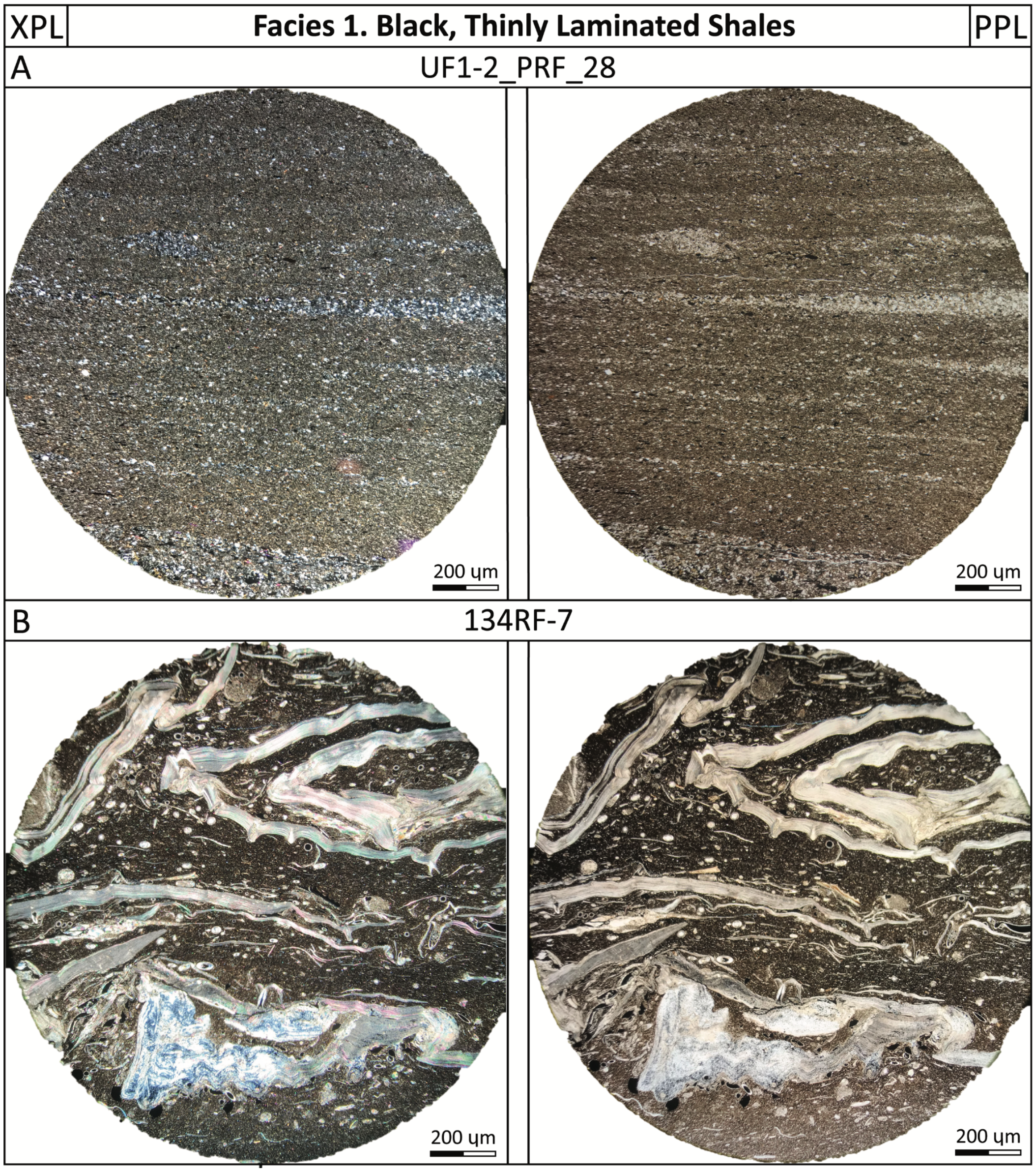

Figure 17. Thin section images of the **A)** Dark gray, laminated, silty shale interval and **B)** Brachiopods, dark-gray, shale interval of Facies 1; note the quartz-filled, silty laminations and burrows in A and the large brachiopod shells in B.

<u>Interpretation</u>

The black, thinly laminated shale facies is interpreted as an offshore marine, prodeltaic deposit. The dark gray to black color, fine-grained composition, and laminated structure of this facies indicates deposition by suspension sediment fallout without traction currents in a low energy offshore marine environment. Lenticular laminae and upwardly fining sets of the first variant suggest episodic deposition in an overall low-energy setting. However, absence of conodonts, pyritic features, and phosphatic material is evidence that this facies is a different variant to the offshore (core) shale described by Heckel (1977, 2008) for the "Kansas-type" cyclothem model.

Additionally, according to Heckel (1977) and Schultz and Coveney (1992), the presence of phosphate is considered evidence for deeper water, offshore environment while its absence is indicative of more nearshore, but still deep marine settings. That is also evidenced by the presence of trace and body fossils, which indicate well oxygenated waters. Nevertheless, the absence of macroscopic plant detritus indicates offshore marine conditions where land-derived organic debris are broken down and/or rare.

Facies 2: Parallel Laminated Sandy Mudstones

<u>Description</u>

Facies 2 is a minor facies that comprises dark gray to black, parallel laminated silty/sandy mudstones, interlaminated with thin, very fine-grained sand lenses (Fig. 18). This facies includes three intervals in Cores 2 and 3, reaching approximately 0.2 ft/0.06 m in Core 2 and roughly 0.4 ft/0.12 m in Core 3. Abundance of sandy laminations vary across the packages. Additional sedimentary structures observed include minor, amorphous, sand-filled features, and rare and very subtle flame structures. This facies displays very low to no fissility. In terms of fossil composition, no trace or body fossils were observed within the facies. This facies is intercalated with the medium to fine grained sandstones of Facies 12 in both cores and the nature of overlying and underlying contacts is sharp (Table 5).

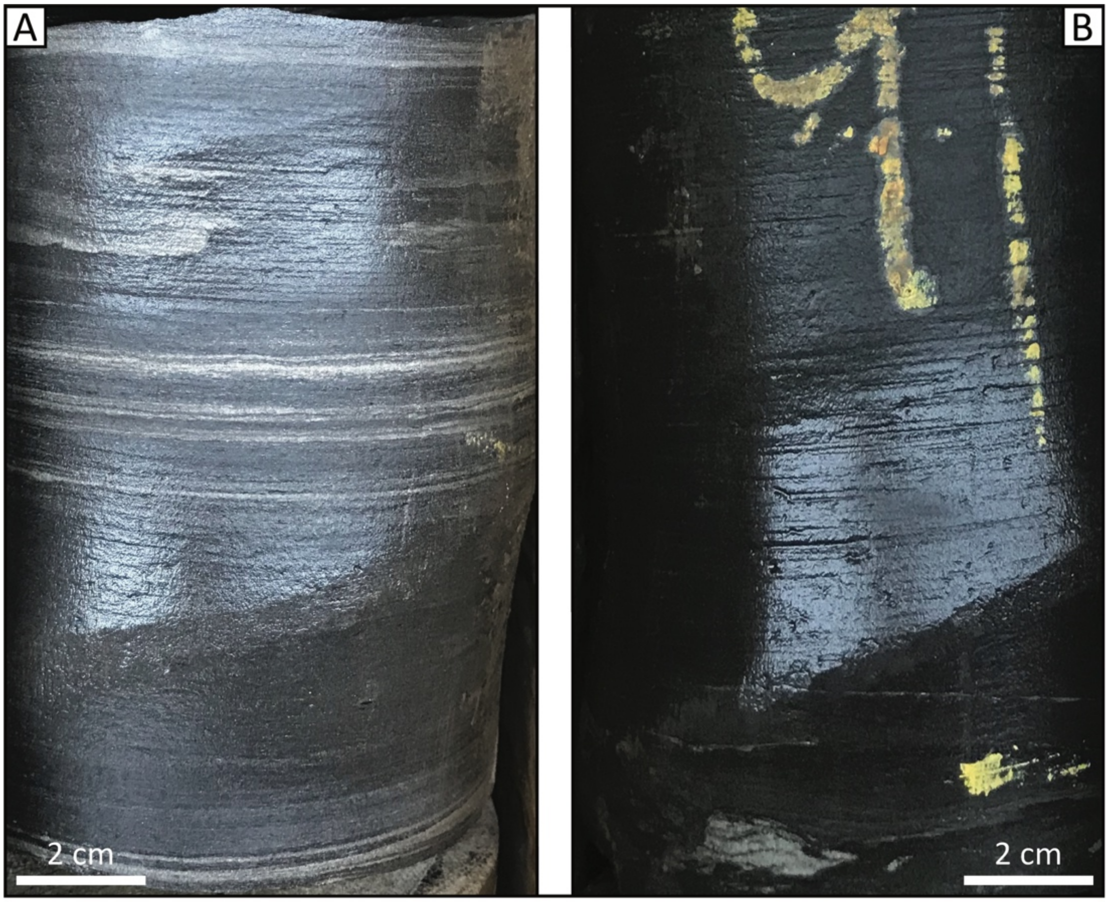

Figure 18. Core images of the parallel laminated sandy mudstones. **A)** Sandier interval with light gray sandy laminations. **B)** Black and laminated interval.

<u>Interpretation</u>

The parallel laminated sandy mudstone facies is interpreted as a tidal deposit. The dark colors, fine-grained composition, and preservation of thin sandstone and mudstone laminations in this facies indicate deposition by both suspension sediment fallout and currents in a relatively low energy environment. The sandy laminae, as well as this facies' vertical relationship with the medium to fine-grained sandstones with mud drapes (Facies 12), indicate deposition caused by tidal currents (Mángano and Buatois, 2004; Desjardinst al., 2012). Subaqueous conditions are also suggested by the absence of root traces or pedogenic features.

Facies 3: Black Carbonaceous Shales

Description

Facies 3 comprises black, planar laminated shales and it occurs as one very thin (0.5 ft/1.5 m) interval in Core 2 (Fig. 19-20). Sedimentary structures present include very thin (<1 mm) laminae (displayed by fissility) to thin (1-3 mm) continuous to discontinuous parallel laminations. Other diagnostic features of this facies include minor carbonate-filled horizontal burrows (Fig. 20A) and abundant carbonaceous lenses (Fig. 20B). Rare trace fossils appear in the form of horizontal, carbonate-filled burrows while rare body fossils include few bivalve fragments. In thin section, the very thin to thin laminations present are more apparent than in core. This facies' upper contact is gradational into the shaly carbonates (Facies 6). The lower contact is gradational with the medium to fine-grained sandstones midcontinent/ mud drapes (Facies 12).

Interpretation

The black carbonaceous shale facies is interpreted as a nearshore to estuarine to swamp deposit. The dark color, fine-grained composition, and preservation of thin laminations in this facies indicate deposition by suspension sediment fallout in a low energy environment. The abundant carbonaceous content, but without the diagnostic features of coalification, and the predominance of silt and carbonate filled clasts are indicative of an environment adjacent to a highly vegetative region but experiencing suspension and occasional current deposition. Furthermore, the vertical relationship with the overlying shaly carbonate facies (Facies 6) suggest proximity to a marine environment.

Figure 19. Core image of the black carbonaceous shale facies. Note gradational contact with the overlying shaly carbonate facies with abundant bivalve fragments (Facies 6).

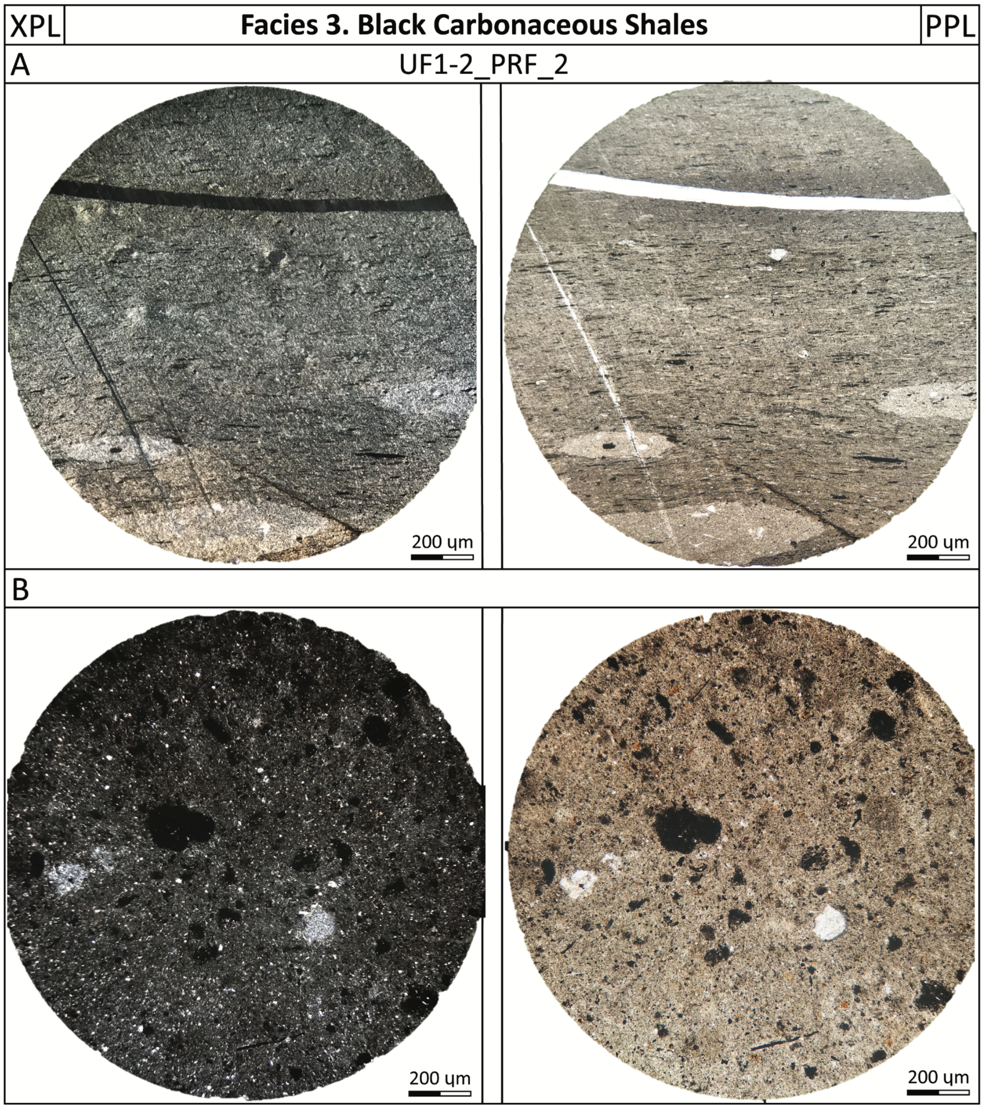

Figure 20. Thin section images of the black carbonaceous shale facies. **A)** Carbonate-filled lenses in very fine-grained clay matrix in which carbonaceous fragments lie along laminations. **B)** Larger, carbonaceous fragments in darker and silty more massive matrix.

Facies 4: Gray Sideritic Shales

<u>Description</u>

The gray sideritic shale facies is composed of medium gray, dark-gray and black shales, silty-shales, and siltstone intervals (Fig. 21-22). This facies occurs twice in Core 2 and thicknesses range from 6.1 ft/1.86 m to 20.85 ft/6.3 m. Sedimentary structures include very thin (>2 mm) parallel horizontal laminae, which display fissility. Intervals of interlaminated mudstone and siltstone bands (10-20 mm thick; Fig. 21A) are present, where silty bands display horizontal, low angle and minor vertical fractures. Additionally, siderite cemented bands (10-20 mm; Fig. 21B) are present throughout. Body fossils in the gray sideritic shales facies are rare; however, an interval of about > 0.5 feet (> 0.2 m) at the base of the lower interval, contains whole bivalve or brachiopod shells.

Figure 21. Core images of the gray sideritic shale facies. **A)** Silty and muddy bands in dark gray interval; note semi-vertical and horizontal fractures in silty bands. **B)** Light gray interval showing a thin siderite band.

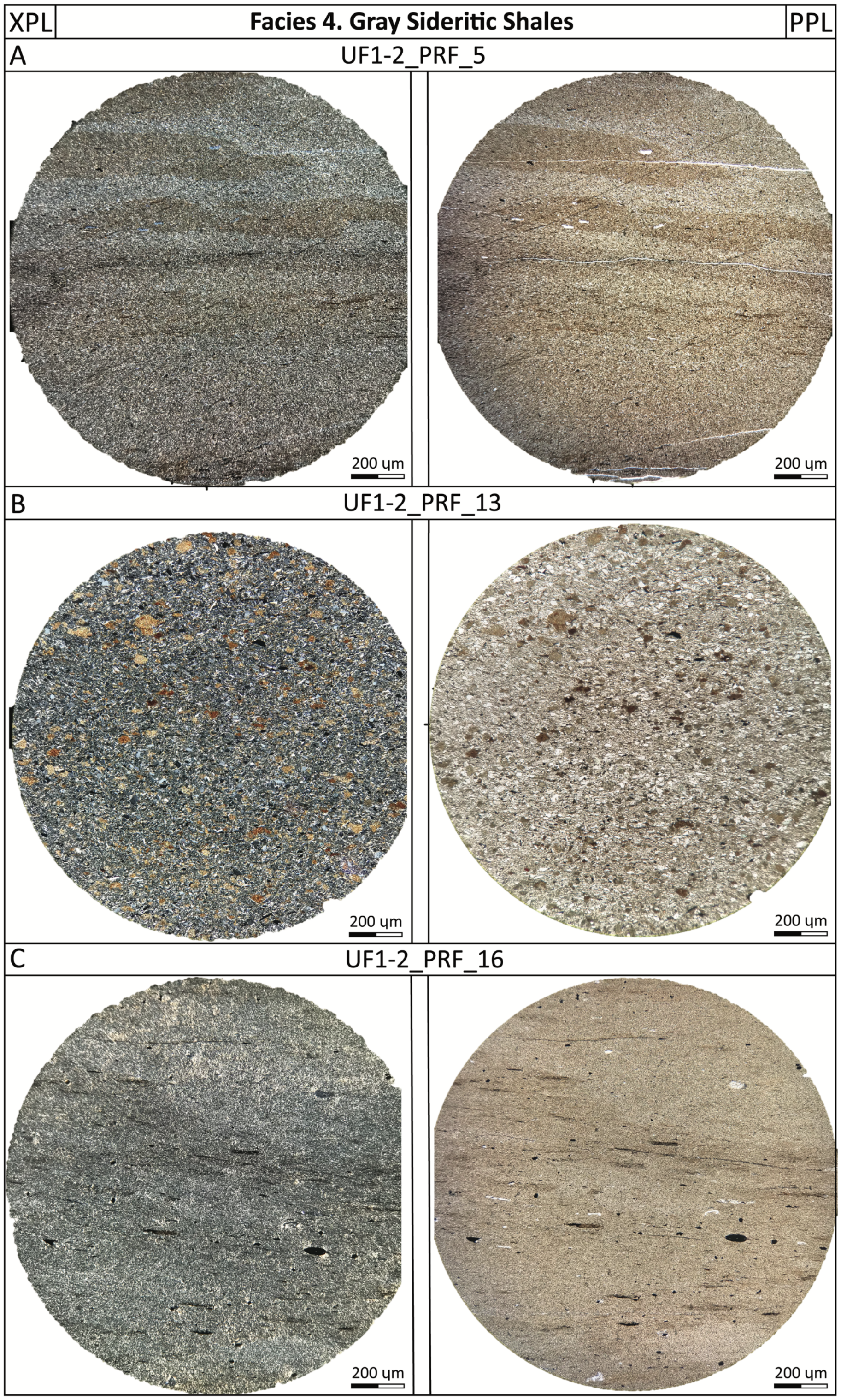

Figure 22. Thin section images of the gray sideritic shale facies. **A)** Quartz rich silty laminae. **B)** Siderite grains (red/orangish) in silt- and clay-sized matrix – lower interval. **C)** Very fine-grained interval showing some burrows and carbonaceous (?) lenses.

Trace fossils in the form of tiny horizontal burrows are present but can only be clearly seen in thin sections (Fig. 22C). Siderite in the form of cement, bands (10-20mm), and very small, microscopic particles are common, and their occurrences increase upward (Fig. 22B). The intervals tend to coarsen up to siltstone/silty shale and upper contacts tend to be gradational with overlying heterolithic siltstone facies (Facies 9) or sharp with the fine-grained sandstone facies (Facies 11). Lower contacts are sharp with the shaly carbonates (Facies 6) or gradational with the skeletal wackstones to packstones facies (Facies 7).

Interpretation

The gray sideritic shale facies is interpreted as being deposited by suspended sediment fallout coupled with episodic low-energy current in a marine or marginal marine environment. Very thin, parallel, horizontal laminations and fine-grained clay composition suggest suspension sediment fallout without traction currents in marine environments with little bioturbation. Minor episodic, repetitive silty bands and laminations might suggest low-energy current deposition. A gradual change from dark gray-black shale, in the lower interval of Core 2, to a medium-, and local lighter -gray color might indicate a change from lower oxygen to more normal oxygen conditions. The low diversity and low occurrence of trace fossils suggest possible stressed conditions, likely caused by oxygen-depleted conditions (Reineck and Singh, 1975; Buatois et al., 1999). The vertical relationship with the shaly carbonate (Facies 6), the skeletal wackestone to packstone (Facies 7) or the heterolithic siltstone facies (Facies 9) also supports deposition in a marine setting (Buatois at al., 1999; Potsma, 1982). This facies is similar to Lange's (2003) "Sideritic Shale Facies" and would be interpreted as part of the "outside shale" in the cyclothem model (Heckel, 1977).

Facies 5: Mottled Shale to Sandstone

Description

The mottled shale to sandstone facies is composed of a variety of siliciclastic lithologies found in Core 2 (Figs. 23-24). This facies comprises friable mudrocks and fine-grained sandstones that are characterized by low to high chroma color changes (light to dark gray and green), and color mottling (green matrix and reddish structures). Thicknesses vary from very thin packages (0.18 m/0.6 ft) to thicker intervals 0.5 m/1.65 ft), with 0.4 m (1.3 ft) being the average. Although bedding and changes in grain size are difficult to observe, the facies appears to form packages of different color and grain size. This facies appears similar to Lange's (2003) "Blocky Mudstone" facies. Most sedimentary structures in this facies are post-depositional, but structures previously found in the parent material (relict structures) may be present within certain intervals including minor thin parallel laminations. Post depositional structures include iron-carbonate (Figs. 23A, 24C) and iron-oxide concretions/patches (Fig. 23A-24B), fabric modifications including pedogenic structures, root traces (rhizoliths) and slickensides (Fig. 23, 24A). Slickenside features are commonly dominant in clay-rich intervals and pedogenic structures occur as platy and angular-blocky mudstone "clods" within most of the packages (Fig. 23B-C).

Fossil constituents include plant fragments (i.e., stems) and root traces. Root traces include minor preserved carbonized root structures (Fig. 23C; 24A), clay and siderite-filled dendritic root systems (rhizoliths) that display an orangish-dark red (rusty) color/mottle (Fig. 23A). Invertebrate body fossils are rare with only one interval containing bivalve shells. Trace fossils of unknown affinity are also present within intervals in contact with or close to the overlying shaly carbonates (Facies 6). Additional post-depositional features typically include calcite or siderite cement and nodules/concretions (Figs. 24B-C).

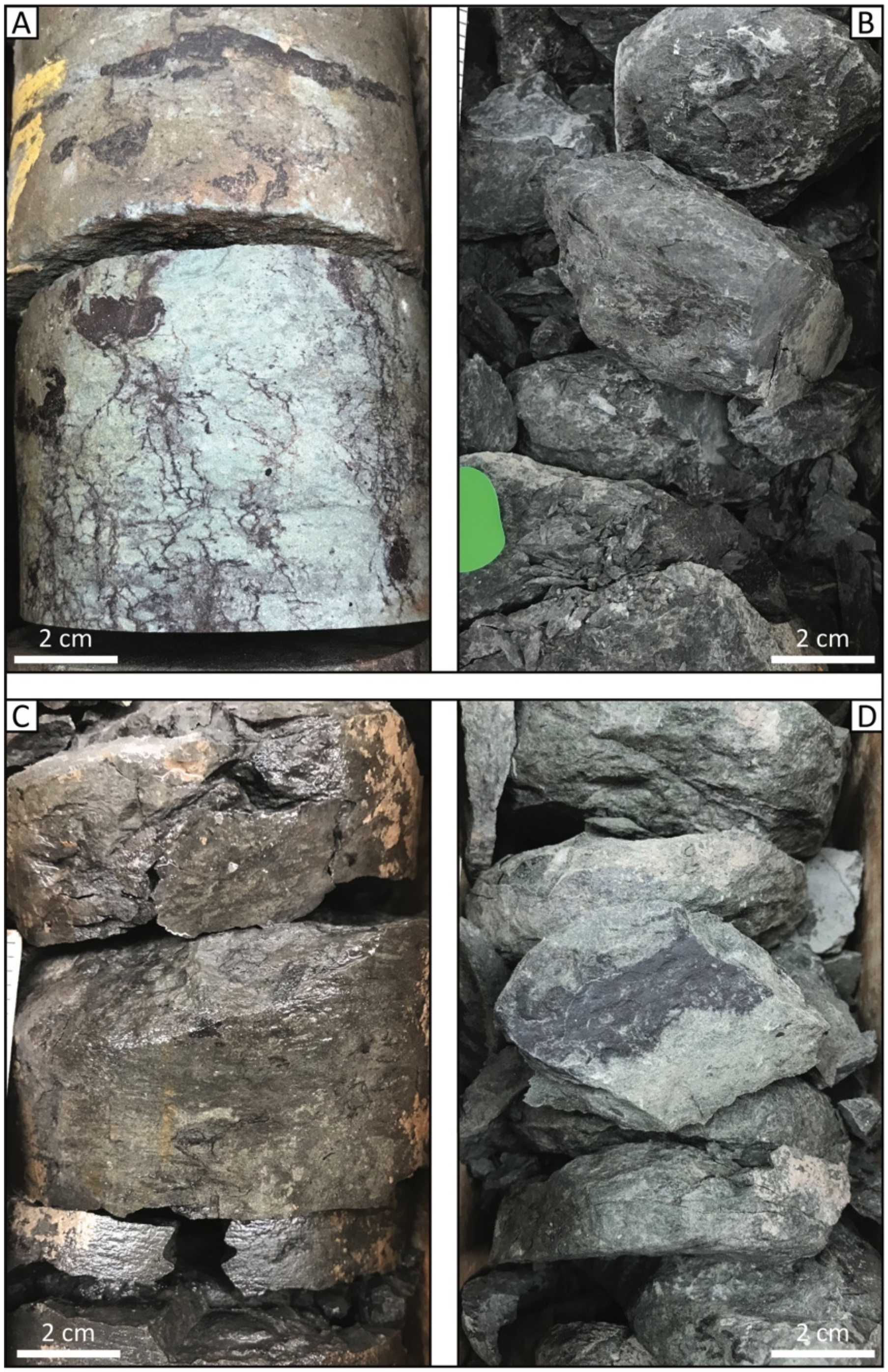

Figure 23. Core images of the mottled mudstone and sandstone facies. **A)** Siderite-filled-dendritic root systems (rhizoliths) displaying an orangish-dark red (rusty) color/mottle in fine-

grained sandstone interval. **B)** Very friable dark-green shale interval showing slickensides. **C)** Small, carbonized root structures in light gray/brownish silty shale interval. **D)** Mudstone "clod" within very friable, light green mudstone interval.

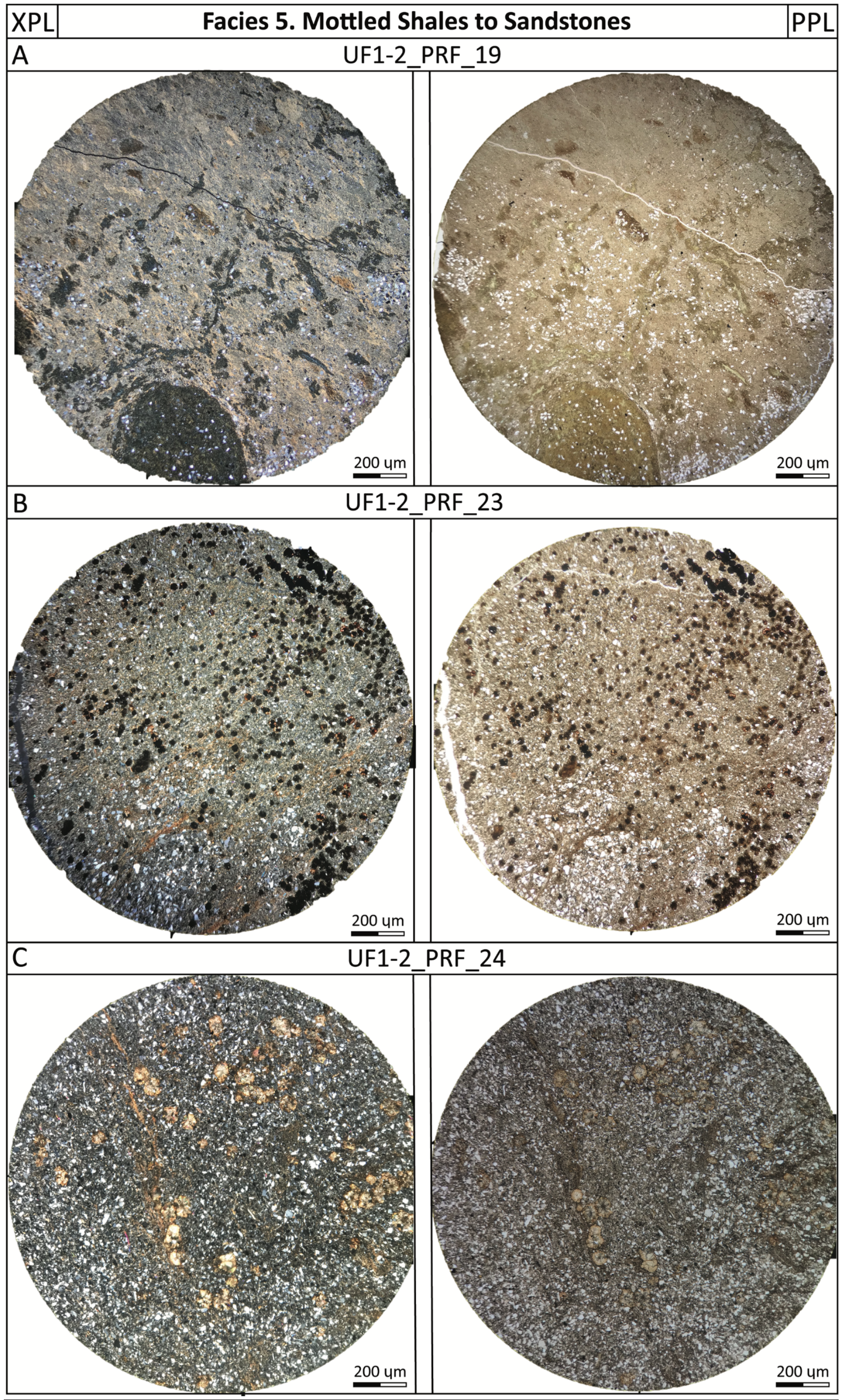

Figure 24. Thin section images of the mottled shales to sandstone facies. **A)** Patchy distribution of quartz and clay blebs interpreted as root traces. **B)** Abundant iron concretions and silt grains and blebs in clay matrix. **C)** Spherulitic siderite concretions within a very fine-grained silty sandstone interval.

Lower contacts display post-depositional pedogenic features overprinting underlying sediments. Typically, the lower contacts are gradational with the heterolithic siltstone (Facies 9) and with the fine-grained sandstone facies (Facies 11), while upper contacts vary between sharp with the wackestone to packstone facies (Facies 7) or gradational (usually bioturbated) with the shaly carbonate facies (Facies 6).

<u>Interpretation</u>

The mottled shales to sandstone facies is interpreted as a paleosol formed from weathering and pedogenic processes during subaerial exposure based on presence of root traces, and horizonation (Retallack, 1990; Boggs, 2012). Pedogenic structures such as platy "clods" may suggest initial disruption of inherent (parental rock) structures, while subangular to angular-blocky peds tend to form from longer periods of pedogenic processes but the lack of strong horizonation suggests overall soil immaturity (Retallack, 1990). Slickensides structures suggest frequent shrink-swell cycles and are characteristic of relatively better developed soils in seasonal environments (wet and dry, Retallack, 1990). The nature of the root traces provides evidence of subaerial exposure, and information regarding the drainability of the soil. Carbonaceous root traces are the most easily recognized and indicate that the environment is waterlogged, poorly drained, usually within anoxic lowland areas. Rhizoliths, rhizoconcetrions, or calcium- and iron-carbonate-lined root traces, on the other hand, suggest well-drained, drier, alkaline soils (Retallack, 1990). Based on the criteria above, the mottled shales to sandstone facies shows evidence of moderately developed Inceptisols, and/or semi-Vertic, and non-oxidized paleosols mostly with poor drainage. This facies was probably formed in an overbank area within an interfluve setting due to its presence above incised valley fill packages of facies 9 and 11.

Facies 6: Shaly Carbonates

Description

The shaly carbonate facies comprises a mottled, orangish to dark red, calcareous mudstone, a mottled fossiliferous packstone, a red and green sandy and fossiliferous packstone, and a black fossiliferous shale interval (Figs. 25-26). This facies occurs once in Core 3 and two times in Core 2 and their thicknesses range from 0.17 m / 0.55 ft to 1.25 m / 4.1 ft. Sedimentary structures observed in core 2 range from structureless to thin (1-3 mm) parallel laminations with thin, minor stylolites. In Core 3, this facies displays sandy/silty planar and wavy bands and discontinuous laminations as well as soft-sediment deformation. Additional features observed include subrounded to rounded (5mm-15mm) carbonate clasts and minor silty/sandy elongated 1-10 mm clasts. The matrix in this facies is typically micritic (Fig. 26).

Body fossils are fragmented and include brachiopod shells, crinoid stems, pelecypods, echinoderms, foraminifera, bryozoans, and minor trilobites (Figs. 25-26). Fossils appear more fragmented in the lower packstone interval of Core 2, whereas abundant whole fossils were observed in the upper packstone bed (Fig. 25A). Whole fossils of the shaly carbonate facies include bryozoa, gastropods and foraminifera (Fig. 26). Post depositional features include red-color staining (mottling). This facies displays a gradational lower contact with the mottled shales to sandstone facies (Facies 5) and the carbonaceous shale (Facies 3; Fig. 25A), and a sharp upper contact with the gray sideritic shale facies (Facies 4) and the conglomerates (Facies 15).

Figure 25. Core images of the shaly carbonate facies. **A)** Packstone interval; note black, shaly interval underlying the interval. **B)** Fossiliferous and sandy packstone interval; note gradational lower contact. Whole bivalve shells are found right above within a black shaly interval of the gray sideritic shale facies (Facies 4).

<u>Interpretation</u>

The shaly carbonate facies is interpreted as being formed in moderate to high energy, marine environments. This interpretation is evidenced by abundant fragmented body fossils, minor trace fossils (only abundant at contacts) and relatively low mud content. Fossil fragmentation might suggest storm transportation while red-staining/mottling where the facies overlies the mottled shales to sandstone facies (Facies 5), might indicate post-depositional alteration by pedogenic processes.

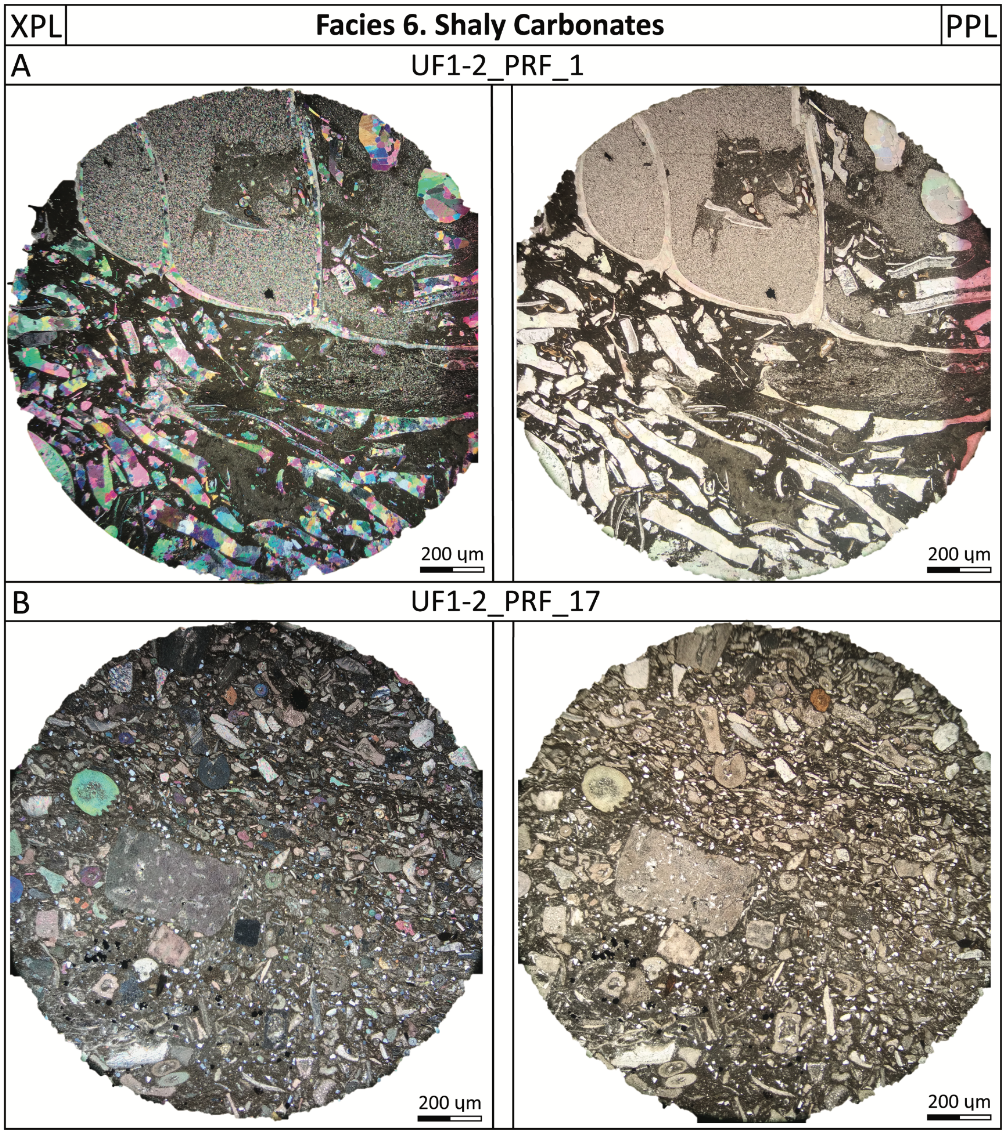

Figure 26. Thin section images of the shaly carbonate facies. **A)** Fossiliferous Packstone; note large gastropod shell and abundant fragmented bivalve shells in micritic cement. **B)** Fossiliferous and sandy packstone; note smaller sizes and different types of fossil fragments and clasts.

The abundance of bryozoans, crinoids and minor brachiopods suggest a normal salinity marine environment (Heckel, 1972). Nevertheless, the upper interval in Core 2 shows very few to rare crinoid fragments but abundant and larger bivalve shell fragments, which along with its overlying relationship with the supratidal carbonaceous shale (Facies 3) might be suggestive of shallow marine environments instead of deeper marine conditions. The interval in Core 3 is interpreted as a high energy environment. This interpretation is supported by the sideritic composition that indicates fresh-water infiltration, mixed sand/silt planar and wavy laminations and soft sediment deformation, and sporadic carbonate clasts and fossil/crinoid-filled silty laminae (storm influence).

Facies 7: Skeletal Wackestones to Packstones

Description

The skeletal wackestone to packstone facies is light-medium tan and gray with micritic calcite matrix (Figs. 27-28). It comprises two intervals of a very thin (1.1 feet / 0.3 m) nodular wackestone occurring above the mottled shales to sandstone facies (Facies 5) and a 0.3 m / 1.1 ft thick laminated packstone occurring right above the wackestone. The intervals are vertically adjacent to each other and located in Core 2. Sedimentary structures in the wackestone include structureless intervals, brecciated intraclasts (nodular appearance; Fig. 27A), thin (1-3 mm) parallel laminations (Fig. 27B), algae, and minor stylolites. Body fossils are sparse and difficult to notice through the naked eye in the wackestone bed, except for some bivalve fragments. Other body fossils observed in thin section include gastropods, possible fusulinids, bryozoa, and possible ostracods (Fig. 28B). Minor bioturbation is common at the top contact with the packstone interval.

In the packstone interval, body fossils, including crinoids and pelecypods (up to 3 mm), are very common (Figs. 27B, 28A). Fossils are fragmented and include brachiopods, crinoid stems, bivalves, echinoderms, foraminifera, bryozoan fragments, and minor trilobites (Fig. 28A). In terms of trace fossil occurrence, it is observed in the upper transition of both intervals in the form of chaotically spread, mottled burrows. This facies displays a sharp upper contact with the gray sideritic facies (Facies 4) and a sharp lower contact with the mottled shales to sandstone facies (Facies 5).

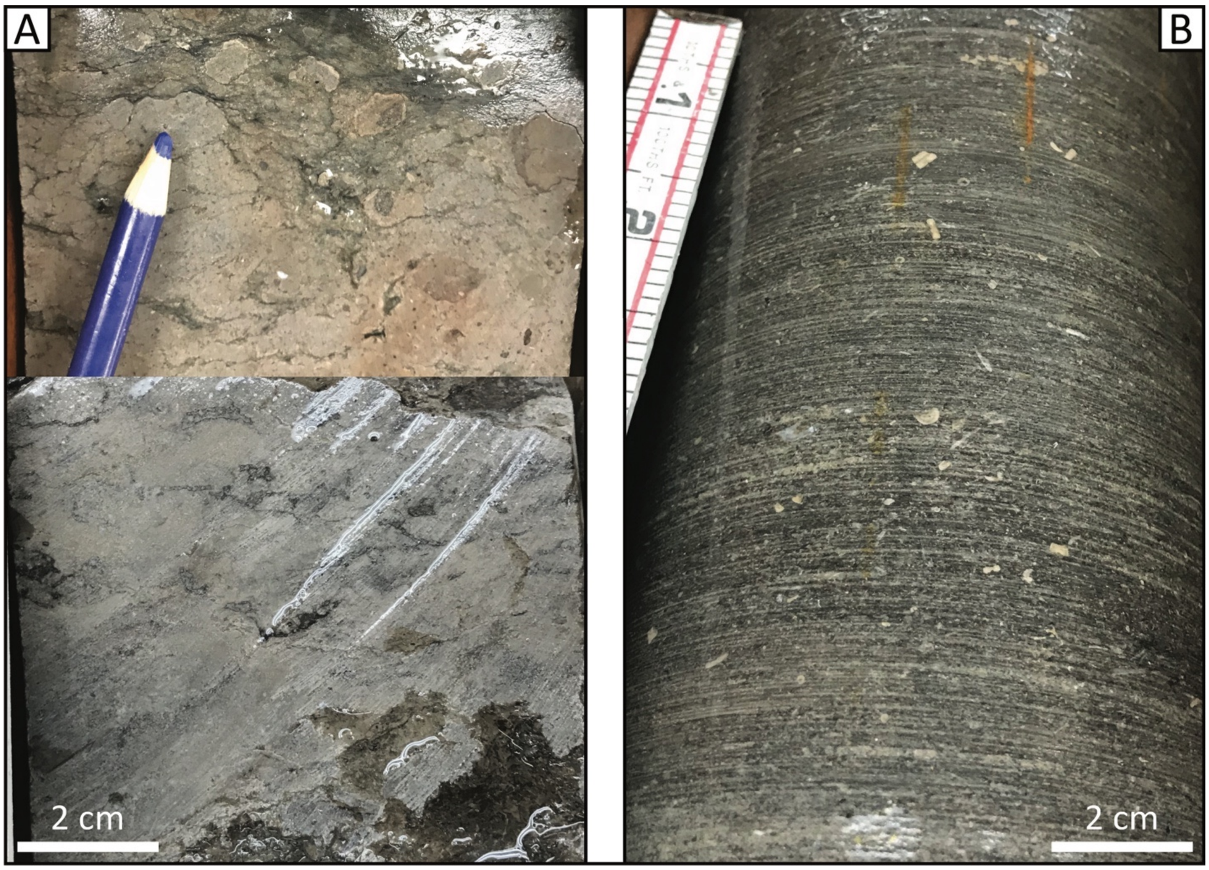

Figure 27. Core images of the skeletal wackestone to packstone facies. **A)** Light gray-tanish, nodular wackestone interval. **B)** Parallel laminated, fossiliferous packstone interval.

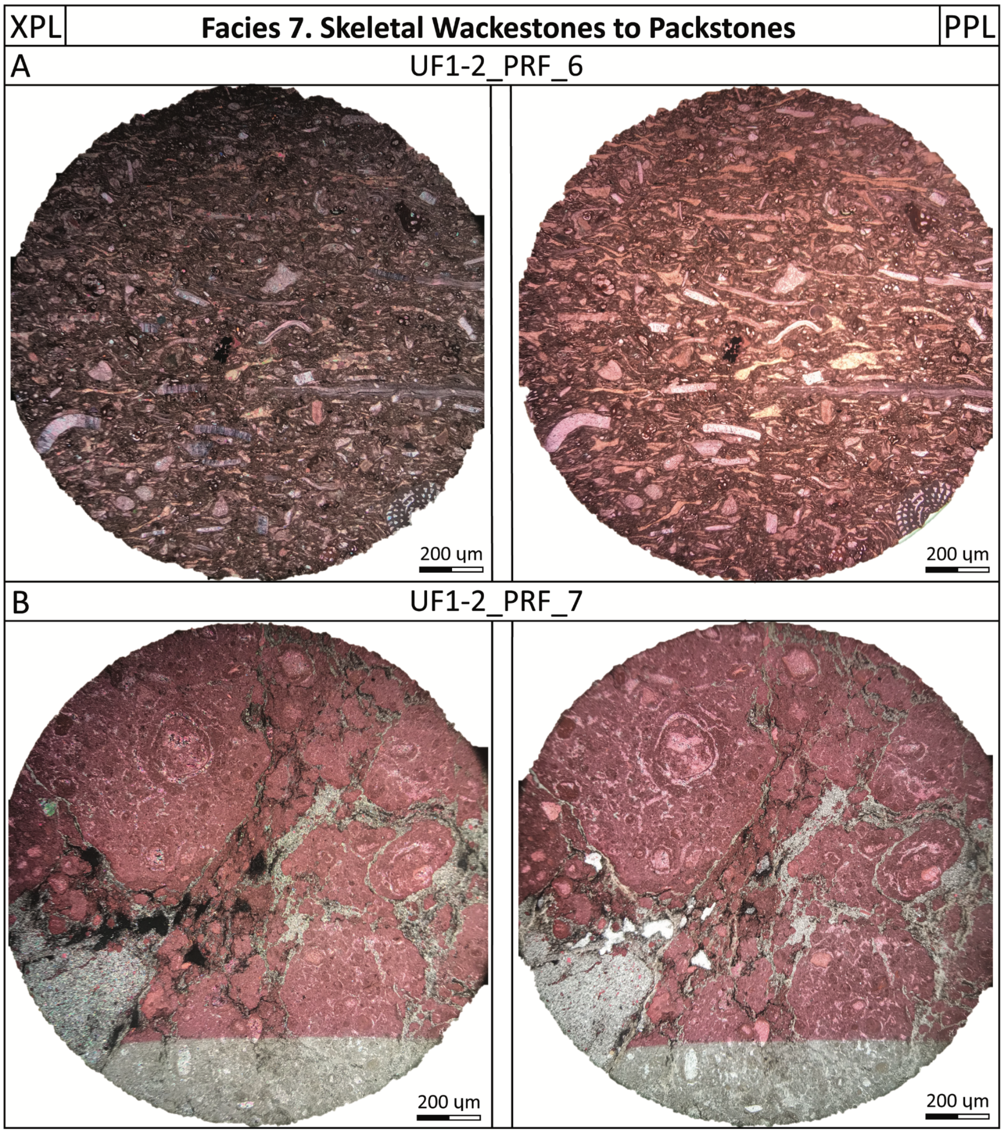

Figure 28. Thin section images of the skeletal wackestone to packstone facies. **A)** Fossiliferous packstone showing forams, bivalve, and gastropod fragments in micritic cement. **B)** Nodular wackestone showing possible pedogenic imprint (voids) and algal composition (circular features).

Interpretation

The skeletal wackestone to packstone facies is interpreted as forming in a variable energy shallow marine environment. In the wackestone interval, the brecciated or nodular appearance, abundant micritic matrix, low faunal abundance and diversity might indicate a shallow water intertidal setting; nevertheless, the minor pedogenic imprint and abundant algae composition suggests a non-marine environment. Episodic high energy currents are indicated by minor fossil fragments and gradational contact with the overlying laminated packstone interval. This latter interval is interpreted as being deposited by episodic storms or other high-energy currents in an overall low-energy intertidal environment. This is evidenced by the association of locally disturbed horizontal laminations with dispersed shell and crinoid fragments and foraminifera. This facies is similar to the "Bioclastic-Packstone-to-Grainstone Facies" of Lange (2003) in southeastern Kansas and would be analogous to the "upper limestone" in Heckel's (1977) cyclothem model.

Facies 8: Burrowed and Interbedded, Sideritic Sandstone and Mudstone

Description

The burrowed and interbedded, sideritic sandstone and mudstone facies occurs only in Core 3 (Figs. 29-30). The entire interval is approximately 55 feet/16.8 m and it is located near the upper portion of the core. The sandstone beds are light to medium gray and thickest toward the base of the facies, ranging from 1 foot/0.3 m to 3.5 feet/1.1 m. In the same interval, the mudstone interbeds are thinner, ranging 2-5 cm. Towards the top of the facies, the mudstone beds reach up to 0.7 feet/0.2 m while the sandstone beds become thinner (Fig. 29B).

Figure 29. Core images of the burrowed and interbedded, sideritic sandstone and mudstone facies. **A)** Massive (above) and light gray fine, heterolithic sandstone. **B)** Heavily bioturbated fine-grained sandstone with mud interbeds. Note siderite composition in matrix and laminations (red material).

Sedimentary structures include mud drapes, wisps, planar laminations, minor faint cross laminations, minor starved ripples (in mudstone beds), serrated laminations, siderite bands, vertical cracks, and stylolites (Fig. 29). Occurrence of mudstone and siderite beds and laminations increases upward in the section. Body fossils are not present in this facies whereas trace fossils are abundant. Trace fossils are present in the form of vertical and flat burrows as well as concentric features filled with sand. Additional characteristics of this facies includes carbonaceous plant material, present in the form of “specks”/filaments within mud and sandstone beds. This facies overlies the interbedded sandstone and mudstone facies (Facies 16). In thin section, this facies shows subrounded-subangular, fine sand of quartz, feldspar and lithic composition (Fig. 30A). The well sorted sand grains are cemented in quartz (overgrowth), calcite and minor clay. Some observed accessory minerals include glauconite, zircon and opaques.

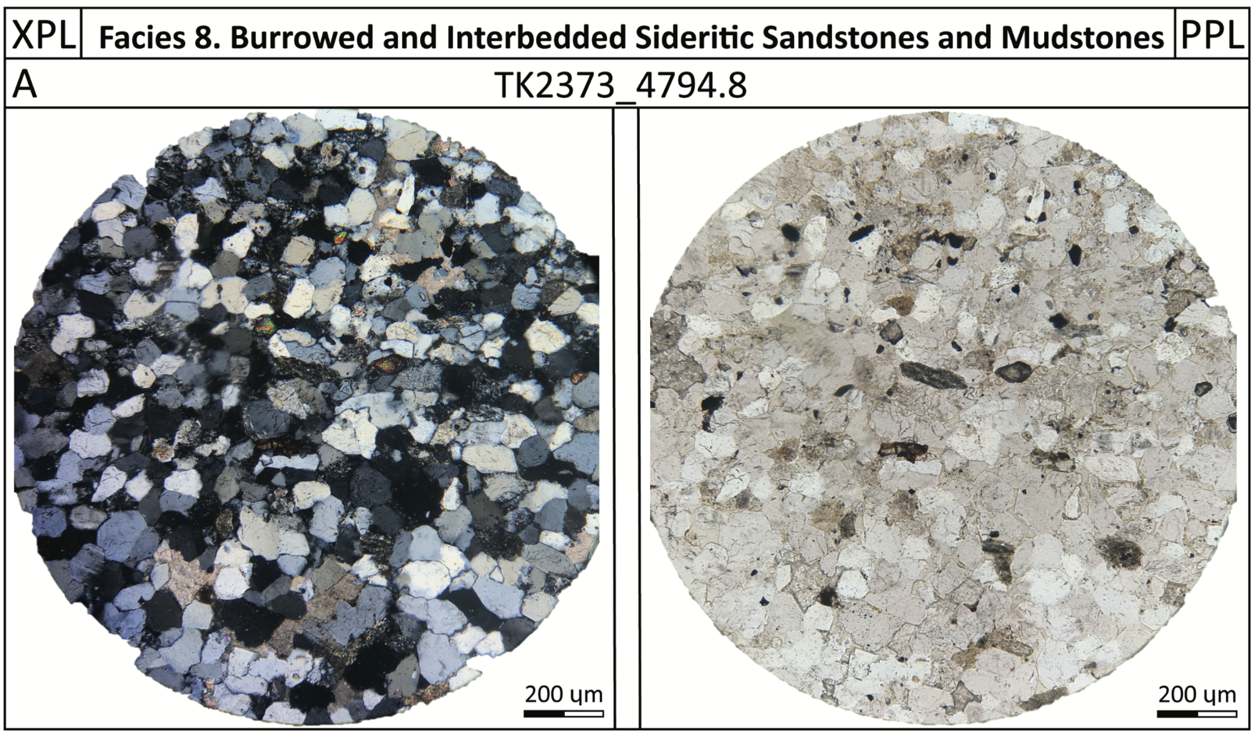

Figure 30. Thin section images of the burrowed and interbedded, sideritic sandstone and mudstone facies. Note abundant quartz grains in quartz overgrowth and calcite cement. High relief grains in PPL (right) are opaque (dense minerals) and zircon grains.

<u>Interpretation</u>

The burrowed and interbedded, sideritic sandstone and mudstone facies is interpreted as a tidal channel fill. The basis for this interpretation lies on the presence of a basal mud-rip up lag and the overall fining upward trend of the package. Additionally, this facies displays an abrupt/sharp contact with the underlying interlaminated and thinly interbedded sandstones and mudstones facies (Facies 16). Trace fossils in this facies are represented in the form of escape features/vertical burrowing, similar to the previous facies, which support a shallower-water setting. The trace-fossil assemblage found in this facies reflect rapid rates of sediment accumulation. Furthermore, this facies displays an array of tidal processes such as preservation of mud drapes and mud layering, and rhythmic lamination styles. The sideritic bands and laminations, may reflect freshwater incursion within an estuary system (Andrews, 1997). The vertical cracks may reflect syneresis cracks and multiple serrated laminations and lamination sets might indicate the shrinkage of sediment without desiccation as well as persistent changes in salinity at the sediment-water interface (Fielding et al., 2020).

Facies 9: Heterolithic Siltstones

Description

The heterolithic siltstone facies comprises three types: a flaser-bedded, green and dark-gray sandy/muddy siltstone, a parallel and lenticularly-laminated, dark gray, muddy siltstone, and a dark green/gray parallel laminated, mudstone and siltstone (Figs. 31-32). The facies is located in Cores 1 and 2. Thicknesses range from 1.54 m / 5.05 ft to and 2.74 m / 9 ft. In general, this facies comprises rhythmic siltstone/very fine sandstone and silty mudstone packages, and it is similar to Lange's (2003) "Interlaminated Sandstone and Siltstone" facies, from coeval deposits in southeast Kansas. The flaser-bedded, green and dark-gray sandy/muddy siltstone interval becomes a more homogeneous, dark green, thinly laminated very-fine silty sandstone upward (Fig. 31). Sedimentary structures include very thin (<1 mm) to thick (3-15 mm) horizontal continuous and discontinuous silt laminae, interlaminated with thin to thick lenticular silty-sand and silty-mud laminae, and abundant unidirectional starved ripple laminations sets (3-15 mm). The flaser-bedded, green and dark-gray sandy/muddy siltstone interval also includes at least two thick flaser and wavy bedding sets (some amalgamated parts; 2-10 cm), very thin (<1 mm) to thin (1-3 mm) sinuous mud drapes, and very thin to thin upwardly fining laminae, and repetitive thin-thick bundled laminated couplets (1-5 mm silty mud, 5-8 mm silt/very fine sand; Fig. 31B).

Reactivation surfaces as well as ill-formed herringbone stratification in silty/very fine sand packages are present but rare. The upper, more homogeneous, 30 cm flaser-bedded interval contains concentric and structureless dark rusty features and planar parallel laminations. The parallel and lenticularly-laminated, dark gray, muddy siltstone variant is composed of thin and faint siderite bands as well as a graded bed (~20 mm thick). Body fossils in the heterolithic siltstone facies are rare, but a 1 cm whole bivalve shell is observed in the upper interval of Core 2. Trace fossils are very abundant in this facies and appear as horizontally oriented individual traces as well as bioturbation in the very thin to thick mud-silty/sandy bands. Some identified trace fossils in this facies include *Planolites (Pl),* and *Nereites (Ne)* (Fig. 31). Possible diagenetic features include siderite features. In thin section, lenticular and wavy parallel lamination sets appear to be disrupted by biologic activity and resemble very small pillow structures (Fig. 32A). Mineral constituents include silt and very fine sand-sized quartz with minor mica, opaques, iron-oxide concretions (Fig. 32B) and clay-silica cement. This facies is overlain by the mottled shales to sandstone facies (Facies 5; sharp contact), and the heterolithic sandstone facies (Facies 10; gradational contact). On the other hand, the lower contacts are gradational with the medium to fine grained sandstones with mud drapes (Facies 12) and the gray sideritic shale facies (Facies 4), and sharp with the rippled sandstone (Facies 13).

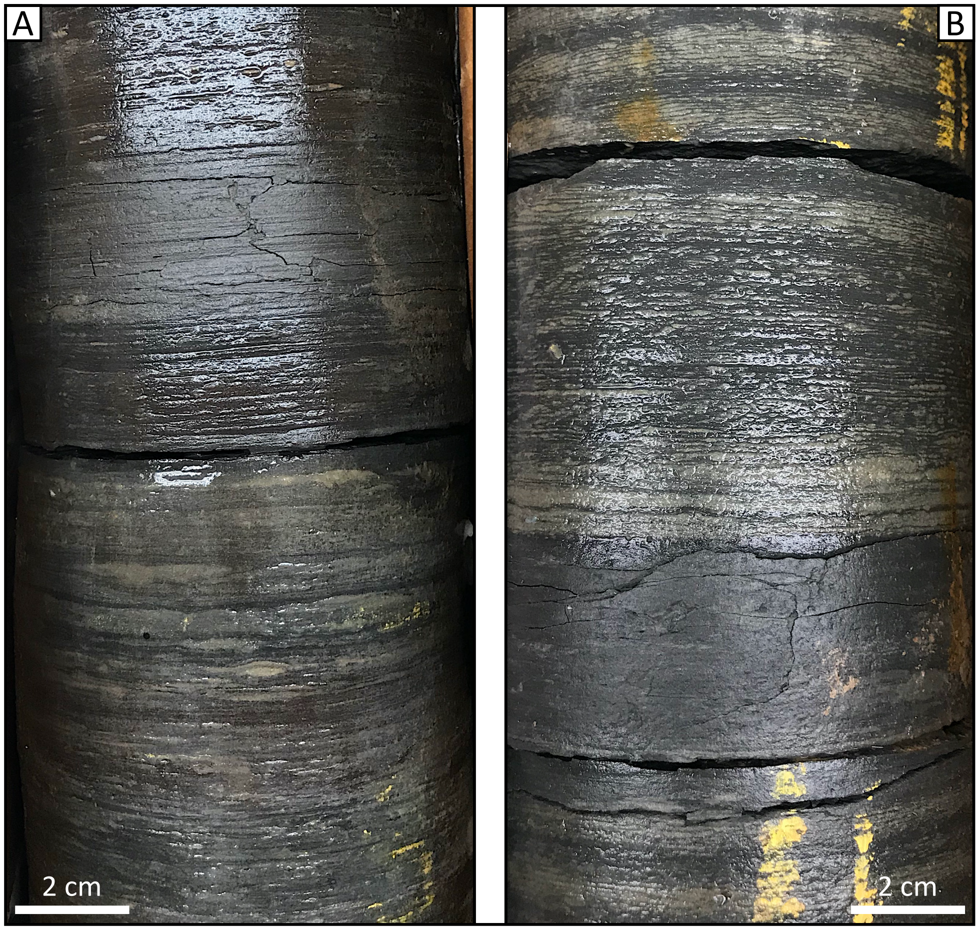

Figure 31. Core images of the heterolithic siltstone facies. **A)** Horizontal burrows in greenish muddy siltstone interval; note red (sideritic) band at lower portion of interval. **B)** Heavily bioturbated greenish interval showing repetitive thin-thick bundled laminated sandy couplets.

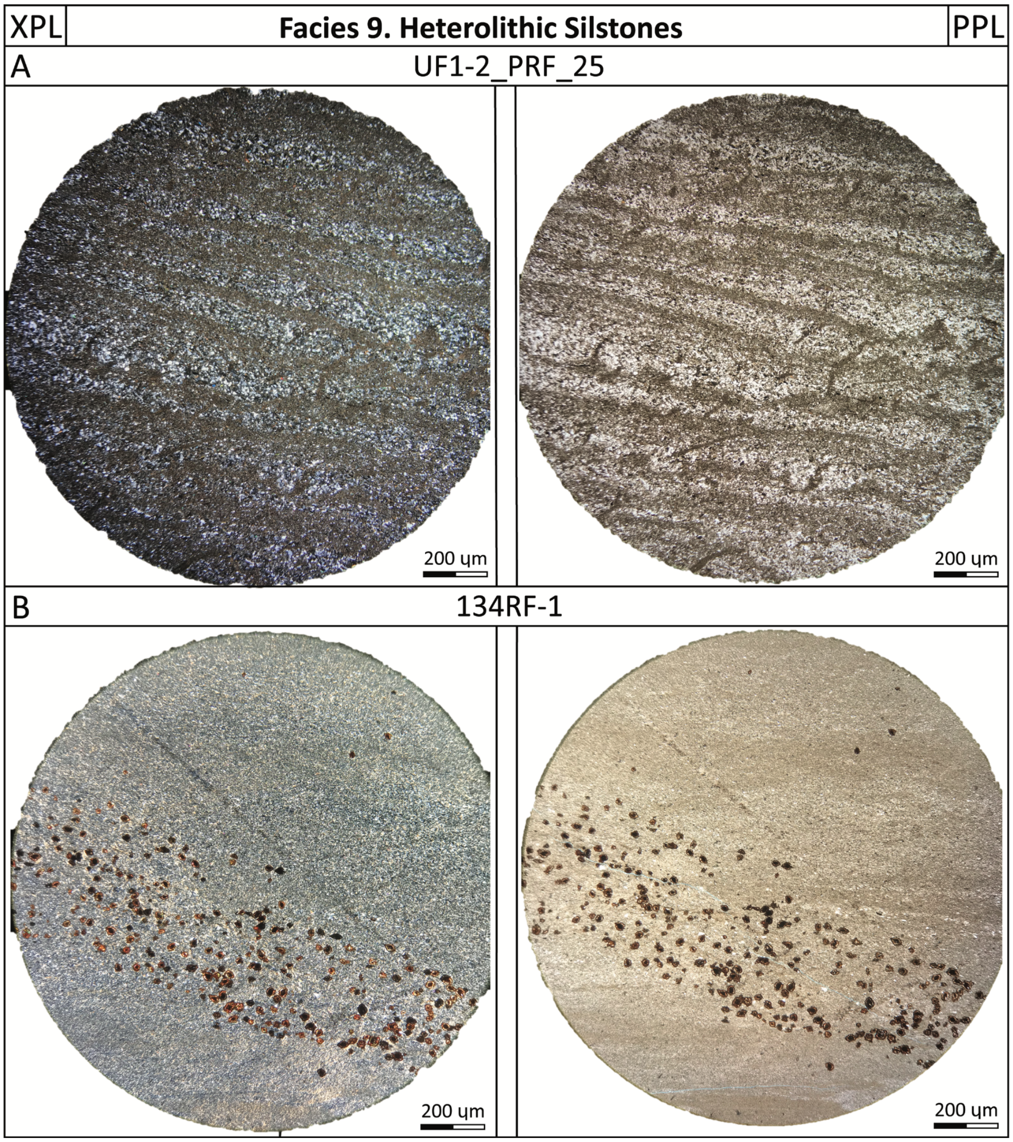

Figure 32. Thin section images of the heterolithic siltstone facies. **A)** Wavy parallel laminations disrupted by biologic activity; silt-rich laminations are quartzose. **B)** Iron-oxide concretions in clay matrix; note quartz-rich, discontinuous laminations.

<u>Interpretation</u>

The heterolithic siltstone facies is interpreted as forming from alternating ebb-tidal flood currents and slackwater sediment (suspension) fallout in lower tidal flat or subtidal coastline environments. Sand/silt layers are laid down during high-energy ebb/flood tidal flow, whereas mud is deposited during low energy slack-water periods in between tidal flows. This interpretation is fundamentally based on sedimentary structures found within the interval that represent tidal processes (Buatois et al., 1999). The presence of mud drapes, repetitive lamination sets and mud-silt couplets, thin-thick cyclic couplets (diurnal or semi-diurnal), and reactivation surfaces, reflect the predominant tidal processes represented. Other indicators of tidal deposits (yet, not exclusive to tidal processes) include minor ill-formed herringbone stratification. Trace fossils such as *Planolites (Pl),* and *Nereites (Ne)* indicate a marginal marine or deltaic environment with moderate sedimentation rates, allowing for the preservation of active burrows (Bouatois et al., 1999). The presence of siderite suggests freshwater infiltration, likely post deposition (Potsma, 1982). Lange (2003) interprets similar deposits as analogous to the "outside shale" in Heckel's (1977) cyclothem model.

Facies 10: Heterolithic Sandstones

Description

The heterolithic sandstone facies is composed of packages of well sorted, very fine- to fine- grained, light to medium tannish-gray sandstone and dark gray, siltstone, and silty mud (Figs. 33-34). The facies is found in all three (3) cores, and consists of interbedded flaser and wavy-bedded sandstone and bioturbated mudstone, interlaminated silty mudstone and sandstone and parallel-laminated silty sandstone (Fig. 33). Thicknesses range from 3.8 ft./1.16 m to 6.3 ft./1.9 m. The interbedded flaser and wavy-bedded sandstone and bioturbated mudstone package displays an overall upwardly fining trend into the bioturbated sandy siltstone facies (Facies 14). Sedimentary structures in that interval include thin to thick (approximately 5-10 cm and 10-20 cm) beds of thin to thick (1-5 mm to 5-10 mm) flaser or wavy stratification interlaminated with very thin to thin (1-5 mm to 5-20 mm) mud drapes. Thin (1-3 cm) unidirectional ripple cross beds (current ripples) are present and locally filled with mud drapes/plant traces. Thin to thick lenticular laminations, minor herringbone stratification and very thin fining upward parallel lamination sets are also prominent.

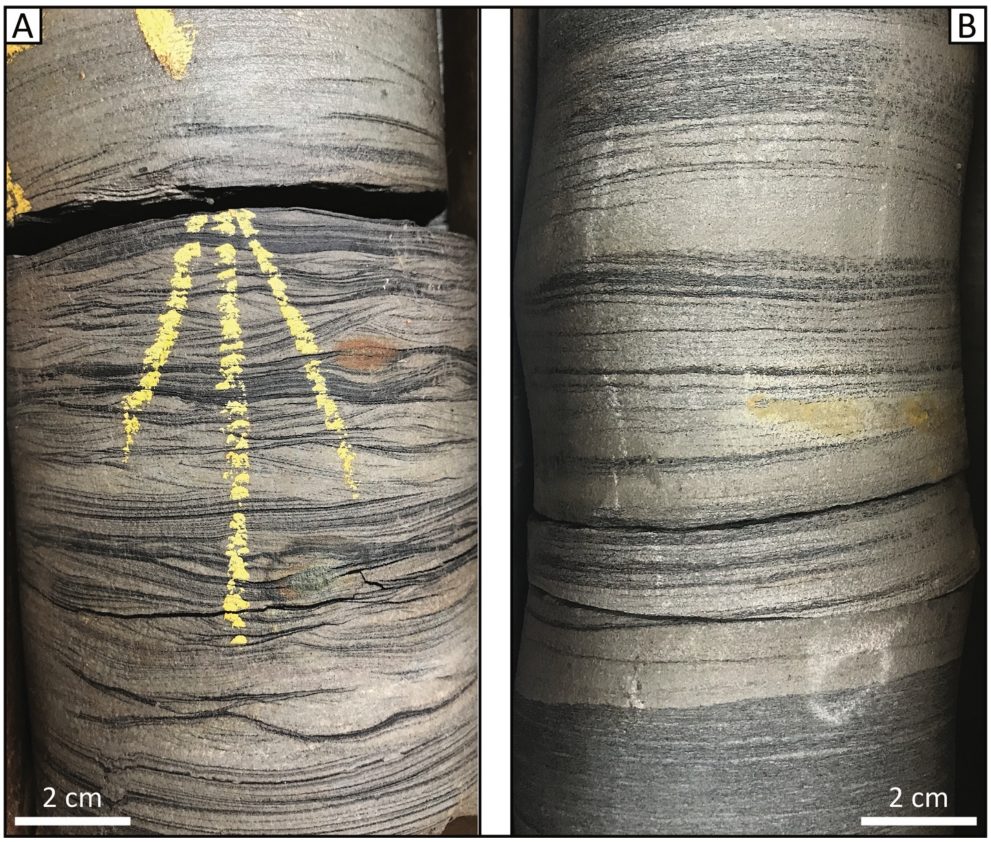

Figure 33. Core images of the heterolithic sandstone facies. **A)** Ripple cross laminations in fine to very fine sandstone interval. **B)** Rhythmic sandstone and mudstone interval.

The interlaminated silty mudstone and sandstone intervals display rhythmic mud-sand lamination sets as well as rare ill-formed herringbone stratification. The parallel-laminated silty sandstone displays more homogeneity as it only contains horizontal and slightly wavy laminations. Sideritic grains and features are dominant in the latter variant. This facies presents a gradational upper contact with the bioturbated sandy siltstone facies and a sharp contact with the parallel laminated mudstone with starved ripples. The basal contacts are consistently gradational with the heterolithic siltstone (Facies 9) and the medium to fine grained sandstones with mud drapes (Facies 12).

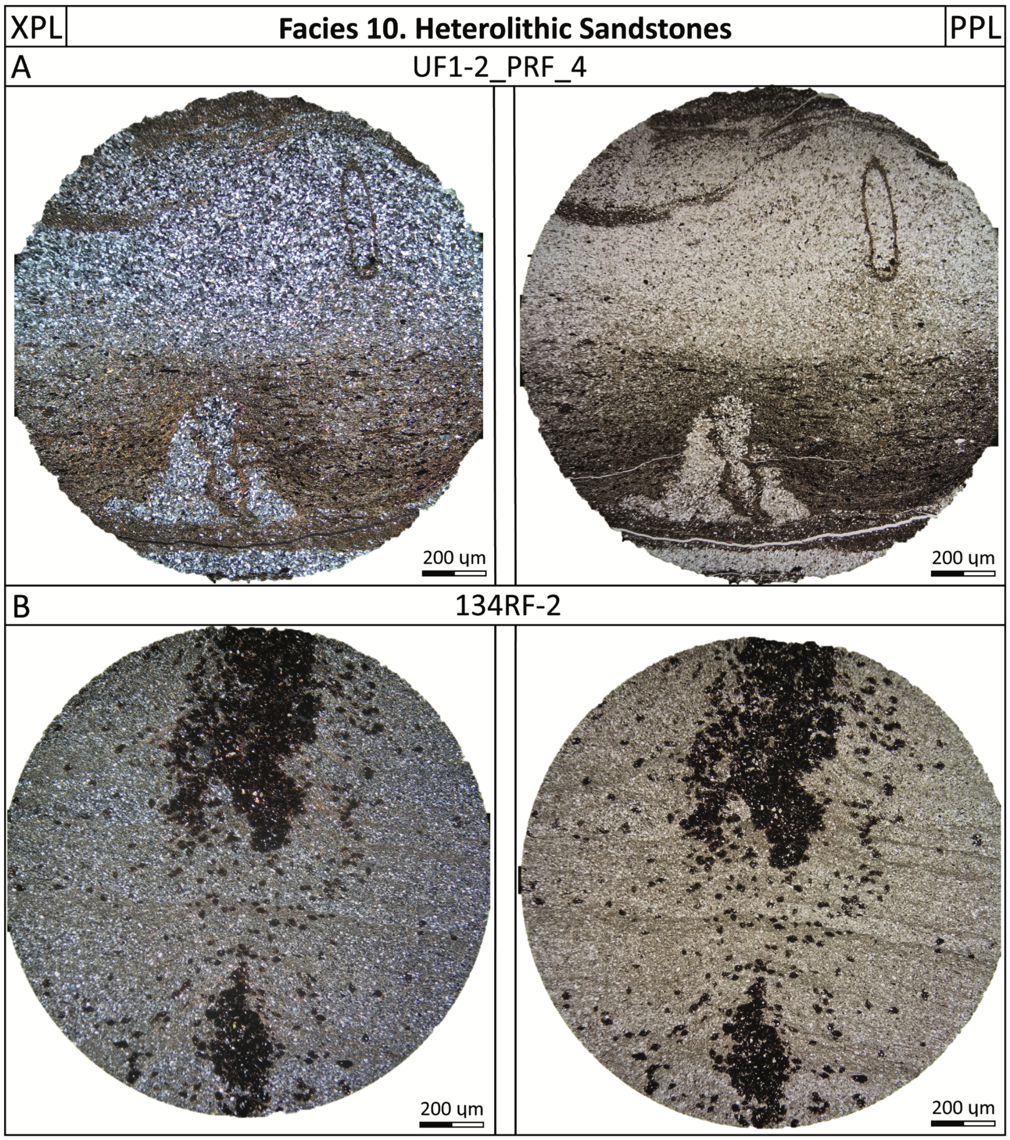

Figure 34. Core images of the heterolithic sandstone facies. **A)** Ripple cross laminations in fine to very fine sandstone interval; note vertical burrows and ripples. **B)** Rhythmic sandstone and mudstone interval; note iron-oxide concretions.

Interpretation

The heterolithic sandstone facies is interpreted as being formed by intermittent ebb-flood tidal currents with slackwater suspension fallout in upper tidal or upper subtidal environments. Numerous sedimentary features, such as flaser, wavy and lenticular ripples, suggest deposition through ebb-tidal flood currents with slackwater suspension deposition. Minor tidal-related structures (non-exclusive) includes herringbone cross stratification. Trace fossils such as *Planolites (Pl),* and *Teichichnus (Te)* suggest a brackish-water, marginal marine, or deltaic environment with moderate sedimentation rates, allowing for the preservation of active burrows (Potsma, 1982; Bouatois et al., 1999).

Facies 11: Fine Grained Sandstone

Description

The fine-grained sandstone facies consists of gray to medium-yellowish gray, silty sand to very-fine to fine-grained sandstone (Figs. 35-36). One variant of this facies occurs in Core 2, comprising a thick interval of 12.45 m (40.87 feet). Grain size varies slightly throughout the interval in the form of alternating beds of very fine to fine sandstone. Sedimentary structures range from structureless (massive; in 0.3-0.9 feet/0.1-0.3 m beds), thin (>1-2 mm) planar and sometimes irregular parallel faint laminations, minor ripple cross-stratification, faint amalgamated ripples, and thin and irregular faint-green laminations (Fig. 35B). A few chaotically dispersed, small (1-3 mm) siderite clasts occur near the upper portion of this facies (Fig. 35A) and a massive, 10mm green band with horizontally aligned siderite/hematite grains also occurs.

Body and trace fossils as well as root/plant fragments were not observed in this facies. In thin section, this facies presents moderate to well sorted, subangular to subrounded, very fine to fine sand-sized grains (Fig. 36). The sand is quartz rich but includes metastable grains, including muscovite, detrital feldspar, biotite, and hornblende. Other phases include pyrite, zircon, hematite, and siderite, and phosphatic grains. Rock fragment-grains are also present including chert, metamorphic, and minor sedimentary lithics. Gilsonite, a solid asphaltic residue (Glass, 1981), is present within certain intervals as cement. Carbonaceous material in the form of randomly oriented specks/filaments is also observed in thin section. The main cement is quartz overgrowths; however, clay and calcite cement also occur. This facies exhibits a sharp lower contact with the gray, sideritic shale facies (Facies 4), and a gradational upper contact with the mottled shales to sandstone facies (Facies 5).

Figure 35. Core images of the fine-grained sandstone facies. **A)** Massive section displaying pedogenic imprint of overlying paleosol/interfluve units (Facies 5). **B)** Faint and greenish cross laminations in fine grained sandstone.

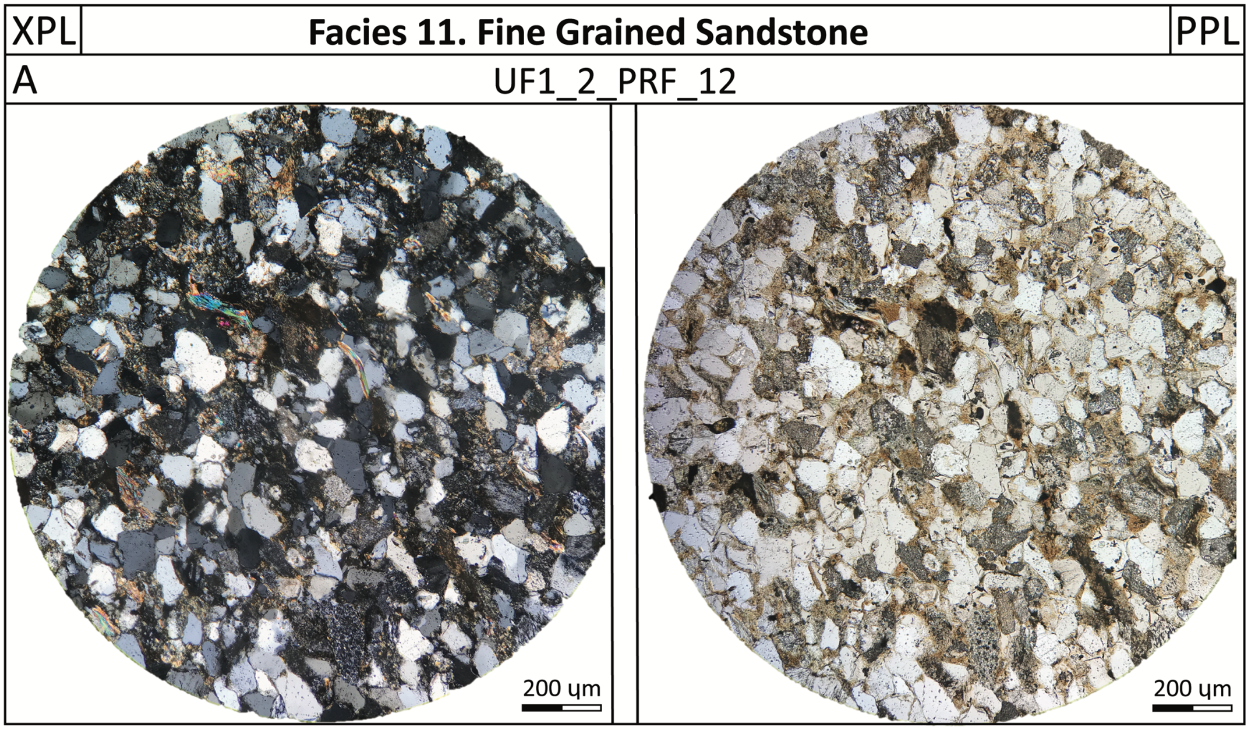

Figure 36. Thin section images of the fine-grained sandstone facies. Note abundant quartz and lithic grains with quartz overgrowths, clay and calcite cement.

Interpretation

The fine-grained sandstone facies is interpreted as forming from unidirectional traction current sedimentation inferred to represent a channel bar. The absence of tidal features previously observed in the other sandstone facies (mud-layered sandstone; features included mud drapes, inclined heterolithic stratification and reactivation surfaces) suggests a relatively constant flow direction in a non-tidal setting. The absence of marine trace and body fossils supports this interpretation as they are suggestive of constant sediment supply and deposition in a non-marine environment. The overall consistent grain-size reflects discharge that must not have been seasonal or prone to large floods.

Facies 12: Medium to Fine-Grained Sandstones with Mud Drapes

Description

The medium to fine grained sandstone with mud drapes facies comprises four components: a light to yellow gray, fine to medium, well sorted sandstone; a light gray, yellowish and greenish fine sandstone; a light gray, fine sandstone with mud laminae; and a medium to fine grained, cross-bedded sandstone (Figs. 37-38). The thickness of this facies ranges from 1.4 ft./0.43 m to 39 feet/11.89 m. This facies occurs in all three (3) cores in association with the parallel laminated sandy mudstone facies (Facies 2). Sedimentary structures include very thin (> 1 cm) to thin (1 cm) horizontal and inclined mud drapes (Fig. 37B), sinuous wispy features that resemble minor faint ripples, and inclined heterolithic stratification (IHS; flaser and lenticular bedding sets). Additional sedimentary structures include faint planar and irregular laminations, low-angle to cross laminations (Fig. 37A), and medium cross-bed sets. The fine sandstone with thin mud drapes contains very few dispersed 1-3 mm mud rip clasts and siderite clasts (1-3 mm) in certain intervals.

Trace fossils are rare and body fossils were not observed except in the upper portion of the light gray, yellowish and greenish fine sandstone, which is in contact with the carbonaceous shale facies above. These body fossils include small fragmented bivalve shells. Some of the rare trace fossils include *Scolicia (Sc), Nereites (Ne)* and *Planolites (Pl)*. Iron-stained root traces are observed throughout the light gray, yellowish and greenish fine sandstone variant in Core 2. Carbonaceous plant material occurs within the fine sandstone with mud laminae in Core 3.

Figure 37. Core images of the medium to fine-grained sandstone with mud drapes facies. **A)** Low to medium angle, cross laminated, medium-grained sand. **B)** Mud drapes within fine to very fine-grained sandstone.

This facies is defined as a sublitharenite based on petrographic analysis and is composed of subangular to subrounded quartz grains, minor feldspar, rock fragments (chert, metamorphic, shale), and clay, quartz overgrowths, and calcite cement. The calcite cement increases upward within the section. This facies presents an upper gradational contact with the heterolithic siltstone (Facies 9), the heterolithic sandstone (Facies 10) and the ripple laminated sandstone facies (Facies 13). The basal contact displays a sharp boundary with the bioturbated sandy siltstone facies (Facies 14), the black thinly laminated shales (Facies 1), or a gradational contact with the conglomerate facies (Facies 15).

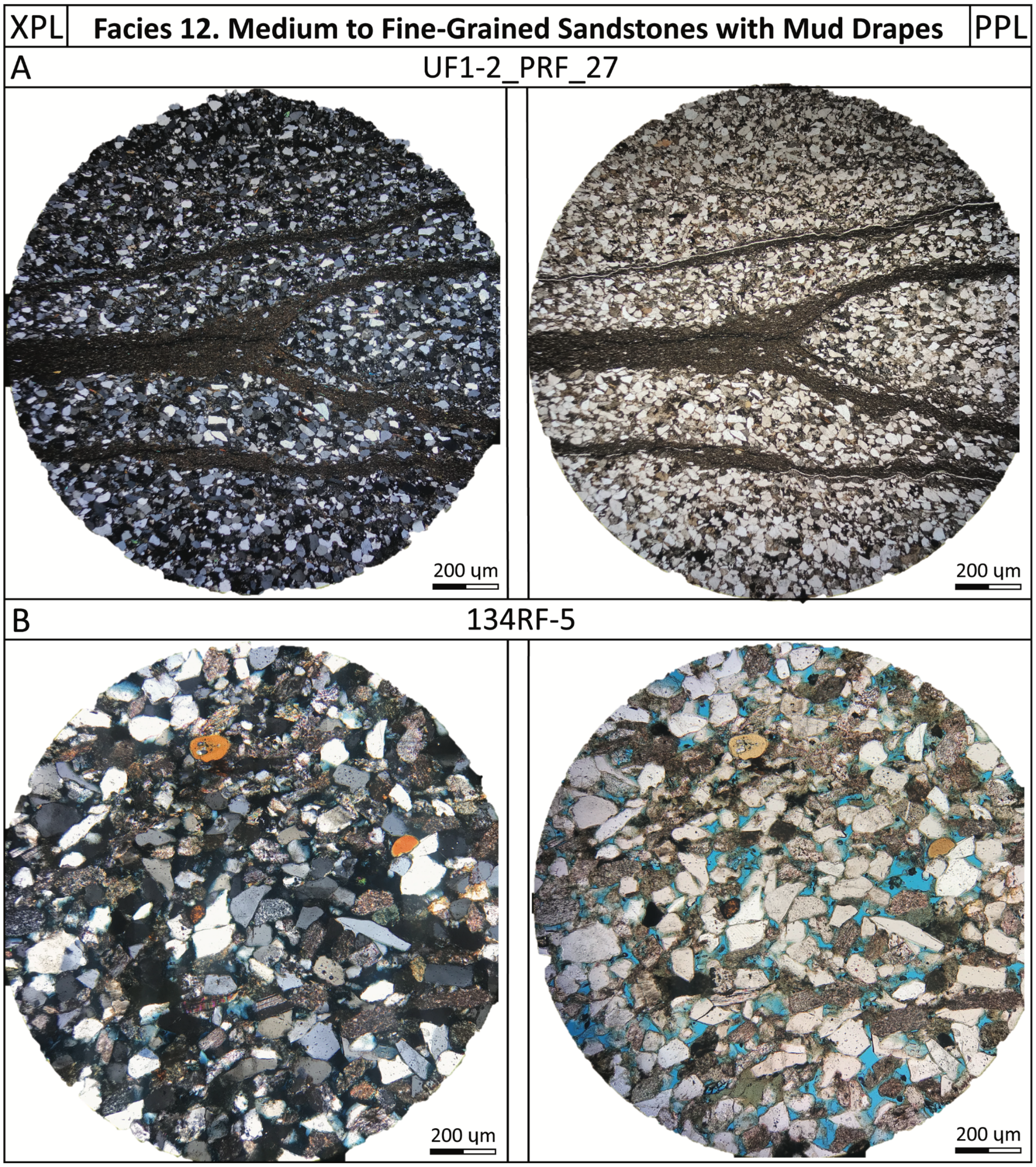

Figure 38. Thin section images of the medium to fine-grained sandstone with mud drapes facies. **A)** Mud drapes in well sorted, fine grained sand laminae. **B)** Note subrounded and well sorted sand grains of quartz, feldspar and lithics. Orange mineral is stained K-feldspar.

Interpretation

The medium to fine grained sandstone with mud drapes facies is interpreted as a channel-fill deposit in a relatively low to moderate energy, tidal environment. Periodic occurrence of mud drapes, minor faint ripples, minor thin and faint flaser as well as lenticular bedding, are indicative of weakly tide-influenced sedimentation (Goodbred and Saito, 2012). The wispy laminations resemble oppositely directed current ripples that have been destroyed by a change in flow velocity; thus, the presence of weakly developed bi-directional current ripples suggests reversing currents as in tidal environments. The variable levels of mud laminae in the different subfacies present are likely caused by the variable amount of mud in the system and fluctuating hydraulic conditions (Boggs, 2012). Therefore, the alternation of thin rippled sandstone and mud also indicates a tidal environment. The presence of *Planolites (Pl), Scolicia (Sc),* and *Nereites (Ne)* indicates marine conditions and thus incursion of marine waters into the channel. The iron-stained root traces and minor color-mottling present in the faintly laminated portion of upper sandstone interval (Core 2), suggest weak pedogenic influence and subaerial exposure. Based on these criteria, the facies is interpreted as a channel fill of a tidal channel deposited in an intertidal environment, but at least in Core 2 the facies experienced some pedogenesis. The overall sharp contact nature with the black, thinly laminated shales, the bioturbated sandy siltstones, and the conglomerate facies, indicate erosion and/or channel incision prior to deposition.

Facies 13: Ripple Laminated Sandstone

<u>Description</u>

Facies 13 comprises one interval of light gray to light green, ripple-laminated, fine-very fine sandstone located in Core 1 (Figs. 39-40). This facies is homogeneous and 10 feet/3 m thick. Sedimentary structures include continuous to discontinuous, sub-parallel laminae, discontinuous laminations in the form of finer "specks"/filaments, abundant ripple-laminations and climbing ripples. Another characteristic of this facies is the common occurrence of red grains (possibly iron oxide concretions), throughout the interval (Fig. 39). Trace or body fossils were not observed. In thin section, this facies is dominated by quartz and feldspars with minor rock fragments, micas, opaques, and glauconite in a quartz, clay and calcite cement (Fig. 40). The sand-sized grains are very fine, subangular-subrounded and moderately to well sorted. The interval overlies (gradational contact) a greenish, slumped, and silty interval of the medium to fine grained sandstone with mud drapes facies (Facies 12). The heterolithic siltstone facies (Facies 9) abruptly overlies this facies.

Figure 39. Core images of the ripple laminated sandstone facies. Note darker, iron-oxide, grains within the interval tracing sedimentary structures.

Interpretation

The ripple laminated sandstone facies is interpreted as the upper part of a tidal channel deposit. The basis for that interpretation includes the vertical relationship with the underlying medium to fine grained, cross bedded sandstone interval of the medium to fine grained sandstone with mud drapes facies (Facies 12), which represent the lower and middle sand body facies. Additional upper sand body characteristics include the abundant ripples and climbing ripple laminations as a result of high energy, unidirectional traction currents in shallow water. The lack of bioturbation is consistent with likely rapid sedimentation, also corroborated by the presence of climbing ripples.

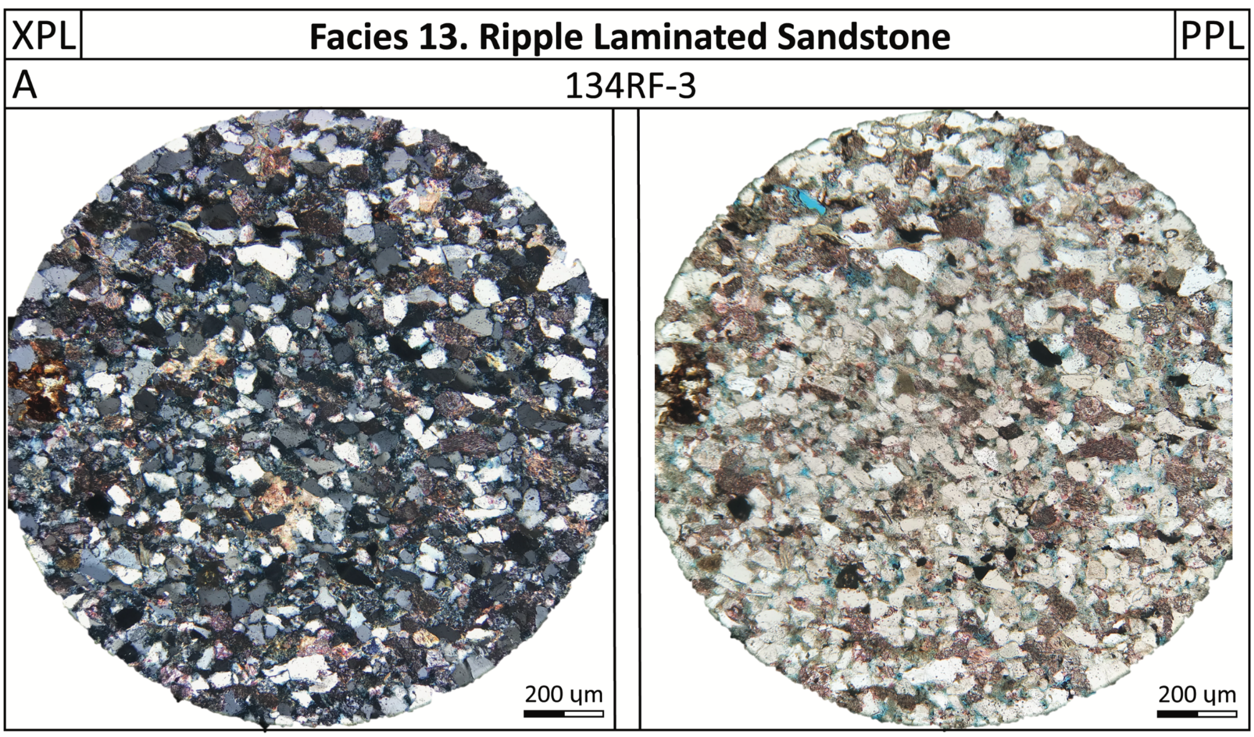

Figure 40. Thin section images of the ripple laminated sandstone facies. Note very fine grained glauconitic, silty sand in silica overgrowth, clay and calcite cement.

Facies 14: Bioturbated Sandy Siltstones

Description

The bioturbated siltstone facies is composed of two intervals: a greenish-light gray, well sorted, highly bioturbated siltstone and a green and dark gray, bioturbated and laminated sandy mudstone and siltstone (Figs. 41-42). The facies occurs in Cores 1 and 2, is approximately 3 feet / 0.9 m thick, and coarsens upward into the medium to fine grained sandstones with mud drapes facies (Facies 12).

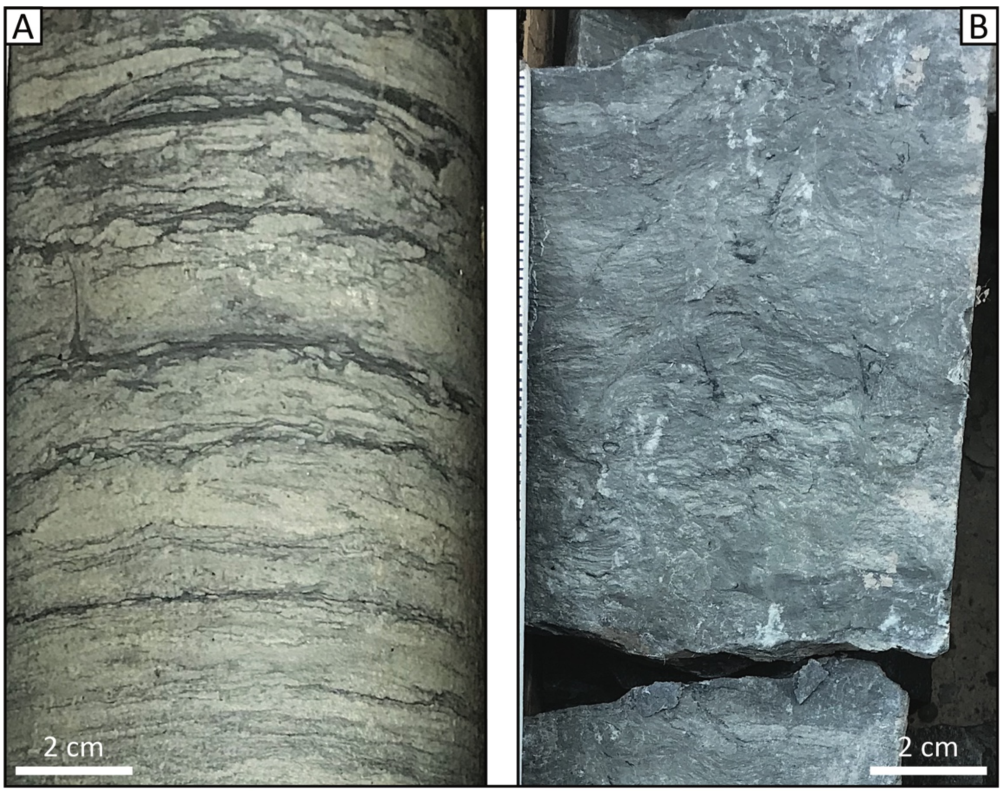

Figure 41. Core images of the bioturbated sandy siltstone facies. Note light ot dark green coloration of intervals. **A)** Moderate bioturbation in preserved mud laminations. **B)** Chaotic interval with few carbonized root traces.

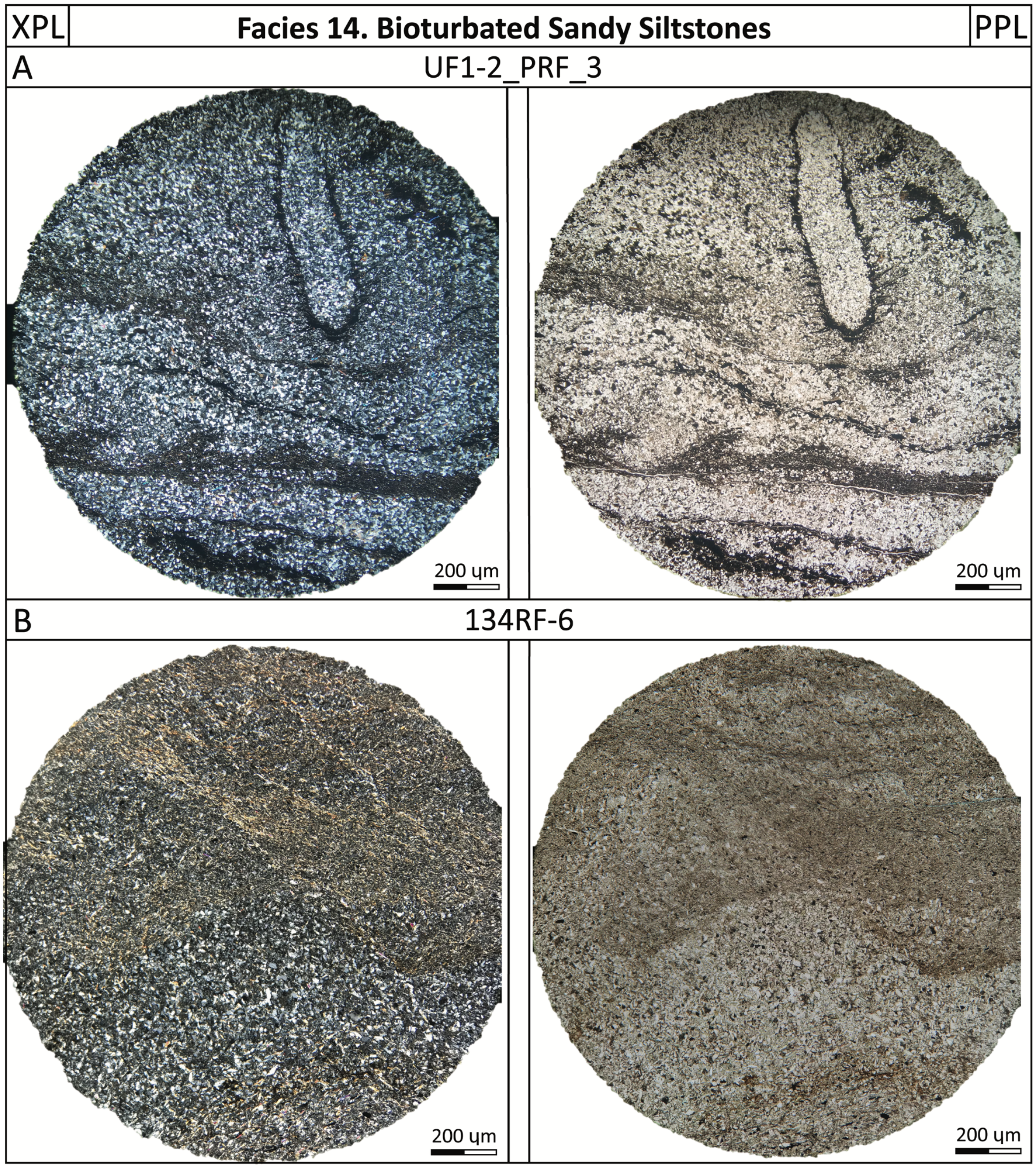

Figure 42. Thin section images of the bioturbated sandy siltstone facies. **A)** Vertical burrow and mud drapes; flame structures (?). **B)** Abundant clay in siltstone interval.

Sedimentary structures present include thin to thick highly bioturbated siltstone beds parted by very thin (>2 mm) to thin (2-5 mm) sinuous and horizontal mud drapes. Minor flaser and wavy stratification are present but lenticular laminae are more common.

However, laminations are commonly disrupted by bioturbation (Figs. 41-42). In the interval in Core 2, parallel laminations become thinner, faint and more planar and discontinuous towards the top and the interval becomes, overall, less bioturbated (Fig. 41A). On the other hand, the interval in Core 1 displays a chaotic texture that grades upward into a more laminated and rhythmic structure (Fig. 41B). Body fossils are rare, but trace fossils and bioturbation are very common and characterize this facies, giving it a mottled appearance throughout the interval. Vertical and horizontal burrows are present but are difficult to identify except for abundant and distinct *Planolite (Pl)* traces. Carbonized plant traces are also present throughout. This facies displays a gradational basal contact with the heterolithic sandstone facies (Facies 10) and a sharp contact with the black, thinly laminated shale facies (Facies 1). Upper contacts are sharp with the medium to fine grained sandstones with mud drapes (Facies 12).

<u>Interpretation</u>

The bioturbated siltstone facies is interpreted as an intertidal (mixed to mud flat) and marginal marine deposit forming from episodic high-energy storm currents and subsequent bioturbation and slackwater sediment fallout. This interpretation is based on its basal contact with the offshore marine/prodeltaic deposit of Facies 1 and with the upper subtidal deposit of Facies 10. Additionally, the facies is both heavily burrowed and displays heterolithic stratification, which are suggestive of tidal environments and occasional storm deposition after which organisms create escape traces. Carbonaceous plant material might suggest proximity to continental or marginal marine environments (Potsma, 1982).

Facies 15: Conglomerate

Description

The conglomerate/breccia facies consists of two types, both in Core 3: a chert-clast conglomerate (Fig. 43A) and a carbonate-clast conglomerate (Fig. 43B). The first consists of orange-brownish, pebble-gravel (2-4 mm), subangular to angular matrix to grain supported chert fragments. The observed thickness is approximately 0.4 feet/0.12 m. The matrix is light-gray to light-tan, fine-grained sandstone. The calcareous conglomerate is medium to dark gray in color and approximately 0.6 feet/0.18 m thick (Fig. 43B). The interval consists of matrix supported, subrounded to angular pebble to (2-4 mm) to cobble (~64 mm) clasts within a calcareous mud matrix. Upper contacts are gradational with overlying medium to fine-grained sandstone with mud drapes facies (Facies 12) and the carbonaceous shale facies (Facies 3). Lower contacts are sharp with the carbonaceous shale facies and the shaly carbonate facies (Facies 6).

Interpretation

The conglomerate facies is interpreted as a channel lag deposit in a channel forming from traction currents and bed load deposition (chert-clast supported interval) as well as from possibly gravity flow (carbonate, matrix-supported interval). The interpretation is evidenced by the overlying channel deposit of Facies 12, its overall thin nature, and the presence of carbonate intraclasts and chert clasts.

Figure 43. Core images of the conglomerate facies. **A)** Clast-supported chert conglomerate. **B)** Matrix-supported carbonate conglomerate.

Facies 16: Interbedded Sandstone and Mudstone

<u>Description</u>

This facies consists of interbedded very fine-grained to fine-grained sandstone and black mudstone, arranged in upwardly coarsening intervals that measure 32 feet/9.75 m (Figs. 44-45). This facies only occurs in Core 3. Sedimentary structures of this facies include lenticular, wavy and flaser bedding, soft sediment deformation, horizontal and low-angle inclined laminations, and ripple cross laminations (Fig. 44A). Additional features include minor siderite nodules and mud rip-up clasts. Highly deformed beds are observed in this facies, ranging from 10 feet/3 m to

2.5 feet/0.76 m thick and containing siderite nodules, mud rip-clasts and a 3 cm siderite band (Fig. 44B). Some of the interlaminated intervals are highly rhythmic on a millimeter to centimeter scale.

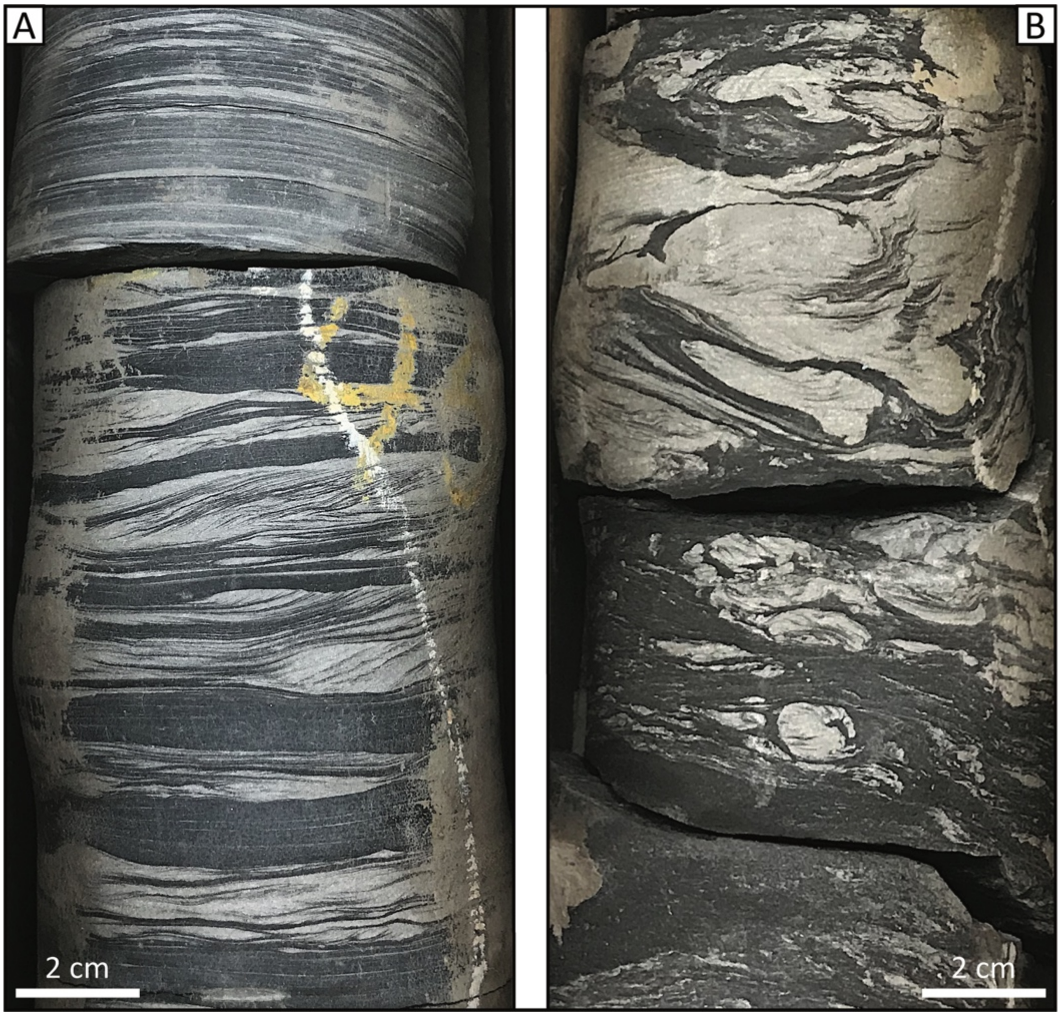

Figure 44. Core images of the interbedded sandstone and mudstone facies. **A)** Ripple cross laminations in rhythmic sand and mud package. **B)** Slumped interval likely caused by higher sedimentation rates.

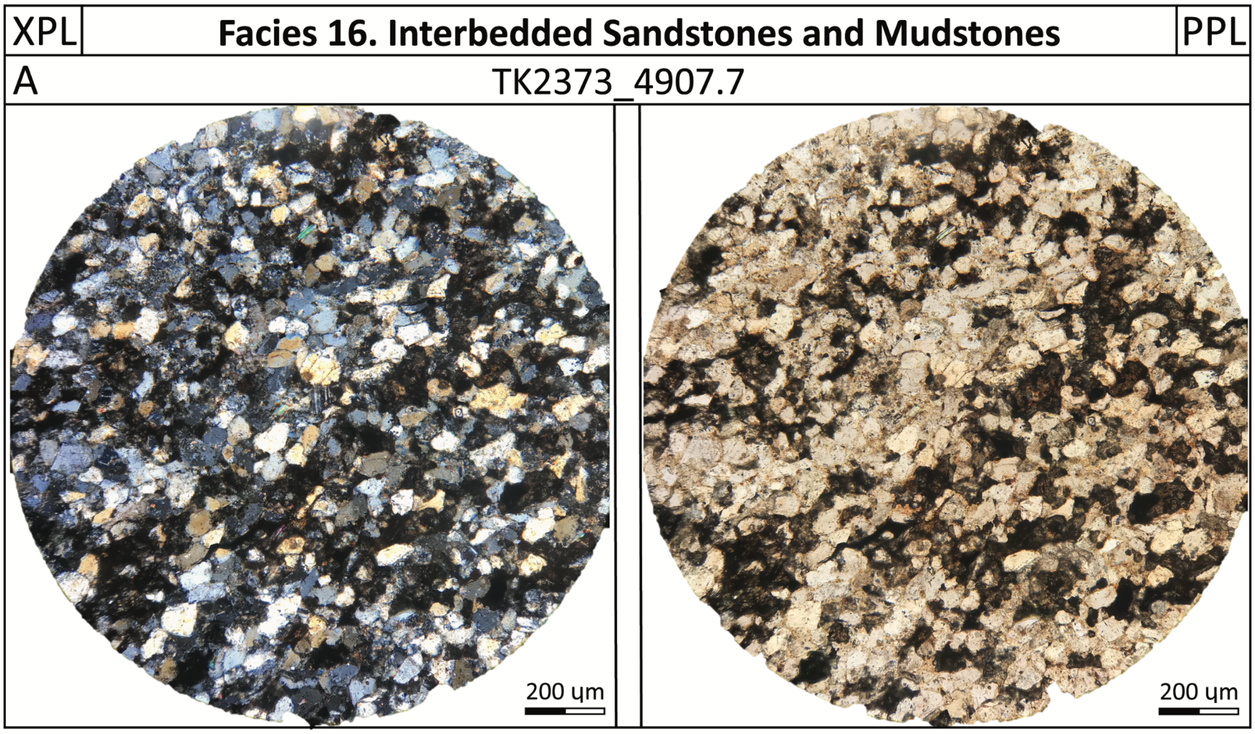

Figure 45. Thin section images of the interbedded sandstone and mudstone facies. Note abundant quartz and minor amounts of feldspar and lithics as well as overall "dirty" appearance.

Body fossils were not observed, and trace fossils are rare in this facies. Minor detrital plant debris was observed in the form of millimeter-scale particles. This facies coarsens upward into a less heterogeneous and less rhythmic sandstone package. Thus, this facies displays a gradational upper contact with the burrowed and interbedded, sideritic sandstone and mudstone facies (Facies 8), whereas the lower contact is gradational with the medium to fine grained sandstones with mud drapes facies (Facies 12). In thin section, this facies is composed of abundant quartz and minor amounts of feldspar and lithics; thus a quartzarenite (Fig. 45). The facies displays a "dirty" appearance likely caused by clay content.

Interpretation

The interbedded sandstone and mudstone facies is interpreted as a distal delta front deposit of a delta that prograded out into open marine waters. This interpretation is supported by the coarsening-upward nature of its intervals and overall coarsening upward trend into the overlying burrowed and interbedded, sideritic sandstones and mudstones facies. Along with the stratigraphic trend, this facies also displays evidence for rapid sedimentation rates, marked by the presence of contorted beds in the middle and upper parts of the package. The facies shows evidence of tidal influence as represented by the common preservation and dominance of mud drapes, heterolithic stratification (e.g. flaser, wavy, lenticular, pinstripe), as well as rhythmic laminations. Another indicator of tidal processes includes the overlying nature of this facies with the medium to fine grained sandstones with mud drapes (Facies 12). The intermittent distribution of trace fossils (represented by escape traces) and common sediment deformation structures and inclined bedding indicate rapid rates of sedimentation, which point to distal areas of a delta front.

Table 5. Distribution and vertical relationships of facies.

		Distribution			**Vertical Relationships**	
No.	**Lithofacies**	**Core 1 (Kay)**	**Core 2 (Logan)**	**Core 3 (Pottaw.)**	**Overlying facies**	**Underlying facies**
1	Black, thinly laminated shales	√	√		Medium to fine-grained sandstones midcontinent/ mud drapes (12) or heterolithic siltstones (9)	N/A
2	Parallel laminated sandy mudstones		√	√	Medium to fine-grained sandstones midcontinent/ mud drapes (12)	Medium to fine-grained sandstones midcontinent/ mud drapes (12)

3	Black carbonaceous shales		√		Shaly carbonates (6)	Medium to fine-grained sandstones midcontinent/ mud drapes (12)
4	Gray sideritic shales		√		Fine-grained sandstones (11) or heterolithic siltstones (9)	Shaly carbonates (6) or skeletal wackstones to packstones (7)
5	Mottled mudstones and sandstones		√		Shaly carbonates (6) or skeletal wackstones to packstones (7)	Fine-grained sandstones (11) or heterolithic siltstones (9)
6	Shaly carbonates		√	√	Gray sideritic shales (4) or N/A	Mottled mudstones and sandstones (5), black carbonaceous shales (3)
7	Skeletal wackstones to grainstones/packstones		√		Gray sideritic shales (4)	Mottled mudstones and sandstones (5)
8	Burrowed and interbedded, sideritic sandstones and mudstones			√	N/A	Interbedded sandstones and mudstones (16)
9	Heterolithic siltstones	√	√		Mottled mudstones and sandstones (5), or heterolithic sandstones (10)	Rippled sandstone (13), gray sideritic shales (4) or medium to fine-grained sandstones midcontinent/ mud drapes (12)
10	Heterolithic sandstones	√	√	√	Interbedded sandstones and mudstones (16) or bioturbated sandy siltstones (14)	Heterolithic siltstones (9), medium to fine grained sandstones with mud drapes (12)
11	Fine grained sandstone		√		Skeletal wackstones to packstones (7)	Gray sideritic shales
12	Medium to fine grained sandstones with mud drapes	√	√	√	Heterolithic siltstones (9),	Bioturbated sandy siltstones (14),

					heterolithic sandstones (10), or ripple laminated sandstones (13)	black thinly laminated shales (1), or conglomerates (15)
13	Ripple laminated sandstone	√			Heterolithic siltstones (9)	Medium to fine-grained sandstones midcontinent/ mud drapes (12)
14	Bioturbated sandy siltstones	√	√		Medium to fine-grained sandstones midcontinent/ mud drapes (12)	Heterolithic sandstones (10) or black, thinly laminated shales (1)
15	Conglomerates			√	Medium to fine-grained sandstones midcontinent/ mud drapes (12) or black carbonaceous shales (3)	Shaly carbonates (6)
16	Interbedded sandstones and mudstones			√	Burrowed and interbedded, sideritic sandstones and mudstones (8)	Medium to fine grained sandstones with mud drapes (12)

CHAPTER VI

SEQUENCE STRATIGRAPHY

Introduction

This chapter presents a detailed, well-core-based sequence stratigraphic analysis of the Red Fork in the study area. The cores were coupled with their respective gamma-ray logs to identify sequence boundaries and related surfaces at the base, top and within the Red Fork interval. Prior to the sequence stratigraphic analysis, I will review key elements of sequence stratigraphy.

Overview of Key Sequence Stratigraphic Concepts

Sequence stratigraphy studies the relationship of rocks within a chronostratigraphic framework of repetitive strata that are genetically related and bounded by surfaces of erosion/deposition/correlative conformities (Van Wagoner et al., 1988; 1990). The most basic stratigraphic unit defined in this methodology is the sequence, which is "a relatively conformable succession of genetically related strata bounded by unconformities and their correlative conformities" (Mitchum, 1977). According to Van Wagoner et al. (1988; 1990), an unconformity is "a surface separating younger from older strata, along which there is evidence of subaerial erosional truncation (and, in some areas, correlative submarine erosion) or subaerial exposure, with a significant hiatus indicated." Sequences are a result of the interplay of sea level change, tectonics, and sediment supply regardless of global sea-level change (McLaughlin Jr., 2005). They are separated by sequence boundaries and can be internally subdivided into system tracts, whose classification depends on their position within a sequence and on the stacking patterns of parasequences and parasequences sets (Mitchum 1977; Van Wagoner et al., 1988).

The fundamental building blocks of sequences are parasequences, the latter defined as a “relatively conformable, genetically related succession of beds or bedsets bounded by marine-flooding surfaces or their correlative surfaces” (Van Wagoner et al., 1988; 1990). Further, a parasequence set is “a succession of genetically related parasequences forming a distinctive stacking pattern bounded by major marine-flooding surfaces and their correlative surfaces” (Van Wagoner, 1995).

There are three types of parasequence-stacking patterns, which are defined by the ratio of the rates of deposition to accommodation. A progradational parasequence set reflects greater deposition relative to accommodation rates and is characterized by an overall shoaling and basinwards advance of a depositional system (Fig. 46). As the well log responses in Figure 46 show, in progradational parasequence sets, younger parasequences are expected to be thicker and coarser than older parasequences. A retrogradational parasequence set represents the contrary; that is, the parasequence stacking patterns exhibit greater accommodation rates in relation to deposition rates, and an overall deepening and landwards retreat of the depositional systems occurs over the parasequence set (Fig. 46). The well-log responses in Figure 46 show that in this parasequence set type, younger parasequences are expected to be thinner than older ones. Lastly, an aggradational parasequence set reflects equal rates of deposition and accommodation, and an overall steady stacking of facies that reflect no significant shifts basinwards or landwards (Fig. 46) (Van Wagoner, 1985; Van Wagoner et al., 1988; 1990; McLaughlin Jr., 2005).

Recognition of stacking patterns and facies trends in parasequence sets is fundamental to the identification of system tracts, which are fundamental sequence components. Systems tracts are defined as "genetically associated stratigraphic units that were deposited during specific phases of the relative sea-level cycle" (Posamentier and Vail, 1988). Systems tracts can be recognized from the overall parasequence set stacking pattern as well as their position in a stratigraphic sequence (McLaughlin, 2005). Commonly defined system tracts include the Lowstand Systems Tracts (LST), the Transgressive Systems Tracts (TST), and the Highstand Systems Tracts (HST) (Fig. 47). Other less common systems tracts (not yet consistently used by sequence stratigraphers) include the Falling Stage Systems Tracts (FSST) and the Forced Regressive Systems Tracts (FRST).

The **Lowstand Systems Tract (LST)** is marked by sedimentary units deposited during the phase of lowest relative sea-level to early rise. It expresses a basinwards shift in facies and overlies the Sequence Boundary (SB) or, in some cases, the Falling Stage Systems Tracts (FSST), and underlies the Transgressive Surface (TS), which is a marine-flooding surface (the maximum regressive surface) (Hunt and Tucker, 1992; Mclaughlin Jr., 2005; Catuneaunu, 2006). In general, lowstand systems tract units show a progradational to aggradational stacking pattern, and in frequent cases, completely or partially characterized by incised valley deposits (Posamentier and Allen, 1999). According to Zaitlin et al. (1994), an incised-valley system is a fluvially incised (eroded) valley and fill that reflects an abrupt basinwards shift in depositional facies across an erosional sequence boundary (Fig. 47).

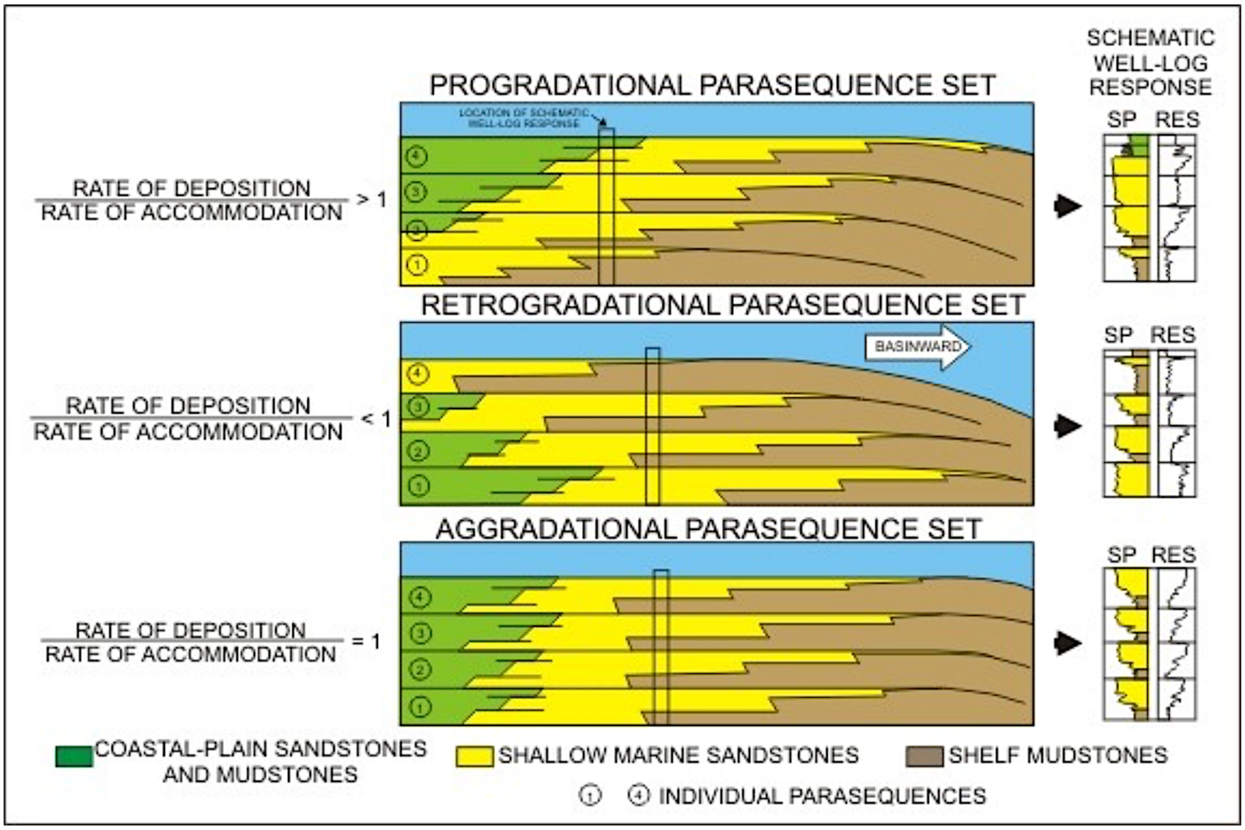

Figure 46. Parasequence stacking patterns in parasequence sets; cross-section and well-log expression (from Van Wagoner et al., 1988; 1990).

The **Transgressive Systems Tract (TST)** contains rocks that were deposited from the onset of landward transgression to the time of maximum coastal transgression and displays a retrogradational parasequence stacking pattern because sediment input is overwhelmed by accommodation space creation (Posamentier and Allen, 1999; McLaughlin, 2005). This systems tract overlies the Transgressive Surface, which lies at the top of the LST in distal areas or the SB in proximal locations, and underlies the maximum flooding surface (mfs), also known as the condensed section (Fig. 47; Van Wagoner et al., 1988).

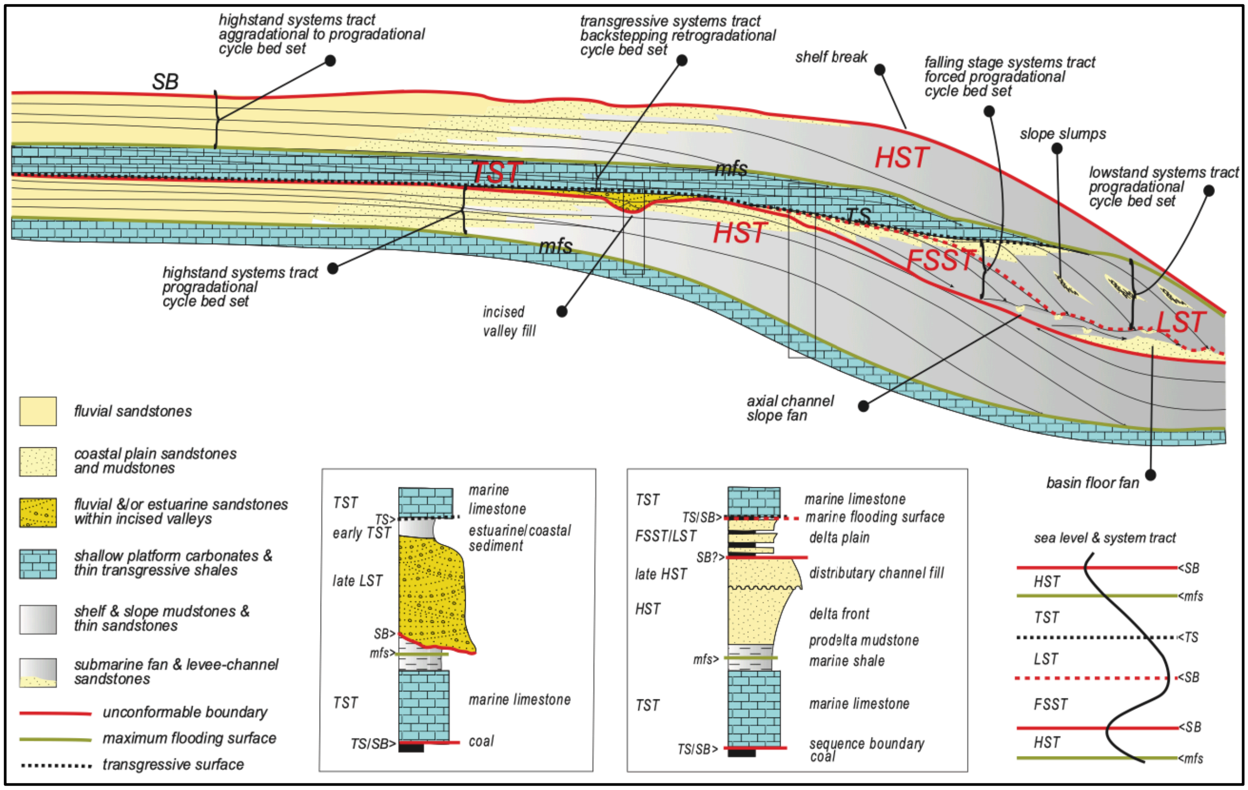

Figure 47. Sequence stratigraphic model and cycles for a mixed carbonate-clastic succession (Catuneanu et al., 2011).

The **Highstand Systems Tract (HST)** is composed of progradational to aggradational deposits that form during a time when sediment input rates coincide or exceed accommodation rates (Posamentier and Allen, 1999). This system tract lies above the maximum flooding surface (mfs) and below a sequence boundary (SB) and represents the upper systems tract of a stratigraphic sequence (Fig. 47; McLaughlin, 2005).

Stratigraphic Markers

Prior to conducting a sequence stratigraphic analysis, it is important to document the existence of widespread stratigraphic markers within the area. The regional markers include the transgressive, carbonate bounding surfaces of the Red Fork Sandstone and the condensed sections with their respective maximum flooding surfaces. A condensed section is "a facies consisting of thin hemipelagic and pelagic sediments accumulated at very slow rates during a long period of time" (Louis et al., 1988). In well logs, condensed sections commonly exhibit high gamma ray values (more than 150 API) and are identified as "hot shales" caused by their high Total Organic Carbon (TOC) signature (Puckette, 1990). On the other hand, the Transgressive Surface (TS) is "the first significant marine flooding surface across the shelf within the sequence" (Van Wagoner et al., 1988).

Pink and Inola Limestones

The Pink Limestone has been interpreted as a major transgression across the Anadarko Shelf and the start of a transgressive-regressive cycle (Houston and Kerr, 2008). In well logs, this limestone marker displays thickness averaging 10 ft (3 m). The facies is present in Core 2 but not within the cored intervals of Cores 1 and 3; for those the limestone is identified in the well log. The limestone is composed of deep and shallow water carbonate facies, an exposure surface and a black "hot shale" in the shelf area (Puckette, 1990). The Inola Limestone is identified as a fossiliferous and dark-gray unit that marks a major transgressive event. The Inola Limestone is an open-marine carbonate to shale deposit containing thin beds of fossiliferous limestones, pyrite, and calcite-filled burrows (Hemish, 1989), and its presence indicates a marine transgression that terminated the underlying Bartlesville Sandstone cycle (Ye and Kerr, 2000). The limestone averages less than 8 ft (2.4 m) in the study area; it was identified in Core 3 and absent in the other two cored intervals but identified in well-logs below the cored interval of Core 1.

Core 1 Stratigraphic Sequence

Two sequences were observed in this core, sequences DG0 and DG1 (Fig. 48). Sequence DG0 only displays a coarsening-upward, progradational parasequence set consisting of offshore marine shales (Facies 1) and marginal marine siltstones (Facies 14). Sequence DG1 starts at 3194.6 ft, where a sequence boundary (SB1) is located and continues to the top of Core 1.

Specifically, at its base, the cored interval contains offshore marine shales (no 1; 3206-3197 ft), characteristic of a condensed section, which occurs in association with the Inola Limestone marker bed (Ye and Kerr, 2000). The Inola Limestone is not present in the cored interval but identified in the gamma-ray well log (~30 ft below the base of Core 1) of a nearby well, which is ~1652 ft north of Core 1 (well 2; Appendix A). Given the characteristics of the Inola Limestone and coeval shales this would reflect the marine transgression prior to regression that led to the deposition of the Red Fork. Therefore, sequence DG0 is a partial sequence in the cored interval, composed of a progradational parasequence set (Pa) which marks the highstand systems tract (HST) bounded by a maximum-flooding surface (mfs1; ~25 ft below the base of Core 1) and by a sequence boundary (SB1) at the top (3194.6 ft). Progradation is marked by the upwardly shallowing trend from offshore marine shale facies (Facies 1) to the shallow/marginal marine siltstones (Facies 14).

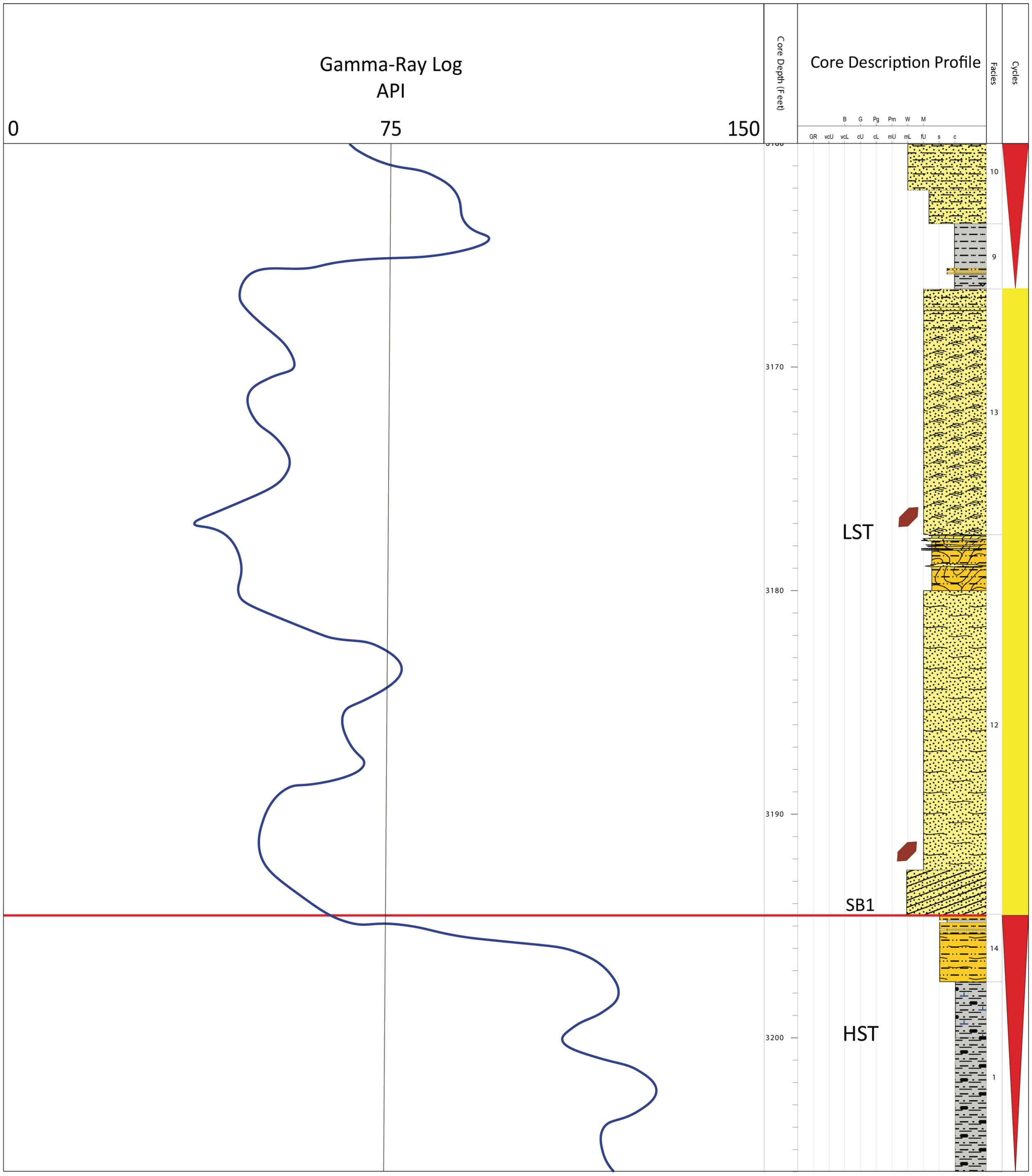

Figure 48. Sequence stratigraphic analysis of Core 1. Refer to Figure 49 for legend.

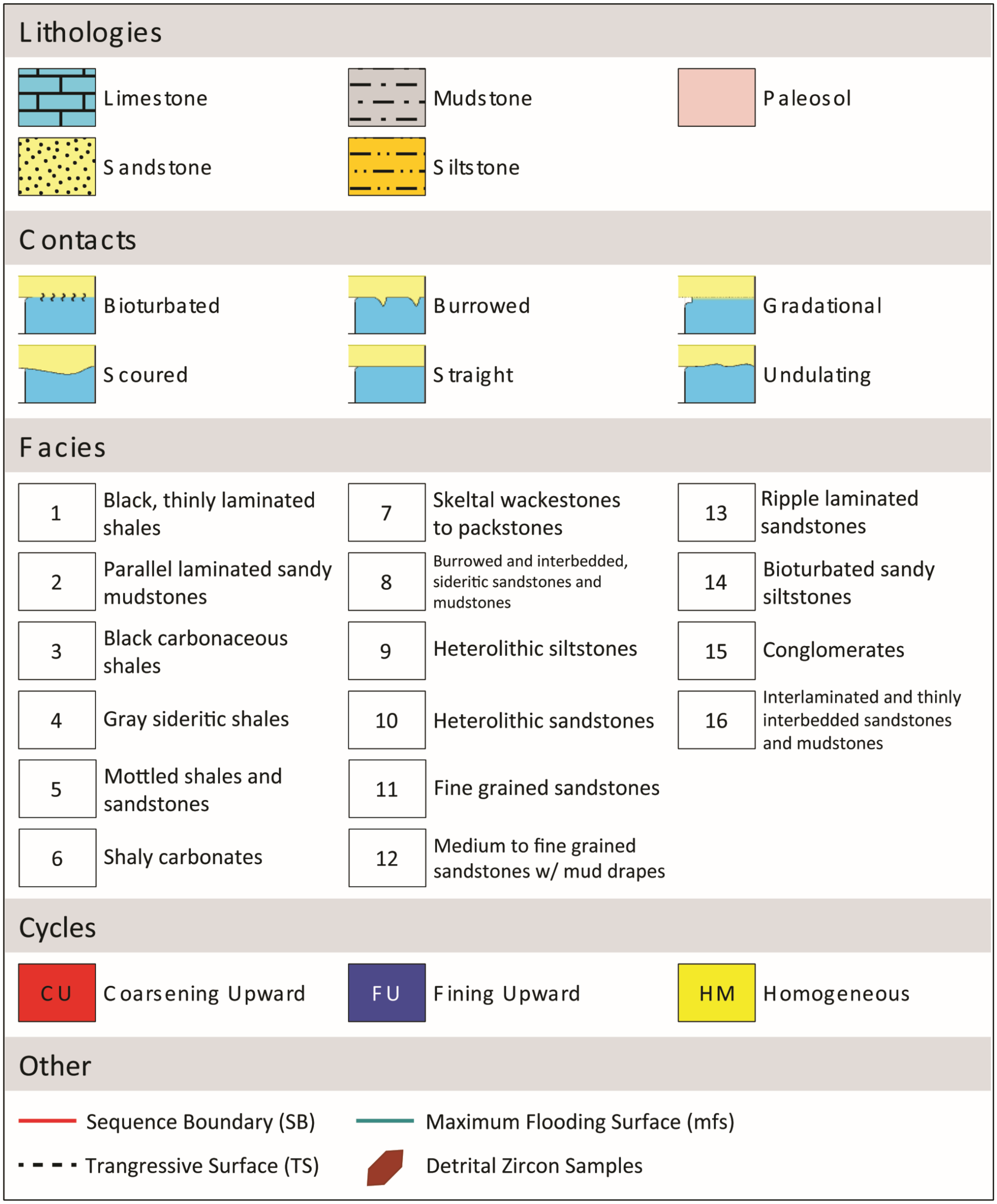

Figure 49. Legend for sequence stratigraphic analysis of cores in the study area (Figures 48, 50 and 51).

Sequence boundary SB1, which marks the start of sequence DG1, is evidenced by the abrupt/sharp contact between the underlying marginal marine siltstones (Facies 14) and the tidal channel sandstones (incised valley fill – IVF; Facies 12). Sequence DG1 is an incomplete sequence defined by an upwardly homogeneous, aggradational parasequence set (Pb). Parasequence set Pb is composed of the lower, middle, and upper channel-fill units of the IVF in Core 1(Facies 12, 13, 10). Parasequence set Pb marks the lowstand systems tract (LST) of the sequence. The onset of the transgressive systems tract (TST) is identified on the gamma-ray log at ~25 ft above the top of Core 1, and the Pink Limestone is identified in the log at ~55 ft above the top of Core 1.

Core 2 Stratigraphic Sequence

At least three (3) sequences were observed in this core, namely UF0, UF1, and UF2 (Fig. 50). Sequence UF0 is similar to sequence DG0 in Core 1 in that at its base, the cored interval contains offshore marine shales (Facies 1) (5237 ft). The Inola Limestone marker was not identified in the associated gamma-ray logs. The present portion of sequence UF0 contains either the transgressive systems tract (TST) or the highstand systems tract (HST), that were possibly partially eroded and thus harder to characterize (only 14 ft present in the GR well log and 1 ft in the core). The interpretation of a TST is preferred over a HST based on the upwardly fining, retrogradational character of log response in the 14ft section and the absence of a marker for a maximum flooding surface.

Sequence boundary (SB2; at 5235.4 ft) marks a fall in sea level, which is supported by the abrupt/sharp facies shift from the underlying offshore marine shales (Facies 1) to the overlying tidal channel-fill (IVF; Facies 12), and the start of sequence UF1. UF1 is composed of at least three parasequence sets, namely Pc, Pd and Pe. Pc is an aggradational parasequence set (Pc) composed of tidal channel deposits (Facies 12). This parasequence set is followed by a fining-upward, retrogradational parasequence set (Pd) that shallows upward from the channel fill/tidal flat deposits (Facies 9) to interfluve deposits (Facies 5). The aggradational parasequence set (Pc) contains the first LST while Pd contains the early TST. This is followed by a transgressive surface (TS) at the base of a shallow marine limestone (Facies 6; at 5208.3 ft) and represents the first marine flooding surface of significant areal extent. The TST consists of an upwardly fining, retrogradational parasequence set (Pd) bounded by the TS at the base and the mfs3 at the top (~5188 ft), which marks the maximum landward extent of transgression (highest GR reading). Following the mfs3, a very thin portion of the HST is present but was almost completely eroded and is capped by SB3.

Sequence UF2 starts at the SB3 and continues upward until the top of the Core 2 (Fig. 50). It is composed of three parasequence sets, namely Pf, Pg, and Ph. Pf is an aggradational parasequence set consisting of channel and interfluve deposits (Facies 11 and 5). This parasequence set contains the LST of sequence UF2. A marine transgression caps the LST, developing thus the TS, which is marked by the deposition of shallow marine beds of the Pink Limestone (Facies 7). The TS is followed by an upwardly fining, retrogradational parasequence set (Pg) composed of the shallow marine limestones (Facies 7) and the offshore marine shales (Facies 4). This parasequence set (Pg) contains the TST of the sequence. The maximum landward extent of transgression is marked by the mfs4 within the offshore marine shale deposit. Above that is an upwardly coarsening, progradational parasequence set (Ph) that is composed of tidal flat deposits (Facies 9, 10, 3). This parasequence set (Ph) contains the HST of sequence UF2.

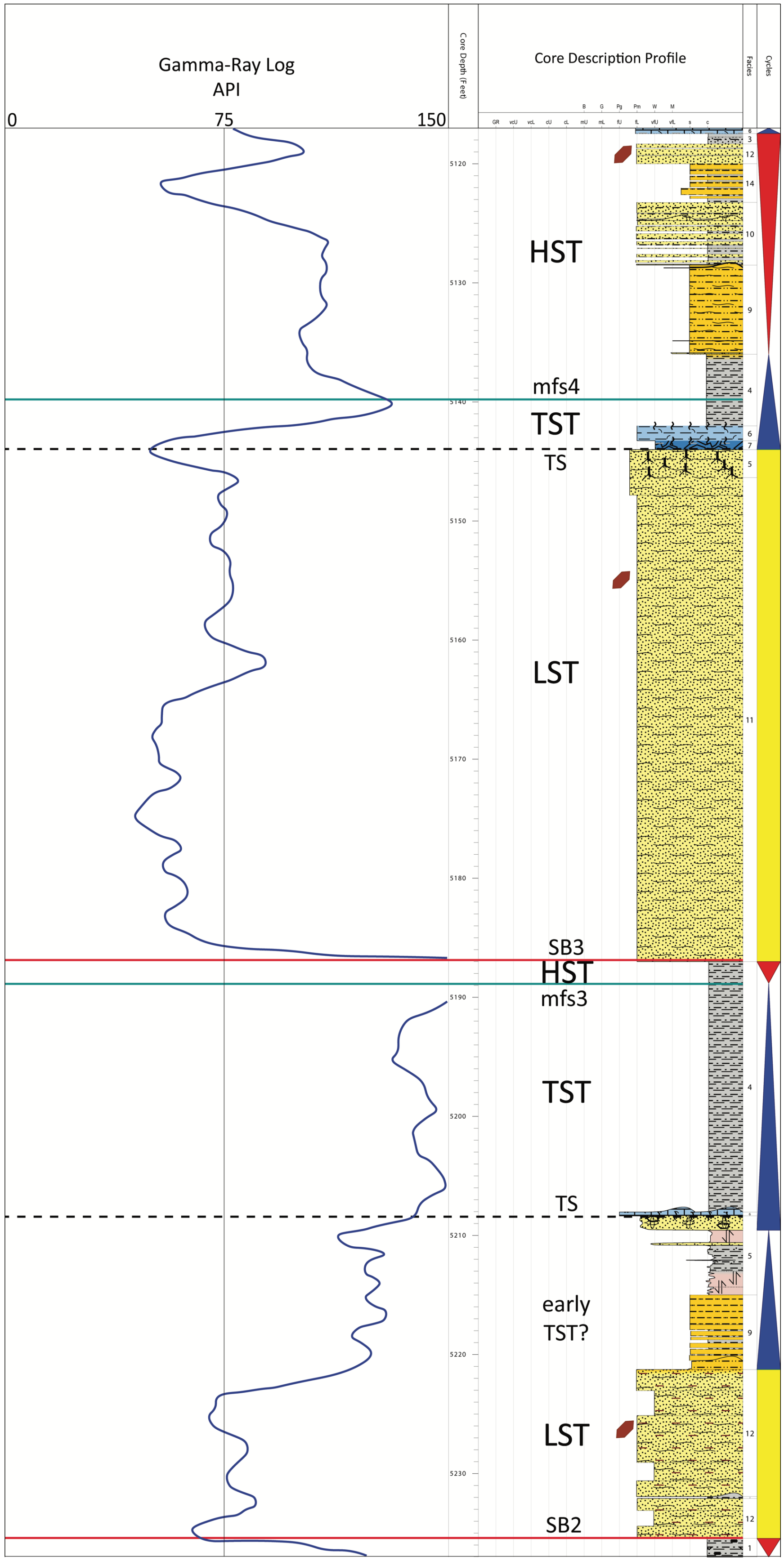
Gamma-Ray Log
API
0
75
150
Core Depth (Feet)
Core Description Profile
Facies
Cycles
HST
mfs4
TST
TS
LST
SB3
HST
mfs3
TST
TS
early
TST?
LST
SB2
5120
5130
5140
5150
5160
5170
5180
5190
5200
5210
5220
5230

Figure 50. Sequence stratigraphic analysis of Core 2. Refer to Figure 49 for legend.

Core 3 Stratigraphic Sequence

Three (3) sequences were observed in this core, namely SF0, SF1, and SF2 (Fig. 51). Sequence SF0 is similar to sequence DG0 in Core 1 and UF0 in Core 2, except for the presence of a shallow marine shaly carbonate deposit (Facies 6) overlying an offshore marine shale package. At its base, the cored interval contains a shallow marine shaly carbonate package (Facies 6; 4920 ft) characteristic of a transgressive section and would correspond to the Inola Limestone marker (Ye and Kerr, 2000). However, from the GR log signature, this package shows an overall aggradational to progradational stacking pattern, which could be interpreted as an HST. Thus, the Inola Limestone base is inferred to be at 5000 ft (~80 ft below the base of Core 3). The TST of sequence SF0 is thin and is capped by mfs5 at ~75 ft below the base of Core 3. An overall upwardly coarsening, progradational parasequence set (Pi) marks the end of sequence SF0 and consists of shallow marine shaly carbonates (Facies 6; base of Core 3). Pi contains the HST of sequence SF0, which is ended/capped by a sequence boundary (SB4) at its top (4914 ft).

Sequence SF1 is composed of at least three (3) parasequence sets, namely Pj, Pk, and Pl. Pj overlies SB4 and consists of an upwardly coarsening, progradational parasequence set. This parasequence set is composed of a basal lag conglomerate (Facies 15) and tidal channel-fill deposits (Facies 12) and contains the LST of sequence SF1. The LST is capped by a transgressive lag (Facies 2), which marks the development of a transgressive surface (TS).

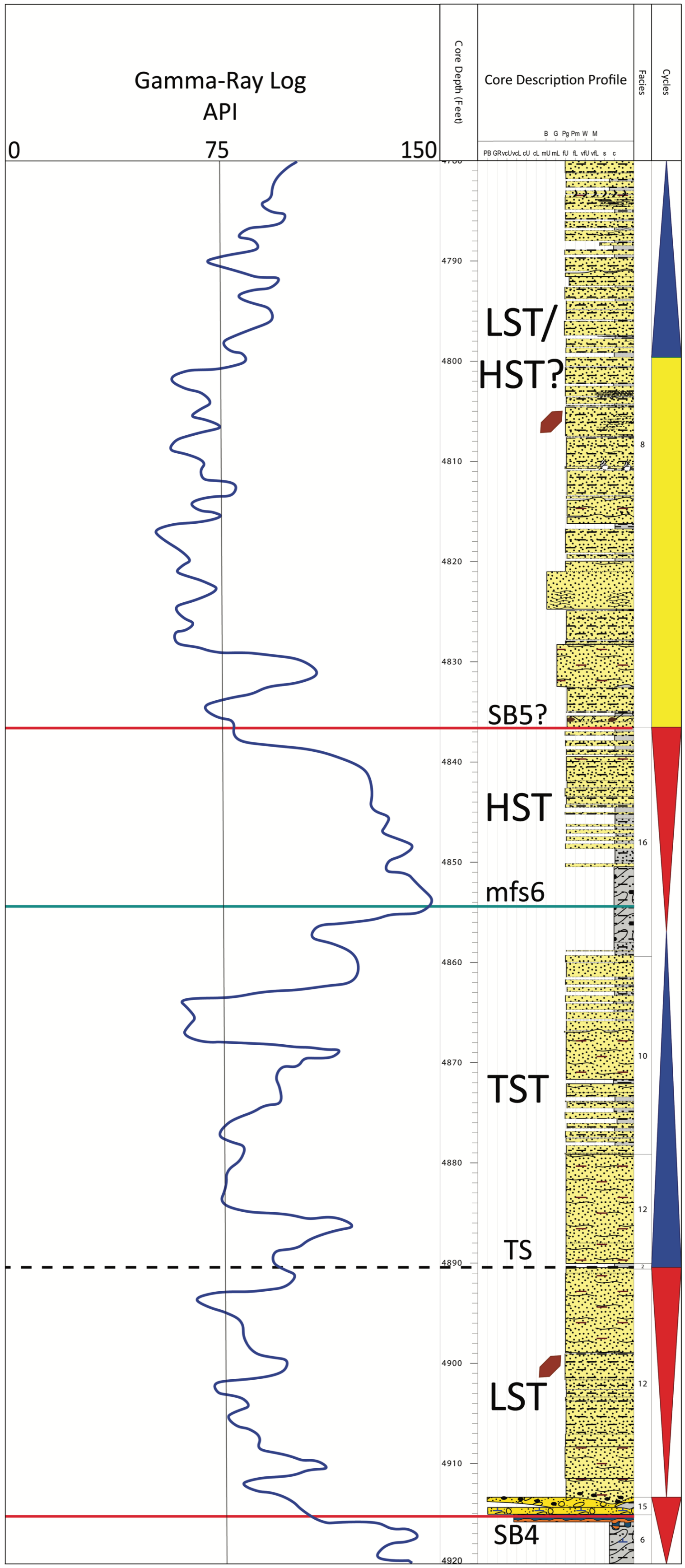
Gamma-Ray Log
API
0
75
150
Core Depth (Feet)
Core Description Profile
Facies
Cycles
4790
4800
4810
4820
4830
4840
4850
4860
4870
4880
4890
4900
4910
4920
LST/
HST?
SB5?
HST
mfs6
TST
TS
LST
SB4
8
16
10
12
12
15
6

Figure 51. Sequence stratigraphic analysis of Core 3. Refer to Figure 49 for legend.

The second parasequence set (Pk) displays an overall upwardly fining stacking pattern and thus a retrogradational trend. It is mainly composed of tidal flat/tidal channel fill deposits (Facies 10, 12) and contains the TST, which is capped by the maximum landward extent of transgression (mfs6). Pl is an overall upwardly coarsening, progradational parasequence set composed of distal delta front deposits (Facies 8). This parasequence set (Pl) contains the highstand systems tract (HST) of the SF1, which possibly ends at ~4836 ft (at SB5). Nevertheless, there's also a possibility that SB5 and sequence SF2 are not not present, and the rest of the package is just a continuation of the HST of sequence SF1.

If sequence SF2 is indeed present, then it starts at ~4836 ft where a lag of rip-up clasts (possibly associated with channelized sands or incised valley) is present and possibly represents a sequence boundary (SB5). Sequence SF2 is composed of an overall aggradational to progradational parasequence set (Pm). The aggradational trend is observed in the cored interval and is composed by tidal channel fill deposits (Facies 16). This parasequence set (Pm) contains the lowstand systems tract (LST), which continues upward. The presence and/or position of the Pink Limestone in this well is not obvious as the resistivity log signature for the Pink Limestone either changes or is absent. However, I infer that the Pink Limestone is found at ~4742 ft, which is ~38 ft above the cored interval. This inference is based on the abrupt lowering of gamma ray response, forming a sharp and the strong resistivity peak, characteristic of the Pink Limestone. Additionally, the serrated gamma ray signature of the overlying shale packages also supports this interpretation as it indicates a continuation in sea level transgression.

CHAPTER VII

PROVENANCE ANALYSIS

Sandstone Modal Composition

Seven thin-section samples of the Red Fork were analyzed for sandstone modal composition determination from a stratigraphically lower (N=2) and a stratigraphically upper (N=5) sandstone of Core 2 (Table 6). Raw point count data appear in Appendix C.

Lower UF1-2 Samples

Thin sections of the Lower UF1-2 (N=2) included two samples from a medium to fine tidal channel deposit (UF1-2_PRF_26 and UF1-2_PRF_27; Figs. 52-53). UF1-2_PRF_26 (Fig. 52) is the higher sample and UF1-2_PRF_27 is 14 ft lower in the interval (Fig. 53).

Compositional changes between the two samples are minor (Table 6; Fig. 54). In UF1-2_PRF_26, quartz account for 81% of the sample while feldspar and lithic fragments account for 10% and 9%, respectively (Figs. 52, 54). In UF1-2_PRF_27, which is stratigraphically lower, quartz accounts for 73% of the sample, with subordinate lithic grains (15%) and feldspar (12%). Overall, quartz grains are predominantly monocrystalline quartz (Qm= 65%), with minor occurrences of polycrystalline quartz (Qp=3%). Plagioclase feldspar is the dominant feldspar in both samples, with rare (observed) to no (zero counts) potassium feldspar (Fig. 54; Appendix C). A large percentage of plagioclase grains are weathered into an unidentified clay mineral (with high relief and birefringence; Figs. 52B and 53B). Calcite replacement of plagioclase grains also occurs (Fig. 53B). Nevertheless, plagioclase decreases upward from 16% in UF1-2_PRF_27 to 12% in UF1-2_PRF_26. Lithic grains are minor, and mostly consist of metamorphic lithic fragments (Lm) and sedimentary lithics (Ls) (Fig. 54). Volcanic lithic fragments (Lv) are rare to non-existent within both samples.

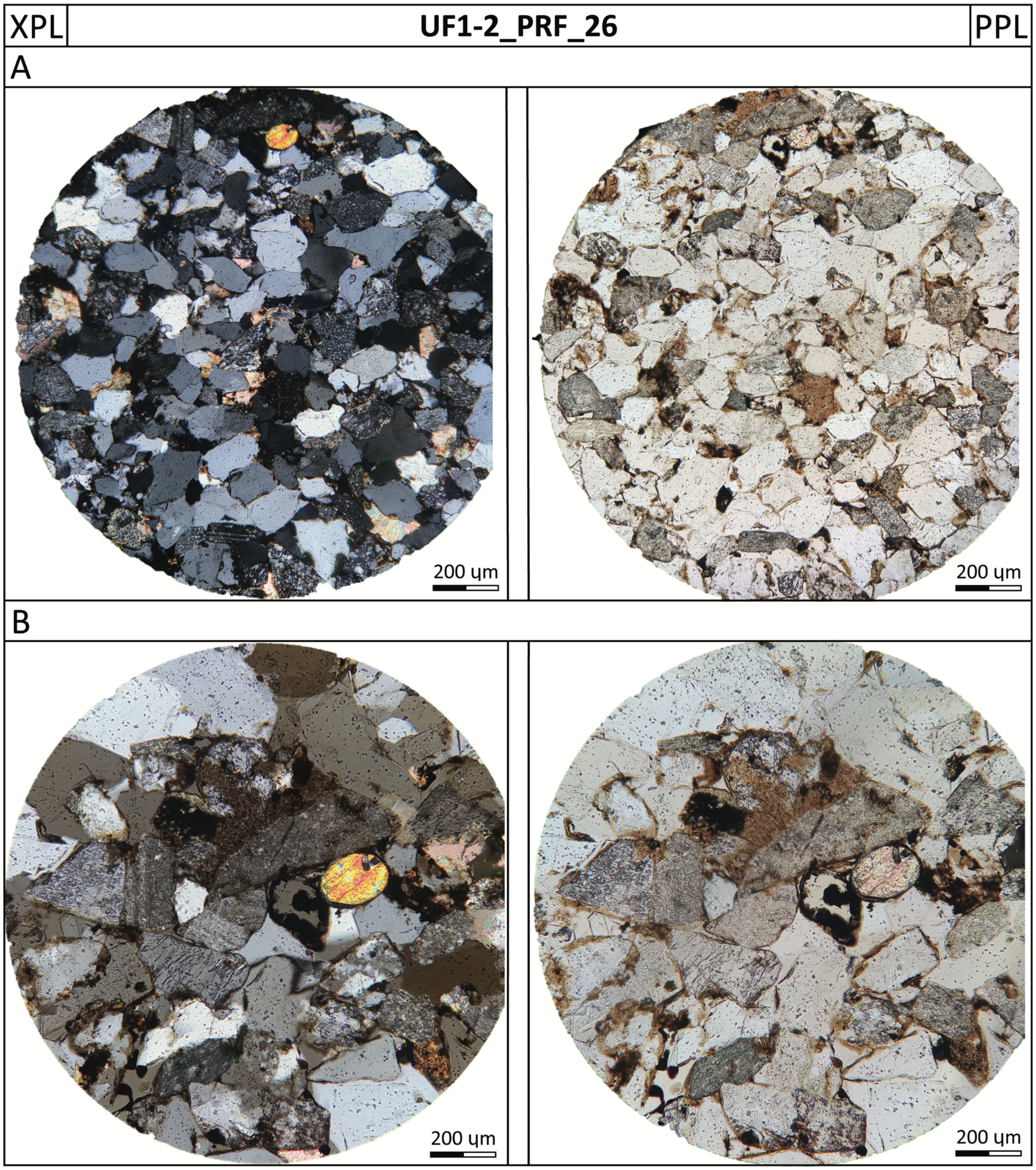

Figure 52. Thin section images (plane light-right and cross polar-left) of the lower UF1-2 (sample 26). **A)** Relative distribution of fine sand-sized grains dominated by monocrystalline quartz with minor plagioclase and lithics. **B)** Altered and dirty looking plagioclase grains and a zircon grain (yellowish) in association with a gilsonite-coated grain.

Table 6. Recalculated point-count data for Desmoinesian Red Fork Sandstone samples from Core 2, Logan County, Oklahoma.

Sample	Depth (feet)	Q – F – L (%)			Qm – F – Lt (%)			Qm – P – K (%)			Lm – Lv – Ls (%)		
UF1-2_PRF_8	5145.2	60	35	6	52	35	13	60	40	0	94	0	6
UF1-2_PRF_9	5187	47	37	16	37	37	26	50	50	0	96	0	4
UF1-2_PRF_10	5194	40	29	31	32	29	39	53	47	0	81	0	19
UF1-2_PRF_11	5201.4	52	34	14	48	34	18	58	42	0	95	0	5
UF1-2_PRF_12	5206.8	72	11	16	60	11	29	84	16	0	90	0	10
UF1-2_PRF_26	5220	81	10	9	73	10	17	88	12	0	71	0	29
UF1-2_PRF_27	5234	73	12	15	60	12	28	84	16	0	64	0	36

Note: *The three categories may not add to 100% because of rounding.*

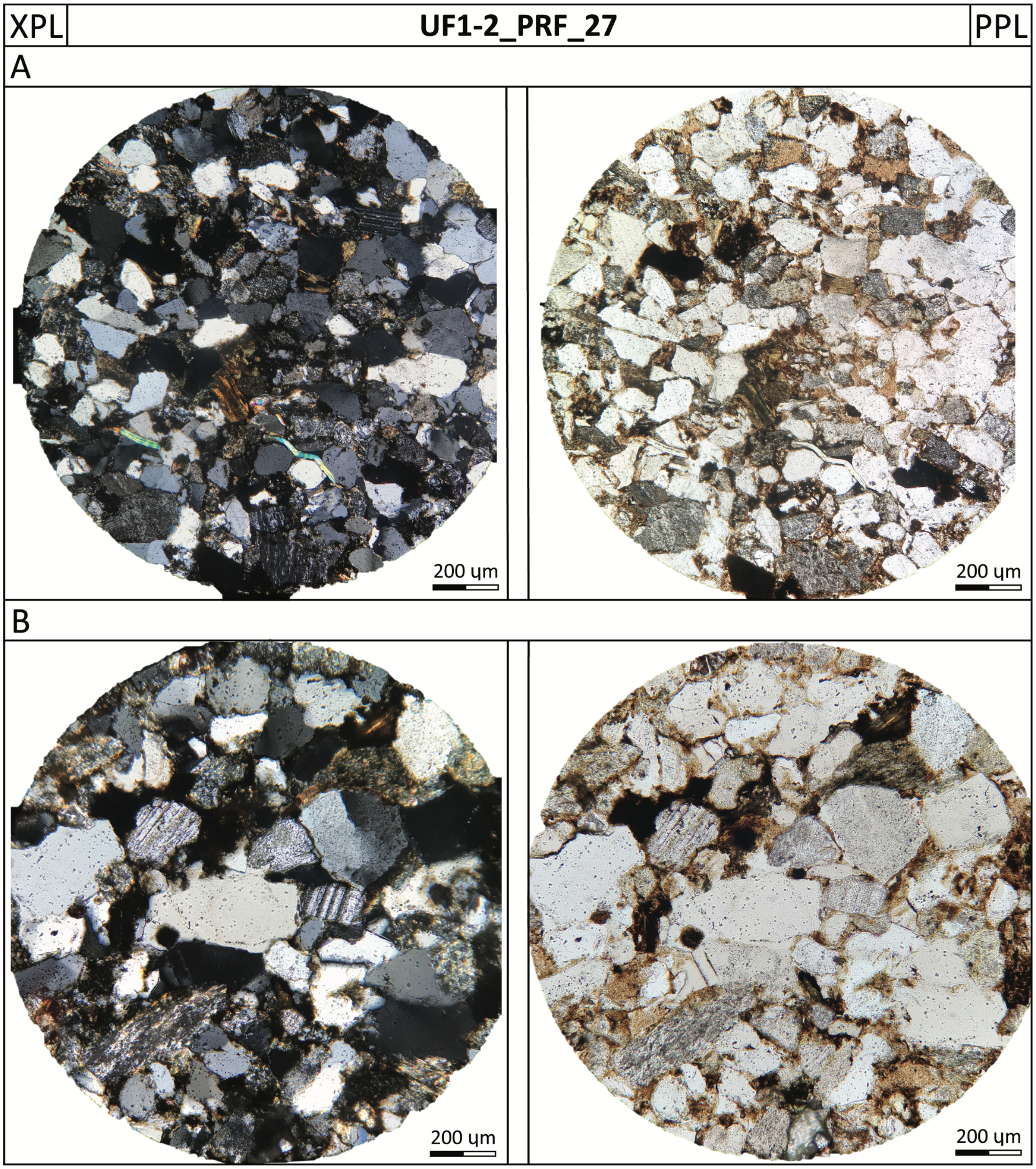

Figure 53. Thin section images (plane light-right and cross polar-left) of the lower UF1-2 (sample 27). **A)** Relative distribution of very fine sand-sized grains dominated by monocrystalline quartz and plagioclase, with minor lithics and micas. **B)** Metamorphic lithics (mica-schist?) in moderately sorted assemblage. Note dirty looking, yet twinned, plagioclase grains and gilsonite material possibly filling void spaces.

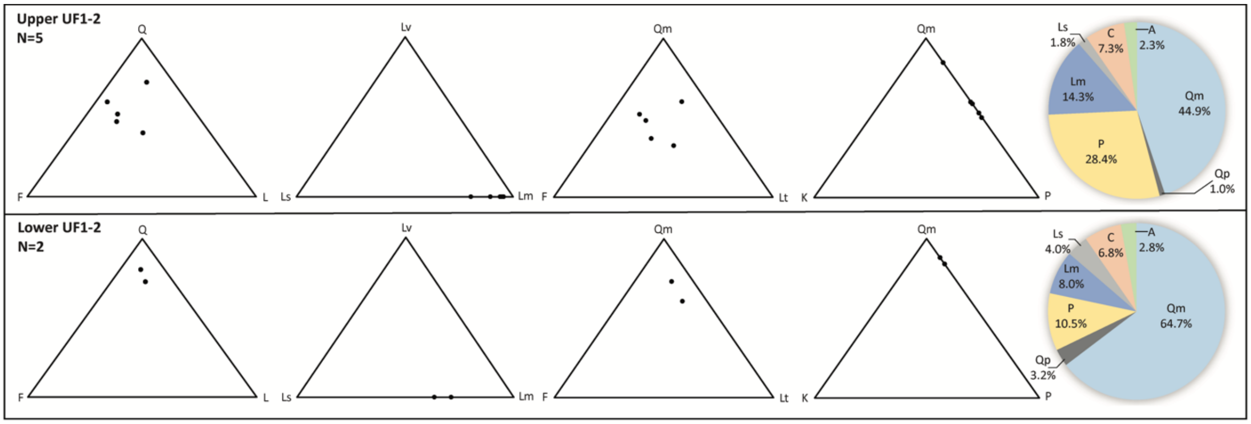

Figure 54. Average framework percentages of the stratigraphically lower and upper samples of the Red Fork in Core 2 shown in pie charts. Sandstone modal compositions depicted on ternary diagrams (from left to right): Standard Q-F-L, Lv-Ls-Lm, Qm-F-Lt, and Qm-K-P. Refer to Table 2 for abbreviations, Appendix C for raw data, and Table 6 for recalculated data used for ternary diagrams.

Upper UF1-2 Samples

Thin sections of the Upper UF1-2 (N=5) include four samples from a very fine sand- to silty-sized channel deposit (UF1-2_PRF_9 to UF1-2_PRF_12; Figs. 55-59) and one sample from a fine, sand-sized interfluve deposit (UF1-2_PRF_8; Fig. 59). All sandstone samples are relatively similar in composition, dominated by quartz (Q), but with subordinate feldspar and minor lithic grains within calcite, clay, and minor silica cement (Table 6).

Compositional differences among the samples are minor. In sample UF1-2_PRF_12, which is stratigraphically lower, quartz makes up 72% of the grains, while feldspar and lithic fragments account for 11% and 17%, respectively (Fig. 55; Table 6). UF1-2_PRF_10 exhibits the lowest quartz content (Q=40%) and more feldspar and lithics (29% and 31%, respectively; Fig. 57; Table 6). UF1-2_PRF_8 contains the lowest number of lithic fragments (6%) while quartz and feldspar grains are abundant (60% and 35%) (Fig. 59; Table 6). Overall, quartz grains are predominantly monocrystalline quartz (Qm= 45%), with very minor occurrences of polycrystalline quartz (Qp=1%). Plagioclase occurrences increase upward from 16% in UF1-

2_PRF_12 to 47% in UF1-2_PRF_9 (Table 6). Lithic grains are minor to abundant, with an overall 91% of metamorphic lithic fragments (Lm) and 9% of sedimentary lithics (Ls) (Table 6; Fig. 55). Volcanic lithic fragments (Lv) are rare to non-existent within the samples.

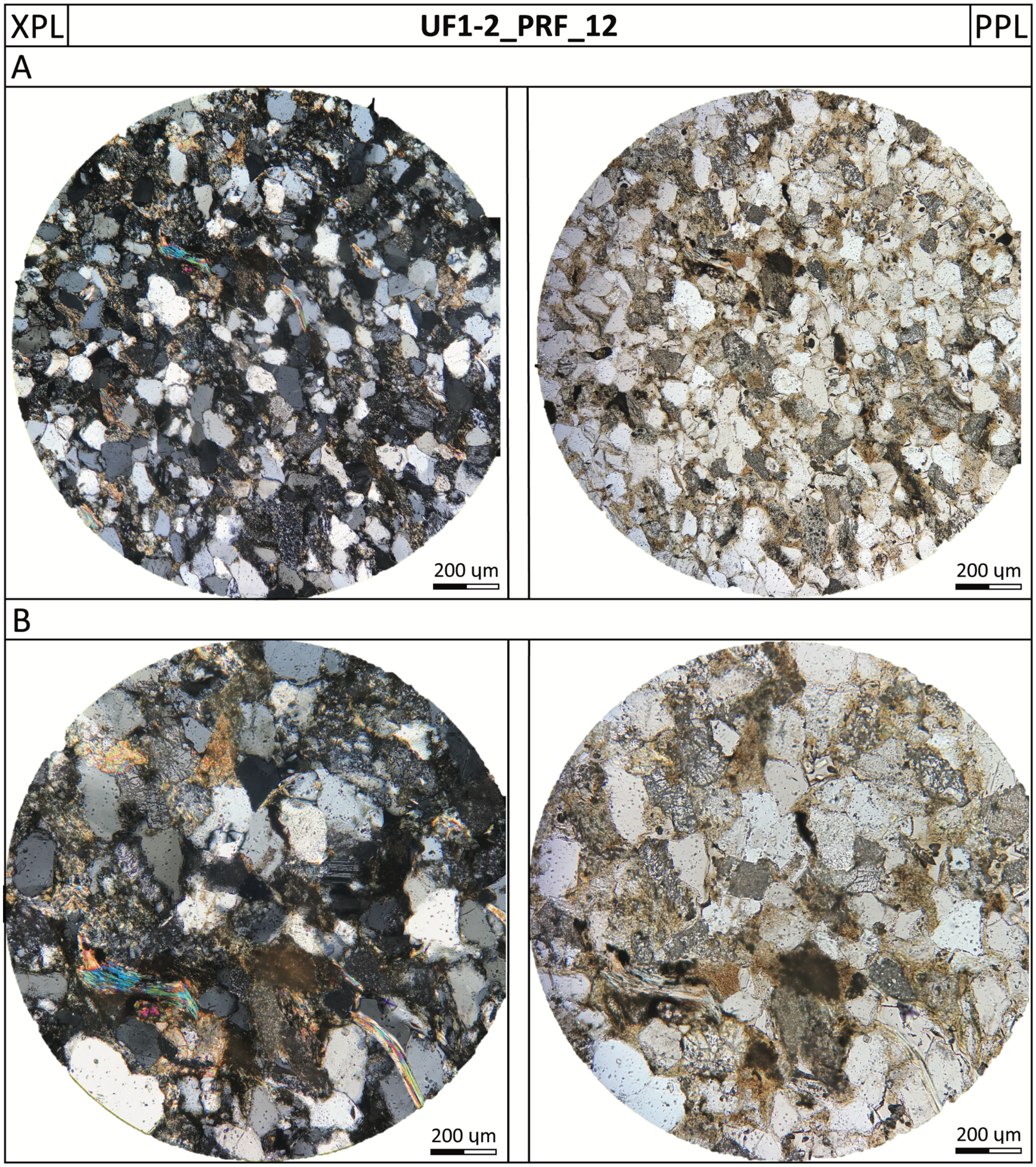

Figure 55. Thin section images (plane light-right and cross polar-left) of the lower UF1-2 (sample 12). **A)** Relative distribution of moderately to well-sorted, very fine sand-sized grains dominated by monocrystalline quartz with subordinate amounts of plagioclase and lithics. **B)** Dirty-looking sample with altered plagioclase, metamorphic lithics (mica-schist?), and minor micas in calcite, clay and silica cement.

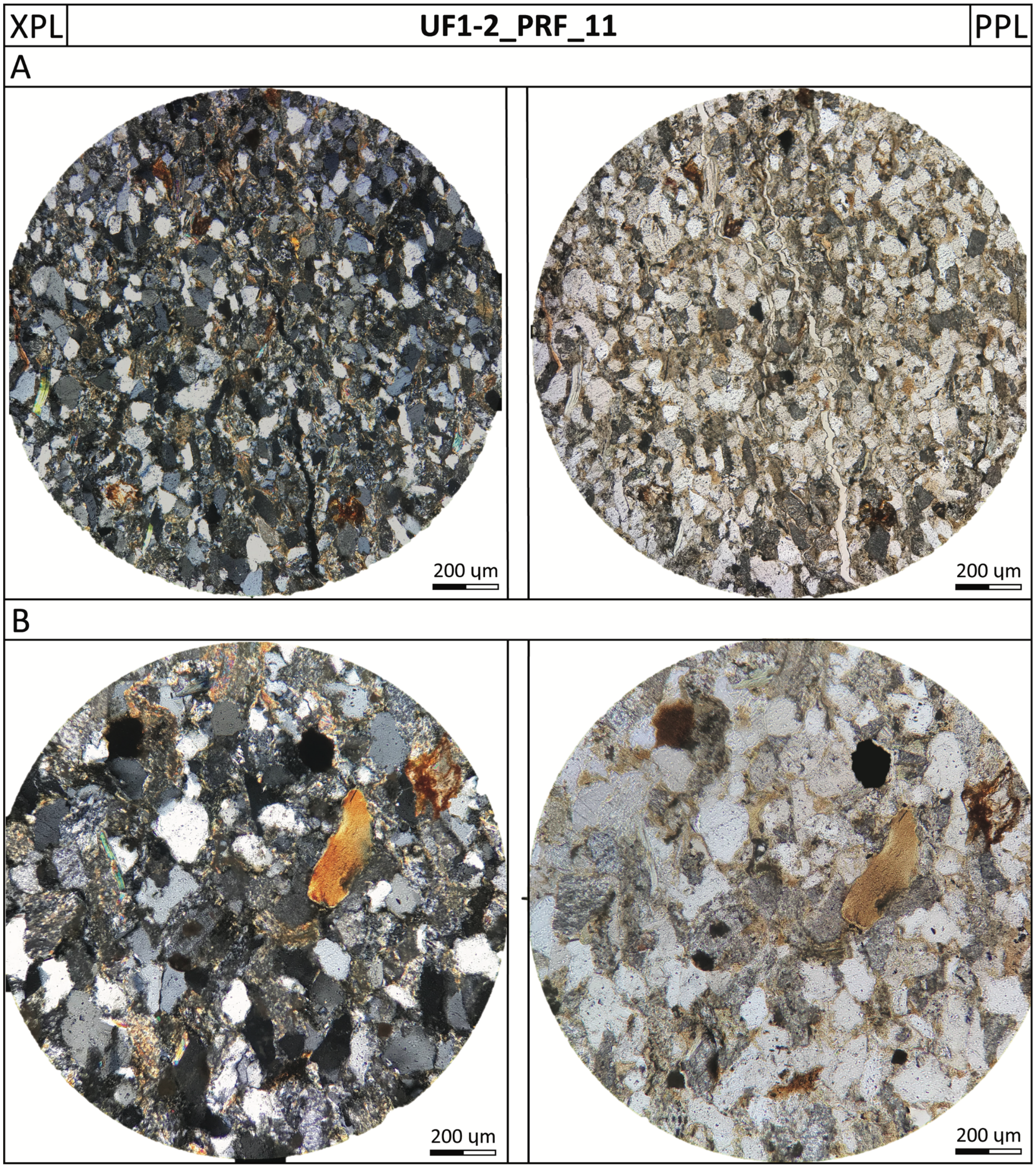

Figure 56. Thin section images (plane light-right and cross polar-left) of the lower UF1-2 (sample 11). **A)** Relative distribution of very fine, silty, sand-sized grains dominated by

monocrystalline quartz and plagioclase; note silica-filled vertical fractures across the sample. **B)** Dirtier-looking slide as plagioclase (altered) amount increases to 34% and quartz decreases to 52%.

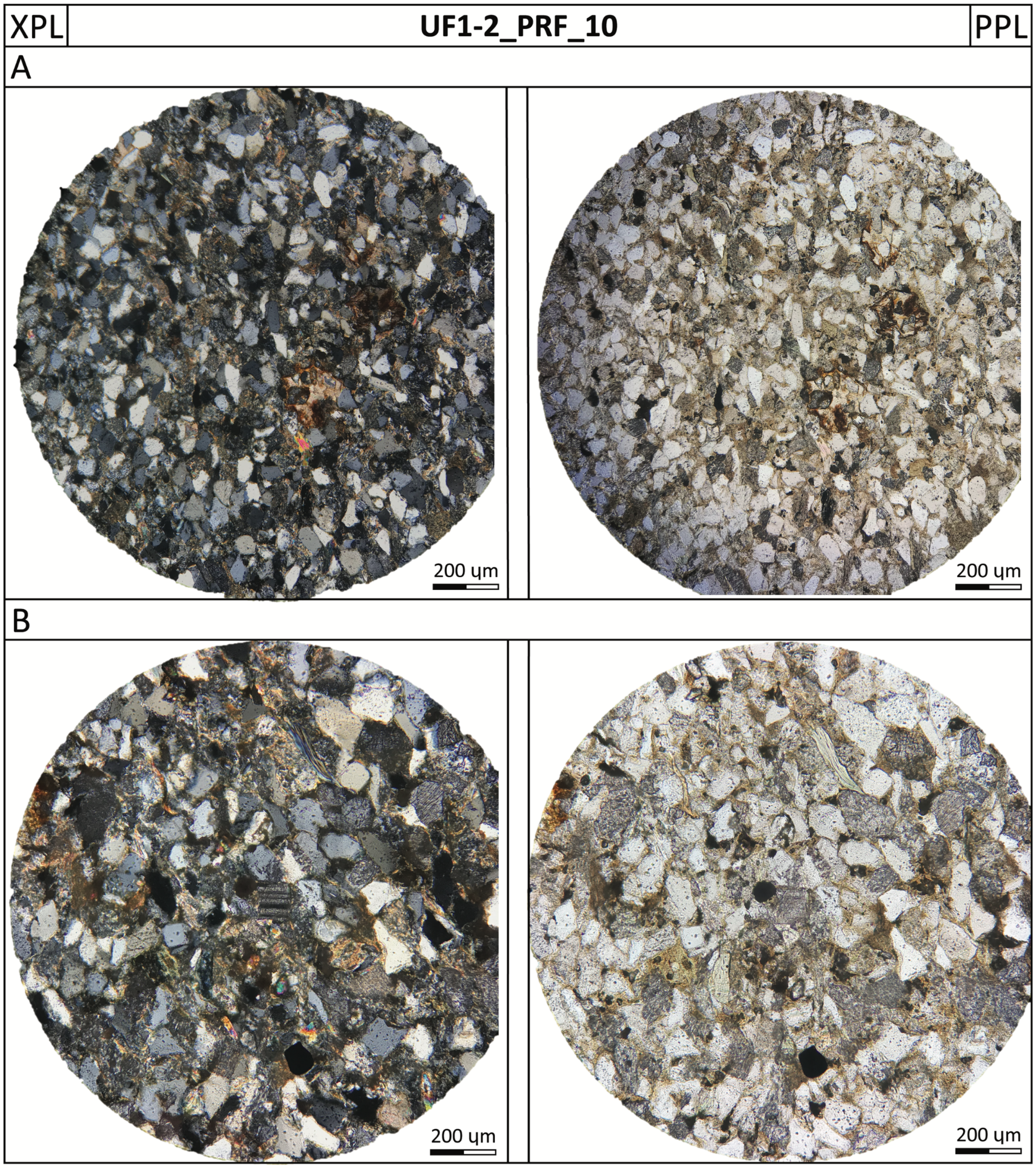

Figure 57. Thin section images (plane light-right and cross polar-left) of the lower UF1-2 (sample 10). **A)** Relative distribution of very fine, silty, sand-sized grains dominated by monocrystalline quartz and plagioclase; note increase in calcite cement. **B)** Augmented figure showing dirty-looking plagioclase grains, monocrystalline quartz, zircon grains (tiny, high-birefringence grains), rare glaucophane (blue, schistose/fibrous grain), and metamorphic lithics.

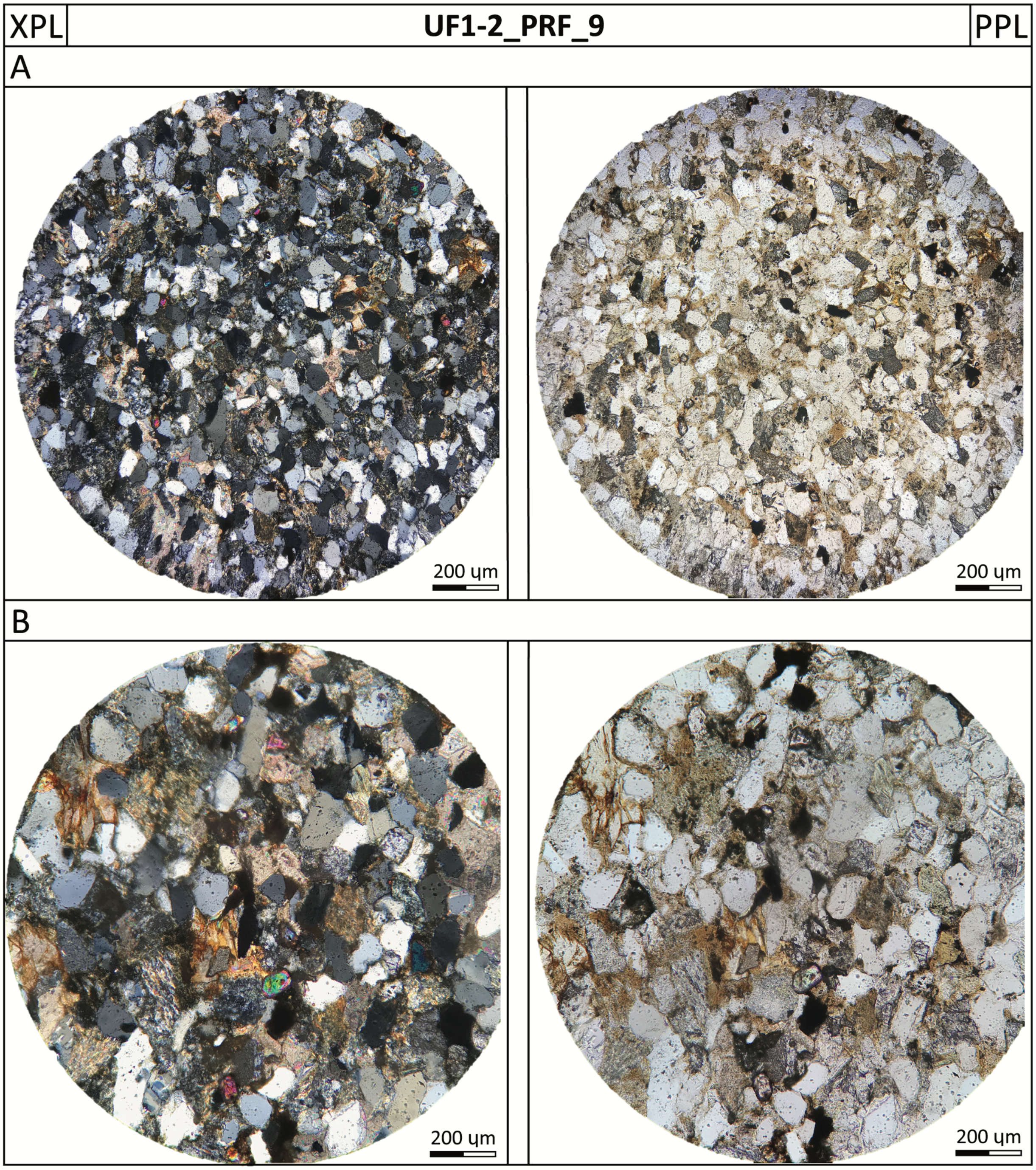

Figure 58. Thin section images (plane light-right and cross polar-left) of the lower UF1-2 (sample 9). **A)** Relative distribution of very fine sand-sized grains dominated by monocrystalline quartz and plagioclase; note higher amounts of calcite through plagioclase alteration. **B)** Metamorphic lithics, opaque/dense minerals, plagioclase, quartz and zircon grains in calcite cement.

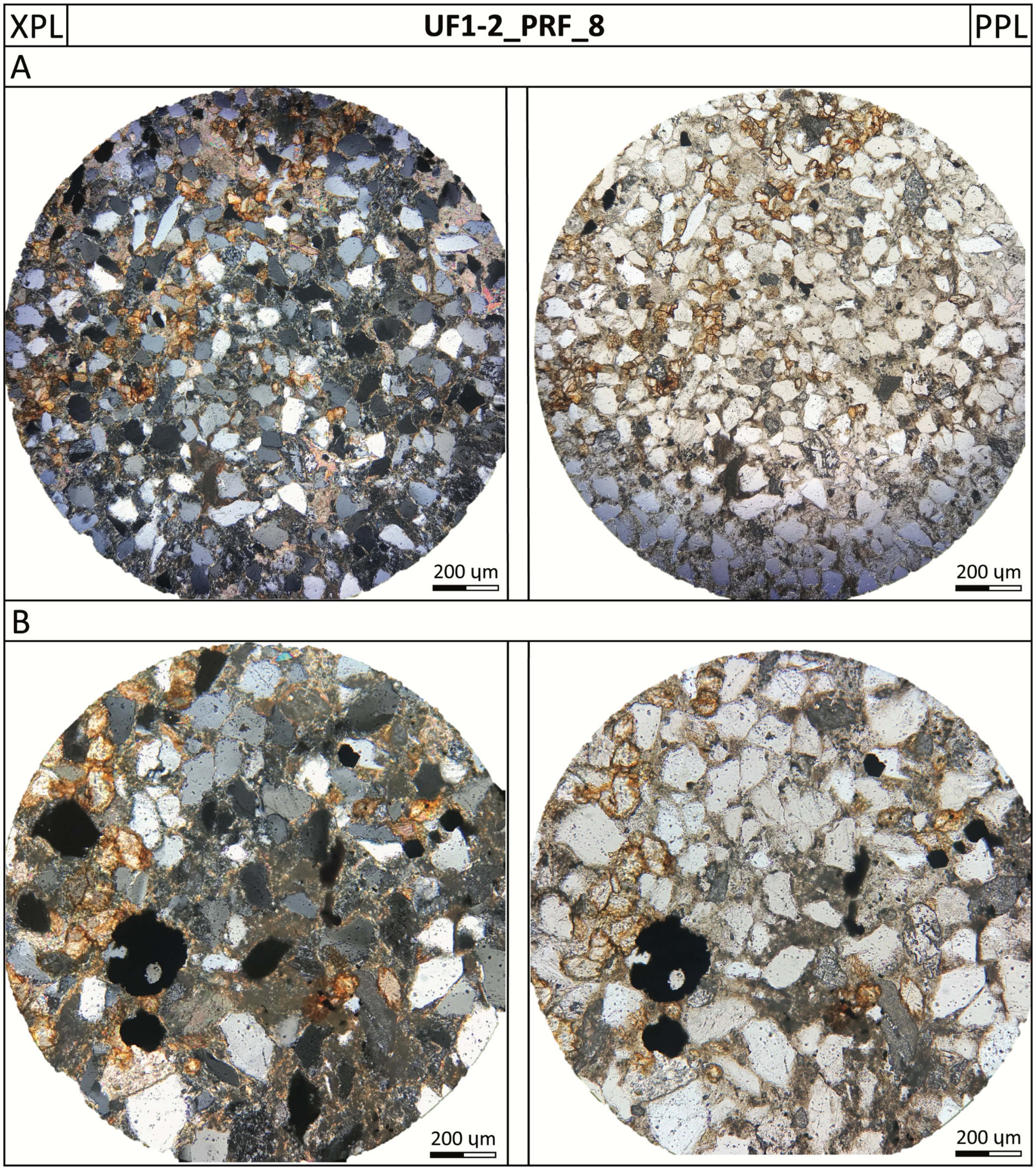

Figure 59. Thin section images (plane light-right and cross polar-left) of the lower UF1-2 (sample 8). **A)** Relative distribution of fine sand-sized grains dominated by monocrystalline quartz and plagioclase; note coarser sand grains and also "spherulithic" siderite (?) minerals. **B)** Opaque and "spherulithic" siderite (?) grains in clay, calcite, and silica cement.

Modal Composition Trends

The petrographic data from Core 2 exhibit only minor variability in composition. The samples range among subarkose, arkose, lithic arkose three feldspathic litharenite compositions (Fig. 60). Using the tectonic discrimination plot (Q-F-L) (Fig. 60 and Table 6; Dickinson 1970 and Dickinson et al., 1983), most samples plot in the recycled orogen provenance field but one (from the upper sample group) plots in the continental block, within the sub-field of transitional continental. When using the Qm-F-Lt ternary diagram, three samples (Lower UF1-2 samples along with the basal Upper UF1-2 (UF1-2_PRF_12)) plot within the quartzose recycled provenance sub-field. Three other Upper UF1-2 samples plot within the dissected arc provenance sub-field and one plot within the transitional continental provenance sub-field (Fig. 60). Few published provenance studies exist on these strata, but Kushner (2018) reported over 90% of Qm for the Upper sandstone sample, whereas in this study, Qm accounts for only 45% (averaged) of the grains in the sandstone. For the Lower sample, Kushner (2018) reported 5% or fewer feldspar grains in a quartzolithic sandstone, which relatively differs from this study's findings of 11% feldspar composition.

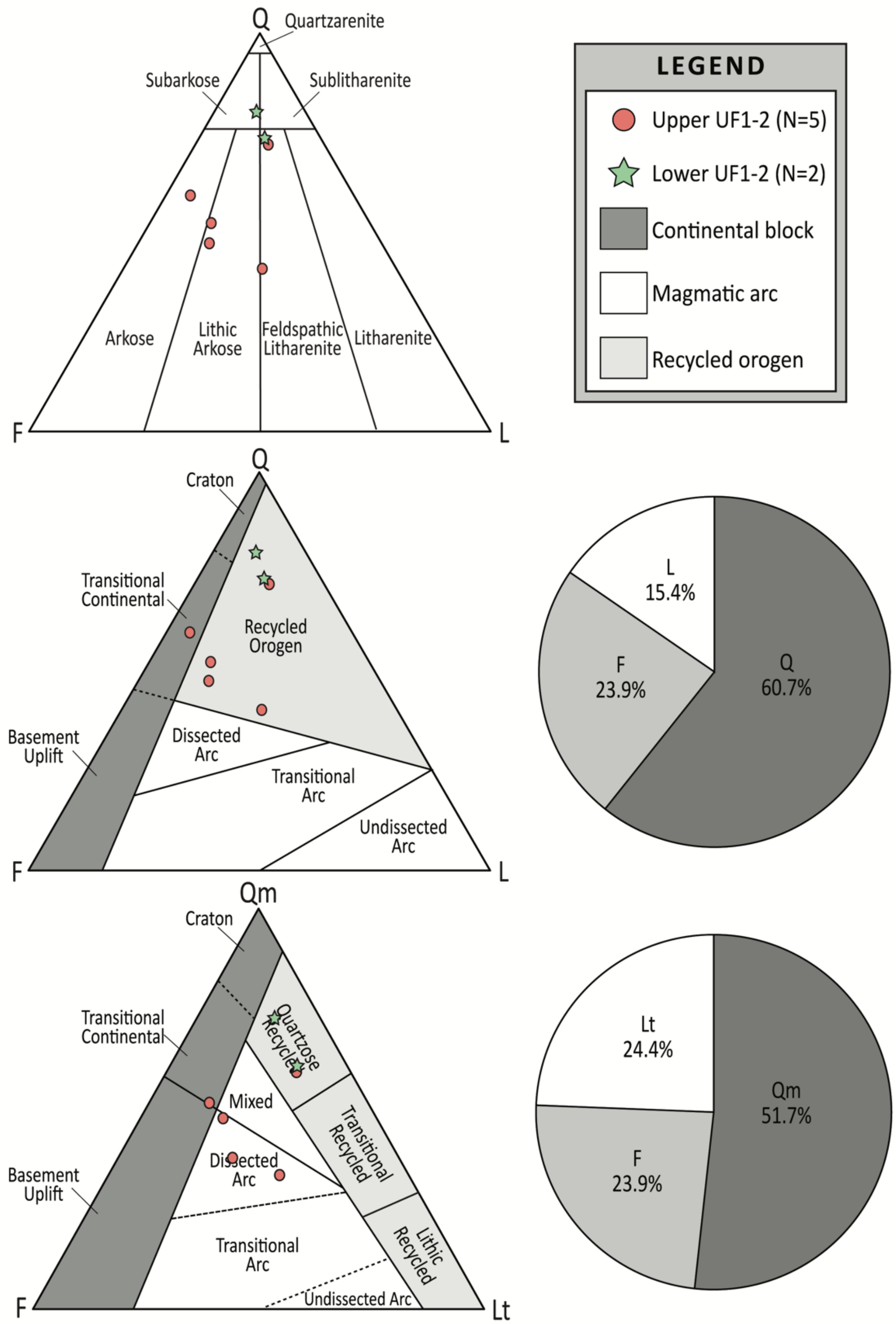

Figure 60. Ternary and pie diagrams of the stratigraphically lower and upper samples of the Red Fork Formation in Core 2. The majority of samples plot in the recycled orogen provenance field and are dominated by quartz (Q). Provenance fields from Dickinson et al. (1983), and Dickinson (1970). Ternary diagram labels defined in Table 2.

Detrital Zircon Geochronology

This chapter presents a detailed, U/Pb detrital zircon provenance analysis of the Red Fork in the study area. Prior to the geochronoly analysis, I will review important concepts of detrital zircon geochronology.

Detrital Zircon Geochronology Overview

Detrital zircon geochronology is used to determine the crystalline or recycled source from which sandstones or sand sediments were derived through weathering prior to their final deposition (Gehrels, 2014). The method has emerged as a fundamental tool for provenance analysis over the past few decades due to its technological advancement which allows for rapid and precise (1-2 sigma uncertainties) determinations of U-Th-Pb ages (Gehrels et al., 2008; Thomas, 2011). The following geochronology basics are my personal notes taken at a Detrital Zircon Short Course presented by George Gehrels at the Geological Society of America 2020 Online Meeting.

Different decay systems are used for provenance analysis depending on their half-lives as well as isotopic composition (some are more efficient for younger systems while others for older ones). These decay systems include: 1) U^{238} / Pb^{206} (Half-life/HL = 4. 468 Ga); U^{235} / Pb^{207} (HL = 0.704 Ga – better for older systems because the rate of decay is faster); 3) Th^{232} / Pb^{208} (HL = 14.01 Ga) and 4) Pb^{206} / Pb^{207} (calculated by taking the slope of systems 1 and 2). For zircon geochronology, the systems used are: 1) U^{238} / Pb^{206}; 2) U^{235} / Pb^{207} and 4) Pb^{206} / Pb207. System 3) Th^{232} / Pb^{208} is not used due to its inefficacy since zircons contain only small proportions of Thorium (Th). The three (3) systems are usually shown on a single diagram called Concordia, which is a curved line connecting equal ages of the systems (Appendix D). If numerous analyses overlap each other in a Concordia plot, the more reliable the analyses are. If analyses are off the Concordia plot, it becomes very difficult to determine their uncertain age (called a discordant analysis; rejected or not considered for provenance analysis). In general, the researcher calculates how discordant a crystal is and determines the appropriate discordance cut-off or filter based on research objectives. A tight filter (0% - 10%) provides good age accuracy but the age distributions are commonly biased, whereas a loose filter (20% - 30%) provides less accurate ages but the age distributions are less biased.

Zircon Age-Distribution Visualization Methods and Data Application

Detrital zircon geochronology has three (3) main applications: 1) sediment provenance determination; 2) maximum depositional age analysis and 3) source terrane characterization. Further, different methods of visualization and representation of age-distribution data exist and include 1) Histograms, 2) Probability Density Plots (PDPs), 3) Cumulative Probability Density Plots (CPDPs), 4) Kernel Density Estimate (KDE), and others. The most used methods of zircon data visualization are 2) Probability Density Plots (PDPs) and 3) Cumulative Probability Density Plots (CPDPs). Probability Density Plots (PDPs) make the best method to show ages (and uncertainties) that have been measured as it displays the sum of individual analyses. The age peaks in Probability Density Plots show/report the most important ages of the sample. On the other hand, Cumulative Probability Density Plots (CPDPs) are less informative than the previous methods as they only consider the best age in the samples and do not account for analytical uncertainties. Finally, this latter method is related to the Kolmogorov-Smirnoff Statistical Test (K-S Test), which compares detrital zircon age distributions from two samples and tests the hypothesis that two distributions are the same. The test is based on CPDPs as it compares the maximum probability difference between two cumulative density functions (Guynn and Gehrels, 2006).

Detrital Zircon Geochronology Results

Of the 1831 detrital zircon grains analyzed from core samples of Kay, Logan and Pottawatomie counties, Oklahoma, a total of 1757 grains yielded concordant ages (<20% discordance or <5% negative discordance) (Fig 61). The entire collection of isotopic measurements, detrital U-Pb zircon ages, and concordia plots are provided in Appendix D. The detrital zircon age data are plotted as probability density plots in Figure 62 (Guynn & Gehrels, 2006; Vermeesch, 2012) with the range of known age terranes highlighted.

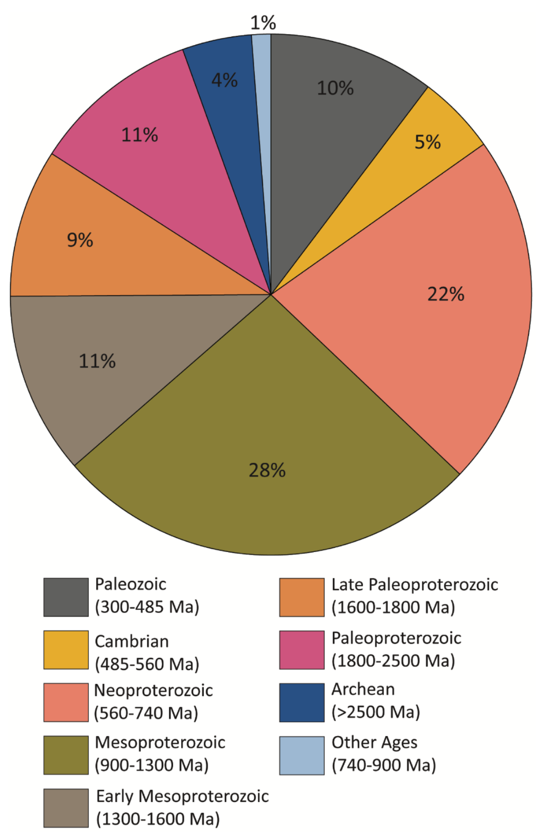

Figure 61. Pie chart showing the relative percentage of detrital zircon grains that fall within each zircon population. All samples were considered including those of Kushner, 2018 (n=2011).

In general, the samples show major groups of Neoproterozoic (~560-740 Ma), Mesoproterozoic (~900-1300 Ma), and Paleozoic (~300-485 Ma) and minor Early Mesoproterozoic (~1,300-1,600 Ma), Late Paleoproterozoic (~1600-1800 Ma), Paleoproterozoic (~1800-2500 Ma) and Archean (>2,500 Ma) (Fig. 61; Table 7). The details of the zircon age data and their variability among the samples are described below.

Kay County Samples

Sample DG-A

This sample is the stratigraphically upper unit (3177 ft) in the Dora Goodson 1 Core, from Kay County, OK. The sample yielded ages with major groups of Neoproterozoic (~560-740 Ma), Mesoproterozoic (~900-1300 Ma), and Paleoproterozoic (~1800-2500 Ma; Fig. 62). Prominent age distribution peaks occur at ~573-657 Ma, ~376-429 Ma, and ~2054-2142 Ma. A total of 307 concordant ages, ranging from 311 ± 4 to 3139 ± 17 Ma, occurred in this unit. The dominant age group of ~560-740 Ma accounts for 36% of the zircons, with two subordinate age groups of ~1800-2500 Ma and ~900-1300 Ma accounting for 20 % and 15% of the grains. One minor age cluster of ~300-485 Ma accounts for 10% of the zircons. The Cambrian population (~485-560 Ma) accounts for another 6% of the U-Pb ages. Other age clusters are made up by 4% or fewer grains (e.g., 4% in ~1300-1600 Ma, and 3% in >2500 Ma).

Table 7. Percentages of U-Pb Ages from samples in this study.

Sample	Paleozoic (300-485 Ma)	Cambrian (~485-560 Ma)	Neoproterozoic (560-740 Ma)	Mesoproterozoic (900-1300 Ma)	Mesoproterozoic (1,300-1,600 Ma)	Paleoproterozoic (1600-1800 Ma)	Paleoproterozoic (1800-2500 Ma)	Archean (>2500 Ma)	Other Ages
DG-A	10	6	36	15	4	5	20	3	1
DG-B	14	8	36	14	9	5	10	2	2
UF-A	9	2	4	29	21	20	8	7	0
UF-B	10	4	38	12	5	10	14	5	2
UF-C	12	8	30	15	11	7	10	5	2
SF-A	10	3	5	48	16	9	3	4	2
SF-B	8	2	5	49	15	9	6	4	2

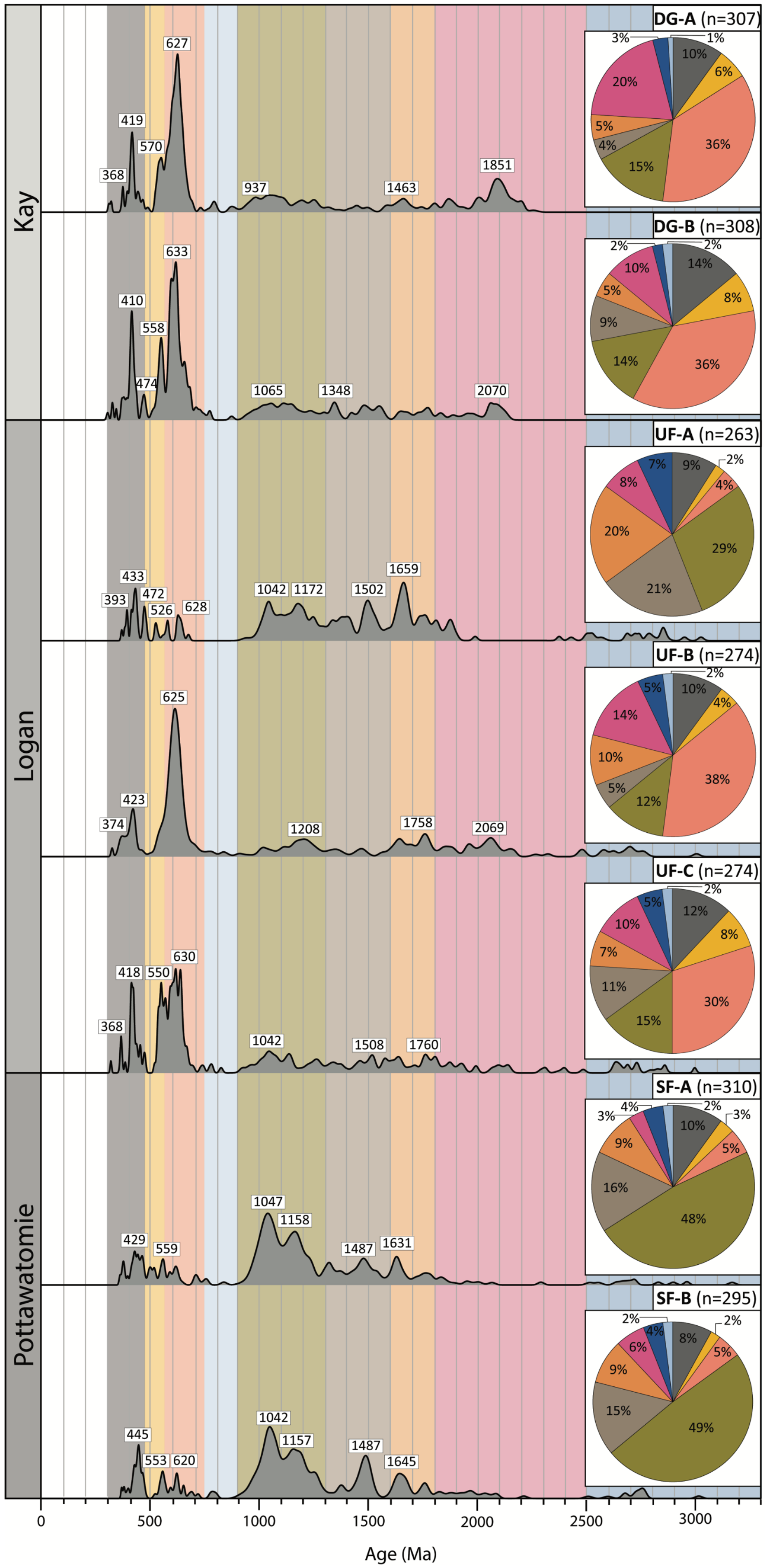

Kay
Logan
Pottawatomie
DG-A (n=307)
DG-B (n=308)
UF-A (n=263)
UF-B (n=274)
UF-C (n=274)
SF-A (n=310)
SF-B (n=295)
Age (Ma)

Figure 62. Probability density plots and pie diagrams of U-Pb detrital zircon distribution for the seven samples of the Red Fork sandstones in the study area. Samples are divided into Paleozoic, Neoproterozoic, Mesoproterozoic, Paleoproterozoic, and Archean age ranges. See Figure 61 for the legend.

Sample DG-B

This sample is the stratigraphically lower unit (3191.5 feet) in the Dora Goodson 1 Core, from Kay County, OK. The sample yielded ages with major groups of Neoproterozoic (~560-740 Ma), Mesoproterozoic (~900-1300 Ma) and Paleozoic (~300-485 Ma; Fig. 62). Dominant age distribution peaks occur at ~591-627 Ma, ~404-434 Ma, and ~545-563 Ma. A total of 308 concordant ages, ranging from 305 ± 5 to 2905 ± 31 Ma, occur in this sample. The dominant age group of ~560-740 Ma accounts for 36% of the zircons. Two subordinate age groups of ~900-1300 Ma and ~300-485 Ma account for 14% and 14%, respectively. The Early Mesoproterozoic (~1300-1600 Ma), Paleoproterozoic (~1800-2500 Ma) and Cambrian (~485-560 Ma) populations account for 9%, 10% and 8% of U-Pb ages, making them minor groups. Other age clusters are made up by 5% or fewer grains (e.g., 5% in ~1600-1800 Ma, and 2% in >2500 Ma).

Logan County Samples

Sample UF-A

This sample is the stratigraphically upper unit (5119.5 feet) in the Universal Flash 1-2 Core, from Logan County, OK. The sample yielded ages with major groups of Mesoproterozoic (~900-1300 Ma), Early Mesoproterozoic (~1300-1600 Ma; Fig. 62) and Late Paleoproterozoic (~1600-1800). Dominant age distribution peaks occur over a wide range, at ~363-678 Ma, ~1007-1883 Ma, and ~2065-2170 Ma. A total yield of 263 concordant ages, ranging from 370 ±

4 to 3139 ± 17 Ma, was analyzed from this sample. Zircons with U-Pb ages of ~900-1300 Ma accounts for 29% of the sample, with two subordinate age populations of ~1300-1600 Ma and ~1600-1800 Ma accounting for 21% and 20% of the grains, respectively. Three minor age clusters of ~300-485 Ma, ~1800-2500 Ma, and >2500 Ma account for 9%, 8% and 7% of concordant ages, respectively. Other age clusters are made up by 4% or fewer grains (e.g., 4% in ~560-740 Ma and 2% in ~485-560 Ma).

Sample UF-B

This sample is stratigraphically from the middle of the section (5154.2 feet) in the Universal Flash 1-2 Core, from Logan County, OK and was first described by Kushner (2018). The sample yielded ages with major groups of Neoproterozoic (~560-740 Ma), Mesoproterozoic (~900-1300 Ma), and Paleoproterozoic (~1800-2500 Ma; Fig. 62). Prominent age distribution peaks are observed at ~534-651 Ma, ~373-479 Ma, and ~1015-1049 Ma. A total of 274 concordant ages, ranging from 320 ± 4 to 2997 ± 8 Ma, occur in this sample. The dominant age group of ~560-740 Ma accounts for 38%, with a subordinate group of ~1800-2500 Ma accounting for 14% of the concordant zircon ages. Three minor age clusters of, ~900-1300 Ma, ~300-485 Ma and ~1600-1800 Ma account for 12%, 10% and 10% of concordant ages, respectively. The Early Mesoproterozoic and Archean populations (~1300-1600 Ma and >2500 Ma) are minor and account for 5% and 5% of zircons, respectively. Other age clusters are made up by 4% or fewer grains (e.g., 4% in ~485-560 Ma).

Sample UF-C

This sample is the stratigraphically lower unit (5226 feet) in the Universal Flash 1-2 Core, from Logan County, OK. The sample yielded ages with major groups of Neoproterozoic (~560-740 Ma), Mesoproterozoic (~900-1300 Ma), Paleozoic (~300-485 Ma) and Early Mesoproterozoic (~1300-1600 Ma; Fig. 62). Prominent age distribution peaks are observed at ~534-651 Ma, ~373-479 Ma, and ~1015-1049 Ma. A total of 274 concordant ages, ranging from 320 ± 4 to 2997 ± 8 Ma, occur in this sample. The dominant age group of ~560-740 Ma accounts for 30%, with a subordinate group of ~900-1300 Ma accounting for 15% of the concordant zircon ages. Three minor age clusters of ~300-485 Ma, ~1300-1600 Ma and ~1800-2500 Ma account for 12%, 11% and 10% of concordant ages, respectively. The Cambrian (~485-560 Ma) and Late Paleoproterozoic populations (~1600-1800 Ma) are minor and account for 8% and 7% of zircons, respectively. Other age clusters are made up of 5% or fewer grains (e.g., 5% in >2500 Ma).

Pottawatomie County Samples

Sample SF-A

This sample is in the stratigraphically upper part (4803 feet) of the State 16 Farris Core, from Pottawatomie County, OK. The sample yielded ages with major groups of Mesoproterozoic (~900-1300 Ma), Early Mesoproterozoic (~1300-1600 Ma), Paleozoic (~300-485 Ma) and Early Paleoproterozoic (~1600-1800 Ma; Fig. 62). Dominant age distribution peaks occur at ~982-1205 Ma, ~391-605 Ma, and ~1294-1657 Ma. A total of 310 concordant ages, ranging from 363 ± 4 to 3169 ± 15 Ma, occur in this sample. The prominent age group of ~900-1300 Ma accounts for 48%, with a subordinate group of ~1300-1600 Ma accounting for 16% of the concordant zircon ages. Two minor age clusters of ~300-485 Ma and ~1600-1800 Ma account for 10% and 9% of concordant ages, respectively. The Neoproterozoic group (~541-900 Ma) accounts for another 5% of zircons. Other age clusters are made up by 4% or fewer grains (e.g., 4% in group >2500 Ma, and 3% in ~1800-2500 Ma and ~485-560 Ma).

Sample SF-B

This sample is the stratigraphically lower fine sandstone unit (4897 feet) in the State 16 Farris Core, from Pottawatomie County, OK. The sample yielded ages with major groups of Mesoproterozoic (~900-1300 Ma), Early Mesoproterozoic (~1300-1600 Ma), Paleozoic (~300-485 Ma) and Late Paleoproterozoic (~1600-1800 Ma; Fig. 62). Prominent age distribution peaks occur at ~1006-1205 Ma, ~420-472 Ma, and ~1452-1519 Ma. A total of 295 concordant ages, ranging from 370 ± 4 to 3016 ± 16 Ma, occur in this unit. The dominant age group of ~900-1300 Ma accounts for 49%, with a subordinate group of ~1300-1600 Ma accounting for 15% of the concordant zircon ages. Two minor age clusters of ~300-485 Ma and ~1600-1800 Ma account for 8% and 9% concordant ages, respectively. Other age groups are made up by 6% or fewer zircon grains (e.g., 6% in group ~1800-2500 Ma, 5% in ~560-740 Ma, and 4% in >2500 Ma).

Comparison of Detrital Zircon Ages by Core

Dora Goodson 1 Core samples (DG-A and DG-B), Kay County, reveal a wide range of age populations and, for the most part, yielded similar proportions of zircon grains in similar age groups (Fig. 62). Prominent distribution peaks for both samples occur at 628-620 Ma and 416-414 Ma. Both samples reveal dominance of Neoproterozoic (~560-740 Ma; 36%) populations, with a subordinate group of Mesoproterozoic (~900-1300 Ma; ~15%) zircons. These samples also both contain Paleozoic (~300-485 Ma) age grains as the second most abundant, differing slightly in percentage (14% to 10% in DG-B vs. DG-A, respectively). On the other hand, the Paleoproterozoic (~1800-2500 Ma) age group is higher (10%) in DG-B compared to DG-A (20%). These two samples yield a *P* value of 0.066 in the K-S statistic (Table 8), suggesting a similar provenance.

Universal Flash 1-2 Core samples (UF-A, UF-B and UF-C), Logan County vary in the relative proportion of zircon age populations (Fig. 62). Prominent peaks of U-Pb ages for these zircon samples include 619-640 Ma and 422 Ma for UF-C, 605 Ma and 427 Ma for UF-B, and 1669 Ma, 437 Ma and 1033 Ma for UF-A. The similarity of samples UF-B and UF-C is indicated both by the similarity in the age distribution peaks as well as the similar percentage of the age groupings in each sample. Samples UF-C and UF-B yielded ages with major groups of Neoproterozoic (~560-740 Ma; 30-38%) zircon grains, with a subordinate group of Mesoproterozoic zircons (~900-1300 Ma; 12-15%) and early Mesoproterozoic grains (1300-1600 Ma; 5-11%). On the other hand, the stratigraphically uppermost sample, UF-A, differs from the other two samples. Sample UF-A shows higher percent of Mesoproterozoic (~900-1300) age grains (29%), which is the dominant group in this sample and a much lower percentage of Neoproterozoic grains (4%). and the UF-A sample also has a higher percentage of Early Mesoproterozoic (~1300-1600 Ma) grains compared to the other two samples. Samples UF-C and UF-B yield a *P* value of 0.344 (Table 8), suggesting similar provenance (Gehrels et al., 2011). However, sample UF-A, when compared to the other two, yields a P value < 0.05, indicating the samples did not come from the same population, and suggesting different provenances (Guynn and Gehrels, 2006).

State 16 Farris Core samples (SF-A and SF-B), Pottawatomie County, reveal a wide range of age groups, but both samples yielded similar percentages of zircons in similar age groups (Fig. 62). Prominent distribution peaks for both samples occur at ~1060 Ma, ~1180 Ma and ~455 Ma. Both samples reveal dominance in Mesoproterozoic groups (~900-1300 Ma; ~49%), with a subordinate group of Late Mesoproterozoic zircons (~1300-1600 Ma; ~16%). Samples SF-A and SF-B yield a *P* value of 0.957 (Table 8), indicating similarities in age distribution and similar provenance (Gehrels et al., 2011).

Table 8. K-S Statistics for Detrital Zircon Data from OK samples.

	SF-B	SF-A	UF-C	UF-B	UF-A	DG-B	DG-A
SF-B		**0.957**	0.000	0.000	0.000	0.000	0.000
SF-A	**0.957**		0.000	0.000	0.000	0.000	0.000
UF-C	0.000	0.000		**0.344**	0.000	**0.276**	**0.279**
UF-B	0.000	0.000	**0.344**		0.000	0.022	**0.800**
UF-A	0.000	0.000	0.000	0.000		0.000	0.000
DG-B	0.000	0.000	**0.276**	0.022	0.000		**0.066**
DG-A	0.000	0.000	**0.279**	**0.800**	0.000	**0.066**	

Note: P values > 0.05 indicate that two zircon groups are statistically indistinguishable and are highlighted in yellow.

Comparison of All Detrital Zircon Samples

Analyzing the cumulative probability plots of the U-Pb ages of detrital zircons for each sample, they fall into three groups or types. Detrital zircon ages for samples DG-A and DG-B from Kay County are very similar to those of samples UF-B and UF-C of Logan County; the four represent the Type 1 group (Fig. 63). The *P* value yielded by those four samples ranges from 0.279-0.800, which suggests similar provenance (Table 8; Gehrels et al., 2011). These samples are dominated by Neoproterozoic (~560-740 Ma) age groups. Samples SF-A and SF-B make up Type 2 group and are dominated by Mesoproterozoic groups (~900-1300 Ma). UF-A is dissimilar to all the others and is alone in Type 3 (Fig. 63).

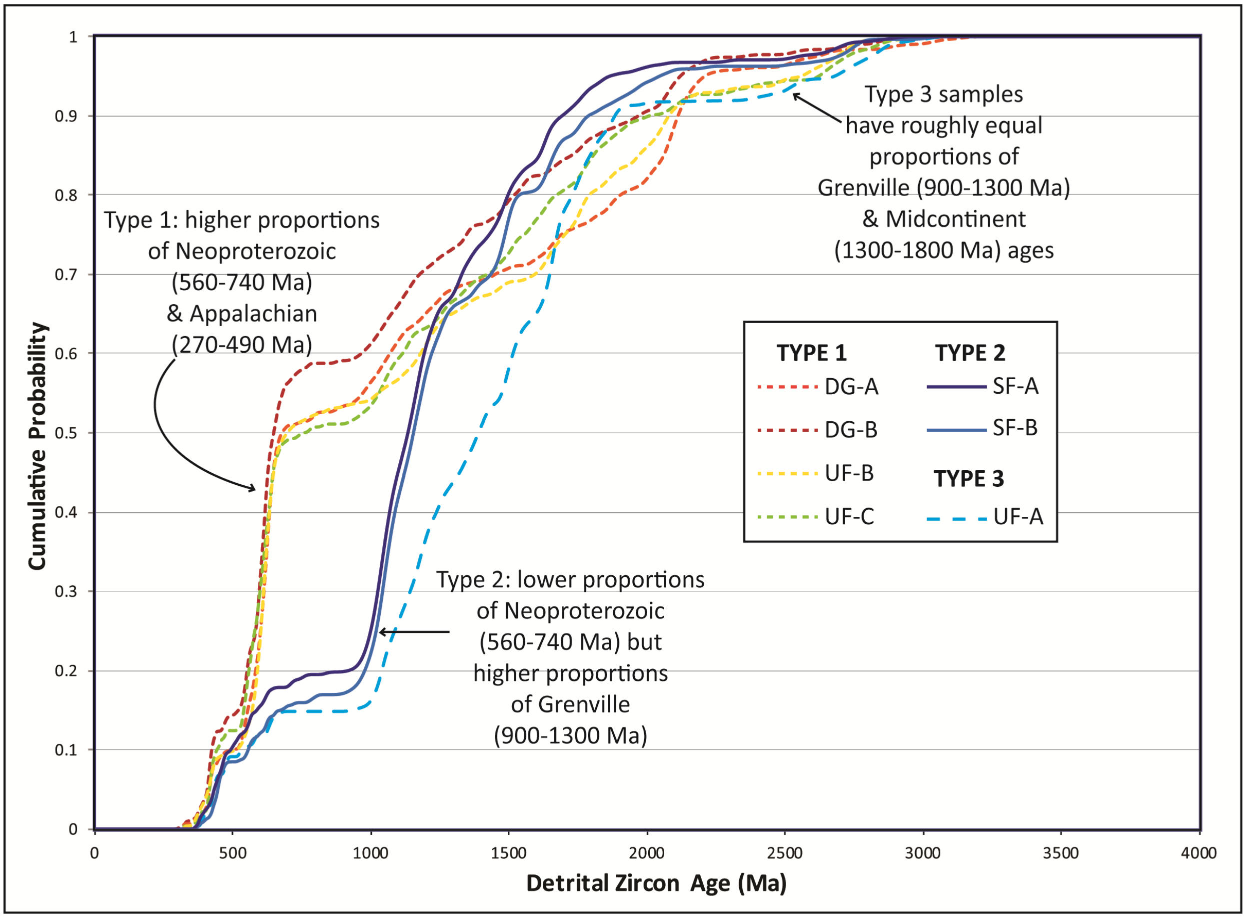

Figure 63. Cumulative probability plot of detrital zircon data.

CHAPTER VIII

DISCUSSION

Potential Source Areas for Detrital Zircons

Detrital zircon geochronology as a provenance analysis tool depends upon comprehensive knowledge of potential sources for the age populations assessed in a study (Gehrels, 2011). U-Pb detrital zircon ages within the Red Fork interval from this study range from Paleozoic (305 Ma) to Archean (3169 Ma) in age. These zircon ages correspond to potential basement provinces and terranes of North America and marginal regions of accreting Gondwanan terranes (Figs. 64-68). Potential source terranes are illustrated in Figure 65. The following text summarizes potential Paleozoic–Archean source terranes that may have contributed detritus during deposition of these Desmoinesian strata.

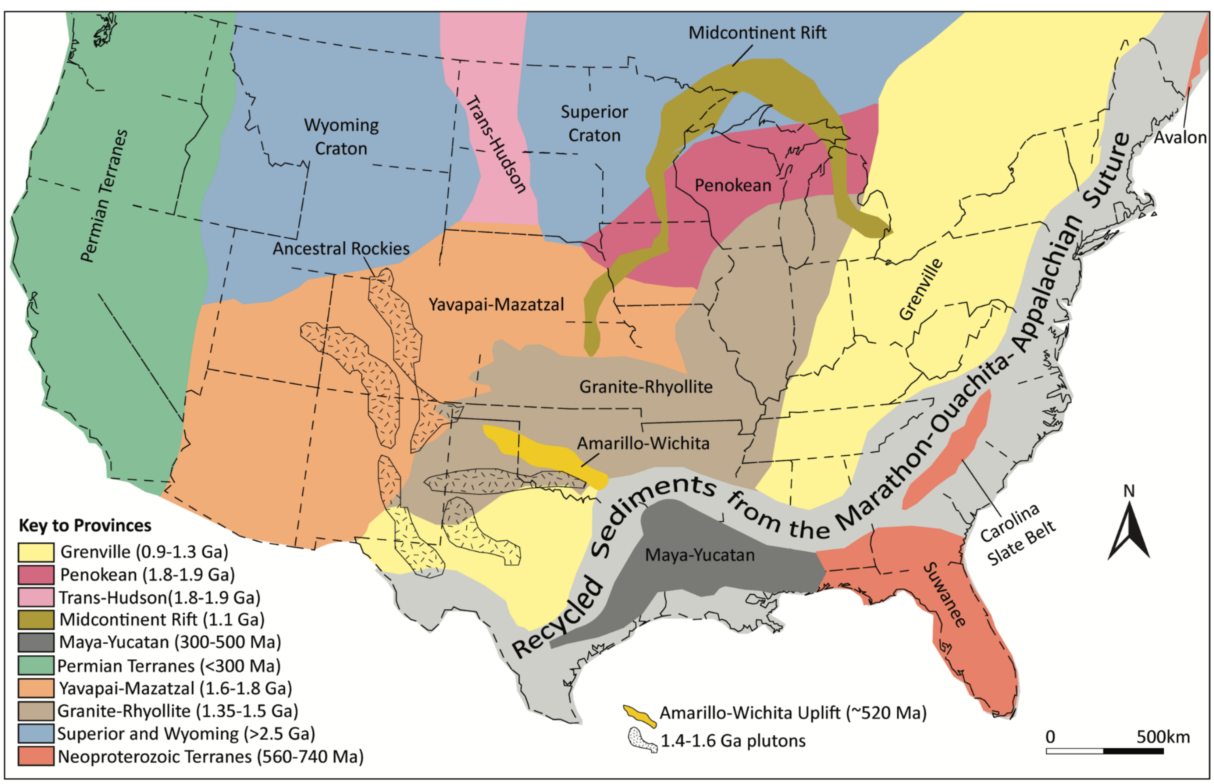

Figure 64. Map showing the main basement provinces in North America (Modified after Soreghan et al., 2002; 2018; Whitmeyer and Karlstrom, 2007).

Zircon Population	Age (Ma)	Basement Province	Age (Ma)
Permian	< 300	Permian Terranes	< 300
Paleozoic	~ 300-485	Appalachian	270-490
		Maya-Yucatan	300-500
Cambrian	~ 485-560	Southern Oklahoma Aulacogen	~ 520-550
Neoproterozoic	~ 560-740	Carolina	560-740
		Sabine	560-740
		Suwanee	560-740
Late Neoproterozoic	~ 740-900	. . .	. . .
Mesoproterozoic	~ 900-1300	Grenville	900-1300
		Midcontinent Rift System	~ 1100
Early Mesoproterozoic	~ 1300-1600	Midcontinent Granite-Rhyollite	1350-1500
Late Paleoproterozoic	~ 1600-1800	Yavapai	1700-1800
		Mazatzal	1600-1700
Paleoproterozoic	~ 1800-2500	Trans-Hudson	1800-1900
		Great Falls	1800-1900
		Penokean	1800-1900
Archean	> 2500	Superior	> 2500
		Wyoming	> 2500

Figure 65. Summary of potential source terranes represented by each zircon age population. Color coordinates with basement terranes and orogenic belts on Figure 64.

Archean (Older Than 2500 Ma)

Archean detrital zircons constitute 4% of sampled zircons in this study and have two potential source regions, which are components of the southernmost Canadian Shield: the Wyoming and the Superior terranes (Figs. 64-65). Both potential source regions (2500-2800 Ma) are located north of Oklahoma; Wyoming terranes lie to the northwest whereas the Superior terrane is north. According to McKee and Oriel (1967) and Sloss (1988), much of the Canadian Shield was not exhumed during late Paleozoic, specifically by Mississippian time; therefore, these zircon grains more likely were sourced from recycling of older, lower-to-mid-Paleozoic strata (Gehrels et al., 2011; Soreghan et al., 2018). Detrital zircon grains of Archean age have been documented from Pennsylvanian strata in the Fort Worth Basin (Alsalem et al., 2018), Marathon-Ouachita system (Sharrah, 2006; Gleason et al., 2007), Illinois and Forest City Basins (Kissock et al., 2018; Thomas et al., 2020); Anadarko Basin (Kushner et al., 2018) and many other areas west and east of Oklahoma (Soreghan et al., 2002; Ericksson et al., 2004; Thomas et al., 2004; Becker et al., 2005; Gehrels et al., 2011).

Paleoproterozoic (1800-2500 Ma)

Paleoproterozoic detrital zircons constitute 10% of sampled zircons in the study area and have many potential source provinces. These include the 1800-1900 Ma Great Falls, Penokean and Trans-Hudson orogenic belts to the north, the latter linking the Wyoming and Superior provinces (Fig. 64; Hoffman, 1989; Van Schmus et al., 1996). About 6.5% of the Paleoproterozoic zircon grains in this study are older than 1900 Ma and thus could suggest source regions such as the 1600-2300 Mojave terrane, along the western margin of Pangaea, and the Trans-Amazonian and Eburian provinces (1950-2250 Ma) that occur south and east of the orogen and were unroofed during the exhumation of Gondwanan provinces (Sharrah, 2006), although inferring direct transport from east of orogenic highlands is problematic. Amazonian-Eburian zircon ages, however, occur in Devonian-Pennsylvanian strata in the Appalachian Foreland Basin, which indicate recycling from peri-Gondwanan terranes (Thomas et al., 2004; Erickson, 2004).

Late Paleoproterozoic-Early Mesoproterozoic (1300-1800 Ma)

Detrital zircons of Late Paleoproterozoic age account for 20% of sampled zircons in this study and have potential origination in uplifts of the Ancestral Rocky Mountains (ARM) and other areas (Figs. 64-65). The primary source regions associated with this age range include the Yavapai (1700-1800 Ma)-Mazatzal (1600-1700 Ma) orogenic belt exhumed in ARM uplifts, the Central Plains orogeny, and the Granite-Rhyolite basement terranes (Figs. 65-66; Kluth, 1986; Hoffman 1989; Van Schmus et al., 1996; Soreghan et al., 2002). Exhumation of the Yavapai-Mazatzal province occurred in the ARM during Pennsylvanian-Permian time while the Central Plains and Granite-Rhyolite terranes were exposed during Cambrian-Mississippian time by a Transcontinental Arch (Van Schmus et al., 1996). Zircon grains of this age are documented throughout Paleozoic strata including those in western U.S. (Soreghan et al., 2002; Gehrels et al., 2011; Kissock et al., 2018). Studies of Cambrian, Ordovician and Pennsylvanian strata in the Marathon and Ouachita orogen, Arbuckle Mountains, Fort Worth Basin, and Oklahoma, also documented zircons of this age (Sharrah 2006; Gleason et al., 2007; Thomas et al. 2016, Alsalem et. al., 2017, Kushner, 2018).

Mesoproterozoic (900-1300 Ma)

Mesoproterozoic zircons account for 26% of sampled grains in this study, making it the most prominent age group, and correspond to two potential source regions: the midcontinent Rift and Grenville terranes (Figs. 64-65). The Grenville orogen (900-1300 Ma), located in parts of southern and eastern North America, developed as a vestige of an orogeny formed during the continent-continent collision that formed the supercontinent Rodinia; on the other hand, the midcontinent Rift System (~1100 Ma) formed as an aulocogen in the breakup of Rodinia and contains bimodal igneous rocks (Hoffman, 1988; Kissock et al., 2018; Wang and Bigdoli, 2019). In Paleozoic time, the Grenville basement was located along the eastern edge of Laurentia (Alsalem et al., 2018), but now the province occupies the western flank of the Appalachians as well as parts of Texas and Mexico (Soreghan et al., 2017). Detrital zircons of Grenvillian age are very prominent and have been documented as a detrital constituent in ancient and modern strata across North America and Canada (Erickson et al., 2004; Becker et al., 2005; Sharrah, 2006; Gehrels, 2011; Alsalem et al., 2018; Kissock et al., 2018; Kushner et al., 2018; Thomas et al., 2020).

Neoproterozoic (560-740 Ma)

Detrital zircons of Neoproterozoic age represent 22% of sampled grains in the study area, making it the second most prominent age population, and can be assigned to two major tectonomagmatic systems with overlapping ages: eastern and southern Laurentia margin magmatism caused by the Rodinia breakup (550-760 Ma) and the peri-Gondwanan provinces (~500-740 Ma; Figs. 64-65; Alsalem et al., 2018). Numerous peri-Gondwanan provinces record Neoproterozoic zircon populations, and these include: the Avalon, Carolina, and Uchee terranes in the Appalachian Mountains, the Suwannee terrane in the Florida subsurface, the Sabine province in eastern Texas and western Louisiana subsurface, and the Yucatan-Maya terrane in southeastern U.S. and Mexico (Mueller et al., 1994; Murphy et al., 2004; Thomas et al., 2004; Sharrah, 2006; Thompson et al., 2012). This age group is documented in several Late Paleozoic basins across North America but typically in lower proportions compared to the Grenville and Appalachian zircon populations (Thomas et al., 2004; Eriksson et al., 2004; Becker et al., 2005;

Sharrah et al., 2006; Gehrels et al., 2011; Alsalem et al., 2018; Kissock et al., 2018; Thomas et al., 2020).

Paleozoic (300-485 Ma)

Detrital zircons of this age were mainly produced during the long-lived Appalachian orogeny (270-490 Ma) that culminated in the suture of Laurentia and Gondwana and represent 10% of the sampled zircon grains in the study area (Figs. 64-65). During that time, eastern Laurentia (Appalachian region) developed three tectonomagmatic systems including the Taconic (420-490 Ma), Acadian (350-420 Ma), and Alleghenian (270-330) orogenies (Miller et al., 2000). Zircons of this age population have been documented in Paleozoic strata in the Appalachian Basins (Eriksson et al., 2004; Thomas et al., 2004; Becker et al., 2005), Michigan Basin (Thomas et al., 2020), Illinois and Forest City Basins (Kissock et al., 2018), Oklahoma, Kansas, and Arkansas (Sharrah, 2006; Kushner et al., 2018; Soreghan et al., 2018), New Mexico, Utah, and Arizona (Soreghan et al., 2002).

Other Ages

Approximately 5% of the sampled zircon grains in this study fall within a 485-560 Ma age range, which correlates to ages of igneous rock within the Cambrian Southern Oklahoma Aulocogen (530-550) and presently makes up the basement of the Wichitas (~520 Ma) uplifts (Figs. 64-65; Wright et al., 1996; Thomas et al., 2016). These igneous rocks formed in the early Paleozoic during the breakup of Rodinia and were uplifted via transpressional tectonics related to the suture of the Pangea supercontinent (Hanson et al., 2013).

Spatial and Temporal Trends

The eight (8) detrital zircon populations contain an overall age range from Paleozoic (305 Ma) to Archean (3169 Ma) and each sample can be classified as one of the three composite types based on distinct differences in one or more dominant age populations (Figs. 63, 66, 67). Type 1 contains a major Neoproterozoic-aged signal from 560 to 740 Ma, and a subordinate Paleozoic-aged signal from 270-485Ma (Appalachian), and includes samples DG-A, DG-B, UF-B, UF-C (Figs. 63, 66, 67). Type 2 contains a dominant Mesoproterozoic-aged signal from 900 to 1300 Ma (Grenvillian) with subordinate Paleozoic (270-485Ma) and Early Mesoproterozoic (1300-1600 Ma) and includes samples SF-A and SF-B. The final assemblage, Type 3 contains roughly equal major populations of Mesoproterozoic-aged signal from 900 to 1300 Ma (29%), Early Mesoproterozoic from 1300 to 1600 Ma (21%) and Late Paleoproterozoic from 1600 to 1800 Ma (20%) and includes sample UF-A. Type 3 is more closely related to Type 2 than to Type 1 assemblages. The Type 1 assemblage dominates in lower zircon samples of the cores in north-central and central Oklahoma (Kay and Logan Counties). However, the upper sample in the Logan County (Core 2) is a Type 3 signature. The Type 2 composite occurs only in Core 3, Pottawatomie County.

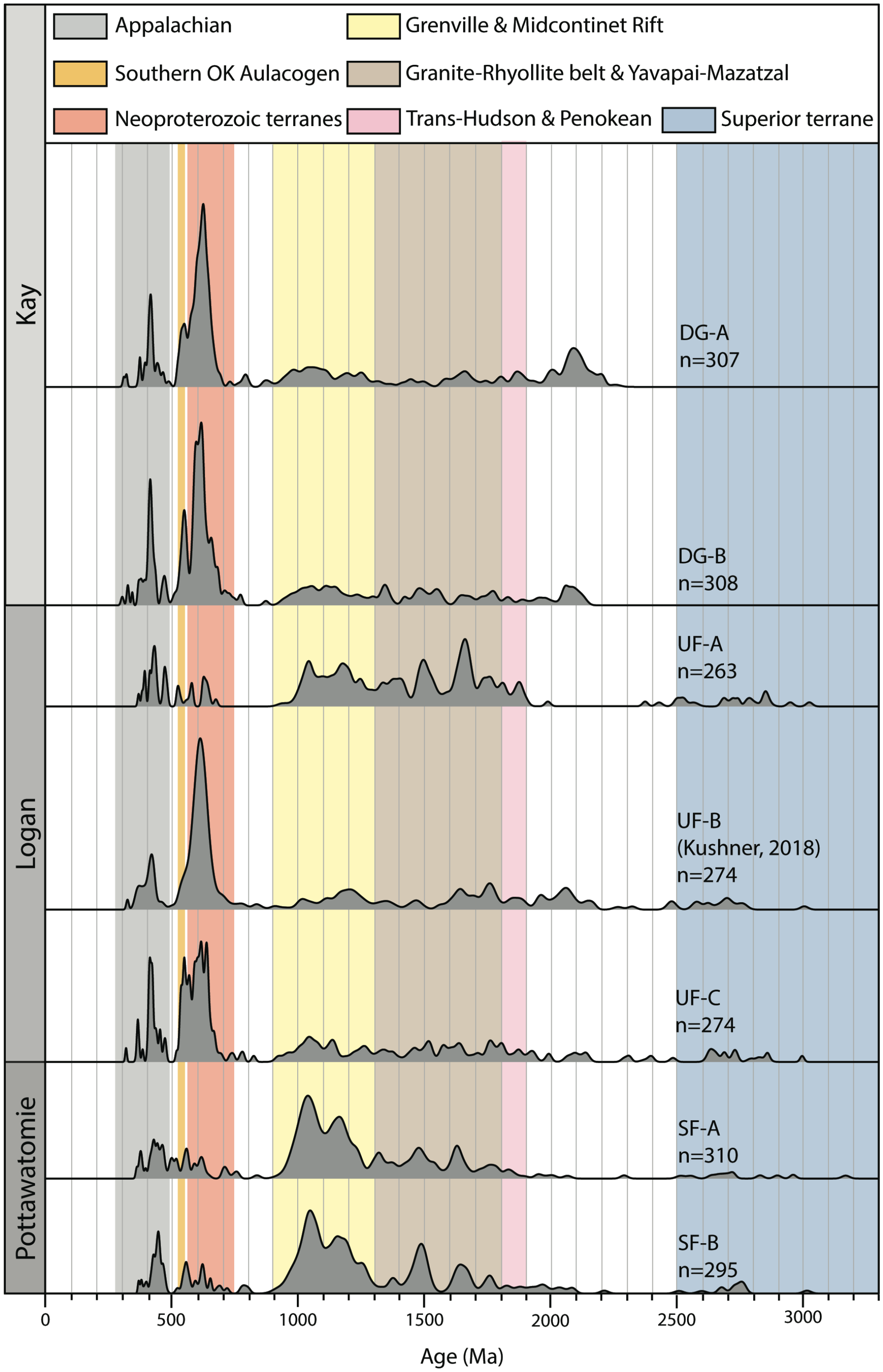

Figure 66. Normalized relative age probability diagrams of detrital zircon data. Colored rectangles illustrate age ranges of potential source terranes discussed in text, and color coordinate with basement terranes and orogenic belts on Figure 65 and 67. n- number of grains.

Provenance Interpretations

Type 1 Provenance

Sandstones containing the Type 1 detrital zircon signature are inferred to have been transported from the northeast during Desmoinesian time. This interpretation is based on this assemblage's dominance of Appalachian- (Taconic-Acadian; 350-490 Ma) and Neoproterozoic- (560-740 Ma) aged zircons (Figs. 66-67). Additionally, point count data for the stratigraphically lower and middle samples in Core 2 show abundant metamorphic lithics, plagioclase feldspar and trace amounts of micas, in addition to the dominant amounts of monocrystalline quartz. Neoproterozoic-aged detrital zircons are not characteristic in the Laurentian midcontinent basement or older Paleozoic strata in the midcontinent (Konstantinou et al., 2014; Kissock et al., 2018; Tunin, 2020). This, along with the sandstones' grain maturity (fine to very fine-grained and subangular-rounded), supports the idea that Type 1 sandstones were likely derived from distant sources to the northeast and transported into the Anadarko Shelf and Basin during the Desmoinesian (Fig. 68). This interpretation agrees with Kushner's (2018) interpretations as well as Tunin's (2020) provenance assessments for Red Fork intervals on the Cherokee platform, west-central OK (Anadarko Basin) and for the Bartlesville Sandstone (below the Inola marker) in the Cherokee platform.

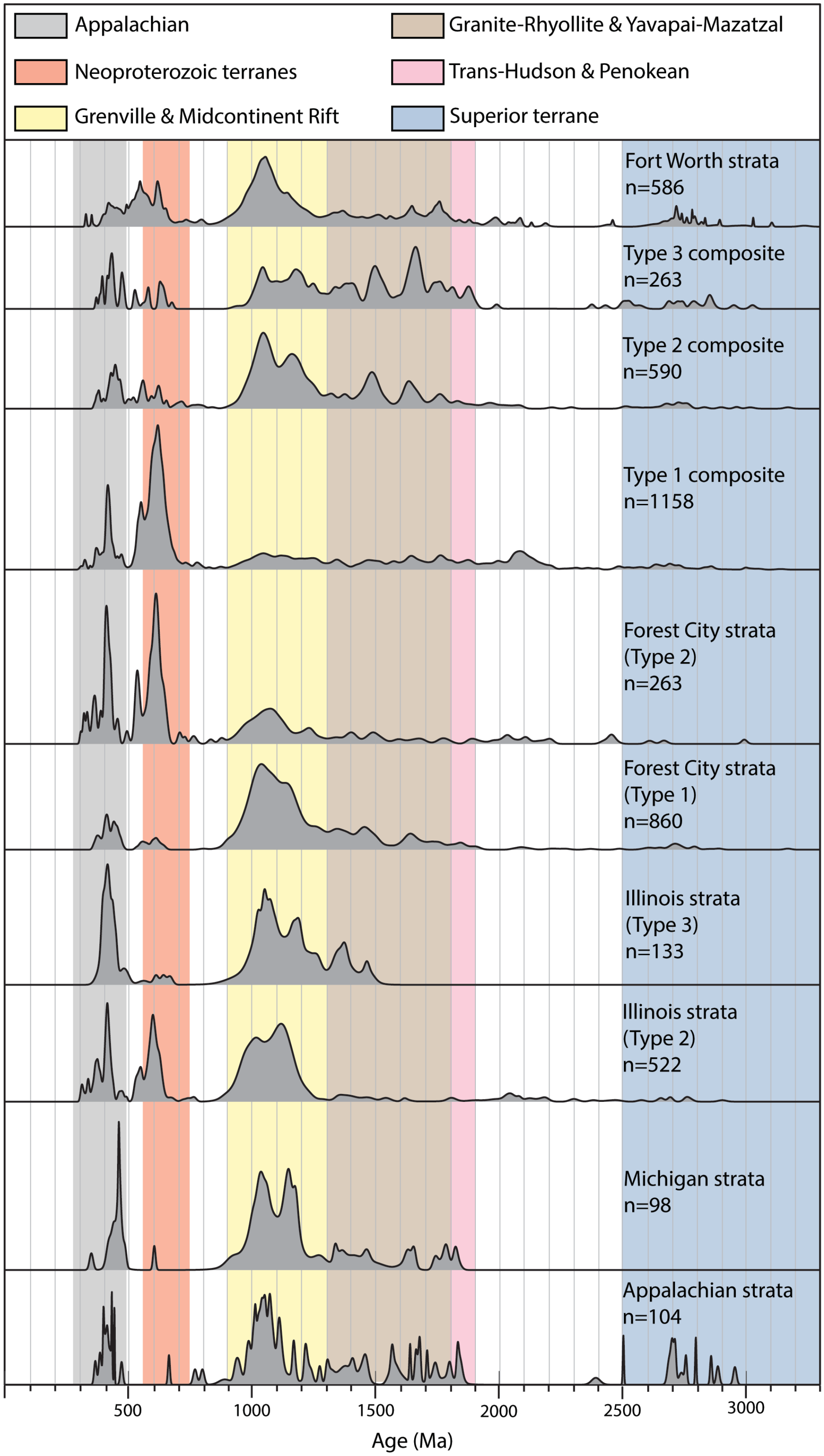

Appalachian
Granite-Rhyollite & Yavapai-Mazatzal
Neoproterozoic terranes
Trans-Hudson & Penokean
Grenville & Midcontinent Rift
Superior terrane
Fort Worth strata
n=586
Type 3 composite
n=263
Type 2 composite
n=590
Type 1 composite
n=1158
Forest City strata
(Type 2)
n=263
Forest City strata
(Type 1)
n=860
Illinois strata
(Type 3)
n=133
Illinois strata
(Type 2)
n=522
Michigan strata
n=98
Appalachian strata
n=104
500
1000
1500
2000
2500
3000
Age (Ma)

Figure 67. Normalized relative age probability diagrams of detrital zircon data from this study (composite of Type 1, 2, and 3), and Middle Pennsylvanian strata from the Appalachian, Michigan, Illinois, Forest City, and Fort Worth basins (Eriksson et al., 2004; Thomas et al., 2004; Kissock et al., 2018; Alsalem et al., 2018). Note that Illinois and Forest City Basins' samples are also categorized in three distinct types. n- number of grains.

Considering the absence of Neoproterozoic zircon grains in Paleozoic clastic wedges of central and southern Appalachian Basin as well as the previously proposed westward transport and south-southwest paleoflow directions (Thomas et al., 2004; Rascoe and Adler, 1983; Kissock et al., 2018; Chapman and Laskowski, 2019), the most probable source for Type 1 populations may be the peri-Gondwanan terranes in the northern part of the Alleghenian orogen. This interpretation is consistent with Kissock's et al. assessment of the stratigraphically higher, Desmoinesian, Floris Formation. in Forest City Basin, central Iowa (2018; Fig. 67). Further evidence relies on the more common presence of Acadian orogenic plutons in northern Appalachians compared to the southern Appalachians (Thomas et al. 2017; Tunin, 2020) that could have yielded the younger (350-485 Ma) zircons common in the Type 1 zircon samples.

Type 2 and 3 Provenance

Sandstones containing the Type 2 and 3 signatures represent deposition from multiple source terranes, based on these assemblage's predominance of Grenville-aged zircons (900-1300 Ma), with subordinate amounts of Granite-Rhyolite- (1300-1600 Ma), Yavapai-Mazatzal-aged grains (1600-1800), and minor amounts of Appalachian- (Taconic-Acadian; 350-490 Ma), and Neoproterozoic (560-740 Ma; Figs. 66-67). In the sandstones represented by the Type 2 and 3 detrital zircon signatures, the high fraction of zircons of Grenville age suggests transport from the Appalachians, most specifically the central Appalachians (Fig. 68). This interpretation is supported by the very similar zircon signature of Paleozoic strata in the central Appalachian Basin (Ericksson et al., 2004; Becker et al., 2005) that show two Grenville peaks, one at ~980-1090 Ma (Ottawan orogeny; Rivers, 1997) and the other at ~1160-1190 Ma (Shawinigan orogeny; Chianzerelli et al., 2010), similar to the age ranges observed in the Type 2 and 3 samples (Fig. 67). This differs from Alsalem's et al. (2018) dataset from Desmoinesian sandstones in the Fort Worth Basin, which show a unimodal Grenvillian peak and low abundance of Shawinigan orogeny ages, characteristic of southern Appalachian zircon signatures (Fig. 67). My interpretation is also different from Tunin's (2020) interpretation of paleogeography of eastern Oklahoma based on provenance of the Taft Sandstone in the Arkoma Shelf, which they interpreted as having been sourced from sandstones fringing the Ozark dome. The small proportions (~5%) of Neoproterozoic zircon grains present in the Type 2 and 3 samples also supports the idea of transport by a mostly east to west system that was separate from the transport of sediment from the northeastern dispersal system active at the time (Thomas et al., 2017; Kissock et al., 2018). Nevertheless, additional potential source terranes need to be considered to account for the subordinate abundance of Granite-Rhyollite and Yavapai-Mazatzal aged grains, which are especially stronger in the stratigraphically higher UF-C (Type 3) sample of Logan County.

During Desmoinesian time, most of the Yavapai-Mazatzal province remained covered, except on basement uplifts associated with the ARM and the Transcontinental Arch (Rascoe and Adler, 1983; Tunin, 2020). The ARM uplifts however, all were bordered by adjacent depositional basins in which most of the local sediment was trapped, and further, a viable pathway for a dispersal system from the west that would traverse the northern and eastern part of the Anadarko Shelf before being deposited along the southeastern margin of the Anadarko shelf is difficult to constrain. Local exposures of the Yavapai-Mazatzal rocks during Desmoinesian were also located in the Nemaha Ridge and Ozark Dome (Whitmeyer and Karlstrom, 2007). The granite, quartzite and rhyolite assemblages in the Nemaha Ridge comprise ages from ~1370 to 1650 Ma, whereas granites and rhyolites of the Yavapai-Mazatzal juvenile crust (only exposed in the vicinity of St. Francois Mountains of eastern Missouri during that time) comprise ages from ~1637 to 1690 Ma ((Bickford et al., 1981; Whitmeyer and Karlstrom, 2007). Additionally, previous studies from Bickford et al. (1981) and Goodge and Vervoot (2007) propose that parts of the Yavapai-Mazatzal juvenile crust could have been emplaced on and around the Ozark Dome by midcontinent granitoid intrusions but later eroded by exhumation of the Dome (Tunin, 2020). These detrital zircon age ranges for the Nemaha Ridge and Ozark Dome match the zircon ages from the Type 2 and 3 samples; given the paleogeography and the evidence that the Nemaha was buried by Red Fork time, the Ozark Dome is the most likely source for these zircon grains, and thus may have been a secondary source of sediment.

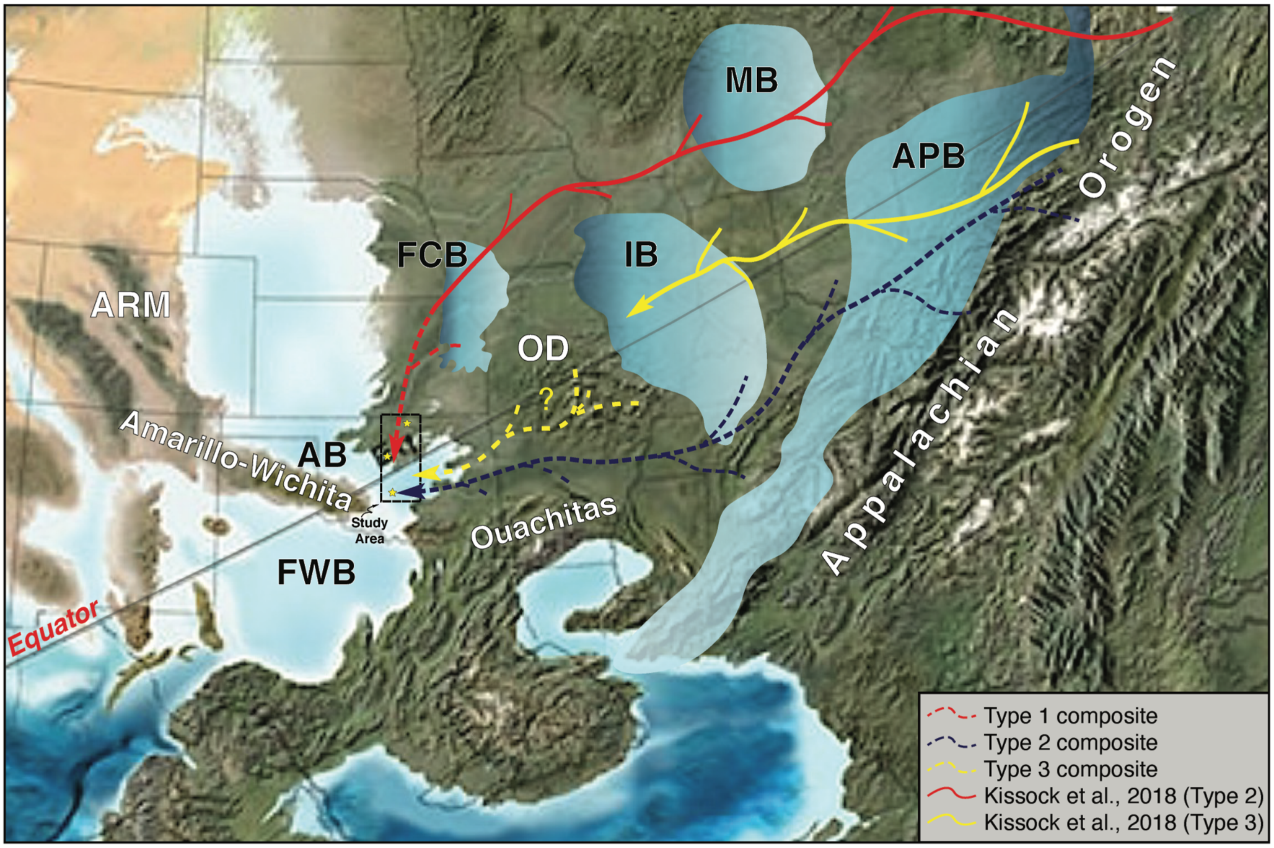

Figure 68. Paleogeographic reconstruction of the Middle-Late Pennsylvanian period (modified from North American Key Time Slices ©2013 Colorado Plateau Geosystems Inc.). AB = Anadarko Basin; FCB = Forest City Basin; IB = Illinois Basin; APB = Appalachian Basin; MB = Michigan Basin; ARM = Ancestral Rocky Mountains; OD = Ozark Dome.

Integrated Sequence Stratigraphy and Provenance Interpretations

Detrital zircon age spectra vary depending on two parameters: their location in the Anadarko Shelf and their position in a sequence stratigraphic framework. The Type 1 zircon signature is contained within the lowstand systems tract (LST) of Cores 1 and 2, which are located in the north and north-central portions of the Anadarko Shelf. The Type 3, on the other hand, is found within the highstand systems tract (HST) of Core 2. Lastly, Type 2, is found only in Core 3, in south-central OK. These spatial and temporal zircon variations point to at least two different possibilities for sediment transport during the Desmoinesian in the Anadarko Shelf and Basin.

The first possibility is related to the multiple stages of Red Fork incision (discussed in Chapter 1) where the sandstones might have been deposited at different times during the Desmoinesian. As noted above, at least five (5) valley incisions have been proposed for the Red Fork in the Anadarko Shelf and adjacent areas (in Chapter 2; Peyton et al., 1998; Lambert, 2006; Davogustto et al., 2013). These interpretations were based primarily on seismic and well data. Sedimentologic evidence of multiple stages of incision were not observed within the cored intervals. Nevertheless, I outline two possibilities: 1) the cored intervals represent different periods of deposition within Red Fork "time" as a single major river system created multiple diachronous incised valley systems across the shelf; and 2) the cored intervals represent two major river systems that coexisted during Red Fork deposition even though the incised valley fills may not be exactly coeval.

The first scenario, in which a major river system created multiple and slightly diachronous incised valleys and channelized sand bodies has been previously put forth by Andrews (1997) and is consistent with the concept of multiple valley incisions as noted above. A major fluvio-deltaic river system, responding to variations in glacioeustasy and autocyclic processes would create slightly diachronous sandstone bodies across the Anadarko Shelf. The provenance of these channel sediments, however, should not be significantly different. Therefore, in testing this hypothesis it is difficult to explain the significant difference in the Type 1 and Type 2 signatures present in the different low-stand sandstones interpreted as incised valley fills during Red Fork deposition. Further, this interpretation is challenged by the presence of Type 3 zircon signature within the HST of Core 2 since the Type 3 zircon population is significantly different from the zircon spectra in the samples in the lower part of the same core.

On the other hand, the second hypothesis, which is preferred, is related to the identification and correlation of regionally transgressive limestone marker beds that bound the Red Fork Sandstone, namely the Inola and Pink Limestones. That is, since the Inola and Pink Limestones are interpreted as units which mark major transgressions that end the Bartlesville (Inola) and Red Fork (Pink) Sandstones' deposition, their identification within this study area and cored intervals indicates that the Red Fork interval, within these horizons, accumulated approximately coevally, regardless of the specific times of incision and filling of the valleys. More importantly, in this scenario, the provenance difference between the LST sandstones in Cores 1 and 2 vs. Core 3 is interpreted to reflect at least two (2) major and contemporaneous river systems that transported sediment into the Anadarko Shelf and Basin during Desmoinesian time (Figs. 68-69). A river that ultimately derived from the northern Appalachians and flowed southwestward into the Anadarko Shelf transported sediment typified by the Type 1 zircon signature into the northern and north-central shelf during sea level lowstand (Fig. 68). However, as these valleys were flooded during transgression, the HST sandstones exhibit a different detrital zircon signature (Type 3) in Core 2, suggesting that sediment from the northeastern source was trapped farther northeast, and sediment accumulation within the incised valley at the location of the core could not keep up with base-level rise. The resulting HST sandstones, interpreted as tidal deposits, were likely derived from well-mixed sources that may have been transported along the shelf from the southeast and the area of core location 3, since the zircon signature of this HST suggests multiple sources including abundant Grenville age grains that is not present in the LST sandstones but is present in Core 3 (Figs. 68-69).

The proposed second river headed primarily in the central Appalachians and flowed mostly west and transported sediment with the Type 2 signature to the eastern margin of the Anadarko Basin. In this case, however, the provenance of the sediment does not appear to change within the core, regardless of sequence stratigraphic position of the sample, suggesting that sediment supply was able to mostly keep up with changes in base level (Figs. 66-67) and that the fluvial system was continuously providing sediment. This is consistent with the predominance of channel fill facies and increase thickness of the sequence displayed in the core. Ultimately the area represented by the core was transgressed, but the cored interval does not display this interval, so I cannot determine if the provenance of the sediment changed.

Middle Pennsylvanian Sediment Pathways into the Anadarko Shelf/Basin

The provenance analysis coupled with a sequence stratigraphic framework for the Desmoinesian strata in Oklahoma, provides new constraints for the ongoing debate on the Middle Pennsylvanian sediment provenance and dispersal patterns in North America (Laurentia supercontinent). U/Pb detrital zircon signatures of Desmoinesian sandstones in Oklahoma support the concept of transcontinental river systems flowing westward from an Appalachian source into central Laurentia sedimentary basins as well as small-scale and local drainage-systems associated with local uplifts, particularly the Ozark Dome. Similarities and differences in zircon signatures within a stratigraphic framework indicate that two large-scale drainage systems, but with likely varying sediment supplies existed during Desmoinesian and provided sediment into the Anadarko Shelf and adjacent areas during times of sea level lowstand. During rising relative sea level, only the south river system was able to keep pace and continued to deliver sediment into the shelf area.

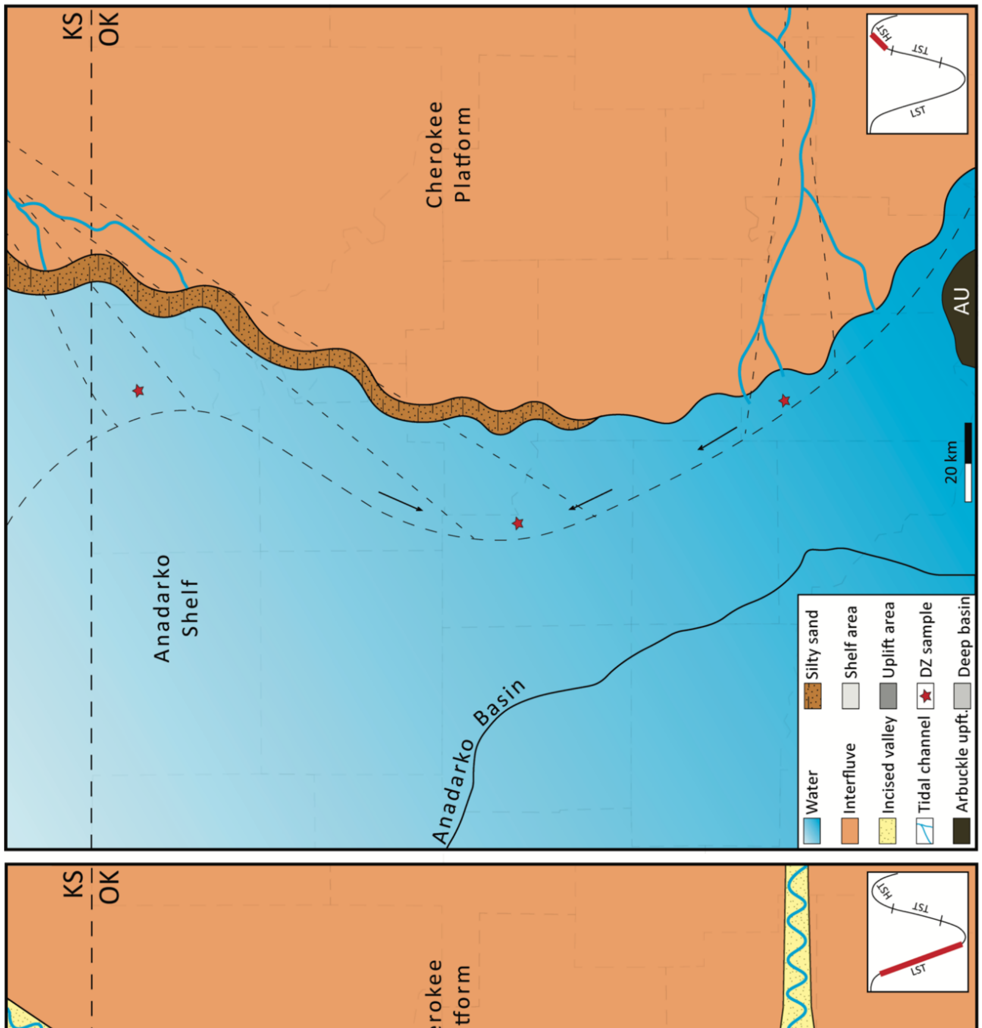

KS
OK
Cherokee Platform
Anadarko Shelf
Anadarko Basin
AU
20 km
LST
TST
HST
Water
Interfluve
Incised valley
Tidal channel
Arbuckle upft.
Silty sand
Shelf area
Uplift area
DZ sample
Deep basin
KS
OK
Cherokee Platform
Anadarko Shelf
Anadarko Basin
AU
20 km
LST
TST
HST
KS
OK
80 km

Figure 69. Schematic paleogeographic reconstruction showing valley incision during sea level lowstand (left) and eastward migration of the shoreline during highstand (right) in the Middle Pennsylvanian. Deltaic progradation continued in the south-central portion of the shelf and mostly countered the sea level rise. Shoreline inference was possible with aid from the work of Moore (1979) and Johnson (2008). AU = Arbuckle Uplift. Inset map of Oklahoma shows major geologic provinces from Johnson (2008).

During Desmoinesian time, lowstand sandstones in north-central and central Oklahoma contain a Type 1 zircon signature, which is characteristic of an Appalachian provenance, except for the low percentage of zircons with Grenvillian ages (Thomas et al., 2017). Based on U/Pb detrital zircon similarities, sandstone compositions, and considering simultaneously continuous sedimentation in those locations, the sands in Cores 1 and 2, which are represented by the Type 1 zircon samples, were likely derived from the same provenance and transported through incised valleys through a shared paleodrainage system across the midcontinent that terminated on the northern Anadarko Shelf. This is consistent with Kissock's et al. (2018) interpretation of a westward migration of transcontinental fluvial systems with headwaters in southeastern New England; thus, marking a connection and continuation of westward and subsequent southward flow of these rivers from the Forrest City Basin into the Anadarko Shelf. This drainage system probably flowed through the Michigan Basin area prior to entering the northern Forest City. During that time, increased sedimentation likely overwhelmed the Bourbon Arch and allowed for the connection of the Forest City Basin with the Cherokee Platform, and the subsequent extension of sedimentation from Kansas into northern Oklahoma. Further, the Nemaha Ridge was likely buried by this time (Tate, 1985; Andrews, 1997; Lambert, 2006 and sources therein). During sea level highstand, the shoreline probably migrated significantly to the north and east, leaving the northeastern Oklahoma shelf far from the direct sediment source of these river systems.

In south-central Oklahoma, lowstand and highstand sandstones contain a Type 2 signature, which are also characteristic of Appalachian type (Thomas et al., 2017) and correspond to those reported in the Fort Worth and Arkoma Basins (Alsalem et al., 2018; Sharrah, 2006). Based on U/Pb detrital zircon similarities, most specifically the high abundance of zircons of Grenville age, the Type 2 zircon grains were likely derived from the same or adjacent Central Appalachian provenance and transported by shared westward paleodrainage systems across the southern portion of the midcontinent into the southern Anadarko Shelf. However, subordinate to minor amounts of Granite-Rhyolite and Yavapai-Mazatzal might indicate small-scale drainage systems from the Ozark Dome.

CHAPTER IX

CONCLUSIONS

In this study, analysis of three cores, supplemented by thirty-three wells (and their respective logs), thin section petrography, and geochronology of detrital zircons allowed for the analysis of the Red Fork interval (lower Cherokee Group), depositional environment, sequence stratigraphy and provenance during Middle Pennsylvanian in the Anadarko Shelf and Basin, Oklahoma. Specifically, 3 cross sections, 16 facies, and 2011 detrital zircon U/Pb ages were reported for the Middle Pennsylvanian strata in the Anadarko Shelf. Based on these data, the sequence stratigraphic framework, and comparisons made with detrital zircon data from coeval Desmoinesian sandstones across the North American Craton, numerous key conclusions are proposed below:

1. The Red Fork Sandstone incised into marine shales of the Bartlesville or lower Pennsylvanian strata throughout the relatively stable Anadarko Shelf. This is interpreted to reflect subaerial exposure of formerly submerged surfaces and subsequent valley downcutting of up to 50 ft into marine shales during sea level drawdown and coeval seaward retreat of the shoreline.
2. Spatial and temporal variations in thickness and facies characteristics of the Red Fork interval, also marked by sequence stratigraphic differences in the study area, are interpreted to demonstrate differences in sedimentation rates and patterns that were

strongly influenced by local tectonics and glacioeustasy that occurred in the Middle Pennsylvanian.

3. Middle Pennsylvanian sandstones in the Anadarko Shelf can be divided into at least three detrital zircon provenance types based on variation in U/Pb age distributions. Specifically:

    a. Type 1 sandstones are classified as sublitharenites to litharenites that are interpreted to reflect sources of sediments in the Northern Appalachians (southeast New England) and sediment transport into the northern Anadarko Shelf and Basin by a southwestwardly flowing transcontinental fluvial system during sea level lowstand.

    b. Type 2 sandstones are classified as quartzarenites that are interpreted to be mainly sourced from the Central Appalachians with possible minor contributions from previously exposed local basement such as the Nemaha Ridge or the Ozark Dome. Type 2 sandstones are interpreted to reflect sediment transport to the southern Anadarko Shelf and Basin by a westwardly flowing transcontinental river system approximately contemporaneous with the northern dispersal systems, during sea level lowstand and highstand.

c. Type 3 sandstones are interpreted as tidal deposits derived from well-mixed sources along the shelf during sea level highstand, after the northern shelf incised valleys were flooded during transgression. The multiple-source character of these sands including the Grenville U/Pb ages absent in the stratigraphically lower LST sandstones is interpreted to reflect that sediment from the northeastern source was trapped farther east, and sediment accumulation at the location of the core could not keep up with base-level rise.

4. Detrital zircon U/Pb age signatures along with sedimentologic characteristics show evidence for connectivity between Northern Appalachian derived fluvial dispersal systems in the Forest City and Illinois Basins as well as the Anadarko Shelf and Basin.

5. U/Pb detrital zircon age data coupled with a sequence stratigraphic framework provide additional constraints for multiple sediment dispersal pathways from the northern and central Appalachians southwestward across the midcontinent and into the Anadarko Shelf and Basin during times of glacioeustatic and tectonic variations in the Middle Pennsylvanian.

REFERENCES

Albano, M. A., 1975, Subsurface stratigraphic analysis, “Cherokee” Group (Pennsylvanian), northeast Cleveland County, Oklahoma: Oklahoma City Geological Society, Shale Shaker, v. 45, p. 94-137.

Alsalem, O.B., Fan, M., Zamora, J., Xiangyang, X., and Griffin, W.R., 2018, Paleozoic sediment dispersal before and during the collision between Laurentia and Gondwana in the Fort Worth Basin, USA: Geosphere, v. 14, p. 325-342.

Andrews, R.D., 1997, Fluvial-dominated deltaic (FDD) oil reservoirs: the Red Fork Play: Oklahoma Geological Survey Special Publication 97-1, 115 p.

Archer, A., and Greb, S.F., 1995, An Amazon-scale drainage system in the early Pennsylvanian of central North America: Geology, v. 103, p. 611-627.

Becker, T.P., 2005, Paleogeographic and Tectonic Implications of the Late Paleozoic Alleghanian Orogen Developed from Isotopic Sedimentary Provenance Proxies from the Appalachian Foreland Basin [Ph.D. Dissertation]: University of Kentucky, Lexington, Kentucky, 214 p.

Belt, E.S., Heckel, P., Lentz, L.J., Bragonier, A., and Lyons, T., 2011, Record of glacial–eustatic sea-level fluctuations in complex middle to late Pennsylvanian facies in the Northern Appalachian Basin and relation to similar events in the midcontinent basin: Sedimentary Geology, v. 238, p. 79–100, doi: 10.1016/j.sedgeo.2011.04.004.

Bickford, M. E., Harrower, K. L., Hoppe, W. J., Nelson, B. K., Nusbaum, R. L., Thomas, J. J., 1981, Rb-Sr and U-Pb geochronology and distribution of rock types in the Precambrian basement of Missouri and Kansas: Geological Society of America Bulletin, part I, v. 92, p. 323-341.

Blakey, R., 2016, Deep time maps: maps of ancient Earth: Colorado Plateau Geosystems, Inc: https://deeptimemaps.com/.

Boggs, S., Jr., 2012, Principles of Sedimentology and Stratigraphy: Pearson, fifth edition, 662 p.

Brown, L. F., 1979, Deltaic sandstone facies in the Midcontinent *in* Pennsylvanian sandstones of the midcontinent: Tulsa Geological Society Special Publication 1, p. 35-63.

Buatois, L.A., Mangano, G., Carr, T.C., 1999, Sedimentology and Ichnology of Paleozoic Estuarine and Shoreface Reservoirs, Morrow Sandstone, Lower Pennsylvanian of Southwest Kansas, USA: Current Research in Earth Sciences, Kansas Geological Survey Bulletin 243, part 1, p. 1-35.

Candler, C. C., 1977, Subsurface stratigraphic analysis of selected sandstones of the “Cherokee” Group, southern Noble County, Oklahoma: Shale Shaker, v. 28, p. 72.

Catuneanu, O., 2006, Principles of Sequence Stratigraphy: Elsevier, first edition, 387 p.

Cecil, C.B., Dulong, F.T., West, R.R., Stamm, R., Wardlaw, B., Edgar, N.T., 2003, Climate controls on the stratigraphy of a Middle Pennsylvanian cyclothem in North America, *in* Cecil, C.B., Edgar, T.N. (eds.), Climate Controls on Stratigraphy: SEPM Special Publication, v. 77, pp. 151–182.

Catuneanu, O., Galloway, W. E., Kendall, C. G. S. C., Miall, A. D., Posamentier, H. W., Strasser, A., and Tucker, M. E., 2011, Sequence Stratigraphy: Methodology and Nomenclature: Newsletters on Stratigraphy, v. 44, no. 3, p. 173–245, doi:10.1127/0078-0421/2011/0011.

Chapman, A. D., & Laskowski, A. K., 2019, Detrital zircon U-Pb data reveal a Mississippian sediment dispersal network originating in the Appalachian orogen, traversing North America along its southern shelf, and reaching as far as the southwest United States: Lithosphere, v. 11, p. 581–587.

Chiarenzelli, J., Regan, S., Peck, W.H., Selleck, B.W., Cousens, B., Baird, G.B., and Shrady, C.H., 2010, Shawinigan arc magmatism in the Adirondack Lowlands as a consequence of closure of the Trans-Adirondack backarc Basin: Geosphere, v. 6, p. 900–916, https://doi.org/10.1130 /GES00576.1.

Davogustto, O., de Matos, M. C., Cabarcas, C., Dao, T., Marfurt K. J., 2013, Resolving subtle stratigraphic features using spectral ridges and phase residues: Interpretation, v. 1, no. 1, p. SA93-SA108.

Desjardins, P. R., Buatois, L. A., Mángano M. G., 2012, Tidal flats and subtidal sand bodies-Chapter 18 *in* Shallow Marine Siliciclatic Systems: Elsevier, Developments in Sedimentoloty, v. 64, p. 529-561.

Davydov, V., Wardlaw, B., & Gradstein, F., 2005, Chapter 5- The Carboniferous Period *in* F. Gradstein, J. Ogg, & A. Smith (eds.), A Geologic Time Scale 2004: Cambridge University Press., p. 222-248, doi:10.1017/CBO9780511536045.016.

Dickinson, R., 1970, Interpreting detrital modes of graywacke and arkose: Journal of Sedimentary Petrology, v. 40, p. 695–707.

Dickinson, MI.R., Beard S.L., Brakenridge, G.R., Erjavec, J.L., Ferguson, R.C., Inman, K.F., Knepp, R.A., Lindberg, F.A., and Ryberg, P.T., 1983, Provenance of North American Phanerozoic sandstones in relation to tectonic setting: Geological Society of America Bulletin, v. 94, p. 222-235.

Dickinson, R., and Gehrels, G.E., 2009, U-Pb ages of detrital zircons in Jurassic eolian and associated sandstones of the Colorado Plateau: Evidence for transcontinental dispersal and intraregional recycling of sediment: Geological Society of America Bulletin, v. 121, p. 408-433.

Dimichele, A., and Phillips, T.L., 1996, Climate change, plant extinctions and vegetational recovery during the Middle-Late Pennsylvanian Transition: The Case of tropical peat-forming environments in North America: Geological Society, London, Special Publications, v. 102, p. 201–221, doi: 10.1144/gsl.sp.1996.001.01.14.

Dimichele, A., Pfefferkorn, and Gastaldo, R.A., 2001, Response of Late Carboniferous and Early Permian Plant Communities to Climate Change: Annual Review of Earth and Planetary Sciences, v. 29, p. 461–487, doi: 10.1146/annurev.earth.29.1.461.

Dogan, N., 1969, A subsurface study of the Middle Pennsylvanian rocks (from the Brown limestone to the Checkerboard limestone) in east-central Oklahoma [M.S. Thesis]: University of Tulsa, Tulsa, Oklahoma, 64 p.

Domeier, M., and Torsvik, T., 2014, Plate tectonics in the late Paleozoic: Geoscience Frontiers, v. 5, p. 303–350, doi: 10.1016/j.gsf.2014.01.002.

Dott, R., 1927, Oil and Gas in Oklahoma - Notes on Pennsylvanian paleogeography with special reference to south-central Oklahoma: Oklahoma Geological Survey Bulletin 40, p. 51-68.

Ettensohn, F.R., Pashin, J.C., Gillian, 2019, Chapter 4-The Appalachian and Black Warrior Basins: Foreland Basins in the Eastern United States *in* The Sedimentary Basins of the United States and Canada: Elsevier, v.5, p. 129-237, https://doi.org/10.1016/S1874-5997(08)00004-X.

Eriksson, K.A., Campbell, I., Palin, J.M., Allen, C.M., and Bock, B., 2004, Evidence for multiple recycling in Neoproterozoic through Pennsylvanian sedimentary rocks of the central Appalachian Basin: Journal of Geology, v. 112, p. 261–276, https://doi.org/10.1086/382758.

Eriksson, K.A., Mcclung, S., and Simpson, E.L., 2019, Sequence stratigraphic expression of greenhouse, transitional and icehouse conditions in siliciclastic successions: Paleozoic examples from the central Appalachian basin, USA: Earth-Science Reviews, v. 188, p. 176–189, doi: 10.1016/j.earscirev.2018.11.010.

Fielding, C.R., Frank, T.D., Birgenheier, L., Rygel, M.C., Jones, A.T., Roberts, J., 2008, Stratigraphic imprint of the Late Palaeozoic Ice Age in eastern Australia: a record of alternating glacial and nonglacial climate regime: Journal of the Geological Society, v. 165, p. 129–140.

Fielding, C.R., Nelson, W. J., Elrick, S. D., 2020, Sequence Stratigraphy of the Late Desmoinesian to Early Missourian (Pennsylvanian) Succession of Southern Illinois: Insights into Controls on Stratal Architecture in an Icehouse Period of Earth History: Journal of Sedimentary Research, v. 90, p. 200-227.

Folarin, K., Turko, M. S., and Carpenter, B. M., 2020, Basement-controlled deformation of sedimentary sequences, Anadarko Shelf, Oklahoma: Basin Research, v. 32, p. 1365-1387, https://doi. org/10.1111/bre.12433.

Frezon, S.E., and Dixon, G., 1975, Texas panhandle and Oklahoma *in* Paleotectonic investigations of the Pennsylvanian system in the United States, Part I: Introduction and regional analyses of the Pennsylvanian system: Oklahoma Geological Survey Professional Paper 853, p. 177-195.

Gehrels, G.E., Victor, V.A., and Pullen, A., 2006, Detrital zircon geochronology by laser-ablation multicollector ICPMS at the Arizona LaserChron Center, *in* Loszewski, T., and Huff (eds.), Geochronology: Emerging Opportunities: The Paleontological Society Papers 12, p. 67–76, https:// doi.org/10.1017/S1089332600001352.

Gehrels, G.E., Valencia, V.A., and Ruiz, J., 2008, Enhanced precision, accuracy, efficiency, and spatial resolutio6rfbv n of U-Pb ages by laser ablation-multicollector-inductively coupled plasma-mass spectrometry: Geochemistry, Geophysics, Geosystems, v. 9, p. 115-150.

Gehrels, G.E., Blakey, R., Karlstrom, K.E., Timmons, J.M., Dickinson, B., and Pecha, M., 2011, Detrital zircon U-Pb geochronology of Paleozoic strata in the Grand Canyon, Arizona: Lithosphere, v. 3, p. 183–200, https://doi .org/10.1130/L121.1.

Gleason, J.D., Gehrels, G.E., Dickinson, R., Patchett, P.J., and Kring, D., 2007, Laurentian sources for detrital zircon grains in turbidite and deltaic sandstones of the Pennsylvanian Haymond Formation, Marathon assemblage, west Texas, U.S.A.: Journal of Sedimentary Research, v. 77, p. 888–900, https://doi.org/10.2110/jsr.2007.084.

Goodbread, S., L., Jr., and Saito, Y., 2012, Tide-Dominated Deltas *in* Davis, R.A, Jr. and Dalrymple, R.W. (eds.), Principles of Tidal Sedimentology: Springer, p. 129-149, doi 10.1007/978-94-007-0123-6_7.

Goodge, J.W., Vervoort, J.D., 2006, Origin of Mesoproterozoic A-type granites in Laurentia: Hf isotope evidence: Earth and Planetary Science Letters, v. 243, p. 711-731.

Graham, S.A., Dickinson, R., and Ingersoll, R.V., 1975, Himalayan-Bengal model for flysch dispersal in the Appalachian-Ouachita system: Geological Society of America Bulletin, v. 86, p. 273–286, https://doi.org/10.1130/0016-7606(1975)86<273: HMFFDI>2.0.CO;2.

Granath, J.W., 1989. Structural evolution of the Ardmore basin, Oklahoma: progressive deformation in the foreland of the Ouachita collision. Tectonics 8 (5).

Guynn, J., and Gehrels, G., 2006, Comparison of detrital zircon age distribution using the K-S test. K-S test instruction of the Arizona LaserChron Center, Retrieved from https://drive.google.com/file/d/0B9ezu34P5h8eZWZmOWUzOTItZDgyZi00NDRiLWI4ZTctNTljNTM5OTU1MGUz/view?hl=en.

Ham, E., 1973, Regional geology of the Arbuckle Mountains, Oklahoma: Oklahoma Geological Survey Guidebook 17, 52 p.

Hanson, R. E., Puckett, R. E. Jr., Keller, G. R., Brueseke, M. E., Bulen, C. L., Mertzman, S. A., Finegan, S. A., & McCleery, D. A., 2013, Intraplate magmatism related to opening of the southern Iapetus Ocean: Cambrian Wichita igneous province in the Southern Oklahoma rift zone: Lithosphere, v. 174, p. 57–70. https://doi.org/10.1016/j.lithos.2012.06.003.

Hatcher Jr., R.D., 1987. Tectonics of the southern and central Appalachian internides: Annual Review of Earth and Planetary Science Letters, v. 15, p. 337–3612.

Hawissa, I. S., 1965, Depositional Environment of the Bartlesville, Red Fork, and the Lower Skinner Sandstones in Portions of Lincoln, Logan, and Payne Counties, Oklahoma [M.S. Thesis,]: University of Tulsa, 35 p.

Hay, 1996, Tectonics and climate: Geologische Rundschau, v. 85, p. 409–437, doi: 10.1007/s005310050086.

Heckel, P.H., 1972, Recognition of Ancient Shallow Marine Environments *in* Rigby, J. K., Hamblin, W. K. (eds.), Recognition of Ancient Sedimentary Environments: SEPM Society for Sedimentary Geology Special Publication, v. 16, p. 226-286.

Heckel, P. H., 1977, Origin of phosphatic black shale facies in Pennsylvanian cyclothems of midcontinent North America: American Association of Petroleum Geologists Bulletin, v. 6, no. 1, p. 1045-1068.

Heckel, P. H., 1980, Paleogeography of Eustatic Model for Deposition of Midcontinent Upper Pennsylvanian Cyclothems, *in*, Paleozoic Paleogeography of West-central United States, T. Fouch and E. Magathan (eds.): Rocky Mountain Section, Society of Economic Paleontologists and Mineralogists, Symposium 1, p. 197-215.

Heckel, P. H., 1994, Evaluation of Evidence for Glacio-Eustatic Control Over Marine Pennsylvanian Cyclothems in North America and Consideration of Possible Tectonic Effects, Tectonic and Eustatic Controls on Sedimentary Cycles, John M. Dennison, Frank R. Ettensohn: SEPM Concepts in Sedimentology and Paleontology, v. 4. https://doi.org/10.2110/csp.94.04.

Heckel, P. H., 2008, Pennsylvanian cyclothems in midcontinent North America as far-field effects of waxing and waning of Gondwana ice sheets, *in* Resolving the Late Paleozoic Ice Age in Time and Space, Christopher R. Fielding, Tracy D. Frank, John L. Isbell (eds.): Geological Society of America Special Paper, v. 441, p. 275-289, https://doi.org/10.1130/SPE441.

Hemish, L. A., 1989, Coal geology of Rogers County and western Mayes County, Oklahoma: Oklahoma Geological Survey Bulletin 144, 118 p.

Hentz, T. F., 1994, Depositional, Structural, and Sequence Framework of the Gas-Bearing Cleveland Formation (Upper Pennsylvanian), Western Anadarko Basin, Texas Panhandle: The University of Texas at Austin, Bureau of Economic Geology, Report of Investigations No. 213, 73 p.

Hoffman, P.F., 1989, Precambrian geology and tectonic history of North America, *in* Bally, A., and Palmer, A.R., (eds.), The Geology of North America-An Overview: Boulder, Colorado: Geological Society of America, Geology of North America, v. A, p. 447–512, https://doi.org/10 .1130/DNAG-GNA-A.447.

Hoffman, P.F., 1991, Did the breakout of Laurentia turn Gondwanaland inside-out: Science, v. 252, p. 1409–1412, https://doi.org/10.1126/science.252.5011.1409.

Houston, C. A., and D. R. Kerr, 2008, Sequence Stratigraphy of the Red Fork Sandstone (Middle Pennsylvanian) in the Vicinity of Southeast Thomas, Squaw Creek, and Bridgeport Fields, Anadarko Basin, Oklahoma, Online Journal for E&P Geoscientists, retrieved in 2020, at https://midcontinent.searchanddiscovery.com/abstracts/html/2008/annual/abstracts/409792.htm.

Hudson, A. S., 1969, Depositional Environment of the Red Fork and Equivalent Sandstones East of the Nemaha Ridge, Kansas and Oklahoma [M.S. Thesis]: University of Tulsa, 80 p.

Hunt, D. and Tucker, M.E., 1992, Stranded Parasequences and the Forced Regressive Wedge System Tract; Deposition during Base Level Fall: Sedimentary Geology, v. 81, p. 1-9, http://dx.doi.org/10.1016/0037-0738(92)90052-S

Ingersoll, R.V., Bullard, T.F., Ford, R.L., Grimm, J.P., Pickle, J.D., and Sares, S., 1984, The effect of grainsize on detrital modes: a test of the Gazzi-Dickinson point-counting method: Journal of Sedimentary Petrology, v. 54, p. 103–116.

Johnson, K.S., 1989, Geologic evolution of the Anadarko Basin: United States Geological Survey Bulletin 1866-A, 28 p.

Johnson, K.S., 1989, Geology of the Southern Midcontinent: Oklahoma Geological Survey Special Publication 89-2, 53 p.

Johnson, K. S., 2008, Earth sciences and mineral resources of Oklahoma: Oklahoma Geological Survey Educational Publication 9, 24 p.

Jordan, L., 1957, Subsurface stratigraphic names of Oklahoma: Oklahoma Geol. Survey Guidebook 6, 220 p.

Kissock, J.K., Malone, D., and Craddock, J.P., 2018, Lower–Middle Pennsylvanian strata in the North American midcontinent record the interplay between erosional unroofing of the Appalachians and eustatic sea-level rise: Geosphere, v. 14, p. 141-161. https://doi.org/10.1130/GES01512.1.

Klein, G., and Hsui, A., 1987, Origin of cratonic basins: Geology, v. 15, p. 1094–1098.

Kluth, C.F., Coney, P.J, 1981, Plate tectonics of the Ancestral Rocky Mountains: Geology, v. 9, no.1, p. 10–15.

Kluth, C.F., 1986, Plate tectonics of the ancestral Rocky Mountains, *in* Peterson, J.A., (eds.), Paleotectonics and Sedimentation in the Rocky Mountain Region: American Association of Petroleum Geologists Memoir 41, p. 353–369.

Konstantinou, A., Wirth, K. R., Vervoort, J. D., Malone, D. H., Davidson, C., and Craddock, J. P., 2014, Provenance of quartz arenites of the early Paleozoic Midcontinent region, USA: Journal of Geology, v. 122, no. 2, p. 201–216, https://doi.org/10.1086/675327.

Kushner, B.E., 2018, Heterogeneity of clastic provenance to the Anadarko Basin and implications for paleomorphology [M.S. thesis]: University of Oklahoma, 61p.

Kutzbach, J., Vavrus, S., Ruddiman, and Philippon-Berthier, G., 2011, Comparisons of atmosphere–ocean simulations of greenhouse gas-induced climate change for pre-industrial and hypothetical ‘no-anthropogenic’ radiative forcing, relative to present day: The Holocene, v. 21, p. 793–801, doi: 10.1177/0959683611400200.

Lambert, N.J, 2006, Interpretation of the upper Red Fork valley in the Anadarko Basin: a comparison study between processed, reprocessed, and high frequency seismic data [M.S. Thesis]: Oklahoma State University, 55 p.

Lange, J. P., 2003, Stratigraphy, Depositional Environments and Coalbed Methane Resources of Cherokee Group Coals (Middle Pennsylvanian), Southeastern Kansas: Kansas Geological Survey Open-File Report 82, 158 p.

Mángano, M.G., Buatois, L.A., 2004, Ichnology of Carboniferous tide-influenced environments and tidal flat variability in the North American Midcontinent *in* McIlroy, D. (ed.), The Application of Ichnology to Palaeoenvironmental and Stratigraphic Analysis: Geological Society of London Special Publication, v. 228, p. 157–178.

McKee, E.D., and Oriel, S.S., 1967, Paleotectonic Investigations of the Permian Systems in the United States: U.S. Geological Survey Professional Paper 515, 268 p.

McKee, E.D., and Crosby, E.J., coordinators, 1975, Paleotectonic investigations of the Pennsylvanian System in the United States: U.S. Geological Survey Professional Paper 853, Part I, 349 p.

McLaughlin, P.P., Jr., 2005, Sequence Stratigraphy *in* R. C. Selley, L. R. M. Cocks, I. R. Plimer, Encyclopedia of Geology: Elsevier, p. 159-173.

Miller, C.F., Hatcher, R.D., Jr., Ayers, J.C., Coath, C.D., and Harrison, T.M., 2000, Age and zircon inheritance of eastern Blue Ridge plutons, southwestern North Carolina and northeastern Georgia, with implications for magma history and evolution of the southern Appalachian orogen: American Journal of Science, v. 300, p. 142–172.

Mitchell, J., 2011, Horizontal drilling of deep Granite Wash reservoirs, Anadarko Basin, Oklahoma and Texas: Shale Shaker, v. 62, p. 118-167.

Mithcum, R.M., Vail, P.R., and Thompson, S., 1977, Seismic stratigraphy and global changes in sea level, Part 2: The depositional sequence as a basic unit for stratigraphic analysis, *in* Payton, C.E (ed.), Seismic stratigraphy applications to hydrocarbon exploration: American Association of Petroleum Geologists Memoir 26, p. 53-62.

Montañez, I.P., and Poulsen, C.J., 2013, The Late Paleozoic Ice Age: An Evolving Paradigm: Annual Review of Earth and Planetary Sciences, v. 41, p. 629–656, doi: 10.1146/annurev.earth.031208.100118.

Moore, G. E.,1979, Pennsylvanian Paleogeography of the Southern Mid-Continent, *in* Hyne, N.J., (ed.), Pennsylvanian sandstones of the mid-continent: Tulsa Geological Society Special Publication 1, p. 2-12.

Mueller, P.A., Heatherington, A.L., Wooden, J.L., Shuster, R.D., Nutman, A.P., and Williams, I.S., 1994, Precambrian zircons from the Florida basement: A Gondwanan connection: Geology, v. 22, p. 119–122, https://doi.org/10.1130/0091-7613(1994)0222.3.CO;2.

Murphy, J.B., Pisarevsky, S.A., Nance, R.D., and Keppie, J.D., 2004, Neoproterozoic–early Paleozoic evolution of peri-Gondwanan terranes: Implications for Laurentia–Gondwana connections: International Journal of Earth Sciences, v. 93, p. 659–682, https://doi.org/10.1007/s00531-004-0412-9.

Park, Barbeau, D. L. Jr., Rickenbaker, A., Bachmann-Krug, D., & Gehrels, G., 2010, Application of foreland basin detrital zircon geochronology to the reconstruction of the Southern and Central Appalachian Orogen: Journal of Geology, v. 118, p. 23–44.

Parrish, J.T., 1993, Climate of the Supercontinent Pangea: The Journal of Geology, v. 101, p. 215–233, doi: 10.1086/648217.

Perry, J., 1989, Tectonic Evolution of the Anadarko Basin Region, Oklahoma: U.S. Geological Survey Bulletin 1866-A, p. 1-19.

Peyton, L., Bottjer, R., and Partyka, G., 1998, Interpretation of incised valleys using new 3-D seismic techniques: A case history using spectral decomposition and coherency: The Leading Edge, v.17, no. 9, p. 1294-1298.

Phillips, T.L., and Peppers, R.A., 1984, Changing patterns of Pennsylvanian coal-swamp vegetation and implications of climatic control on coal occurrence: International Journal of Coal Geology, v. 3, p. 205–255, doi: 10.1016/0166-5162(84)90019-3.

Posamentier, H. W., Jervey, M. T., Vail, P. R., 1988, Eustatic controls on clastic deposition I: conceptual framework *in* C. K. Wilgus, B. S. Hastings, C. St. C. C. Kendall, *et al.* (eds.), Sea-Level Changes: An Integrated Approach: Society of Economic Paleontologists and Mineralogists, Special Publication 42, p. 109-124.

Posamentier, H. W., and Allen, G. P., 1999, Siliciclastic sequence stratigraphy: concepts and applications: SEPM Concepts in Sedimentology and Paleontology 7, p. 210.

Postma, D., 1982, Pyrite and siderite formation in brackish and freshwater swamp sediments: American Journal of Science, v. 282, p. 1151-1183.

Poulsen, C. J., Pollard, D., Montañez, I.P., Rowley, D., 2007, Late Paleozoic tropical climate response to Gondwanan deglaciation: Geology, v. 7. 35, no. 9, p. 771–774; doi: 10.1130/G23841A.1.

Powell, B.N., Gilbert, M.C., and Fischer, J.F., 1980, Lithostratigraphic classification of basement rocks of the Wichita Province, Oklahoma – Summary: Geological Society of America Bulletin, v. 91, p. 509-514.

Price, J.D., 2016, The Wichita Mountains: insights into the evolution of southern Oklahoma: SIPES Quarterly, v. 52, p. 23-27.

Puckette, J.O., Anderson, C., and Al-Shaieb, Z., 2000, The Deep-marine Red Fork sandstone: A submarine-fan complex: Oklahoma Geological Survey Circular 103, p. 177- 184.

Puckette, J.O., and Al-Shaieb, Z., 2002, The Red Fork sandstone: Overview of marine and deep-marine reservoirs: Oklahoma Geological Survey Circular 108, p. 119-133.

Puckette, J.O., 2003, Lower Skinner Valley Fill Sandstones: Attractive Exploration Targets on the Northeast Oklahoma Platform, Search and Discovery Article #10050

Puckette J.O., 2016, Influence of Provenance and Sediment Supply on Sandstone Composition and Depositional Styles: Pennsylvanian Upper Morrowan and Cherokee, Oklahoma: Why Are These Sandstones so Different? Search and Discovery Article #51223.

Pulling, D. M., 1979, Subsurface stratigraphic and structural analysis, Cherokee Group, Pottawatomie County, Oklahoma: Shale Shaker, v. 29, p. 124-137.

Qie, W., Algeo, T.J., Luo, G., and Herrmann, A., 2019, Global events of the Late Paleozoic (Early Devonian to Middle Permian): A review: Palaeogeography, Palaeoclimatology, Palaeoecology, v. 531, p. 109259, doi: 10.1016/j.palaeo.2019.109259.

Rascoe, B., Adler, F. J., 1983, Permo-Carboniferous hydrocarbon accumulations, Midcontinent, U.S.A.: American Association of Petroleum Geologists Bulletin, v. 67, p. 979-1001.

Reineck, H. E., Singh, I. B., 1980, Depositional Sedimentary Environments: Springer, Berlin, 551 p.

Retallack, G. J., 1990, Soils of the Past—An Introduction to Paleopedology: Boston, Unwin Hyman, 520 p.

Root, S., and Onasch, C.M., 1999, Structure and tectonic evolution of the transitional region between the central Appalachian foreland and interior cratonic basins: Tectonophysics, v. 305, no. 1–3, p. 205–223, doi:10.1016/S0040-1951(99)00022-0.

Schultz, R. B., Coveney, Jr., R.M., 1992, Time-dependent changes for Midcontinent Pennsylvanian black shales U.S.A.: Chemical Geology, v. 99, no. 1–3, p. 83-100.

Sharrah, K.L., 2006, Comparative study of the sedimentology and provenance of the Atoka Formation in the frontal Ouachita thrust belt, Oklahoma [M.S. thesis]: University of Tulsa, 268 p.

Shulman, C., 1966, Stratigraphic analysis of the Cherokee Group in adjacent portions of Lincoln, Logan, and Oklahoma Counties, Oklahoma: Shale Shaker Digest, v. 16, no. 2, p. 126-140.

Sloss, L. L., 1963. Sequences in the cratonic interior of North America. Geological Society of America Bulletin, v. 74, p. 93–114. https://doi.org/10.1130/0016-7606(1963)74[93:SITCIO]2.0.CO;2

Sloss, L.L., 1988, Tectonic evolution of the craton in Phanerozoic time, in Sloss, L.L. (ed.), Sedimentary Cover—North American Craton: U.S.: Boulder, Colorado, Geological Society of America, The Geology of North America, v. D-2, p. 25–51.

Soreghan, G.S., 1994, Stratigraphic responses to geologic processes: Late Pennsylvanian eustasy and tectonics in the Pedregosa and Orogrande Basins: Geological Society of America Bulletin, v. 106, p. 1195-1211.

Soreghan, G.S., 1994, The impact of glacioclimatic change on Pennsylvanian cyclostratigraphy, *in*, Embry, A.F., Beauchamp, B., and Glass, D.J. (eds.), Pangea–Global environments and resources: Canadian Society of Petroleum Geologists Memoir 17, p. 523-543.

Soreghan, M.J., Soreghan, G.S., and Hamilton, M.A., 2002, Paleowinds inferred from detrital-zircon geochronology of Upper Paleozoic loessite, western equatorial Pangea: Geology, v. 30, p. 695–698, https://doi.org/10.1130/0091-7613(2002)0302.0.CO;2.

Soreghan, G. S., Keller, G. R., Gilbert, M. C., Chase, C.G., and Sweet, D. E., 2012, Load-induced subsidence of the Ancestral Rocky Mountains recorded by preservation of Permian landscapes: Geosphere, v. 8, no. 3, p. 654-668.

Soreghan, G.S., and Soreghan, M.J., 2013, Tracing clastic delivery to the Permian Delaware Basin, U.S.A.: Implications for paleogeography and circulation in westernmost equatorial Pangea: Journal of Sedimentary Research, v. 83, p. 786–802, https://doi.org/10.2110/jsr.2013.63.

Soreghan, M.J., Swift, M.M., and Soreghan, G.S., 2018, Provenance of Permian eolian and related strata in the North American midcontinent: Tectonic and climatic controls on sediment dispersal in western tropical Pangea, *in,* Ingersoll, R.V., Lawton, T.F., and Graham, S.A., eds., Tectonics, Sedimentary Basins, and Provenance: A Celebration of William R. Dickinson's Career: Geological Society of America Special Paper 540, p. 1–27, https://doi.org/10.1130/2018.2540(28).

Suarez, Y., K.J. Marfurt, and M. Falk, 2008, Seismic attribute-assisted interpretation of channel geometries and infill lithology: A case study of Anadarko Basin Red Fork channels, 78th Annual International Meeting, SEG, Expanded Abstracts, p. 1-4.

Tate, L., 1985, The Depositional Environment, Petrology, Diagenesis, and Petroleum Geology of the Red Fork Sandstone in Central Oklahoma [M.S. Thesis]: Oklahoma State University, p. 1-190.

Thomas, A., 1977, Evolution of Ouachita-Appalachian salients and recesses from restaints and promontories in the continental margin: American Journal of Science, v. 277, p. 1233-1278.

Thomas, A., Becker, T.P., Samson, S.D., and Hamilton, M.A., 2004, Detrital zircon evidence of a recycled orogenic foreland provenance for Alleghenian clastic-wedge sandstones: The Journal of Geology, v. 112, p. 23–37.

Thomas, W. A., 2011, Detrital-zircon Geochronology and Sedimentary Provenance, Lithosphere, v. 3, no. 4, p. 304-308.

Thomas, A., Gehrels, G.E., and Romero, M.C., 2016, Detrital zircons from crystalline rocks along the Southern Oklahoma fault system, Wichita and Arbuckle Mountains, USA: Geosphere, v. 12, p. 1224–1234, https://doi.org/10.1130/GES01316.1.

Thomas, A., Gehrels, G.E., Greb, S.F., Nadon, G.C., Satkoski, A.M., and Romero, M.C., 2017, Detrital zircons and sediment dispersal in the Appalachian foreland: Geosphere, v. 13, p 2206-2230.

Thomas, A., Gehrels, G.E., Sundell, K.E., Greb, S.F., Finzel, E.S., Clark, R.J., Malone, D., Hampton, B.A., Romero, M.C., 2020, Detrital zircons and sediment dispersal in the eastern midcontinent of North America. Geosphere, v. 16, p. 817–843. doi: https://doi.org/10.1130/GES02152.1.

Tunin, Z. T., 2020, Detrital Zircon Geochronology and Provenance Analysis of the Desmoinesian (Middle Pennsylvanian) Bartlesville and Red Fork Sandstones, Cherokee

Platform and Anadarko Basin, Oklahoma [M.S. Thesis]: Oklahoma State University, Stillwater, Oklahoma, 97 p.

Turko, M., 2019, Structural Analysis of the Wichita Uplift and Structures in the Southeast Anadarko Basin, Southern Oklahoma [PhD Dissertation]: University of Oklahoma, p. 1-188.

Turko, M., Mitra, S., 2021, Macroscopic structural styles in the southeastern Anadarko Basin, southern Oklahoma: Elsevier, Marine and Petroleum Geology, v. 125, p. 1-18.

Turner, G.L., 1957, Paleozoic stratigraphy of the Fort Worth basin, *in* 1957 Joint Field Trip Guidebook: Abilene Geological Society and Fort Worth Geological Society, p. 57–7.

Van Schmus, R., Bickford, M.E., Sims, P.K., Anderson, J.L., Shearer, C.K., and Treves, S.B., 1993, Proterozoic geology of the western midcontinent region, *in* Reed, J.C., Bickford, M.E., Houston, R.S., Link, P.K., Rankin, D., Sims, P.K., and Van Schmus, R. (eds.), Precambrian Conterminous U.S.: Boulder, Colorado, Geological Society of America, Geology of North America, v. C, no. 2, p. 239–259.

Van Schmus, R., Bickford, M.E., and Turek, A., 1996, Proterozoic geology of the east-central midcontinent basement, *in* van der Pluijm, B.A., and Catacosinos, P.A., (eds.), Basement and Basins of Eastern North America: Geological Society of America Special Paper 308, p. 7–32, https://doi .org/10.1130/0-8137-2308-6.7.

Van Wagoner, J. C., 1985, Reservoir Facies Distribution as Controlled by Sea-Level Change: SEPM Mid-Year Meeting, Golden, Colorado, p. 91-92.

Van Wagoner, J.C., Posamentier, H.W., Mitchum, R.M., Vail, P.R., Sarg, J.F., Loutit, T.S., and Hardenbol, J., 1988, An overview of sequence stratigraphy and key definitions, *in* C. W. Wilgus et. al. (eds.), Sea level changes, an integrated approach: Society of Economic Paleontologists and Mineralogists Special Publication 42, p. 39-45.

Van Wagoner, J.C., Mitchum, R.M., Campion, K.M., and Rahmanian, V.D., 1990, Siliciclastic Sequence Stratigraphy in Well Logs, Cores, and Outcrops: AAPG Methods in Exploration Series 7, 55 p.

Van Wagoner, J.C., 1995, Sequence stratigraphy and marine to nonmarine facies architecture of foreland basin strata, Book Cliffs, Utah, USA *in* Van Wagoner, J. C., Bertram, G. T. (eds.), Sequence Stratigraphy of Foreland Basin Deposits: Outcrop and Subsurface Examples from the Cretaceous of North America: American Association of Petroleum Geologists, Memoir 64, v. 64, p. 137-223.

Verish, N. P., 1979, Reservoir trends, depositional environments, and petroleum geology of selected Cherokee sandstones in T11-13N, R4-5E: Shale Shaker, v. 29, no. 9, p. 209-236.

Vermeesch, P., 2012, On the visualization of detrital age distributions, Chemical Geology, v. 312, p. 190–194.

Visher, G.S., Saitta S.B., 1971, Pennsylvanian Delta Patterns and Petroleum Occurrences in Eastern Oklahoma: AAPG Bulletin, v. 55, no. 8, p. 1206-1230, doi: 10.1306/819a3cd4-16c5-11d7-8645000102c1865d.

Walker, r. k., 1982, Structural geology and distribution of lower and middle Pennsylvanian sandstones in adjacent portions of Lincoln, Okfuskee, Seminole, and Pottawatomie Counties, Oklahoma [M.S. Thesis]: Oklahoma State University, 56 p.

Wallet, B. C., Davugustto, O., Daber, R., Marfurt K. J, 2012, Using an HSV color map to visualize spectral phase and magnitude information for an incised valley system in the Anadarko Basin, Oklahoma, USA: SEG Las Vegas 2021 Annual Meeting, p. 1-6, doi http://dx.doi.org/10.1190/segam2012-0497.1.

Wang, W., and Bidgoli, T. S., 2019, Detrital Zircon Geochronologic Constraints on Patterns and Drivers of Continental-Scale Sediment Dispersal in the Late Mississippian: Geochemistry, Geophysics, Geosystems, v. 20, p. 5522-5543.

Whitmeyer, S. J., & Karlstrom, K. E., 2007, Tectonic Model for the Proterozoic Growth of North America: Geosphere, v. 3, p. 220–259. https://doi.org/10.1130/GES00055.1

Withrow, P.C., 1968, Depositional Environments of Pennsylvanian Red Fork Sandstone in Northeastern Anadarko Basin, Oklahoma: AAPG Bulletin, v. 52, no. 9, p. 1638-1654, doi: 10.1306/5d25c4c1-16c1-11d7-8645000102c1865d.

Wright, J. E., Hogan, J. P., and Gilbert, M. C., 1996, The Southern Oklahoma Aulacogen: Not just Another BLIP: American Geophysical Union Transactions, v. 77, no. 46, p. F845.

Xie, X., Patrick M. O'Connor, P.M., and Alsleben, 2016, Carboniferous Sediment Dispersal in the Appalachian–Ouachita juncture: Provenance of Selected Late Mississippian Sandstones in the Black Warrior Basin, Mississippi, United States: Sedimentary Geology, v. 342, p. 191-201.

Ye, L., and Kerr, D., 2000, Sequence Stratigraphy of the Middle Pennsylvanian Bartlesville Sandstone, Northeastern Oklahoma: A Case of an Underfilled Incised Valley: American Association of Petroleum Geologists Bulletin, v. 84, no. 8, p. 1185–1204.

Zaitlin, B. A., Dalrymple, R. W., and Boyd, R., 1994, The Stratigraphic Organization of Incised-Valley Systems Associated with Relative Sea-Level Change *in* R. W. Dalrymple, and B. A. Zaitlin, (eds.), Incised-Valley Systems: Origin and Sedimentary Sequences: SEPM Special Publication 51, p. 45–60.

APPENDICES

APPENDIX A: STRATIGRAPHIC CROSS SECTIONS

Table 9. Well information for this study's stratigraphic cross sections.

Well ID	API	Well Name	Operator	Tw, Rg, Sec, Q	Latitude	Longitude	County	TVD (ft)
1	3507124 8810000	FORD 1	BLUE OX PARTNERS LLC	29N 4E 27 SE NE SE	36.960325	-96.850988	KAY	3345
2	3507123 3380000	LARRY 1	QUAIL OIL&GAS LLC	28N 3E 13 SW4	36.901697	-96.935448	KAY	3274
3	3507124 6840000	STEICHEN D 2	CEJA CORPORATION	25N 1E 13 NE NW NW	36.651	-97.153746	KAY	4144
4	3507124 3920000	SALTFORK 6	DAVIS GARRY OIL LLC	25N 1E 35 SW SW NW	36.602948	-97.172745	KAY	4634
5	3510323 5960000	NEW BLISS 1	XANADU EXPLORATION COMPANY	24N 1E 2 SW4 SE4	36.581502	-97.16542	NOBLE	4730
6	3510323 3010000	COCKRELL 1	EOG RESOURCES	23N 1E 8 NW4 NE4	36.49021	-97.216746	NOBLE	5000
7	3510321 9730000	VOSS 1	VALIDUS INC	22N 1E 30 SW4 NW4	36.355686	-97.243821	NOBLE	4923
8	3510324 5420000	HARTSUC K SWD	DORADO ENERGY LLC	20N 1W 9 SW SW SW	36.217582	-97.316543	NOBLE	6675
9	3508321 2820000	MEYER 1	NERCO OIL & GAS, INC.	19N 2W 1 CNW4 NE4	36.15741	-97.361175	LOGAN	5363
10	3508322 2060000	WEBB 1	SANDSTONE RESOURCES, INC.	19N 2W 25 NE4 NE4	36.098616	-97.357695	LOGAN	5560
11	3508320 9270000	J R FLASCH	UNIVERSAL DRILLING CO., INC.	17N 2W 2 SE4 NW4	35.980172	-97.382009	LOGAN	5640
12	3508323 9550000	CANNON	ELDER CRAIG OIL AND GAS LLC	16N 2W 14 SE SW SW	35.856548	-97.387005	LOGAN	5759
13	3508323 8990000	EEA 1	GLB EXPLORATION INC	15N 2W 22 NW SE SW	35.756682	-97.40234	LOGAN	7000
14	3510921 5850000	SNEED 1-27	DSM EXPLORATION INC	14N 2W 27 NE SE NW	35.66243	-97.399992	OK	6078
15	3510921 4570000	AGAR 1-32	ALPINE OIL & GAS INC	14N 1W 32 SE NW SE	35.642537	-97.323523	OK	6450
16	3510920 9650000	CLEMENTS 30-1	EL DORADO DRILLING INC	13N 1E 30 W2 NE NW	35.578129	-97.241574	OK	5850
17	3510921 9700000	DAVIS 1-11	INDIAN OIL CO	13N 1W 11 N2 SE NE	35.618964	-97.266818	OK	5750
18	3510920 6030000	CANAAN 2	AMSTAR OIL	12N 1E 8 SW NE NE	35.533499	-97.215266	OK	6176
19	3512522 4870000	HIGDON	REGENCY EXPLORATION INC	11N 2E 28 N2 NW4 NE	35.404894	-97.096466	PWTOMIE	6025
20	3512520 9620000	HALBERT 1	EASON OIL COMPANY	11N 2E 34 NW4 SW4	35.383147	-97.085998	PWTOMIE	5760
21	3512521 0550000	STATE16 FARRIS 1	TRIAD ENERGY CORP OF TEXAS	10N 3E 16 SW4 SW4	35.33418	-96.99757	PWTOMIE	5168
22	3512522 0870000	MARY HARTLEY 1	BLUE QUAIL ENTERPRISES INC	10N 3E 25 SW4 SW4	35.306933	-96.940211	PWTOMIE	5438

23	3508120 7990000	NELSON ORR ET AL 1	JEFFERSON-WILLIAMS ENERGY CORP	15N 2E 16 SE	35.769578	-97.093319	LINCOLN	5270
24	3508121 8780000	NICKELL 10-1	TEX-OK PETROLEUM INCORPORATED	13N 4E 10 SW	35.613752	-96.872342	LINCOLN	5875
25	3508122 5980000	LEGAKO 1	C & C EXPLORATION	14N 3E 6 NE SE NW	35.719341	-97.026868	LINCOLN	5175
26	3508321 0900000	HOPFER 1	ALPHA DRILLING INCORPORATED	19N 3W 25 C NE NE	36.099652	-97.463418	LOGAN	5757
27	3508320 6170000	BROWN 3	DARNELL BOBBY J	18N 2W 29 C SE NE	36.008695	-97.427289	LOGAN	5757
28	3508320 9270000	J R FLASCH	UNIVERSAL DRILLING COMPANY	17N 2W 4 SE NW			LOGAN	5640
29	3508320 5300000	PRIESS 1	BLUEBELL OIL & GAS CO	17N 1W 8 SW SW NE	35.964516	-97.325608	LOGAN	5166
30	3504720 5970000	POPE 1	DUNCAN W & ANDERSON R C	24N 7W 10 SW NW	36.575156	-97.93888	GRFIELD	6505
31	3504720 5200000	GROENDY KE A-1	JONES & PELLOW OIL CO	23N 7W 12 C NE SE	36.483203	-97.891943	GRFIELD	6850
32	3504720 5500000	WOODRIN G AIRPORT 1	CLEARY PETROLEUM CORP	22N 6W 24 C S2 NW	36.37062	-97.796168	GRFIELD	6836
33	3504720 3930000	BENTZ-4 1	RODMAN GAS COMPANY & BASIN PETROLEUM	20N 4W 4 C SE SE	36.233901	-97.623681	GRFIELD	6707

**Tw = township; Rg = range; Sec = section; Q = quarter; TVD = total vertical depth*

Noble County Cross Section

The Noble County cross section is also a northeast-southwest section crossing the northern portion of the study area from T.24N., R.1E. to T.20N., R.1W. (Fig. 70). Sandstones of the Red Fork are not well developed in wells of this cross section as Gamma-Ray (GR) log patterns lack characteristic blocky/bell shapes suggestive of channelized sandstone packages. However, thin fining-upward sequences of less than 10 ft exist is wells 5 and 8. The Inola Limestone is present in this area, but its correlation lacks accuracy due to a loss of its characteristic GR log pattern towards the southwest (Fig. 70). The Bartlesville Sandstone is also present in this area. Non-channel deposits of the Red Fork Sandstone are illustrated in all the wells and they display characteristic interbedded “ratty” sandstone/shale and gamma-ray “hugging” shale (with no distinct fining- or coarsening-upward trends) patterns suggestive of marginal marine to marine (prodeltaic) deposits. Thinning of the Red Fork interval is observed from wells 5, 6, 7, to well 8. The section thins out from 330 ft in well 5 to approximately 250 ft in well 8 (Fig. 70).

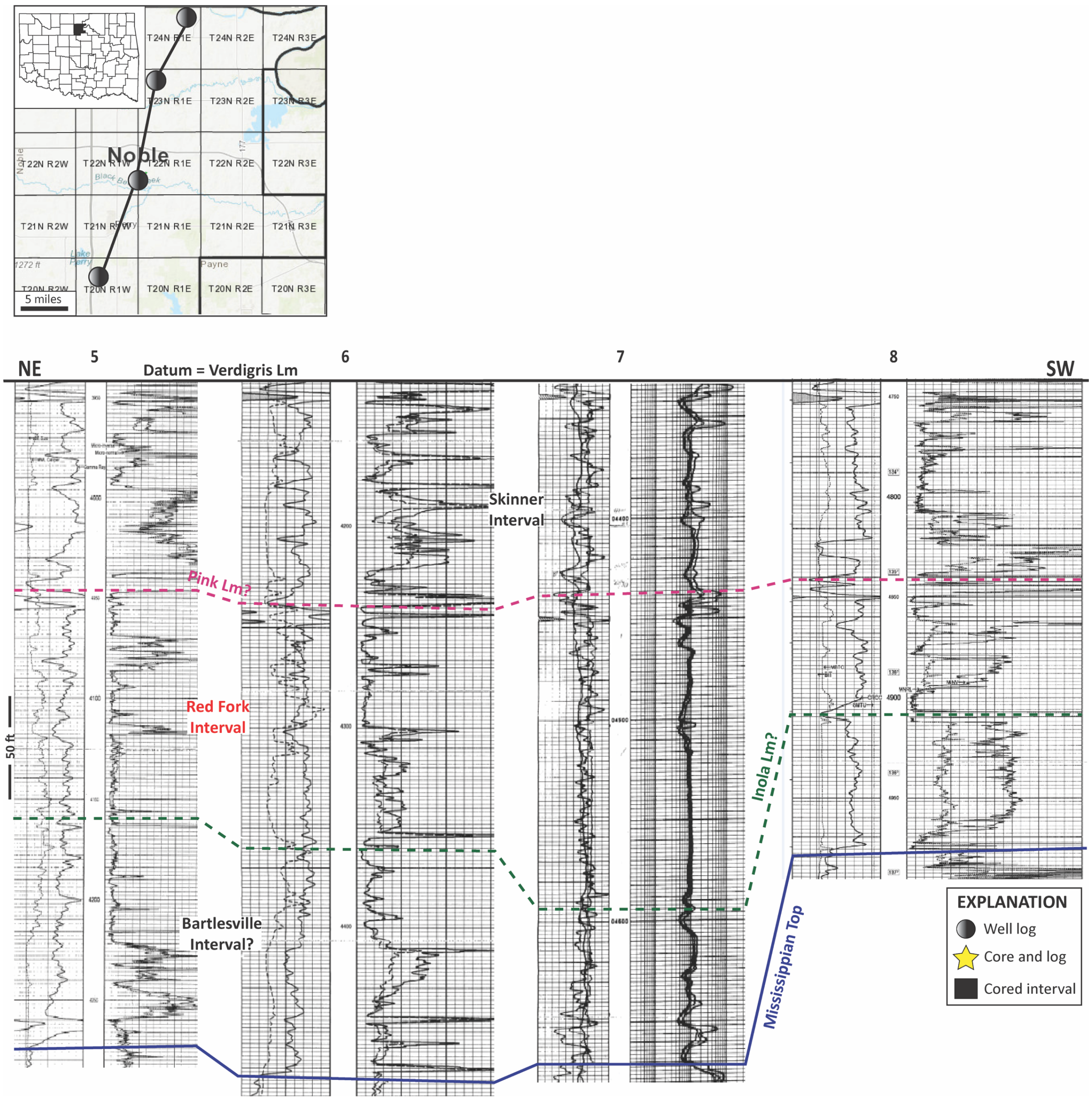

Figure 70. Northeast-southwest stratigraphic cross section of the middle and lower Cherokee Group in Noble County. The Verdigris Limestone is the stratigraphic datum. IVF = incised valley fill. The left and right logs are Gamma-Ray (GR) and Resistivity logs, respectively.

Garfield County Cross Section

The Garfield County cross section is a northwest-southeast section crossing the extreme northern portion of the study area from T.24N., R.7W. to T.20N., R.4W. (Fig. 71). The Red Fork Sandstone is well developed in wells 30, 31, and 33, displaying a blocky well log pattern, characteristic fining upward sequence that cuts underlying strata (abrupt basal contact), indicative of channel-fill (incised valley fill) deposits. That suggestion is also supported by the overall valley incision (lateral) pattern displayed by the lower Mississippian top correlation. Sand packages in wells 30 and 33 are minor channel deposits due to their low thicknesses. Thickness of the channel-fill deposits range from 10 ft to 35 ft. Non-channel deposits of the Red Fork Sandstone are illustrated in all wells and they display coarsening upward sequence trend, characteristic interbedded "ratty" sandstone/shale and gamma-ray "hugging" shale (with no distinct fining- or coarsening-upward trends) patterns suggestive of marginal marine to marine deposits.

A significant feature observed in this cross section is overall thickening and thinning of the Cherokee interval from the base of the Verdigris Limestone to top of the Mississippian Limestone. The interval thickens from 250 ft in well 30 to 310 ft in well 32 and thins back to 280 ft in well 4. Similarly, the Red Fork interval displays a thinning-thickening pattern from the Pink Limestone to the Inola Limestone. The section thickens from 70 ft in well 30 to 100 ft in well 32 and thins back to 55 ft in well 3.

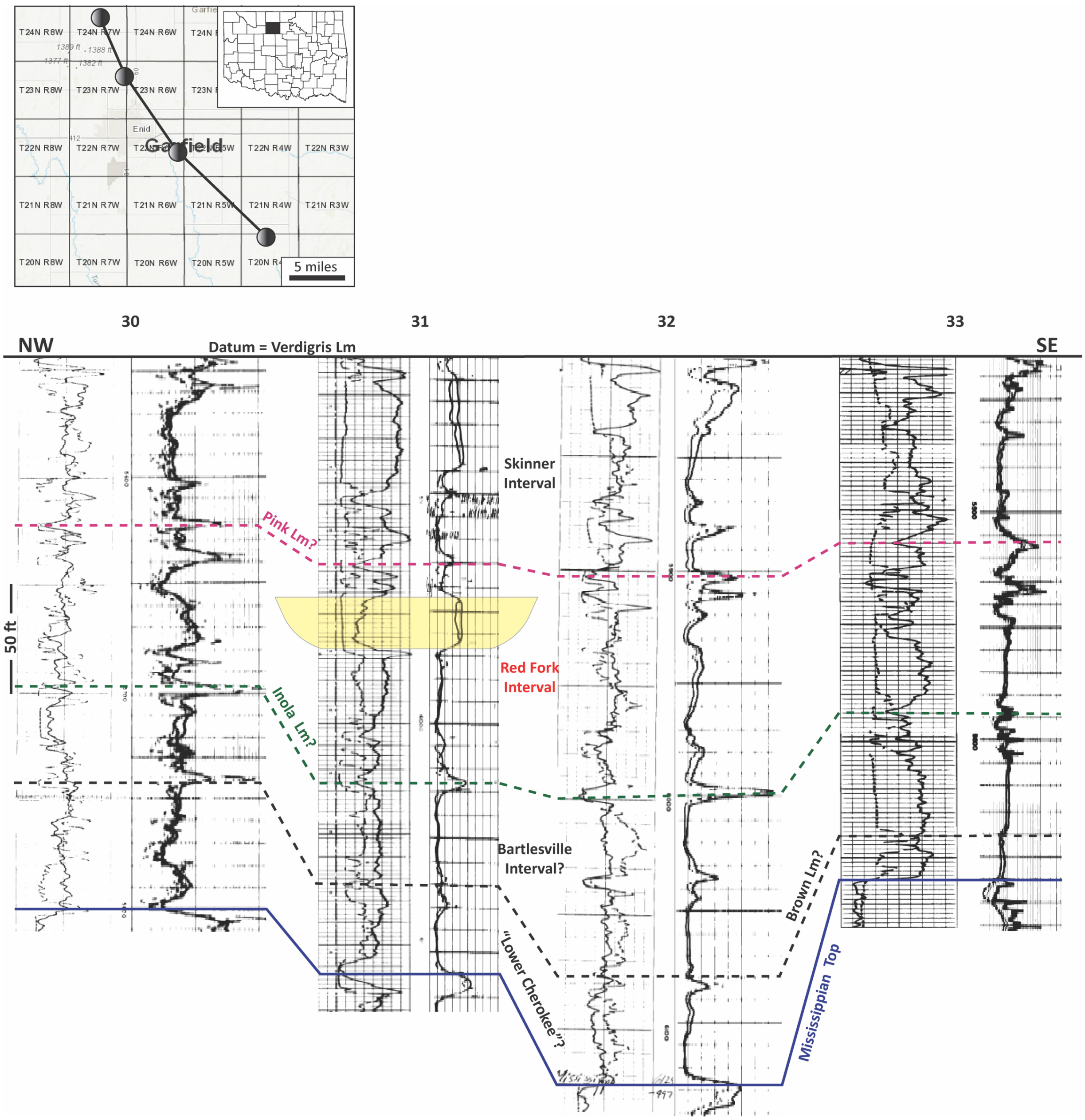

Figure 71. Northwest-southeast stratigraphic cross section of the middle and lower Cherokee Group in Garfield County. The Verdigris Limestone is the stratigraphic datum. IVF = incised valley fill. The left and right logs are Gamma-Ray (GR) and Resistivity logs, respectively.

Oklahoma County Cross Section

The Oklahoma County cross section is also a northwest-southeast section crossing the northern portion of the study area from T.14N., R.2W. to T.12N., R.1E. (Fig. 72). Sandstones of the Red Fork are not well developed in wells of this cross section as Gamma-Ray (GR) log patterns lack characteristic blocky/bell shapes suggestive of channelized sandstone packages. However, very minor fining-upward sequences of less than 5 ft exist on these wells. The Inola Limestone is present throughout this area. Non-channel deposits of the Red Fork Sandstone are dominant in the area and they display characteristic interbedded “ratty” sandstone/shale and gamma-ray “hugging” shale (with no distinct fining- or coarsening-upward trends) patterns suggestive of marginal marine to marine (prodeltaic) deposits. Thickening of the Red Fork interval is observed from northwest to southeast wells. The section thickens out from 90 ft in well 14 to approximately150 ft in well 16 and thins a little down to 130 ft in well 18 (Fig. 72).

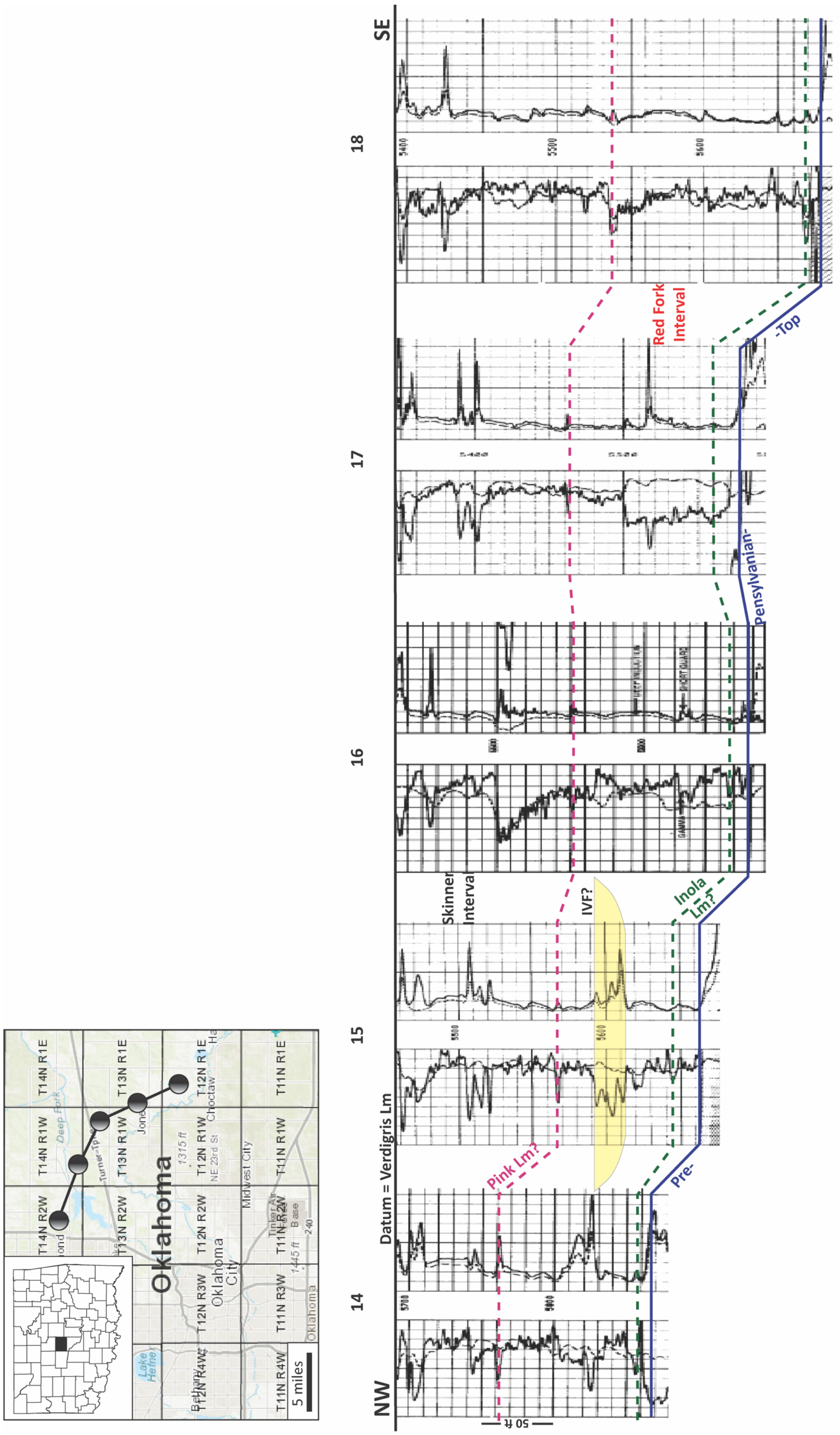

NW
SE
Datum = Verdigris Lm
14
15
16
17
18
Pink Lm?
IVF?
Skinner Interval
Inola Lm?
Red Fork Interval
Pre-
Pensylvanian-
-Top
50 ft
Oklahoma
5 miles

Figure 72. Northwest-southeast stratigraphic cross section of the middle and lower Cherokee Group in Oklahoma County. The Verdigris Limestone is the stratigraphic datum. IVF = incised valley fill. The left and right logs are Gamma-Ray (GR) and Resistivity logs, respectively.

Lincoln County Cross Section

The Lincoln County cross section is a northwest-southeast section crossing the central portion of the study area from T.15N., R.2E. to T.13N., R.4E. (Fig. 20). The Red Fork Sandstone is well developed in well 24, displaying a blocky well log pattern, characteristic fining upward sequence that cuts underlying strata (abrupt basal contact), indicative of channel-fill (incised valley fill) deposits. The channel-fill deposit is 50 ft thick and contains two minor, less than 5 ft thick shaly beds. Non-channel deposits of the Red Fork Sandstone are illustrated in all wells and they display coarsening upward sequence trend, characteristic interbedded “ratty” sandstone/shale and gamma-ray “hugging” shale (with no distinct fining- or coarsening-upward trends) patterns suggestive of marginal marine to marine deposits.

A prominent feature observed in this cross section is overall thickening and thinning of the Cherokee interval from the base of the Verdigris Limestone to top of the Mississippian Limestone. The interval thickens from 350 ft in well 23 to 430 ft in well 24 and thins back to 350 ft in well 25. However, the Red Fork interval displays a pretty uniform thickness with only a 10 ft difference from well 23 (110 ft thick) to 24 (120 ft thick) and a 20 ft difference with well 25 (100 ft thick).

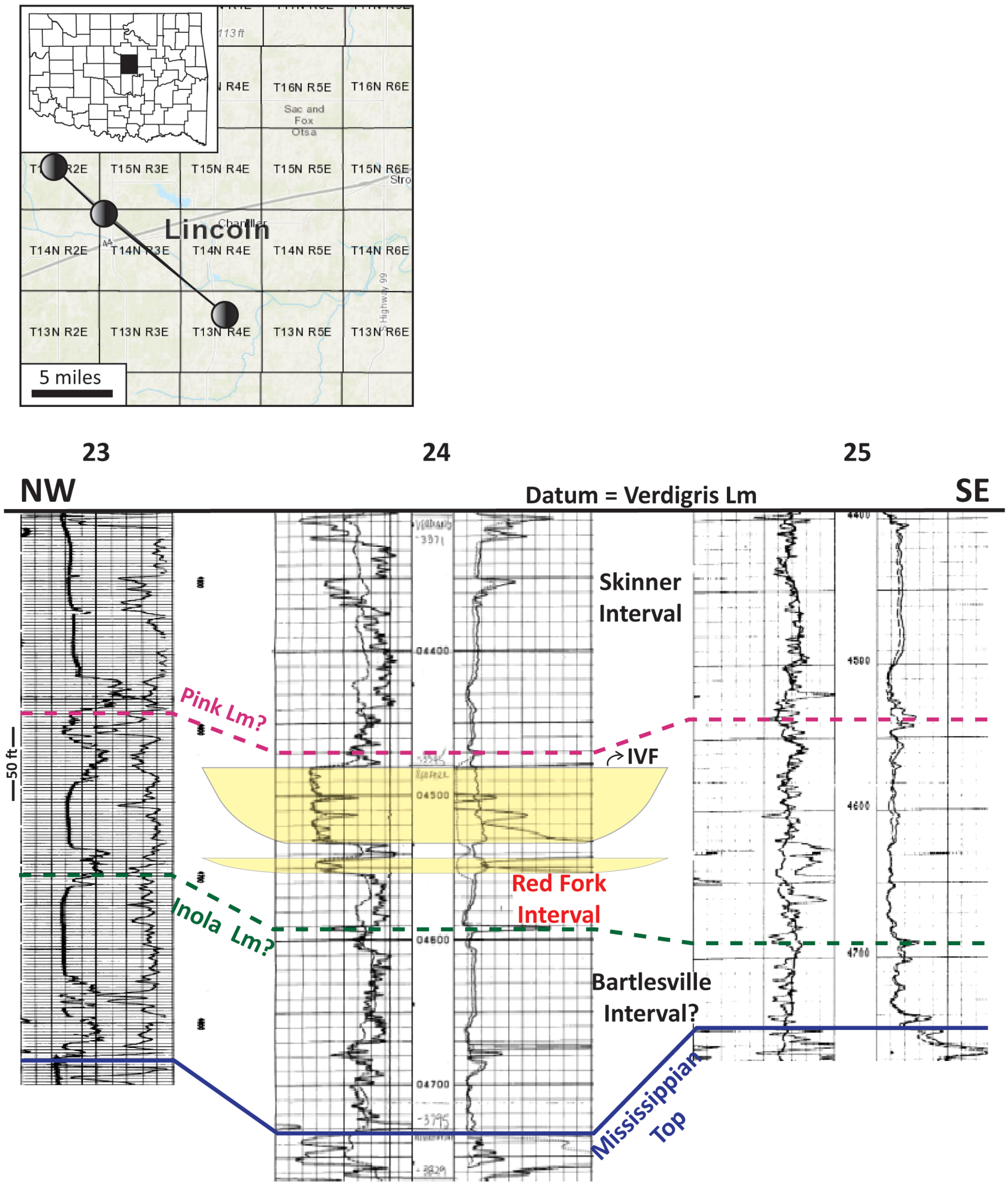

Figure 73. Northwest-southeast stratigraphic cross section of the middle and lower Cherokee Group in Lincoln County. The Verdigris Limestone is the stratigraphic datum. IVF = incised valley fill. The left and right logs are Gamma-Ray (GR) and Resistivity logs, respectively.

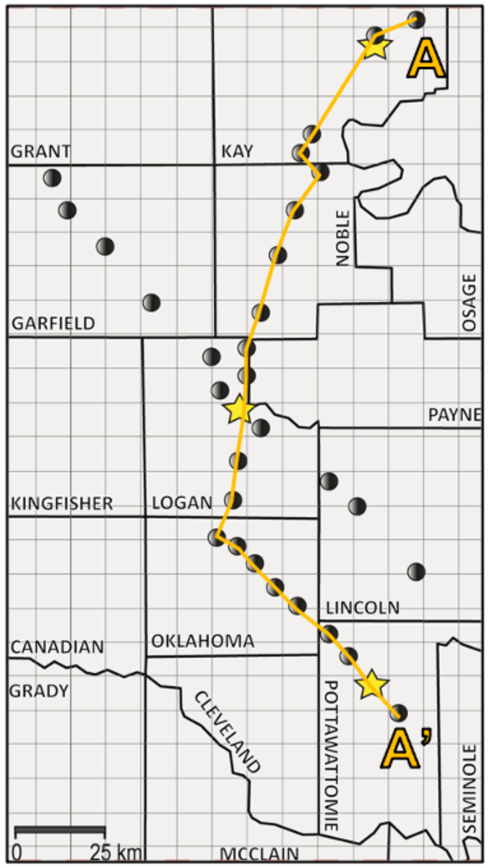

Figure 74. North-South (A-A') stratigraphic cross section of the middle and lower Cherokee Group in the study area. Yellow star= core location. Black circles= well log data location.

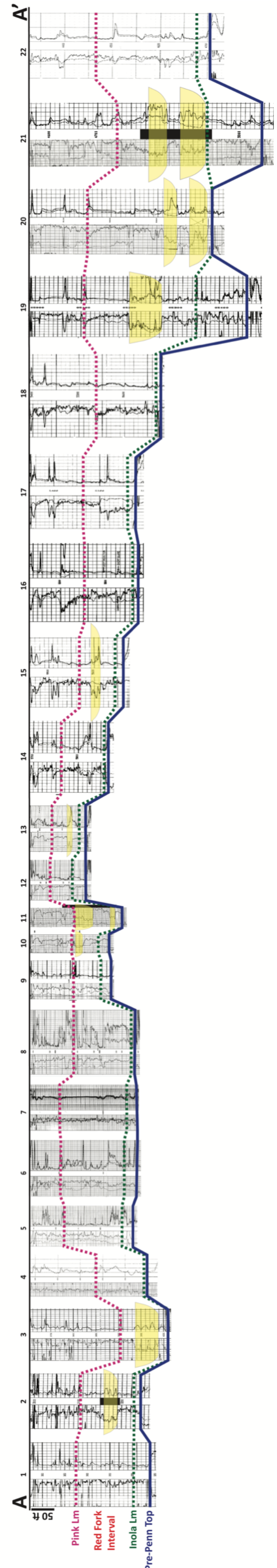
A
A'
50 ft
Pink Lm
Red Fork Interval
Inola Lm
Pre-Penn Top
1
2
3
4
5
6
7
8
9
10
11
12
13
14
15
16
17
18
19
20
21
22

Figure 75. North-South (A-A') stratigraphic cross section of the middle and lower Cherokee Group in the study area. The Verdigris Limestone is the stratigraphic datum. IVF = incised valley fill. The left and right logs are Gamma-Ray (GR) and Resistivity logs, respectively.

APPENDIX B: CORE / FACIES IMAGES & DESCRIPTIONS

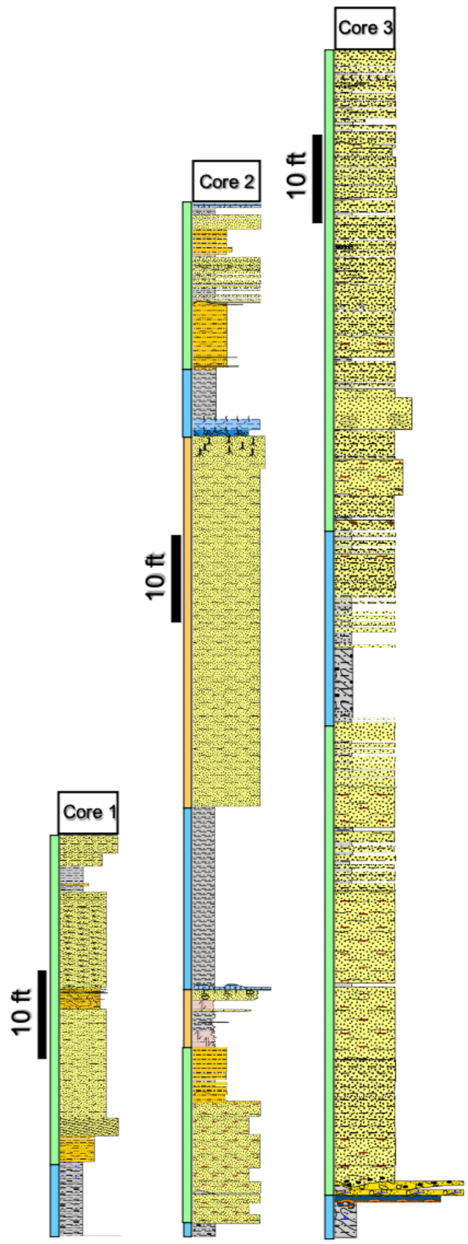

Code	Lithofacies	Depositional Process	Sedimentary Environment
	Mottled shales and sandstones	Pedogenesis of existing lithologies	Paleosol; interfluve
	Fine grained sandstone	Unidirectional tractive currents	Channel bar deposit
	Conglomerates	High energy, unidirectional tractive currents	Channel bar (basal lag)
	Black carbonaceous shales	Peat growth/accumulation without coalification	Supratidal flat / swamp
	Ripple laminated sandstone	Migration of subaqueous, unidirectional flow ripples	Tidal channel (upper unit)
	Medium to fine grained sandstones with mud drapes	Tidal currents, migration of subaqueous, bidirectional flow ripples, and slackwater sediment fallout	Tidal channel, subtidal, intertidal, or supratidal channels
	Parallel laminated sandy mudstones	Sediment fallout and low energy tidal currents	Tidal channel
	Bioturbated sandy siltstones	Storm current sediment reworking; bioturbation	Marginal marine (intertidal-supratidal); storm deposits
	Heterolithic sandstones	High energy tidal currents; slackwater sediment fallout	Upper tidal flat, channel, or coastline (subtidal-intertidal)
	Heterolithic siltstones	Low energy tidal currents and slackwater fallout; bioturbation	Lower tidal flat or subtidal coastline
	Burrowed and interbedded, sideritic sandstones and mudstones	Migration of subaqueous, bidirectional flow ripples, high-energy tidal currents; slackwater sediment fallout; bioturbation	Tidal channel; proximal delta front?
	Interlaminated and thinly interbedded sandstones and mudstones	Migration of subaqueous, bidirectional flow ripples and dunes, high-energy tidal currents; slackwater sediment fallout;	Distal delta front of tidal delta
	Skeletal wackstones to packstones	Low to high energy carbonate production; current reworking	Shallow marine; storm deposit
	Shaly carbonates	High energy carbonate reworking; current reworking	Shallow / deep marine; transgressive lag
	Gray sideritic shales	Low energy sediment fallout; sediment reworking	Marine
	Black, thinly laminated shales	Low energy sediment fallout; sediment reworking	Offshore marine; prodelta

Marine | Marginal marine | Non-marine

Figure 76. Summary of core descriptions and interpretations of the depositional environments. Refer to Figure 49 or Table 4 for the numbering of the lithofacies.

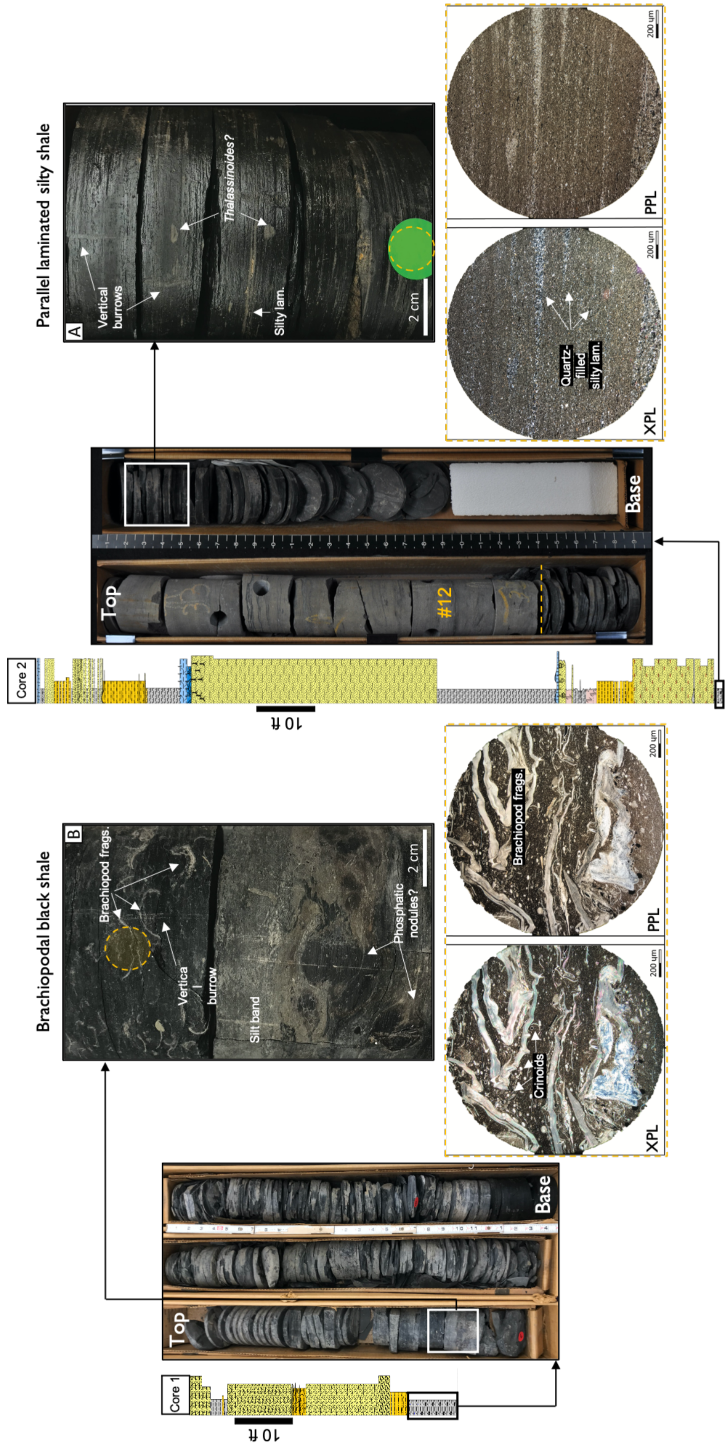

Figure 77. Core and thin section images and descriptions of the black, thinly laminated shales (Facies 1). Refer to Figure 49 or Table 4 for the explanation of facies numbers.

Figure 78. Core and thin section images and descriptions of the parallel laminated sandy mudstones (Facies 2). Refer to Figure 49 or Table 4 for the explanation of facies numbers.

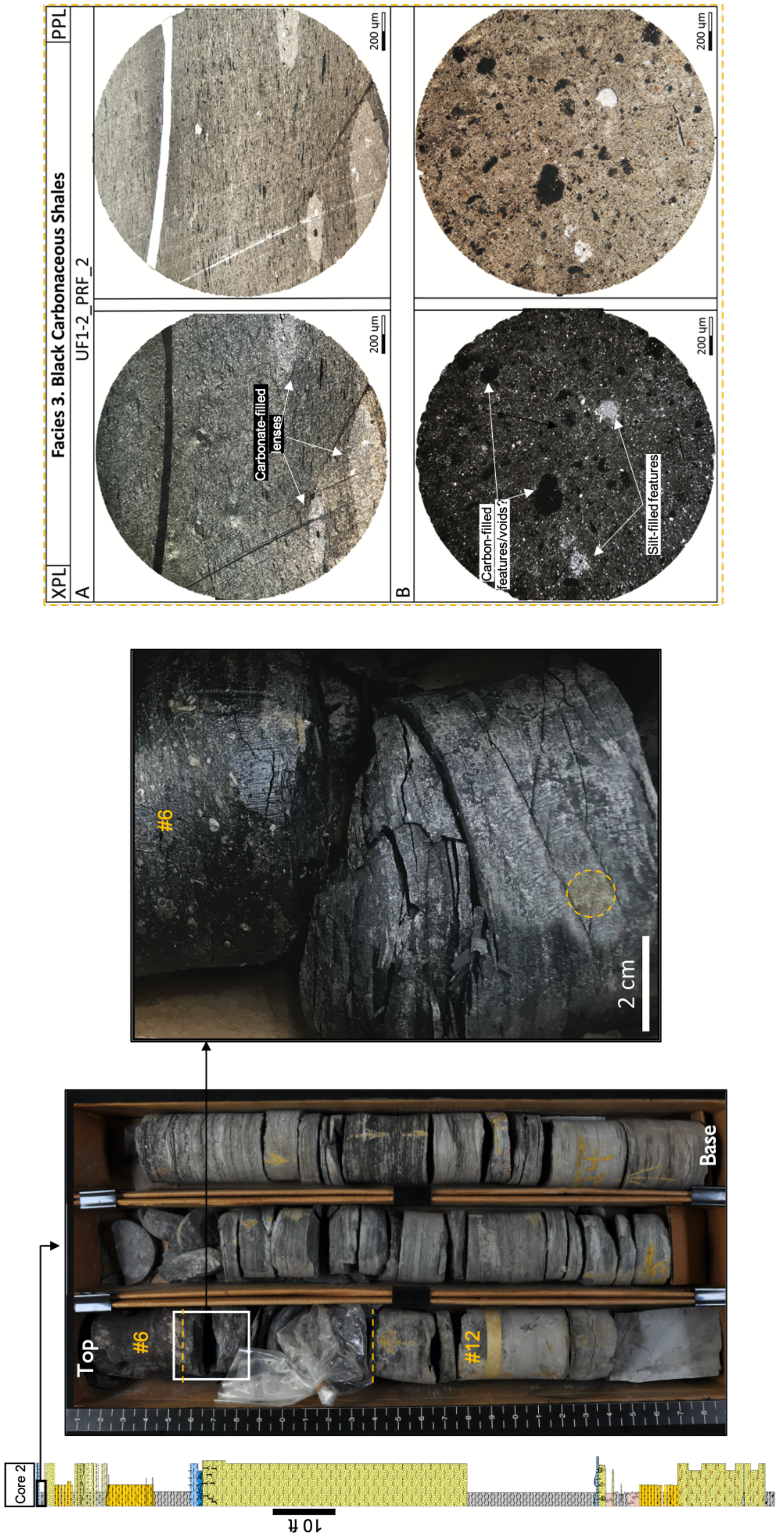

Figure 79. Core and thin section images and descriptions of the black, carbonaceous shales (Facies 3). Refer to Figure 49 or Table 4 for the explanation of facies numbers.

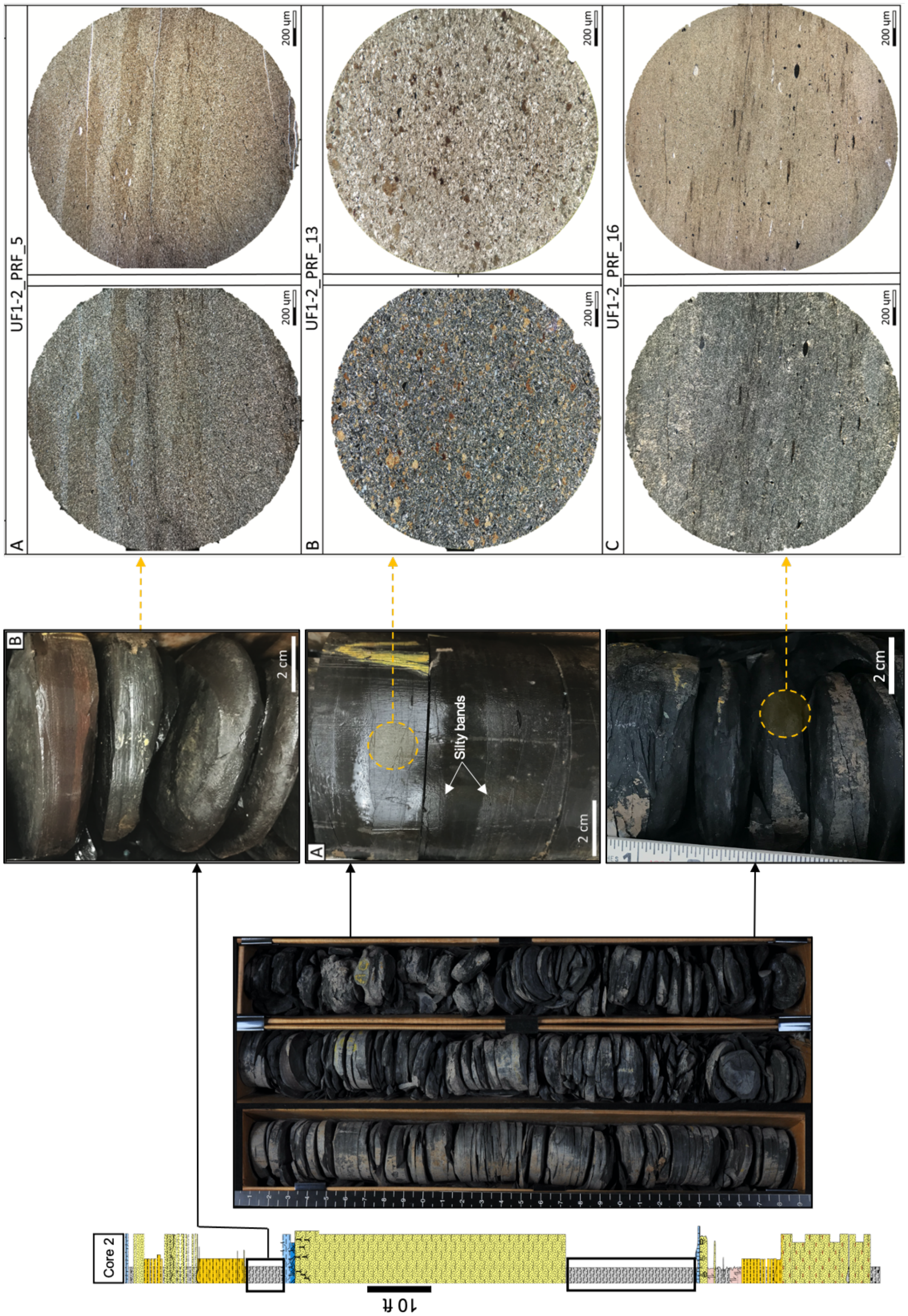

Figure 80. Core and thin section images and descriptions of the gray, sideritic shales (Facies 4). Refer to Figure 49 or Table 4 for the explanation of facies numbers.

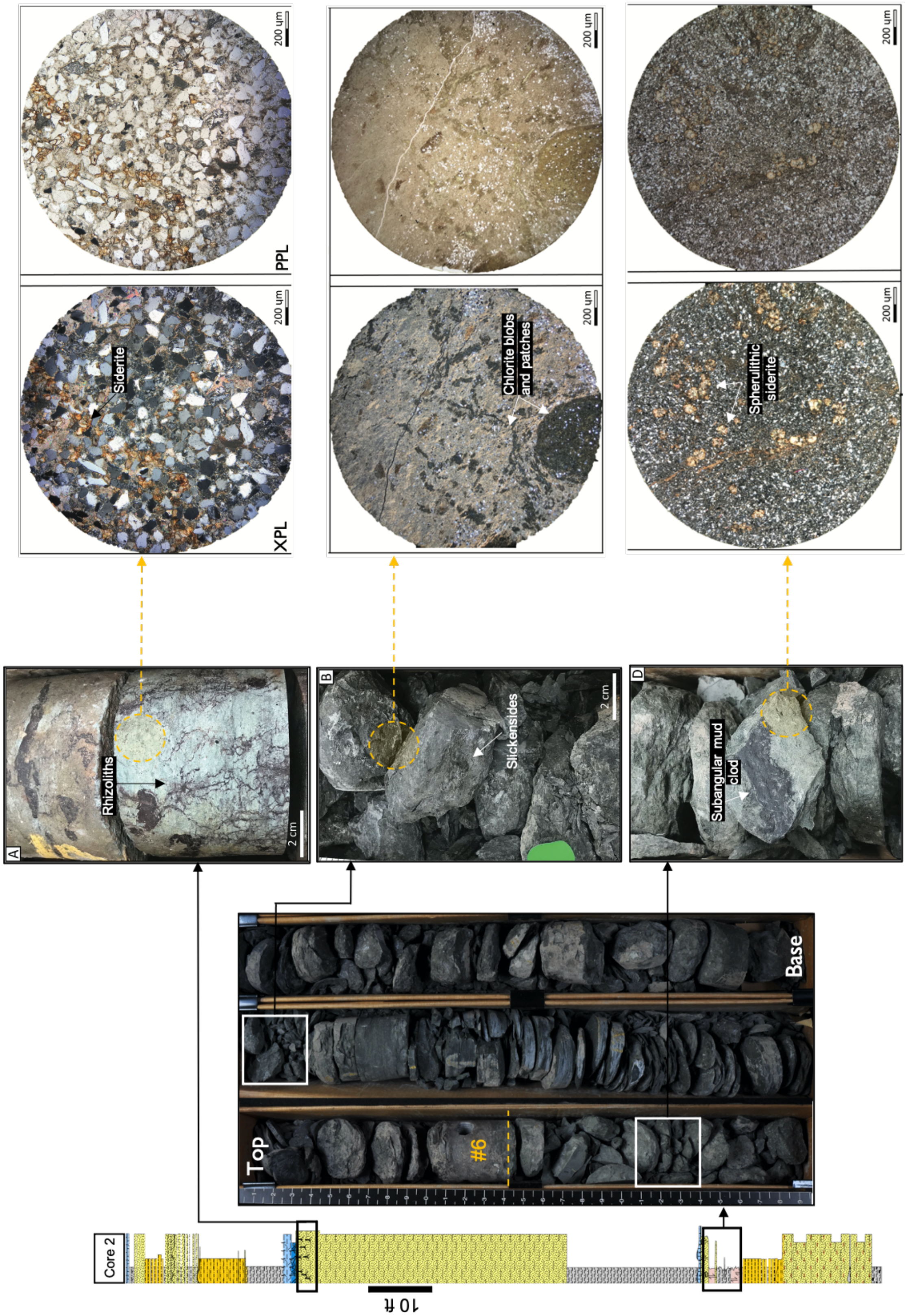

Figure 81. Core and thin section images and descriptions of the mottled shales to sandstones (Facies 5). Refer to Figure 49 or Table 4 for the explanation of facies numbers.

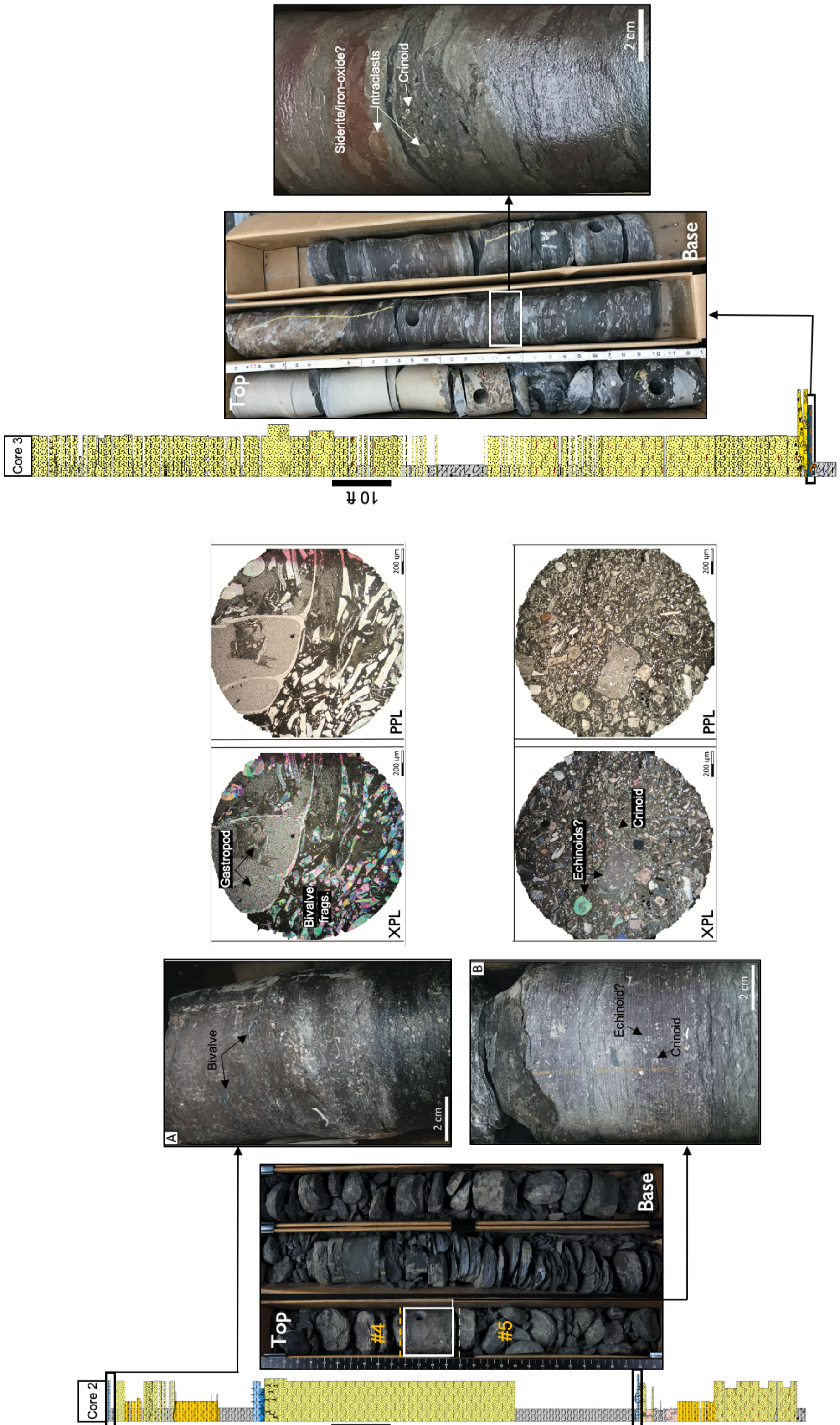

Figure 82. Core and thin section images and descriptions of the shaly carbonates (Facies 6). Refer to Figure 49 or Table 4 for the explanation of facies numbers.

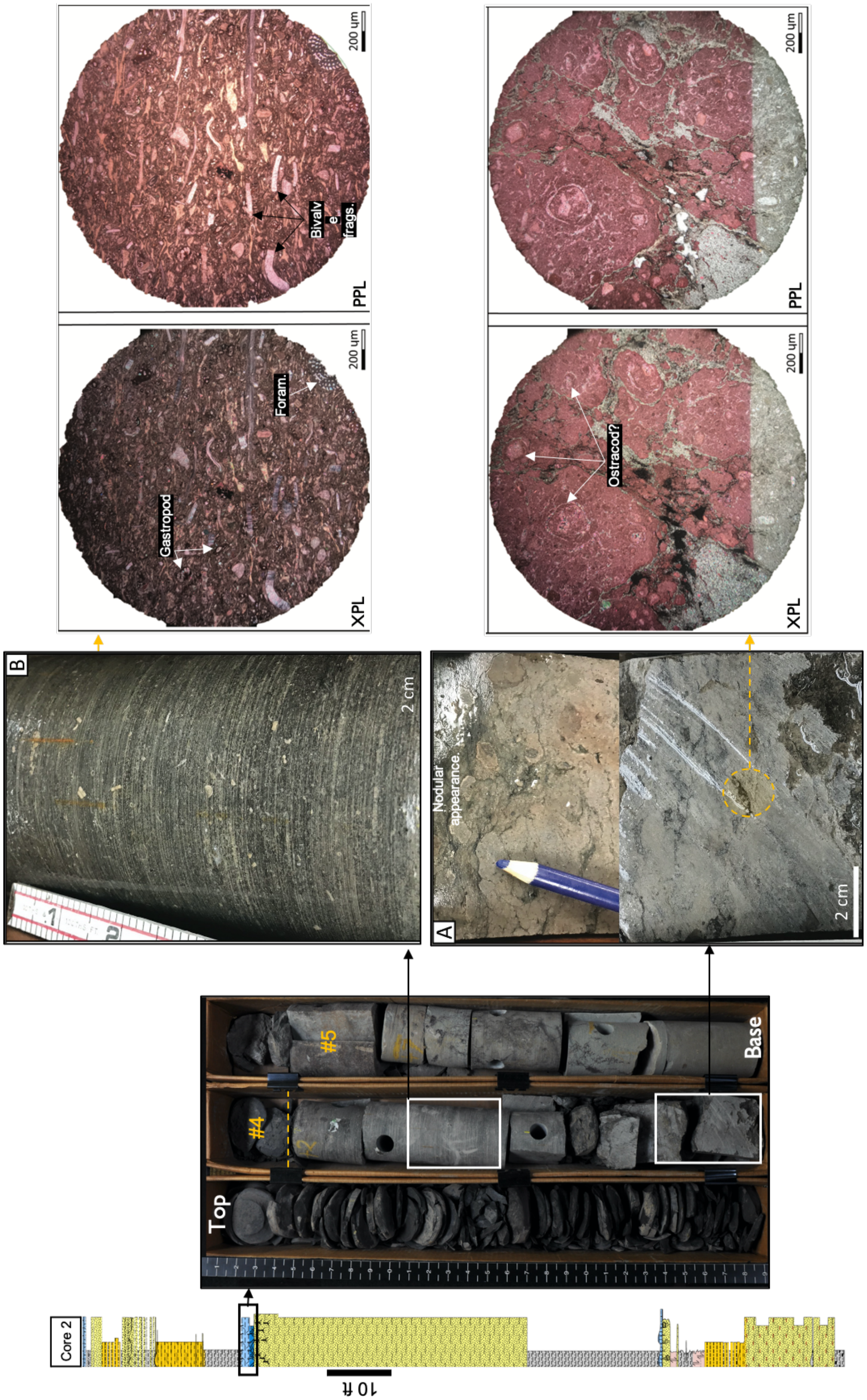

Figure 83. Core and thin section images and descriptions of the skeletal wackestones to packstones (Facies 7). Refer to Figure 49 or Table 4 for the explanation of facies numbers.

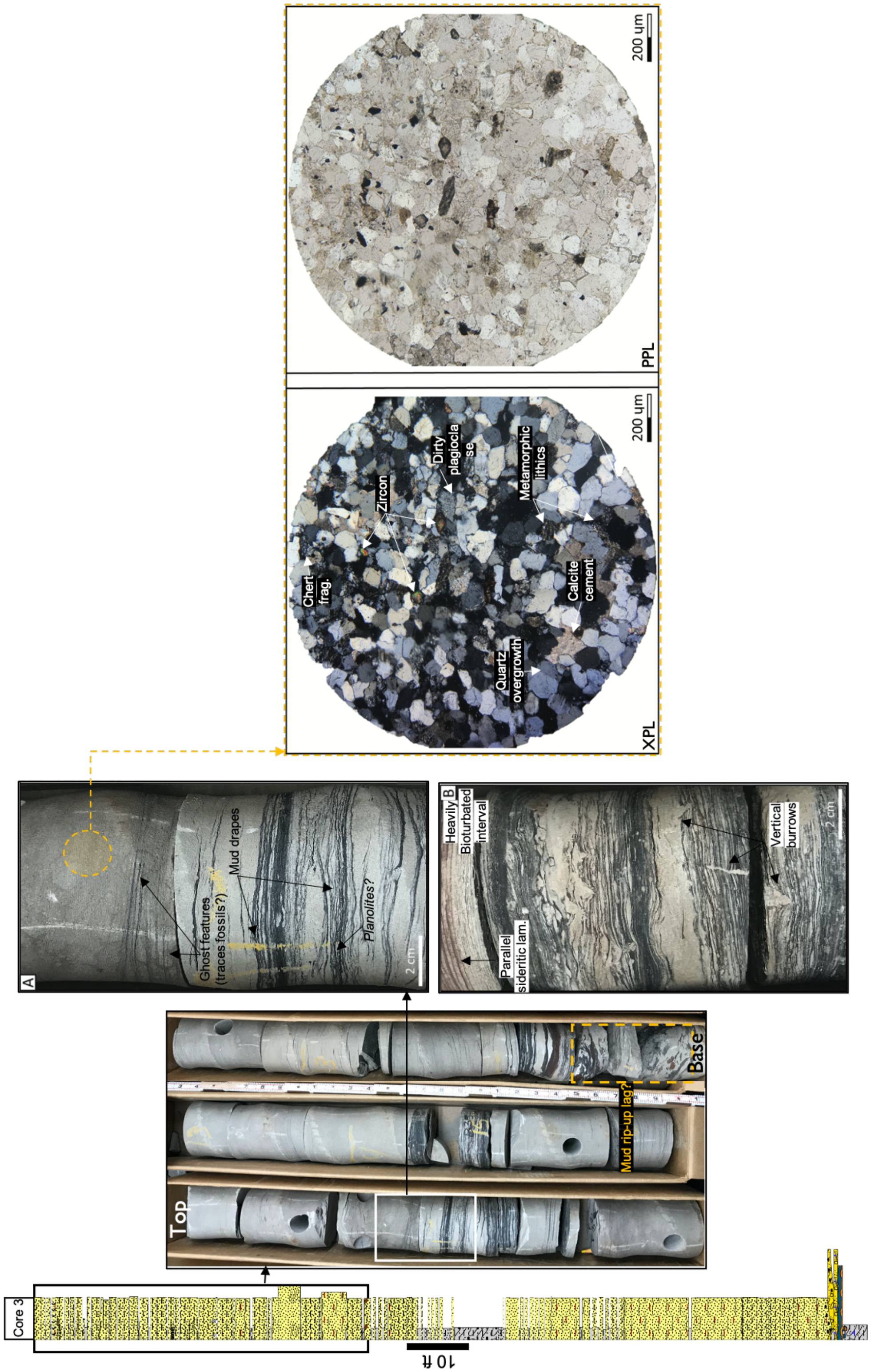

Figure 84. Core and thin section images and descriptions of the burrowed and interbedded, sideritic sandstones and mudstones (Facies 8). Refer to Figure 49 or Table 4 for the explanation of facies numbers.

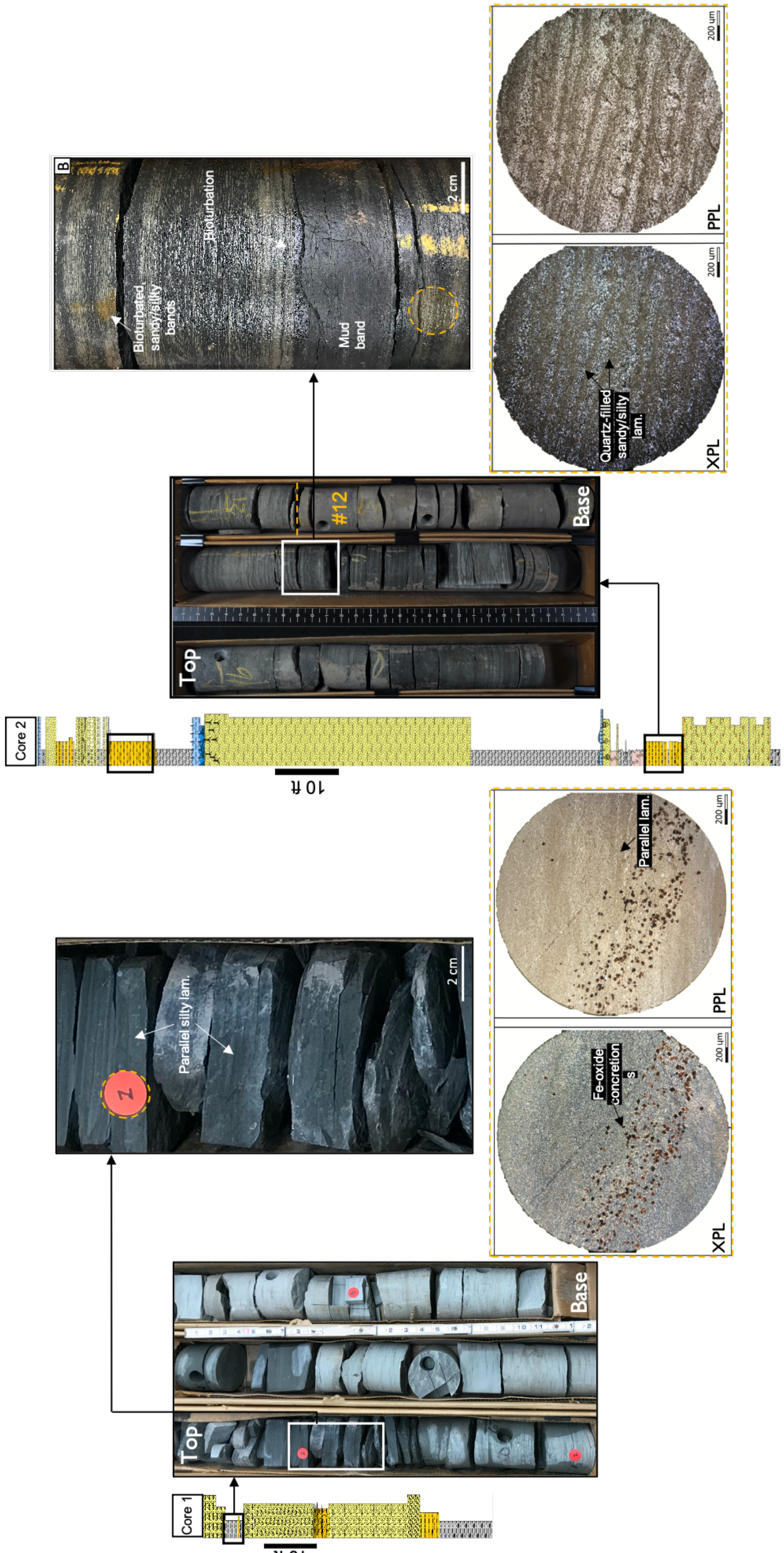

Figure 85. Core and thin section images and descriptions of the heterolithic siltstones (Facies 9). Refer to Figure 49 or Table 4 for the explanation of facies numbers.

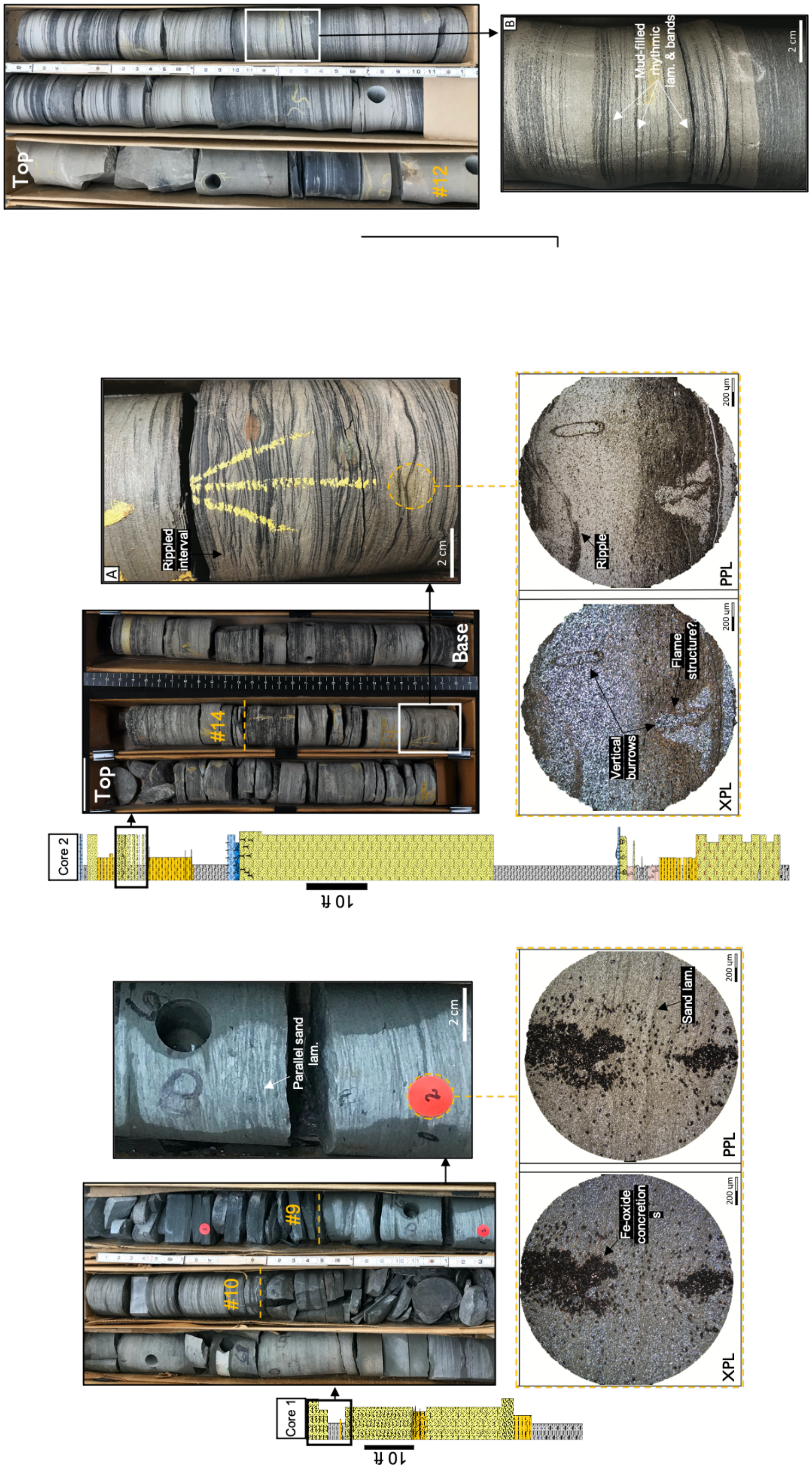

Figure 86. Core and thin section images and descriptions of the heterolithic sandstones (Facies 10). Refer to Figure 49 or Table 4 for the explanation of facies numbers.

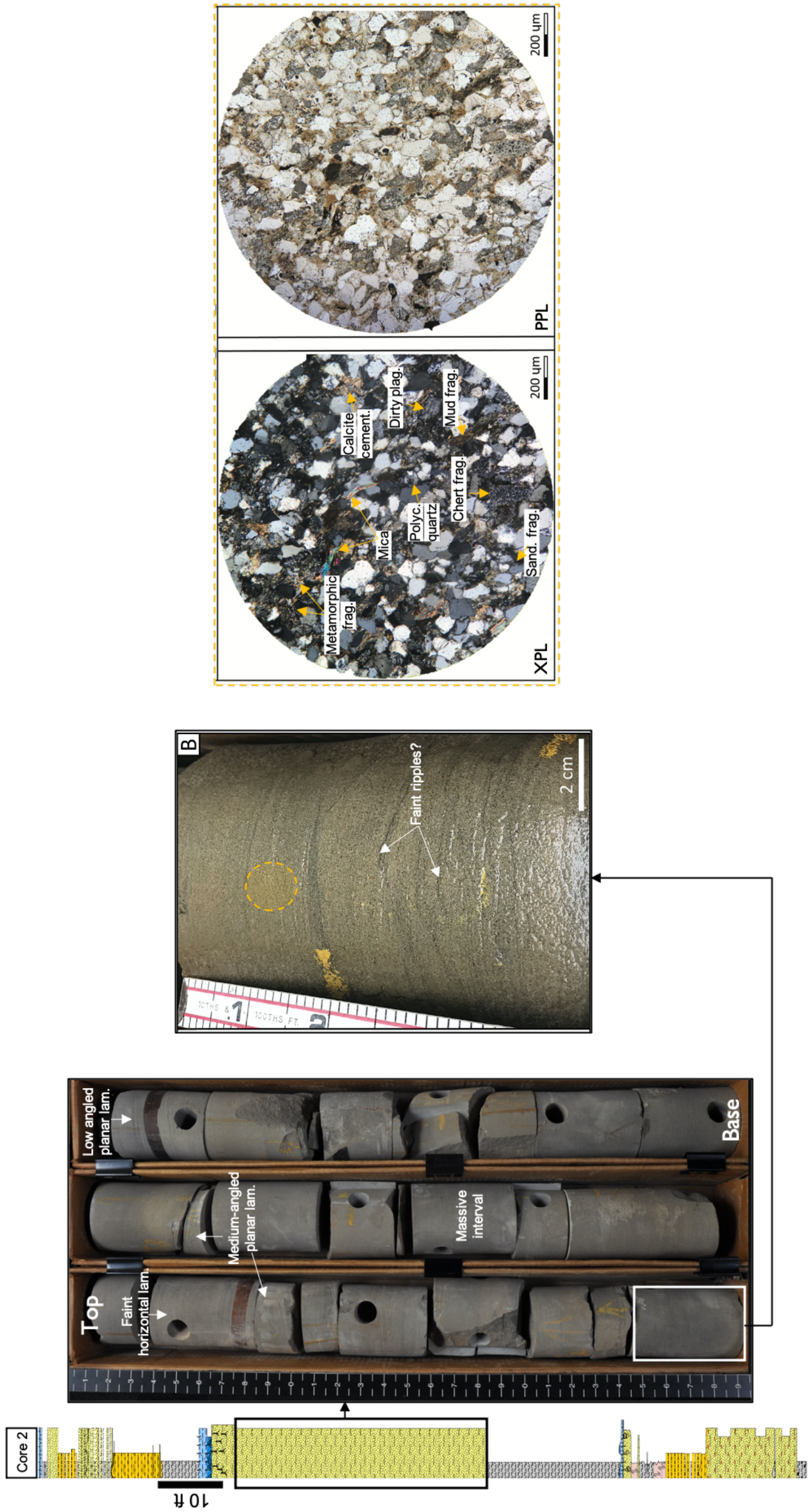

Figure 87. Core and thin section images and descriptions of the fine-grained sandstones (Facies 11). Refer to Figure 49 or Table 4 for the explanation of facies numbers.

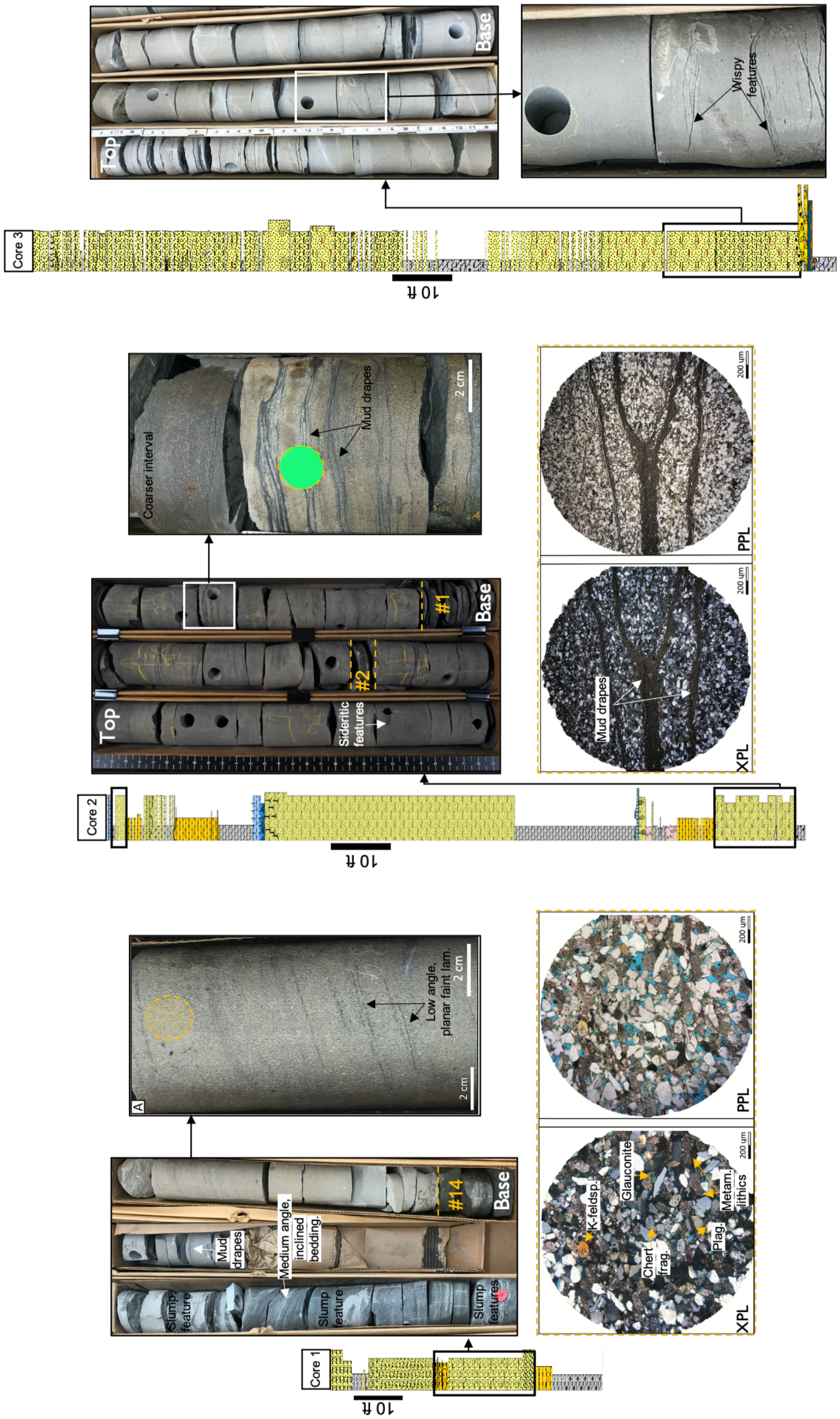

Figure 88. Core and thin section images and descriptions of the medium to fine grained sandstones with mud drapes (Facies 12). Refer to Figure 49 or Table 4 for the explanation of facies numbers.

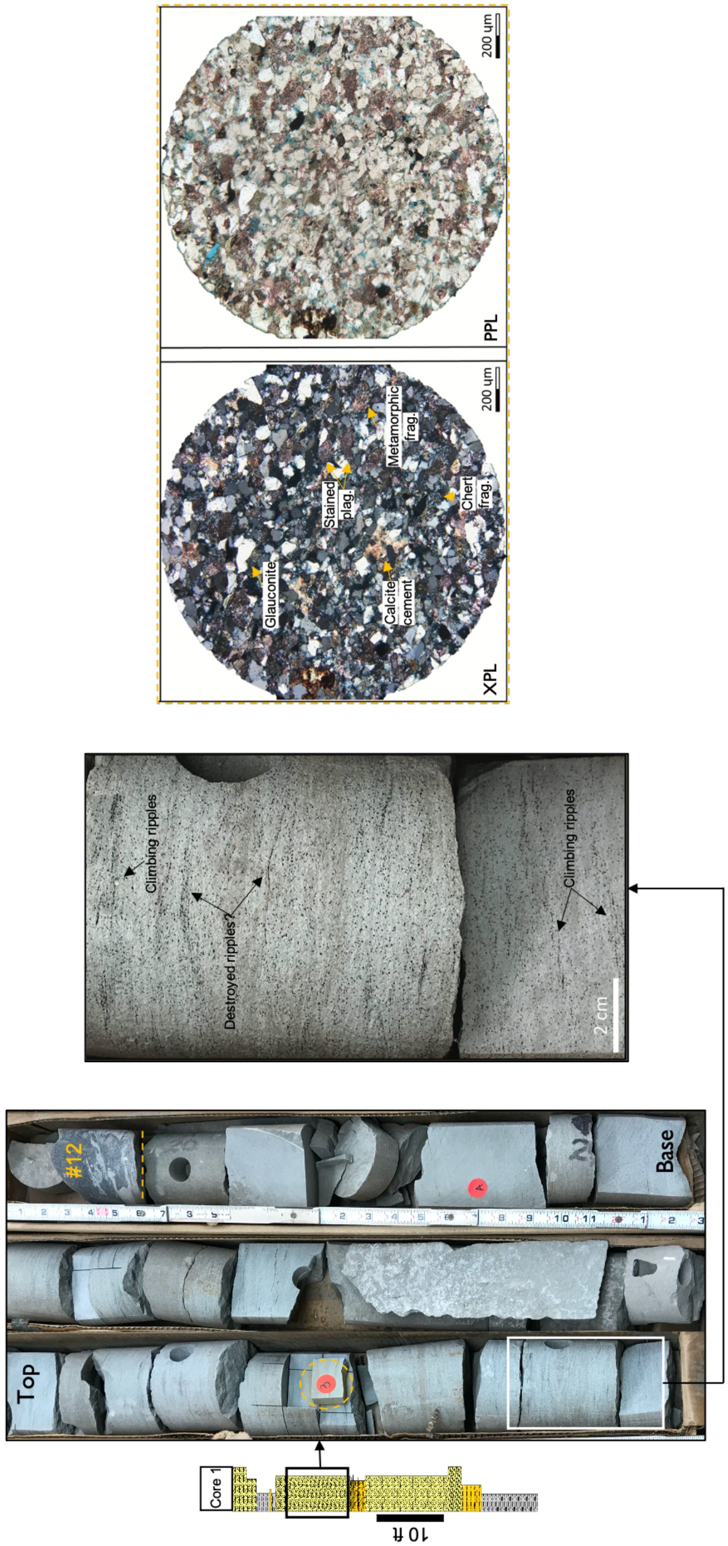

Figure 89. Core and thin section images and descriptions of the ripple laminated sandstone (Facies 13). Refer to Figure 49 or Table 4 for the explanation of facies numbers.

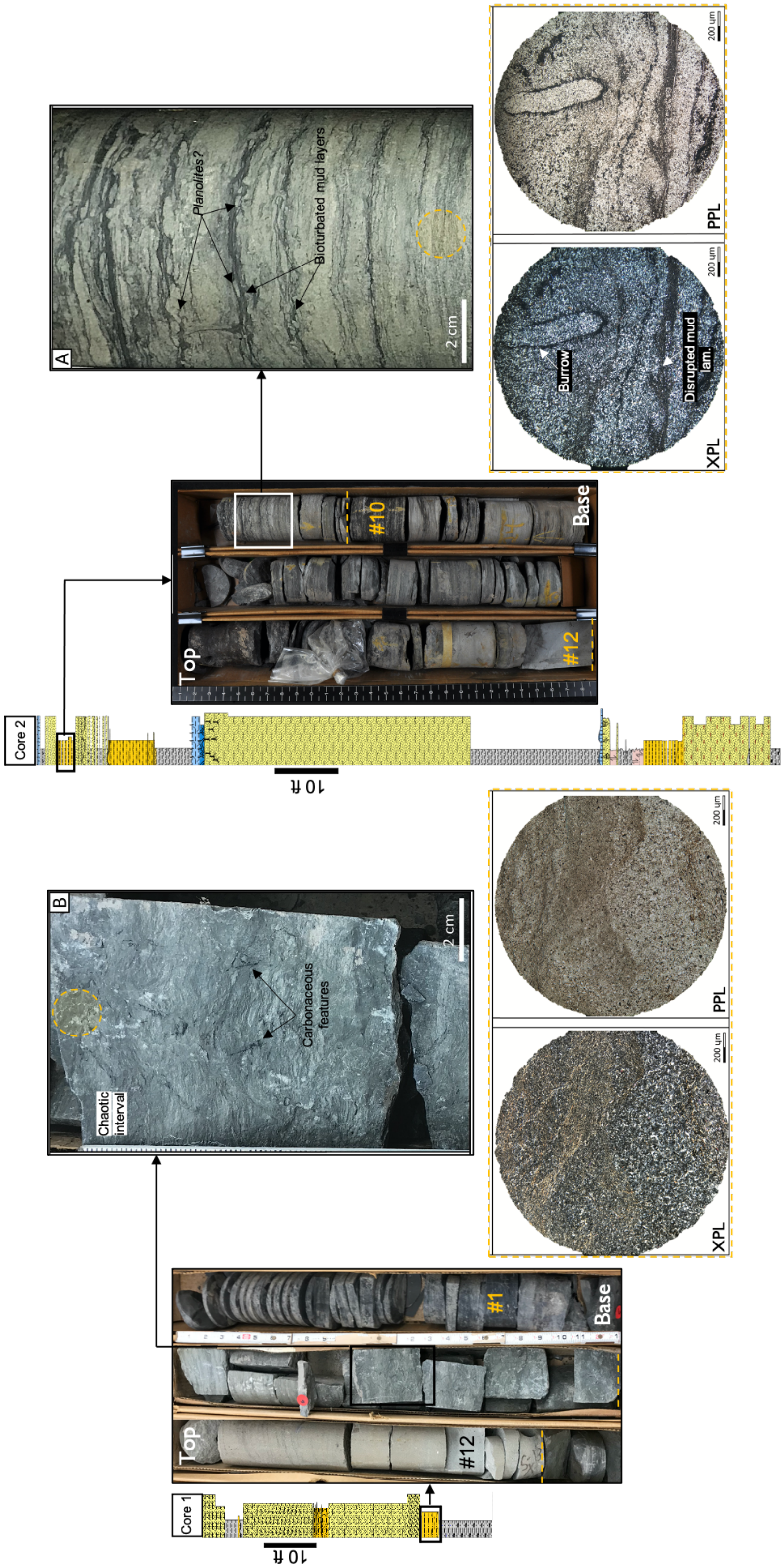

Figure 90. Core and thin section images and descriptions of the bioturbated sandy siltstones (Facies 14). Refer to Figure 49 or Table 4 for the explanation of facies numbers.

Figure 91. Core and thin section images and descriptions of the conglomerates (Facies 15). Refer to Figure 49 or Table 4 for the explanation of facies numbers.

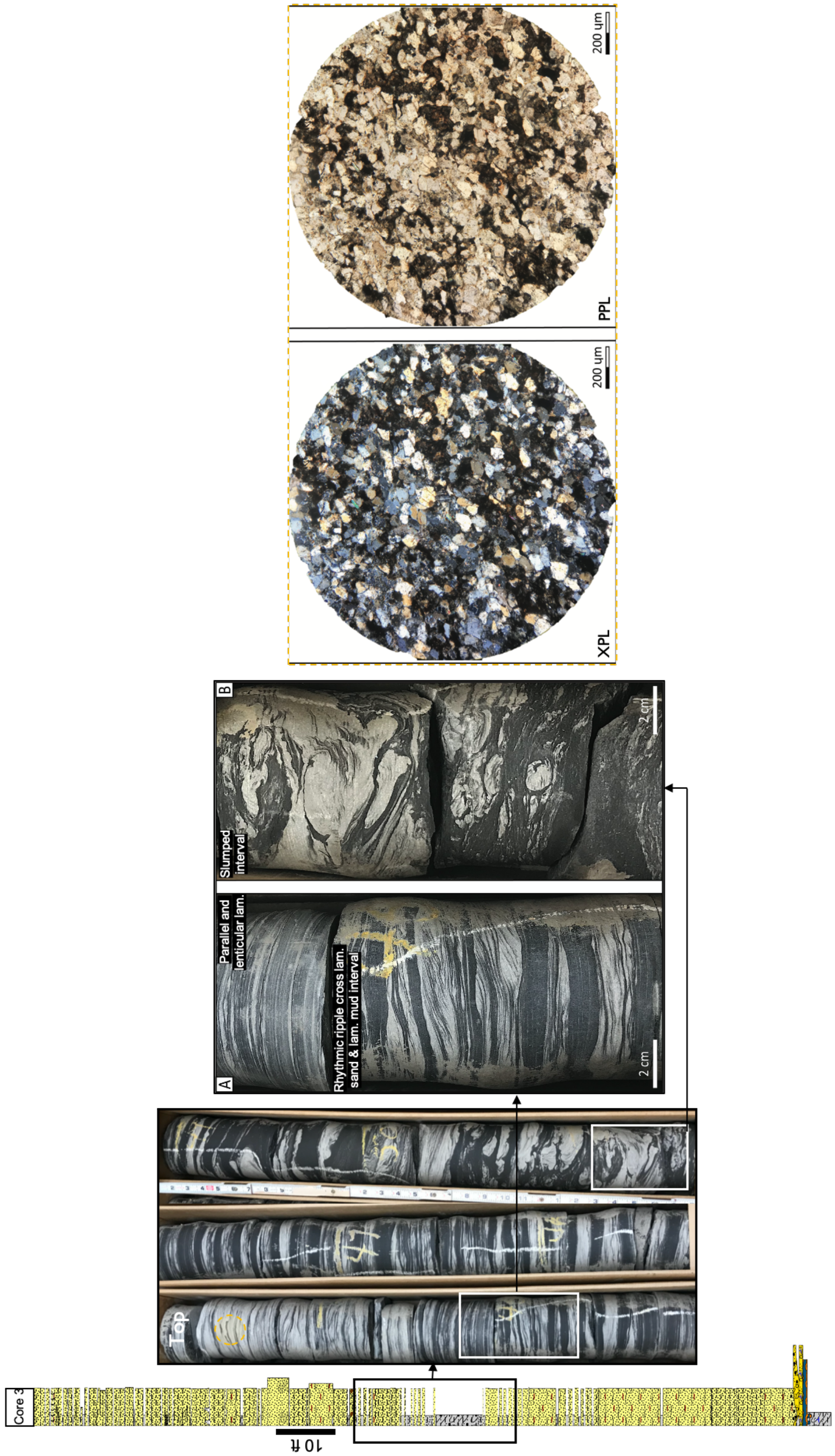

Figure 91. Core and thin section images and descriptions of the interbedded sandstones and mudstones (Facies 16). Refer to Figure 49 or Table 4 for the explanation of facies numbers.

APPENDIX C: POINT-COUNT DATA

Table 10. Raw modal point-count data for Desmoinesian Red Fork Sandstone samples from Core 2, Logan County, Oklahoma.

Sample	Depth (feet)	Qm	Qp	P	K	Lm	Lsm	Lss	Chert	Lv	Op	M	Other
UF1-2_PRF_8	5145.2	155	0	104	0	16	0	1	23	0	0	0	1
UF1-2_PRF_9	5187	107	2	107	0	44	0	2	29	0	0	0	9
UF1-2_PRF_10	5194	94	4	84	0	72	3	14	19	0	0	0	10
UF1-2_PRF_11	5201.4	138	2	98	98	39	2	0	9	0	0	2	10
UF1-2_PRF_12	5206.8	179	7	33	0	44	5	0	29	0	0	1	2
UF1-2_PRF_26	5220	217	11	30	0	20	2	6	12	0	0	0	2
UF1-2_PRF_27	5234	171	8	33	0	28	3	13	29	0	1	5	9

*M=Mica grains; Op= Opaque grains (dense minerals); Other=accessory minerals=chlorite, clays, hematite, zircon.

APPENDIX D: U/PB DETRITAL ZIRCON DATA

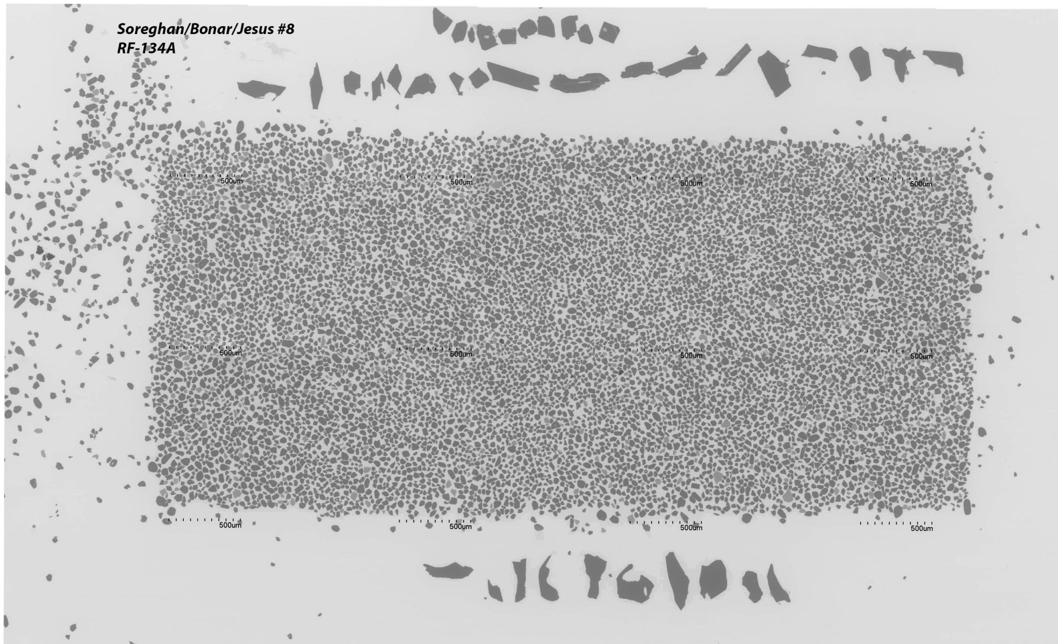

Figure 92. BSE inverted image of mounted zircon grains from sample DG-A (Core 1).

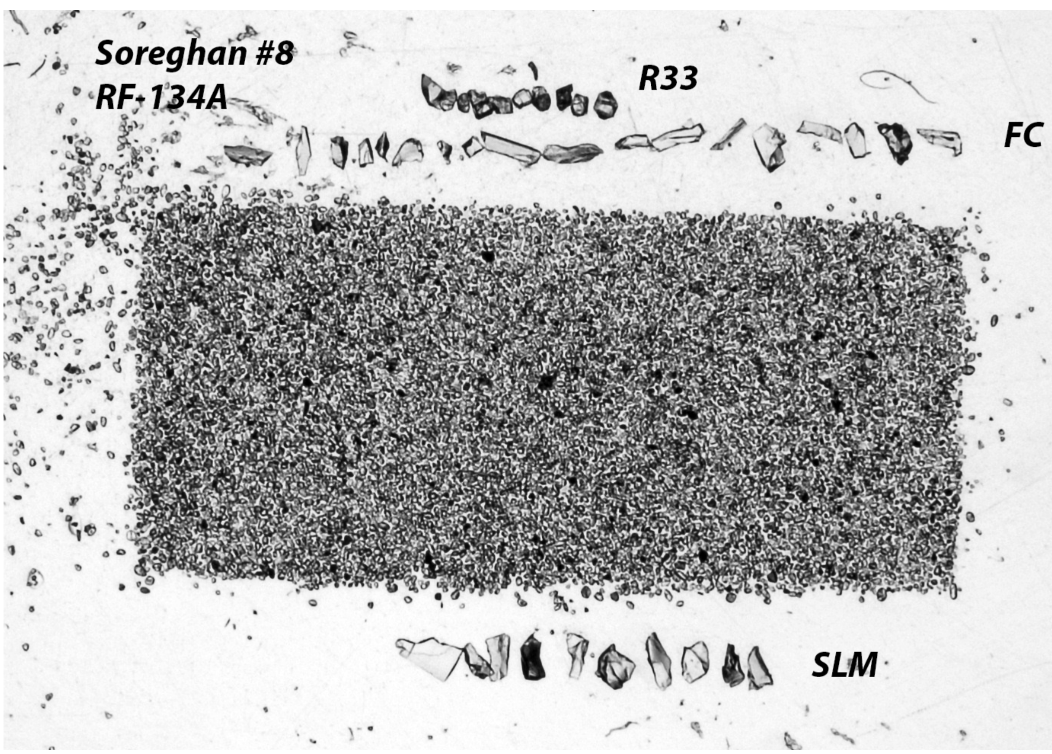

Figure 93. CL image of mounted zircon grains from sample DG-A (Core 1).

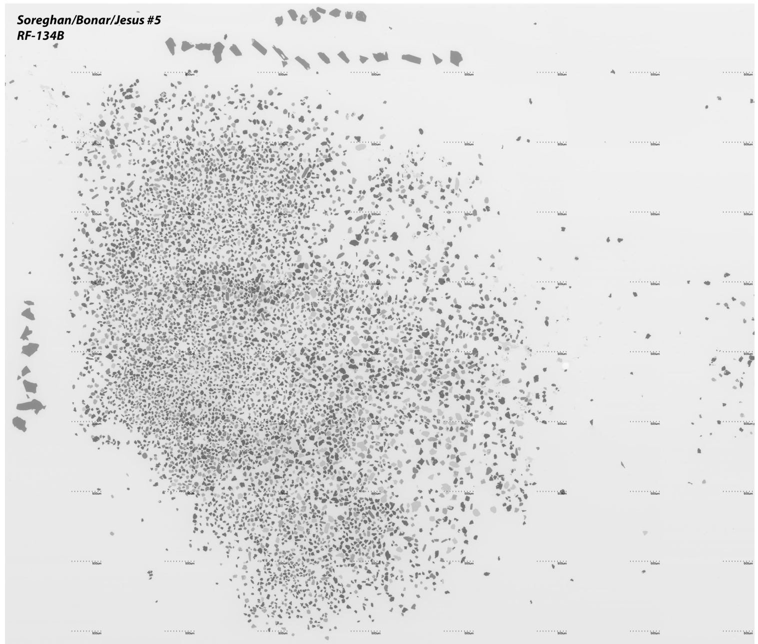

Figure 94. BSE inverted image of mounted zircon grains from sample DG-B (Core 1).

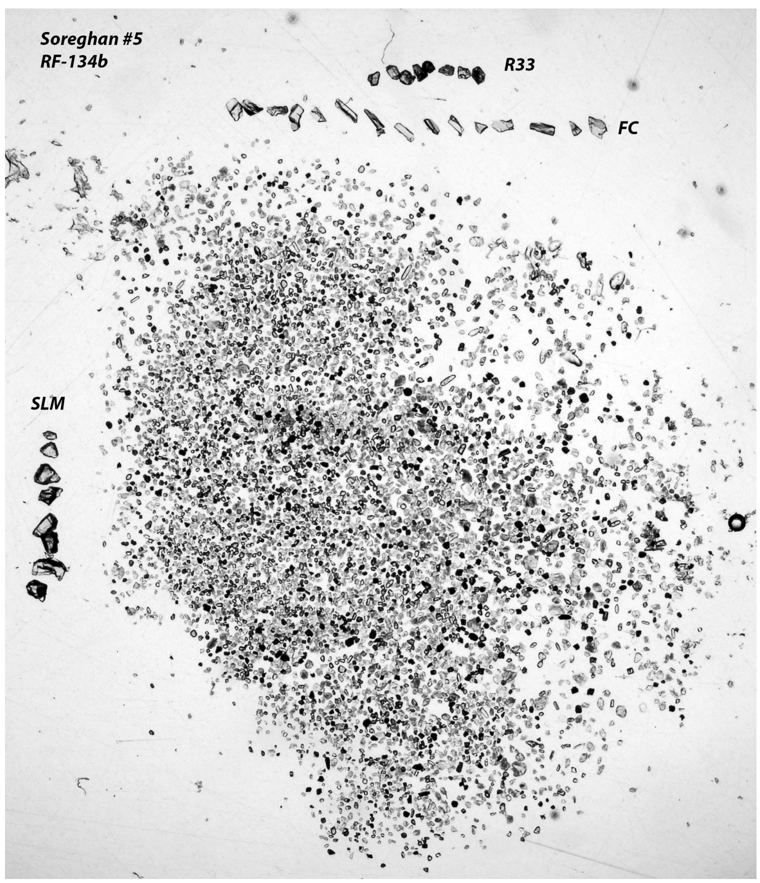

Figure 95. CL image of mounted zircon grains from sample DG-B (Core 1).

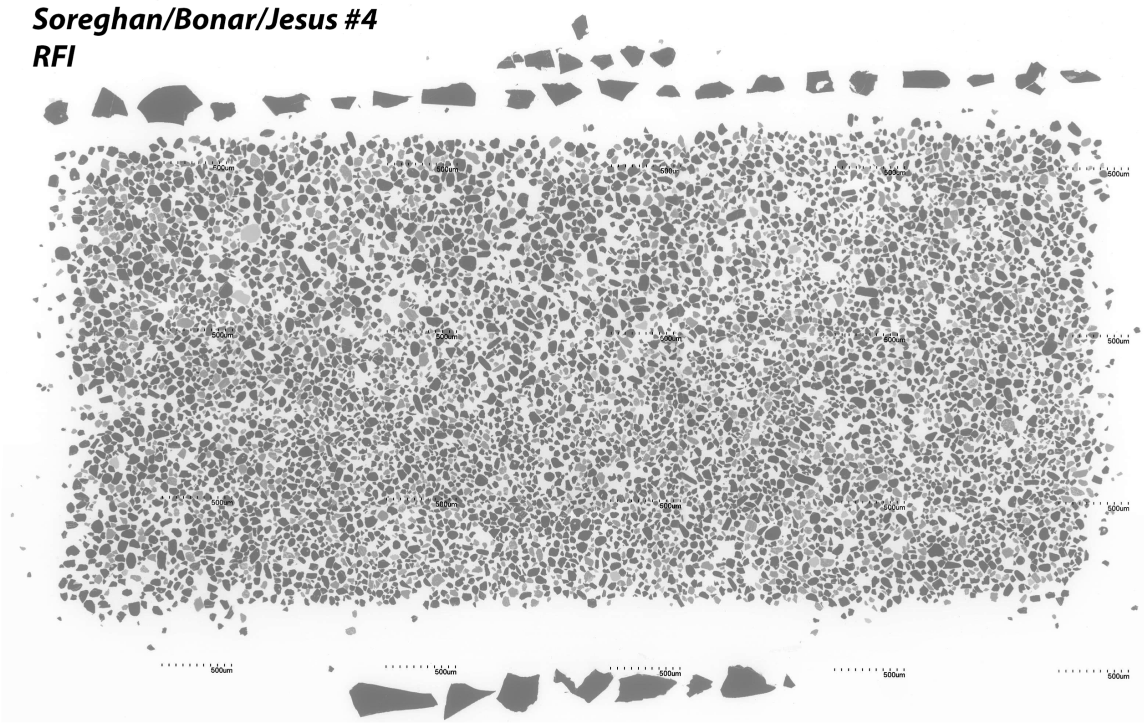

Figure 96. BSE inverted image of mounted zircon grains from sample SF-A (Core 3).

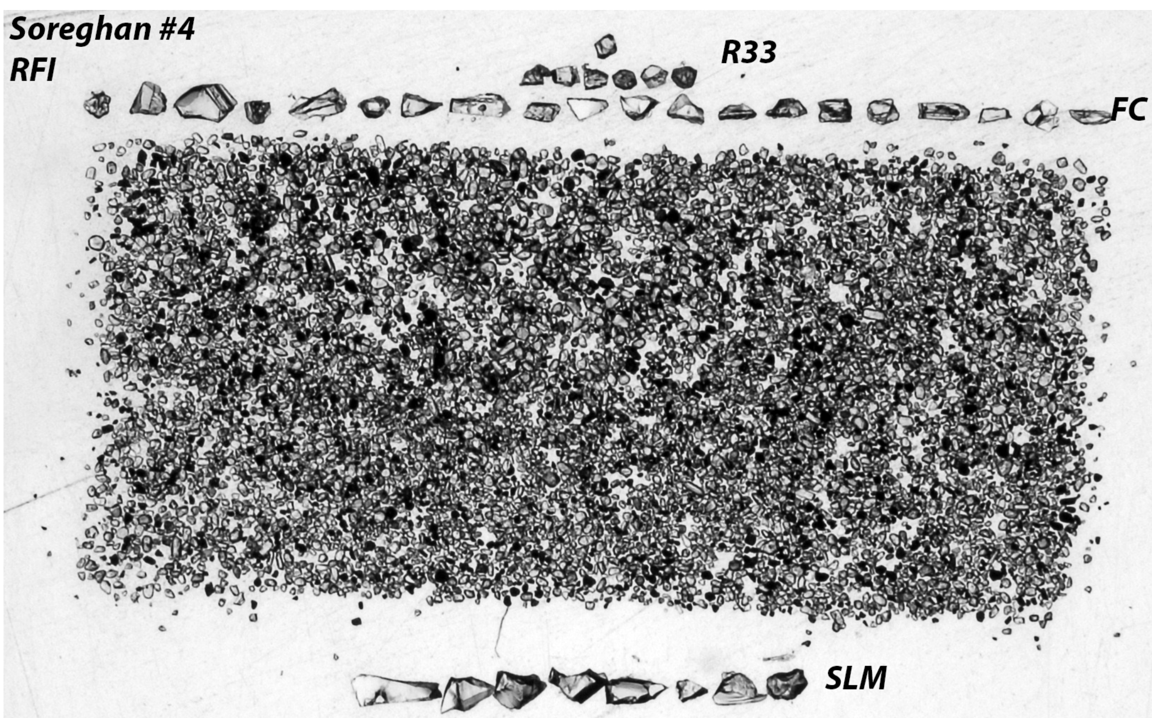

Figure 97. CL image of mounted zircon grains from sample SF-A (Core 3).

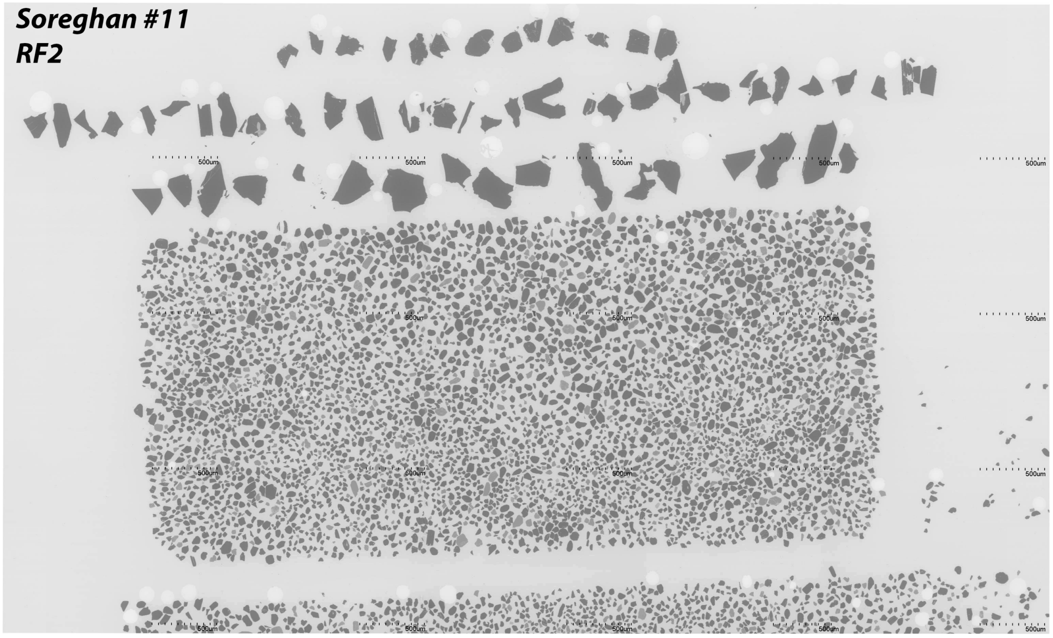

Figure 98. BSE inverted image of mounted zircon grains from sample SF-B (Core 3).

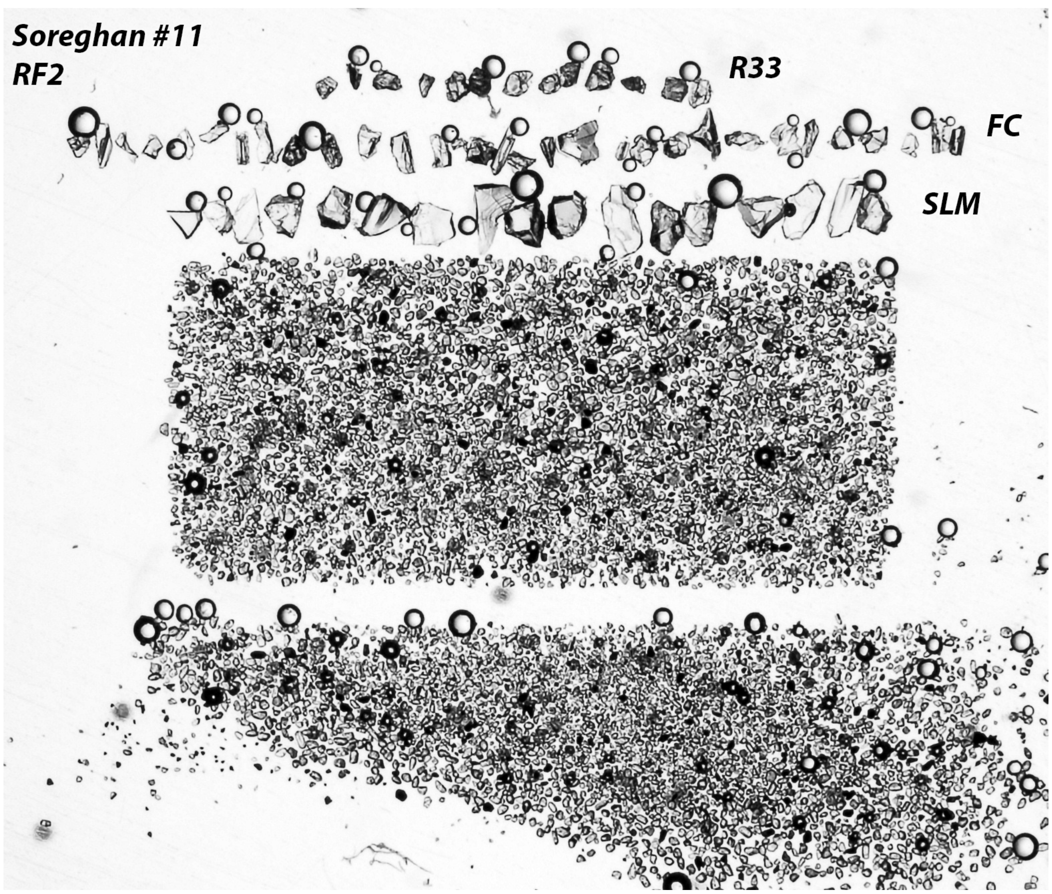

Figure 99. CL image of mounted zircon grains from sample SF-B (Core 3).

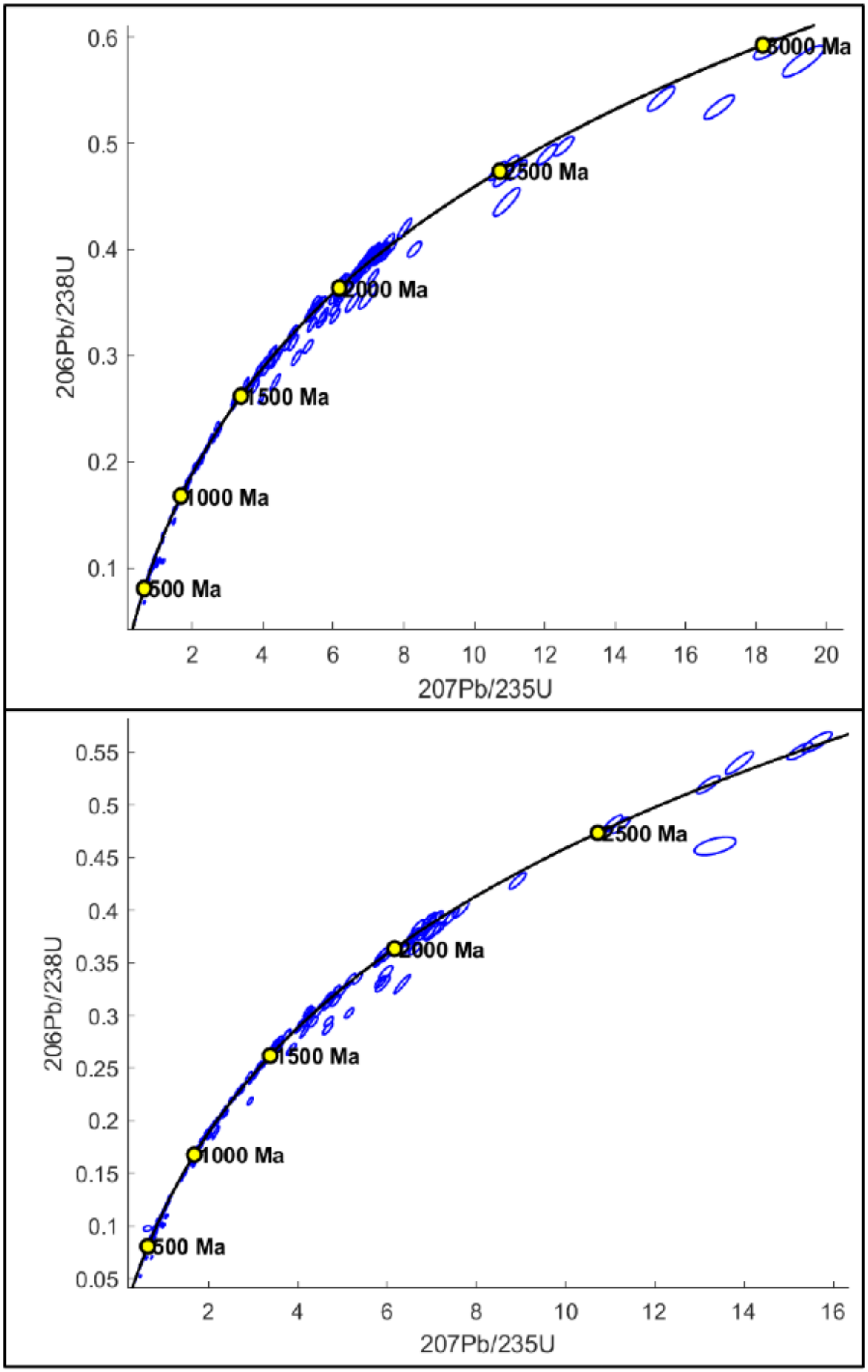

Figure 100. Concordia diagrams of samples from Core 1. Top = DG-A; Bottom = DG-B.

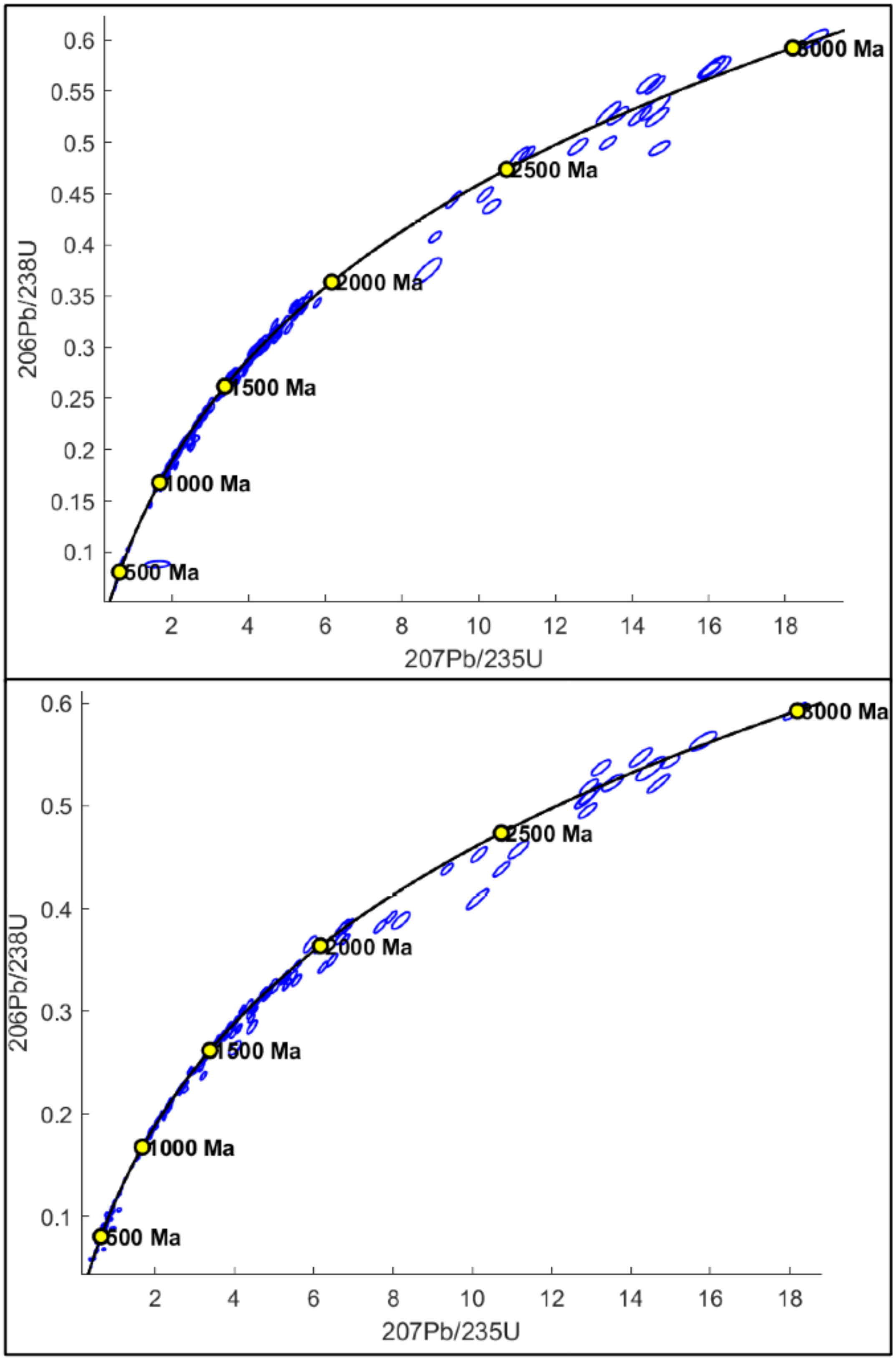

Figure 101. Concordia diagrams of samples from Core 2. Top = UF-A; Bottom = UF-C. Note: UF-B was analyzed from Kushner's (2018) work.

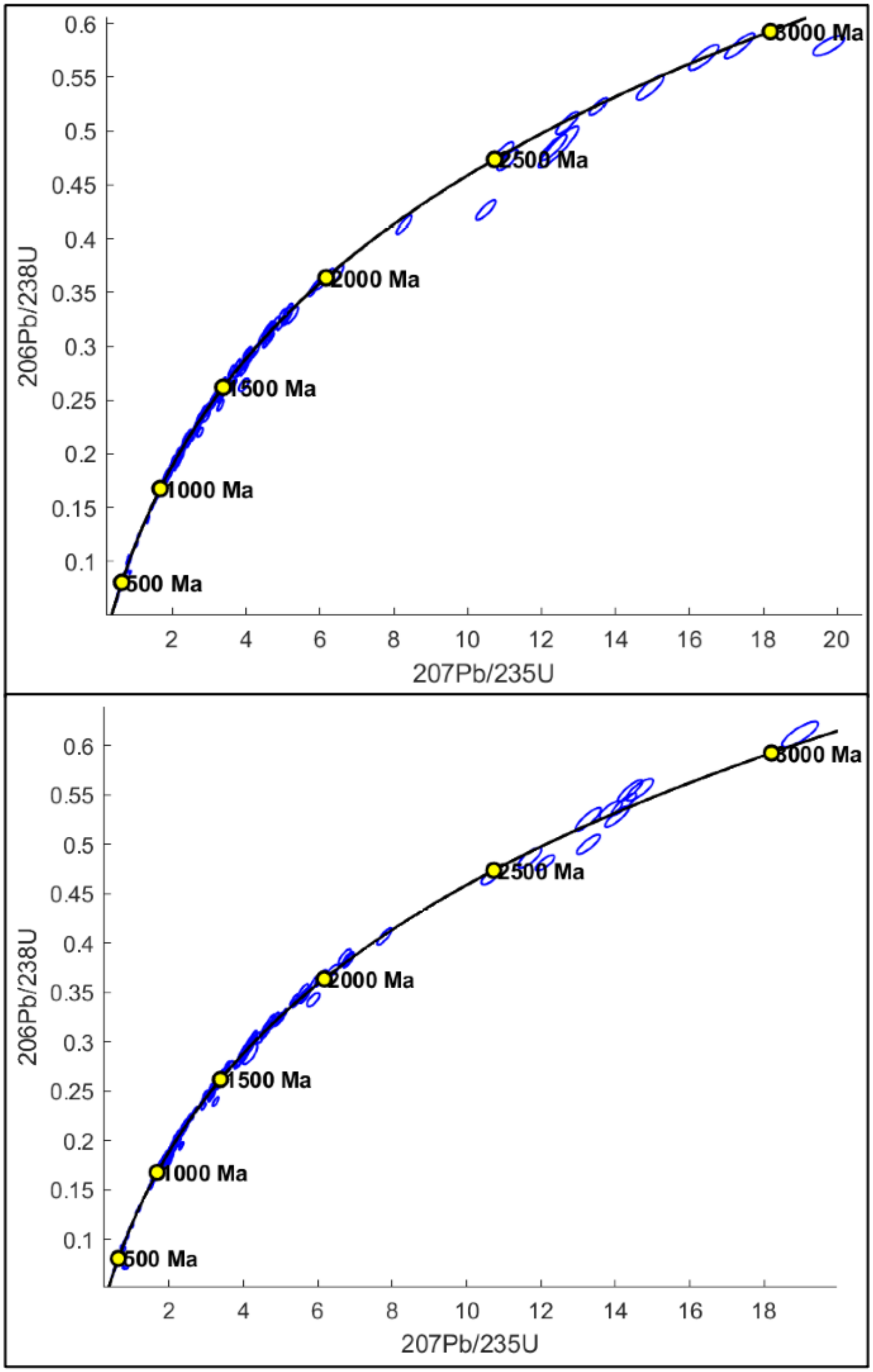

Figure 102. Concordia diagrams of samples from Core 3. Top = SF-A; Bottom = SF-B.

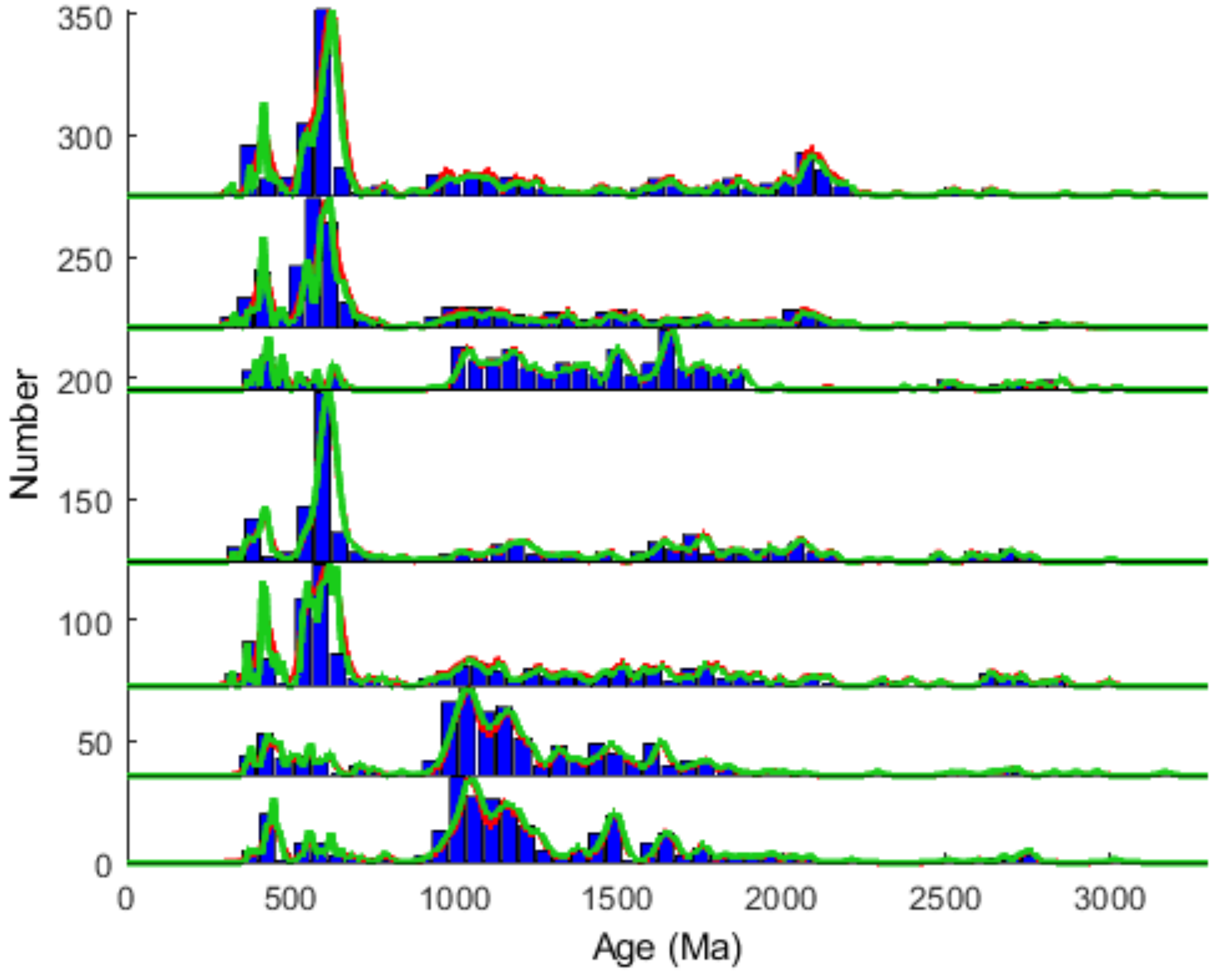

Figure 103. Probability density plot (green line), Kernel density estimate (red line) and histograms of the analyzed detrital zircon data. From bottom to the top: Samples SF-B, SF-A, UF-C, UF-B, UF-A, DG-B, DG-A.

Sample: DG-A						Isotope Ratios					Apparent Ages (Ma)								
Analysis	**U (ppm)**	**206Pb /204Pb**	**U /Th**	**206Pb /207Pb**	**± (%)**	**207Pb /235U**	**± (%)**	**206Pb /238U**	**± (%)**	**err. corr.**	**206Pb /238U**	**± (Ma)**	**207Pb /235U**	**± (Ma)**	**206Pb /207Pb**	**± (Ma)**	**Best Age**	**± (Ma)**	**Conc. (%)**
1	222	153611.2	1.3	17.8	1.1	0.6	1.6	0.1	1.2	0.8	462.5	5.4	461.0	6.0	453.5	23.8	**462.5**	**5.4**	102.0
100	31	186093.2	3.9	7.4	1.0	7.4	1.6	0.4	1.3	0.8	2163.4	23.5	2166.9	14.3	2170.3	16.8	**2170.3**	**16.8**	99.7
101	240	104613.5	1.3	15.5	1.0	1.1	1.6	0.1	1.3	0.8	731.3	8.7	736.4	8.5	752.2	21.4	**731.3**	**8.7**	97.2
102	178	676571.5	0.8	18.3	1.2	0.5	1.8	0.1	1.3	0.7	377.3	4.9	380.1	5.8	396.9	27.5	**377.3**	**4.9**	95.1
103	109	71696.7	1.9	14.4	1.0	1.5	1.7	0.2	1.4	0.8	925.5	11.9	920.8	10.4	909.6	20.9	**909.6**	**20.9**	101.8
104	254	2368976.4	6.9	7.7	0.9	7.0	1.7	0.4	1.4	0.8	2134.0	25.8	2115.5	14.9	2097.4	15.8	**2097.4**	**15.8**	101.7
105	95	84124.1	1.6	16.1	1.2	0.9	2.0	0.1	1.6	0.8	651.9	9.7	658.0	9.5	678.9	25.1	**651.9**	**9.7**	96.0
106	108	1221328.4	1.2	16.7	1.1	0.8	1.9	0.1	1.6	0.8	575.7	8.6	580.6	8.5	599.8	24.5	**575.7**	**8.6**	96.0
107	406	367705.8	8.9	9.3	1.0	4.4	1.7	0.3	1.3	0.8	1694.1	19.6	1718.2	13.7	1747.8	18.4	**1747.8**	**18.4**	96.9
108	85	71749.0	1.1	18.0	1.8	0.5	2.3	0.1	1.4	0.6	415.7	5.5	418.1	7.8	431.4	40.2	**415.7**	**5.5**	96.4
109	112	97429.1	2.5	7.6	0.9	7.1	1.5	0.4	1.2	0.8	2130.7	22.5	2127.9	13.5	2125.1	15.3	**2125.1**	**15.3**	100.3
11	371	135992.0	14.7	16.4	0.9	0.9	1.5	0.1	1.2	0.8	645.4	7.2	645.0	7.1	643.7	19.6	**645.4**	**7.2**	100.3
110	42	18899.8	2.3	15.7	1.5	0.9	2.0	0.1	1.3	0.7	611.9	7.6	638.4	9.4	733.4	31.8	**611.9**	**7.6**	83.4
111	166	164393.1	3.5	12.6	1.2	2.2	1.7	0.2	1.2	0.7	1187.3	13.4	1185.9	11.9	1183.4	23.3	**1183.4**	**23.3**	100.3
112	93	63671.9	1.0	16.3	1.2	0.9	1.8	0.1	1.3	0.7	623.0	7.7	627.8	8.4	645.2	26.8	**623.0**	**7.7**	96.6
113	121	208839.9	3.1	7.8	0.9	6.7	1.7	0.4	1.4	0.9	2078.3	25.4	2073.6	14.7	2068.8	15.1	**2068.8**	**15.1**	100.5
114	63	191484.6	1.3	8.6	0.8	5.4	1.5	0.3	1.3	0.8	1881.1	20.6	1888.8	13.0	1897.2	14.9	**1897.2**	**14.9**	99.1
115	187	32378.8	1.7	16.5	1.3	0.8	2.0	0.1	1.6	0.8	615.2	9.5	616.1	9.4	619.0	27.0	**615.2**	**9.5**	99.4
116	243	174613.9	1.6	16.6	1.0	0.7	1.8	0.1	1.5	0.8	537.1	7.8	552.3	7.7	615.2	21.0	**537.1**	**7.8**	87.3
117	119	64372.3	1.1	16.4	0.9	0.9	1.4	0.1	1.1	0.8	622.6	6.7	626.8	6.7	641.8	19.3	**622.6**	**6.7**	97.0
118	237	857540.9	14.0	4.3	0.9	17.0	1.7	0.5	1.4	0.8	2758.6	31.7	2932.2	16.0	3053.6	14.2	**3053.6**	**14.2**	90.3
119	88	42686.4	1.6	16.4	1.1	0.9	1.7	0.1	1.3	0.8	647.9	7.9	644.2	8.0	631.4	23.3	**647.9**	**7.9**	102.6
12	257	144913.2	22.1	13.0	0.8	2.0	1.5	0.2	1.3	0.8	1135.0	13.1	1128.3	10.2	1115.5	16.4	**1115.5**	**16.4**	101.7
120	363	369943.0	38.6	12.7	0.8	2.2	1.2	0.2	1.0	0.8	1172.6	10.2	1169.5	8.5	1163.7	15.3	**1163.7**	**15.3**	100.8
121	98	46253.3	1.5	16.6	1.3	0.8	1.9	0.1	1.3	0.7	619.4	7.9	617.7	8.6	611.2	27.8	**619.4**	**7.9**	101.3
122	227	51339.6	2.5	16.6	1.1	0.8	1.9	0.1	1.6	0.8	593.7	8.9	596.1	8.7	605.1	24.4	**593.7**	**8.9**	98.1
123	139	119791.7	2.9	7.6	0.8	7.0	1.3	0.4	1.1	0.8	2092.9	18.8	2108.5	11.5	2123.7	13.3	**2123.7**	**13.3**	98.5
124	115	174301.7	2.1	16.6	1.2	0.8	1.7	0.1	1.2	0.7	621.0	7.3	618.0	7.8	607.1	25.0	**621.0**	**7.3**	102.3
125	65	130705.0	3.2	4.1	1.1	19.3	2.0	0.6	1.7	0.8	2938.0	39.8	3058.8	19.4	3139.2	17.5	**3139.2**	**17.5**	93.6
126	950	984272.9	2.0	16.7	0.8	0.8	1.7	0.1	1.5	0.9	611.8	8.9	608.2	7.8	594.7	16.8	**611.8**	**8.9**	102.9

127	274	46208.5	1.1	16.7	0.9	0.8	1.6	0.1	1.3	0.8	611.8	7.6	608.3	7.2	595.2	19.4	**611.8**	**7.6**	102.8
128	292	365853.4	1.6	18.2	1.1	0.5	1.6	0.1	1.2	0.7	408.7	4.6	407.9	5.3	403.1	23.8	**408.7**	**4.6**	101.4
129	69	23268.4	1.2	18.6	2.0	0.4	2.4	0.1	1.4	0.6	371.4	4.9	369.1	7.5	354.4	45.0	**371.4**	**4.9**	104.8
13	336	71667.1	0.8	16.9	1.0	0.8	1.5	0.1	1.1	0.7	604.3	6.6	598.8	6.9	578.2	22.1	**604.3**	**6.6**	104.5
130	206	152803.8	3.9	10.2	1.0	3.7	1.8	0.3	1.5	0.8	1552.6	20.7	1569.7	14.2	1592.8	18.0	**1592.8**	**18.0**	97.5
131	282	228524.6	4.9	8.0	1.0	5.3	1.7	0.3	1.3	0.8	1734.4	20.4	1866.9	14.3	2017.8	17.8	**2017.8**	**17.8**	86.0
132	414	160499.0	2.1	18.2	1.0	0.5	1.5	0.1	1.1	0.7	418.3	4.4	417.0	5.1	410.1	23.0	**418.3**	**4.4**	102.0
133	208	43772.6	2.3	16.8	1.1	0.8	2.0	0.1	1.6	0.8	594.9	9.2	593.0	8.9	585.6	24.5	**594.9**	**9.2**	101.6
134	244	5400934.5	1.5	16.0	0.9	0.9	1.7	0.1	1.4	0.8	631.5	8.3	643.1	8.0	684.3	20.2	**631.5**	**8.3**	92.3
135	55	15372.2	1.3	18.2	1.9	0.4	2.3	0.1	1.2	0.5	322.2	3.8	333.1	6.5	409.8	43.3	**322.2**	**3.8**	78.6
136	37	11849.9	1.6	17.2	1.7	0.8	2.2	0.1	1.5	0.7	597.1	8.4	584.8	9.9	537.3	36.6	**597.1**	**8.4**	111.1
137	211	157571.9	5.3	16.4	1.1	0.8	1.6	0.1	1.1	0.7	577.0	6.2	588.4	7.0	632.9	23.7	**577.0**	**6.2**	91.2
138	385	52663.1	3.3	17.8	1.2	0.5	2.0	0.1	1.6	0.8	418.0	6.6	423.8	7.1	455.4	27.5	**418.0**	**6.6**	91.8
139	455	187419.1	2.3	16.6	1.0	0.9	1.7	0.1	1.4	0.8	632.0	8.5	628.7	8.1	616.8	21.2	**632.0**	**8.5**	102.5
14	405	177347.8	4.2	13.2	0.9	1.9	1.9	0.2	1.6	0.9	1081.8	16.2	1083.1	12.4	1085.8	18.6	**1085.8**	**18.6**	99.6
140	248	7738797.4	2.0	16.3	0.8	0.9	1.4	0.1	1.2	0.8	640.2	7.4	641.7	6.9	646.9	17.0	**640.2**	**7.4**	99.0
141	1228	1898697.2	9.3	10.7	0.8	3.5	1.7	0.3	1.6	0.9	1555.6	21.5	1528.9	13.8	1492.1	14.8	**1492.1**	**14.8**	104.3
142	223	73951.7	1.0	18.2	0.9	0.5	1.4	0.1	1.2	0.8	424.4	4.8	422.5	5.0	411.8	19.2	**424.4**	**4.8**	103.1
143	224	68212.1	1.6	16.8	0.9	0.7	1.4	0.1	1.1	0.8	552.4	5.7	559.2	6.2	586.8	20.6	**552.4**	**5.7**	94.1
144	199	48219.1	2.0	17.9	1.3	0.5	2.0	0.1	1.5	0.8	415.9	6.2	420.3	6.9	444.8	28.6	**415.9**	**6.2**	93.5
145	151	71901.4	3.3	15.4	0.7	1.2	1.6	0.1	1.4	0.9	799.7	10.7	791.5	8.8	768.2	15.5	**799.7**	**10.7**	104.1
146	247	181523.6	1.4	16.7	0.8	0.7	1.6	0.1	1.3	0.8	525.3	6.6	539.9	6.5	602.0	18.0	**525.3**	**6.6**	87.3
147	117	207182.2	1.7	16.9	1.5	0.7	1.8	0.1	1.1	0.6	540.3	5.8	546.6	7.8	573.0	31.8	**540.3**	**5.8**	94.3
148	89	156278.6	1.9	9.1	1.1	4.8	2.0	0.3	1.6	0.8	1793.1	25.4	1792.5	16.5	1791.9	20.0	**1791.9**	**20.0**	100.1
149	68	119211.8	1.1	6.6	1.0	8.3	1.6	0.4	1.2	0.8	2169.0	22.3	2264.9	14.2	2352.6	16.9	**2352.6**	**16.9**	92.2
15	86	119166.0	3.0	7.8	1.0	6.8	1.5	0.4	1.2	0.8	2102.8	21.7	2092.0	13.7	2081.4	17.1	**2081.4**	**17.1**	101.0
151	265	1197979.1	3.4	6.1	0.8	10.7	1.5	0.5	1.3	0.8	2501.0	26.0	2494.1	13.9	2488.6	13.8	**2488.6**	**13.8**	100.5
152	156	175477.3	4.0	12.7	0.9	2.1	1.6	0.2	1.4	0.8	1140.7	14.4	1150.1	11.2	1167.8	17.3	**1167.8**	**17.3**	97.7
153	227	632410.8	1.8	4.9	0.9	15.3	1.7	0.5	1.4	0.8	2792.0	32.5	2834.5	16.1	2864.9	14.5	**2864.9**	**14.5**	97.5
154	163	58234.9	62.6	16.2	0.9	1.0	1.7	0.1	1.4	0.8	693.0	9.2	686.4	8.4	664.7	19.8	**693.0**	**9.2**	104.3
155	87	178469.8	3.1	7.5	0.9	7.3	1.7	0.4	1.4	0.8	2163.7	26.3	2153.9	15.2	2144.6	16.2	**2144.6**	**16.2**	100.9
156	412	162384.2	9.1	17.0	0.9	0.7	1.4	0.1	1.0	0.7	524.5	5.2	532.2	5.8	565.0	20.4	**524.5**	**5.2**	92.8
157	277	156971.3	2.3	8.8	1.0	4.9	1.9	0.3	1.6	0.8	1750.8	24.4	1795.6	15.9	1848.2	18.1	**1848.2**	**18.1**	94.7
158	116	38840.7	2.9	16.5	1.3	0.9	1.7	0.1	1.1	0.6	650.0	6.8	644.6	8.2	625.6	28.1	**650.0**	**6.8**	103.9
159	103	11410465.3	2.4	5.8	0.8	11.2	1.6	0.5	1.3	0.8	2504.7	27.2	2542.5	14.5	2572.8	14.0	**2572.8**	**14.0**	97.4
16	64	173855.7	6.5	9.0	0.8	4.0	1.4	0.3	1.2	0.8	1487.7	16.0	1626.6	11.6	1811.3	14.0	**1811.3**	**14.0**	82.1

160	539	183043.9	19.5	16.8	1.1	0.8	2.2	0.1	1.9	0.9	580.1	10.7	580.0	9.7	579.9	23.1	**580.1**	**10.7**	100.0
161	235	54199.7	2.3	17.2	1.0	0.7	1.6	0.1	1.2	0.7	569.1	6.4	563.1	6.8	538.5	23.0	**569.1**	**6.4**	105.7
162	746	333522.4	80.0	8.1	0.8	5.7	1.6	0.3	1.4	0.9	1877.1	23.1	1934.7	14.0	1996.9	13.9	**1996.9**	**13.9**	94.0
163	147	177384.2	1.4	8.0	0.7	6.2	1.6	0.4	1.4	0.9	1994.8	23.5	2008.5	13.6	2022.7	13.1	**2022.7**	**13.1**	98.6
164	265	402921.1	4.2	11.8	0.9	2.6	1.5	0.2	1.2	0.8	1295.4	14.3	1303.2	11.1	1316.1	17.0	**1316.1**	**17.0**	98.4
165	217	3276402.5	2.9	7.6	0.8	7.2	1.5	0.4	1.3	0.9	2152.1	23.1	2132.8	13.2	2114.2	13.6	**2114.2**	**13.6**	101.8
166	147	267397.7	4.3	13.6	0.9	1.7	1.3	0.2	0.9	0.7	1022.3	8.8	1024.1	8.5	1027.9	18.7	**1027.9**	**18.7**	99.5
167	174	68332.8	1.1	16.7	1.0	0.8	1.7	0.1	1.4	0.8	604.5	8.2	603.4	8.0	599.4	22.3	**604.5**	**8.2**	100.8
168	206	102089.9	3.0	13.0	0.9	2.0	1.6	0.2	1.3	0.8	1129.5	13.9	1127.3	11.0	1123.0	17.7	**1123.0**	**17.7**	100.6
169	53	19365.7	1.2	13.1	1.2	2.1	1.9	0.2	1.4	0.8	1147.5	15.2	1133.8	12.8	1107.7	23.6	**1107.7**	**23.6**	103.6
17	185	45620.7	1.9	16.4	0.9	0.9	1.6	0.1	1.4	0.8	622.9	8.0	625.1	7.5	633.2	18.6	**622.9**	**8.0**	98.4
170	217	22041.2	1.9	18.5	1.0	0.5	2.0	0.1	1.8	0.9	419.0	7.2	412.3	6.8	375.3	21.6	**419.0**	**7.2**	111.6
171	376	439153.9	4.8	9.7	1.0	4.1	1.6	0.3	1.2	0.8	1624.2	17.6	1648.3	12.9	1679.2	18.4	**1679.2**	**18.4**	96.7
172	133	153493.3	2.9	7.5	1.1	7.3	1.8	0.4	1.5	0.8	2151.1	27.3	2151.9	16.4	2152.7	18.8	**2152.7**	**18.8**	99.9
173	151	191612.2	1.3	9.6	1.1	4.2	1.7	0.3	1.3	0.8	1660.3	18.5	1675.8	13.7	1695.4	20.0	**1695.4**	**20.0**	97.9
174	329	66307.0	1.2	17.6	0.9	0.6	1.4	0.1	1.1	0.8	451.9	4.9	456.5	5.3	479.7	19.3	**451.9**	**4.9**	94.2
175	196	175694.6	1.9	16.7	1.1	0.8	1.8	0.1	1.5	0.8	604.1	8.6	602.3	8.4	595.7	23.2	**604.1**	**8.6**	101.4
176	131	3441113.8	1.4	16.0	1.0	0.9	1.7	0.1	1.3	0.8	667.6	8.2	671.5	8.2	684.7	22.3	**667.6**	**8.2**	97.5
177	91	37990.1	1.2	16.7	1.7	0.8	2.1	0.1	1.2	0.6	600.9	7.0	601.5	9.4	603.7	36.2	**600.9**	**7.0**	99.5
178	224	58456.3	1.7	18.2	1.0	0.5	1.5	0.1	1.1	0.7	427.5	4.7	424.6	5.3	408.7	22.6	**427.5**	**4.7**	104.6
179	43	15534.2	1.8	16.3	1.4	0.9	2.0	0.1	1.5	0.7	626.6	8.8	633.2	9.5	656.6	29.5	**626.6**	**8.8**	95.4
18	391	182868.0	1.3	16.5	1.0	0.9	1.7	0.1	1.4	0.8	640.0	8.5	636.2	8.1	622.8	21.3	**640.0**	**8.5**	102.8
180	96	67596.6	1.9	17.1	1.0	0.7	1.7	0.1	1.3	0.8	532.8	6.6	534.4	6.9	541.5	22.7	**532.8**	**6.6**	98.4
181	259	174097.7	0.9	16.6	1.0	0.9	1.7	0.1	1.4	0.8	631.5	8.5	626.4	8.1	608.3	21.4	**631.5**	**8.5**	103.8
182	224	454445.9	1.6	16.7	0.8	0.8	1.6	0.1	1.3	0.8	623.0	7.7	617.8	7.2	598.9	18.3	**623.0**	**7.7**	104.0
183	425	238744.9	2.0	16.9	0.9	0.8	1.5	0.1	1.2	0.8	578.3	6.4	576.3	6.5	568.4	19.5	**578.3**	**6.4**	101.7
184	309	1430687.1	14.8	5.6	0.9	12.1	1.6	0.5	1.3	0.8	2568.4	27.8	2610.0	14.9	2642.3	14.9	**2642.3**	**14.9**	97.2
185	277	2647388.7	1.4	8.8	0.9	5.3	1.8	0.3	1.6	0.9	1885.3	25.9	1874.2	15.4	1862.0	15.4	**1862.0**	**15.4**	101.3
186	257	57064.5	1.3	16.3	1.3	0.8	1.8	0.1	1.3	0.7	610.0	7.8	620.1	8.6	657.0	27.2	**610.0**	**7.8**	92.8
187	123	198871.1	1.4	13.5	0.9	1.7	1.6	0.2	1.3	0.8	1017.5	12.6	1023.5	10.5	1036.2	19.1	**1036.2**	**19.1**	98.2
188	101	202300.8	2.4	7.8	0.8	7.0	1.4	0.4	1.2	0.8	2147.9	21.7	2114.4	12.6	2081.9	13.5	**2081.9**	**13.5**	103.2
189	458	276220.5	27.3	16.8	0.9	0.8	2.1	0.1	1.9	0.9	571.7	10.3	574.4	9.0	585.5	18.5	**571.7**	**10.3**	97.6
19	58	184303.2	1.5	11.4	0.9	2.8	1.6	0.2	1.4	0.8	1326.6	16.4	1342.6	12.1	1368.3	16.7	**1368.3**	**16.7**	96.9
190	160	212143.0	2.0	8.5	0.8	5.7	1.5	0.3	1.3	0.9	1929.2	21.8	1925.4	13.1	1921.3	13.7	**1921.3**	**13.7**	100.4
191	174	20557818.0	2.8	7.2	0.7	8.0	1.7	0.4	1.5	0.9	2260.1	28.7	2233.9	14.9	2210.0	11.9	**2210.0**	**11.9**	102.3
192	218	193633.9	0.7	18.1	1.0	0.5	1.5	0.1	1.1	0.7	421.0	4.4	421.7	5.2	425.0	23.0	**421.0**	**4.4**	99.1

193	287	63714.4	2.7	16.5	0.8	0.8	1.2	0.1	0.9	0.8	599.1	5.1	603.8	5.4	621.3	16.9	**599.1**	**5.1**	96.4
194	104	156164.7	1.5	15.8	1.7	0.9	2.2	0.1	1.3	0.6	605.0	7.7	628.8	10.2	715.7	36.4	**605.0**	**7.7**	84.5
195	79	13125.8	1.7	15.8	2.0	0.9	2.5	0.1	1.5	0.6	612.2	8.7	634.7	11.6	715.8	41.4	**612.2**	**8.7**	85.5
196	278	1051731.0	1.8	11.0	0.7	3.2	1.5	0.3	1.3	0.9	1454.9	16.7	1451.1	11.3	1445.6	13.5	**1445.6**	**13.5**	100.6
197	161	1804971.5	7.7	7.8	0.8	6.6	1.5	0.4	1.3	0.9	2047.9	22.2	2065.1	13.0	2082.3	13.3	**2082.3**	**13.3**	98.3
198	196	382938.5	4.0	7.7	0.9	6.7	1.4	0.4	1.1	0.8	2051.2	19.5	2073.6	12.6	2095.9	15.6	**2095.9**	**15.6**	97.9
199	138	98182.8	2.1	16.5	1.5	0.9	1.9	0.1	1.2	0.6	631.9	7.3	629.9	8.9	622.5	31.7	**631.9**	**7.3**	101.5
2	105	139372.9	2.5	7.6	0.7	7.1	1.4	0.4	1.2	0.9	2120.5	20.8	2121.5	12.0	2122.4	12.4	**2122.4**	**12.4**	99.9
20	187	270738.7	1.8	17.0	0.9	0.7	1.6	0.1	1.4	0.8	546.2	7.1	548.7	6.9	558.7	19.3	**546.2**	**7.1**	97.8
200	714	331589.3	19.0	13.9	0.9	1.6	1.9	0.2	1.6	0.9	979.0	14.8	980.0	11.8	982.3	18.6	**982.3**	**18.6**	99.7
201	165	738280.6	5.7	13.4	0.9	1.9	1.7	0.2	1.5	0.9	1074.7	14.4	1070.2	11.2	1061.1	17.2	**1061.1**	**17.2**	101.3
202	157	114259.7	1.3	16.4	1.0	0.9	1.4	0.1	1.0	0.7	626.7	6.0	627.9	6.7	632.1	21.7	**626.7**	**6.0**	99.1
203	114	67470.8	0.7	16.3	1.3	0.9	1.9	0.1	1.4	0.7	649.7	8.4	650.9	8.9	655.1	27.4	**649.7**	**8.4**	99.2
204	175	17867.6	2.2	14.0	2.2	1.1	2.7	0.1	1.6	0.6	656.3	9.7	731.9	14.0	970.9	44.6	**656.3**	**9.7**	67.6
205	131	50974.3	2.3	16.4	1.8	0.7	2.2	0.1	1.2	0.6	546.3	6.5	565.5	9.6	643.5	39.5	**546.3**	**6.5**	84.9
206	493	191086.9	43.0	16.6	0.8	0.8	1.7	0.1	1.5	0.9	601.1	8.5	602.2	7.8	606.2	18.2	**601.1**	**8.5**	99.1
207	448	298732.5	1.6	17.8	1.0	0.6	1.5	0.1	1.1	0.7	469.0	4.9	467.7	5.5	461.2	21.6	**469.0**	**4.9**	101.7
208	251	100254.8	1.4	17.2	1.1	0.7	1.6	0.1	1.2	0.8	549.2	6.3	547.5	6.8	540.4	23.0	**549.2**	**6.3**	101.6
209	91	54085.2	3.5	14.7	1.0	1.4	1.8	0.1	1.4	0.8	883.2	11.9	880.6	10.4	873.9	21.0	**883.2**	**11.9**	101.1
21	92	23926.1	0.9	12.6	2.2	1.2	2.6	0.1	1.4	0.5	651.3	8.5	785.3	14.2	1187.5	43.5	**1187.5**	**43.5**	54.8
210	103	556571.3	1.4	16.2	1.1	0.9	2.3	0.1	2.1	0.9	634.7	12.5	642.3	11.0	669.2	22.5	**634.7**	**12.5**	94.8
211	111	72548.2	2.3	13.8	0.9	1.7	1.7	0.2	1.4	0.8	1027.3	13.6	1018.3	10.8	999.1	18.1	**999.1**	**18.1**	102.8
212	98	190841.2	2.1	13.0	1.0	1.9	1.5	0.2	1.1	0.7	1079.9	11.2	1090.5	10.0	1111.9	19.9	**1111.9**	**19.9**	97.1
213	149	9640948.4	2.1	7.0	1.2	7.0	2.5	0.4	2.2	0.9	1961.9	37.3	2109.6	22.2	2256.8	20.5	**2256.8**	**20.5**	86.9
214	114	224198.8	7.4	7.8	1.0	6.3	1.7	0.4	1.4	0.8	1986.0	23.1	2025.2	14.5	2065.4	16.8	**2065.4**	**16.8**	96.2
215	446	488088.0	6.8	10.9	1.0	3.3	1.8	0.3	1.5	0.8	1492.9	19.7	1479.0	13.8	1459.2	18.8	**1459.2**	**18.8**	102.3
216	258	198643.0	2.6	10.0	0.8	3.9	1.3	0.3	1.1	0.8	1603.0	15.2	1609.3	10.9	1617.5	15.2	**1617.5**	**15.2**	99.1
217	325	7542186.3	3.4	13.2	0.9	1.9	1.5	0.2	1.2	0.8	1101.9	11.9	1095.7	9.9	1083.4	18.1	**1083.4**	**18.1**	101.7
218	129	83446.1	3.4	8.3	1.0	5.0	1.9	0.3	1.6	0.9	1681.4	24.1	1811.9	16.0	1965.5	17.2	**1965.5**	**17.2**	85.5
219	273	182908.5	2.1	17.1	1.0	0.8	1.6	0.1	1.3	0.8	586.5	7.3	578.1	7.2	545.1	21.3	**586.5**	**7.3**	107.6
22	169	101416.6	2.3	9.8	1.0	4.2	1.6	0.3	1.2	0.8	1670.3	17.8	1665.7	12.7	1660.0	18.0	**1660.0**	**18.0**	100.6
220	375	1030813.4	2.8	11.2	0.7	3.2	1.7	0.3	1.5	0.9	1481.8	20.3	1453.5	13.2	1412.4	14.0	**1412.4**	**14.0**	104.9
221	306	183185.7	1.3	18.2	1.1	0.5	1.6	0.1	1.2	0.7	413.6	4.8	412.7	5.4	407.5	24.0	**413.6**	**4.8**	101.5
222	50	29406.9	2.3	7.6	0.9	7.1	1.4	0.4	1.0	0.8	2134.5	19.0	2123.3	12.3	2112.5	15.7	**2112.5**	**15.7**	101.0
223	224	51788.4	1.4	16.4	1.0	0.9	1.5	0.1	1.2	0.8	648.9	7.4	646.0	7.3	635.9	20.6	**648.9**	**7.4**	102.0
224	66	47294.2	1.7	9.8	0.8	4.1	1.6	0.3	1.4	0.9	1661.2	19.9	1659.6	12.9	1657.5	14.6	**1657.5**	**14.6**	100.2

225	64	25023.9	1.0	16.1	1.4	0.9	1.9	0.1	1.2	0.7	622.7	7.4	634.0	8.9	674.4	30.2	**622.7**	**7.4**	92.3
226	370	1686983.4	3.5	8.1	1.1	5.7	1.8	0.3	1.5	0.8	1858.5	23.8	1929.9	15.7	2007.3	18.9	**2007.3**	**18.9**	92.6
227	231	189617.3	2.4	16.5	0.9	0.9	1.6	0.1	1.3	0.8	627.0	8.1	627.0	7.6	627.0	19.5	**627.0**	**8.1**	100.0
229	108	27572.9	1.8	17.3	1.4	0.7	1.9	0.1	1.3	0.7	541.4	6.9	538.3	8.0	525.3	30.4	**541.4**	**6.9**	103.1
23	92	40151.4	1.5	17.0	1.3	0.7	1.7	0.1	1.2	0.7	536.6	5.9	540.0	7.2	554.2	27.6	**536.6**	**5.9**	96.8
230	261	52101.5	1.6	18.6	1.2	0.4	1.5	0.1	0.9	0.6	375.5	3.1	373.0	4.6	357.3	26.9	**375.5**	**3.1**	105.1
231	126	183942.7	1.9	8.4	0.8	5.4	1.6	0.3	1.4	0.9	1834.8	21.8	1884.1	13.4	1938.9	13.5	**1938.9**	**13.5**	94.6
232	139	72671.7	1.4	16.5	1.1	0.9	1.7	0.1	1.3	0.7	660.1	7.9	652.4	8.2	626.1	24.8	**660.1**	**7.9**	105.4
233	233	4331390.7	1.5	16.0	1.2	0.8	1.7	0.1	1.2	0.7	551.3	6.1	578.3	7.3	686.3	25.5	**551.3**	**6.1**	80.3
234	152	99025.7	3.0	7.7	0.8	6.8	1.4	0.4	1.2	0.8	2066.5	20.6	2082.1	12.4	2097.6	13.8	**2097.6**	**13.8**	98.5
235	101	35631.1	1.5	14.0	1.2	1.5	1.8	0.2	1.3	0.7	938.0	11.2	945.2	10.8	962.0	24.6	**962.0**	**24.6**	97.5
236	106	99284.3	0.9	9.9	1.0	3.8	1.9	0.3	1.6	0.8	1545.6	21.5	1589.7	14.9	1648.7	18.4	**1648.7**	**18.4**	93.7
237	161	1279105.9	2.6	6.0	1.0	10.8	1.8	0.5	1.5	0.8	2481.5	30.1	2509.4	16.4	2532.0	16.7	**2532.0**	**16.7**	98.0
238	92	136327.2	2.8	16.1	1.0	0.9	1.6	0.1	1.3	0.8	647.6	8.2	652.9	7.9	671.2	20.7	**647.6**	**8.2**	96.5
239	135	386664.8	16.5	9.4	0.8	4.4	1.8	0.3	1.6	0.9	1670.7	23.9	1703.5	14.9	1744.0	14.3	**1744.0**	**14.3**	95.8
240	389	231457.3	2.3	13.3	0.8	1.8	1.8	0.2	1.6	0.9	1056.5	16.0	1061.4	12.1	1071.4	16.7	**1071.4**	**16.7**	98.6
241	349	1045889.1	1.6	17.8	1.2	0.5	1.9	0.1	1.5	0.8	441.5	6.3	444.0	6.8	456.8	25.8	**441.5**	**6.3**	96.7
242	174	50854.0	2.0	16.3	0.9	0.9	1.4	0.1	1.0	0.8	628.8	6.3	633.5	6.5	650.0	19.1	**628.8**	**6.3**	96.7
243	169	197114.4	0.9	16.5	1.0	0.8	1.4	0.1	1.0	0.7	597.7	5.8	602.4	6.4	620.0	21.1	**597.7**	**5.8**	96.4
244	51	16275.7	1.0	16.4	1.4	0.9	2.0	0.1	1.4	0.7	640.2	8.5	640.7	9.4	642.5	30.3	**640.2**	**8.5**	99.7
245	547	1290916.7	2.7	12.5	0.9	2.2	1.8	0.2	1.6	0.9	1191.6	17.4	1195.0	12.8	1201.3	17.2	**1201.3**	**17.2**	99.2
246	116	161790.2	1.5	13.9	1.2	1.6	1.6	0.2	1.1	0.7	967.0	9.5	970.6	9.9	978.8	24.2	**978.8**	**24.2**	98.8
248	298	3580251.5	1.7	7.6	0.9	7.1	1.4	0.4	1.1	0.8	2137.2	20.9	2124.2	12.9	2111.7	15.4	**2111.7**	**15.4**	101.2
249	318	168354.6	2.2	17.0	0.7	0.7	1.5	0.1	1.3	0.9	560.5	7.0	561.1	6.5	563.5	16.2	**560.5**	**7.0**	99.5
25	99	201542.2	2.3	7.3	0.8	7.6	1.4	0.4	1.1	0.8	2179.2	20.0	2189.2	12.3	2198.5	14.6	**2198.5**	**14.6**	99.1
250	104	53243.5	6.8	16.4	1.4	0.8	2.3	0.1	1.8	0.8	619.8	10.4	624.6	10.5	642.1	30.5	**619.8**	**10.4**	96.5
251	79	5672652.0	1.5	12.5	1.0	2.2	1.5	0.2	1.1	0.7	1151.4	11.7	1166.5	10.5	1194.7	20.3	**1194.7**	**20.3**	96.4
252	169	1927881.8	7.0	16.4	1.0	0.8	1.5	0.1	1.1	0.7	616.3	6.7	620.2	7.0	634.4	21.6	**616.3**	**6.7**	97.1
253	168	83077.0	1.7	13.9	0.9	1.6	1.5	0.2	1.2	0.8	957.4	11.1	966.2	9.5	986.3	18.0	**986.3**	**18.0**	97.1
254	710	241935.2	1.7	18.0	0.8	0.5	1.8	0.1	1.6	0.9	395.9	6.2	401.4	6.0	433.0	18.8	**395.9**	**6.2**	91.4
255	563	1798988.2	1.3	12.1	0.9	2.5	1.8	0.2	1.5	0.9	1288.9	18.0	1277.6	12.8	1258.7	16.7	**1258.7**	**16.7**	102.4
256	39	239160.3	4.1	7.6	1.1	7.2	1.6	0.4	1.3	0.8	2145.6	23.0	2134.8	14.6	2124.4	18.5	**2124.4**	**18.5**	101.0
257	227	191467.7	1.7	16.6	1.0	0.8	1.8	0.1	1.5	0.8	610.1	8.6	611.1	8.2	614.9	21.7	**610.1**	**8.6**	99.2
258	338	89753.9	5.3	16.3	0.8	0.8	1.6	0.1	1.3	0.8	610.4	7.8	617.7	7.3	644.8	18.1	**610.4**	**7.8**	94.7
259	380	2467803.0	4.1	9.7	0.8	4.3	1.8	0.3	1.6	0.9	1701.3	24.2	1688.0	14.8	1671.6	14.6	**1671.6**	**14.6**	101.8
26	166	48562.5	7.5	16.4	1.0	0.9	2.0	0.1	1.7	0.9	641.9	10.5	642.2	9.6	643.5	22.2	**641.9**	**10.5**	99.8

260	202	2222266.9	2.9	8.2	0.8	6.2	1.5	0.4	1.3	0.8	2028.9	22.2	2009.9	13.2	1990.5	14.2	**1990.5**	**14.2**	101.9
261	168	31316.1	6.0	13.4	1.1	1.5	1.7	0.1	1.3	0.8	866.8	10.9	924.6	10.4	1065.1	21.7	**1065.1**	**21.7**	81.4
263	96	129592.7	2.2	7.8	1.2	6.8	1.7	0.4	1.3	0.7	2104.6	23.2	2092.0	15.4	2079.5	20.4	**2079.5**	**20.4**	101.2
264	154	65047.9	1.4	16.8	1.0	0.8	1.7	0.1	1.4	0.8	573.0	7.5	575.5	7.5	585.5	21.7	**573.0**	**7.5**	97.9
265	371	129179.8	1.1	16.2	1.0	0.9	1.6	0.1	1.3	0.8	663.9	8.0	663.5	7.8	662.1	21.0	**663.9**	**8.0**	100.3
266	146	80914.0	1.0	16.7	1.1	0.8	1.8	0.1	1.4	0.8	565.1	7.5	570.6	7.8	592.5	24.3	**565.1**	**7.5**	95.4
267	213	132156.9	2.5	16.6	1.0	0.8	1.5	0.1	1.2	0.8	600.8	6.9	601.9	7.0	605.6	21.0	**600.8**	**6.9**	99.2
268	696	420280.4	9.4	5.6	1.1	10.9	2.3	0.4	2.0	0.9	2371.5	39.7	2516.5	21.2	2635.7	18.1	**2635.7**	**18.1**	90.0
269	476	165172.0	1.2	18.3	0.9	0.5	1.4	0.1	1.1	0.8	440.2	4.6	433.7	5.0	399.5	20.9	**440.2**	**4.6**	110.2
27	111	113316.2	2.4	7.8	0.8	6.7	1.4	0.4	1.2	0.8	2061.8	21.3	2069.1	12.7	2076.3	13.7	**2076.3**	**13.7**	99.3
270	392	90605.0	2.4	18.2	0.8	0.5	1.3	0.1	0.9	0.8	408.9	3.8	409.5	4.2	412.9	18.3	**408.9**	**3.8**	99.0
271	130	125832.6	2.9	9.8	1.0	4.3	1.6	0.3	1.2	0.7	1703.6	17.3	1684.5	12.8	1660.7	19.2	**1660.7**	**19.2**	102.6
272	580	205657.3	2.2	16.4	0.9	0.9	1.7	0.1	1.4	0.8	675.4	9.0	667.5	8.2	640.8	19.7	**675.4**	**9.0**	105.4
273	106	24560.5	1.7	16.7	1.1	0.9	2.0	0.1	1.6	0.8	636.5	10.0	627.7	9.3	596.1	24.0	**636.5**	**10.0**	106.8
274	168	51519.7	1.6	16.4	1.1	0.9	1.7	0.1	1.3	0.8	626.8	7.6	628.0	7.9	632.3	24.0	**626.8**	**7.6**	99.1
275	46	238025.7	2.2	11.9	1.0	2.7	1.6	0.2	1.3	0.8	1351.5	15.5	1328.0	11.9	1290.2	19.1	**1290.2**	**19.1**	104.8
276	139	188432.6	3.7	7.7	0.8	6.9	1.3	0.4	1.0	0.8	2096.6	18.1	2092.6	11.5	2088.5	14.3	**2088.5**	**14.3**	100.4
277	98	31219.5	1.3	16.7	1.2	0.8	1.6	0.1	1.0	0.6	585.0	5.3	588.3	6.9	600.8	26.6	**585.0**	**5.3**	97.4
279	204	52908.2	1.2	17.0	0.8	0.8	1.4	0.1	1.1	0.8	574.0	6.2	570.8	6.1	558.1	18.2	**574.0**	**6.2**	102.9
28	272	403823.6	3.3	12.4	0.8	2.3	1.7	0.2	1.5	0.9	1207.4	16.8	1209.8	12.3	1214.1	16.3	**1214.1**	**16.3**	99.4
280	88	59382.0	0.8	16.5	1.1	0.9	1.8	0.1	1.5	0.8	626.5	8.8	625.0	8.6	619.5	23.7	**626.5**	**8.8**	101.1
281	410	1688613.6	109.1	10.3	0.8	3.7	1.3	0.3	1.1	0.8	1568.1	14.6	1570.9	10.5	1574.6	14.6	**1574.6**	**14.6**	99.6
282	183	64246.1	1.9	16.6	1.2	0.8	1.8	0.1	1.3	0.8	586.7	7.5	592.2	8.0	613.5	25.2	**586.7**	**7.5**	95.6
283	138	153284.3	1.7	8.7	0.9	5.4	1.4	0.3	1.1	0.8	1905.8	17.6	1889.6	11.9	1871.8	16.0	**1871.8**	**16.0**	101.8
284	598	140177.3	8.3	7.7	0.7	6.1	1.5	0.3	1.3	0.9	1872.8	21.8	1983.3	13.3	2100.6	12.9	**2100.6**	**12.9**	89.2
285	106	48306.9	1.0	9.9	0.8	3.9	1.4	0.3	1.2	0.8	1612.4	17.5	1621.9	11.7	1634.3	14.3	**1634.3**	**14.3**	98.7
286	253	1525099.8	7.3	7.8	0.9	6.4	1.6	0.4	1.3	0.8	1998.6	22.0	2038.7	13.9	2079.5	16.4	**2079.5**	**16.4**	96.1
287	143	101156.7	2.3	15.9	1.0	0.9	1.7	0.1	1.4	0.8	645.2	8.7	657.1	8.3	698.4	21.0	**645.2**	**8.7**	92.4
288	296	807190.9	1.5	16.6	1.0	0.8	1.6	0.1	1.2	0.8	590.8	6.7	595.2	7.1	611.9	22.5	**590.8**	**6.7**	96.5
289	62	310591.4	2.6	16.2	1.0	0.9	1.6	0.1	1.2	0.8	648.9	7.7	652.1	7.8	663.1	22.4	**648.9**	**7.7**	97.9
29	222	64114.8	3.2	18.1	1.1	0.5	1.8	0.1	1.4	0.8	421.8	5.9	421.5	6.2	419.7	24.0	**421.8**	**5.9**	100.5
290	372	282029.5	2.3	9.1	0.9	4.7	1.6	0.3	1.4	0.9	1745.7	21.3	1768.5	13.7	1795.5	15.5	**1795.5**	**15.5**	97.2
291	99	185262.0	1.5	8.8	0.8	5.5	1.5	0.3	1.3	0.8	1932.4	20.9	1898.2	13.0	1861.0	15.2	**1861.0**	**15.2**	103.8
292	161	223653.4	1.4	7.7	1.0	7.0	1.7	0.4	1.4	0.8	2144.3	26.0	2115.0	15.3	2086.7	17.0	**2086.7**	**17.0**	102.8
293	949	1243947.8	0.3	17.6	0.9	0.6	1.9	0.1	1.7	0.9	488.7	8.2	488.2	7.5	485.6	19.1	**488.7**	**8.2**	100.6
294	100	138842.5	0.5	9.0	0.8	4.9	1.6	0.3	1.4	0.8	1784.9	21.1	1795.3	13.4	1807.4	15.3	**1807.4**	**15.3**	98.8

295	68	15213.1	2.3	16.5	1.4	0.8	1.9	0.1	1.4	0.7	606.9	7.9	610.5	8.9	623.9	29.9	**606.9**	**7.9**	97.3
296	205	2520642.8	2.2	16.3	1.0	0.9	1.6	0.1	1.2	0.8	626.6	7.5	632.6	7.4	653.8	20.8	**626.6**	**7.5**	95.8
297	83	168430.9	2.3	14.3	2.2	1.0	2.5	0.1	1.3	0.5	631.0	7.5	697.8	12.6	919.5	44.5	**631.0**	**7.5**	68.6
298	71	154118.6	1.8	10.6	0.9	3.4	1.6	0.3	1.3	0.8	1494.8	17.2	1500.4	12.3	1508.1	16.8	**1508.1**	**16.8**	99.1
299	82	8047.4	1.9	14.7	2.3	0.6	2.7	0.1	1.4	0.5	422.4	5.8	498.2	10.7	863.3	48.3	**422.4**	**5.8**	48.9
3	113	60610.5	2.0	16.5	0.8	0.9	1.4	0.1	1.2	0.8	632.9	7.1	631.9	6.8	628.4	17.8	**632.9**	**7.1**	100.7
30	93	51964.0	2.0	16.2	1.2	0.9	1.8	0.1	1.4	0.8	672.8	9.0	671.7	9.0	668.1	25.5	**672.8**	**9.0**	100.7
300	537	65354012.7	3.3	10.2	0.8	3.9	2.1	0.3	1.9	0.9	1615.9	27.4	1604.2	16.8	1588.8	15.7	**1588.8**	**15.7**	101.7
301	36	15328.6	1.9	16.7	1.7	0.8	2.2	0.1	1.3	0.6	596.0	7.6	596.8	9.8	599.6	37.1	**596.0**	**7.6**	99.4
302	153	498438.8	1.0	16.7	1.4	0.8	1.9	0.1	1.3	0.7	614.6	7.7	611.8	8.9	601.5	30.6	**614.6**	**7.7**	102.2
304	374	77829.3	3.5	12.1	1.0	2.4	1.7	0.2	1.3	0.8	1242.5	14.9	1247.0	12.0	1254.6	20.0	**1254.6**	**20.0**	99.0
305	212	75209.9	7.0	13.4	0.8	1.8	1.4	0.2	1.2	0.8	1021.1	11.2	1030.5	9.2	1050.4	15.7	**1050.4**	**15.7**	97.2
306	326	5491294.9	231.0	7.9	0.9	6.2	1.6	0.4	1.3	0.8	1953.3	22.6	2003.8	14.1	2056.2	16.0	**2056.2**	**16.0**	95.0
307	132	118952.7	3.2	5.5	0.9	12.5	1.5	0.5	1.2	0.8	2601.9	25.8	2645.8	13.9	2679.7	14.1	**2679.7**	**14.1**	97.1
308	198	35870.8	1.7	18.0	1.5	0.5	1.9	0.1	1.1	0.6	446.9	4.9	444.9	6.7	434.8	32.9	**446.9**	**4.9**	102.8
309	185	185105.6	3.6	12.1	0.9	2.4	1.6	0.2	1.3	0.8	1249.6	15.2	1253.5	11.7	1260.2	18.0	**1260.2**	**18.0**	99.2
31	295	90442.6	1.5	13.9	0.9	1.6	1.8	0.2	1.5	0.8	957.0	13.3	964.3	11.0	981.1	19.2	**981.1**	**19.2**	97.5
310	105	81441.5	2.6	7.3	0.9	7.5	1.5	0.4	1.1	0.8	2147.3	20.8	2167.1	13.0	2185.9	15.7	**2185.9**	**15.7**	98.2
311	99	112939.5	1.0	16.6	1.2	0.8	1.6	0.1	1.1	0.7	622.6	6.3	618.9	7.6	605.0	26.6	**622.6**	**6.3**	102.9
312	92	27931.7	0.8	16.5	1.2	0.9	1.8	0.1	1.3	0.7	639.0	8.0	634.7	8.4	619.2	25.7	**639.0**	**8.0**	103.2
313	174	178732.0	1.3	14.0	1.1	1.6	1.5	0.2	1.1	0.7	988.7	9.8	981.4	9.5	965.0	21.5	**965.0**	**21.5**	102.5
314	246	218782.9	1.7	8.8	1.0	5.3	1.6	0.3	1.2	0.8	1874.9	20.2	1871.5	13.4	1867.7	17.3	**1867.7**	**17.3**	100.4
315	225	164313.3	1.3	16.2	1.1	0.9	1.6	0.1	1.1	0.7	615.7	6.7	626.1	7.3	664.0	22.8	**615.7**	**6.7**	92.7
32	262	84086.9	1.0	18.1	0.9	0.5	1.8	0.1	1.5	0.9	413.6	6.2	414.7	6.1	420.6	20.5	**413.6**	**6.2**	98.3
33	152	164771.3	1.6	16.6	1.3	0.8	1.7	0.1	1.2	0.7	557.4	6.2	568.8	7.6	614.7	28.2	**557.4**	**6.2**	90.7
34	142	65879.8	1.2	16.1	1.3	0.9	1.8	0.1	1.3	0.7	676.2	8.4	676.5	9.1	677.6	28.0	**676.2**	**8.4**	99.8
35	67	105063.9	2.3	7.4	0.9	7.5	1.8	0.4	1.6	0.9	2194.4	28.9	2175.7	16.3	2158.2	16.4	**2158.2**	**16.4**	101.7
36	377	175742.7	2.3	14.6	1.0	1.4	1.7	0.1	1.4	0.8	866.2	11.0	872.8	9.8	889.4	20.4	**866.2**	**11.0**	97.4
37	198	105250.9	4.3	13.3	0.9	1.8	1.7	0.2	1.4	0.8	1055.9	13.6	1059.4	11.0	1066.7	18.4	**1066.7**	**18.4**	99.0
38	123	186795.5	1.6	7.7	0.7	7.2	1.3	0.4	1.2	0.9	2165.6	21.6	2135.0	12.0	2105.6	11.6	**2105.6**	**11.6**	102.8
39	148	186685.5	0.7	8.0	1.0	6.2	1.8	0.4	1.5	0.8	1978.5	25.1	2002.9	15.7	2028.1	18.3	**2028.1**	**18.3**	97.6
4	173	167212.5	5.3	16.9	1.1	0.8	1.7	0.1	1.2	0.7	588.0	6.8	583.9	7.4	568.0	24.9	**588.0**	**6.8**	103.5
40	130	62135.6	3.9	11.0	1.1	3.2	1.8	0.3	1.5	0.8	1462.5	19.7	1455.2	14.2	1444.5	20.0	**1444.5**	**20.0**	101.2
41	18	19311.6	3.3	14.0	2.1	1.7	2.6	0.2	1.6	0.6	1002.6	15.1	992.3	16.7	969.6	42.2	**969.6**	**42.2**	103.4
42	177	181531.6	4.8	7.9	0.8	6.6	1.5	0.4	1.3	0.9	2059.8	22.8	2057.5	13.2	2055.2	13.5	**2055.2**	**13.5**	100.2
43	49	47313.2	1.1	18.2	1.8	0.5	2.3	0.1	1.5	0.6	397.2	5.7	399.3	7.6	411.2	39.5	**397.2**	**5.7**	96.6

45	155	37453.2	3.8	16.8	1.1	0.7	1.9	0.1	1.6	0.8	553.3	8.3	559.0	8.3	582.3	24.2	**553.3**	**8.3**	95.0
46	41	111814.4	1.6	16.6	1.6	0.8	2.0	0.1	1.2	0.6	596.7	7.0	599.0	9.2	608.1	35.0	**596.7**	**7.0**	98.1
47	109	204371.9	4.8	13.6	0.7	1.7	1.6	0.2	1.4	0.9	1008.4	12.8	1014.9	10.0	1028.9	15.2	**1028.9**	**15.2**	98.0
48	265	95045.8	3.0	15.5	1.3	1.0	1.8	0.1	1.3	0.7	662.2	8.1	683.1	9.1	752.7	27.7	**662.2**	**8.1**	88.0
49	230	50229.4	1.6	18.2	1.0	0.5	1.6	0.1	1.2	0.8	414.9	5.0	414.5	5.5	412.0	23.3	**414.9**	**5.0**	100.7
5	45	33197.5	2.0	15.5	1.5	1.2	2.0	0.1	1.3	0.6	795.6	9.9	786.6	11.1	761.3	32.5	**795.6**	**9.9**	104.5
50	86	41454.3	1.9	16.6	1.4	0.8	1.9	0.1	1.3	0.7	557.8	7.1	569.0	8.3	613.7	30.0	**557.8**	**7.1**	90.9
51	202	165727.9	1.5	16.4	1.0	0.9	1.5	0.1	1.1	0.7	629.3	6.7	631.0	7.0	637.2	21.5	**629.3**	**6.7**	98.7
52	265	195206.7	2.7	16.4	1.2	0.9	1.8	0.1	1.3	0.7	631.1	8.0	632.1	8.5	635.9	26.4	**631.1**	**8.0**	99.2
53	554	166967.1	10.8	16.6	0.9	0.8	1.8	0.1	1.6	0.9	623.6	9.3	622.0	8.5	616.0	20.3	**623.6**	**9.3**	101.2
54	242	146002.8	1.7	16.4	0.9	0.9	1.4	0.1	1.1	0.8	641.8	6.7	641.7	6.7	641.2	19.4	**641.8**	**6.7**	100.1
55	663	182010.7	2.4	16.6	0.9	0.9	1.7	0.1	1.4	0.8	647.5	8.6	640.5	8.0	615.9	19.8	**647.5**	**8.6**	105.1
56	173	598933.5	1.6	16.5	0.8	0.8	1.6	0.1	1.4	0.9	599.7	8.2	603.9	7.5	619.8	17.9	**599.7**	**8.2**	96.8
57	686	250601.5	1.7	16.2	1.1	0.9	1.9	0.1	1.6	0.8	648.9	9.7	652.8	9.2	666.3	23.4	**648.9**	**9.7**	97.4
58	32	74744.1	2.5	6.0	0.8	11.0	1.4	0.5	1.1	0.8	2529.0	23.7	2526.0	13.2	2523.5	14.3	**2523.5**	**14.3**	100.2
59	137	53457.0	1.3	16.6	1.0	0.8	1.6	0.1	1.2	0.7	580.1	6.6	587.6	7.1	616.4	22.7	**580.1**	**6.6**	94.1
6	84	103519.4	2.2	7.4	1.0	6.6	2.0	0.4	1.7	0.9	1936.5	29.2	2052.7	17.8	2171.5	17.6	**2171.5**	**17.6**	89.2
60	308	2189482.0	39.8	7.9	0.8	6.0	1.5	0.3	1.3	0.8	1908.7	21.4	1983.0	13.4	2061.4	14.7	**2061.4**	**14.7**	92.6
61	137	47085.2	1.2	16.4	1.0	0.8	1.6	0.1	1.2	0.8	609.5	7.2	616.6	7.4	642.9	21.7	**609.5**	**7.2**	94.8
62	70	22245.9	1.8	16.8	1.2	0.8	1.7	0.1	1.2	0.7	589.7	6.9	588.3	7.7	582.8	26.5	**589.7**	**6.9**	101.2
63	921	3127216.6	8.4	8.7	0.9	4.4	2.1	0.3	1.9	0.9	1565.3	26.9	1703.9	17.7	1878.8	16.4	**1878.8**	**16.4**	83.3
64	305	183458.4	2.7	12.5	0.7	2.3	1.4	0.2	1.2	0.8	1201.4	12.8	1198.3	9.6	1192.7	14.3	**1192.7**	**14.3**	100.7
65	348	151528.2	5.2	16.1	0.9	0.9	1.5	0.1	1.2	0.8	636.2	7.5	645.7	7.3	678.7	19.4	**636.2**	**7.5**	93.7
66	266	159467.3	2.8	7.5	0.7	7.2	1.4	0.4	1.2	0.9	2143.7	22.7	2139.0	12.8	2134.4	12.4	**2134.4**	**12.4**	100.4
67	209	540254.4	4.0	7.2	0.7	7.1	1.4	0.4	1.3	0.9	2048.8	22.4	2127.2	12.9	2203.8	11.9	**2203.8**	**11.9**	93.0
68	385	452597.7	2.2	17.8	1.0	0.5	1.6	0.1	1.3	0.8	416.5	5.3	422.2	5.6	452.9	21.6	**416.5**	**5.3**	92.0
69	173	419440.3	1.5	8.6	0.8	5.6	1.5	0.3	1.3	0.9	1928.0	21.5	1911.5	13.0	1893.7	13.9	**1893.7**	**13.9**	101.8
7	68	47054.5	1.2	13.9	1.2	1.7	1.7	0.2	1.2	0.7	1009.9	11.2	1000.0	11.0	978.3	25.4	**978.3**	**25.4**	103.2
70	180	179695.6	1.8	9.6	0.9	4.2	1.5	0.3	1.2	0.8	1656.0	17.5	1678.7	12.5	1707.2	17.4	**1707.2**	**17.4**	97.0
71	169	188392.4	2.1	14.9	1.0	1.2	2.0	0.1	1.8	0.9	767.1	12.7	785.0	11.0	836.2	20.2	**767.1**	**12.7**	91.7
72	205	443424.5	1.8	4.4	0.9	18.3	1.5	0.6	1.1	0.8	2985.2	26.6	3007.7	14.1	3022.8	15.2	**3022.8**	**15.2**	98.8
73	145	234722.1	2.7	14.2	0.7	1.5	1.4	0.2	1.2	0.9	921.2	10.6	927.8	8.7	943.5	14.6	**943.5**	**14.6**	97.6
74	161	192101.4	1.2	16.6	1.1	0.9	1.6	0.1	1.2	0.8	632.2	7.3	629.1	7.6	617.6	22.8	**632.2**	**7.3**	102.4
76	106	59661.0	3.4	13.6	1.1	1.8	1.5	0.2	1.0	0.7	1035.9	9.8	1031.0	9.8	1020.7	22.6	**1020.7**	**22.6**	101.5
77	281	313583.3	2.7	11.7	0.9	2.6	1.5	0.2	1.1	0.8	1289.5	13.0	1303.9	10.7	1327.7	18.2	**1327.7**	**18.2**	97.1
78	207	74951.9	11.7	16.6	0.9	0.8	1.6	0.1	1.3	0.8	616.6	7.5	615.7	7.3	612.4	20.1	**616.6**	**7.5**	100.7

79	459	627990.2	2.4	18.1	1.2	0.5	1.7	0.1	1.3	0.7	394.4	4.9	397.7	5.7	416.5	25.9	**394.4**	**4.9**	94.7
8	89	225571.2	3.4	13.6	0.9	1.8	1.5	0.2	1.2	0.8	1042.4	11.6	1039.1	9.7	1032.1	18.0	**1032.1**	**18.0**	101.0
80	119	168969.0	0.9	17.0	1.0	0.8	1.6	0.1	1.2	0.7	574.1	6.4	572.0	6.8	563.6	22.7	**574.1**	**6.4**	101.9
82	725	286144.8	3.6	12.2	0.8	2.4	1.5	0.2	1.3	0.9	1239.6	14.6	1242.8	10.9	1248.4	15.5	**1248.4**	**15.5**	99.3
83	196	168642.4	0.9	17.1	1.2	0.7	2.0	0.1	1.6	0.8	554.5	8.3	553.8	8.3	551.0	25.8	**554.5**	**8.3**	100.6
84	266	355816.1	1.2	13.5	1.0	1.8	1.6	0.2	1.2	0.8	1075.9	11.8	1063.3	10.4	1037.4	20.9	**1037.4**	**20.9**	103.7
85	259	350853.6	14.0	12.2	0.9	2.4	1.5	0.2	1.2	0.8	1244.5	13.7	1243.8	10.7	1242.7	17.1	**1242.7**	**17.1**	100.1
86	38	39053.4	0.9	7.4	1.1	7.2	1.5	0.4	1.1	0.7	2129.4	19.4	2142.2	13.6	2154.5	19.0	**2154.5**	**19.0**	98.8
87	475	385096.6	14.3	13.1	1.4	1.8	2.4	0.2	1.9	0.8	1034.3	18.5	1055.0	15.7	1098.2	27.9	**1098.2**	**27.9**	94.2
88	257	774624.6	2.4	16.2	0.9	0.9	1.7	0.1	1.5	0.9	623.9	8.8	632.4	8.1	663.0	18.8	**623.9**	**8.8**	94.1
89	372	3832797.4	1.3	8.1	1.0	6.3	1.6	0.4	1.3	0.8	2028.1	22.0	2018.9	13.9	2009.4	17.0	**2009.4**	**17.0**	100.9
9	687	178472.2	2.2	18.8	1.2	0.4	1.9	0.0	1.5	0.8	311.7	4.6	314.5	5.2	335.4	26.8	**311.7**	**4.6**	92.9
90	29	30339.1	1.8	10.0	1.2	4.0	1.9	0.3	1.4	0.8	1653.6	21.1	1643.0	15.3	1629.5	22.4	**1629.5**	**22.4**	101.5
91	69	18113.6	1.3	16.8	1.1	0.8	1.8	0.1	1.4	0.8	608.2	8.3	602.6	8.2	581.3	24.0	**608.2**	**8.3**	104.6
92	184	194808.2	2.5	16.2	1.3	0.9	1.7	0.1	1.1	0.7	660.3	7.1	662.2	8.3	668.4	27.4	**660.3**	**7.1**	98.8
93	258	2061156.2	0.8	15.3	0.8	1.2	1.5	0.1	1.3	0.8	787.9	9.7	787.8	8.4	787.2	17.1	**787.9**	**9.7**	100.1
94	37	158153.6	2.5	13.1	1.3	1.8	1.8	0.2	1.3	0.7	1040.5	12.4	1062.1	11.9	1106.8	25.1	**1106.8**	**25.1**	94.0
95	61	82121.0	2.0	16.3	1.4	0.9	1.8	0.1	1.2	0.6	633.2	7.1	636.6	8.7	648.9	30.2	**633.2**	**7.1**	97.6
96	86	82051.0	2.5	8.1	0.9	6.0	1.4	0.4	1.0	0.7	1952.0	17.1	1977.6	11.9	2004.4	16.3	**2004.4**	**16.3**	97.4
97	159	81099.5	2.3	16.0	1.0	1.0	1.6	0.1	1.2	0.8	692.2	7.9	690.6	7.8	685.5	21.2	**692.2**	**7.9**	101.0
98	46	75653.5	3.0	12.3	1.4	2.3	2.1	0.2	1.5	0.7	1184.2	16.3	1201.5	14.5	1232.7	27.4	**1232.7**	**27.4**	96.1
99	357	176914.5	5.7	16.1	1.1	0.9	1.8	0.1	1.4	0.8	615.4	8.3	629.8	8.3	682.1	22.7	**615.4**	**8.3**	90.2
xx	611	333892.7	6.0	17.1	1.0	0.7	2.2	0.1	2.0	0.9	536.6	10.3	539.3	9.4	551.1	22.2	**536.6**	**10.3**	97.4
xx	515	262649.8	2.0	13.1	1.1	1.8	2.3	0.2	2.0	0.9	1004.1	18.2	1036.3	14.7	1104.8	22.8	**1104.8**	**22.8**	90.9
xx	227	140936.4	7.1	16.9	1.0	0.7	1.5	0.1	1.1	0.7	536.5	5.8	543.6	6.4	573.3	22.5	**536.5**	**5.8**	93.6

Sample: DG-B						Isotope Ratios					Apparent Ages (Ma)								
Analysis	**U (ppm)**	**206Pb /204Pb**	**U /Th**	**206Pb /207Pb**	**± (%)**	**207Pb /235U**	**± (%)**	**206Pb /238U**	**± (%)**	**err. corr.**	**206Pb /238U**	**± (Ma)**	**207Pb /235U**	**± (Ma)**	**206Pb /207Pb**	**± (Ma)**	**Best Age**	**± (Ma)**	**Conc. (%)**
10	382	37394.7	2.8	8.6	1.0	4.7	1.4	0.3	1.0	0.7	1663.4	14.7	1766.2	11.7	1890.1	17.6	**1890.1**	**17.6**	88.1
100	620	442228.7	1.3	16.4	0.7	0.8	1.5	0.1	1.3	0.9	598.6	7.2	605.8	6.7	632.8	15.9	**598.6**	**7.2**	94.6
101	183	263784.2	1.0	7.5	0.9	6.9	1.4	0.4	1.1	0.8	2070.5	19.7	2103.7	12.5	2136.2	15.2	**2136.2**	**15.2**	96.9
102	196	64606.8	1.1	16.3	1.0	0.9	1.7	0.1	1.4	0.8	622.2	8.1	629.5	8.0	656.1	21.7	**622.2**	**8.1**	94.8
103	459	360032.0	2.6	10.9	0.7	3.2	1.6	0.3	1.4	0.9	1460.8	18.0	1462.5	12.1	1464.8	14.0	**1464.8**	**14.0**	99.7
104	70	12960.2	1.0	16.5	1.3	0.8	1.9	0.1	1.3	0.7	617.8	7.9	619.5	8.6	625.5	27.4	**617.8**	**7.9**	98.8
105	196	103324.4	3.9	13.1	0.8	2.0	1.5	0.2	1.3	0.9	1122.8	13.1	1115.9	10.1	1102.5	15.5	**1102.5**	**15.5**	101.8
106	105	117417.6	1.2	7.6	0.9	7.1	1.8	0.4	1.6	0.9	2122.4	28.9	2118.6	16.2	2114.9	15.4	**2114.9**	**15.4**	100.4
107	174	39937.9	0.9	16.0	1.1	0.9	1.6	0.1	1.1	0.7	655.3	7.0	662.3	7.7	686.0	23.5	**655.3**	**7.0**	95.5
108	205	26896.7	1.6	18.1	0.9	0.5	1.3	0.1	0.9	0.7	414.3	3.7	415.2	4.4	420.3	20.6	**414.3**	**3.7**	98.6
109	229	63052.6	2.0	16.5	0.9	0.8	1.5	0.1	1.2	0.8	611.7	6.9	613.3	6.8	619.0	19.6	**611.7**	**6.9**	98.8
11	114	94186.4	1.6	9.7	0.9	4.2	1.5	0.3	1.2	0.8	1661.9	17.3	1668.2	12.1	1676.1	16.4	**1676.1**	**16.4**	99.1
110	216	115393.4	0.5	17.1	0.9	0.7	1.6	0.1	1.3	0.8	553.1	6.8	551.8	6.7	546.1	19.8	**553.1**	**6.8**	101.3
111	277	57539.7	1.1	18.0	1.0	0.5	1.7	0.1	1.3	0.8	417.4	5.4	419.5	5.8	431.1	22.5	**417.4**	**5.4**	96.8
112	215	567728.3	2.8	13.6	0.9	1.7	1.6	0.2	1.3	0.8	1008.2	11.7	1015.9	10.0	1032.5	18.5	**1032.5**	**18.5**	97.6
113	154	308273.0	1.9	7.6	0.9	6.8	1.5	0.4	1.2	0.8	2069.4	21.1	2088.3	13.2	2106.9	15.7	**2106.9**	**15.7**	98.2
114	72	29789.3	1.0	16.4	1.1	0.9	1.5	0.1	1.0	0.7	647.2	6.3	644.1	7.2	633.4	23.6	**647.2**	**6.3**	102.2
115	255	133002.3	1.2	16.3	1.0	0.8	1.6	0.1	1.3	0.8	603.4	7.5	612.8	7.5	647.5	21.1	**603.4**	**7.5**	93.2
116	242	113283.7	1.2	15.8	0.8	0.8	1.4	0.1	1.2	0.8	591.9	6.6	619.0	6.7	719.1	17.9	**591.9**	**6.6**	82.3
117	924	1903980.6	6.9	10.8	0.8	3.3	1.7	0.3	1.5	0.9	1469.5	20.0	1473.4	13.2	1479.0	14.4	**1479.0**	**14.4**	99.4
118	793	88269.2	0.7	18.5	0.8	0.4	1.9	0.0	1.8	0.9	305.3	5.3	313.8	5.3	377.5	18.3	**305.3**	**5.3**	80.9
119	94	60654.9	2.4	12.9	1.1	2.0	1.6	0.2	1.1	0.7	1110.8	11.3	1119.7	10.6	1137.2	22.1	**1137.2**	**22.1**	97.7
12	132	39273.1	1.5	18.1	1.1	0.5	1.6	0.1	1.1	0.7	425.1	4.7	424.6	5.5	421.6	25.0	**425.1**	**4.7**	100.8
120	196	104035.0	1.0	8.9	0.8	4.9	1.5	0.3	1.3	0.8	1763.3	19.3	1793.9	12.6	1829.7	14.8	**1829.7**	**14.8**	96.4
121	256	1237813.4	6.6	10.4	0.8	3.6	1.7	0.3	1.5	0.9	1547.8	20.5	1545.6	13.5	1542.6	15.6	**1542.6**	**15.6**	100.3
122	105	29206.2	1.9	16.4	1.1	0.8	1.8	0.1	1.3	0.8	618.0	7.9	623.2	8.2	642.0	24.4	**618.0**	**7.9**	96.3

123	34	13155.4	1.0	13.6	1.5	1.7	1.9	0.2	1.1	0.6	1004.4	10.5	1011.4	11.9	1026.6	29.7	**1026.6**	**29.7**	97.8
124	363	91750.2	2.5	11.9	0.6	2.6	1.2	0.2	1.0	0.9	1294.7	12.0	1296.1	8.6	1298.5	11.2	**1298.5**	**11.2**	99.7
125	42	33466.1	2.5	16.9	1.6	0.8	2.0	0.1	1.1	0.6	606.8	6.3	598.7	8.9	568.2	35.7	**606.8**	**6.3**	106.8
126	151	23199.1	1.0	16.5	1.1	0.8	1.6	0.1	1.2	0.8	615.4	7.3	617.2	7.5	623.6	22.8	**615.4**	**7.3**	98.7
127	761	94271.5	0.9	7.2	0.6	6.3	1.9	0.3	1.8	0.9	1838.8	29.1	2024.1	16.9	2218.8	10.7	**2218.8**	**10.7**	82.9
129	103	280469.0	1.5	16.6	1.3	0.8	1.7	0.1	1.2	0.7	592.6	6.8	597.4	7.9	615.8	27.4	**592.6**	**6.8**	96.2
13	112	171513.9	2.9	12.3	0.9	2.3	1.7	0.2	1.4	0.8	1227.1	15.8	1226.6	12.1	1225.6	18.5	**1225.6**	**18.5**	100.1
130	180	100666.7	25.6	10.3	0.9	2.9	1.4	0.2	1.1	0.8	1275.2	12.7	1390.5	10.9	1572.0	17.4	**1572.0**	**17.4**	81.1
131	15	6959.8	1.7	16.7	2.5	0.9	2.9	0.1	1.3	0.5	646.4	8.1	635.7	13.5	597.9	55.0	**646.4**	**8.1**	108.1
132	462	106979.9	0.6	17.1	1.0	0.7	2.1	0.1	1.8	0.9	508.7	9.0	516.5	8.5	551.1	22.8	**508.7**	**9.0**	92.3
133	217	109939.8	3.1	15.4	0.9	1.0	1.4	0.1	1.1	0.8	714.3	7.4	727.5	7.5	768.3	19.6	**714.3**	**7.4**	93.0
134	106	315413.1	1.4	10.4	0.9	3.7	1.6	0.3	1.3	0.8	1596.4	17.9	1580.0	12.5	1558.1	17.2	**1558.1**	**17.2**	102.5
135	800	220029.4	0.5	16.5	0.8	0.8	1.7	0.1	1.5	0.9	617.0	8.7	619.8	7.7	630.3	16.3	**617.0**	**8.7**	97.9
136	190	115824.3	3.0	16.4	0.8	0.9	1.4	0.1	1.1	0.8	623.5	6.7	626.8	6.5	638.8	17.8	**623.5**	**6.7**	97.6
137	62	16055.2	1.4	16.5	1.1	0.8	1.7	0.1	1.2	0.7	606.2	7.1	610.4	7.7	625.6	24.5	**606.2**	**7.1**	96.9
138	135	28924.0	1.3	18.0	1.5	0.4	1.8	0.1	1.0	0.6	344.9	3.5	356.3	5.5	431.1	34.1	**344.9**	**3.5**	80.0
139	93	135294.6	1.0	16.3	1.2	0.9	1.7	0.1	1.2	0.7	625.7	7.4	632.2	8.0	655.5	24.8	**625.7**	**7.4**	95.5
14	88	117385.0	1.4	18.0	1.4	0.5	1.8	0.1	1.1	0.6	418.9	4.5	420.5	6.2	429.5	31.4	**418.9**	**4.5**	97.5
140	376	113585.5	1.2	16.2	0.8	0.9	1.3	0.1	1.0	0.8	657.1	6.4	658.6	6.2	663.6	16.2	**657.1**	**6.4**	99.0
141	36	487108.2	1.8	13.4	1.3	1.8	2.0	0.2	1.4	0.7	1056.4	14.0	1058.8	12.9	1063.8	27.0	**1063.8**	**27.0**	99.3
142	141	49936.8	3.2	17.2	1.2	0.7	1.8	0.1	1.4	0.8	556.2	7.4	552.6	7.8	537.4	26.1	**556.2**	**7.4**	103.5
143	187	124056.4	2.3	12.7	0.9	2.2	1.3	0.2	1.0	0.7	1178.0	10.4	1175.3	9.3	1170.2	18.3	**1170.2**	**18.3**	100.7
144	94	17043.8	4.4	13.3	1.2	1.7	1.6	0.2	1.1	0.7	976.5	10.1	1007.0	10.3	1074.1	23.6	**1074.1**	**23.6**	90.9
145	377	44189.2	0.8	16.9	1.0	0.7	1.9	0.1	1.6	0.9	523.6	8.2	532.9	7.9	573.1	21.5	**523.6**	**8.2**	91.4
146	96	83005.6	3.8	12.1	1.1	2.5	1.5	0.2	1.0	0.7	1278.7	11.6	1274.1	10.6	1266.4	20.9	**1266.4**	**20.9**	101.0
147	90	369231.1	3.3	12.8	1.0	2.1	1.7	0.2	1.4	0.8	1155.9	14.7	1151.5	11.6	1143.1	19.0	**1143.1**	**19.0**	101.1
148	193	268265.5	2.6	11.6	0.6	2.7	1.5	0.2	1.3	0.9	1336.3	16.3	1339.8	11.0	1345.5	12.0	**1345.5**	**12.0**	99.3
149	296	110068.3	1.1	16.3	1.1	0.9	1.4	0.1	0.9	0.6	638.4	5.2	639.7	6.5	644.2	23.0	**638.4**	**5.2**	99.1
15	101	130781.3	3.2	14.3	1.1	1.4	1.7	0.1	1.3	0.8	873.7	10.5	886.9	9.9	919.9	21.8	**873.7**	**10.5**	95.0
150	881	138863.8	5.3	16.8	0.8	0.8	1.6	0.1	1.4	0.9	566.0	7.5	570.5	6.9	588.4	16.3	**566.0**	**7.5**	96.2

151	172	7702.7	1.6	13.4	1.1	0.7	1.7	0.1	1.4	0.8	435.5	5.8	550.9	7.4	1061.7	21.7	**435.5**	**5.8**	41.0
152	280	245581.0	3.3	7.3	0.7	7.4	1.6	0.4	1.5	0.9	2143.2	27.2	2166.0	14.8	2187.6	12.2	**2187.6**	**12.2**	98.0
153	305	375326.0	1.0	16.4	0.8	0.8	1.2	0.1	1.0	0.8	599.0	5.6	606.3	5.7	633.6	16.2	**599.0**	**5.6**	94.5
154	211	139299.5	3.8	9.9	0.9	4.1	1.4	0.3	1.1	0.8	1649.2	16.2	1646.2	11.5	1642.3	16.2	**1642.3**	**16.2**	100.4
155	369	129264.5	3.8	16.3	0.9	0.8	1.4	0.1	1.1	0.8	603.2	6.1	612.0	6.3	644.9	18.6	**603.2**	**6.1**	93.5
156	137	9781403.0	1.5	16.4	1.0	0.9	1.6	0.1	1.3	0.8	660.4	8.0	654.8	7.8	635.4	21.4	**660.4**	**8.0**	103.9
157	122	82672.2	1.0	15.8	2.0	0.8	2.3	0.1	1.2	0.5	553.8	6.5	588.0	10.4	722.2	41.8	**553.8**	**6.5**	76.7
158	40	27681.2	1.6	16.4	1.5	0.9	1.8	0.1	1.1	0.6	656.5	6.6	653.4	8.9	642.7	32.4	**656.5**	**6.6**	102.2
159	200	15468.9	1.1	18.4	1.0	0.4	1.5	0.1	1.1	0.7	368.5	4.1	371.3	4.8	388.8	22.9	**368.5**	**4.1**	94.8
16	165	117859.9	1.0	7.4	0.7	7.2	1.4	0.4	1.1	0.8	2091.5	20.1	2133.2	12.1	2173.5	13.1	**2173.5**	**13.1**	96.2
160	99	150080.0	1.4	16.1	1.0	0.9	1.4	0.1	1.0	0.7	663.0	6.5	667.3	6.9	681.9	20.7	**663.0**	**6.5**	97.2
161	179	336052.7	2.1	16.3	1.3	0.9	1.8	0.1	1.3	0.7	638.8	7.7	642.6	8.5	656.0	27.1	**638.8**	**7.7**	97.4
164	238	69133.3	34.2	17.0	0.8	0.7	1.4	0.1	1.1	0.8	531.7	5.8	535.9	5.8	553.6	18.1	**531.7**	**5.8**	96.1
165	155	94451.9	1.0	13.5	1.0	1.8	1.4	0.2	1.1	0.7	1043.6	10.2	1040.9	9.3	1035.2	19.3	**1035.2**	**19.3**	100.8
166	57	20718.8	1.9	16.1	1.3	0.9	1.7	0.1	1.2	0.7	622.1	7.0	635.5	8.2	683.5	26.9	**622.1**	**7.0**	91.0
167	49	7997.6	1.3	17.2	1.5	0.8	1.9	0.1	1.1	0.6	594.4	6.4	583.2	8.4	539.7	33.1	**594.4**	**6.4**	110.1
168	252	90134.7	3.9	9.2	0.7	4.7	1.5	0.3	1.3	0.9	1777.1	20.4	1774.8	12.6	1772.1	13.2	**1772.1**	**13.2**	100.3
169	292	90454.5	2.6	16.4	0.8	0.9	1.4	0.1	1.2	0.8	637.3	7.1	637.4	6.6	637.8	16.3	**637.3**	**7.1**	99.9
17	282	47195.5	1.9	18.0	0.9	0.5	1.3	0.1	1.0	0.8	408.0	3.8	411.8	4.4	432.8	19.0	**408.0**	**3.8**	94.3
170	82	37244.1	1.7	11.5	1.1	2.7	1.5	0.2	1.1	0.7	1330.3	13.0	1338.0	11.5	1350.4	21.1	**1350.4**	**21.1**	98.5
171	524	2436107.0	1.2	9.5	0.6	4.2	1.6	0.3	1.5	0.9	1617.6	21.1	1665.0	13.1	1725.3	11.6	**1725.3**	**11.6**	93.8
172	609	382263.3	1.1	13.0	0.7	2.0	1.8	0.2	1.6	0.9	1133.6	16.7	1128.2	12.0	1117.8	14.5	**1117.8**	**14.5**	101.4
173	147	86434.8	0.9	16.1	1.1	0.9	1.8	0.1	1.4	0.8	627.0	8.3	636.8	8.3	671.8	23.2	**627.0**	**8.3**	93.3
174	87	114604.8	8.1	7.7	0.9	7.0	1.4	0.4	1.1	0.8	2129.0	20.0	2116.3	12.8	2104.1	16.3	**2104.1**	**16.3**	101.2
175	471	714612.2	1.4	9.4	0.9	4.5	1.9	0.3	1.6	0.9	1720.8	24.2	1728.7	15.4	1738.2	17.0	**1738.2**	**17.0**	99.0
176	40	41962.9	3.6	8.1	0.8	5.2	1.3	0.3	1.0	0.8	1703.1	15.5	1844.9	11.2	2008.7	14.4	**2008.7**	**14.4**	84.8
177	326	512349.2	1.3	16.5	0.8	0.8	1.4	0.1	1.1	0.8	618.6	6.6	620.7	6.3	628.1	16.6	**618.6**	**6.6**	98.5
178	185	97071.5	1.8	12.9	1.0	2.1	1.5	0.2	1.2	0.8	1141.0	12.3	1135.9	10.6	1126.1	19.9	**1126.1**	**19.9**	101.3
179	108	86994.1	1.4	8.7	0.9	5.3	1.4	0.3	1.1	0.8	1865.5	17.9	1875.3	11.9	1886.2	15.4	**1886.2**	**15.4**	98.9
18	165	26562.2	3.5	18.1	1.1	0.5	1.6	0.1	1.2	0.8	417.7	5.0	419.1	5.6	426.4	24.2	**417.7**	**5.0**	98.0

180	376	66729.8	2.6	17.0	0.8	0.8	1.4	0.1	1.1	0.8	593.3	6.4	585.6	6.2	556.1	17.4	**593.3**	**6.4**	106.7
181	182	25233.5	3.5	16.0	1.0	0.9	1.4	0.1	1.1	0.7	668.5	6.8	674.6	7.1	695.1	20.5	**668.5**	**6.8**	96.2
182	6	2066.4	0.7	21.4	9.0	0.6	9.2	0.1	1.8	0.2	601.4	10.1	495.4	36.1	31.6	NA	**601.4**	**10.1**	1904.4
183	152	35560.9	1.4	16.2	1.0	0.9	1.4	0.1	1.0	0.7	615.1	5.6	625.1	6.6	661.3	22.2	**615.1**	**5.6**	93.0
184	140	67277.2	1.1	18.2	1.1	0.5	1.5	0.1	1.0	0.7	411.2	4.2	411.2	5.2	411.6	24.8	**411.2**	**4.2**	99.9
185	92	989655.5	2.9	4.9	0.8	15.6	1.4	0.6	1.2	0.8	2865.6	26.9	2854.9	13.6	2847.4	13.3	**2847.4**	**13.3**	100.6
186	775	100639.4	1.7	17.3	0.6	0.7	1.8	0.1	1.7	0.9	515.1	8.5	516.6	7.4	523.2	13.7	**515.1**	**8.5**	98.4
187	120	70515.3	1.1	16.9	1.0	0.7	1.6	0.1	1.3	0.8	551.3	6.6	554.4	6.8	567.4	21.5	**551.3**	**6.6**	97.2
188	197	118623.9	0.9	13.4	0.7	1.7	1.2	0.2	1.0	0.8	1001.6	9.0	1019.0	7.6	1056.5	13.7	**1056.5**	**13.7**	94.8
189	16	3795.2	0.3	17.0	2.4	0.7	2.9	0.1	1.5	0.5	533.2	7.9	538.5	12.1	561.0	53.3	**533.2**	**7.9**	95.0
19	50	42347.1	0.5	17.0	1.5	0.8	2.0	0.1	1.3	0.7	577.5	7.1	574.7	8.6	563.6	32.2	**577.5**	**7.1**	102.5
190	366	111911.9	0.9	15.4	0.8	1.1	1.4	0.1	1.1	0.8	729.2	7.3	739.4	7.1	770.6	17.7	**729.2**	**7.3**	94.6
191	102	170404.4	2.4	8.2	0.9	6.1	1.4	0.4	1.0	0.8	1998.5	18.0	1990.7	11.8	1982.6	15.2	**1982.6**	**15.2**	100.8
192	282	153289.5	2.8	7.7	0.7	6.8	1.4	0.4	1.2	0.9	2087.6	22.1	2088.8	12.7	2089.9	12.9	**2089.9**	**12.9**	99.9
193	542	5273843.9	5.0	14.2	0.7	1.4	1.9	0.1	1.7	0.9	883.3	14.4	900.0	11.3	941.1	15.2	**941.1**	**15.2**	93.9
194	293	55062.9	5.0	17.7	0.9	0.5	1.4	0.1	1.1	0.8	416.9	4.4	425.2	4.9	470.4	19.2	**416.9**	**4.4**	88.6
195	86	17961.4	1.5	16.9	1.2	0.7	1.6	0.1	1.1	0.7	547.1	5.7	552.0	7.0	571.9	27.2	**547.1**	**5.7**	95.7
196	309	47351.4	1.5	17.7	0.8	0.6	1.7	0.1	1.5	0.9	480.3	7.0	478.2	6.5	468.1	17.3	**480.3**	**7.0**	102.6
197	356	105504.9	0.9	16.6	1.0	0.8	1.8	0.1	1.5	0.8	616.4	8.6	616.1	8.2	614.9	21.6	**616.4**	**8.6**	100.2
198	456	889258.5	1.9	11.1	0.5	3.0	1.4	0.2	1.3	0.9	1383.6	16.6	1398.1	10.9	1420.3	10.1	**1420.3**	**10.1**	97.4
199	41	45815.0	0.4	7.8	1.1	6.6	1.8	0.4	1.4	0.8	2053.3	25.3	2058.2	15.9	2063.0	19.2	**2063.0**	**19.2**	99.5
2	724	397981.7	1.5	18.1	1.0	0.5	2.0	0.1	1.7	0.9	406.9	6.7	409.9	6.8	426.6	23.4	**406.9**	**6.7**	95.4
20	1960	1971401.3	12.5	18.3	0.9	0.5	1.8	0.1	1.5	0.8	397.9	5.7	398.6	5.8	402.8	21.0	**397.9**	**5.7**	98.8
200	41	108113.0	1.2	16.2	1.5	0.9	1.9	0.1	1.2	0.6	664.2	7.8	663.4	9.3	660.8	31.4	**664.2**	**7.8**	100.5
201	1312	1734390.1	13.3	12.1	1.0	2.2	2.4	0.2	2.2	0.9	1115.0	22.7	1168.0	16.9	1267.6	19.5	**1267.6**	**19.5**	88.0
202	332	197320.1	4.1	5.4	0.8	13.2	1.3	0.5	1.1	0.8	2697.0	23.6	2693.9	12.5	2691.6	12.8	**2691.6**	**12.8**	100.2
203	78	135906.2	1.6	15.8	1.1	1.0	1.6	0.1	1.2	0.7	666.7	7.7	678.8	8.1	719.2	23.2	**666.7**	**7.7**	92.7
205	337	193188.5	19.1	9.9	0.8	4.0	1.6	0.3	1.3	0.8	1638.8	18.9	1641.7	12.7	1645.3	15.7	**1645.3**	**15.7**	99.6
206	132	121736.3	1.5	12.3	0.9	2.4	1.6	0.2	1.3	0.8	1224.3	14.1	1228.2	11.3	1235.0	18.6	**1235.0**	**18.6**	99.1
207	741	176931.6	4.6	16.8	1.0	0.8	2.0	0.1	1.8	0.9	583.9	10.0	583.2	9.1	580.3	21.3	**583.9**	**10.0**	100.6

208	406	277998.1	4.1	7.9	0.9	6.7	1.4	0.4	1.1	0.8	2095.2	19.6	2072.9	12.4	2050.8	15.5	**2050.8**	**15.5**	102.2
209	99	5519.8	1.3	4.8	2.0	13.4	2.3	0.5	1.2	0.5	2444.7	25.1	2705.1	22.0	2905.8	31.9	**2905.8**	**31.9**	84.1
21	269	65824.9	2.5	16.1	1.2	0.9	1.8	0.1	1.4	0.8	615.4	8.1	629.7	8.4	681.3	24.6	**615.4**	**8.1**	90.3
210	196	174173.0	1.0	6.6	0.7	8.9	1.4	0.4	1.2	0.9	2297.1	23.3	2330.7	12.9	2360.1	12.5	**2360.1**	**12.5**	97.3
211	56	70617.4	2.8	10.6	1.1	3.5	2.3	0.3	2.0	0.9	1554.1	27.9	1535.0	18.3	1508.8	21.3	**1508.8**	**21.3**	103.0
213	207	27624.2	1.4	18.1	0.9	0.5	1.8	0.1	1.6	0.9	423.2	6.4	422.9	6.2	421.3	19.9	**423.2**	**6.4**	100.5
214	86	9312.1	1.2	17.8	1.0	0.7	1.6	0.1	1.2	0.8	555.6	6.5	536.9	6.7	457.8	23.3	**555.6**	**6.5**	121.4
215	661	114221.1	4.1	12.5	0.9	2.2	1.9	0.2	1.6	0.9	1177.7	17.7	1184.3	13.3	1196.2	18.5	**1196.2**	**18.5**	98.5
216	175	15442.8	1.1	18.2	1.1	0.5	1.8	0.1	1.4	0.8	425.4	5.9	422.7	6.3	408.1	25.3	**425.4**	**5.9**	104.2
217	202	54277.7	1.4	16.5	0.9	0.8	1.4	0.1	1.1	0.8	592.1	6.4	599.8	6.5	628.9	18.8	**592.1**	**6.4**	94.2
218	49	27483.6	1.4	15.9	2.6	0.8	2.9	0.1	1.3	0.4	551.1	7.0	583.1	13.1	709.9	55.9	**551.1**	**7.0**	77.6
219	80	23124.7	3.7	13.4	1.1	1.9	1.7	0.2	1.3	0.8	1082.5	12.9	1072.9	11.3	1053.6	22.2	**1053.6**	**22.2**	102.7
22	209	69731.8	1.3	16.4	0.8	0.8	1.2	0.1	0.9	0.8	594.1	5.0	602.5	5.3	634.4	16.5	**594.1**	**5.0**	93.6
220	84	20883.7	2.0	18.5	1.5	0.5	2.2	0.1	1.6	0.7	392.0	5.9	389.2	7.1	372.5	34.5	**392.0**	**5.9**	105.2
221	435	130865.8	1.9	8.5	0.9	4.7	1.6	0.3	1.3	0.8	1629.9	18.6	1762.2	13.1	1922.9	15.9	**1922.9**	**15.9**	84.8
222	170	928012.5	1.2	7.8	0.9	5.9	1.5	0.3	1.2	0.8	1848.3	19.1	1954.7	12.9	2069.4	15.7	**2069.4**	**15.7**	89.3
223	174	52668.1	1.5	16.5	1.1	0.8	1.6	0.1	1.2	0.7	603.9	6.9	607.8	7.5	622.4	24.0	**603.9**	**6.9**	97.0
224	38	32272.8	1.3	14.1	1.8	1.0	2.2	0.1	1.3	0.6	617.6	7.5	695.1	11.1	954.5	36.7	**617.6**	**7.5**	64.7
225	96	42835.3	1.6	15.6	1.3	1.1	1.8	0.1	1.3	0.7	771.4	9.2	764.3	9.8	743.7	27.6	**771.4**	**9.2**	103.7
226	192	65406.8	3.9	13.7	1.0	1.6	1.8	0.2	1.5	0.8	963.0	13.4	979.2	11.2	1015.7	19.6	**1015.7**	**19.6**	94.8
227	111	94038.6	1.8	16.3	1.1	0.8	1.5	0.1	1.1	0.7	615.2	6.4	622.6	7.1	649.8	22.7	**615.2**	**6.4**	94.7
228	119	37733.7	3.4	12.4	0.8	2.3	1.7	0.2	1.5	0.9	1199.9	16.1	1202.8	11.9	1208.1	16.1	**1208.1**	**16.1**	99.3
229	280	82262.0	1.4	8.3	0.7	5.8	1.4	0.4	1.2	0.9	1945.0	19.6	1949.8	11.9	1955.0	12.9	**1955.0**	**12.9**	99.5
23	78	171375.3	1.7	9.2	0.7	4.9	1.3	0.3	1.1	0.8	1807.5	16.8	1794.0	10.6	1778.4	12.4	**1778.4**	**12.4**	101.6
230	129	239778.7	1.5	16.4	1.0	0.8	1.7	0.1	1.4	0.8	603.4	8.3	610.2	8.0	635.7	21.5	**603.4**	**8.3**	94.9
231	32	8051.7	0.5	16.8	2.4	0.7	2.8	0.1	1.5	0.5	538.0	7.8	548.3	11.9	591.3	51.2	**538.0**	**7.8**	91.0
232	94	36318.3	1.6	12.7	1.1	2.1	1.5	0.2	1.1	0.7	1164.6	11.5	1164.5	10.6	1164.3	21.5	**1164.3**	**21.5**	100.0
233	148	20183.9	0.7	16.6	1.0	0.9	1.4	0.1	1.0	0.7	627.4	5.7	625.1	6.3	616.8	20.6	**627.4**	**5.7**	101.7
234	42	18075630.1	1.0	7.2	0.9	7.6	1.6	0.4	1.2	0.8	2172.4	23.0	2190.7	13.9	2207.9	15.9	**2207.9**	**15.9**	98.4
235	219	146856.6	1.5	5.0	0.7	15.3	1.2	0.6	1.0	0.8	2830.5	22.1	2831.4	11.6	2832.0	12.1	**2832.0**	**12.1**	100.0

236	98	25111.3	2.8	13.1	1.1	1.7	1.8	0.2	1.4	0.8	954.6	12.8	1001.6	11.4	1106.0	21.4	**1106.0**	**21.4**	86.3
237	487	670796.2	2.9	8.2	0.8	6.0	1.6	0.4	1.4	0.9	1976.5	24.3	1977.9	14.2	1979.3	13.9	**1979.3**	**13.9**	99.9
238	361	399114.8	2.5	12.8	0.6	2.1	1.2	0.2	1.0	0.8	1153.2	10.3	1153.0	8.0	1152.7	12.6	**1152.7**	**12.6**	100.0
239	162	113397.4	2.5	9.7	0.9	4.3	1.5	0.3	1.1	0.8	1687.0	16.8	1685.6	12.1	1683.8	17.5	**1683.8**	**17.5**	100.2
24	236	416241.7	3.0	10.8	0.7	3.4	1.4	0.3	1.2	0.9	1512.4	16.0	1495.8	10.8	1472.4	13.6	**1472.4**	**13.6**	102.7
240	245	57479.7	0.8	16.3	1.0	0.9	1.5	0.1	1.2	0.8	621.7	6.9	628.2	7.2	651.8	21.6	**621.7**	**6.9**	95.4
241	155	18774.6	1.6	16.7	0.8	0.8	1.2	0.1	0.9	0.8	580.4	5.2	583.6	5.4	596.2	16.6	**580.4**	**5.2**	97.3
242	18	30055.7	4.3	13.9	1.9	1.7	2.5	0.2	1.6	0.7	991.7	15.0	990.5	15.9	987.8	38.7	**987.8**	**38.7**	100.4
243	249	920011.3	1.4	18.1	1.1	0.5	1.6	0.1	1.1	0.7	377.0	4.2	382.5	5.0	415.9	24.2	**377.0**	**4.2**	90.6
244	635	164392.6	2.1	18.1	0.7	0.5	1.4	0.1	1.2	0.9	419.6	5.1	419.9	4.9	421.6	15.4	**419.6**	**5.1**	99.5
245	148	81311.8	2.2	16.7	1.3	0.8	1.7	0.1	1.1	0.7	603.3	6.2	601.4	7.5	594.3	27.3	**603.3**	**6.2**	101.5
246	104	341800.7	1.6	16.8	1.0	0.7	1.4	0.1	1.0	0.7	562.2	5.3	565.9	6.1	581.1	22.1	**562.2**	**5.3**	96.7
247	66	99388.4	1.0	9.2	0.9	4.7	1.4	0.3	1.1	0.8	1744.9	17.5	1760.6	12.0	1779.1	15.9	**1779.1**	**15.9**	98.1
248	356	2914932.6	1.1	16.2	1.0	0.8	1.7	0.1	1.4	0.8	607.2	7.9	619.5	7.8	664.9	20.6	**607.2**	**7.9**	91.3
249	85	26760.2	0.7	16.4	1.2	0.7	1.8	0.1	1.3	0.7	548.6	6.9	565.3	7.8	633.1	26.2	**548.6**	**6.9**	86.7
25	280	329641.7	2.5	11.0	0.9	3.0	1.6	0.2	1.3	0.8	1409.0	17.0	1420.1	12.2	1436.6	16.5	**1436.6**	**16.5**	98.1
250	79	358257.5	3.8	12.6	0.8	2.2	1.4	0.2	1.2	0.8	1172.8	12.3	1176.3	9.7	1182.9	15.5	**1182.9**	**15.5**	99.1
251	286	63018.7	1.1	16.5	0.9	0.8	1.5	0.1	1.2	0.8	615.9	7.0	618.5	6.8	627.8	18.8	**615.9**	**7.0**	98.1
252	68	315423.1	2.3	10.7	0.9	3.3	1.3	0.3	1.0	0.7	1478.2	13.1	1483.6	10.5	1491.3	17.1	**1491.3**	**17.1**	99.1
253	897	516283.0	4.3	12.8	0.8	2.1	1.6	0.2	1.3	0.8	1145.1	13.7	1144.9	10.7	1144.5	16.8	**1144.5**	**16.8**	100.1
254	226	172946.5	2.5	14.0	0.7	1.6	1.5	0.2	1.4	0.9	980.7	12.5	978.9	9.7	974.7	14.3	**974.7**	**14.3**	100.6
256	109	429524.0	1.9	6.0	0.7	11.1	1.3	0.5	1.1	0.8	2538.7	22.4	2528.5	12.0	2520.3	12.0	**2520.3**	**12.0**	100.7
257	156	142939.4	1.0	8.9	0.9	5.2	1.7	0.3	1.4	0.9	1851.9	23.1	1847.0	14.2	1841.6	15.4	**1841.6**	**15.4**	100.6
258	27	29295.6	1.7	15.5	1.7	1.1	2.1	0.1	1.2	0.6	748.3	8.8	752.3	11.4	764.2	36.6	**748.3**	**8.8**	97.9
259	198	138586.8	0.9	16.3	1.1	0.8	1.6	0.1	1.2	0.7	595.9	6.8	606.8	7.5	648.0	24.0	**595.9**	**6.8**	92.0
26	35	5341259.3	2.2	12.0	1.2	2.4	1.8	0.2	1.3	0.7	1213.5	14.8	1234.2	12.9	1270.6	23.5	**1270.6**	**23.5**	95.5
260	74	22911.9	1.7	18.7	1.5	0.5	1.9	0.1	1.3	0.7	381.9	4.7	377.3	6.1	349.3	32.9	**381.9**	**4.7**	109.3
261	60	112168.3	3.4	11.7	1.1	2.7	1.8	0.2	1.5	0.8	1335.3	18.1	1334.5	13.7	1333.2	20.7	**1333.2**	**20.7**	100.2
262	293	6064925.8	4.0	11.6	0.8	2.7	1.4	0.2	1.1	0.8	1339.5	13.4	1339.0	10.1	1338.2	15.2	**1338.2**	**15.2**	100.1
263	61	54682.1	0.9	11.8	1.1	2.7	1.6	0.2	1.1	0.7	1320.1	13.4	1316.6	11.7	1310.8	21.8	**1310.8**	**21.8**	100.7

264	300	37047.5	1.7	18.2	0.8	0.5	1.4	0.1	1.1	0.8	428.0	4.8	425.3	4.9	410.4	18.5	**428.0**	**4.8**	104.3
265	94	38710.3	2.7	16.7	1.4	0.8	1.7	0.1	1.0	0.6	588.5	5.7	590.0	7.6	595.5	29.4	**588.5**	**5.7**	98.8
266	194	1124993.3	5.1	9.6	1.0	3.9	1.7	0.3	1.4	0.8	1530.7	19.1	1604.7	13.9	1703.4	18.6	**1703.4**	**18.6**	89.9
267	250	428369.4	2.2	11.6	0.7	2.7	1.3	0.2	1.1	0.8	1332.7	13.4	1335.5	9.8	1339.9	13.7	**1339.9**	**13.7**	99.5
268	42	4852.7	1.9	16.6	1.5	0.8	1.9	0.1	1.1	0.6	624.0	6.4	620.6	8.6	608.1	32.5	**624.0**	**6.4**	102.6
269	138	93761.8	2.3	10.6	1.0	3.4	1.6	0.3	1.3	0.8	1518.8	17.3	1514.7	12.9	1508.9	19.4	**1508.9**	**19.4**	100.7
27	125	201144.9	2.5	7.7	1.0	5.9	1.8	0.3	1.5	0.8	1838.9	24.1	1961.9	15.6	2094.1	17.4	**2094.1**	**17.4**	87.8
270	178	362407.1	1.9	10.4	0.9	3.6	1.4	0.3	1.1	0.8	1562.3	15.2	1553.3	11.5	1541.1	17.6	**1541.1**	**17.6**	101.4
271	107	35076.4	1.6	16.9	1.2	0.7	1.6	0.1	1.1	0.7	552.6	5.9	555.3	6.9	566.4	25.7	**552.6**	**5.9**	97.6
273	258	236689.3	1.1	16.2	1.0	0.9	1.7	0.1	1.4	0.8	633.8	8.5	639.4	8.3	659.2	22.4	**633.8**	**8.5**	96.1
274	118	37308.4	2.0	13.7	1.0	1.7	1.6	0.2	1.2	0.8	1025.6	11.5	1020.5	10.0	1009.6	19.7	**1009.6**	**19.7**	101.6
275	246	185931.1	0.9	16.4	0.9	0.8	1.6	0.1	1.3	0.8	613.4	7.3	619.5	7.2	641.6	19.8	**613.4**	**7.3**	95.6
276	107	82548.3	1.8	15.3	1.0	1.1	1.4	0.1	1.1	0.7	774.6	7.7	777.1	7.8	784.4	20.5	**774.6**	**7.7**	98.7
277	302	118731.4	2.0	18.1	1.0	0.5	1.5	0.1	1.1	0.7	417.9	4.4	418.0	5.1	418.8	22.6	**417.9**	**4.4**	99.8
278	168	47201.4	2.9	10.4	0.9	3.6	1.6	0.3	1.4	0.8	1537.8	18.8	1541.9	13.0	1547.4	17.0	**1547.4**	**17.0**	99.4
279	154	564473.1	1.8	16.1	1.0	1.0	1.5	0.1	1.1	0.7	704.2	7.2	698.7	7.4	681.2	20.9	**704.2**	**7.2**	103.4
28	120	201042.7	1.3	7.5	1.0	7.0	1.8	0.4	1.5	0.8	2076.9	26.9	2115.4	16.3	2153.0	17.9	**2153.0**	**17.9**	96.5
280	16	5300.1	1.2	13.9	2.1	1.7	2.3	0.2	1.0	0.4	997.3	9.4	992.1	14.8	980.7	42.9	**980.7**	**42.9**	101.7
281	163	112880.5	0.7	16.5	1.1	0.9	1.6	0.1	1.2	0.7	627.5	7.0	627.7	7.4	628.2	22.8	**627.5**	**7.0**	99.9
282	457	66206.6	1.4	15.8	0.8	1.1	1.9	0.1	1.7	0.9	733.7	11.7	728.9	9.8	714.3	17.9	**733.7**	**11.7**	102.7
283	79	306584.4	2.9	7.7	1.0	7.0	1.5	0.4	1.2	0.8	2127.0	21.3	2105.8	13.6	2085.2	17.4	**2085.2**	**17.4**	102.0
284	146	1884962.8	3.6	10.7	1.0	3.4	1.7	0.3	1.4	0.8	1517.1	18.5	1505.1	13.2	1488.2	18.7	**1488.2**	**18.7**	101.9
285	694	83881.4	1.3	17.9	0.7	0.6	1.6	0.1	1.5	0.9	470.9	6.7	467.7	6.1	452.0	16.0	**470.9**	**6.7**	104.2
286	107	63325.3	1.2	16.4	1.3	0.8	1.7	0.1	1.1	0.7	595.4	6.4	603.9	7.7	635.8	27.3	**595.4**	**6.4**	93.7
287	382	174390.4	3.0	16.9	1.0	0.8	1.6	0.1	1.2	0.8	593.5	7.0	589.3	7.2	573.3	22.7	**593.5**	**7.0**	103.5
288	422	67064.0	1.0	18.1	1.0	0.5	1.7	0.1	1.4	0.8	407.8	5.4	410.1	5.7	423.5	22.5	**407.8**	**5.4**	96.3
289	170	77427.4	1.7	18.1	1.0	0.5	1.7	0.1	1.3	0.8	434.7	5.6	433.1	5.9	424.5	22.8	**434.7**	**5.6**	102.4
29	28	25688.3	1.7	15.8	1.4	1.0	1.7	0.1	1.1	0.6	686.3	7.2	693.4	8.8	716.5	28.7	**686.3**	**7.2**	95.8
290	865	60452.0	2.2	16.6	1.0	0.8	1.9	0.1	1.6	0.8	572.6	8.6	580.1	8.3	609.5	21.9	**572.6**	**8.6**	93.9
291	22	3128.6	3.0	17.7	4.9	0.6	5.1	0.1	1.6	0.3	473.7	7.2	472.4	19.4	466.2	108.4	**473.7**	**7.2**	101.6

292	181	208604.9	2.5	13.3	0.8	1.9	1.4	0.2	1.1	0.8	1068.9	10.9	1067.7	8.9	1065.3	15.7	**1065.3**	**15.7**	100.3
294	233	279475.7	0.8	8.4	0.9	5.9	1.8	0.4	1.5	0.9	1963.4	25.9	1955.4	15.3	1947.0	15.7	**1947.0**	**15.7**	100.8
295	238	122964.4	1.6	16.4	1.1	0.8	1.8	0.1	1.5	0.8	615.9	8.7	619.3	8.4	631.7	22.6	**615.9**	**8.7**	97.5
296	85	32502.1	2.0	16.4	1.0	0.9	1.6	0.1	1.2	0.8	650.8	7.3	649.2	7.5	643.9	22.0	**650.8**	**7.3**	101.1
297	302	79353.5	2.5	12.2	0.7	2.3	1.3	0.2	1.1	0.8	1212.9	11.6	1221.4	9.0	1236.3	13.6	**1236.3**	**13.6**	98.1
298	247	100155.7	2.3	16.3	0.7	0.9	1.3	0.1	1.1	0.9	654.6	6.8	652.6	6.1	645.8	14.0	**654.6**	**6.8**	101.4
299	161	513115.0	1.9	9.3	0.9	4.4	1.4	0.3	1.1	0.8	1661.8	16.5	1704.1	11.7	1756.4	15.7	**1756.4**	**15.7**	94.6
3	185	35256.2	1.4	18.0	1.1	0.5	1.5	0.1	1.1	0.7	437.8	4.7	436.3	5.5	428.4	23.6	**437.8**	**4.7**	102.2
30	225	55703.0	2.7	16.6	1.0	0.9	1.8	0.1	1.5	0.8	636.1	9.0	631.2	8.5	613.9	22.4	**636.1**	**9.0**	103.6
300	66	8880.3	0.9	17.4	1.8	0.7	2.1	0.1	1.1	0.5	555.4	5.7	545.9	8.8	506.8	39.2	**555.4**	**5.7**	109.6
301	975	108632.8	5.9	15.6	0.8	1.0	1.7	0.1	1.5	0.9	710.9	10.2	718.1	8.9	740.6	17.7	**710.9**	**10.2**	96.0
302	119	14447.2	1.5	17.4	1.6	0.7	2.2	0.1	1.6	0.7	543.1	8.3	536.0	9.3	506.0	34.7	**543.1**	**8.3**	107.3
303	37	16195.3	1.9	9.3	0.8	4.7	1.5	0.3	1.2	0.8	1771.9	19.1	1762.5	12.4	1751.3	15.1	**1751.3**	**15.1**	101.2
304	165	139292.0	2.1	16.3	1.2	0.9	1.7	0.1	1.2	0.7	660.2	7.4	658.5	8.0	652.7	24.7	**660.2**	**7.4**	101.2
305	56	66438.6	2.9	16.4	1.2	0.8	1.9	0.1	1.4	0.8	597.4	8.1	605.1	8.5	634.2	26.2	**597.4**	**8.1**	94.2
306	912	90021.4	5.1	18.3	0.8	0.5	1.7	0.1	1.5	0.9	383.1	5.7	385.4	5.5	399.2	18.0	**383.1**	**5.7**	96.0
308	183	30531.4	2.6	16.4	1.2	0.8	1.7	0.1	1.2	0.7	585.8	6.7	597.1	7.6	640.6	25.4	**585.8**	**6.7**	91.4
309	34	49362.5	4.0	15.8	1.8	0.6	2.3	0.1	1.5	0.6	433.5	6.2	481.5	8.8	717.1	37.2	**433.5**	**6.2**	60.5
31	52	8020.5	0.9	16.8	1.5	0.8	2.1	0.1	1.5	0.7	617.6	8.6	611.1	9.6	586.7	32.3	**617.6**	**8.6**	105.3
310	55	66129.8	0.9	17.0	1.7	0.8	2.2	0.1	1.4	0.6	608.7	8.3	599.5	10.1	564.7	37.1	**608.7**	**8.3**	107.8
311	657	1015663.3	2.4	7.9	0.5	6.6	1.6	0.4	1.5	0.9	2048.5	25.8	2052.7	13.8	2056.9	9.7	**2056.9**	**9.7**	99.6
312	187	1183159.9	5.0	11.1	1.0	3.1	1.8	0.3	1.5	0.8	1443.0	19.7	1438.2	13.9	1431.2	18.7	**1431.2**	**18.7**	100.8
313	40	32163.1	1.0	16.0	1.6	1.0	2.0	0.1	1.2	0.6	682.1	7.6	684.0	10.0	690.3	34.6	**682.1**	**7.6**	98.8
314	288	36298.0	0.6	16.5	0.9	0.8	1.3	0.1	1.0	0.7	610.6	5.6	614.3	6.0	627.9	19.0	**610.6**	**5.6**	97.2
315	65	72218.1	1.7	18.4	1.7	0.4	2.0	0.1	1.2	0.6	370.9	4.2	372.6	6.4	383.5	37.5	**370.9**	**4.2**	96.7
32	99	88674.8	3.4	11.5	0.9	2.9	1.7	0.2	1.4	0.8	1396.5	17.7	1383.9	12.7	1364.4	17.8	**1364.4**	**17.8**	102.4
33	139	233480.1	6.2	9.9	0.9	4.2	1.5	0.3	1.2	0.8	1709.1	18.5	1679.1	12.5	1641.8	16.6	**1641.8**	**16.6**	104.1
34	152	175669.0	0.7	17.0	1.1	0.7	1.4	0.1	1.0	0.7	546.8	5.0	549.8	6.0	562.4	23.1	**546.8**	**5.0**	97.2
35	205	54609.9	9.0	18.1	1.3	0.5	1.9	0.1	1.3	0.7	412.2	5.3	413.4	6.4	419.9	30.0	**412.2**	**5.3**	98.2
36	204	65663.0	2.1	18.4	0.9	0.5	1.6	0.1	1.4	0.8	392.9	5.2	391.6	5.2	384.2	19.6	**392.9**	**5.2**	102.3

37	150	8830.8	0.8	14.3	1.6	1.1	2.1	0.1	1.3	0.6	669.5	8.4	730.8	11.0	923.5	33.6	**669.5**	**8.4**	72.5
38	213	93487.3	3.9	9.7	1.0	4.3	1.6	0.3	1.2	0.8	1702.9	17.8	1688.5	12.8	1670.6	18.3	**1670.6**	**18.3**	101.9
39	356	39686.4	1.8	16.9	0.8	0.8	1.2	0.1	0.9	0.8	586.4	5.1	583.3	5.3	571.4	16.6	**586.4**	**5.1**	102.6
4	125	18748.8	1.2	14.9	1.3	0.9	1.9	0.1	1.4	0.7	624.5	8.2	671.9	9.4	834.2	27.6	**624.5**	**8.2**	74.9
40	77	24999.1	1.3	12.8	1.3	2.0	1.8	0.2	1.3	0.7	1099.4	12.8	1118.7	12.4	1156.5	26.2	**1156.5**	**26.2**	95.1
41	84	55452.8	1.6	16.5	1.0	0.8	1.6	0.1	1.3	0.8	622.2	7.5	622.0	7.6	621.1	22.3	**622.2**	**7.5**	100.2
42	59	14552.7	2.7	18.2	1.5	0.5	1.8	0.1	1.0	0.5	411.9	4.0	411.7	6.2	410.7	34.2	**411.9**	**4.0**	100.3
43	150	71522.0	1.8	15.7	0.9	1.0	1.3	0.1	0.9	0.7	684.7	5.9	696.6	6.5	735.2	19.7	**684.7**	**5.9**	93.1
44	232	183229.0	5.7	11.5	0.8	2.8	1.4	0.2	1.2	0.8	1337.8	14.6	1343.2	10.8	1351.9	15.2	**1351.9**	**15.2**	99.0
45	159	39284.4	1.4	17.3	0.8	0.7	1.6	0.1	1.4	0.9	546.9	7.4	542.2	6.9	522.8	18.6	**546.9**	**7.4**	104.6
46	655	406771.7	3.4	9.2	1.1	4.7	1.9	0.3	1.6	0.8	1766.8	25.2	1775.0	16.3	1784.7	19.4	**1784.7**	**19.4**	99.0
47	174	30614.8	2.1	16.7	1.2	0.8	1.7	0.1	1.2	0.7	586.0	6.8	588.1	7.5	596.2	24.9	**586.0**	**6.8**	98.3
48	347	76844.3	1.0	18.0	0.9	0.5	1.5	0.1	1.2	0.8	419.8	4.8	421.4	5.0	430.0	19.4	**419.8**	**4.8**	97.6
49	71	28945.3	1.6	16.1	1.4	1.0	1.9	0.1	1.3	0.7	679.9	8.2	679.1	9.3	676.2	29.3	**679.9**	**8.2**	100.6
5	231	111347.8	2.0	12.9	1.0	2.0	1.6	0.2	1.3	0.8	1107.5	13.3	1115.6	11.0	1131.5	19.4	**1131.5**	**19.4**	97.9
50	41	5688.4	2.3	16.2	3.0	0.8	3.2	0.1	1.2	0.4	578.8	6.9	596.3	14.6	663.3	63.8	**578.8**	**6.9**	87.3
51	99	76529.6	3.2	10.8	1.0	3.5	1.7	0.3	1.5	0.8	1549.5	20.0	1521.6	13.8	1483.0	18.3	**1483.0**	**18.3**	104.5
52	152	34061.5	1.8	16.5	1.1	0.9	1.5	0.1	1.0	0.7	626.5	5.8	626.2	7.0	624.9	24.3	**626.5**	**5.8**	100.3
53	187	49926.5	0.8	16.5	1.2	0.9	1.6	0.1	1.1	0.7	630.5	6.4	629.7	7.5	626.7	25.8	**630.5**	**6.4**	100.6
54	26	10043.6	1.8	17.5	1.9	0.6	2.3	0.1	1.3	0.5	470.0	5.7	475.4	8.8	501.5	42.9	**470.0**	**5.7**	93.7
55	459	101303.1	2.1	16.8	1.0	0.8	1.5	0.1	1.1	0.7	606.1	6.3	601.2	6.6	582.6	21.2	**606.1**	**6.3**	104.0
56	97	40767.9	3.2	16.3	1.0	0.9	1.6	0.1	1.2	0.8	641.8	7.5	643.9	7.6	651.3	21.7	**641.8**	**7.5**	98.5
57	231	112206.5	2.9	16.5	0.8	0.9	1.6	0.1	1.4	0.9	652.8	8.6	645.2	7.7	618.8	17.6	**652.8**	**8.6**	105.5
58	51	7133.8	1.1	17.4	1.7	0.8	2.2	0.1	1.4	0.6	605.3	7.9	585.9	9.6	511.7	36.4	**605.3**	**7.9**	118.3
59	759	244175.4	4.9	17.9	0.8	0.5	1.6	0.1	1.4	0.9	417.9	5.5	422.0	5.5	444.1	18.0	**417.9**	**5.5**	94.1
6	185	1244766.3	3.2	10.3	0.8	3.8	1.4	0.3	1.1	0.8	1602.6	15.8	1584.9	11.1	1561.4	15.4	**1561.4**	**15.4**	102.6
60	220	264885.3	1.3	5.4	0.7	13.9	1.5	0.5	1.3	0.9	2784.7	29.6	2743.0	14.2	2712.4	12.1	**2712.4**	**12.1**	102.7
61	52	46673.3	1.6	7.9	1.3	6.7	1.9	0.4	1.5	0.8	2093.5	26.3	2076.5	17.1	2059.8	22.1	**2059.8**	**22.1**	101.6
62	124	47314.0	2.7	16.1	1.2	0.9	1.9	0.1	1.5	0.8	612.4	8.6	627.4	8.9	682.2	25.7	**612.4**	**8.6**	89.8
63	357	541907.5	1.8	16.4	0.7	0.8	1.2	0.1	1.0	0.8	601.3	5.9	608.3	5.6	634.2	14.5	**601.3**	**5.9**	94.8

64	684	131113.9	4.0	16.1	0.7	1.0	1.4	0.1	1.2	0.9	683.0	8.0	681.5	6.9	676.6	14.3	**683.0**	**8.0**	100.9
65	104	176758.0	1.5	9.0	0.9	5.0	1.4	0.3	1.1	0.8	1805.5	16.7	1815.1	11.7	1826.2	16.3	**1826.2**	**16.3**	98.9
66	288	52234.7	1.0	16.2	1.0	0.9	1.5	0.1	1.2	0.8	627.6	6.9	634.4	7.2	658.5	20.9	**627.6**	**6.9**	95.3
67	337	118718.1	2.6	11.5	0.9	2.8	1.4	0.2	1.0	0.8	1335.8	12.7	1342.1	10.4	1352.2	17.7	**1352.2**	**17.7**	98.8
68	115	56947.5	2.7	16.3	0.9	0.9	1.6	0.1	1.3	0.8	678.2	8.5	673.1	8.0	656.1	20.0	**678.2**	**8.5**	103.4
69	177	112575.1	2.3	16.2	1.1	0.9	1.6	0.1	1.2	0.7	637.8	7.1	644.1	7.7	666.2	23.7	**637.8**	**7.1**	95.7
7	1210	87469.7	3.1	17.7	0.9	0.5	1.8	0.1	1.6	0.9	408.6	6.2	417.8	6.2	468.6	20.6	**408.6**	**6.2**	87.2
70	417	319090.7	30.9	14.1	0.9	1.5	1.9	0.2	1.7	0.9	913.5	14.5	927.6	11.7	961.5	18.5	**961.5**	**18.5**	95.0
71	12	18547.6	3.5	13.7	2.1	1.7	2.5	0.2	1.4	0.5	1026.4	12.9	1023.5	16.3	1017.4	43.3	**1017.4**	**43.3**	100.9
72	67	19945.4	1.4	16.9	1.3	0.7	1.8	0.1	1.2	0.7	558.4	6.4	560.7	7.7	570.0	28.4	**558.4**	**6.4**	98.0
73	330	81930.8	1.7	18.0	1.0	0.5	1.6	0.1	1.3	0.8	421.3	5.2	424.0	5.5	438.6	21.2	**421.3**	**5.2**	96.1
74	85	123963.8	0.9	16.8	1.5	0.7	1.9	0.1	1.2	0.6	563.2	6.6	567.9	8.4	587.0	32.2	**563.2**	**6.6**	95.9
75	87	115240.3	2.7	16.6	1.4	0.8	1.9	0.1	1.3	0.7	590.0	7.6	593.8	8.6	608.3	29.7	**590.0**	**7.6**	97.0
76	61	41167.7	2.9	7.8	1.0	6.5	1.7	0.4	1.4	0.8	2010.3	24.8	2041.3	15.3	2072.8	17.4	**2072.8**	**17.4**	97.0
77	294	99272.1	1.7	18.1	1.1	0.5	1.8	0.1	1.4	0.8	413.4	5.6	415.4	6.1	426.4	24.6	**413.4**	**5.6**	96.9
78	119	43464.1	1.7	7.6	0.9	6.6	1.3	0.4	0.9	0.7	1996.7	16.0	2062.3	11.2	2128.5	15.1	**2128.5**	**15.1**	93.8
79	121	2122022.3	2.9	17.1	1.2	0.7	2.0	0.1	1.5	0.8	547.9	8.1	548.7	8.3	551.7	26.4	**547.9**	**8.1**	99.3
8	359	44974.7	2.7	16.6	0.8	0.8	1.4	0.1	1.2	0.8	598.7	6.8	602.0	6.5	614.3	16.8	**598.7**	**6.8**	97.5
80	142	491496.6	2.4	10.4	1.0	3.6	1.7	0.3	1.3	0.8	1545.4	18.4	1546.6	13.3	1548.3	19.0	**1548.3**	**19.0**	99.8
81	98	50072.2	1.4	16.1	0.9	0.9	1.4	0.1	1.1	0.8	641.1	6.5	648.4	6.6	673.9	18.9	**641.1**	**6.5**	95.1
82	44	236283.4	1.5	13.9	1.2	1.6	1.7	0.2	1.3	0.7	973.6	11.4	978.9	10.7	990.6	23.5	**990.6**	**23.5**	98.3
83	53	11335.0	1.1	18.5	1.6	0.6	1.9	0.1	1.1	0.6	461.0	4.9	447.0	6.9	375.4	35.1	**461.0**	**4.9**	122.8
84	356	954934.0	1.7	5.9	0.8	11.2	1.3	0.5	1.1	0.8	2531.3	22.0	2542.6	12.1	2551.7	12.7	**2551.7**	**12.7**	99.2
85	289	593963.6	3.6	7.9	1.1	6.0	1.7	0.3	1.4	0.8	1888.2	22.5	1971.4	15.2	2059.9	18.9	**2059.9**	**18.9**	91.7
86	94	47886.1	3.1	13.3	0.9	2.0	1.5	0.2	1.2	0.8	1116.6	12.5	1101.0	10.4	1070.3	18.9	**1070.3**	**18.9**	104.3
87	142	183992.8	2.5	10.6	0.8	3.5	1.4	0.3	1.2	0.8	1550.4	16.3	1531.6	11.4	1505.8	15.6	**1505.8**	**15.6**	103.0
88	1629	13763.6	3.6	15.3	1.0	0.5	1.6	0.1	1.3	0.8	329.1	4.2	392.4	5.4	784.4	20.7	**329.1**	**4.2**	42.0
89	558	199929.5	1.3	16.7	0.6	0.8	1.4	0.1	1.3	0.9	597.1	7.4	598.2	6.5	602.2	13.7	**597.1**	**7.4**	99.2
9	339	67257.4	2.3	18.8	1.1	0.4	1.7	0.1	1.3	0.8	325.9	4.0	326.6	4.6	331.6	24.0	**325.9**	**4.0**	98.3
90	88	48800.4	0.9	16.2	1.2	0.9	1.6	0.1	1.0	0.7	620.0	6.1	630.1	7.5	666.4	25.7	**620.0**	**6.1**	93.0

91	214	117166.3	2.1	13.1	0.7	2.0	1.3	0.2	1.1	0.8	1100.8	11.1	1102.7	8.7	1106.3	13.8	**1106.3**	**13.8**	99.5
92	88	64991.2	1.9	16.3	1.2	0.9	1.5	0.1	1.0	0.6	621.9	5.7	627.2	7.1	646.2	24.8	**621.9**	**5.7**	96.3
93	112	98697.7	1.0	13.7	1.0	1.7	1.5	0.2	1.1	0.7	1014.9	10.5	1012.7	9.7	1007.8	20.7	**1007.8**	**20.7**	100.7
94	60	15478.8	1.8	16.8	1.1	0.8	1.7	0.1	1.2	0.7	615.2	7.2	607.8	7.7	580.2	24.9	**615.2**	**7.2**	106.0
95	343	162035.7	2.8	13.1	0.9	2.0	1.5	0.2	1.3	0.8	1105.3	12.8	1102.8	10.4	1097.9	18.0	**1097.9**	**18.0**	100.7
96	327	72453.6	1.9	16.8	0.8	0.8	1.3	0.1	1.1	0.8	592.9	6.1	591.4	6.0	585.9	17.8	**592.9**	**6.1**	101.2
97	160	51392.7	1.4	17.2	0.9	0.7	1.4	0.1	1.1	0.8	540.6	5.6	539.0	6.0	532.4	20.3	**540.6**	**5.6**	101.5
98	373	119690.1	1.9	16.6	0.8	0.8	1.4	0.1	1.1	0.8	591.6	6.1	596.0	6.2	612.7	18.1	**591.6**	**6.1**	96.6
99	25	8232.6	1.2	13.5	1.7	1.8	1.9	0.2	0.8	0.4	1072.2	8.1	1062.0	12.2	1041.0	33.5	**1041.0**	**33.5**	103.0
xx	219	114121.0	6.3	16.9	0.9	0.7	1.6	0.1	1.3	0.8	539.1	6.9	545.2	6.7	570.7	19.5	**539.1**	**6.9**	94.5
xx	212	18490557.4	6.6	17.2	1.0	0.7	1.6	0.1	1.3	0.8	539.1	6.7	538.3	6.9	535.1	22.3	**539.1**	**6.7**	100.7

Sample: UF-A						Isotope Ratios					Apparent Ages (Ma)								
Analysis	**U (ppm)**	**206Pb /204Pb**	**U /Th**	**206Pb /207Pb**	**± (%)**	**207Pb /235U**	**± (%)**	**206Pb/ 238U**	**± (%)**	**err. corr.**	**206Pb /238U**	**± (Ma)**	**207Pb /235U**	**± (Ma)**	**206Pb /207Pb**	**± (Ma)**	**Best Age**	**± (Ma)**	**Conc. (%)**
1	422	663080.0	2.8	13.3	0.7	1.9	1.2	0.2	1.0	0.8	1076.6	9.8	1075.8	8.0	1074.2	13.9	**1074.2**	**13.9**	100.2
10	86	52063.1	1.1	13.6	0.8	1.7	1.3	0.2	1.1	0.8	979.5	9.8	995.2	8.5	1029.8	16.2	**1029.8**	**16.2**	95.1
100	177	101267.1	4.0	8.6	0.7	5.4	1.2	0.3	1.0	0.8	1875.4	16.6	1888.9	10.5	1903.7	12.0	**1903.7**	**12.0**	98.5
101	46	11216.9	3.4	8.7	0.7	5.3	1.4	0.3	1.2	0.9	1866.5	18.9	1869.1	11.7	1872.1	12.9	**1872.1**	**12.9**	99.7
102	77	38779.1	3.3	11.2	0.9	2.9	1.4	0.2	1.1	0.8	1357.8	13.6	1379.2	10.8	1412.4	17.3	**1412.4**	**17.3**	96.1
103	62	52574.4	3.4	11.9	0.9	2.5	1.4	0.2	1.1	0.8	1244.0	12.3	1262.2	10.0	1293.4	16.8	**1293.4**	**16.8**	96.2
104	122	35217.9	2.7	13.5	0.8	1.8	1.3	0.2	1.0	0.8	1037.6	9.4	1041.2	8.3	1048.9	16.2	**1048.9**	**16.2**	98.9
105	47	27094.5	3.5	12.7	1.3	2.1	2.0	0.2	1.5	0.8	1130.8	15.8	1143.3	13.9	1166.9	26.5	**1166.9**	**26.5**	96.9
106	31	6082.5	2.4	11.5	1.5	2.9	1.8	0.2	1.0	0.6	1383.5	12.7	1376.2	13.5	1364.8	28.2	**1364.8**	**28.2**	101.4
107	116	18273.4	3.2	16.0	0.8	1.0	1.4	0.1	1.1	0.8	675.7	7.1	679.4	6.8	691.6	17.0	**675.7**	**7.1**	97.7
108	63	14596.3	3.6	13.5	0.9	1.7	1.3	0.2	0.9	0.7	1014.7	8.9	1025.1	8.3	1047.5	17.6	**1047.5**	**17.6**	96.9
109	15	10845.9	3.8	12.6	1.4	2.2	1.7	0.2	1.1	0.6	1183.1	11.6	1181.5	12.1	1178.7	26.9	**1178.7**	**26.9**	100.4
11	383	105696.0	4.0	13.2	0.7	1.9	1.1	0.2	0.9	0.8	1065.0	8.7	1072.6	7.5	1088.0	14.0	**1088.0**	**14.0**	97.9
110	163	39921.3	1.8	18.3	1.0	0.5	1.5	0.1	1.1	0.7	392.9	4.3	393.6	4.9	397.5	22.1	**392.9**	**4.3**	98.9
111	72	13867.4	3.0	11.9	0.7	2.5	1.3	0.2	1.1	0.8	1250.5	12.7	1267.5	9.8	1296.5	14.5	**1296.5**	**14.5**	96.5
112	82	120212.3	5.5	9.8	0.7	4.0	1.2	0.3	1.0	0.8	1611.1	14.3	1629.1	9.8	1652.4	12.5	**1652.4**	**12.5**	97.5
113	89	47257.5	3.2	11.2	0.9	3.0	1.5	0.2	1.2	0.8	1389.8	15.1	1398.5	11.3	1411.9	16.7	**1411.9**	**16.7**	98.4
114	84	26745.6	2.0	10.0	0.7	3.9	1.0	0.3	0.8	0.8	1599.7	11.2	1608.8	8.3	1620.7	12.2	**1620.7**	**12.2**	98.7
115	124	43147.4	1.4	13.3	0.7	1.8	1.3	0.2	1.1	0.8	1026.2	10.4	1040.3	8.5	1070.0	14.4	**1070.0**	**14.4**	95.9
117	212	34970.2	5.8	12.3	0.8	2.4	1.3	0.2	1.0	0.8	1238.5	11.7	1236.4	9.3	1232.7	15.3	**1232.7**	**15.3**	100.5
118	102	13788.4	3.3	13.5	1.2	1.7	1.7	0.2	1.3	0.7	1010.5	11.9	1020.2	11.1	1041.0	23.6	**1041.0**	**23.6**	97.1
119	73	422503.0	2.0	5.3	0.7	13.6	1.3	0.5	1.1	0.8	2725.9	24.7	2724.4	12.6	2723.3	12.0	**2723.3**	**12.0**	100.1
12	403	89982.6	6.9	8.6	1.0	5.5	1.5	0.3	1.1	0.7	1903.1	18.1	1896.2	12.6	1888.7	17.6	**1888.7**	**17.6**	100.8
120	51	14619.8	3.3	12.6	0.7	2.2	1.2	0.2	0.9	0.8	1193.4	9.8	1187.1	8.2	1175.8	14.8	**1175.8**	**14.8**	101.5
121	280	208384.6	1.9	9.2	0.6	4.7	1.3	0.3	1.2	0.9	1743.9	17.6	1758.4	11.0	1775.8	11.3	**1775.8**	**11.3**	98.2
122	81	24594.3	1.9	11.7	1.1	2.6	1.4	0.2	0.9	0.6	1278.8	9.9	1299.4	10.0	1333.6	20.6	**1333.6**	**20.6**	95.9

123	20	5723.0	3.1	12.9	0.8	2.1	1.1	0.2	0.8	0.7	1166.1	8.6	1153.9	7.6	1131.0	15.0	**1131.0**	**15.0**	103.1
124	257	372082.1	3.4	12.7	0.8	2.2	1.6	0.2	1.4	0.9	1190.9	15.5	1181.9	11.3	1165.5	15.5	**1165.5**	**15.5**	102.2
125	176	110983.4	2.4	12.1	0.8	2.4	1.4	0.2	1.1	0.8	1232.7	12.9	1241.9	9.9	1257.8	14.7	**1257.8**	**14.7**	98.0
126	349	216675.3	11.1	9.4	0.8	4.5	1.3	0.3	1.0	0.8	1726.7	15.3	1733.3	10.7	1741.1	14.7	**1741.1**	**14.7**	99.2
127	48	12945.7	3.2	10.2	0.7	3.8	1.2	0.3	1.0	0.8	1576.8	14.1	1582.4	10.0	1590.0	13.8	**1590.0**	**13.8**	99.2
128	49	93154.1	2.2	10.5	0.8	3.6	1.3	0.3	1.0	0.8	1564.8	14.5	1550.7	10.4	1531.6	14.7	**1531.6**	**14.7**	102.2
129	657	565614.6	3.6	5.2	0.7	13.4	1.1	0.5	0.8	0.8	2612.8	17.9	2706.4	10.0	2777.0	10.7	**2777.0**	**10.7**	94.1
13	60	65136.3	1.7	11.2	0.7	3.0	1.3	0.2	1.1	0.8	1387.4	14.1	1397.3	10.2	1412.3	14.1	**1412.3**	**14.1**	98.2
130	111	36349.5	4.9	12.5	1.0	2.1	1.4	0.2	0.9	0.7	1136.1	9.8	1158.0	9.6	1199.2	20.1	**1199.2**	**20.1**	94.7
131	124	105610.7	4.0	10.6	0.7	3.3	1.5	0.3	1.3	0.9	1475.5	16.7	1491.1	11.5	1513.3	14.0	**1513.3**	**14.0**	97.5
132	98	20266.0	1.6	9.8	0.8	4.0	1.2	0.3	0.9	0.7	1624.9	13.3	1641.9	10.1	1663.7	15.4	**1663.7**	**15.4**	97.7
133	130	50479.6	4.1	11.3	0.9	2.8	1.9	0.2	1.7	0.9	1316.8	19.7	1342.8	14.0	1384.5	17.3	**1384.5**	**17.3**	95.1
134	107	70701.6	2.4	10.5	0.9	3.4	1.4	0.3	1.1	0.8	1481.6	14.3	1506.2	11.0	1540.9	16.9	**1540.9**	**16.9**	96.2
135	227	84637.2	4.1	13.8	0.8	1.6	1.4	0.2	1.2	0.8	968.4	10.7	979.2	9.1	1003.4	16.7	**1003.4**	**16.7**	96.5
136	28	17126.2	1.5	11.0	1.3	3.0	1.7	0.2	1.2	0.7	1389.1	14.5	1413.8	13.2	1451.1	24.2	**1451.1**	**24.2**	95.7
137	86	30477.4	4.1	12.3	0.9	2.2	1.8	0.2	1.6	0.9	1153.1	16.5	1177.5	12.7	1222.6	18.6	**1222.6**	**18.6**	94.3
138	124	55111.3	7.4	12.7	0.7	2.0	1.2	0.2	1.0	0.8	1113.2	10.0	1129.6	8.2	1161.2	14.0	**1161.2**	**14.0**	95.9
139	382	107793.9	5.2	10.0	0.7	4.1	1.3	0.3	1.1	0.8	1671.9	15.8	1647.2	10.6	1615.7	13.7	**1615.7**	**13.7**	103.5
14	194	80808.7	3.0	10.2	0.6	3.7	1.2	0.3	1.0	0.8	1557.8	13.7	1573.4	9.4	1594.4	11.9	**1594.4**	**11.9**	97.7
140	50	33578.4	1.9	9.8	0.7	4.3	1.3	0.3	1.1	0.8	1700.9	15.8	1684.7	10.6	1664.6	13.6	**1664.6**	**13.6**	102.2
141	65	123343.2	2.7	11.4	0.8	2.5	1.2	0.2	1.0	0.8	1191.3	10.4	1259.0	8.9	1376.6	15.1	**1376.6**	**15.1**	86.5
142	31	34422.0	2.5	11.5	1.0	2.7	1.6	0.2	1.3	0.8	1315.9	15.0	1329.2	11.9	1350.5	19.0	**1350.5**	**19.0**	97.4
143	48	137740.5	2.7	9.8	0.6	4.1	1.4	0.3	1.3	0.9	1658.4	18.4	1663.6	11.6	1670.2	12.0	**1670.2**	**12.0**	99.3
144	162	98671.0	3.0	10.0	0.9	3.9	1.7	0.3	1.5	0.9	1611.8	20.9	1617.7	13.9	1625.3	16.5	**1625.3**	**16.5**	99.2
145	80	39897.2	3.0	9.3	0.9	4.7	1.6	0.3	1.3	0.8	1763.8	20.8	1763.5	13.5	1763.1	16.4	**1763.1**	**16.4**	100.0
146	54	532932.4	3.3	8.8	0.8	5.2	1.6	0.3	1.3	0.9	1864.6	21.8	1860.7	13.4	1856.3	14.5	**1856.3**	**14.5**	100.4
147	151	78188.6	1.6	9.1	0.8	4.7	1.5	0.3	1.3	0.9	1762.0	19.9	1775.3	12.6	1790.9	14.1	**1790.9**	**14.1**	98.4
148	51	33494.3	3.3	10.7	0.8	3.2	1.4	0.3	1.1	0.8	1452.3	14.2	1467.9	10.7	1490.6	15.9	**1490.6**	**15.9**	97.4
149	86	40537.5	3.0	11.1	0.7	2.9	1.6	0.2	1.5	0.9	1354.4	18.0	1380.0	12.2	1419.8	12.7	**1419.8**	**12.7**	95.4
15	56	22448.4	3.6	8.7	0.9	5.2	1.3	0.3	1.0	0.7	1842.5	15.4	1854.7	11.2	1868.5	16.3	**1868.5**	**16.3**	98.6

150	166	36470.6	176.1	13.5	0.9	1.7	1.5	0.2	1.2	0.8	994.9	10.7	1010.6	9.4	1044.6	17.9	**1044.6**	**17.9**	95.2
151	118	210320.8	3.5	9.1	0.8	4.9	1.5	0.3	1.3	0.9	1812.1	21.0	1808.1	12.9	1803.5	13.8	**1803.5**	**13.8**	100.5
152	49	39922.2	2.0	9.5	0.9	4.3	1.4	0.3	1.1	0.8	1672.5	16.0	1692.2	11.9	1716.7	17.4	**1716.7**	**17.4**	97.4
153	134	24510.0	2.1	8.2	0.6	5.8	1.1	0.3	0.9	0.8	1902.4	15.2	1944.7	9.6	1990.0	10.8	**1990.0**	**10.8**	95.6
154	183	85276.6	1.1	13.1	0.7	2.0	1.2	0.2	1.0	0.8	1105.9	10.6	1106.8	8.3	1108.4	13.2	**1108.4**	**13.2**	99.8
156	18	41011.8	2.2	11.2	1.0	2.9	1.7	0.2	1.3	0.8	1353.7	16.3	1373.3	12.6	1403.9	19.2	**1403.9**	**19.2**	96.4
157	87	28328.0	4.1	12.5	1.0	2.2	1.5	0.2	1.2	0.8	1186.6	12.6	1189.5	10.6	1194.8	19.0	**1194.8**	**19.0**	99.3
158	98	38163.0	2.1	12.8	0.9	2.1	1.4	0.2	1.1	0.8	1158.6	11.3	1157.9	9.8	1156.6	18.5	**1156.6**	**18.5**	100.2
159	39	13093.3	3.0	12.5	1.0	2.2	1.7	0.2	1.4	0.8	1181.2	14.7	1186.8	11.9	1197.0	20.1	**1197.0**	**20.1**	98.7
16	60	32134.7	1.8	9.7	0.7	4.3	1.0	0.3	0.8	0.8	1685.4	12.0	1686.5	8.6	1687.8	12.2	**1687.8**	**12.2**	99.9
161	101	38723.7	7.5	9.0	0.8	5.2	1.3	0.3	1.0	0.8	1882.5	15.9	1854.7	11.0	1823.7	15.4	**1823.7**	**15.4**	103.2
162	269	561745.7	9.8	12.5	0.6	2.2	1.5	0.2	1.4	0.9	1158.5	14.6	1173.8	10.5	1202.1	12.3	**1202.1**	**12.3**	96.4
163	191	223209.7	2.8	9.9	0.7	4.0	1.8	0.3	1.6	0.9	1619.9	23.4	1628.9	14.3	1640.5	12.4	**1640.5**	**12.4**	98.7
164	90	336181.2	2.9	9.0	0.9	4.8	1.4	0.3	1.1	0.8	1745.4	17.5	1778.3	12.1	1817.2	15.7	**1817.2**	**15.7**	96.0
165	143	520024.6	3.1	13.5	0.7	1.8	1.5	0.2	1.3	0.9	1051.2	12.7	1050.1	9.8	1047.7	14.8	**1047.7**	**14.8**	100.3
166	29	5095.5	1.5	13.5	1.5	1.9	1.9	0.2	1.2	0.6	1089.1	12.0	1076.1	12.8	1050.0	30.3	**1050.0**	**30.3**	103.7
167	31	18832.5	2.1	9.7	0.9	4.3	1.4	0.3	1.1	0.8	1707.9	15.8	1692.2	11.4	1672.9	16.7	**1672.9**	**16.7**	102.1
168	33	33374.3	2.9	13.5	1.1	1.9	1.6	0.2	1.1	0.7	1081.3	11.2	1067.9	10.3	1040.8	21.7	**1040.8**	**21.7**	103.9
169	29	4675.6	0.9	17.8	3.1	0.7	3.5	0.1	1.6	0.5	559.2	8.5	539.1	14.5	455.3	68.6	**559.2**	**8.5**	122.8
17	576	303057.0	2.1	12.2	0.7	2.4	1.4	0.2	1.2	0.9	1247.3	13.6	1247.2	10.0	1247.1	14.0	**1247.1**	**14.0**	100.0
170	87	182624.4	3.2	13.5	0.6	1.8	1.2	0.2	1.0	0.9	1051.3	9.9	1049.8	7.6	1046.5	11.3	**1046.5**	**11.3**	100.5
171	50	658239.6	1.9	13.0	1.2	1.9	1.7	0.2	1.2	0.7	1054.5	11.6	1076.7	11.1	1121.9	23.5	**1121.9**	**23.5**	94.0
172	292	256083.6	1.9	17.4	1.2	0.5	1.6	0.1	1.1	0.7	395.7	4.3	413.1	5.5	511.9	25.7	**395.7**	**4.3**	77.3
173	122	146714.5	2.2	12.6	0.7	2.0	1.3	0.2	1.0	0.8	1090.9	10.5	1123.7	8.7	1187.5	14.6	**1187.5**	**14.6**	91.9
175	209	39523.2	3.2	18.1	0.7	0.5	1.2	0.1	1.0	0.8	394.5	3.9	397.8	4.1	416.6	16.0	**394.5**	**3.9**	94.7
176	113	13195.6	1.4	18.6	1.2	0.4	1.7	0.1	1.1	0.7	370.1	4.0	369.1	5.2	362.6	27.8	**370.1**	**4.0**	102.1
177	65	11113.5	3.7	12.2	0.7	2.4	1.3	0.2	1.0	0.8	1221.8	11.4	1231.3	9.0	1248.0	14.5	**1248.0**	**14.5**	97.9
178	38	12351.7	0.9	9.7	1.0	4.4	1.6	0.3	1.3	0.8	1720.1	19.1	1705.8	13.2	1688.2	18.1	**1688.2**	**18.1**	101.9
179	364	36664.1	4.5	10.8	0.8	3.2	1.4	0.3	1.1	0.8	1448.8	14.7	1461.8	10.8	1480.7	15.2	**1480.7**	**15.2**	97.8
18	75	81540.9	1.6	4.4	0.8	18.8	1.3	0.6	1.0	0.8	3035.1	24.4	3029.2	12.2	3025.3	12.3	**3025.3**	**12.3**	100.3

180	171	843.4	0.9	7.5	13.1	1.6	13.3	0.1	2.3	0.2	543.9	12.2	975.8	83.3	2138.0	229.3	**2138.0**	**229.3**	25.4
181	22	50257.8	1.2	8.7	0.9	5.4	1.3	0.3	1.0	0.7	1883.1	15.5	1877.0	11.3	1870.2	16.7	**1870.2**	**16.7**	100.7
182	133	13753.7	2.9	17.7	0.8	0.6	1.4	0.1	1.2	0.8	482.8	5.5	480.0	5.4	466.2	17.1	**482.8**	**5.5**	103.6
183	26	10204.4	3.0	18.0	1.7	0.5	2.3	0.1	1.5	0.7	428.1	6.2	428.8	8.0	432.4	38.8	**428.1**	**6.2**	99.0
184	117	61256.7	2.5	9.0	0.7	4.7	1.4	0.3	1.2	0.9	1739.6	18.4	1774.4	11.8	1815.6	13.2	**1815.6**	**13.2**	95.8
185	121	39212.9	1.0	9.9	0.6	4.1	1.2	0.3	1.0	0.9	1657.8	15.2	1653.4	9.8	1647.8	11.1	**1647.8**	**11.1**	100.6
186	161	31540.0	2.1	18.2	0.8	0.5	1.3	0.1	1.0	0.8	383.6	3.7	386.6	4.2	404.4	18.6	**383.6**	**3.7**	94.9
188	61	25359.8	4.6	13.7	1.0	1.8	1.6	0.2	1.2	0.8	1036.8	11.2	1030.7	10.1	1017.8	20.8	**1017.8**	**20.8**	101.9
189	38	47004.7	2.0	11.7	1.1	2.7	1.6	0.2	1.1	0.7	1344.2	12.9	1336.3	11.6	1323.5	22.1	**1323.5**	**22.1**	101.6
19	139	46445.5	1.6	9.7	0.7	4.1	1.3	0.3	1.1	0.8	1631.3	15.8	1650.1	10.6	1674.2	13.0	**1674.2**	**13.0**	97.4
190	140	53515.1	5.0	13.7	0.9	1.7	1.3	0.2	1.0	0.7	1006.9	9.4	1010.3	8.6	1017.6	18.1	**1017.6**	**18.1**	98.9
191	77	78752.3	1.2	9.8	0.7	4.2	1.3	0.3	1.1	0.8	1663.0	15.7	1665.7	10.7	1669.1	13.7	**1669.1**	**13.7**	99.6
192	62	29982.9	1.1	5.3	0.5	14.6	1.2	0.6	1.0	0.9	2852.0	23.8	2789.7	11.0	2744.9	8.5	**2744.9**	**8.5**	103.9
193	65	18186.1	2.1	18.1	1.4	0.5	1.8	0.1	1.1	0.6	414.4	4.3	416.0	6.0	424.5	30.9	**414.4**	**4.3**	97.6
194	17	32246.3	1.8	12.5	1.2	2.2	1.5	0.2	0.9	0.6	1176.5	9.8	1181.9	10.4	1191.7	23.2	**1191.7**	**23.2**	98.7
195	29	9830.3	2.8	13.2	0.9	1.7	1.6	0.2	1.3	0.8	994.9	12.2	1025.9	10.4	1092.7	18.1	**1092.7**	**18.1**	91.1
196	122	286164.1	2.2	10.4	0.9	3.5	1.5	0.3	1.2	0.8	1504.7	16.1	1520.7	12.0	1543.0	17.7	**1543.0**	**17.7**	97.5
197	54	23088.2	3.3	12.6	0.7	2.2	1.4	0.2	1.2	0.9	1179.1	12.8	1179.3	9.8	1179.6	14.6	**1179.6**	**14.6**	100.0
198	202	123325.7	0.9	10.6	0.7	3.3	1.0	0.3	0.8	0.8	1457.1	10.1	1477.7	7.9	1507.3	12.3	**1507.3**	**12.3**	96.7
199	1228	240077.7	2.3	12.7	0.8	1.9	1.2	0.2	0.8	0.7	1042.3	7.8	1081.5	7.8	1161.2	16.7	**1161.2**	**16.7**	89.8
2	98	108599.6	1.6	9.3	0.6	4.5	1.1	0.3	0.9	0.8	1698.2	13.6	1726.5	9.1	1760.9	11.1	**1760.9**	**11.1**	96.4
20	301	2320848.1	6.2	10.0	0.5	4.1	1.3	0.3	1.2	0.9	1679.2	17.9	1658.0	10.8	1631.3	10.1	**1631.3**	**10.1**	102.9
200	125	23721.7	3.8	11.8	0.8	2.6	1.5	0.2	1.2	0.8	1284.5	14.5	1296.8	10.8	1317.0	15.2	**1317.0**	**15.2**	97.5
201	195	944253.0	2.2	9.3	0.7	4.7	1.3	0.3	1.1	0.8	1773.3	17.0	1770.0	11.0	1766.1	13.2	**1766.1**	**13.2**	100.4
202	82	25429.0	1.8	17.8	1.0	0.5	1.5	0.1	1.2	0.8	424.5	5.0	429.2	5.4	454.2	21.2	**424.5**	**5.0**	93.5
203	204	107670.2	3.7	12.6	0.7	2.3	1.5	0.2	1.4	0.9	1216.6	15.3	1203.9	10.9	1181.2	13.6	**1181.2**	**13.6**	103.0
204	111	370484.9	1.7	5.0	0.9	14.6	1.8	0.5	1.6	0.9	2758.6	35.2	2788.8	17.0	2810.6	14.3	**2810.6**	**14.3**	98.2
205	170	261166.6	4.1	13.5	0.7	1.8	1.4	0.2	1.2	0.9	1035.6	11.6	1040.1	9.2	1049.6	14.7	**1049.6**	**14.7**	98.7
206	28	35258.5	1.4	13.7	1.2	1.7	1.5	0.2	1.0	0.6	1019.9	9.0	1019.0	9.8	1017.1	24.2	**1017.1**	**24.2**	100.3
207	279	70381.1	2.9	9.7	0.6	3.9	1.1	0.3	0.9	0.8	1569.6	12.5	1615.2	8.8	1675.1	11.3	**1675.1**	**11.3**	93.7

208	110	225505.6	1.9	9.6	0.7	4.3	1.1	0.3	0.9	0.8	1704.6	13.5	1699.3	9.3	1692.9	12.5	**1692.9**	**12.5**	100.7
209	223	121975.3	10.0	10.3	0.8	3.6	1.6	0.3	1.3	0.9	1539.7	18.5	1549.7	12.5	1563.5	15.4	**1563.5**	**15.4**	98.5
21	96	32362.6	2.3	9.9	0.7	4.0	1.1	0.3	0.9	0.8	1618.0	12.6	1628.2	9.1	1641.3	13.0	**1641.3**	**13.0**	98.6
210	102	45460.5	2.3	12.4	0.6	2.3	1.2	0.2	1.0	0.9	1223.0	11.4	1219.1	8.4	1212.4	11.8	**1212.4**	**11.8**	100.9
211	287	236125.3	1.2	17.4	0.7	0.6	1.2	0.1	1.0	0.8	471.6	4.4	477.6	4.6	506.7	16.3	**471.6**	**4.4**	93.1
212	137	15252.5	3.4	17.7	1.3	0.6	1.7	0.1	1.1	0.7	473.7	5.2	472.5	6.4	466.6	27.9	**473.7**	**5.2**	101.5
213	20	36078.5	4.3	12.9	1.1	2.0	1.8	0.2	1.4	0.8	1101.1	14.5	1112.7	12.1	1135.5	21.3	**1135.5**	**21.3**	97.0
214	121	91286.8	2.2	4.9	0.7	14.7	1.3	0.5	1.2	0.9	2720.0	25.7	2792.8	12.7	2845.8	10.9	**2845.8**	**10.9**	95.6
215	45	10344.3	1.9	17.1	1.1	0.8	1.4	0.1	0.9	0.6	581.9	4.9	574.3	6.1	544.5	23.3	**581.9**	**4.9**	106.9
216	214	66739.8	3.2	10.7	0.6	3.5	1.2	0.3	1.1	0.9	1557.2	14.6	1531.1	9.5	1495.3	11.0	**1495.3**	**11.0**	104.1
217	61	14704.5	1.3	16.3	1.1	0.9	1.6	0.1	1.1	0.7	635.8	6.7	640.1	7.6	655.1	24.5	**635.8**	**6.7**	97.0
218	148	227366.5	9.4	11.1	1.0	2.5	1.7	0.2	1.4	0.8	1190.2	15.3	1279.3	12.7	1432.4	19.5	**1432.4**	**19.5**	83.1
219	278	13377.4	87.0	18.4	0.8	0.5	1.3	0.1	1.1	0.8	436.9	4.6	429.6	4.6	390.4	17.0	**436.9**	**4.6**	111.9
22	39	6466.3	3.2	16.3	1.3	0.9	1.8	0.1	1.2	0.7	640.5	7.5	641.8	8.6	646.1	28.5	**640.5**	**7.5**	99.1
220	369	2325814.2	57.5	13.1	0.9	2.0	1.4	0.2	1.1	0.8	1118.7	10.9	1113.1	9.2	1102.2	17.0	**1102.2**	**17.0**	101.5
221	84	34886.4	1.4	9.5	0.6	4.5	1.4	0.3	1.3	0.9	1734.2	19.0	1730.4	11.7	1725.8	11.7	**1725.8**	**11.7**	100.5
222	85	6893.0	3.5	18.3	1.2	0.5	1.8	0.1	1.3	0.7	428.8	5.3	423.6	6.1	395.4	26.7	**428.8**	**5.3**	108.5
223	146	225612.9	4.0	10.8	0.7	3.3	1.4	0.3	1.2	0.9	1492.4	16.5	1486.6	11.0	1478.5	12.7	**1478.5**	**12.7**	100.9
224	451	163074.1	6.5	6.3	0.8	8.9	1.2	0.4	0.9	0.8	2205.0	16.5	2324.1	10.7	2430.4	13.2	**2430.4**	**13.2**	90.7
225	400	88301.2	16.4	12.9	0.7	2.1	1.2	0.2	0.9	0.8	1136.6	9.9	1135.1	8.0	1132.3	13.5	**1132.3**	**13.5**	100.4
226	36	32894.2	3.0	9.8	0.7	4.2	1.5	0.3	1.3	0.9	1704.3	18.8	1683.6	12.0	1657.8	13.8	**1657.8**	**13.8**	102.8
229	46	59688.6	3.1	4.9	0.7	16.1	1.3	0.6	1.1	0.9	2927.6	26.5	2883.8	12.4	2853.3	10.6	**2853.3**	**10.6**	102.6
23	86	22342.3	2.0	9.7	0.6	4.3	1.1	0.3	0.9	0.8	1695.6	12.7	1692.2	8.8	1688.0	11.9	**1688.0**	**11.9**	100.5
230	8	18005.9	0.7	13.1	1.7	2.1	2.3	0.2	1.5	0.6	1152.6	15.4	1137.4	15.4	1108.5	34.2	**1108.5**	**34.2**	104.0
231	41	12567.0	1.9	17.6	1.4	0.6	1.9	0.1	1.3	0.7	466.2	5.9	469.8	7.1	487.2	29.9	**466.2**	**5.9**	95.7
232	71	138166.1	3.3	8.7	0.6	5.4	1.4	0.3	1.3	0.9	1872.7	20.7	1877.6	12.2	1883.0	11.6	**1883.0**	**11.6**	99.4
233	12	10414.0	2.8	13.6	1.7	1.8	2.1	0.2	1.2	0.6	1045.4	11.2	1040.3	13.5	1029.5	34.7	**1029.5**	**34.7**	101.5
234	166	105658.8	3.9	10.7	0.7	3.3	1.4	0.3	1.3	0.9	1485.2	16.6	1492.3	11.2	1502.4	13.0	**1502.4**	**13.0**	98.9
236	68	53898.6	2.3	8.9	0.7	5.3	1.4	0.3	1.2	0.9	1897.0	20.0	1872.3	12.2	1844.9	13.5	**1844.9**	**13.5**	102.8
237	148	56519.9	1.2	5.4	0.7	13.4	1.6	0.5	1.4	0.9	2736.4	31.1	2707.0	14.7	2685.1	11.6	**2685.1**	**11.6**	101.9

238	48	30330.7	3.4	11.2	1.1	2.9	1.6	0.2	1.2	0.7	1372.1	14.8	1384.9	12.1	1404.7	20.3	**1404.7**	**20.3**	97.7
239	90	33520.4	5.0	13.5	0.7	1.8	1.1	0.2	0.9	0.8	1027.2	8.4	1031.4	7.1	1040.4	13.4	**1040.4**	**13.4**	98.7
24	53	13286.7	2.3	13.6	1.0	1.7	1.5	0.2	1.1	0.7	1009.9	10.7	1015.6	9.9	1027.8	20.7	**1027.8**	**20.7**	98.3
240	58	217383.9	1.6	10.8	0.9	3.5	1.4	0.3	1.0	0.8	1546.0	14.3	1517.1	10.8	1477.0	16.8	**1477.0**	**16.8**	104.7
241	179	38145.5	2.4	11.4	0.7	2.8	1.3	0.2	1.1	0.8	1368.2	13.3	1368.7	9.6	1369.3	13.3	**1369.3**	**13.3**	99.9
242	224	46871.1	2.9	10.8	0.7	3.4	1.4	0.3	1.2	0.9	1530.6	16.2	1512.4	10.7	1487.0	12.7	**1487.0**	**12.7**	102.9
243	58	75636.1	1.1	10.6	1.6	3.3	1.9	0.3	1.0	0.5	1464.5	13.6	1484.6	14.8	1513.4	29.9	**1513.4**	**29.9**	96.8
244	53	48288.8	2.9	8.7	0.8	5.5	1.5	0.3	1.3	0.8	1925.5	21.0	1904.4	13.1	1881.3	15.3	**1881.3**	**15.3**	102.3
245	45	17327.5	1.1	11.9	0.9	2.6	1.5	0.2	1.2	0.8	1306.2	14.2	1300.5	10.8	1291.1	16.7	**1291.1**	**16.7**	101.2
246	104	30243.1	1.8	17.4	1.1	0.6	1.8	0.1	1.4	0.8	441.2	5.8	452.4	6.4	509.7	24.6	**441.2**	**5.8**	86.6
247	97	46271.8	3.7	10.7	0.6	3.4	1.3	0.3	1.1	0.9	1509.3	14.9	1505.8	10.0	1500.8	11.7	**1500.8**	**11.7**	100.6
248	403	144343.4	2.8	10.8	0.6	3.4	1.2	0.3	1.0	0.8	1529.8	13.7	1507.2	9.4	1475.6	12.3	**1475.6**	**12.3**	103.7
249	66	11794.9	2.4	10.4	0.9	3.6	2.6	0.3	2.5	0.9	1539.1	33.8	1543.1	20.8	1548.5	16.6	**1548.5**	**16.6**	99.4
25	159	38139.6	1.4	9.3	0.8	4.6	1.5	0.3	1.3	0.8	1725.4	19.3	1742.2	12.7	1762.4	15.4	**1762.4**	**15.4**	97.9
250	83	34865.7	4.0	10.0	0.7	3.9	1.1	0.3	0.9	0.8	1611.2	13.0	1616.7	9.1	1623.8	12.5	**1623.8**	**12.5**	99.2
251	56	28479.3	3.9	14.2	0.9	1.6	1.4	0.2	1.1	0.8	958.3	9.7	951.9	8.9	937.3	19.0	**937.3**	**19.0**	102.2
252	98	126393.2	2.4	6.0	0.6	11.3	1.2	0.5	1.0	0.9	2565.4	21.4	2544.8	11.1	2528.3	10.4	**2528.3**	**10.4**	101.5
253	126	25304.8	1.4	17.3	0.9	0.6	1.4	0.1	1.1	0.8	481.1	5.2	487.6	5.5	518.0	19.5	**481.1**	**5.2**	92.9
254	204	26755.9	1.5	18.0	0.9	0.5	1.4	0.1	1.1	0.8	431.3	4.6	431.9	4.9	435.0	19.2	**431.3**	**4.6**	99.1
255	166	117162.3	5.2	17.1	1.1	0.5	1.5	0.1	1.0	0.7	412.9	4.1	433.6	5.2	545.3	23.1	**412.9**	**4.1**	75.7
256	35	12080.7	4.0	11.3	1.0	3.0	1.5	0.2	1.2	0.8	1419.0	15.1	1407.1	11.8	1389.2	19.1	**1389.2**	**19.1**	102.1
258	129	38147.1	10.0	13.2	0.9	1.9	1.3	0.2	1.0	0.8	1064.3	9.8	1071.4	8.8	1085.7	17.5	**1085.7**	**17.5**	98.0
259	86	45729.0	2.6	13.0	0.7	1.9	1.3	0.2	1.1	0.8	1084.8	10.9	1095.9	8.9	1117.9	14.9	**1117.9**	**14.9**	97.0
26	169	403933.5	4.2	12.4	0.6	2.1	1.2	0.2	1.0	0.8	1134.9	10.1	1158.9	8.0	1204.1	12.5	**1204.1**	**12.5**	94.3
260	146	48668.1	83.6	5.4	0.8	12.6	1.3	0.5	1.1	0.8	2596.6	23.1	2649.2	12.4	2689.7	12.5	**2689.7**	**12.5**	96.5
261	43	21845.3	1.8	16.2	1.3	0.9	1.7	0.1	1.1	0.6	650.3	6.7	654.2	8.2	667.8	27.9	**650.3**	**6.7**	97.4
262	85	32343.2	4.5	12.6	0.7	2.1	1.2	0.2	1.0	0.8	1158.2	10.4	1163.8	8.3	1174.1	13.7	**1174.1**	**13.7**	98.6
263	98	16973.4	6.4	18.3	1.1	0.5	1.7	0.1	1.2	0.7	415.9	4.8	412.9	5.6	396.1	25.7	**415.9**	**4.8**	105.0
264	51	9948.0	2.3	17.0	1.5	0.8	1.8	0.1	1.0	0.5	628.8	5.7	615.1	8.2	565.4	32.8	**628.8**	**5.7**	111.2
265	101	32957.4	2.0	16.5	0.9	0.9	1.4	0.1	1.1	0.8	640.7	6.7	637.5	6.6	626.2	18.7	**640.7**	**6.7**	102.3

266	68	39702.1	2.8	13.4	1.0	1.9	1.4	0.2	1.0	0.7	1087.7	9.7	1079.0	9.1	1061.4	19.5	**1061.4**	**19.5**	102.5
267	54	10293.8	1.8	17.8	1.7	0.6	2.0	0.1	1.1	0.5	474.5	5.0	472.4	7.6	462.7	37.1	**474.5**	**5.0**	102.5
268	27	11433.3	3.6	9.1	0.9	5.2	1.5	0.3	1.2	0.8	1886.6	20.3	1848.7	13.0	1806.3	16.4	**1806.3**	**16.4**	104.4
269	91	77587.4	1.1	9.8	0.7	4.2	1.3	0.3	1.1	0.8	1678.5	16.5	1667.1	11.0	1652.7	13.6	**1652.7**	**13.6**	101.6
27	96	857816.9	1.6	9.9	0.8	3.7	1.4	0.3	1.2	0.8	1527.1	16.6	1573.9	11.6	1637.2	14.3	**1637.2**	**14.3**	93.3
270	257	20187086.5	3.5	10.7	0.7	3.4	1.3	0.3	1.1	0.8	1495.0	14.9	1496.7	10.4	1499.0	13.8	**1499.0**	**13.8**	99.7
271	163	87335.7	1.3	5.1	0.6	14.2	1.4	0.5	1.2	0.9	2725.7	26.7	2763.7	12.9	2791.5	10.4	**2791.5**	**10.4**	97.6
272	19	7020.7	4.6	6.1	0.8	11.1	1.5	0.5	1.2	0.8	2555.2	25.9	2529.2	13.8	2508.4	14.0	**2508.4**	**14.0**	101.9
273	7	4743.6	2.3	11.5	1.8	2.5	2.8	0.2	2.2	0.8	1221.2	24.0	1270.3	20.2	1354.4	34.2	**1354.4**	**34.2**	90.2
275	11	65417.8	2.3	10.6	0.9	3.6	1.6	0.3	1.3	0.8	1562.2	18.6	1542.8	12.7	1516.3	16.3	**1516.3**	**16.3**	103.0
28	163	21359.5	4.5	12.0	0.8	2.1	1.5	0.2	1.3	0.9	1091.6	12.7	1155.0	10.2	1276.0	14.8	**1276.0**	**14.8**	85.5
29	160	72303.0	1.7	9.3	0.7	4.5	1.1	0.3	0.9	0.8	1693.1	13.3	1724.2	9.5	1762.2	13.0	**1762.2**	**13.0**	96.1
3	194	168446.4	3.9	9.4	0.7	4.5	1.3	0.3	1.0	0.8	1708.6	15.3	1724.6	10.5	1744.1	13.7	**1744.1**	**13.7**	98.0
30	242	25979.5	3.1	13.1	0.7	1.9	1.4	0.2	1.2	0.9	1085.5	12.2	1089.7	9.4	1098.1	13.6	**1098.1**	**13.6**	98.9
31	178	41991.0	2.4	16.1	0.6	0.9	1.2	0.1	1.1	0.9	626.0	6.5	635.9	5.9	671.0	12.7	**626.0**	**6.5**	93.3
32	339	2806617.3	3.8	9.4	0.7	4.6	1.1	0.3	0.9	0.8	1759.6	13.4	1747.8	9.1	1733.8	12.1	**1733.8**	**12.1**	101.5
33	137	30080.5	3.8	16.0	0.8	0.9	1.2	0.1	0.9	0.7	623.4	5.1	637.2	5.7	686.3	18.0	**623.4**	**5.1**	90.8
34	128	39386.9	0.9	17.1	0.8	0.7	1.3	0.1	1.0	0.8	522.3	4.8	527.3	5.3	549.1	18.4	**522.3**	**4.8**	95.1
35	67	860115.2	1.6	12.8	0.8	2.1	1.7	0.2	1.5	0.9	1158.9	15.8	1156.4	11.6	1151.5	15.7	**1151.5**	**15.7**	100.6
36	54	19428.5	0.9	13.7	0.9	1.7	1.6	0.2	1.4	0.8	1006.4	12.7	1009.2	10.4	1015.1	18.0	**1015.1**	**18.0**	99.1
37	85	39566.0	2.1	11.6	0.7	2.7	1.2	0.2	1.0	0.8	1343.5	11.7	1341.3	8.7	1337.8	12.6	**1337.8**	**12.6**	100.4
38	52	38567.7	2.6	12.6	1.0	2.2	1.3	0.2	0.9	0.7	1173.2	9.8	1174.3	9.2	1176.4	19.1	**1176.4**	**19.1**	99.7
39	61	67216.6	3.4	11.4	0.7	2.8	1.3	0.2	1.0	0.8	1359.1	12.5	1363.4	9.5	1370.1	14.3	**1370.1**	**14.3**	99.2
4	162	35600.7	11.1	17.0	1.0	0.7	1.6	0.1	1.2	0.8	535.2	6.4	539.3	6.6	556.9	21.2	**535.2**	**6.4**	96.1
40	82	55472.9	1.9	13.1	0.9	1.9	1.6	0.2	1.3	0.8	1088.8	13.1	1092.4	10.7	1099.7	18.4	**1099.7**	**18.4**	99.0
41	84	52225.5	15.3	10.1	1.0	3.6	1.5	0.3	1.1	0.7	1527.4	14.9	1560.1	11.8	1604.7	18.7	**1604.7**	**18.7**	95.2
42	240	96473.1	5.8	9.5	0.6	4.7	1.4	0.3	1.3	0.9	1798.8	19.7	1761.0	11.8	1716.5	11.8	**1716.5**	**11.8**	104.8
43	174	16025.5	3.5	16.8	1.0	0.8	1.6	0.1	1.2	0.8	580.4	6.8	581.2	7.0	584.4	21.5	**580.4**	**6.8**	99.3
44	62	18889.0	1.9	10.8	0.7	3.4	1.2	0.3	1.0	0.8	1524.1	13.9	1505.4	9.7	1479.2	12.9	**1479.2**	**12.9**	103.0
45	200	60490.3	2.5	8.7	0.7	5.0	1.3	0.3	1.1	0.9	1782.1	17.8	1826.1	11.3	1876.7	12.6	**1876.7**	**12.6**	95.0

46	13	23369.1	1.4	9.5	1.1	4.4	1.5	0.3	1.0	0.7	1706.8	14.8	1713.3	12.3	1721.3	20.5	**1721.3**	**20.5**	99.2
47	160	23393.7	2.0	13.0	0.8	2.0	1.3	0.2	1.1	0.8	1111.7	10.7	1115.6	9.0	1123.3	16.3	**1123.3**	**16.3**	99.0
48	31	5149.1	2.3	17.7	1.9	0.7	2.3	0.1	1.2	0.5	575.7	6.8	554.7	9.7	469.4	41.8	**575.7**	**6.8**	122.7
49	65	30126.9	1.1	9.7	0.9	4.1	1.4	0.3	1.1	0.8	1644.8	16.5	1660.8	11.7	1681.1	15.9	**1681.1**	**15.9**	97.8
5	28	58724.7	1.3	13.3	1.1	1.9	1.6	0.2	1.2	0.7	1107.8	12.4	1095.9	11.0	1072.3	22.2	**1072.3**	**22.2**	103.3
50	51	35484.3	1.3	9.9	0.9	4.1	1.4	0.3	1.1	0.8	1666.3	15.5	1656.0	11.3	1642.9	16.7	**1642.9**	**16.7**	101.4
51	442	248580.9	4.6	10.5	0.9	3.5	1.4	0.3	1.0	0.8	1523.7	14.2	1527.1	10.7	1531.8	16.3	**1531.8**	**16.3**	99.5
52	148	34575.8	8.6	9.4	0.6	4.4	1.3	0.3	1.1	0.9	1680.0	16.8	1705.9	10.8	1737.7	11.7	**1737.7**	**11.7**	96.7
53	67	13324.8	1.6	12.2	0.9	2.4	1.5	0.2	1.2	0.8	1241.2	13.9	1240.5	10.8	1239.2	16.9	**1239.2**	**16.9**	100.2
54	286	408833.4	3.6	17.8	0.9	0.6	1.6	0.1	1.3	0.8	443.1	5.7	445.3	5.8	456.3	20.0	**443.1**	**5.7**	97.1
55	37	38814.1	1.6	9.9	0.7	4.0	1.4	0.3	1.2	0.9	1633.6	17.7	1640.6	11.4	1649.7	12.6	**1649.7**	**12.6**	99.0
56	281	100162.7	3.3	12.2	0.6	2.4	1.2	0.2	1.0	0.9	1253.8	11.3	1252.6	8.4	1250.5	11.8	**1250.5**	**11.8**	100.3
57	51	33017.7	1.8	9.2	0.9	4.7	1.4	0.3	1.0	0.7	1765.2	16.0	1768.6	11.7	1772.5	17.2	**1772.5**	**17.2**	99.6
58	113	18937.1	1.5	17.8	1.0	0.5	1.5	0.1	1.1	0.7	434.7	4.7	439.1	5.4	462.1	22.9	**434.7**	**4.7**	94.1
59	37	77252.9	2.3	10.5	0.8	3.6	1.3	0.3	1.1	0.8	1556.5	14.7	1544.4	10.3	1527.9	14.3	**1527.9**	**14.3**	101.9
6	135	47423.9	3.4	9.0	0.6	4.8	1.0	0.3	0.8	0.8	1754.2	12.3	1783.1	8.5	1817.0	11.2	**1817.0**	**11.2**	96.5
61	65	57632.1	1.3	9.1	0.7	4.9	1.2	0.3	0.9	0.8	1794.2	14.1	1796.9	9.7	1800.0	13.3	**1800.0**	**13.3**	99.7
62	111	248744.7	2.0	9.8	0.7	3.9	1.4	0.3	1.2	0.9	1588.9	16.6	1621.2	11.0	1663.4	12.6	**1663.4**	**12.6**	95.5
64	77	91709.5	3.1	12.0	0.9	2.4	1.5	0.2	1.2	0.8	1234.2	13.2	1249.2	10.5	1275.3	17.0	**1275.3**	**17.0**	96.8
65	13	7257.7	1.4	5.3	0.8	14.4	1.4	0.6	1.1	0.8	2856.2	25.2	2778.4	13.0	2722.4	13.6	**2722.4**	**13.6**	104.9
66	300	55897.6	6.0	6.0	1.6	8.7	2.7	0.4	2.2	0.8	2051.5	39.0	2303.9	24.7	2535.8	26.1	**2535.8**	**26.1**	80.9
67	36	25120.7	3.4	4.9	1.0	16.2	1.6	0.6	1.3	0.8	2918.6	31.0	2886.8	15.6	2864.7	15.7	**2864.7**	**15.7**	101.9
68	86	4296.7	2.7	18.3	1.2	0.5	1.7	0.1	1.2	0.7	434.6	4.9	427.9	5.9	391.7	27.0	**434.6**	**4.9**	110.9
69	132	31793.2	2.4	9.8	0.7	4.1	1.3	0.3	1.1	0.9	1632.9	16.5	1645.5	10.9	1661.6	13.0	**1661.6**	**13.0**	98.3
7	56	270600.9	2.6	9.9	0.9	4.2	1.7	0.3	1.4	0.9	1683.4	21.2	1667.6	13.7	1647.7	16.0	**1647.7**	**16.0**	102.2
70	46	111496.6	4.1	9.7	0.9	4.0	1.4	0.3	1.1	0.8	1619.9	16.4	1642.7	11.8	1672.0	16.3	**1672.0**	**16.3**	96.9
71	53	13129.5	2.9	11.3	0.9	3.0	1.3	0.2	0.9	0.7	1397.9	11.6	1395.6	9.8	1392.1	17.2	**1392.1**	**17.2**	100.4
72	137	242360.6	3.4	12.2	0.7	2.3	1.1	0.2	0.8	0.7	1207.8	8.5	1218.6	7.6	1237.8	14.6	**1237.8**	**14.6**	97.6
73	62	37293.1	2.3	9.8	1.0	4.1	1.6	0.3	1.2	0.8	1634.3	17.5	1645.7	12.9	1660.3	19.1	**1660.3**	**19.1**	98.4
74	66	281455.4	2.4	6.1	0.7	10.2	1.3	0.4	1.1	0.8	2391.4	22.2	2450.1	12.3	2499.2	12.4	**2499.2**	**12.4**	95.7

76	180	28626.5	2.8	10.3	0.7	3.6	1.2	0.3	1.0	0.8	1537.0	13.9	1553.7	9.8	1576.5	13.2	**1576.5**	**13.2**	97.5
77	176	32638.4	1.5	17.7	0.9	0.5	1.3	0.1	1.0	0.7	425.5	4.0	433.0	4.7	473.2	19.7	**425.5**	**4.0**	89.9
78	155	46698.7	1.9	12.1	0.8	2.3	1.2	0.2	0.9	0.8	1193.1	10.1	1216.9	8.7	1259.2	15.9	**1259.2**	**15.9**	94.7
79	84	144366.6	1.6	9.8	1.0	4.1	1.8	0.3	1.6	0.8	1632.8	22.4	1648.7	15.0	1669.0	18.2	**1669.0**	**18.2**	97.8
8	52	28349.2	2.9	4.6	0.8	14.7	1.2	0.5	0.9	0.8	2589.9	19.5	2796.8	11.4	2949.7	12.4	**2949.7**	**12.4**	87.8
80	97	31120.7	3.2	11.7	0.6	2.7	1.3	0.2	1.1	0.9	1311.8	13.2	1319.8	9.5	1332.7	12.4	**1332.7**	**12.4**	98.4
81	87	70057.6	5.9	9.4	0.8	4.6	1.6	0.3	1.4	0.9	1751.2	21.2	1748.3	13.4	1744.8	14.9	**1744.8**	**14.9**	100.4
82	39	5198.1	1.0	11.1	2.1	2.6	2.3	0.2	1.0	0.4	1232.3	11.2	1304.2	17.2	1424.6	40.5	**1424.6**	**40.5**	86.5
83	16	255497.2	1.5	4.9	0.8	16.0	1.2	0.6	0.9	0.8	2910.4	21.2	2877.1	11.2	2853.9	12.2	**2853.9**	**12.2**	102.0
84	372	34273.3	3.0	5.8	1.0	10.3	1.4	0.4	1.0	0.7	2339.9	20.3	2465.4	13.4	2570.4	17.0	**2570.4**	**17.0**	91.0
85	114	31519.5	3.6	10.5	0.8	3.4	1.3	0.3	1.1	0.8	1472.2	13.9	1494.3	10.3	1525.7	14.6	**1525.7**	**14.6**	96.5
86	56	14501.9	2.0	11.3	0.9	2.8	1.4	0.2	1.1	0.8	1349.6	13.3	1365.6	10.7	1390.7	17.6	**1390.7**	**17.6**	97.0
88	102	36585.4	2.3	10.8	0.8	3.4	1.6	0.3	1.3	0.8	1498.2	17.6	1493.3	12.2	1486.4	16.0	**1486.4**	**16.0**	100.8
89	27	1708079.3	1.3	10.6	0.9	3.5	1.4	0.3	1.0	0.8	1526.9	14.2	1521.0	10.7	1512.7	16.5	**1512.7**	**16.5**	100.9
9	164	106528.5	3.2	11.6	0.8	2.7	1.4	0.2	1.2	0.8	1298.9	14.1	1318.2	10.5	1349.8	14.9	**1349.8**	**14.9**	96.2
90	248	2057111.8	3.9	10.7	0.8	3.3	1.3	0.3	1.0	0.8	1481.6	13.4	1490.7	9.9	1503.5	14.3	**1503.5**	**14.3**	98.5
91	17	29400.9	1.3	9.8	1.1	4.2	1.5	0.3	1.0	0.7	1685.6	15.4	1672.1	12.6	1655.1	20.9	**1655.1**	**20.9**	101.8
92	46	62166.9	1.5	6.6	0.6	9.3	1.4	0.4	1.2	0.9	2368.7	24.3	2372.2	12.6	2375.2	10.7	**2375.2**	**10.7**	99.7
93	52	9704.6	3.7	13.9	1.1	1.4	1.6	0.1	1.1	0.7	876.8	9.4	906.3	9.5	978.8	22.2	**978.8**	**22.2**	89.6
94	613	86844.5	17.4	13.6	0.8	1.8	1.4	0.2	1.1	0.8	1071.1	11.0	1057.8	9.0	1030.5	15.8	**1030.5**	**15.8**	103.9
95	140	17391825.5	1.8	9.8	0.7	4.0	1.1	0.3	0.9	0.8	1621.7	13.1	1640.6	9.2	1665.0	12.3	**1665.0**	**12.3**	97.4
96	18	30454.1	0.9	11.7	1.1	2.7	1.6	0.2	1.2	0.7	1340.1	14.3	1336.2	11.9	1329.9	20.8	**1329.9**	**20.8**	100.8
97	81	16608.3	1.4	12.4	0.9	2.2	1.4	0.2	1.1	0.7	1146.4	11.1	1168.9	9.8	1210.9	18.6	**1210.9**	**18.6**	94.7
98	214	25908.3	2.0	12.8	0.7	2.1	1.3	0.2	1.1	0.8	1136.0	11.0	1142.3	8.7	1154.3	14.0	**1154.3**	**14.0**	98.4
99	81	31549.3	5.0	12.5	0.8	2.2	1.3	0.2	1.0	0.8	1167.1	11.1	1177.4	9.2	1196.3	15.9	**1196.3**	**15.9**	97.6
xx	213	33262.1	4.3	16.8	0.7	0.7	1.2	0.1	1.0	0.8	527.7	4.8	539.4	4.8	589.2	14.2	**527.7**	**4.8**	89.6
xx	1906	586749.1	2.8	12.9	0.6	1.7	1.4	0.2	1.2	0.9	967.5	10.8	1020.4	8.7	1135.7	12.6	**1135.7**	**12.6**	85.2
60	308	2189482.0	39.8	7.9	0.8	6.0	1.5	0.3	1.3	0.8	1908.7	21.4	1983.0	13.4	2061.4	14.7	**2061.4**	**14.7**	92.6
61	137	47085.2	1.2	16.4	1.0	0.8	1.6	0.1	1.2	0.8	609.5	7.2	616.6	7.4	642.9	21.7	**609.5**	**7.2**	94.8
62	70	22245.9	1.8	16.8	1.2	0.8	1.7	0.1	1.2	0.7	589.7	6.9	588.3	7.7	582.8	26.5	**589.7**	**6.9**	101.2

63	921	3127216.6	8.4	8.7	0.9	4.4	2.1	0.3	1.9	0.9	1565.3	26.9	1703.9	17.7	1878.8	16.4	**1878.8**	**16.4**	83.3
64	305	183458.4	2.7	12.5	0.7	2.3	1.4	0.2	1.2	0.8	1201.4	12.8	1198.3	9.6	1192.7	14.3	**1192.7**	**14.3**	100.7
65	348	151528.2	5.2	16.1	0.9	0.9	1.5	0.1	1.2	0.8	636.2	7.5	645.7	7.3	678.7	19.4	**636.2**	**7.5**	93.7
66	266	159467.3	2.8	7.5	0.7	7.2	1.4	0.4	1.2	0.9	2143.7	22.7	2139.0	12.8	2134.4	12.4	**2134.4**	**12.4**	100.4
67	209	540254.4	4.0	7.2	0.7	7.1	1.4	0.4	1.3	0.9	2048.8	22.4	2127.2	12.9	2203.8	11.9	**2203.8**	**11.9**	93.0
68	385	452597.7	2.2	17.8	1.0	0.5	1.6	0.1	1.3	0.8	416.5	5.3	422.2	5.6	452.9	21.6	**416.5**	**5.3**	92.0
69	173	419440.3	1.5	8.6	0.8	5.6	1.5	0.3	1.3	0.9	1928.0	21.5	1911.5	13.0	1893.7	13.9	**1893.7**	**13.9**	101.8
7	68	47054.5	1.2	13.9	1.2	1.7	1.7	0.2	1.2	0.7	1009.9	11.2	1000.0	11.0	978.3	25.4	**978.3**	**25.4**	103.2
70	180	179695.6	1.8	9.6	0.9	4.2	1.5	0.3	1.2	0.8	1656.0	17.5	1678.7	12.5	1707.2	17.4	**1707.2**	**17.4**	97.0
71	169	188392.4	2.1	14.9	1.0	1.2	2.0	0.1	1.8	0.9	767.1	12.7	785.0	11.0	836.2	20.2	**767.1**	**12.7**	91.7
72	205	443424.5	1.8	4.4	0.9	18.3	1.5	0.6	1.1	0.8	2985.2	26.6	3007.7	14.1	3022.8	15.2	**3022.8**	**15.2**	98.8
73	145	234722.1	2.7	14.2	0.7	1.5	1.4	0.2	1.2	0.9	921.2	10.6	927.8	8.7	943.5	14.6	**943.5**	**14.6**	97.6
74	161	192101.4	1.2	16.6	1.1	0.9	1.6	0.1	1.2	0.8	632.2	7.3	629.1	7.6	617.6	22.8	**632.2**	**7.3**	102.4
76	106	59661.0	3.4	13.6	1.1	1.8	1.5	0.2	1.0	0.7	1035.9	9.8	1031.0	9.8	1020.7	22.6	**1020.7**	**22.6**	101.5
77	281	313583.3	2.7	11.7	0.9	2.6	1.5	0.2	1.1	0.8	1289.5	13.0	1303.9	10.7	1327.7	18.2	**1327.7**	**18.2**	97.1
78	207	74951.9	11.7	16.6	0.9	0.8	1.6	0.1	1.3	0.8	616.6	7.5	615.7	7.3	612.4	20.1	**616.6**	**7.5**	100.7
79	459	627990.2	2.4	18.1	1.2	0.5	1.7	0.1	1.3	0.7	394.4	4.9	397.7	5.7	416.5	25.9	**394.4**	**4.9**	94.7
8	89	225571.2	3.4	13.6	0.9	1.8	1.5	0.2	1.2	0.8	1042.4	11.6	1039.1	9.7	1032.1	18.0	**1032.1**	**18.0**	101.0
80	119	168969.0	0.9	17.0	1.0	0.8	1.6	0.1	1.2	0.7	574.1	6.4	572.0	6.8	563.6	22.7	**574.1**	**6.4**	101.9
82	725	286144.8	3.6	12.2	0.8	2.4	1.5	0.2	1.3	0.9	1239.6	14.6	1242.8	10.9	1248.4	15.5	**1248.4**	**15.5**	99.3
83	196	168642.4	0.9	17.1	1.2	0.7	2.0	0.1	1.6	0.8	554.5	8.3	553.8	8.3	551.0	25.8	**554.5**	**8.3**	100.6
84	266	355816.1	1.2	13.5	1.0	1.8	1.6	0.2	1.2	0.8	1075.9	11.8	1063.3	10.4	1037.4	20.9	**1037.4**	**20.9**	103.7
85	259	350853.6	14.0	12.2	0.9	2.4	1.5	0.2	1.2	0.8	1244.5	13.7	1243.8	10.7	1242.7	17.1	**1242.7**	**17.1**	100.1
86	38	39053.4	0.9	7.4	1.1	7.2	1.5	0.4	1.1	0.7	2129.4	19.4	2142.2	13.6	2154.5	19.0	**2154.5**	**19.0**	98.8
87	475	385096.6	14.3	13.1	1.4	1.8	2.4	0.2	1.9	0.8	1034.3	18.5	1055.0	15.7	1098.2	27.9	**1098.2**	**27.9**	94.2
88	257	774624.6	2.4	16.2	0.9	0.9	1.7	0.1	1.5	0.9	623.9	8.8	632.4	8.1	663.0	18.8	**623.9**	**8.8**	94.1
89	372	3832797.4	1.3	8.1	1.0	6.3	1.6	0.4	1.3	0.8	2028.1	22.0	2018.9	13.9	2009.4	17.0	**2009.4**	**17.0**	100.9
9	687	178472.2	2.2	18.8	1.2	0.4	1.9	0.0	1.5	0.8	311.7	4.6	314.5	5.2	335.4	26.8	**311.7**	**4.6**	92.9
90	29	30339.1	1.8	10.0	1.2	4.0	1.9	0.3	1.4	0.8	1653.6	21.1	1643.0	15.3	1629.5	22.4	**1629.5**	**22.4**	101.5
91	69	18113.6	1.3	16.8	1.1	0.8	1.8	0.1	1.4	0.8	608.2	8.3	602.6	8.2	581.3	24.0	**608.2**	**8.3**	104.6

92	184	194808.2	2.5	16.2	1.3	0.9	1.7	0.1	1.1	0.7	660.3	7.1	662.2	8.3	668.4	27.4	**660.3**	**7.1**	98.8
93	258	2061156.2	0.8	15.3	0.8	1.2	1.5	0.1	1.3	0.8	787.9	9.7	787.8	8.4	787.2	17.1	**787.9**	**9.7**	100.1
94	37	158153.6	2.5	13.1	1.3	1.8	1.8	0.2	1.3	0.7	1040.5	12.4	1062.1	11.9	1106.8	25.1	**1106.8**	**25.1**	94.0
95	61	82121.0	2.0	16.3	1.4	0.9	1.8	0.1	1.2	0.6	633.2	7.1	636.6	8.7	648.9	30.2	**633.2**	**7.1**	97.6
96	86	82051.0	2.5	8.1	0.9	6.0	1.4	0.4	1.0	0.7	1952.0	17.1	1977.6	11.9	2004.4	16.3	**2004.4**	**16.3**	97.4
97	159	81099.5	2.3	16.0	1.0	1.0	1.6	0.1	1.2	0.8	692.2	7.9	690.6	7.8	685.5	21.2	**692.2**	**7.9**	101.0
98	46	75653.5	3.0	12.3	1.4	2.3	2.1	0.2	1.5	0.7	1184.2	16.3	1201.5	14.5	1232.7	27.4	**1232.7**	**27.4**	96.1
99	357	176914.5	5.7	16.1	1.1	0.9	1.8	0.1	1.4	0.8	615.4	8.3	629.8	8.3	682.1	22.7	**615.4**	**8.3**	90.2
xx	611	333892.7	6.0	17.1	1.0	0.7	2.2	0.1	2.0	0.9	536.6	10.3	539.3	9.4	551.1	22.2	**536.6**	**10.3**	97.4
xx	515	262649.8	2.0	13.1	1.1	1.8	2.3	0.2	2.0	0.9	1004.1	18.2	1036.3	14.7	1104.8	22.8	**1104.8**	**22.8**	90.9
xx	227	140936.4	7.1	16.9	1.0	0.7	1.5	0.1	1.1	0.7	536.5	5.8	543.6	6.4	573.3	22.5	**536.5**	**5.8**	93.6

Sample: UF-C						**Isotope Ratios**					**Apparent Ages (Ma)**								
Analysis	**U (ppm)**	**206Pb /204Pb**	**U /Th**	**206Pb /207Pb**	**± (%)**	**207Pb /235U**	**± (%)**	**206Pb /238U**	**± (%)**	**err. corr.**	**206Pb /238U**	**± (Ma)**	**207Pb/ 235U**	**± (Ma)**	**206Pb /207Pb**	**± (Ma)**	**Best Age**	**± (Ma)**	**Conc. (%)**
1	255	16482.3	0.4	17.2	0.9	0.7	1.3	0.1	0.9	0.7	520.5	4.7	522.8	5.2	532.7	18.8	**520.5**	**4.7**	97.7
10	179	11150.2	2.7	18.1	0.9	0.5	1.3	0.1	0.9	0.7	421.3	3.8	421.4	4.6	422.2	21.0	**421.3**	**3.8**	99.8
100	53	19527.4	1.5	12.2	1.0	2.4	1.6	0.2	1.3	0.8	1238.4	14.1	1242.3	11.3	1249.2	18.7	**1249.2**	**18.7**	99.1
101	138	12588.9	1.9	14.1	0.9	1.6	1.2	0.2	0.9	0.7	995.7	8.2	983.9	7.8	957.5	17.5	**957.5**	**17.5**	104.0
102	352	17789.9	0.7	17.1	0.7	0.6	1.1	0.1	0.9	0.8	443.0	3.8	460.5	4.2	548.9	15.7	**443.0**	**3.8**	80.7
103	78	45629.4	2.2	6.9	0.7	7.7	1.3	0.4	1.1	0.8	2090.1	20.2	2194.5	12.1	2293.5	12.4	**2293.5**	**12.4**	91.1
104	228	27311.9	1.9	17.0	1.0	0.8	1.6	0.1	1.2	0.8	572.5	6.8	568.8	7.0	553.7	22.0	**572.5**	**6.8**	103.4
106	359	2915.8	2.2	13.3	3.9	0.7	4.0	0.1	0.7	0.2	425.4	3.0	542.5	16.6	1070.8	78.1	**425.4**	**3.0**	39.7
107	151	14842.4	2.0	9.5	0.7	4.1	1.1	0.3	0.9	0.8	1609.7	12.5	1655.6	8.9	1714.3	12.0	**1714.3**	**12.0**	93.9
108	188	131936.1	0.9	6.5	0.6	9.4	1.1	0.4	0.8	0.8	2343.8	16.6	2374.0	9.7	2399.9	10.9	**2399.9**	**10.9**	97.7
109	342	45129.8	3.4	12.1	0.7	2.2	1.1	0.2	0.9	0.8	1157.3	9.8	1194.3	8.1	1262.1	13.3	**1262.1**	**13.3**	91.7
11	335	31196.2	1.7	17.8	0.7	0.6	1.1	0.1	0.9	0.8	456.8	3.8	456.2	4.1	452.9	16.2	**456.8**	**3.8**	100.9
110	252	617778.8	1.3	9.8	0.7	4.2	1.2	0.3	1.0	0.8	1684.0	15.0	1671.6	9.9	1656.1	12.1	**1656.1**	**12.1**	101.7
111	165	29371.2	1.0	15.9	0.9	0.9	1.4	0.1	1.1	0.8	667.1	6.7	676.9	6.9	709.7	19.4	**667.1**	**6.7**	94.0
112	229	9519.9	1.2	17.8	1.4	0.5	1.7	0.1	0.9	0.5	426.1	3.6	431.5	5.9	460.1	31.7	**426.1**	**3.6**	92.6
113	168	26835.0	3.1	10.9	0.6	3.2	1.1	0.3	0.9	0.8	1463.8	11.8	1462.8	8.5	1461.3	11.8	**1461.3**	**11.8**	100.2
114	282	487510.1	1.1	6.1	0.7	10.2	1.3	0.5	1.1	0.8	2407.8	22.1	2450.0	12.2	2485.3	12.1	**2485.3**	**12.1**	96.9
115	326	42964.6	2.4	5.4	0.7	12.8	1.3	0.5	1.2	0.9	2641.4	25.2	2668.4	12.7	2688.9	11.3	**2688.9**	**11.3**	98.2
116	191	30530.9	2.2	7.5	0.7	6.5	1.4	0.3	1.3	0.9	1933.4	21.0	2040.3	12.6	2150.1	12.1	**2150.1**	**12.1**	89.9
117	227	13561.9	1.5	16.6	1.2	0.8	1.5	0.1	1.0	0.6	603.1	5.5	605.6	7.0	614.8	26.1	**603.1**	**5.5**	98.1
118	264	8282.3	2.2	18.0	1.0	0.6	1.4	0.1	0.9	0.7	454.2	4.1	449.9	5.0	428.0	22.3	**454.2**	**4.1**	106.1
119	1005	37012.7	1.8	16.5	0.6	0.8	1.1	0.1	0.9	0.8	620.6	5.3	620.3	5.0	618.9	12.3	**620.6**	**5.3**	100.3
12	566	100946.7	3.4	16.8	0.6	0.8	1.1	0.1	0.9	0.8	619.8	5.3	611.6	5.1	581.3	13.7	**619.8**	**5.3**	106.6
121	72	10325.7	1.3	16.2	1.3	0.8	1.7	0.1	1.0	0.6	550.1	5.3	571.5	7.3	657.7	28.5	**550.1**	**5.3**	83.6
122	426	23488.6	0.9	16.6	0.6	0.8	1.0	0.1	0.8	0.8	590.5	4.7	594.8	4.7	611.4	13.9	**590.5**	**4.7**	96.6

123	620	109944.9	1.2	16.2	0.6	0.9	1.1	0.1	0.9	0.8	636.2	5.5	642.1	5.3	662.8	13.7	**636.2**	**5.5**	96.0
124	32	8173.6	2.5	15.5	1.4	1.1	1.8	0.1	1.2	0.6	732.6	8.0	737.4	9.4	752.2	28.7	**732.6**	**8.0**	97.4
126	535	144078.2	2.0	13.4	0.7	1.9	1.2	0.2	1.0	0.8	1097.8	9.9	1084.7	7.8	1058.5	13.2	**1058.5**	**13.2**	103.7
127	780	60075.9	8.9	12.9	0.6	2.0	1.1	0.2	1.0	0.9	1112.7	10.0	1121.4	7.8	1138.3	12.0	**1138.3**	**12.0**	97.7
128	119	36319.3	1.4	4.9	0.9	15.8	1.4	0.6	1.1	0.8	2879.3	25.3	2865.7	13.6	2856.1	14.9	**2856.1**	**14.9**	100.8
13	135	43441.4	2.9	16.7	0.9	0.8	1.4	0.1	1.0	0.7	590.4	5.7	592.7	6.2	601.6	20.0	**590.4**	**5.7**	98.1
130	834	246890.9	9.3	6.5	1.1	8.2	1.8	0.4	1.4	0.8	2115.4	25.0	2253.1	16.2	2380.6	19.3	**2380.6**	**19.3**	88.9
131	344	44442.3	2.0	16.2	0.8	0.8	1.3	0.1	1.0	0.8	605.0	6.0	616.5	6.0	659.0	16.5	**605.0**	**6.0**	91.8
132	84	8613.7	2.0	13.7	1.0	1.7	1.3	0.2	0.9	0.7	1009.8	8.2	1010.3	8.5	1011.5	20.3	**1011.5**	**20.3**	99.8
133	365	44758.4	1.8	17.1	0.9	0.7	1.2	0.1	0.8	0.7	537.9	4.2	540.5	5.1	551.6	19.6	**537.9**	**4.2**	97.5
134	215	8822.4	1.9	18.0	1.2	0.5	1.5	0.1	1.0	0.7	411.1	4.0	415.4	5.3	439.3	25.8	**411.1**	**4.0**	93.6
135	17	1804.1	1.3	18.1	3.0	0.8	3.3	0.1	1.3	0.4	627.6	7.9	585.7	14.6	426.6	67.0	**627.6**	**7.9**	147.1
136	250	46938.1	5.5	15.9	0.8	0.9	1.4	0.1	1.2	0.8	641.3	7.0	653.9	6.6	697.7	16.1	**641.3**	**7.0**	91.9
137	350	35478.6	1.3	8.7	0.6	5.3	1.3	0.3	1.1	0.9	1858.4	18.1	1863.8	10.8	1869.8	10.7	**1869.8**	**10.7**	99.4
138	500	35805.2	0.9	16.7	0.7	0.8	1.4	0.1	1.2	0.9	583.8	6.6	586.1	6.2	594.9	15.5	**583.8**	**6.6**	98.1
14	177	38522.8	1.7	17.8	2.2	0.5	2.4	0.1	0.9	0.4	366.1	3.2	379.2	7.6	460.1	49.6	**366.1**	**3.2**	79.6
140	56	3122.3	1.1	16.2	1.0	0.9	1.4	0.1	1.0	0.7	636.4	6.0	643.4	6.7	668.1	21.2	**636.4**	**6.0**	95.3
141	62	6020.7	2.3	12.0	0.9	2.4	1.4	0.2	1.1	0.8	1211.4	12.3	1236.0	10.3	1279.2	17.8	**1279.2**	**17.8**	94.7
142	253	7359.6	1.5	16.9	0.7	0.8	1.3	0.1	1.1	0.8	591.2	6.0	588.0	5.7	575.5	15.5	**591.2**	**6.0**	102.7
143	389	20529.0	1.0	16.9	1.1	0.5	1.3	0.1	0.8	0.6	411.2	3.3	436.7	4.8	573.0	23.2	**411.2**	**3.3**	71.8
144	105	7266.2	0.9	15.5	1.0	0.9	1.3	0.1	0.9	0.7	630.2	5.5	657.8	6.5	753.4	20.8	**630.2**	**5.5**	83.6
145	248	140459.9	2.8	12.8	0.8	2.1	1.2	0.2	0.9	0.7	1142.3	9.4	1143.9	8.2	1147.0	15.9	**1147.0**	**15.9**	99.6
146	306	53184.8	2.2	17.9	0.8	0.5	1.2	0.1	0.9	0.7	412.9	3.7	417.2	4.2	441.3	18.1	**412.9**	**3.7**	93.6
147	55	83466.9	2.9	11.4	0.9	2.8	1.3	0.2	0.9	0.7	1331.9	11.1	1349.6	9.5	1377.7	16.8	**1377.7**	**16.8**	96.7
148	333	64069.0	5.4	10.7	0.8	3.3	1.5	0.3	1.3	0.9	1458.8	17.0	1472.7	11.9	1492.6	15.1	**1492.6**	**15.1**	97.7
149	216	313371 0.6	1.8	7.5	0.6	6.8	1.1	0.4	0.9	0.9	2029.4	16.5	2084.5	9.9	2139.3	10.2	**2139.3**	**10.2**	94.9
15	109	11136.1	1.2	15.8	1.3	0.9	1.7	0.1	1.0	0.6	636.3	6.4	653.6	8.1	713.9	28.0	**636.3**	**6.4**	89.1
150	82	6660.6	1.1	11.2	1.1	3.0	1.4	0.2	0.9	0.6	1394.2	11.7	1397.0	10.9	1401.2	21.1	**1401.2**	**21.1**	99.5
151	928	36334.1	4.6	16.0	0.9	0.8	1.5	0.1	1.2	0.8	556.3	6.4	582.6	6.6	686.2	18.8	**556.3**	**6.4**	81.1

152	628	107019.0	2.1	13.3	0.8	1.9	1.5	0.2	1.3	0.8	1062.6	12.4	1066.3	10.0	1074.0	16.5	**1074.0**	**16.5**	98.9
153	313	40590.2	7.3	14.3	0.6	1.4	1.0	0.2	0.8	0.8	902.5	6.9	907.9	6.1	921.3	12.1	**921.3**	**12.1**	98.0
154	210	29339.3	0.8	10.2	0.6	3.7	1.1	0.3	0.9	0.8	1558.5	13.1	1566.7	9.0	1577.7	11.3	**1577.7**	**11.3**	98.8
155	246	15182.6	2.9	17.0	1.1	0.7	1.6	0.1	1.2	0.7	554.3	6.3	556.1	7.0	563.5	24.5	**554.3**	**6.3**	98.4
156	578	34468.4	2.0	16.7	0.6	0.9	1.1	0.1	0.9	0.8	655.1	5.7	643.3	5.3	602.3	13.2	**655.1**	**5.7**	108.8
157	569	75422.6	2.4	13.5	0.7	1.9	1.4	0.2	1.2	0.9	1082.8	11.8	1068.6	9.0	1039.9	13.8	**1039.9**	**13.8**	104.1
158	154	54136.6	8.6	7.7	0.8	6.7	1.3	0.4	1.0	0.8	2033.0	17.5	2069.0	11.3	2105.1	14.1	**2105.1**	**14.1**	96.6
159	162	36775.6	3.0	12.0	0.7	2.3	1.3	0.2	1.1	0.9	1199.8	12.4	1226.6	9.5	1274.1	13.6	**1274.1**	**13.6**	94.2
16	55	39957.6	1.6	5.1	0.9	14.5	1.7	0.5	1.4	0.8	2767.9	32.0	2783.0	16.0	2794.0	14.8	**2794.0**	**14.8**	99.1
160	128	5799.8	1.6	16.3	1.2	1.0	1.7	0.1	1.3	0.7	698.7	8.3	686.8	8.7	648.2	25.7	**698.7**	**8.3**	107.8
161	198	19653.0	1.6	16.4	0.7	0.9	1.2	0.1	1.0	0.8	636.8	5.8	635.9	5.7	632.8	16.0	**636.8**	**5.8**	100.6
162	28	6023.8	2.6	10.6	1.0	3.4	1.4	0.3	1.0	0.7	1513.0	13.4	1512.1	11.1	1510.9	18.8	**1510.9**	**18.8**	100.1
163	91	10095.1	1.0	17.0	1.3	0.7	1.7	0.1	1.1	0.6	535.7	5.5	541.1	7.0	564.0	27.6	**535.7**	**5.5**	95.0
164	261	61727.3	0.9	8.1	0.6	6.1	1.3	0.4	1.2	0.9	1994.4	19.9	1994.8	11.3	1995.2	10.0	**1995.2**	**10.0**	100.0
165	181	30342.9	2.0	17.0	1.1	0.5	1.5	0.1	1.1	0.7	369.9	3.9	397.2	5.0	559.0	23.4	**369.9**	**3.9**	66.2
166	377	300177.4	1.6	16.0	0.8	0.8	1.4	0.1	1.1	0.8	603.4	6.4	622.1	6.4	690.5	17.4	**603.4**	**6.4**	87.4
167	447	37203.2	0.9	17.4	0.7	0.6	1.3	0.1	1.1	0.8	475.5	5.1	480.6	5.1	504.9	15.6	**475.5**	**5.1**	94.2
168	123	7960.7	2.6	13.0	0.9	1.9	1.4	0.2	1.1	0.8	1057.6	10.4	1076.3	9.1	1114.3	17.2	**1114.3**	**17.2**	94.9
169	263	18911.1	0.4	16.4	0.8	0.8	1.3	0.1	1.0	0.8	598.3	5.5	605.4	5.7	632.2	17.4	**598.3**	**5.5**	94.6
17	36	24605.9	2.0	13.9	1.5	1.6	1.8	0.2	0.9	0.5	941.9	8.0	954.9	11.0	984.9	30.8	**984.9**	**30.8**	95.6
171	244	49141.9	2.4	12.8	0.7	2.1	1.3	0.2	1.1	0.9	1171.0	12.1	1163.1	9.1	1148.5	13.3	**1148.5**	**13.3**	102.0
172	135	29208.1	1.7	8.7	0.6	5.3	1.4	0.3	1.2	0.9	1847.7	20.0	1862.6	12.0	1879.1	11.5	**1879.1**	**11.5**	98.3
173	1762	31223.6	1.3	16.5	0.9	0.9	1.5	0.1	1.2	0.8	639.4	7.2	634.9	7.0	618.6	19.6	**639.4**	**7.2**	103.4
174	322	261318.6	2.2	16.3	0.7	0.9	1.2	0.1	0.9	0.8	641.4	5.7	644.7	5.7	656.4	15.9	**641.4**	**5.7**	97.7
175	299	14858.1	1.4	16.7	0.9	0.7	1.5	0.1	1.2	0.8	546.4	6.1	556.1	6.2	595.8	18.9	**546.4**	**6.1**	91.7
176	106	51156.0	2.4	5.0	0.8	15.0	1.1	0.5	0.8	0.7	2796.3	17.1	2813.8	10.1	2826.4	12.3	**2826.4**	**12.3**	98.9
178	238	60982.3	2.5	9.9	0.8	3.9	1.3	0.3	1.1	0.8	1591.3	15.5	1610.1	10.9	1634.8	14.4	**1634.8**	**14.4**	97.3
179	468	30584.3	0.8	17.9	0.8	0.5	1.3	0.1	1.1	0.8	435.5	4.5	436.9	4.7	444.0	17.0	**435.5**	**4.5**	98.1

18	172	53038.4	1.7	11.7	0.8	2.7	1.3	0.2	1.1	0.8	1321.9	12.8	1323.7	10.0	1326.7	15.9	**1326.7**	**15.9**	99.6
181	332	92443.0	3.1	13.4	0.8	1.8	1.4	0.2	1.2	0.8	1063.4	11.9	1061.1	9.5	1056.5	15.6	**1056.5**	**15.6**	100.6
182	46	11878.8	2.0	7.8	0.9	6.8	1.6	0.4	1.3	0.8	2086.4	22.3	2080.0	13.8	2073.7	16.4	**2073.7**	**16.4**	100.6
183	419	26514.5	15.2	16.6	0.9	0.9	1.3	0.1	0.9	0.7	668.1	5.8	656.2	6.1	615.6	18.7	**668.1**	**5.8**	108.5
184	138	19951.7	2.5	16.5	0.7	0.8	1.1	0.1	0.9	0.8	571.9	4.7	582.0	4.9	621.5	14.9	**571.9**	**4.7**	92.0
185	114	45107.5	1.7	10.2	0.8	3.7	1.4	0.3	1.1	0.8	1567.1	15.8	1571.9	11.3	1578.4	15.9	**1578.4**	**15.9**	99.3
186	68	5673.4	3.0	13.1	1.5	1.9	1.8	0.2	1.1	0.6	1089.9	10.7	1094.2	12.1	1102.7	29.2	**1102.7**	**29.2**	98.8
187	129	5775.2	3.1	16.8	1.4	0.6	1.7	0.1	1.0	0.6	420.2	4.2	446.4	6.2	584.0	30.0	**420.2**	**4.2**	72.0
188	158	57863.0	2.5	8.8	0.7	5.0	1.3	0.3	1.1	0.8	1804.7	17.4	1824.9	11.2	1848.0	13.0	**1848.0**	**13.0**	97.7
189	125	625188.4	1.8	4.9	0.5	14.7	1.3	0.5	1.2	0.9	2706.9	25.7	2795.4	12.1	2859.8	8.4	**2859.8**	**8.4**	94.7
19	261	125959.3	1.0	16.5	0.7	0.8	1.3	0.1	1.1	0.9	624.4	6.6	624.4	6.1	624.4	14.5	**624.4**	**6.6**	100.0
190	296	13875.9	1.9	15.9	1.1	0.8	1.6	0.1	1.1	0.7	592.1	6.3	616.0	7.2	705.0	23.2	**592.1**	**6.3**	84.0
191	105	12158.9	1.0	15.6	1.5	0.9	1.8	0.1	1.0	0.5	606.5	5.6	635.7	8.4	740.9	31.6	**606.5**	**5.6**	81.9
192	415	27912.6	2.3	16.5	0.9	0.8	1.3	0.1	1.0	0.8	570.7	5.4	581.8	5.8	625.4	18.4	**570.7**	**5.4**	91.3
193	406	22941.8	1.1	17.8	0.8	0.5	1.2	0.1	0.8	0.7	427.8	3.5	431.7	4.1	452.9	17.4	**427.8**	**3.5**	94.5
194	200	38667.1	0.8	16.6	0.7	0.7	1.1	0.1	0.8	0.7	550.3	4.1	562.2	4.6	610.5	15.7	**550.3**	**4.1**	90.1
195	374	34870.5	4.8	12.4	0.9	2.3	1.4	0.2	1.0	0.7	1213.6	11.6	1211.8	9.9	1208.5	18.5	**1208.5**	**18.5**	100.4
196	39	9381.3	0.6	16.7	1.9	0.6	2.3	0.1	1.2	0.5	474.7	5.7	496.7	9.0	599.6	41.6	**474.7**	**5.7**	79.2
197	83	26889.1	1.4	15.4	1.2	0.9	1.5	0.1	0.9	0.6	640.8	5.4	671.1	7.2	774.2	24.6	**640.8**	**5.4**	82.8
198	1802	170373.7	3.9	9.1	0.8	4.4	1.2	0.3	1.0	0.8	1656.3	13.9	1717.7	10.3	1793.5	14.4	**1793.5**	**14.4**	92.4
199	156	3375.8	1.1	13.5	3.2	1.1	3.4	0.1	1.0	0.3	653.4	6.5	747.8	17.8	1041.8	64.5	**653.4**	**6.5**	62.7
2	340	38401.4	1.6	17.5	0.9	0.5	1.5	0.1	1.1	0.8	411.8	4.4	424.1	5.0	491.8	20.7	**411.8**	**4.4**	83.7
20	43	6769.9	6.1	13.0	1.3	2.0	1.7	0.2	1.2	0.7	1134.8	12.2	1130.6	11.8	1122.6	25.4	**1122.6**	**25.4**	101.1
200	173	48150.4	0.5	5.3	0.7	14.2	1.3	0.5	1.1	0.9	2814.1	25.6	2766.2	12.4	2731.4	11.1	**2731.4**	**11.1**	103.0
201	170	24814.7	0.5	16.4	0.8	0.8	1.3	0.1	1.0	0.8	616.6	5.8	621.2	6.0	637.8	17.8	**616.6**	**5.8**	96.7
202	190	7715.3	1.1	16.1	1.6	0.8	1.9	0.1	1.0	0.5	582.1	5.6	602.9	8.6	682.0	34.4	**582.1**	**5.6**	85.4
203	430	52686.1	20.2	8.2	0.8	5.6	1.4	0.3	1.1	0.8	1839.2	18.0	1910.9	11.8	1989.7	13.9	**1989.7**	**13.9**	92.4
204	302	23175.8	3.3	18.1	1.0	0.5	1.5	0.1	1.0	0.7	386.1	3.9	391.5	4.7	423.9	23.0	**386.1**	**3.9**	91.1
205	58	10456.3	2.6	13.7	1.3	1.7	1.8	0.2	1.2	0.7	987.8	11.0	997.5	11.2	1018.8	26.0	**1018.8**	**26.0**	97.0

206	332	16698.6	227.7	16.5	0.7	0.8	1.4	0.1	1.2	0.9	616.5	7.1	619.2	6.5	628.9	15.5	**616.5**	**7.1**	98.0
207	101	19448.9	1.5	16.0	1.1	0.8	1.6	0.1	1.1	0.7	543.1	5.8	571.7	7.0	687.4	24.2	**543.1**	**5.8**	79.0
208	857	77423.6	4.2	9.3	0.7	4.7	1.4	0.3	1.2	0.9	1776.6	19.3	1770.5	12.1	1763.2	13.6	**1763.2**	**13.6**	100.8
209	533	128890.8	1.0	16.1	0.8	0.8	1.2	0.1	0.9	0.8	601.1	5.1	617.5	5.5	678.1	16.7	**601.1**	**5.1**	88.6
210	279	305998.9	1.2	9.4	0.7	4.5	1.3	0.3	1.1	0.8	1710.3	16.7	1726.9	11.0	1747.0	13.0	**1747.0**	**13.0**	97.9
212	14	2150.4	1.7	19.6	4.7	0.5	4.9	0.1	1.5	0.3	470.2	6.6	432.6	17.4	237.2	108.5	**470.2**	**6.6**	198.2
213	92	3658.5	2.2	17.4	1.6	0.7	2.2	0.1	1.5	0.7	563.8	8.1	553.8	9.5	512.8	35.8	**563.8**	**8.1**	109.9
214	243	21642.0	0.9	8.8	1.0	4.4	1.9	0.3	1.5	0.8	1615.4	22.1	1720.8	15.5	1851.4	18.9	**1851.4**	**18.9**	87.3
215	155	9068.9	2.1	7.6	0.7	6.2	1.3	0.3	1.1	0.9	1901.8	18.9	2010.4	11.7	2123.8	11.9	**2123.8**	**11.9**	89.5
216	74	7123.9	59.9	13.3	1.5	1.8	1.8	0.2	1.0	0.6	1054.6	9.7	1061.0	11.9	1074.0	30.1	**1074.0**	**30.1**	98.2
217	151	38488.6	2.7	12.1	1.2	2.4	1.6	0.2	1.1	0.7	1242.2	12.8	1246.4	11.7	1253.7	23.0	**1253.7**	**23.0**	99.1
218	173	38137.7	1.4	16.0	0.9	1.0	1.6	0.1	1.3	0.8	686.0	8.8	688.3	8.2	695.7	19.8	**686.0**	**8.8**	98.6
219	314	130503.8	1.6	13.0	0.8	1.9	1.4	0.2	1.1	0.8	1065.6	11.1	1082.9	9.2	1118.0	15.9	**1118.0**	**15.9**	95.3
22	65	23847.0	2.2	10.8	0.9	3.3	1.5	0.3	1.2	0.8	1465.2	16.0	1469.7	11.7	1476.3	16.7	**1476.3**	**16.7**	99.2
220	263	23554.9	1.6	16.7	0.8	0.7	1.4	0.1	1.2	0.8	538.8	6.0	549.3	5.9	592.7	16.5	**538.8**	**6.0**	90.9
223	527	487237.3	2.7	9.5	0.8	4.1	1.3	0.3	1.1	0.8	1607.1	15.0	1655.5	11.0	1717.4	15.3	**1717.4**	**15.3**	93.6
224	366	39410.7	2.8	17.5	0.8	0.5	1.3	0.1	1.0	0.8	421.4	4.1	433.0	4.6	495.5	18.3	**421.4**	**4.1**	85.0
225	172	148723.9	1.4	9.7	0.8	4.4	1.4	0.3	1.2	0.8	1721.3	17.7	1705.3	11.8	1685.7	15.1	**1685.7**	**15.1**	102.1
226	1283	408541.9	4.3	9.7	1.0	4.0	1.5	0.3	1.1	0.7	1584.4	15.0	1628.6	11.8	1686.2	18.2	**1686.2**	**18.2**	94.0
227	805	36323.8	3.7	18.3	0.8	0.5	1.3	0.1	1.0	0.8	414.0	4.1	412.1	4.4	401.4	17.4	**414.0**	**4.1**	103.1
228	261	23703.6	1.2	16.3	0.9	0.8	1.5	0.1	1.2	0.8	573.6	6.6	590.2	6.8	654.6	19.8	**573.6**	**6.6**	87.6
23	110	5620612.3	3.1	16.4	1.0	0.8	1.4	0.1	0.9	0.7	616.8	5.3	621.3	6.3	637.8	21.5	**616.8**	**5.3**	96.7
230	146	6796.3	2.2	17.2	1.1	0.7	1.6	0.1	1.2	0.7	536.4	5.9	535.2	6.8	530.0	25.1	**536.4**	**5.9**	101.2
231	105	19899.0	2.5	14.0	0.9	1.5	1.5	0.2	1.1	0.8	938.0	10.0	946.2	9.0	965.2	18.6	**965.2**	**18.6**	97.2
232	146	6159.1	0.8	16.5	1.5	0.8	1.8	0.1	0.9	0.5	614.9	5.5	618.1	8.2	629.8	32.4	**614.9**	**5.5**	97.6
233	65	24215.7	0.9	17.2	1.2	0.5	1.8	0.1	1.3	0.7	421.1	5.5	439.4	6.5	536.5	26.8	**421.1**	**5.5**	78.5
234	424	39951.4	0.6	5.6	0.8	10.1	1.8	0.4	1.6	0.9	2212.4	30.0	2446.8	16.4	2647.7	12.7	**2647.7**	**12.7**	83.6
235	122	6635.4	2.7	18.5	1.6	0.5	2.0	0.1	1.1	0.5	406.3	4.2	401.1	6.5	371.6	37.0	**406.3**	**4.2**	109.3
236	970	172896.9	5.5	9.0	0.8	4.9	1.4	0.3	1.1	0.8	1778.1	17.5	1794.0	11.8	1812.4	15.0	**1812.4**	**15.0**	98.1

237	63	8537.6	1.7	9.9	0.9	4.0	1.5	0.3	1.3	0.8	1632.3	18.1	1633.8	12.4	1635.8	16.2	**1635.8**	**16.2**	99.8
238	95	20498.8	137.6	17.1	1.1	0.8	1.5	0.1	1.0	0.7	621.1	6.0	606.3	6.7	551.5	23.0	**621.1**	**6.0**	112.6
239	127	12839.2	1.1	17.5	0.9	0.6	1.4	0.1	1.1	0.8	434.5	4.5	445.4	5.1	501.9	20.6	**434.5**	**4.5**	86.6
24	257	38809.5	4.1	12.3	0.8	2.3	1.3	0.2	1.0	0.8	1206.1	11.5	1216.7	9.1	1235.5	14.8	**1235.5**	**14.8**	97.6
240	209	43374.6	2.2	10.6	0.6	3.4	1.0	0.3	0.8	0.8	1507.8	10.5	1510.8	7.7	1515.1	11.3	**1515.1**	**11.3**	99.5
241	183	23962.9	1.2	9.1	0.6	4.8	1.3	0.3	1.1	0.9	1767.1	17.1	1785.3	10.7	1806.5	11.2	**1806.5**	**11.2**	97.8
242	95	19192.5	1.5	15.5	2.0	0.9	2.1	0.1	0.8	0.4	644.8	5.1	670.2	10.5	756.5	41.4	**644.8**	**5.1**	85.2
243	143	13392.9	1.7	11.4	0.6	2.7	1.1	0.2	0.9	0.8	1318.6	10.6	1340.0	8.0	1374.4	11.4	**1374.4**	**11.4**	95.9
244	562	18601.6	16.4	18.2	1.0	0.5	1.7	0.1	1.3	0.8	413.9	5.2	413.3	5.6	410.3	22.7	**413.9**	**5.2**	100.9
245	281	35872.5	5.1	16.4	0.7	0.8	1.0	0.1	0.8	0.8	590.5	4.5	600.1	4.7	636.6	14.1	**590.5**	**4.5**	92.8
246	292	45269.7	2.0	16.4	0.8	0.8	1.2	0.1	0.9	0.7	621.6	5.3	624.1	5.6	633.2	17.5	**621.6**	**5.3**	98.2
247	421	108687.5	1.7	5.6	0.6	10.7	1.3	0.4	1.1	0.9	2344.2	21.7	2500.4	11.8	2629.8	10.2	**2629.8**	**10.2**	89.1
248	86	21249.4	1.7	13.3	1.0	1.9	1.5	0.2	1.1	0.8	1071.9	11.2	1071.6	10.0	1071.0	20.0	**1071.0**	**20.0**	100.1
249	357	49602.4	110.1	9.3	0.6	4.7	1.3	0.3	1.1	0.9	1758.1	17.1	1760.4	10.7	1763.1	11.8	**1763.1**	**11.8**	99.7
25	128	26988.0	1.2	10.2	0.8	3.9	1.4	0.3	1.2	0.8	1615.0	16.6	1604.8	11.3	1591.5	14.7	**1591.5**	**14.7**	101.5
250	176	11066.4	1.4	16.8	1.3	0.7	1.7	0.1	1.2	0.7	536.6	6.2	547.2	7.4	591.6	27.5	**536.6**	**6.2**	90.7
251	451	413081.5	10.6	6.8	0.6	7.9	1.2	0.4	1.1	0.9	2130.7	19.2	2225.1	10.9	2313.2	9.9	**2313.2**	**9.9**	92.1
253	412	88947.0	2.2	10.3	0.9	3.7	1.4	0.3	1.1	0.8	1572.0	15.5	1569.8	11.6	1566.9	17.3	**1566.9**	**17.3**	100.3
254	472	20006.5	1.1	16.1	0.8	0.9	1.3	0.1	1.1	0.8	618.8	6.5	631.1	6.3	675.2	16.2	**618.8**	**6.5**	91.7
255	767	30107.5	2.4	17.0	0.7	0.8	1.2	0.1	1.0	0.8	577.7	5.3	574.8	5.1	563.7	14.2	**577.7**	**5.3**	102.5
256	37	13529.0	1.2	11.2	1.8	2.7	2.0	0.2	0.9	0.5	1301.5	10.6	1339.9	14.7	1401.7	33.9	**1401.7**	**33.9**	92.9
257	62	12943.5	2.4	10.2	1.0	3.2	1.5	0.2	1.1	0.7	1372.5	13.9	1461.7	11.6	1593.9	18.6	**1593.9**	**18.6**	86.1
258	63	4606.2	1.9	16.8	1.5	0.8	1.8	0.1	1.0	0.5	604.6	5.5	600.6	8.1	585.9	32.8	**604.6**	**5.5**	103.2
259	330	73652.6	2.8	16.5	0.6	0.7	1.0	0.1	0.8	0.8	549.7	4.4	564.3	4.5	623.8	13.9	**549.7**	**4.4**	88.1
26	1000	173537.0	5.1	9.9	0.7	4.2	1.2	0.3	0.9	0.8	1699.1	14.1	1673.0	9.7	1640.4	13.3	**1640.4**	**13.3**	103.6
260	502	175233.6	1.0	13.2	0.8	1.9	1.3	0.2	1.1	0.8	1072.1	10.8	1075.2	9.0	1081.3	15.9	**1081.3**	**15.9**	99.2
261	141	443850.1	1.4	5.4	0.6	13.0	1.4	0.5	1.3	0.9	2663.2	28.4	2677.8	13.5	2688.9	9.7	**2688.9**	**9.7**	99.0
262	340	637998.1	2.1	16.3	1.0	0.8	1.5	0.1	1.1	0.8	594.5	6.2	605.9	6.7	648.8	20.6	**594.5**	**6.2**	91.6

263	404	344570.3	241.3	13.6	0.8	1.8	1.4	0.2	1.2	0.8	1041.6	11.3	1038.5	9.2	1032.1	16.1	**1032.1**	**16.1**	100.9
264	243	61974.0	1.6	16.2	0.6	0.9	1.3	0.1	1.1	0.9	635.2	7.0	642.7	6.1	669.0	11.9	**635.2**	**7.0**	95.0
265	442	35738.4	3.3	12.4	0.7	2.4	1.4	0.2	1.2	0.9	1238.8	13.2	1231.9	9.8	1219.7	13.8	**1219.7**	**13.8**	101.6
266	401	86849.4	1.7	11.0	0.7	3.0	1.2	0.2	1.0	0.8	1402.9	12.2	1418.1	9.1	1441.1	13.0	**1441.1**	**13.0**	97.4
267	67	12075.3	2.8	16.5	1.1	0.8	1.7	0.1	1.3	0.8	569.9	6.9	580.8	7.3	623.9	23.0	**569.9**	**6.9**	91.3
268	352	272540.8	1.7	15.8	0.7	0.9	1.2	0.1	1.0	0.8	643.3	6.2	659.5	6.0	715.2	15.2	**643.3**	**6.2**	90.0
269	572	760364.4	2.1	12.8	0.6	2.1	1.3	0.2	1.2	0.9	1138.7	12.0	1140.4	9.0	1143.6	12.7	**1143.6**	**12.7**	99.6
27	76	32542.1	1.7	11.7	0.9	2.7	1.3	0.2	1.0	0.8	1308.8	11.8	1317.7	9.7	1332.3	16.6	**1332.3**	**16.6**	98.2
270	72	24641.9	1.2	9.0	0.8	4.8	1.3	0.3	1.0	0.8	1768.3	15.6	1789.2	10.6	1813.6	13.7	**1813.6**	**13.7**	97.5
271	23	2886.0	2.4	9.1	1.7	4.0	2.4	0.3	1.7	0.7	1512.2	23.5	1636.6	19.8	1800.4	31.1	**1800.4**	**31.1**	84.0
272	121	7322.5	2.0	16.5	1.0	0.9	1.4	0.1	1.0	0.7	626.5	5.7	624.9	6.3	619.2	20.7	**626.5**	**5.7**	101.2
273	363	29580.4	2.5	16.1	0.9	0.9	1.5	0.1	1.3	0.8	670.2	8.0	671.6	7.6	676.4	19.2	**670.2**	**8.0**	99.1
274	294	23402.2	0.9	18.3	1.1	0.4	1.9	0.1	1.5	0.8	365.2	5.2	370.0	5.8	400.3	25.6	**365.2**	**5.2**	91.2
275	201	36849.9	2.6	8.4	0.9	5.4	1.6	0.3	1.4	0.8	1853.1	22.0	1892.2	13.9	1935.4	15.5	**1935.4**	**15.5**	95.7
276	173	37333.4	2.4	11.5	0.7	2.7	1.4	0.2	1.2	0.9	1295.4	14.0	1316.8	10.0	1351.8	12.5	**1351.8**	**12.5**	95.8
277	161	30984.0	0.7	14.8	1.2	0.9	1.5	0.1	0.9	0.6	598.6	5.0	653.6	7.2	848.4	25.2	**598.6**	**5.0**	70.6
278	151	94719.4	1.6	8.7	0.8	5.3	1.2	0.3	0.9	0.7	1860.1	14.4	1872.7	10.4	1886.7	14.9	**1886.7**	**14.9**	98.6
279	294	4208132.1	1.7	5.3	0.6	12.9	1.2	0.5	1.0	0.8	2594.1	20.7	2672.8	11.0	2732.8	10.5	**2732.8**	**10.5**	94.9
28	111	6304.8	2.0	17.5	1.2	0.7	1.5	0.1	1.0	0.6	569.2	5.4	554.5	6.6	494.7	26.0	**569.2**	**5.4**	115.1
280	196	10617.5	1.8	15.1	0.7	1.2	1.3	0.1	1.1	0.8	773.6	7.7	782.4	7.0	807.7	15.5	**773.6**	**7.7**	95.8
281	249	160178.1	2.4	10.5	0.6	3.4	1.0	0.3	0.8	0.8	1485.1	10.6	1502.1	8.0	1526.1	11.8	**1526.1**	**11.8**	97.3
282	55	8757.2	1.4	11.8	1.0	2.6	1.3	0.2	0.9	0.7	1295.0	10.6	1299.3	9.7	1306.3	18.9	**1306.3**	**18.9**	99.1
283	78	8383.8	0.8	16.2	1.7	0.7	2.0	0.1	1.1	0.5	537.8	5.5	563.8	8.6	670.0	35.9	**537.8**	**5.5**	80.3
284	570	33884.6	1.3	17.9	0.7	0.5	1.3	0.1	1.1	0.8	438.7	4.5	440.7	4.6	451.0	15.5	**438.7**	**4.5**	97.3
286	33	5184.7	1.3	16.1	1.5	0.8	1.9	0.1	1.2	0.6	589.0	6.7	607.4	8.7	676.9	31.9	**589.0**	**6.7**	87.0
287	120	15190.4	1.9	16.1	0.9	0.9	1.8	0.1	1.5	0.9	618.2	8.9	631.7	8.3	680.2	19.6	**618.2**	**8.9**	90.9
288	200	56923.6	3.3	16.1	0.9	0.9	1.5	0.1	1.2	0.8	670.2	7.9	673.2	7.5	683.2	19.2	**670.2**	**7.9**	98.1
289	550	36846.1	32.9	16.7	0.8	0.8	1.2	0.1	0.9	0.7	611.6	5.4	609.4	5.6	601.0	17.7	**611.6**	**5.4**	101.8
290	87	2199707.0	1.2	8.4	0.7	5.3	1.4	0.3	1.2	0.9	1819.9	18.8	1873.0	11.7	1932.4	12.1	**1932.4**	**12.1**	94.2

291	133	12766.4	1.2	15.3	0.9	1.2	1.3	0.1	0.9	0.7	784.5	6.8	785.3	6.9	787.8	18.1	**784.5**	**6.8**	99.6
292	118	9653.8	1.3	16.5	1.0	0.6	1.4	0.1	1.0	0.7	417.4	3.9	451.1	5.0	626.5	21.4	**417.4**	**3.9**	66.6
293	98	9468.5	1.5	9.3	1.0	4.4	1.7	0.3	1.4	0.8	1686.0	20.7	1717.9	14.4	1757.0	18.9	**1757.0**	**18.9**	96.0
3	116	372134.9	1.6	17.1	0.9	0.7	1.4	0.1	1.0	0.7	553.0	5.3	550.6	5.8	540.8	20.5	**553.0**	**5.3**	102.3
31	114	14572.1	1.9	16.9	1.2	0.8	1.6	0.1	1.1	0.7	604.9	6.5	597.5	7.4	569.3	25.6	**604.9**	**6.5**	106.3
33	119	44678.2	3.5	16.5	1.2	0.8	1.9	0.1	1.5	0.8	604.7	8.7	609.0	8.7	625.0	24.8	**604.7**	**8.7**	96.7
34	165	40139.2	2.6	10.3	0.7	3.6	1.4	0.3	1.3	0.9	1533.2	17.6	1548.3	11.5	1568.9	12.2	**1568.9**	**12.2**	97.7
36	1297	55435.3	3.9	18.4	0.8	0.5	1.5	0.1	1.2	0.8	420.5	5.0	415.6	5.0	388.6	18.3	**420.5**	**5.0**	108.2
38	372	15648.3	0.9	16.2	0.9	0.8	1.3	0.1	0.9	0.7	590.8	5.4	604.8	5.9	657.4	18.7	**590.8**	**5.4**	89.9
39	420	135333.7	1.3	10.1	0.6	3.9	1.3	0.3	1.1	0.9	1616.7	16.0	1612.1	10.2	1606.1	10.7	**1606.1**	**10.7**	100.7
40	98	38467.5	2.1	4.5	0.5	18.1	1.1	0.6	0.9	0.9	2997.8	22.6	2997.1	10.3	2996.6	8.1	**2996.6**	**8.1**	100.0
41	103	4701.7	1.6	16.8	1.2	0.8	1.5	0.1	0.9	0.6	616.5	5.4	608.8	7.0	580.3	26.3	**616.5**	**5.4**	106.2
42	23	13640.0	1.2	10.7	1.6	3.4	1.9	0.3	1.1	0.6	1501.1	14.3	1501.9	15.1	1503.1	30.3	**1503.1**	**30.3**	99.9
43	139	175357.0	2.9	12.6	0.7	2.2	1.2	0.2	1.0	0.8	1168.3	10.4	1174.1	8.5	1184.9	14.7	**1184.9**	**14.7**	98.6
44	79	10072.3	0.8	17.1	1.0	0.7	1.6	0.1	1.2	0.8	557.9	6.5	556.1	6.7	548.5	21.3	**557.9**	**6.5**	101.7
45	135	12148.3	1.5	16.9	1.1	0.8	1.6	0.1	1.2	0.7	598.0	6.7	593.6	7.3	577.2	24.2	**598.0**	**6.7**	103.6
46	44	3450.0	1.3	17.5	1.2	0.8	1.5	0.1	0.9	0.6	608.8	5.2	584.7	6.6	491.9	26.1	**608.8**	**5.2**	123.8
48	41	5405.1	2.7	14.1	1.5	1.6	1.9	0.2	1.2	0.6	974.6	11.0	968.2	12.0	953.6	30.5	**953.6**	**30.5**	102.2
49	164	13650.8	1.0	17.6	1.2	0.5	1.5	0.1	0.9	0.6	423.4	3.8	433.8	5.4	489.2	26.7	**423.4**	**3.8**	86.5
5	323	91982.5	0.8	13.7	0.7	1.6	1.0	0.2	0.8	0.7	953.3	6.8	969.7	6.5	1007.1	14.2	**1007.1**	**14.2**	94.7
50	203	526761.1	2.9	7.8	0.9	6.7	1.5	0.4	1.2	0.8	2073.5	21.1	2071.7	13.2	2069.8	15.8	**2069.8**	**15.8**	100.2
51	82	93214.4	1.0	15.9	1.1	0.9	1.5	0.1	1.0	0.7	653.9	6.3	665.9	7.1	707.0	22.4	**653.9**	**6.3**	92.5
52	104	76107.9	3.3	13.5	0.7	1.8	1.3	0.2	1.1	0.8	1021.4	10.0	1027.7	8.2	1041.0	14.3	**1041.0**	**14.3**	98.1
53	276	42816.1	1.9	16.1	1.0	0.9	1.6	0.1	1.3	0.8	651.3	8.1	656.0	7.9	672.1	20.9	**651.3**	**8.1**	96.9
54	145	6474.8	1.3	18.7	1.4	0.5	1.6	0.1	0.9	0.5	415.1	3.5	404.9	5.4	347.3	30.9	**415.1**	**3.5**	119.5
55	145	73818.8	2.8	5.6	0.9	11.2	1.5	0.5	1.3	0.8	2428.2	25.4	2536.6	14.1	2624.5	14.2	**2624.5**	**14.2**	92.5
56	221	18172.9	4.5	10.7	0.8	3.2	1.5	0.2	1.2	0.8	1416.4	15.7	1450.8	11.3	1501.6	14.7	**1501.6**	**14.7**	94.3
57	22	3544.1	1.0	13.8	1.8	1.7	2.1	0.2	1.1	0.5	1004.0	10.4	999.9	13.3	990.9	36.0	**990.9**	**36.0**	101.3
58	146	25970.9	2.8	9.9	0.8	4.0	1.2	0.3	0.9	0.8	1626.9	13.0	1633.5	9.8	1641.9	14.6	**1641.9**	**14.6**	99.1

59	1045	64054.1	1.1	16.6	0.8	0.9	1.4	0.1	1.1	0.8	642.1	6.7	635.0	6.5	610.0	17.4	**642.1**	**6.7**	105.3
6	126	29049.8	1.7	10.9	0.7	3.2	1.2	0.3	1.1	0.8	1459.1	13.7	1461.5	9.6	1465.0	12.6	**1465.0**	**12.6**	99.6
60	91	25546.5	1.3	10.6	0.8	3.5	1.2	0.3	0.9	0.7	1531.9	11.8	1526.8	9.4	1519.7	15.6	**1519.7**	**15.6**	100.8
61	59	14238.1	1.6	5.6	0.7	13.2	1.2	0.5	0.9	0.8	2771.8	21.3	2697.3	11.3	2641.9	12.3	**2641.9**	**12.3**	104.9
62	133	10569.3	1.0	17.5	1.3	0.7	1.9	0.1	1.4	0.7	552.0	7.2	541.9	7.8	499.7	28.2	**552.0**	**7.2**	110.5
63	315	5470665.2	5.1	9.0	0.7	5.0	1.3	0.3	1.1	0.8	1820.3	17.8	1814.2	11.3	1807.2	13.2	**1807.2**	**13.2**	100.7
64	156	34274.8	5.1	9.2	0.8	4.8	1.4	0.3	1.2	0.8	1777.9	18.1	1777.8	12.1	1777.8	15.3	**1777.8**	**15.3**	100.0
65	364	55384.5	2.0	13.5	0.7	1.7	1.2	0.2	1.0	0.8	1005.9	9.5	1017.3	8.0	1042.0	14.2	**1042.0**	**14.2**	96.5
66	23	4486.9	3.0	12.9	1.8	2.0	2.1	0.2	1.0	0.5	1106.5	10.0	1116.8	14.0	1137.0	36.1	**1137.0**	**36.1**	97.3
68	131	19665.1	1.8	9.3	0.6	4.6	1.3	0.3	1.1	0.9	1746.6	17.6	1751.3	10.7	1756.8	10.5	**1756.8**	**10.5**	99.4
69	381	60454.1	1.5	9.2	0.7	4.5	1.2	0.3	0.9	0.8	1694.6	14.0	1730.8	9.6	1774.9	12.5	**1774.9**	**12.5**	95.5
7	122	10075.3	2.7	16.7	1.4	0.8	1.9	0.1	1.3	0.7	619.4	7.5	615.7	8.8	602.1	31.0	**619.4**	**7.5**	102.9
70	41	32005.0	1.5	8.5	1.1	5.9	1.8	0.4	1.5	0.8	2006.9	25.5	1962.4	15.8	1915.8	18.9	**1915.8**	**18.9**	104.8
71	87	125792.3	2.6	10.5	0.6	3.6	1.2	0.3	1.1	0.9	1553.6	14.8	1541.2	9.7	1524.3	11.4	**1524.3**	**11.4**	101.9
72	179	2525.7	1.4	13.0	5.0	0.9	5.1	0.1	0.9	0.2	548.9	4.7	673.2	25.1	1114.6	100.3	**548.9**	**4.7**	49.3
73	456	56628.2	2.0	13.2	0.6	1.9	1.1	0.2	0.9	0.8	1084.4	8.5	1083.2	7.0	1080.8	12.2	**1080.8**	**12.2**	100.3
75	127	28719.1	1.9	11.6	0.8	2.9	1.3	0.2	1.0	0.8	1398.6	12.7	1376.2	9.5	1341.7	14.6	**1341.7**	**14.6**	104.2
76	454	34342.5	0.8	18.0	1.1	0.4	1.6	0.1	1.1	0.7	320.3	3.5	333.8	4.4	428.4	24.2	**320.3**	**3.5**	74.8
77	108	36218.4	1.1	7.7	0.7	6.9	1.3	0.4	1.1	0.9	2091.8	20.5	2094.4	11.8	2096.9	11.8	**2096.9**	**11.8**	99.8
78	39	4346.7	2.8	13.5	1.0	1.8	1.3	0.2	0.9	0.7	1036.2	8.6	1038.4	8.7	1043.1	20.2	**1043.1**	**20.2**	99.3
79	109	6045.9	1.6	16.0	0.9	0.9	1.2	0.1	0.8	0.6	636.0	4.8	646.8	5.9	684.8	20.2	**636.0**	**4.8**	92.9
8	251	197856.8	4.1	10.0	0.7	3.8	1.1	0.3	0.9	0.8	1567.1	12.1	1588.0	8.8	1615.8	12.4	**1615.8**	**12.4**	97.0
80	1104	146003.7	2.5	16.6	0.7	0.9	1.4	0.1	1.2	0.9	639.1	7.6	633.7	6.7	614.6	15.4	**639.1**	**7.6**	104.0
82	260	39798.9	1.6	17.8	1.0	0.6	1.5	0.1	1.0	0.7	452.1	4.6	452.8	5.4	456.3	23.2	**452.1**	**4.6**	99.1
83	241	8877.2	1.3	15.2	1.2	1.1	1.6	0.1	1.1	0.7	745.4	7.5	759.2	8.4	800.1	24.1	**745.4**	**7.5**	93.2
84	26	30433.7	3.1	11.8	1.2	2.6	1.6	0.2	1.0	0.7	1296.4	12.2	1299.6	11.5	1305.0	23.0	**1305.0**	**23.0**	99.3
85	155	12289.9	1.9	16.3	0.9	0.9	1.1	0.1	0.7	0.7	644.0	4.5	646.7	5.4	656.1	18.3	**644.0**	**4.5**	98.1
86	184	44203.6	2.2	5.3	0.8	13.5	1.3	0.5	1.0	0.8	2710.4	22.9	2718.0	12.6	2723.7	13.9	**2723.7**	**13.9**	99.5
87	127	29181.7	1.8	17.1	1.1	0.7	1.5	0.1	1.0	0.7	536.6	5.1	539.8	6.2	553.2	23.9	**536.6**	**5.1**	97.0

88	48	8435.4	1.5	11.0	0.9	3.3	1.5	0.3	1.2	0.8	1513.8	15.5	1485.0	11.4	1444.1	17.1	**1444.1**	**17.1**	104.8
89	492	110192.2	2.7	15.1	0.8	1.2	1.3	0.1	1.0	0.8	825.6	8.0	820.9	7.3	808.1	16.4	**825.6**	**8.0**	102.2
9	170	24225.0	31.1	16.5	1.1	0.8	1.6	0.1	1.2	0.8	570.2	6.7	581.7	7.2	626.5	23.0	**570.2**	**6.7**	91.0
90	123	39406.7	3.6	12.1	0.8	2.3	1.3	0.2	1.0	0.8	1196.9	11.1	1217.9	9.1	1255.3	15.4	**1255.3**	**15.4**	95.3
91	95	46350.3	2.5	12.9	0.7	2.1	1.2	0.2	1.0	0.8	1149.8	10.5	1142.4	8.2	1128.3	13.4	**1128.3**	**13.4**	101.9
92	892	33434.3	1.3	16.0	0.7	0.8	1.5	0.1	1.3	0.9	562.0	7.2	588.5	6.7	691.9	14.4	**562.0**	**7.2**	81.2
93	147	58613.8	4.6	5.5	0.7	12.9	1.2	0.5	0.9	0.8	2695.1	20.9	2675.4	11.0	2660.6	11.4	**2660.6**	**11.4**	101.3
94	160	155772.9	12.8	8.5	0.8	5.6	1.2	0.3	0.9	0.8	1912.8	15.5	1914.0	10.4	1915.3	13.8	**1915.3**	**13.8**	99.9
95	291	45818.5	1.3	16.7	0.6	0.8	1.2	0.1	1.0	0.9	612.2	6.1	608.3	5.6	593.7	13.5	**612.2**	**6.1**	103.1
96	478	16353.9	2.8	16.7	1.0	0.9	1.7	0.1	1.4	0.8	634.7	8.2	628.1	8.0	604.5	22.6	**634.7**	**8.2**	105.0
97	70	39250.2	2.6	9.9	0.8	4.0	1.4	0.3	1.2	0.8	1645.1	16.8	1640.6	11.4	1634.8	14.5	**1634.8**	**14.5**	100.6
98	141	23068.6	3.3	13.7	0.8	1.7	1.3	0.2	1.0	0.8	1000.1	9.5	1002.8	8.2	1008.8	15.7	**1008.8**	**15.7**	99.1
99	543	117345.4	0.9	16.4	1.1	0.8	1.7	0.1	1.3	0.8	584.1	7.3	594.9	7.6	636.4	23.1	**584.1**	**7.3**	91.8
xx	116	28383.9	8.4	17.2	0.9	0.7	1.4	0.1	1.1	0.8	562.0	5.8	557.0	6.2	536.9	20.8	**562.0**	**5.8**	104.7
xx	233	23676.2	6.8	16.8	0.7	0.7	1.3	0.1	1.1	0.9	548.9	5.8	554.9	5.5	579.9	14.6	**548.9**	**5.8**	94.6
xx	64	2199.0	3.8	18.9	1.8	0.7	2.3	0.1	1.4	0.6	562.4	7.5	518.6	9.1	329.8	40.2	**562.4**	**7.5**	170.5
xx	598	31297.4	6.3	17.3	0.8	0.7	1.4	0.1	1.1	0.8	558.1	6.1	550.6	5.9	519.8	17.9	**558.1**	**6.1**	107.4
xx	435	227235.8	4.4	16.8	0.9	0.8	1.6	0.1	1.3	0.8	570.8	7.3	572.8	7.0	580.5	19.6	**570.8**	**7.3**	98.3
70	180	179695.6	1.8	9.6	0.9	4.2	1.5	0.3	1.2	0.8	1656.0	17.5	1678.7	12.5	1707.2	17.4	**1707.2**	**17.4**	97.0
71	169	188392.4	2.1	14.9	1.0	1.2	2.0	0.1	1.8	0.9	767.1	12.7	785.0	11.0	836.2	20.2	**767.1**	**12.7**	91.7
72	205	443424.5	1.8	4.4	0.9	18.3	1.5	0.6	1.1	0.8	2985.2	26.6	3007.7	14.1	3022.8	15.2	**3022.8**	**15.2**	98.8
73	145	234722.1	2.7	14.2	0.7	1.5	1.4	0.2	1.2	0.9	921.2	10.6	927.8	8.7	943.5	14.6	**943.5**	**14.6**	97.6
74	161	192101.4	1.2	16.6	1.1	0.9	1.6	0.1	1.2	0.8	632.2	7.3	629.1	7.6	617.6	22.8	**632.2**	**7.3**	102.4
76	106	59661.0	3.4	13.6	1.1	1.8	1.5	0.2	1.0	0.7	1035.9	9.8	1031.0	9.8	1020.7	22.6	**1020.7**	**22.6**	101.5
77	281	313583.3	2.7	11.7	0.9	2.6	1.5	0.2	1.1	0.8	1289.5	13.0	1303.9	10.7	1327.7	18.2	**1327.7**	**18.2**	97.1
78	207	74951.9	11.7	16.6	0.9	0.8	1.6	0.1	1.3	0.8	616.6	7.5	615.7	7.3	612.4	20.1	**616.6**	**7.5**	100.7
79	459	627990.2	2.4	18.1	1.2	0.5	1.7	0.1	1.3	0.7	394.4	4.9	397.7	5.7	416.5	25.9	**394.4**	**4.9**	94.7
8	89	225571.2	3.4	13.6	0.9	1.8	1.5	0.2	1.2	0.8	1042.4	11.6	1039.1	9.7	1032.1	18.0	**1032.1**	**18.0**	101.0

80	119	168969.0	0.9	17.0	1.0	0.8	1.6	0.1	1.2	0.7	574.1	6.4	572.0	6.8	563.6	22.7	**574.1**	**6.4**	101.9
82	725	286144.8	3.6	12.2	0.8	2.4	1.5	0.2	1.3	0.9	1239.6	14.6	1242.8	10.9	1248.4	15.5	**1248.4**	**15.5**	99.3
83	196	168642.4	0.9	17.1	1.2	0.7	2.0	0.1	1.6	0.8	554.5	8.3	553.8	8.3	551.0	25.8	**554.5**	**8.3**	100.6
84	266	355816.1	1.2	13.5	1.0	1.8	1.6	0.2	1.2	0.8	1075.9	11.8	1063.3	10.4	1037.4	20.9	**1037.4**	**20.9**	103.7
85	259	350853.6	14.0	12.2	0.9	2.4	1.5	0.2	1.2	0.8	1244.5	13.7	1243.8	10.7	1242.7	17.1	**1242.7**	**17.1**	100.1
86	38	39053.4	0.9	7.4	1.1	7.2	1.5	0.4	1.1	0.7	2129.4	19.4	2142.2	13.6	2154.5	19.0	**2154.5**	**19.0**	98.8
87	475	385096.6	14.3	13.1	1.4	1.8	2.4	0.2	1.9	0.8	1034.3	18.5	1055.0	15.7	1098.2	27.9	**1098.2**	**27.9**	94.2
88	257	774624.6	2.4	16.2	0.9	0.9	1.7	0.1	1.5	0.9	623.9	8.8	632.4	8.1	663.0	18.8	**623.9**	**8.8**	94.1
89	372	3832797.4	1.3	8.1	1.0	6.3	1.6	0.4	1.3	0.8	2028.1	22.0	2018.9	13.9	2009.4	17.0	**2009.4**	**17.0**	100.9
9	687	178472.2	2.2	18.8	1.2	0.4	1.9	0.0	1.5	0.8	311.7	4.6	314.5	5.2	335.4	26.8	**311.7**	**4.6**	92.9
90	29	30339.1	1.8	10.0	1.2	4.0	1.9	0.3	1.4	0.8	1653.6	21.1	1643.0	15.3	1629.5	22.4	**1629.5**	**22.4**	101.5
91	69	18113.6	1.3	16.8	1.1	0.8	1.8	0.1	1.4	0.8	608.2	8.3	602.6	8.2	581.3	24.0	**608.2**	**8.3**	104.6
92	184	194808.2	2.5	16.2	1.3	0.9	1.7	0.1	1.1	0.7	660.3	7.1	662.2	8.3	668.4	27.4	**660.3**	**7.1**	98.8
93	258	2061156.2	0.8	15.3	0.8	1.2	1.5	0.1	1.3	0.8	787.9	9.7	787.8	8.4	787.2	17.1	**787.9**	**9.7**	100.1
94	37	158153.6	2.5	13.1	1.3	1.8	1.8	0.2	1.3	0.7	1040.5	12.4	1062.1	11.9	1106.8	25.1	**1106.8**	**25.1**	94.0
95	61	82121.0	2.0	16.3	1.4	0.9	1.8	0.1	1.2	0.6	633.2	7.1	636.6	8.7	648.9	30.2	**633.2**	**7.1**	97.6
96	86	82051.0	2.5	8.1	0.9	6.0	1.4	0.4	1.0	0.7	1952.0	17.1	1977.6	11.9	2004.4	16.3	**2004.4**	**16.3**	97.4
97	159	81099.5	2.3	16.0	1.0	1.0	1.6	0.1	1.2	0.8	692.2	7.9	690.6	7.8	685.5	21.2	**692.2**	**7.9**	101.0
98	46	75653.5	3.0	12.3	1.4	2.3	2.1	0.2	1.5	0.7	1184.2	16.3	1201.5	14.5	1232.7	27.4	**1232.7**	**27.4**	96.1
99	357	176914.5	5.7	16.1	1.1	0.9	1.8	0.1	1.4	0.8	615.4	8.3	629.8	8.3	682.1	22.7	**615.4**	**8.3**	90.2
xx	611	333892.7	6.0	17.1	1.0	0.7	2.2	0.1	2.0	0.9	536.6	10.3	539.3	9.4	551.1	22.2	**536.6**	**10.3**	97.4
xx	515	262649.8	2.0	13.1	1.1	1.8	2.3	0.2	2.0	0.9	1004.1	18.2	1036.3	14.7	1104.8	22.8	**1104.8**	**22.8**	90.9
xx	227	140936.4	7.1	16.9	1.0	0.7	1.5	0.1	1.1	0.7	536.5	5.8	543.6	6.4	573.3	22.5	**536.5**	**5.8**	93.6

Sample: SF-A						Isotope Ratios					Apparent Ages (Ma)								
Analysis	**U (ppm)**	**206Pb /204Pb**	**U /Th**	**206Pb /207Pb**	**± (%)**	**207Pb/ 235U**	**± (%)**	**206Pb /238U**	**± (%)**	**err. corr.**	**206Pb /238U**	**± (Ma)**	**207Pb /235U**	**± (Ma)**	**206Pb /207Pb**	**± (Ma)**	**Best Age**	**± (Ma)**	**Conc. (%)**
1	172	500841.2	2.7	11.2	0.8	2.9	1.6	0.2	1.3	0.8	1384.5	16.4	1394.7	11.8	1410.3	15.8	**1410.3**	**15.8**	98.2
10	120	1960914.0	1.6	8.8	0.9	5.1	1.7	0.3	1.5	0.9	1820.3	23.2	1837.5	14.6	1857.0	16.1	**1857.0**	**16.1**	98.0
100	102	164134.6	1.3	5.3	0.7	13.5	1.2	0.5	1.0	0.8	2711.9	22.5	2718.4	11.5	2723.3	11.1	**2723.3**	**11.1**	99.6
102	65	58306.7	2.6	12.5	1.4	2.4	2.1	0.2	1.6	0.8	1250.1	17.9	1230.0	14.8	1194.9	26.7	**1194.9**	**26.7**	104.6
103	320	47887.8	4.3	18.1	1.0	0.5	1.9	0.1	1.6	0.8	429.5	6.8	429.2	6.7	427.5	23.0	**429.5**	**6.8**	100.5
104	78	76423.8	3.7	11.7	0.8	2.7	1.4	0.2	1.2	0.8	1344.7	14.5	1339.3	10.8	1330.7	15.7	**1330.7**	**15.7**	101.1
105	209	180765.4	2.8	11.4	0.9	2.8	1.5	0.2	1.2	0.8	1350.3	15.1	1360.7	11.6	1377.0	17.9	**1377.0**	**17.9**	98.1
106	57	35251.2	2.5	12.7	1.3	2.1	1.8	0.2	1.3	0.7	1153.2	13.6	1159.9	12.8	1172.4	26.1	**1172.4**	**26.1**	98.4
107	57	24768.7	2.7	13.9	1.4	1.6	2.0	0.2	1.4	0.7	988.7	13.1	987.4	12.8	984.5	29.3	**984.5**	**29.3**	100.4
108	348	1264243.6	1.5	5.6	0.9	10.5	1.7	0.4	1.4	0.9	2291.5	27.6	2479.5	15.6	2637.5	14.7	**2637.5**	**14.7**	86.9
109	429	726296.5	2.2	12.8	0.8	2.1	1.5	0.2	1.3	0.8	1145.5	13.4	1144.2	10.4	1141.8	16.1	**1141.8**	**16.1**	100.3
11	250	354563.8	3.9	12.5	1.1	2.2	1.9	0.2	1.6	0.8	1168.5	16.9	1180.5	13.3	1202.5	20.8	**1202.5**	**20.8**	97.2
110	212	419838.9	1.9	10.9	0.9	3.3	1.6	0.3	1.3	0.8	1479.9	16.8	1475.6	12.2	1469.3	17.7	**1469.3**	**17.7**	100.7
111	245	196093.7	4.2	12.7	0.9	2.1	1.8	0.2	1.6	0.9	1158.1	16.5	1161.7	12.6	1168.5	18.5	**1168.5**	**18.5**	99.1
112	122	20454.3	2.1	18.1	1.4	0.6	1.9	0.1	1.3	0.7	467.6	5.8	459.2	7.0	417.2	30.8	**467.6**	**5.8**	112.1
113	266	168320.3	1.0	17.8	1.1	0.5	1.7	0.1	1.2	0.7	397.8	4.6	407.5	5.6	462.9	25.5	**397.8**	**4.6**	85.9
114	223	84279.9	7.7	13.3	0.9	1.8	1.8	0.2	1.5	0.9	1048.0	14.5	1055.4	11.5	1070.9	18.3	**1070.9**	**18.3**	97.9
115	127	474811.9	1.6	13.8	1.2	1.6	1.9	0.2	1.4	0.8	975.6	12.8	983.7	11.9	1001.9	25.3	**1001.9**	**25.3**	97.4
116	601	672808.8	6.5	13.1	0.8	1.9	1.8	0.2	1.7	0.9	1079.7	16.5	1090.0	12.2	1110.6	15.1	**1110.6**	**15.1**	97.2
117	87	12952.8	2.6	15.5	1.5	1.0	2.3	0.1	1.6	0.7	710.6	11.0	723.0	11.7	761.5	32.6	**710.6**	**11.0**	93.3
118	10	18848.1	2.4	10.3	1.8	3.7	2.8	0.3	2.2	0.8	1554.3	29.9	1561.6	22.2	1571.4	32.8	**1571.4**	**32.8**	98.9
119	60	22957.4	3.1	13.5	1.1	1.7	1.8	0.2	1.4	0.8	1010.1	13.1	1018.1	11.6	1035.4	23.2	**1035.4**	**23.2**	97.6
12	87	40214.1	4.5	12.3	1.1	2.3	1.9	0.2	1.6	0.8	1177.2	16.7	1198.0	13.5	1235.7	21.8	**1235.7**	**21.8**	95.3
120	131	180102.3	2.9	4.6	0.7	17.4	1.5	0.6	1.4	0.9	2945.8	32.1	2954.8	14.8	2961.0	11.8	**2961.0**	**11.8**	99.5
121	56	97531.2	2.3	12.4	1.2	2.4	1.8	0.2	1.4	0.8	1256.6	15.8	1242.2	13.0	1217.4	23.4	**1217.4**	**23.4**	103.2
122	423	398025.1	1.8	13.7	0.9	1.7	1.6	0.2	1.3	0.8	997.8	12.2	1003.0	10.2	1014.4	18.5	**1014.4**	**18.5**	98.4

123	73	117828.1	0.9	9.9	1.1	4.1	1.7	0.3	1.3	0.8	1655.3	19.4	1646.8	14.1	1636.0	20.7	**1636.0**	**20.7**	101.2
124	67	171874.9	2.9	5.0	0.9	14.9	1.6	0.5	1.4	0.9	2785.4	31.3	2811.6	15.5	2830.4	13.9	**2830.4**	**13.9**	98.4
125	179	261330.3	2.5	13.3	0.8	1.8	1.5	0.2	1.3	0.8	1051.7	12.5	1058.7	10.1	1073.2	16.6	**1073.2**	**16.6**	98.0
126	46	18437.6	0.8	11.6	1.0	2.6	2.2	0.2	1.9	0.9	1271.4	21.9	1297.7	15.8	1341.3	20.0	**1341.3**	**20.0**	94.8
127	188	77829.3	1.7	13.4	1.0	1.7	1.6	0.2	1.3	0.8	1009.1	11.8	1024.6	10.3	1058.0	19.9	**1058.0**	**19.9**	95.4
128	263	171304.2	3.1	13.4	0.9	1.8	1.4	0.2	1.1	0.8	1041.1	10.9	1047.1	9.3	1059.4	17.2	**1059.4**	**17.2**	98.3
129	63	156184.1	3.3	13.8	1.3	1.7	1.9	0.2	1.3	0.7	1007.5	12.4	1002.7	11.9	992.2	26.7	**992.2**	**26.7**	101.5
13	169	930780.6	2.4	13.5	1.1	1.8	1.5	0.2	1.1	0.7	1055.5	10.6	1050.7	10.1	1040.8	21.9	**1040.8**	**21.9**	101.4
130	177	87004.8	1.9	10.0	0.9	4.1	1.5	0.3	1.2	0.8	1663.3	17.4	1645.6	12.1	1623.1	16.8	**1623.1**	**16.8**	102.5
131	42	20618.6	1.4	11.7	1.3	2.7	1.9	0.2	1.4	0.7	1354.2	16.8	1341.7	14.1	1321.7	25.2	**1321.7**	**25.2**	102.5
132	64	1435380.2	2.3	13.7	1.0	1.8	1.6	0.2	1.3	0.8	1034.7	12.3	1028.9	10.4	1016.4	19.6	**1016.4**	**19.6**	101.8
133	100	78074.5	1.2	13.5	1.0	1.8	1.4	0.2	1.0	0.7	1046.1	9.7	1045.2	9.3	1043.2	20.4	**1043.2**	**20.4**	100.3
134	468	69842.2	3.8	17.3	0.9	0.6	1.6	0.1	1.3	0.8	502.0	6.4	506.1	6.3	524.4	18.8	**502.0**	**6.4**	95.7
135	85	392755.1	1.2	11.5	1.0	2.8	1.5	0.2	1.1	0.7	1341.3	13.4	1350.3	11.2	1364.4	19.5	**1364.4**	**19.5**	98.3
136	96	79917.0	1.4	13.8	1.0	1.7	1.9	0.2	1.6	0.8	1017.5	15.1	1011.3	12.1	997.9	20.5	**997.9**	**20.5**	102.0
137	90	147401.7	0.7	5.4	1.1	12.5	2.9	0.5	2.7	0.9	2550.6	56.2	2639.4	27.3	2708.3	18.9	**2708.3**	**18.9**	94.2
138	72	25405.4	2.1	18.0	1.8	0.6	2.6	0.1	1.8	0.7	459.7	8.1	456.0	9.4	437.8	39.8	**459.7**	**8.1**	105.0
139	235	107807.2	2.9	13.3	1.0	1.9	1.5	0.2	1.1	0.7	1069.8	11.2	1068.5	10.1	1065.7	20.7	**1065.7**	**20.7**	100.4
14	128	122382.4	1.4	9.9	1.0	4.0	1.5	0.3	1.2	0.8	1618.8	16.9	1628.9	12.4	1642.0	18.2	**1642.0**	**18.2**	98.6
140	155	226513.2	1.3	13.9	0.9	1.6	1.4	0.2	1.0	0.7	989.2	9.5	987.5	8.9	983.9	19.3	**983.9**	**19.3**	100.5
141	156	68967.9	2.6	12.9	0.9	2.1	1.7	0.2	1.4	0.8	1164.7	15.2	1156.4	11.6	1140.8	17.8	**1140.8**	**17.8**	102.1
142	39	27442.8	3.0	12.9	1.2	2.0	1.9	0.2	1.5	0.8	1107.7	14.8	1116.1	12.7	1132.5	23.6	**1132.5**	**23.6**	97.8
143	384	990039.1	9.1	9.8	0.7	4.0	1.4	0.3	1.2	0.8	1608.2	16.8	1629.0	11.3	1656.0	13.8	**1656.0**	**13.8**	97.1
144	273	850813.3	3.4	13.5	0.8	1.7	1.4	0.2	1.1	0.8	1002.7	10.0	1014.8	8.7	1041.2	16.7	**1041.2**	**16.7**	96.3
145	1845	1299797.7	1.5	13.1	1.0	2.0	2.0	0.2	1.7	0.9	1104.2	17.0	1101.3	13.2	1095.6	20.3	**1095.6**	**20.3**	100.8
146	115	71730.5	1.3	12.8	1.1	2.1	1.8	0.2	1.5	0.8	1143.5	15.2	1147.9	12.6	1156.3	21.9	**1156.3**	**21.9**	98.9
147	280	204102.3	2.1	13.4	0.9	1.8	1.5	0.2	1.1	0.8	1043.5	11.0	1048.4	9.5	1058.8	18.1	**1058.8**	**18.1**	98.6
148	113	2377386.5	2.6	8.1	0.9	6.2	1.5	0.4	1.2	0.8	2009.3	20.9	2009.2	13.3	2009.1	16.4	**2009.1**	**16.4**	100.0
149	647	283522.3	2.4	16.9	1.0	0.8	1.9	0.1	1.6	0.9	620.8	9.6	611.8	8.7	578.7	21.0	**620.8**	**9.6**	107.3
150	283	154238.6	1.6	13.8	1.0	1.6	2.2	0.2	1.9	0.9	974.4	17.4	981.0	13.6	995.6	19.8	**995.6**	**19.8**	97.9

151	21	14392.0	1.7	13.7	1.7	1.7	2.5	0.2	1.8	0.7	985.2	16.6	993.1	16.0	1010.6	35.5	**1010.6**	**35.5**	97.5
152	50	13601.0	1.2	12.8	1.5	1.8	2.0	0.2	1.2	0.6	977.3	11.1	1030.0	12.7	1143.7	30.5	**1143.7**	**30.5**	85.5
153	172	549491.2	2.2	12.6	0.8	2.2	1.5	0.2	1.3	0.9	1197.7	13.9	1190.0	10.4	1175.9	14.9	**1175.9**	**14.9**	101.9
154	195	127819.6	2.2	10.7	0.8	3.3	1.5	0.3	1.3	0.8	1458.2	16.3	1472.0	11.7	1492.1	15.8	**1492.1**	**15.8**	97.7
155	280	164013.2	3.9	12.9	0.9	2.0	1.7	0.2	1.5	0.9	1116.5	15.3	1124.9	11.8	1141.1	17.8	**1141.1**	**17.8**	97.8
156	48	440370.6	0.7	13.8	1.2	1.7	2.3	0.2	1.9	0.8	1010.3	17.9	1008.3	14.6	1003.9	25.1	**1003.9**	**25.1**	100.6
157	250	253452.8	1.8	12.5	0.8	2.2	1.5	0.2	1.2	0.8	1163.4	12.9	1175.3	10.2	1197.1	16.4	**1197.1**	**16.4**	97.2
159	87	177197.5	1.8	16.7	1.7	0.8	2.4	0.1	1.8	0.7	585.2	9.9	586.9	10.9	593.4	36.7	**585.2**	**9.9**	98.6
16	153	49799.4	2.4	18.2	1.5	0.5	2.0	0.1	1.3	0.7	430.6	5.6	426.4	7.1	403.9	34.5	**430.6**	**5.6**	106.6
160	143	19384.2	1.7	16.6	1.2	0.8	1.9	0.1	1.5	0.8	625.6	8.8	621.5	8.9	606.4	26.3	**625.6**	**8.8**	103.2
161	249	79690.2	2.7	13.8	0.9	1.7	1.4	0.2	1.0	0.7	1000.3	9.7	1001.6	8.9	1004.3	19.0	**1004.3**	**19.0**	99.6
162	118	27303.3	2.5	13.4	1.0	1.7	1.8	0.2	1.4	0.8	1009.3	13.5	1025.9	11.3	1061.5	20.1	**1061.5**	**20.1**	95.1
163	252	143956.0	2.3	12.5	0.9	2.3	1.9	0.2	1.7	0.9	1221.8	18.6	1212.4	13.3	1195.8	17.1	**1195.8**	**17.1**	102.2
164	117	57368.3	1.0	9.2	1.8	3.9	2.3	0.3	1.5	0.6	1511.3	20.2	1621.6	18.7	1767.8	32.1	**1767.8**	**32.1**	85.5
165	93	34754.4	1.5	15.4	1.3	0.8	2.0	0.1	1.5	0.8	521.3	7.6	571.1	8.6	774.3	26.6	**521.3**	**7.6**	67.3
166	200	24034.0	2.6	16.7	1.3	0.8	1.8	0.1	1.3	0.7	561.0	6.9	569.4	7.8	603.1	27.2	**561.0**	**6.9**	93.0
167	98	196821.0	1.5	9.7	0.9	4.0	2.0	0.3	1.7	0.9	1590.4	24.5	1625.8	15.9	1671.9	16.6	**1671.9**	**16.6**	95.1
168	268	323796.9	1.5	18.2	1.0	0.5	2.0	0.1	1.8	0.9	381.5	6.5	384.7	6.5	404.1	22.2	**381.5**	**6.5**	94.4
169	86	87726.8	1.5	4.8	0.9	16.4	1.6	0.6	1.4	0.8	2901.2	32.2	2899.6	15.7	2898.6	14.3	**2898.6**	**14.3**	100.1
17	89	75622.2	3.8	13.7	1.1	1.7	1.8	0.2	1.5	0.8	1011.6	13.8	1013.6	11.6	1017.8	21.4	**1017.8**	**21.4**	99.4
170	86	96223.9	3.4	12.6	1.0	2.1	1.8	0.2	1.5	0.8	1156.5	15.6	1162.2	12.3	1172.9	19.8	**1172.9**	**19.8**	98.6
171	215	111774.7	2.8	10.8	0.9	3.3	1.6	0.3	1.3	0.8	1495.0	17.9	1489.2	12.8	1481.0	17.6	**1481.0**	**17.6**	100.9
172	696	507344.2	5.6	16.3	1.0	0.9	2.1	0.1	1.9	0.9	643.4	11.6	646.3	10.2	656.6	20.4	**643.4**	**11.6**	98.0
173	85	44504.8	2.3	10.9	1.0	3.3	1.6	0.3	1.2	0.8	1476.2	16.3	1473.6	12.4	1469.9	19.0	**1469.9**	**19.0**	100.4
174	387	182896.1	4.5	14.3	1.2	1.5	1.9	0.2	1.5	0.8	907.8	12.3	912.7	11.2	924.4	23.8	**924.4**	**23.8**	98.2
175	113	3166150.5	1.5	10.5	0.9	3.5	1.5	0.3	1.3	0.8	1511.0	16.9	1521.0	12.2	1535.0	17.1	**1535.0**	**17.1**	98.4
176	406	499537.9	4.1	13.2	1.0	1.9	1.8	0.2	1.5	0.8	1070.8	14.9	1074.7	12.0	1082.8	20.2	**1082.8**	**20.2**	98.9
177	272	66977.5	4.8	13.6	0.9	1.7	1.7	0.2	1.4	0.8	1013.3	13.0	1015.5	10.7	1020.3	18.9	**1020.3**	**18.9**	99.3
178	338	971728.3	88.8	17.0	0.9	0.7	1.6	0.1	1.4	0.8	559.2	7.2	558.2	7.0	554.3	20.2	**559.2**	**7.2**	100.9
179	169	161220.7	2.4	13.9	0.9	1.7	1.9	0.2	1.7	0.9	1016.4	15.6	1004.3	11.9	977.7	17.5	**977.7**	**17.5**	104.0

18	392	296486.9	2.5	17.2	1.3	0.6	2.3	0.1	1.9	0.8	474.7	8.9	484.9	8.9	533.4	27.7	**474.7**	**8.9**	89.0
180	76	42815.4	2.5	13.5	1.2	1.8	1.9	0.2	1.5	0.8	1022.9	14.0	1030.2	12.2	1045.8	23.3	**1045.8**	**23.3**	97.8
181	77	11081.5	2.1	17.1	2.6	0.6	3.1	0.1	1.7	0.5	471.8	7.7	485.0	12.0	548.0	57.2	**471.8**	**7.7**	86.1
182	123	685775.8	1.9	11.1	1.3	3.0	1.8	0.2	1.3	0.7	1406.9	17.0	1414.0	14.1	1424.8	24.2	**1424.8**	**24.2**	98.7
183	349	170152.6	8.2	13.5	0.8	1.8	1.4	0.2	1.2	0.8	1034.8	11.2	1038.6	9.4	1046.7	16.9	**1046.7**	**16.9**	98.9
184	94	52754.9	2.0	10.8	0.8	3.3	1.6	0.3	1.4	0.9	1472.6	18.5	1476.7	12.7	1482.5	15.9	**1482.5**	**15.9**	99.3
185	220	111439.6	2.3	11.4	0.8	2.9	1.5	0.2	1.3	0.8	1399.6	16.3	1392.6	11.6	1381.9	15.8	**1381.9**	**15.8**	101.3
186	425	116097.2	1.2	18.5	1.0	0.4	1.6	0.1	1.2	0.8	362.7	4.3	363.4	4.9	368.0	23.1	**362.7**	**4.3**	98.6
187	205	363356.6	2.6	12.3	0.8	2.4	1.6	0.2	1.4	0.9	1260.9	16.0	1249.4	11.5	1229.7	15.6	**1229.7**	**15.6**	102.5
188	248	194765.0	3.3	10.9	0.8	3.3	1.7	0.3	1.6	0.9	1482.9	20.9	1471.0	13.6	1454.0	14.5	**1454.0**	**14.5**	102.0
189	823	14132499.8	2.7	16.5	0.9	0.8	1.8	0.1	1.5	0.9	595.2	8.7	601.9	8.1	627.3	19.2	**595.2**	**8.7**	94.9
19	75	1202069.5	1.0	8.9	0.9	5.1	1.6	0.3	1.2	0.8	1855.3	20.0	1842.9	13.3	1829.0	17.2	**1829.0**	**17.2**	101.4
190	487	289180.9	0.7	11.7	0.6	2.7	1.5	0.2	1.4	0.9	1330.3	16.7	1326.2	11.3	1319.7	12.1	**1319.7**	**12.1**	100.8
191	95	42369.6	0.7	14.0	1.2	1.6	2.1	0.2	1.7	0.8	961.0	15.1	964.9	12.9	973.9	24.2	**973.9**	**24.2**	98.7
192	75	99287.5	1.5	12.4	1.2	2.1	1.8	0.2	1.3	0.7	1111.7	13.6	1147.6	12.4	1216.0	23.8	**1216.0**	**23.8**	91.4
193	101	467156.6	1.3	9.8	1.0	4.1	1.8	0.3	1.5	0.8	1637.6	21.0	1649.2	14.4	1664.0	18.6	**1664.0**	**18.6**	98.4
194	107	56224.8	1.5	8.9	0.9	5.0	1.8	0.3	1.5	0.9	1801.5	24.2	1814.5	14.9	1829.5	15.5	**1829.5**	**15.5**	98.5
195	308	1716784.0	2.6	10.7	1.2	3.3	2.2	0.3	1.8	0.8	1491.8	23.9	1491.3	16.9	1490.5	22.6	**1490.5**	**22.6**	100.1
196	216	327566.7	1.1	10.0	0.8	3.9	1.8	0.3	1.6	0.9	1605.4	22.8	1615.7	14.5	1629.1	14.8	**1629.1**	**14.8**	98.5
197	103	169799.3	3.3	13.7	1.0	1.7	1.8	0.2	1.5	0.8	997.0	13.5	1000.7	11.4	1008.8	20.9	**1008.8**	**20.9**	98.8
198	276	226258.6	3.4	17.3	0.9	0.7	1.4	0.1	1.1	0.8	517.7	5.5	519.1	5.8	525.2	19.6	**517.7**	**5.5**	98.6
199	250	170275.8	4.2	10.4	0.9	3.5	1.9	0.3	1.7	0.9	1517.4	22.9	1528.5	15.2	1543.8	17.3	**1543.8**	**17.3**	98.3
2	268	82940.8	3.6	13.5	1.0	1.8	1.6	0.2	1.2	0.8	1065.4	12.1	1056.3	10.3	1037.7	19.5	**1037.7**	**19.5**	102.7
20	225	181849.8	2.6	13.5	1.2	1.8	2.0	0.2	1.6	0.8	1032.4	15.2	1037.2	12.9	1047.5	24.0	**1047.5**	**24.0**	98.6
200	200	91435.3	2.2	10.6	0.9	3.6	1.5	0.3	1.3	0.8	1577.1	17.8	1550.6	12.3	1514.6	16.6	**1514.6**	**16.6**	104.1
201	318	283050.0	6.2	12.2	1.2	2.2	1.9	0.2	1.5	0.8	1134.5	15.5	1172.7	13.2	1243.8	23.1	**1243.8**	**23.1**	91.2
202	170	35214.1	2.3	17.7	1.2	0.6	1.9	0.1	1.5	0.8	448.9	6.4	452.5	6.9	471.3	26.3	**448.9**	**6.4**	95.2
203	108	82360.4	1.7	11.4	0.9	2.7	1.8	0.2	1.6	0.9	1299.2	18.4	1326.4	13.3	1370.7	17.0	**1370.7**	**17.0**	94.8
204	87	30258.7	1.2	13.2	1.2	1.7	1.8	0.2	1.4	0.8	982.2	12.7	1017.1	11.8	1092.9	23.9	**1092.9**	**23.9**	89.9
205	225	943455.4	4.4	13.5	1.2	1.8	1.9	0.2	1.6	0.8	1019.0	14.7	1028.6	12.6	1049.1	23.5	**1049.1**	**23.5**	97.1

206	20	18150.3	0.5	13.7	1.3	1.7	2.0	0.2	1.6	0.8	1020.3	14.7	1020.2	13.0	1019.9	25.7	**1019.9**	**25.7**	100.0
207	1114	334014.9	7.0	9.2	1.0	4.8	2.0	0.3	1.8	0.9	1788.0	27.5	1779.5	16.9	1769.6	17.8	**1769.6**	**17.8**	101.0
208	243	100276.0	1.9	15.4	1.0	1.1	1.7	0.1	1.4	0.8	761.3	10.0	765.2	9.1	776.6	20.1	**761.3**	**10.0**	98.0
209	296	163776.6	2.4	5.4	1.0	12.3	1.9	0.5	1.7	0.9	2547.9	35.1	2629.1	18.1	2692.3	15.9	**2692.3**	**15.9**	94.6
21	235	287566.1	3.2	18.1	1.3	0.5	2.2	0.1	1.8	0.8	441.9	7.5	439.6	7.7	427.4	28.1	**441.9**	**7.5**	103.4
210	34	21752.0	2.4	13.5	1.3	1.7	1.9	0.2	1.4	0.7	1018.9	12.9	1025.8	12.1	1040.7	25.6	**1040.7**	**25.6**	97.9
211	1067	2358940.8	7.4	12.6	0.9	2.1	2.2	0.2	2.0	0.9	1150.9	21.1	1158.9	15.2	1173.8	18.2	**1173.8**	**18.2**	98.1
212	28	65961.6	2.8	13.8	1.5	1.7	2.3	0.2	1.8	0.8	1018.1	16.6	1011.8	14.9	998.3	30.8	**998.3**	**30.8**	102.0
213	95	61841.2	1.1	16.3	1.2	0.8	1.8	0.1	1.3	0.7	565.1	7.0	582.9	7.9	652.7	26.4	**565.1**	**7.0**	86.6
214	200	165482.2	3.7	12.6	1.0	2.1	1.6	0.2	1.2	0.8	1149.2	12.9	1161.7	11.0	1185.0	20.2	**1185.0**	**20.2**	97.0
215	369	1263730.3	2.8	12.8	0.9	2.1	1.6	0.2	1.3	0.8	1130.1	13.6	1135.0	11.0	1144.4	18.8	**1144.4**	**18.8**	98.8
216	56	17142.8	2.8	13.5	1.3	1.8	1.8	0.2	1.2	0.7	1037.5	11.5	1037.1	11.6	1036.3	26.6	**1036.3**	**26.6**	100.1
217	51	56964.2	4.4	13.0	1.3	1.9	2.0	0.2	1.5	0.8	1048.7	14.6	1069.6	13.3	1112.3	26.5	**1112.3**	**26.5**	94.3
218	109	54225.3	2.1	17.7	1.6	0.5	2.1	0.1	1.3	0.6	416.7	5.2	425.9	7.2	475.7	35.5	**416.7**	**5.2**	87.6
219	268	196916.3	3.4	7.8	0.9	6.5	1.8	0.4	1.6	0.9	2013.9	27.1	2040.5	15.9	2067.4	16.0	**2067.4**	**16.0**	97.4
22	268	197431.3	59.2	13.1	0.8	1.9	1.5	0.2	1.3	0.9	1066.5	12.5	1076.8	9.9	1097.8	15.5	**1097.8**	**15.5**	97.2
220	165	645887.8	3.8	9.7	1.0	4.1	1.7	0.3	1.4	0.8	1645.9	20.2	1660.8	14.1	1679.7	18.8	**1679.7**	**18.8**	98.0
221	80	31497.5	1.5	12.1	1.1	2.3	2.0	0.2	1.6	0.8	1165.1	17.4	1196.8	13.9	1254.6	21.8	**1254.6**	**21.8**	92.9
222	108	491402.6	1.5	12.6	1.3	2.1	1.9	0.2	1.4	0.7	1150.1	14.8	1158.0	13.1	1172.7	25.1	**1172.7**	**25.1**	98.1
223	209	32057.1	1.1	18.4	1.1	0.5	1.9	0.1	1.6	0.8	376.6	5.8	378.5	6.0	389.9	23.8	**376.6**	**5.8**	96.6
224	350	166343.9	2.1	9.9	0.9	4.0	1.6	0.3	1.4	0.8	1623.6	19.7	1631.3	13.3	1641.3	16.5	**1641.3**	**16.5**	98.9
225	132	56338.2	3.5	13.3	0.9	1.8	2.0	0.2	1.7	0.9	1021.3	16.2	1036.6	12.7	1069.0	19.0	**1069.0**	**19.0**	95.5
226	54	94610.2	1.3	12.4	1.2	2.3	1.8	0.2	1.4	0.8	1206.8	15.0	1208.2	12.8	1210.8	23.3	**1210.8**	**23.3**	99.7
227	92	412437.4	0.6	9.2	1.2	4.6	1.6	0.3	1.2	0.7	1731.4	17.9	1756.1	13.8	1785.6	21.0	**1785.6**	**21.0**	97.0
228	234	733470.9	1.5	13.5	1.0	1.8	1.4	0.2	1.0	0.7	1052.0	9.3	1050.1	8.9	1046.2	19.4	**1046.2**	**19.4**	100.6
229	127	15249.5	0.8	14.4	1.9	0.9	2.3	0.1	1.3	0.6	554.4	6.8	629.4	10.7	909.0	39.0	**554.4**	**6.8**	61.0
23	148	293988.1	3.0	10.7	1.0	3.3	1.5	0.3	1.2	0.8	1484.3	16.1	1490.5	12.1	1499.3	18.1	**1499.3**	**18.1**	99.0
230	161	199566.2	1.1	18.3	1.5	0.5	2.1	0.1	1.5	0.7	434.8	6.1	428.6	7.2	395.7	32.9	**434.8**	**6.1**	109.9
231	450	2961328.4	2.3	12.4	0.8	2.2	1.5	0.2	1.3	0.8	1144.5	13.4	1166.2	10.7	1206.6	16.7	**1206.6**	**16.7**	94.9
232	526	163173.1	2.3	16.8	1.0	0.7	1.7	0.1	1.4	0.8	547.8	7.1	555.7	7.3	588.3	22.6	**547.8**	**7.1**	93.1

233	209	428978.7	3.8	10.0	1.0	3.6	1.8	0.3	1.5	0.8	1510.0	20.4	1558.3	14.5	1624.5	18.6	**1624.5**	**18.6**	93.0
234	92	103358.7	2.2	13.1	1.0	1.9	1.5	0.2	1.0	0.7	1045.7	10.1	1066.0	9.7	1107.7	20.6	**1107.7**	**20.6**	94.4
235	143	172091.5	1.6	13.3	1.1	1.8	1.8	0.2	1.4	0.8	1041.3	13.7	1051.6	11.9	1073.1	22.4	**1073.1**	**22.4**	97.0
236	162	198176.2	1.4	14.0	0.9	1.5	1.5	0.2	1.2	0.8	941.7	10.7	948.6	9.4	964.6	18.8	**964.6**	**18.8**	97.6
237	115	150376.7	2.4	13.3	0.9	1.7	1.6	0.2	1.3	0.8	985.8	11.6	1015.3	10.0	1079.3	18.4	**1079.3**	**18.4**	91.3
238	302	90131.6	4.9	13.3	1.2	1.8	1.7	0.2	1.2	0.7	1047.4	11.8	1054.9	11.1	1070.5	23.7	**1070.5**	**23.7**	97.8
239	20	29381.2	2.3	13.4	1.7	1.7	2.2	0.2	1.5	0.7	1001.7	13.5	1018.5	14.3	1054.9	33.7	**1054.9**	**33.7**	95.0
24	523	477454.3	3.1	13.8	1.0	1.7	1.7	0.2	1.4	0.8	1000.5	12.9	998.0	11.0	992.5	21.1	**992.5**	**21.1**	100.8
240	68	39557.0	1.9	9.3	0.9	4.6	1.5	0.3	1.2	0.8	1741.0	18.1	1747.8	12.4	1755.9	16.3	**1755.9**	**16.3**	99.2
241	164	91140.5	4.7	12.8	1.0	1.9	1.8	0.2	1.5	0.8	1072.4	14.5	1096.3	11.7	1144.1	19.0	**1144.1**	**19.0**	93.7
242	380	165376.5	2.1	17.6	1.0	0.5	1.7	0.1	1.3	0.8	429.1	5.4	437.1	5.9	479.0	22.9	**429.1**	**5.4**	89.6
243	62	28879.2	1.6	13.9	1.4	1.6	1.8	0.2	1.1	0.6	958.8	9.8	967.8	11.3	988.1	29.4	**988.1**	**29.4**	97.0
244	627	285724.8	11.9	12.8	1.0	2.1	1.9	0.2	1.6	0.9	1156.9	16.9	1151.8	12.9	1142.2	19.4	**1142.2**	**19.4**	101.3
245	64	94529.9	2.4	10.6	1.2	3.4	1.9	0.3	1.4	0.8	1487.5	19.1	1500.8	14.8	1519.6	23.2	**1519.6**	**23.2**	97.9
246	282	1312843.1	1.8	13.5	0.7	1.8	1.6	0.2	1.4	0.9	1038.3	13.4	1037.8	10.2	1036.7	14.6	**1036.7**	**14.6**	100.2
247	384	1258799.8	4.4	10.8	0.9	3.2	1.5	0.3	1.2	0.8	1440.6	15.8	1455.5	11.6	1477.4	16.2	**1477.4**	**16.2**	97.5
248	109	147298.5	0.1	13.5	1.0	1.7	1.6	0.2	1.3	0.8	1018.7	12.6	1025.0	10.6	1038.4	19.3	**1038.4**	**19.3**	98.1
249	133	89584.9	3.2	10.5	1.0	3.4	1.5	0.3	1.2	0.8	1502.4	15.6	1511.5	11.9	1524.1	18.0	**1524.1**	**18.0**	98.6
25	82	407823.4	1.9	11.6	0.9	2.8	1.7	0.2	1.4	0.8	1385.3	17.3	1365.1	12.6	1333.7	18.3	**1333.7**	**18.3**	103.9
250	206	673562.3	4.2	10.3	0.8	3.7	1.9	0.3	1.7	0.9	1596.6	24.0	1580.5	15.2	1559.2	15.9	**1559.2**	**15.9**	102.4
251	116	191781.5	1.1	6.0	1.0	10.9	1.8	0.5	1.5	0.8	2522.7	31.5	2518.3	16.7	2514.7	16.5	**2514.7**	**16.5**	100.3
252	486	777553.6	2.9	9.5	1.0	4.4	1.7	0.3	1.4	0.8	1726.9	20.9	1720.1	14.3	1711.9	19.2	**1711.9**	**19.2**	100.9
253	314	78564.4	1.6	18.1	1.3	0.5	2.1	0.1	1.6	0.8	427.7	6.7	426.3	7.2	418.7	28.8	**427.7**	**6.7**	102.2
254	1096	976863.1	2.0	13.0	0.8	2.0	1.7	0.2	1.4	0.9	1110.1	14.7	1115.1	11.2	1125.0	16.4	**1125.0**	**16.4**	98.7
255	331	289787.8	5.1	9.2	0.8	4.6	1.8	0.3	1.6	0.9	1721.0	24.7	1747.7	15.1	1779.8	14.0	**1779.8**	**14.0**	96.7
256	60	452179.4	1.5	11.7	1.1	2.7	1.7	0.2	1.3	0.8	1324.0	15.9	1321.5	12.6	1317.5	20.6	**1317.5**	**20.6**	100.5
257	40	27016.3	1.3	13.4	1.2	1.8	1.9	0.2	1.5	0.8	1028.7	14.3	1040.2	12.3	1064.5	23.4	**1064.5**	**23.4**	96.6
258	127	1127281.5	2.9	12.7	0.8	2.1	1.4	0.2	1.1	0.8	1139.9	11.6	1146.6	9.5	1159.2	16.5	**1159.2**	**16.5**	98.3
259	92	54538.6	2.8	10.7	1.0	3.3	1.8	0.3	1.5	0.8	1457.7	19.7	1476.0	13.9	1502.3	18.0	**1502.3**	**18.0**	97.0
26	172	216033.9	0.9	17.3	1.2	0.7	1.7	0.1	1.3	0.7	508.1	6.2	509.4	6.9	515.1	25.6	**508.1**	**6.2**	98.6

260	56	10855962.0	2.1	11.1	1.3	2.9	1.9	0.2	1.5	0.8	1360.7	18.0	1389.9	14.6	1434.9	24.0	**1434.9**	**24.0**	94.8
261	412	230103.2	1.8	13.3	0.7	1.8	1.5	0.2	1.3	0.9	1045.1	12.1	1054.8	9.6	1075.0	15.0	**1075.0**	**15.0**	97.2
263	85	63313.9	2.8	13.0	1.1	2.0	2.1	0.2	1.8	0.9	1126.2	18.3	1125.9	14.1	1125.5	21.3	**1125.5**	**21.3**	100.1
264	56	190018.7	1.5	5.9	1.0	11.1	1.7	0.5	1.3	0.8	2497.1	27.9	2530.0	15.6	2556.4	16.5	**2556.4**	**16.5**	97.7
265	142	188658.3	2.1	8.4	0.8	5.8	1.5	0.4	1.3	0.9	1952.6	22.4	1951.4	13.4	1950.2	14.1	**1950.2**	**14.1**	100.1
266	525	168559.0	2.3	13.1	0.8	1.9	1.5	0.2	1.2	0.9	1055.7	12.1	1071.1	9.7	1102.5	15.2	**1102.5**	**15.2**	95.8
267	322	236998.8	3.5	12.2	1.1	2.3	1.8	0.2	1.5	0.8	1201.2	16.0	1216.2	12.9	1242.8	21.1	**1242.8**	**21.1**	96.7
268	179	52683.8	2.7	12.7	1.1	2.1	1.6	0.2	1.2	0.7	1137.3	12.3	1145.5	10.9	1161.2	21.3	**1161.2**	**21.3**	97.9
269	313	306695.7	3.1	12.7	0.9	2.2	1.6	0.2	1.3	0.8	1177.6	14.1	1172.0	11.1	1161.5	18.1	**1161.5**	**18.1**	101.4
27	155	141495.8	3.1	13.3	0.8	1.9	1.3	0.2	1.1	0.8	1065.7	10.4	1066.9	8.8	1069.4	16.0	**1069.4**	**16.0**	99.6
271	99	106811.3	1.9	10.0	1.1	4.0	1.7	0.3	1.3	0.8	1645.9	19.1	1638.2	14.0	1628.2	20.5	**1628.2**	**20.5**	101.1
272	166	153394.3	3.3	11.0	0.9	3.1	1.7	0.2	1.5	0.9	1415.4	19.0	1424.1	13.2	1437.2	16.6	**1437.2**	**16.6**	98.5
273	339	229268.6	2.1	13.6	1.0	1.8	1.5	0.2	1.1	0.7	1043.7	10.3	1039.1	9.6	1029.6	20.6	**1029.6**	**20.6**	101.4
274	242	148227.6	1.9	18.2	1.0	0.5	1.6	0.1	1.2	0.8	420.8	5.1	419.1	5.6	409.5	23.2	**420.8**	**5.1**	102.8
275	76	137493.8	0.7	17.5	1.3	0.6	1.8	0.1	1.2	0.7	465.2	5.5	471.3	6.6	500.7	27.9	**465.2**	**5.5**	92.9
276	307	1233296.5	2.2	12.6	1.0	2.1	2.0	0.2	1.7	0.9	1135.0	18.2	1150.8	13.7	1180.7	19.1	**1180.7**	**19.1**	96.1
277	110	129339.7	1.3	10.0	0.8	3.8	1.6	0.3	1.3	0.8	1579.8	18.5	1602.1	12.6	1631.5	15.3	**1631.5**	**15.3**	96.8
278	192	292232.4	1.6	9.5	1.1	4.6	2.0	0.3	1.6	0.8	1767.4	25.1	1748.8	16.4	1726.6	20.3	**1726.6**	**20.3**	102.4
279	141	149393.0	3.8	14.0	1.1	1.6	2.0	0.2	1.7	0.8	969.2	15.0	970.9	12.5	974.8	22.5	**974.8**	**22.5**	99.4
28	92	155055.9	2.0	10.8	1.1	3.4	1.6	0.3	1.3	0.8	1521.1	17.0	1500.5	12.8	1471.6	20.1	**1471.6**	**20.1**	103.4
280	111	100054.3	2.5	12.3	1.1	2.3	1.7	0.2	1.4	0.8	1204.8	15.0	1212.4	12.2	1225.9	20.9	**1225.9**	**20.9**	98.3
281	66	66519.2	1.7	18.4	1.7	0.4	2.2	0.1	1.5	0.7	374.9	5.3	376.1	7.0	383.0	37.9	**374.9**	**5.3**	97.9
282	136	77117.0	2.1	11.2	1.0	3.1	1.5	0.3	1.1	0.7	1439.3	14.7	1429.6	11.8	1415.0	19.8	**1415.0**	**19.8**	101.7
283	269	175133.2	2.2	15.9	1.1	1.0	1.7	0.1	1.3	0.8	705.8	8.7	704.8	8.6	701.7	22.9	**705.8**	**8.7**	100.6
284	274	257431.8	1.8	13.2	0.8	2.0	1.6	0.2	1.3	0.9	1108.1	13.6	1103.8	10.5	1095.2	16.1	**1095.2**	**16.1**	101.2
285	93	26059.1	2.3	13.4	1.0	1.9	1.7	0.2	1.4	0.8	1080.7	13.6	1071.7	11.2	1053.4	20.3	**1053.4**	**20.3**	102.6
286	56	22454.8	1.3	13.2	1.2	1.8	1.7	0.2	1.1	0.7	1040.9	11.0	1053.7	10.9	1080.3	24.0	**1080.3**	**24.0**	96.4
287	114	135047.0	3.5	12.5	1.1	2.1	1.7	0.2	1.3	0.8	1149.1	13.6	1165.0	11.9	1194.7	22.3	**1194.7**	**22.3**	96.2
288	166	610005.0	1.9	9.5	0.9	4.5	1.4	0.3	1.1	0.8	1756.2	16.7	1738.9	11.6	1718.1	16.1	**1718.1**	**16.1**	102.2
289	98	284185.8	2.2	4.0	1.0	19.8	1.4	0.6	1.1	0.7	2946.5	24.9	3080.4	13.8	3168.9	15.2	**3168.9**	**15.2**	93.0

29	81	98068.6	1.8	13.1	1.0	2.0	1.6	0.2	1.3	0.8	1113.7	13.0	1112.4	11.0	1109.7	20.3	**1109.7**	**20.3**	100.4
290	126	56624.1	5.3	16.9	0.9	0.8	1.6	0.1	1.3	0.8	610.2	7.8	601.5	7.4	568.9	20.5	**610.2**	**7.8**	107.3
291	211	104232.5	3.0	12.6	0.9	2.2	1.7	0.2	1.4	0.8	1197.0	15.3	1191.4	11.8	1181.4	18.2	**1181.4**	**18.2**	101.3
292	311	1484681.4	2.9	12.7	0.7	2.1	1.4	0.2	1.2	0.8	1159.3	12.5	1163.2	9.7	1170.4	14.9	**1170.4**	**14.9**	99.1
293	288	73817.1	2.2	13.5	1.1	1.8	1.9	0.2	1.6	0.8	1054.1	15.4	1051.1	12.5	1044.8	21.5	**1044.8**	**21.5**	100.9
294	735	11069844.7	13.7	9.3	0.9	4.7	2.0	0.3	1.8	0.9	1761.5	28.1	1759.0	16.8	1756.0	15.6	**1756.0**	**15.6**	100.3
295	85	94134.9	0.6	16.2	1.6	0.8	2.1	0.1	1.4	0.7	614.1	8.5	624.1	9.9	660.6	33.5	**614.1**	**8.5**	93.0
296	375	350502.6	6.6	10.1	0.8	3.6	1.6	0.3	1.4	0.9	1503.9	19.1	1549.5	13.0	1612.2	15.2	**1612.2**	**15.2**	93.3
297	130	290933.0	2.2	12.6	1.0	2.2	1.7	0.2	1.4	0.8	1191.3	15.1	1188.7	11.9	1184.1	19.3	**1184.1**	**19.3**	100.6
298	124	149937.8	2.7	11.0	1.3	2.8	1.8	0.2	1.3	0.7	1282.9	15.1	1343.5	13.8	1441.3	25.1	**1441.3**	**25.1**	89.0
299	341	81415.0	1.7	18.3	0.8	0.5	1.7	0.1	1.5	0.9	381.3	5.6	383.7	5.5	397.9	18.9	**381.3**	**5.6**	95.8
3	172	162599.1	2.6	12.8	1.1	2.2	1.7	0.2	1.3	0.8	1183.2	14.6	1173.2	12.0	1154.8	21.4	**1154.8**	**21.4**	102.5
30	437	868190.6	2.9	11.1	0.9	3.1	1.6	0.3	1.4	0.8	1450.8	17.7	1441.2	12.4	1427.0	16.3	**1427.0**	**16.3**	101.7
300	131	86918.2	1.3	13.0	0.9	2.0	1.5	0.2	1.2	0.8	1106.9	12.6	1112.0	10.2	1122.1	17.2	**1122.1**	**17.2**	98.6
301	68	61472.7	1.0	13.7	0.9	1.7	1.4	0.2	1.1	0.8	980.8	10.1	991.3	9.2	1014.5	18.8	**1014.5**	**18.8**	96.7
302	47	54085.6	1.8	13.6	1.1	1.7	1.8	0.2	1.4	0.8	1013.8	12.8	1020.1	11.3	1033.6	22.2	**1033.6**	**22.2**	98.1
303	131	246550.9	1.7	5.5	0.8	12.7	1.6	0.5	1.4	0.8	2645.4	29.3	2657.0	15.0	2665.9	14.0	**2665.9**	**14.0**	99.2
304	148	64494.7	2.3	12.9	1.1	2.2	2.0	0.2	1.7	0.8	1180.0	18.0	1165.8	13.9	1139.4	22.0	**1139.4**	**22.0**	103.6
305	272	97351.0	4.4	13.7	0.9	1.7	1.4	0.2	1.1	0.8	1027.9	10.7	1024.9	9.3	1018.3	18.2	**1018.3**	**18.2**	100.9
306	81	18900.1	2.6	17.1	1.7	0.7	2.3	0.1	1.6	0.7	544.6	8.4	544.2	9.9	542.6	37.3	**544.6**	**8.4**	100.4
307	267	446474.2	2.5	10.4	0.6	3.3	1.7	0.3	1.6	0.9	1455.5	20.3	1490.9	13.2	1541.6	12.0	**1541.6**	**12.0**	94.4
308	403	1370388.4	3.9	18.3	1.1	0.5	1.7	0.1	1.2	0.7	411.2	4.9	409.8	5.6	401.3	25.3	**411.2**	**4.9**	102.5
309	56	52639.2	3.5	13.6	0.9	1.8	1.7	0.2	1.4	0.8	1059.5	13.6	1047.8	11.0	1023.5	18.9	**1023.5**	**18.9**	103.5
31	168	140143.9	4.8	10.1	0.9	4.0	1.4	0.3	1.1	0.8	1656.0	16.3	1635.8	11.6	1610.0	16.7	**1610.0**	**16.7**	102.9
310	307	2532383.3	2.0	13.6	1.0	1.7	1.8	0.2	1.5	0.8	1026.8	14.3	1025.9	11.6	1024.1	19.9	**1024.1**	**19.9**	100.3
311	445	184557.5	4.7	11.9	0.8	2.6	1.4	0.2	1.1	0.8	1313.9	13.6	1308.5	10.1	1299.7	14.7	**1299.7**	**14.7**	101.1
312	391	192254.6	3.0	12.9	0.8	2.1	1.5	0.2	1.3	0.9	1133.4	14.0	1132.7	10.6	1131.4	15.3	**1131.4**	**15.3**	100.2
313	35	54153.3	1.9	6.9	0.8	8.3	1.7	0.4	1.5	0.9	2228.7	27.3	2261.8	15.1	2291.9	14.1	**2291.9**	**14.1**	97.2
314	270	7397167.7	2.2	11.9	0.7	2.5	1.6	0.2	1.4	0.9	1253.4	15.7	1270.0	11.3	1298.3	14.2	**1298.3**	**14.2**	96.5
315	288	169787.2	3.4	13.6	1.0	1.8	1.7	0.2	1.4	0.8	1045.9	13.2	1041.5	11.2	1032.3	20.9	**1032.3**	**20.9**	101.3

32	105	475180.4	2.4	12.9	1.1	2.1	1.7	0.2	1.2	0.7	1156.5	13.1	1147.6	11.4	1130.9	21.9	**1130.9**	**21.9**	102.3
33	72	17400.1	1.7	16.3	1.7	0.8	2.2	0.1	1.3	0.6	564.8	7.2	581.3	9.7	646.4	37.4	**564.8**	**7.2**	87.4
34	67	79082.0	2.8	12.4	1.2	2.2	2.1	0.2	1.7	0.8	1148.8	18.2	1169.5	14.8	1207.9	24.3	**1207.9**	**24.3**	95.1
35	110	565467.9	2.8	11.5	0.9	2.9	1.5	0.2	1.1	0.8	1388.8	14.0	1376.9	11.1	1358.4	18.3	**1358.4**	**18.3**	102.2
36	255	98619.2	2.9	17.4	0.9	0.7	1.6	0.1	1.3	0.8	525.2	6.7	521.0	6.6	502.6	20.2	**525.2**	**6.7**	104.5
37	313	118595.9	4.8	12.9	1.0	2.0	1.5	0.2	1.1	0.8	1125.2	11.8	1128.0	10.2	1133.4	19.1	**1133.4**	**19.1**	99.3
38	352	197717.1	2.7	11.9	0.8	2.4	1.5	0.2	1.3	0.8	1228.8	14.1	1254.9	10.9	1299.9	16.0	**1299.9**	**16.0**	94.5
39	54	33186.9	2.5	13.5	1.2	1.8	1.7	0.2	1.3	0.8	1017.4	12.3	1027.5	11.3	1049.2	23.2	**1049.2**	**23.2**	97.0
4	230	72787.9	1.0	16.8	0.8	0.8	1.5	0.1	1.3	0.8	589.9	7.3	589.3	6.8	586.9	17.7	**589.9**	**7.3**	100.5
40	2602	504367.9	6.7	18.2	0.8	0.5	1.6	0.1	1.4	0.9	444.7	6.0	439.0	5.8	409.2	18.9	**444.7**	**6.0**	108.7
41	149	65818.9	3.3	13.8	1.1	1.7	2.0	0.2	1.6	0.8	999.4	15.3	997.9	12.5	994.5	21.7	**994.5**	**21.7**	100.5
42	149	70155.2	2.6	15.7	1.2	1.0	1.8	0.1	1.4	0.8	719.3	9.6	721.5	9.5	728.5	25.1	**719.3**	**9.6**	98.7
43	1357	958284.4	3.0	13.6	1.0	1.8	2.0	0.2	1.8	0.9	1028.7	17.0	1029.3	13.2	1030.5	19.8	**1030.5**	**19.8**	99.8
44	664	928308.4	4.2	10.0	0.8	4.0	1.8	0.3	1.6	0.9	1627.5	22.6	1627.2	14.3	1626.7	14.8	**1626.7**	**14.8**	100.1
45	263	3343438.6	3.3	9.4	1.0	4.6	1.7	0.3	1.4	0.8	1768.8	21.1	1757.1	14.1	1743.2	18.2	**1743.2**	**18.2**	101.5
46	86	186484.0	2.6	10.2	1.0	3.7	1.5	0.3	1.1	0.7	1570.1	15.7	1580.5	12.3	1594.4	19.5	**1594.4**	**19.5**	98.5
47	33	21533.0	2.5	8.2	1.2	6.0	1.7	0.4	1.2	0.7	1976.1	20.2	1975.7	14.7	1975.2	21.3	**1975.2**	**21.3**	100.0
48	98	63806.1	2.2	12.7	1.2	2.1	1.7	0.2	1.2	0.7	1135.2	12.2	1145.2	11.6	1164.2	24.1	**1164.2**	**24.1**	97.5
49	843	921264.3	7.4	13.7	1.0	1.8	2.0	0.2	1.7	0.9	1063.6	16.9	1048.7	13.0	1017.8	19.9	**1017.8**	**19.9**	104.5
5	95	26244.3	1.4	17.6	1.4	0.6	1.9	0.1	1.3	0.7	499.7	6.2	497.7	7.3	488.9	29.9	**499.7**	**6.2**	102.2
50	351	106239.9	1.1	17.8	0.9	0.6	1.5	0.1	1.2	0.8	492.2	5.6	486.5	5.9	459.4	21.0	**492.2**	**5.6**	107.2
51	92	23081.6	2.8	14.1	1.2	1.6	1.7	0.2	1.2	0.7	996.8	11.0	982.8	10.7	951.7	24.8	**951.7**	**24.8**	104.7
52	54	27263.2	1.2	12.5	1.0	2.3	1.7	0.2	1.4	0.8	1197.6	14.9	1198.0	12.1	1198.8	20.6	**1198.8**	**20.6**	99.9
53	29	18801.3	0.8	10.8	1.4	3.3	2.0	0.3	1.4	0.7	1471.0	18.0	1471.6	15.2	1472.4	26.5	**1472.4**	**26.5**	99.9
54	187	171984.9	2.7	13.4	1.0	1.8	1.6	0.2	1.3	0.8	1067.4	12.8	1062.4	10.8	1052.4	19.9	**1052.4**	**19.9**	101.4
55	108	18936.2	1.3	13.7	1.1	1.7	1.9	0.2	1.5	0.8	1024.8	14.4	1023.1	12.0	1019.5	21.6	**1019.5**	**21.6**	100.5
56	149	38873.0	1.4	10.2	1.0	3.3	1.8	0.2	1.5	0.8	1413.9	18.5	1483.1	13.7	1583.5	18.3	**1583.5**	**18.3**	89.3
57	93	140445.3	1.9	12.8	1.2	2.1	2.3	0.2	2.0	0.9	1144.3	21.2	1147.8	16.1	1154.5	23.2	**1154.5**	**23.2**	99.1
58	665	210943.8	9.4	12.3	0.8	2.4	1.8	0.2	1.6	0.9	1250.0	18.4	1242.6	12.8	1229.8	15.0	**1229.8**	**15.0**	101.6
59	204	176324.4	2.2	11.9	0.9	2.5	1.5	0.2	1.2	0.8	1274.5	14.0	1279.8	10.9	1288.6	17.3	**1288.6**	**17.3**	98.9

6	409	418132.2	2.1	15.8	1.1	1.1	2.0	0.1	1.7	0.8	748.8	11.9	742.3	10.7	723.0	24.2	**748.8**	**11.9**	103.6
60	256	323779.5	0.8	10.7	1.0	3.4	1.4	0.3	1.0	0.7	1492.3	13.2	1496.0	10.7	1501.3	18.0	**1501.3**	**18.0**	99.4
61	867	1876168.0	349.7	13.2	1.0	2.0	1.9	0.2	1.7	0.9	1114.3	17.1	1107.0	13.1	1092.6	20.0	**1092.6**	**20.0**	102.0
62	120	15723.6	1.4	17.1	1.5	0.6	2.0	0.1	1.4	0.7	456.2	6.0	470.5	7.6	541.0	32.3	**456.2**	**6.0**	84.3
63	124	54930.4	2.0	11.6	0.9	2.7	1.8	0.2	1.6	0.9	1332.0	19.2	1334.2	13.6	1337.7	17.6	**1337.7**	**17.6**	99.6
64	210	192162.6	2.8	11.7	0.8	2.7	1.4	0.2	1.2	0.8	1334.7	14.2	1328.1	10.5	1317.5	15.2	**1317.5**	**15.2**	101.3
65	187	199716.4	1.7	9.1	0.7	5.0	1.3	0.3	1.0	0.8	1836.8	16.6	1816.4	10.6	1793.1	12.8	**1793.1**	**12.8**	102.4
66	871	503135.3	2.3	12.2	0.8	2.4	1.8	0.2	1.6	0.9	1231.1	17.9	1234.0	12.9	1239.2	16.5	**1239.2**	**16.5**	99.3
67	216	2900917.3	2.8	10.9	1.0	3.2	1.8	0.3	1.5	0.8	1468.7	19.1	1465.8	13.9	1461.7	19.7	**1461.7**	**19.7**	100.5
68	129	88303.0	1.2	16.2	0.9	0.9	1.7	0.1	1.4	0.9	622.6	8.5	632.1	7.8	666.4	18.3	**622.6**	**8.5**	93.4
7	123	27363.3	2.6	12.2	1.1	2.5	1.4	0.2	1.0	0.7	1280.0	11.4	1264.9	10.4	1239.3	20.6	**1239.3**	**20.6**	103.3
70	130	51537.9	1.3	12.7	1.0	2.2	1.8	0.2	1.4	0.8	1179.2	15.3	1176.3	12.2	1170.9	20.3	**1170.9**	**20.3**	100.7
71	184	167869.7	1.3	8.9	1.0	5.1	1.8	0.3	1.5	0.8	1836.2	23.5	1837.8	15.1	1839.6	18.3	**1839.6**	**18.3**	99.8
72	158	63471.7	2.1	13.4	1.0	1.8	1.8	0.2	1.4	0.8	1062.1	14.0	1059.0	11.6	1052.8	20.9	**1052.8**	**20.9**	100.9
73	248	187812.2	1.8	9.9	0.7	4.0	1.4	0.3	1.2	0.9	1640.7	17.6	1637.2	11.3	1632.7	12.5	**1632.7**	**12.5**	100.5
74	96	197641.4	1.8	8.6	1.1	5.3	1.9	0.3	1.6	0.8	1834.5	25.3	1863.0	16.3	1895.0	19.0	**1895.0**	**19.0**	96.8
75	164	181167.9	5.3	14.2	1.0	1.3	2.0	0.1	1.8	0.9	838.7	13.8	864.9	11.8	932.8	20.6	**838.7**	**13.8**	89.9
76	231	262802.5	1.5	9.9	1.0	4.0	1.9	0.3	1.6	0.9	1631.5	23.2	1634.9	15.2	1639.3	17.9	**1639.3**	**17.9**	99.5
77	78	34942.9	1.1	13.0	1.1	1.8	1.6	0.2	1.2	0.7	1011.8	10.9	1043.9	10.3	1111.7	21.5	**1111.7**	**21.5**	91.0
78	246	298783.6	2.0	12.2	0.9	2.3	2.1	0.2	1.9	0.9	1189.5	20.6	1211.5	14.8	1250.9	17.7	**1250.9**	**17.7**	95.1
79	494	391693.2	3.2	11.7	0.6	2.7	1.3	0.2	1.1	0.9	1333.5	13.8	1329.5	9.6	1323.1	11.4	**1323.1**	**11.4**	100.8
80	135	223030.4	2.2	12.7	0.9	2.1	1.6	0.2	1.3	0.8	1141.9	13.9	1151.3	11.2	1168.9	18.7	**1168.9**	**18.7**	97.7
81	169	163507.4	5.1	12.7	1.0	2.1	1.7	0.2	1.4	0.8	1156.6	14.4	1161.1	11.6	1169.3	19.6	**1169.3**	**19.6**	98.9
82	353	310878.6	1.1	10.8	0.8	3.1	1.2	0.2	1.0	0.8	1420.8	12.6	1441.9	9.6	1473.1	14.4	**1473.1**	**14.4**	96.4
83	435	136008.8	2.6	17.9	1.2	0.6	1.9	0.1	1.5	0.8	458.3	6.6	456.9	7.0	449.8	26.3	**458.3**	**6.6**	101.9
84	200	61961.2	4.1	11.4	0.9	2.8	1.7	0.2	1.5	0.9	1349.6	18.4	1361.8	13.0	1381.0	16.5	**1381.0**	**16.5**	97.7
85	233	1387368.2	3.3	12.8	0.9	2.2	1.7	0.2	1.4	0.8	1172.8	14.7	1165.1	11.5	1150.8	18.5	**1150.8**	**18.5**	101.9
86	307	43562.2	1.7	17.9	1.1	0.5	1.5	0.1	1.0	0.7	443.9	4.4	444.9	5.3	450.1	23.5	**443.9**	**4.4**	98.6
88	67	582190.3	0.4	13.4	1.2	1.8	1.9	0.2	1.4	0.8	1036.3	13.7	1041.8	12.2	1053.4	24.1	**1053.4**	**24.1**	98.4
89	249	253437.4	3.9	11.7	0.9	2.7	1.9	0.2	1.6	0.9	1337.3	19.8	1334.0	14.0	1328.6	18.2	**1328.6**	**18.2**	100.6

9	163	180675.6	1.9	11.5	0.7	2.7	1.5	0.2	1.3	0.9	1294.2	15.1	1317.0	10.9	1354.3	14.0	**1354.3**	**14.0**	95.6
90	95	50153.2	1.2	11.7	0.8	2.7	1.5	0.2	1.3	0.8	1316.4	15.0	1317.2	11.0	1318.5	15.2	**1318.5**	**15.2**	99.8
91	189	276715.6	2.5	10.7	0.8	3.4	1.3	0.3	1.0	0.8	1493.1	13.8	1495.7	10.1	1499.4	14.7	**1499.4**	**14.7**	99.6
92	376	265557.1	2.8	16.9	0.9	0.7	1.5	0.1	1.2	0.8	562.7	6.7	565.3	6.7	576.0	19.8	**562.7**	**6.7**	97.7
93	126	28570.4	2.3	17.9	1.2	0.5	2.0	0.1	1.6	0.8	430.6	6.5	433.2	6.9	446.8	26.4	**430.6**	**6.5**	96.4
94	1225	161548.0	1.2	17.7	0.9	0.6	1.9	0.1	1.6	0.9	471.5	7.4	471.1	7.1	469.0	20.6	**471.5**	**7.4**	100.5
95	328	168385.5	4.6	13.4	1.0	1.8	1.9	0.2	1.6	0.9	1044.3	15.8	1046.3	12.5	1050.7	19.9	**1050.7**	**19.9**	99.4
96	99	69029.7	1.3	17.3	1.2	0.6	1.7	0.1	1.3	0.7	460.0	5.8	470.7	6.6	523.2	25.4	**460.0**	**5.8**	87.9
97	714	948389.0	7.7	9.6	0.9	4.3	1.9	0.3	1.7	0.9	1672.7	24.5	1685.3	15.6	1701.0	16.7	**1701.0**	**16.7**	98.3
98	231	578919.6	4.0	12.6	0.9	2.2	1.7	0.2	1.4	0.8	1171.3	15.5	1175.4	12.1	1183.2	18.8	**1183.2**	**18.8**	99.0
99	43	23042.2	1.6	13.2	1.2	2.0	1.8	0.2	1.4	0.8	1147.6	14.4	1129.1	12.3	1093.6	23.6	**1093.6**	**23.6**	104.9
xx	620	176870.1	5.3	17.7	1.0	0.8	3.0	0.1	2.8	0.9	624.7	16.9	593.3	13.6	475.2	22.7	**624.7**	**16.9**	131.5
xx	9255	3270241.3	0.6	18.2	1.0	0.5	2.0	0.1	1.8	0.9	387.2	6.7	391.1	6.6	414.2	21.9	**387.2**	**6.7**	93.5
xx	6332	746429.0	0.7	18.3	0.9	0.5	1.9	0.1	1.6	0.9	402.7	6.4	401.5	6.2	394.3	20.3	**402.7**	**6.4**	102.1

Sample: SF-B						Isotope Ratios					Apparent Ages (Ma)								
Analysis	U (ppm)	206Pb /204Pb	U /Th	206Pb /207Pb	± (%)	207Pb /235U	± (%)	206Pb /238U	± (%)	err. corr.	206Pb /238U	± (Ma)	207Pb /235U	± (Ma)	206Pb /207Pb	± (Ma)	Best Age	± (Ma)	Conc. (%)
1	50	62545.1	1.0	13.3	0.9	1.8	1.7	0.2	1.4	0.8	1043.4	13.9	1055.1	11.2	1079.2	18.2	**1079.2**	**18.2**	96.7
10	56	63558.8	0.6	13.6	1.0	1.7	1.7	0.2	1.4	0.8	1001.6	13.2	1007.6	11.1	1020.6	20.5	**1020.6**	**20.5**	98.1
100	128	105891.2	2.8	12.2	0.8	2.5	1.4	0.2	1.1	0.8	1265.7	12.6	1259.8	9.9	1249.7	16.3	**1249.7**	**16.3**	101.3
101	230	415520.7	2.8	9.9	0.9	4.1	1.4	0.3	1.1	0.8	1655.5	16.7	1646.8	11.7	1635.8	16.1	**1635.8**	**16.1**	101.2
102	164	109521.9	1.1	9.7	0.8	4.2	1.7	0.3	1.5	0.9	1665.1	21.5	1671.7	13.7	1680.0	15.1	**1680.0**	**15.1**	99.1
103	125	90672.9	3.6	13.3	1.0	1.9	1.5	0.2	1.1	0.7	1067.1	10.7	1071.3	9.8	1080.0	20.2	**1080.0**	**20.2**	98.8
104	119	116323.8	2.6	12.5	1.0	2.3	1.6	0.2	1.3	0.8	1236.9	14.1	1224.6	11.2	1203.0	19.0	**1203.0**	**19.0**	102.8
105	32	21954.6	0.9	14.0	1.1	1.6	2.0	0.2	1.7	0.8	980.1	15.5	974.4	12.8	961.6	23.1	**961.6**	**23.1**	101.9
106	172	91807.7	3.3	13.7	0.9	1.7	1.6	0.2	1.4	0.8	988.1	12.5	995.4	10.5	1011.4	18.9	**1011.4**	**18.9**	97.7
107	220	16007551.7	4.1	11.4	1.0	2.9	1.5	0.2	1.2	0.8	1374.0	14.7	1375.8	11.7	1378.7	19.1	**1378.7**	**19.1**	99.7
109	22	2180425.6	1.6	17.2	1.9	0.6	2.2	0.1	1.1	0.5	473.5	5.0	483.0	8.3	528.6	40.7	**473.5**	**5.0**	89.6
11	54	91435.2	2.4	12.8	1.2	2.2	1.9	0.2	1.4	0.7	1201.3	15.3	1184.9	13.1	1155.0	24.7	**1155.0**	**24.7**	104.0
110	212	158491.0	2.8	12.2	0.9	2.4	1.5	0.2	1.2	0.8	1238.2	13.6	1240.5	10.9	1244.4	18.3	**1244.4**	**18.3**	99.5
111	718	208190.6	2.4	18.0	0.8	0.6	1.6	0.1	1.4	0.9	450.3	6.2	448.3	5.8	438.4	16.8	**450.3**	**6.2**	102.7
112	72	190432.3	4.5	13.6	1.1	1.7	1.8	0.2	1.4	0.8	1021.4	12.8	1022.5	11.4	1024.9	22.9	**1024.9**	**22.9**	99.7
113	69	188816.2	3.5	13.5	0.8	1.8	1.4	0.2	1.1	0.8	1048.3	11.0	1046.8	9.0	1043.8	15.4	**1043.8**	**15.4**	100.4
114	37	86866.6	1.3	11.5	1.0	2.3	1.7	0.2	1.4	0.8	1146.4	14.7	1220.0	12.3	1352.7	19.7	**1352.7**	**19.7**	84.7
115	160	488406.1	4.6	8.0	1.1	6.4	1.5	0.4	1.0	0.7	2042.2	17.2	2034.9	13.0	2027.5	19.6	**2027.5**	**19.6**	100.7
116	23	53849.4	4.5	12.8	1.5	2.2	2.1	0.2	1.4	0.7	1191.0	15.0	1174.9	14.3	1145.3	30.1	**1145.3**	**30.1**	104.0
117	9	4245.6	1.3	17.9	3.3	0.6	3.6	0.1	1.2	0.3	464.6	5.5	462.1	13.2	449.7	74.3	**464.6**	**5.5**	103.3
118	464	503140.0	2.9	12.7	0.8	2.1	1.5	0.2	1.2	0.8	1153.6	13.1	1155.1	10.1	1157.7	15.5	**1157.7**	**15.5**	99.6
119	290	1202140.9	2.6	10.6	0.9	3.4	1.5	0.3	1.2	0.8	1501.5	16.1	1503.8	11.8	1507.1	16.8	**1507.1**	**16.8**	99.6
12	330	221553.5	5.4	12.5	0.8	2.2	1.4	0.2	1.2	0.8	1182.4	12.5	1186.1	9.8	1192.8	15.7	**1192.8**	**15.7**	99.1
120	41	271203.9	1.3	4.4	1.0	19.0	1.7	0.6	1.4	0.8	3076.6	34.2	3039.9	16.5	3015.8	15.9	**3015.8**	**15.9**	102.0
121	47	445535.1	1.4	5.3	0.8	14.4	1.5	0.6	1.3	0.9	2843.1	30.3	2775.9	14.5	2727.4	12.6	**2727.4**	**12.6**	104.2
122	63	131297.1	1.5	17.1	1.5	0.7	1.9	0.1	1.1	0.6	559.3	6.1	557.5	8.1	550.1	33.0	**559.3**	**6.1**	101.7

123	23	47575.6	1.0	12.5	1.4	2.2	1.9	0.2	1.4	0.7	1186.0	14.6	1187.8	13.6	1191.1	27.7	**1191.1**	**27.7**	99.6
124	82	154863.9	1.3	13.9	1.0	1.6	1.4	0.2	1.0	0.7	986.1	9.3	984.5	8.9	981.0	19.7	**981.0**	**19.7**	100.5
125	115	56642.3	2.0	11.7	0.7	2.7	1.2	0.2	1.0	0.8	1339.4	12.1	1336.5	9.1	1331.9	13.6	**1331.9**	**13.6**	100.6
126	117	125820.6	1.8	12.7	0.9	2.1	1.3	0.2	0.9	0.7	1148.6	9.3	1155.9	8.9	1169.7	18.6	**1169.7**	**18.6**	98.2
127	35	132686.9	2.8	7.7	0.8	6.8	1.5	0.4	1.3	0.8	2087.7	22.4	2089.2	13.1	2090.7	13.7	**2090.7**	**13.7**	99.9
128	41	35461.9	3.8	12.7	1.1	2.2	1.5	0.2	1.0	0.7	1182.9	11.3	1174.1	10.6	1158.0	22.1	**1158.0**	**22.1**	102.2
129	14	53923.4	0.8	6.1	1.0	10.6	1.6	0.5	1.2	0.7	2473.1	23.9	2493.0	14.5	2509.1	17.6	**2509.1**	**17.6**	98.6
13	44	82928.9	5.6	9.3	1.0	4.6	1.8	0.3	1.5	0.8	1755.4	22.6	1758.2	14.7	1761.4	17.9	**1761.4**	**17.9**	99.7
130	95	88724.3	0.7	17.0	1.2	0.7	1.6	0.1	1.1	0.7	556.6	5.7	556.4	6.8	555.3	25.7	**556.6**	**5.7**	100.2
131	119	43450.8	1.1	17.7	1.1	0.5	1.6	0.1	1.2	0.7	437.6	5.1	442.1	5.9	465.6	24.6	**437.6**	**5.1**	94.0
132	46	34770.1	1.2	17.2	1.4	0.7	1.9	0.1	1.3	0.7	560.3	7.0	555.4	8.2	535.0	30.6	**560.3**	**7.0**	104.7
133	130	156112.2	2.6	12.7	0.8	2.2	1.3	0.2	1.1	0.8	1199.9	11.5	1185.6	9.3	1159.5	16.2	**1159.5**	**16.2**	103.5
134	56	351289.5	1.4	5.5	0.9	13.3	1.7	0.5	1.5	0.9	2722.9	33.2	2698.9	16.3	2680.9	14.3	**2680.9**	**14.3**	101.6
135	169	1023538.6	1.9	10.0	0.9	4.0	1.6	0.3	1.3	0.8	1654.9	18.7	1641.4	13.0	1624.2	17.7	**1624.2**	**17.7**	101.9
136	90	852716.3	2.1	13.3	1.0	1.8	1.6	0.2	1.2	0.8	1041.0	11.9	1049.5	10.3	1067.1	19.6	**1067.1**	**19.6**	97.6
137	334	236872.0	8.3	18.6	0.9	0.4	1.3	0.1	1.0	0.7	370.3	3.6	368.7	4.1	358.3	19.8	**370.3**	**3.6**	103.4
138	103	2098028.1	1.0	12.3	1.0	2.4	1.9	0.2	1.6	0.9	1249.3	18.1	1238.6	13.3	1219.9	19.1	**1219.9**	**19.1**	102.4
139	61	132895.4	1.8	13.8	1.1	1.6	1.6	0.2	1.2	0.7	984.5	11.0	988.9	10.3	998.6	22.1	**998.6**	**22.1**	98.6
14	64	16535.3	2.1	17.9	1.5	0.6	2.0	0.1	1.4	0.7	444.3	6.1	445.3	7.4	450.6	32.5	**444.3**	**6.1**	98.6
140	235	458417.9	2.4	5.5	0.9	12.1	1.4	0.5	1.1	0.8	2532.8	22.6	2612.7	13.0	2675.2	14.4	**2675.2**	**14.4**	94.7
141	20	20086.4	3.2	9.8	1.0	4.2	1.6	0.3	1.3	0.8	1689.5	19.5	1679.4	13.5	1666.8	18.1	**1666.8**	**18.1**	101.4
142	203	150369.9	1.2	10.8	1.1	3.1	1.9	0.2	1.5	0.8	1413.1	19.5	1442.2	14.4	1485.3	20.4	**1485.3**	**20.4**	95.1
143	57	245137.4	2.4	11.0	0.8	3.2	1.5	0.3	1.2	0.8	1450.9	16.0	1450.7	11.4	1450.5	15.4	**1450.5**	**15.4**	100.0
144	57	39516.8	3.3	11.1	0.9	3.1	1.6	0.3	1.4	0.8	1458.2	17.8	1443.3	12.6	1421.3	17.2	**1421.3**	**17.2**	102.6
145	85	156448.7	0.9	9.9	0.9	4.2	1.7	0.3	1.5	0.9	1713.2	22.9	1682.5	14.4	1644.5	15.9	**1644.5**	**15.9**	104.2
146	93	244424.8	1.6	13.5	0.9	1.7	1.9	0.2	1.6	0.9	1017.3	15.5	1026.2	12.2	1045.3	19.1	**1045.3**	**19.1**	97.3
147	270	309078.8	3.9	12.5	0.7	2.2	1.3	0.2	1.1	0.8	1171.4	11.9	1178.6	9.3	1191.9	14.5	**1191.9**	**14.5**	98.3
148	16	24377.3	1.7	12.9	1.5	2.1	2.0	0.2	1.4	0.7	1158.6	14.4	1149.9	13.9	1133.4	29.6	**1133.4**	**29.6**	102.2
149	461	271792.9	3.0	13.8	0.8	1.7	1.6	0.2	1.3	0.9	991.6	12.3	995.4	9.9	1003.9	16.2	**1003.9**	**16.2**	98.8
15	104	97989.0	2.9	11.0	0.9	3.2	1.7	0.3	1.5	0.9	1451.7	19.0	1446.4	13.2	1438.7	16.8	**1438.7**	**16.8**	100.9

150	96	139561.3	5.2	12.6	0.8	2.2	1.4	0.2	1.1	0.8	1187.7	12.1	1182.9	9.6	1174.1	15.9	**1174.1**	**15.9**	101.2
151	42	83075.8	1.0	8.6	1.0	5.6	1.9	0.4	1.6	0.9	1936.8	26.6	1914.4	16.1	1890.2	17.7	**1890.2**	**17.7**	102.5
152	91	100652.5	1.7	16.4	1.3	0.8	1.7	0.1	1.2	0.7	592.7	6.6	601.4	7.9	634.2	28.1	**592.7**	**6.6**	93.5
153	23	16653.0	1.6	16.9	1.6	0.8	2.1	0.1	1.4	0.7	596.6	7.8	592.6	9.3	577.1	34.0	**596.6**	**7.8**	103.4
154	63	59029.8	2.0	12.4	0.9	2.4	1.8	0.2	1.5	0.8	1267.6	17.3	1249.7	12.7	1219.1	18.4	**1219.1**	**18.4**	104.0
155	247	209387.4	29.3	5.2	0.8	13.3	1.6	0.5	1.3	0.8	2614.2	28.2	2699.3	14.7	2763.7	13.8	**2763.7**	**13.8**	94.6
156	139	870083.3	3.0	9.3	0.7	4.6	1.3	0.3	1.1	0.9	1726.7	17.2	1741.9	11.0	1760.1	12.5	**1760.1**	**12.5**	98.1
157	54	98621.5	0.6	5.2	0.8	14.2	1.6	0.5	1.4	0.9	2787.2	30.8	2765.1	14.8	2749.0	12.7	**2749.0**	**12.7**	101.4
158	73	66427.1	2.0	17.9	1.1	0.6	2.2	0.1	1.9	0.9	475.3	8.5	470.8	8.2	448.8	24.7	**475.3**	**8.5**	105.9
159	45	42287.8	1.5	13.5	1.2	1.7	1.8	0.2	1.4	0.8	1022.0	13.5	1027.0	11.9	1037.8	23.8	**1037.8**	**23.8**	98.5
161	36	195911.9	4.4	5.2	0.8	14.0	1.6	0.5	1.4	0.9	2733.7	30.1	2752.6	14.7	2766.4	12.5	**2766.4**	**12.5**	98.8
162	38	42953.1	1.7	13.8	1.4	1.7	1.9	0.2	1.3	0.7	1009.1	11.9	1004.7	12.0	995.1	28.0	**995.1**	**28.0**	101.4
163	38	150681.2	2.4	13.2	0.9	1.9	2.0	0.2	1.8	0.9	1102.1	17.9	1096.2	13.3	1084.6	18.3	**1084.6**	**18.3**	101.6
164	223	152874.4	3.1	12.1	1.2	2.3	2.0	0.2	1.6	0.8	1167.4	17.3	1197.7	14.1	1252.9	23.0	**1252.9**	**23.0**	93.2
165	126	644720.7	2.2	10.9	1.1	3.2	1.6	0.3	1.2	0.7	1467.5	15.7	1466.2	12.7	1464.2	21.2	**1464.2**	**21.2**	100.2
166	53	24361.8	1.8	13.1	1.0	2.0	1.7	0.2	1.3	0.8	1127.0	13.5	1120.4	11.3	1107.6	20.4	**1107.6**	**20.4**	101.8
167	100	63805.8	3.2	12.5	0.8	2.2	1.4	0.2	1.2	0.8	1161.0	12.7	1172.3	10.0	1193.1	15.7	**1193.1**	**15.7**	97.3
168	72	109609.8	3.8	12.9	1.0	2.1	1.6	0.2	1.2	0.8	1147.7	12.8	1144.8	10.7	1139.2	19.3	**1139.2**	**19.3**	100.7
169	40	11218.1	3.4	17.5	1.3	0.6	2.0	0.1	1.5	0.8	460.8	6.8	467.5	7.4	500.4	27.6	**460.8**	**6.8**	92.1
170	103	2276687.3	1.5	7.8	0.9	6.8	1.5	0.4	1.2	0.8	2095.2	22.1	2086.6	13.7	2078.1	16.2	**2078.1**	**16.2**	100.8
171	46	41127.6	1.8	16.5	1.4	0.8	1.8	0.1	1.1	0.6	622.0	6.8	622.7	8.3	625.1	29.7	**622.0**	**6.8**	99.5
172	150	1394755.4	1.8	18.0	1.1	0.5	2.1	0.1	1.8	0.9	392.7	6.9	398.0	6.9	429.1	23.6	**392.7**	**6.9**	91.5
173	31	18328.2	2.7	12.2	1.5	2.5	2.0	0.2	1.4	0.7	1276.7	15.8	1265.9	14.6	1247.7	28.9	**1247.7**	**28.9**	102.3
174	105	1284405.2	2.0	12.7	0.9	2.1	1.5	0.2	1.2	0.8	1119.1	12.4	1134.4	10.4	1163.7	18.4	**1163.7**	**18.4**	96.2
175	120	200768.9	0.8	9.2	0.8	4.8	1.6	0.3	1.4	0.9	1805.9	21.6	1790.8	13.5	1773.3	15.1	**1773.3**	**15.1**	101.8
176	96	315948.9	3.5	10.6	0.9	3.4	1.6	0.3	1.4	0.8	1504.4	18.7	1512.0	12.9	1522.6	16.3	**1522.6**	**16.3**	98.8
177	86	186836.7	3.6	9.9	0.9	3.9	1.9	0.3	1.6	0.9	1593.5	23.3	1614.4	15.3	1641.8	17.3	**1641.8**	**17.3**	97.1
178	55	26816.3	2.2	12.6	1.0	2.2	1.5	0.2	1.1	0.8	1164.5	12.2	1168.5	10.6	1176.0	19.9	**1176.0**	**19.9**	99.0
179	48	1396971.6	3.0	13.2	1.2	1.9	1.7	0.2	1.3	0.7	1059.4	12.6	1069.1	11.5	1088.9	23.3	**1088.9**	**23.3**	97.3
18	56	77729.6	1.9	11.3	1.0	3.0	1.8	0.2	1.5	0.8	1401.7	18.8	1396.9	13.5	1389.6	18.4	**1389.6**	**18.4**	100.9

180	161	99057.9	1.4	12.6	1.0	2.2	1.7	0.2	1.3	0.8	1172.3	14.5	1175.0	11.7	1179.9	20.1	**1179.9**	**20.1**	99.4
181	151	142147.5	1.9	11.1	1.0	2.9	1.4	0.2	1.0	0.7	1359.1	12.4	1388.1	10.9	1433.0	19.6	**1433.0**	**19.6**	94.8
182	364	83124.2	2.1	17.0	0.8	0.7	1.9	0.1	1.7	0.9	524.4	8.4	531.0	7.7	559.7	18.4	**524.4**	**8.4**	93.7
183	75	92176.3	5.1	14.0	1.2	1.5	1.7	0.2	1.2	0.7	938.2	10.4	948.6	10.3	972.6	24.1	**972.6**	**24.1**	96.5
184	266	121670.9	3.9	11.4	0.8	3.0	1.4	0.2	1.1	0.8	1423.3	13.9	1404.5	10.3	1376.1	15.4	**1376.1**	**15.4**	103.4
185	92	325381.7	2.2	12.9	1.0	1.9	1.6	0.2	1.3	0.8	1050.0	12.2	1078.5	10.6	1136.7	19.5	**1136.7**	**19.5**	92.4
186	48	183187.1	2.7	10.0	0.9	4.1	1.6	0.3	1.3	0.8	1679.2	18.7	1658.4	12.8	1632.1	17.1	**1632.1**	**17.1**	102.9
187	85	517509.9	3.5	13.4	1.0	1.8	1.6	0.2	1.2	0.8	1059.3	12.1	1061.0	10.5	1064.6	20.0	**1064.6**	**20.0**	99.5
188	108	120543.9	1.1	9.8	1.1	4.0	1.9	0.3	1.5	0.8	1619.1	21.2	1633.7	15.1	1652.4	21.0	**1652.4**	**21.0**	98.0
189	305	3820652.6	3.6	13.5	0.9	1.7	1.5	0.2	1.2	0.8	1018.7	11.7	1026.0	10.0	1041.5	18.6	**1041.5**	**18.6**	97.8
19	22	26572.5	4.5	12.4	1.1	2.4	1.8	0.2	1.4	0.8	1243.0	16.0	1229.6	13.0	1206.2	22.6	**1206.2**	**22.6**	103.0
190	155	61187.9	2.3	12.3	1.1	2.1	1.8	0.2	1.4	0.8	1130.2	14.6	1162.5	12.2	1223.1	21.0	**1223.1**	**21.0**	92.4
191	434	164807.2	3.0	12.1	0.9	2.5	1.8	0.2	1.5	0.8	1292.8	17.7	1282.7	13.0	1265.8	18.4	**1265.8**	**18.4**	102.1
192	151	323545.7	1.9	12.5	1.1	2.2	1.6	0.2	1.2	0.7	1160.9	12.8	1171.8	11.4	1192.1	21.8	**1192.1**	**21.8**	97.4
193	76	53323.9	2.9	13.9	1.2	1.5	2.0	0.2	1.6	0.8	923.8	13.7	940.6	12.0	980.2	23.5	**980.2**	**23.5**	94.3
194	327	108028.9	1.6	17.8	1.1	0.6	1.6	0.1	1.1	0.7	441.6	4.9	445.1	5.7	463.5	24.5	**441.6**	**4.9**	95.3
195	84	127373.1	3.8	13.1	1.1	2.0	1.6	0.2	1.2	0.8	1119.6	12.7	1115.8	11.0	1108.5	21.1	**1108.5**	**21.1**	101.0
196	201	121464.4	15.8	12.5	1.0	2.1	1.6	0.2	1.3	0.8	1140.4	13.1	1157.8	11.0	1190.4	19.4	**1190.4**	**19.4**	95.8
197	19	8297.3	2.2	14.3	1.2	1.6	1.8	0.2	1.3	0.7	975.1	12.2	961.8	11.2	931.5	24.9	**931.5**	**24.9**	104.7
198	60	73829.0	2.4	13.3	0.8	1.9	1.3	0.2	1.0	0.8	1082.7	9.7	1077.7	8.3	1067.6	15.9	**1067.6**	**15.9**	101.4
199	69	61604.2	2.8	13.3	1.1	1.8	1.8	0.2	1.4	0.8	1061.6	14.1	1063.3	12.0	1067.0	22.3	**1067.0**	**22.3**	99.5
2	36	89790.8	3.7	13.8	1.1	1.7	1.7	0.2	1.3	0.8	1023.9	11.9	1017.0	10.6	1002.2	21.7	**1002.2**	**21.7**	102.2
20	48	422404.4	3.1	12.7	1.1	2.2	1.9	0.2	1.5	0.8	1170.4	15.8	1168.2	13.0	1164.1	22.8	**1164.1**	**22.8**	100.5
200	192	136102.2	1.3	17.7	1.1	0.6	1.7	0.1	1.3	0.8	450.5	5.5	454.4	6.2	474.0	24.8	**450.5**	**5.5**	95.0
201	401	604347.2	6.3	16.4	0.9	0.9	1.8	0.1	1.6	0.9	621.4	9.4	625.2	8.6	638.9	20.1	**621.4**	**9.4**	97.3
202	109	37685.6	5.7	13.0	0.9	2.0	1.4	0.2	1.1	0.8	1127.5	11.4	1125.4	9.8	1121.4	18.4	**1121.4**	**18.4**	100.5
203	191	1086375.7	1.7	11.0	1.0	3.1	1.7	0.3	1.4	0.8	1440.2	18.3	1443.5	13.4	1448.5	19.3	**1448.5**	**19.3**	99.4
204	57	37771.5	1.6	13.9	1.3	1.7	1.9	0.2	1.3	0.7	1003.1	12.0	997.0	11.8	983.6	27.4	**983.6**	**27.4**	102.0
205	86	198029.8	2.7	10.7	0.8	3.5	1.6	0.3	1.4	0.9	1562.7	19.9	1536.6	13.0	1500.8	14.9	**1500.8**	**14.9**	104.1
206	87	135101.9	3.1	9.0	0.8	4.9	1.6	0.3	1.4	0.9	1802.8	22.4	1807.0	13.6	1811.7	13.7	**1811.7**	**13.7**	99.5

207	61	298198.6	2.5	13.4	1.2	1.9	1.8	0.2	1.3	0.7	1076.7	13.1	1072.1	12.0	1062.7	24.7	**1062.7**	**24.7**	101.3
208	93	198039.5	1.7	9.7	1.0	4.1	1.7	0.3	1.4	0.8	1630.0	20.6	1647.9	14.2	1670.7	18.3	**1670.7**	**18.3**	97.6
209	182	288177.4	67.0	11.8	0.8	2.7	1.4	0.2	1.2	0.8	1328.6	13.9	1318.8	10.4	1302.8	15.7	**1302.8**	**15.7**	102.0
21	75	488247.3	2.1	8.2	1.0	6.1	1.6	0.4	1.2	0.8	2007.7	21.0	1994.8	13.6	1981.4	17.4	**1981.4**	**17.4**	101.3
210	77	119646.7	2.3	13.1	1.1	1.9	1.7	0.2	1.3	0.8	1095.2	13.3	1097.3	11.3	1101.4	21.1	**1101.4**	**21.1**	99.4
211	108	139992.2	1.1	8.8	0.8	5.4	1.4	0.3	1.2	0.8	1897.2	19.2	1879.2	12.3	1859.4	15.0	**1859.4**	**15.0**	102.0
212	731	776871.7	8.0	16.3	0.8	0.9	1.6	0.1	1.4	0.9	626.3	8.1	632.2	7.4	653.2	17.2	**626.3**	**8.1**	95.9
213	158	60838.2	2.6	13.4	1.2	1.8	1.6	0.2	1.1	0.7	1062.3	10.6	1059.0	10.5	1052.3	23.9	**1052.3**	**23.9**	100.9
215	36	54893.7	1.8	9.4	1.0	4.6	1.7	0.3	1.3	0.8	1757.9	20.6	1747.7	14.1	1735.5	18.7	**1735.5**	**18.7**	101.3
216	358	507740.7	2.7	8.9	0.8	5.0	1.7	0.3	1.5	0.9	1820.8	23.5	1827.4	14.1	1835.0	13.9	**1835.0**	**13.9**	99.2
217	171	118603.4	4.2	13.6	1.0	1.7	1.9	0.2	1.6	0.9	1010.6	15.0	1014.1	12.1	1021.6	20.2	**1021.6**	**20.2**	98.9
218	32	16398.4	1.4	17.7	2.1	0.6	2.5	0.1	1.3	0.5	448.1	5.6	451.1	9.0	466.4	46.3	**448.1**	**5.6**	96.1
22	198	148896.3	6.4	12.9	1.1	2.1	1.8	0.2	1.5	0.8	1130.3	15.1	1133.0	12.4	1138.0	21.5	**1138.0**	**21.5**	99.3
220	77	64597.8	1.5	15.2	1.4	1.2	1.9	0.1	1.3	0.7	804.4	9.5	804.3	10.3	804.0	28.4	**804.4**	**9.5**	100.1
221	107	131192.6	3.8	10.2	1.0	3.3	1.7	0.2	1.3	0.8	1384.7	16.4	1469.6	12.9	1594.5	19.0	**1594.5**	**19.0**	86.8
222	59	59145.7	4.9	16.5	1.1	0.9	1.5	0.1	0.9	0.6	653.7	5.8	647.1	7.0	624.0	24.5	**653.7**	**5.8**	104.8
223	34	29948.0	1.5	10.7	1.0	3.5	1.7	0.3	1.3	0.8	1527.8	17.7	1516.7	13.0	1501.4	19.4	**1501.4**	**19.4**	101.8
224	292	1557090.8	2.9	10.6	0.9	3.4	1.5	0.3	1.2	0.8	1514.0	15.7	1510.4	11.5	1505.4	16.9	**1505.4**	**16.9**	100.6
225	192	36451.7	2.1	17.8	1.2	0.5	1.8	0.1	1.3	0.7	427.4	5.2	431.9	6.2	455.9	27.3	**427.4**	**5.2**	93.8
226	23	140381.4	3.2	12.3	1.3	2.4	1.8	0.2	1.3	0.7	1239.9	15.1	1237.3	13.2	1232.8	25.0	**1232.8**	**25.0**	100.6
227	70	237487.9	1.3	13.1	1.1	1.9	1.7	0.2	1.3	0.8	1091.5	13.4	1095.8	11.5	1104.2	21.3	**1104.2**	**21.3**	98.9
228	20	7053.9	1.3	13.8	1.5	1.6	2.0	0.2	1.4	0.7	967.6	12.5	977.0	12.8	998.2	30.4	**998.2**	**30.4**	96.9
23	208	154711.3	5.0	13.4	1.0	1.8	1.9	0.2	1.6	0.9	1058.6	15.6	1055.9	12.3	1050.3	19.6	**1050.3**	**19.6**	100.8
230	122	152228.7	2.5	12.8	0.9	2.1	1.5	0.2	1.3	0.8	1161.0	13.5	1154.6	10.6	1142.6	17.0	**1142.6**	**17.0**	101.6
231	99	131671.4	3.5	12.6	1.1	2.1	1.6	0.2	1.2	0.7	1128.0	12.0	1146.1	10.9	1180.7	21.4	**1180.7**	**21.4**	95.5
232	113	193470.1	3.7	13.5	0.8	1.8	1.4	0.2	1.1	0.8	1027.6	10.7	1033.9	9.0	1047.2	16.3	**1047.2**	**16.3**	98.1
234	50	52330.1	2.8	18.0	1.4	0.5	2.1	0.1	1.6	0.7	424.9	6.4	425.4	7.3	428.6	31.5	**424.9**	**6.4**	99.1
235	310	659791.5	85.0	13.5	0.9	1.8	1.8	0.2	1.6	0.9	1040.3	15.5	1041.0	12.0	1042.4	18.0	**1042.4**	**18.0**	99.8
236	105	159153.2	2.9	12.8	1.1	2.2	1.6	0.2	1.1	0.7	1181.1	12.2	1171.6	11.2	1154.2	22.7	**1154.2**	**22.7**	102.3
237	329	2054976.8	4.3	16.4	0.9	0.9	1.5	0.1	1.2	0.8	623.9	7.3	627.4	7.1	640.1	19.5	**623.9**	**7.3**	97.5

239	90	72331.0	3.7	13.3	1.1	1.8	1.5	0.2	1.1	0.7	1058.1	10.3	1060.7	9.8	1066.1	21.1	**1066.1**	**21.1**	99.3
24	30	49021.9	1.5	15.9	1.4	0.9	2.2	0.1	1.6	0.7	629.1	9.7	644.9	10.3	700.6	30.6	**629.1**	**9.7**	89.8
240	23	120682.3	1.4	18.4	2.4	0.5	2.8	0.1	1.4	0.5	427.3	5.8	421.0	9.6	386.6	54.0	**427.3**	**5.8**	110.5
241	236	115558.2	16.1	12.9	1.1	2.0	1.6	0.2	1.2	0.8	1120.2	12.8	1122.6	11.1	1127.4	21.0	**1127.4**	**21.0**	99.4
242	87	61099.8	1.4	10.5	1.1	3.6	1.8	0.3	1.4	0.8	1565.9	20.0	1554.2	14.3	1538.4	20.2	**1538.4**	**20.2**	101.8
243	122	103442.3	1.8	10.7	1.0	3.3	1.5	0.3	1.1	0.7	1464.6	14.0	1478.0	11.4	1497.3	19.1	**1497.3**	**19.1**	97.8
244	23	136453.1	2.9	13.5	1.1	1.7	1.6	0.2	1.2	0.8	1000.3	11.6	1013.0	10.5	1040.4	21.4	**1040.4**	**21.4**	96.2
246	282	417288.0	5.5	8.7	0.8	5.4	1.3	0.3	1.0	0.8	1886.2	16.8	1883.4	11.3	1880.3	14.7	**1880.3**	**14.7**	100.3
247	203	409800.7	2.3	10.7	0.9	3.4	1.6	0.3	1.3	0.8	1511.9	17.8	1506.4	12.5	1498.7	17.0	**1498.7**	**17.0**	100.9
248	41	31289.5	1.0	10.0	1.0	4.1	1.9	0.3	1.6	0.8	1660.5	22.8	1646.3	15.1	1628.2	18.8	**1628.2**	**18.8**	102.0
249	141	477212.3	1.8	13.7	1.0	1.7	1.5	0.2	1.1	0.7	989.5	10.0	996.4	9.5	1011.6	20.5	**1011.6**	**20.5**	97.8
25	81	549171.3	3.2	13.3	1.0	1.8	1.5	0.2	1.1	0.7	1033.2	10.3	1047.1	9.6	1076.2	20.2	**1076.2**	**20.2**	96.0
250	56	31409.0	5.3	13.5	1.0	1.8	1.7	0.2	1.4	0.8	1032.9	13.5	1034.9	11.3	1039.1	20.4	**1039.1**	**20.4**	99.4
251	60	33012.7	1.2	10.6	0.9	3.4	1.7	0.3	1.4	0.9	1478.6	18.7	1495.2	13.0	1518.9	16.5	**1518.9**	**16.5**	97.3
252	24	11986.5	1.0	17.6	2.2	0.7	2.5	0.1	1.3	0.5	569.1	7.0	552.4	10.7	484.3	47.8	**569.1**	**7.0**	117.5
253	255	270913.8	1.9	17.9	1.0	0.6	1.6	0.1	1.3	0.8	449.7	5.5	449.9	5.8	451.2	21.8	**449.7**	**5.5**	99.7
254	72	2160254.9	1.9	7.9	0.9	6.7	1.6	0.4	1.3	0.8	2106.2	22.9	2075.2	14.0	2044.5	16.6	**2044.5**	**16.6**	103.0
255	174	265564.5	14.7	13.0	0.8	2.0	1.3	0.2	1.0	0.8	1094.2	10.3	1101.9	8.8	1117.2	16.2	**1117.2**	**16.2**	97.9
256	103	144205.1	1.0	9.8	0.9	4.1	1.5	0.3	1.3	0.8	1647.2	18.4	1652.5	12.5	1659.4	16.1	**1659.4**	**16.1**	99.3
258	397	768497.2	8.9	10.0	0.8	3.9	2.0	0.3	1.8	0.9	1629.5	25.6	1623.2	15.9	1615.1	15.5	**1615.1**	**15.5**	100.9
259	19	9895.3	1.8	13.6	1.4	1.7	2.1	0.2	1.5	0.7	995.8	14.3	1005.3	13.4	1026.0	28.7	**1026.0**	**28.7**	97.1
26	29	34305.1	1.2	9.9	1.3	4.2	1.9	0.3	1.3	0.7	1693.8	19.7	1674.0	15.2	1649.3	24.1	**1649.3**	**24.1**	102.7
260	85	114109.3	6.7	12.7	1.1	2.2	1.9	0.2	1.5	0.8	1207.5	16.2	1189.9	13.0	1157.9	22.4	**1157.9**	**22.4**	104.3
261	100	178073.0	4.7	13.2	0.9	2.0	1.4	0.2	1.0	0.7	1111.4	10.3	1102.3	9.1	1084.3	18.1	**1084.3**	**18.1**	102.5
262	214	147543.6	1.2	9.6	0.8	4.4	1.4	0.3	1.2	0.8	1711.6	17.8	1703.2	11.8	1692.9	14.8	**1692.9**	**14.8**	101.1
263	87	20020.6	1.2	18.0	1.3	0.6	1.7	0.1	1.2	0.7	454.2	5.2	451.3	6.4	436.5	28.7	**454.2**	**5.2**	104.1
265	457	702537.2	4.3	9.3	0.8	4.7	1.7	0.3	1.4	0.9	1767.7	22.2	1763.1	13.9	1757.5	15.2	**1757.5**	**15.2**	100.6
266	80	41025.2	3.1	13.5	1.0	1.8	1.7	0.2	1.3	0.8	1034.2	12.3	1035.8	10.8	1039.2	21.1	**1039.2**	**21.1**	99.5
267	86	143709.5	2.3	13.6	0.9	1.8	1.3	0.2	0.9	0.7	1054.2	8.6	1046.8	8.4	1031.4	19.1	**1031.4**	**19.1**	102.2
268	67	147361.6	3.2	15.5	1.2	1.0	1.7	0.1	1.2	0.7	694.4	7.9	710.3	8.7	760.8	25.6	**694.4**	**7.9**	91.3

269	11	29152.8	1.1	13.5	2.0	1.9	2.5	0.2	1.6	0.6	1079.6	15.6	1069.3	16.7	1048.3	39.7	**1048.3**	**39.7**	103.0
27	63	46137.8	4.5	13.4	1.1	1.9	1.6	0.2	1.2	0.8	1101.4	12.2	1089.2	10.7	1064.9	21.2	**1064.9**	**21.2**	103.4
270	210	130390.5	5.1	13.7	0.9	1.8	1.7	0.2	1.5	0.9	1036.2	14.1	1030.2	11.2	1017.5	18.1	**1017.5**	**18.1**	101.8
271	256	298779.1	2.1	12.0	0.8	2.5	1.4	0.2	1.2	0.8	1279.2	13.7	1276.5	10.4	1271.9	15.8	**1271.9**	**15.8**	100.6
272	99	125494.7	2.6	11.3	1.1	3.0	1.6	0.2	1.2	0.7	1418.6	15.1	1408.0	12.4	1392.0	21.4	**1392.0**	**21.4**	101.9
273	123	71584.2	2.5	12.6	0.9	2.1	1.4	0.2	1.1	0.8	1142.7	11.1	1158.2	9.5	1187.3	17.4	**1187.3**	**17.4**	96.2
274	152	1362639.2	2.7	10.7	0.9	3.4	1.4	0.3	1.0	0.8	1504.4	14.0	1501.9	10.7	1498.2	16.6	**1498.2**	**16.6**	100.4
275	101	39233.7	1.6	15.7	0.9	1.0	1.5	0.1	1.3	0.8	720.2	8.5	721.8	8.0	727.1	19.4	**720.2**	**8.5**	99.1
276	78	92264.3	2.7	13.4	1.2	1.8	1.7	0.2	1.2	0.7	1032.9	11.0	1040.3	11.1	1055.9	25.2	**1055.9**	**25.2**	97.8
277	28	373624.6	7.4	5.3	0.9	13.9	1.5	0.5	1.1	0.8	2763.3	24.7	2741.4	13.8	2725.4	15.6	**2725.4**	**15.6**	101.4
278	55	2234160.9	5.2	5.2	1.0	14.7	1.7	0.6	1.3	0.8	2847.8	30.8	2792.8	15.8	2753.3	16.3	**2753.3**	**16.3**	103.4
279	49	571167.2	2.0	10.8	1.0	3.3	1.8	0.3	1.4	0.8	1488.8	19.0	1486.0	13.8	1482.0	19.9	**1482.0**	**19.9**	100.5
28	33	66779.4	2.7	10.8	0.9	3.4	1.6	0.3	1.4	0.8	1523.1	18.5	1505.5	12.9	1480.7	17.1	**1480.7**	**17.1**	102.9
280	408	413984.5	1.5	18.0	1.0	0.5	1.8	0.1	1.5	0.8	432.5	6.5	432.6	6.5	433.3	22.5	**432.5**	**6.5**	99.8
281	121	34452465.3	1.8	10.8	0.8	3.4	1.4	0.3	1.2	0.8	1518.0	15.9	1504.0	11.3	1484.3	15.7	**1484.3**	**15.7**	102.3
282	61	149962.4	3.2	12.8	1.0	2.1	1.6	0.2	1.3	0.8	1150.7	14.0	1147.9	11.3	1142.5	19.3	**1142.5**	**19.3**	100.7
283	144	44926.7	1.2	15.6	0.9	1.1	1.5	0.1	1.3	0.8	776.8	9.2	769.3	8.3	747.5	18.9	**776.8**	**9.2**	103.9
284	44	83013.0	2.7	10.8	0.9	3.3	1.5	0.3	1.3	0.8	1486.4	16.7	1484.7	12.0	1482.4	16.8	**1482.4**	**16.8**	100.3
285	283	247805.6	6.2	13.4	0.9	1.8	1.4	0.2	1.1	0.8	1047.2	10.5	1048.2	9.4	1050.1	19.1	**1050.1**	**19.1**	99.7
286	159	644065.3	2.1	12.1	0.7	2.5	1.4	0.2	1.2	0.9	1257.6	14.0	1258.8	10.1	1260.7	13.3	**1260.7**	**13.3**	99.8
287	26	27069.6	3.0	13.3	1.4	1.8	1.8	0.2	1.2	0.7	1043.2	11.6	1053.7	11.9	1075.5	27.3	**1075.5**	**27.3**	97.0
288	206	1786183.8	2.4	13.2	1.0	1.9	1.5	0.2	1.2	0.8	1081.8	11.8	1083.7	10.1	1087.7	19.1	**1087.7**	**19.1**	99.5
289	86	40311.9	1.4	18.1	1.0	0.5	1.7	0.1	1.3	0.8	429.5	5.5	428.3	5.8	422.2	22.6	**429.5**	**5.5**	101.7
290	213	258401.3	4.0	12.3	0.9	2.3	1.5	0.2	1.1	0.8	1225.6	12.4	1225.1	10.3	1224.2	18.3	**1224.2**	**18.3**	100.1
291	33	24610.7	2.5	13.3	1.5	1.9	2.0	0.2	1.3	0.6	1065.1	12.3	1068.7	12.9	1076.0	30.2	**1076.0**	**30.2**	99.0
292	31	230038.6	2.5	7.2	0.9	7.8	1.7	0.4	1.4	0.8	2200.8	26.0	2207.3	15.0	2213.4	15.8	**2213.4**	**15.8**	99.4
294	281	103776.6	9.0	16.1	0.8	0.9	1.3	0.1	1.0	0.8	654.6	6.3	658.4	6.2	671.3	16.5	**654.6**	**6.3**	97.5
295	194	295794.4	3.2	13.2	0.7	1.8	1.5	0.2	1.3	0.9	1053.8	12.5	1062.4	9.6	1080.3	13.7	**1080.3**	**13.7**	97.5
296	38	112293.6	2.9	10.7	1.1	3.4	1.9	0.3	1.6	0.8	1513.8	21.1	1509.1	15.0	1502.6	20.9	**1502.6**	**20.9**	100.7
297	181	215924.4	5.3	11.8	1.1	2.6	1.6	0.2	1.1	0.7	1300.4	13.4	1301.6	11.5	1303.6	20.9	**1303.6**	**20.9**	99.8

298	182	148858.0	2.9	13.5	1.1	1.8	2.0	0.2	1.6	0.8	1062.5	16.1	1056.6	12.8	1044.4	21.3	**1044.4**	**21.3**	101.7
299	70	81445.6	4.6	16.8	1.3	0.7	1.8	0.1	1.2	0.7	547.4	6.5	554.1	7.6	581.8	27.3	**547.4**	**6.5**	94.1
3	33	19337.2	1.2	13.3	1.4	1.9	1.9	0.2	1.3	0.7	1098.2	12.9	1090.8	12.7	1076.2	28.3	**1076.2**	**28.3**	102.0
30	136	119671.0	1.0	15.0	0.9	1.2	1.5	0.1	1.2	0.8	789.8	9.3	799.6	8.4	827.1	18.3	**789.8**	**9.3**	95.5
300	189	172485.0	2.3	14.0	0.9	1.6	1.7	0.2	1.5	0.9	989.2	13.8	981.5	10.9	964.3	17.8	**964.3**	**17.8**	102.6
301	152	95872.3	2.0	17.9	1.2	0.6	1.8	0.1	1.3	0.7	448.6	5.7	448.2	6.4	446.2	26.2	**448.6**	**5.7**	100.5
302	36	225698.4	1.8	12.2	1.3	2.5	1.8	0.2	1.2	0.7	1275.9	14.3	1266.0	13.2	1249.1	26.3	**1249.1**	**26.3**	102.1
303	40	134293.6	2.3	10.0	1.0	3.9	1.7	0.3	1.4	0.8	1583.7	19.3	1603.7	13.5	1630.0	17.9	**1630.0**	**17.9**	97.2
304	155	812094.2	2.7	13.3	0.8	1.9	1.5	0.2	1.2	0.8	1060.6	12.0	1067.0	9.6	1080.1	15.5	**1080.1**	**15.5**	98.2
305	36	42579.3	1.1	13.5	1.1	1.9	1.7	0.2	1.3	0.8	1082.0	13.4	1070.3	11.5	1046.5	22.3	**1046.5**	**22.3**	103.4
307	65	1117911.8	12.1	10.8	0.9	3.4	1.8	0.3	1.5	0.8	1520.5	20.1	1500.2	13.8	1471.8	18.0	**1471.8**	**18.0**	103.3
308	79	20080.2	1.7	17.7	1.4	0.6	1.7	0.1	1.0	0.6	466.0	4.6	467.9	6.4	476.9	30.1	**466.0**	**4.6**	97.7
309	74	131241.6	1.7	12.9	0.9	2.0	1.6	0.2	1.3	0.8	1111.7	13.6	1118.8	10.9	1132.6	17.7	**1132.6**	**17.7**	98.2
31	247	270936.3	7.9	12.5	0.8	2.2	1.6	0.2	1.4	0.9	1198.1	15.4	1195.6	11.5	1191.1	16.4	**1191.1**	**16.4**	100.6
310	97	87976.9	4.6	13.1	0.9	2.0	1.6	0.2	1.3	0.8	1097.3	13.3	1100.7	10.6	1107.3	17.1	**1107.3**	**17.1**	99.1
311	78	135113.1	3.1	10.9	1.0	3.2	1.8	0.3	1.4	0.8	1465.8	18.9	1467.4	13.6	1469.6	19.1	**1469.6**	**19.1**	99.7
312	173	131776.0	1.6	9.7	0.9	4.3	1.5	0.3	1.2	0.8	1699.6	17.6	1687.9	12.2	1673.4	16.5	**1673.4**	**16.5**	101.6
313	78	85068.0	2.0	12.4	1.0	2.3	1.6	0.2	1.3	0.8	1191.9	14.0	1198.5	11.5	1210.5	19.8	**1210.5**	**19.8**	98.5
314	146	27819.6	4.0	18.1	1.2	0.5	1.6	0.1	1.1	0.7	416.9	4.6	416.7	5.6	415.6	26.3	**416.9**	**4.6**	100.3
315	111	122701.7	5.2	9.2	0.9	4.8	1.5	0.3	1.2	0.8	1776.5	18.3	1776.3	12.3	1776.0	15.9	**1776.0**	**15.9**	100.0
32	154	180907.2	2.5	8.5	1.0	5.7	1.8	0.3	1.5	0.8	1920.6	24.7	1924.8	15.3	1929.3	17.2	**1929.3**	**17.2**	99.5
33	151	252483.6	7.6	12.7	1.0	2.1	2.0	0.2	1.7	0.9	1138.4	18.2	1147.7	13.8	1165.2	19.7	**1165.2**	**19.7**	97.7
34	43	444469.7	2.5	10.9	1.0	3.2	1.5	0.3	1.1	0.8	1465.8	15.1	1461.5	11.7	1455.1	18.5	**1455.1**	**18.5**	100.7
35	183	351120.6	1.9	13.5	0.8	1.8	1.3	0.2	1.0	0.8	1053.4	9.9	1050.1	8.3	1043.3	15.5	**1043.3**	**15.5**	101.0
36	83	98169.6	3.0	10.8	0.9	3.3	1.9	0.3	1.7	0.9	1481.6	22.1	1481.0	14.9	1480.2	17.6	**1480.2**	**17.6**	100.1
37	67	364400.1	2.2	12.0	1.0	2.5	1.7	0.2	1.4	0.8	1249.5	16.5	1259.9	12.6	1277.7	19.1	**1277.7**	**19.1**	97.8
38	50	149316.4	1.3	11.4	0.8	2.9	1.7	0.2	1.5	0.9	1407.2	18.5	1394.1	12.6	1374.1	15.5	**1374.1**	**15.5**	102.4
39	163	242324.9	3.2	9.0	0.8	5.0	1.6	0.3	1.3	0.8	1803.5	20.5	1814.3	13.1	1826.8	15.2	**1826.8**	**15.2**	98.7
4	12	83849.2	81900.2	16.1	3.9	0.8	4.3	0.1	1.7	0.4	557.1	9.1	580.3	18.8	672.6	83.4	**557.1**	**9.1**	82.8
40	40	25678.0	0.8	8.0	1.4	5.9	1.9	0.3	1.3	0.7	1899.9	21.4	1957.6	16.3	2019.2	24.1	**2019.2**	**24.1**	94.1

41	158	52052.4	2.2	12.6	0.8	2.2	1.7	0.2	1.4	0.9	1154.6	15.2	1166.2	11.6	1187.9	16.7	**1187.9**	**16.7**	97.2
42	77	443690.6	2.3	12.2	0.9	2.0	2.4	0.2	2.2	0.9	1073.7	22.2	1131.3	16.4	1243.7	17.3	**1243.7**	**17.3**	86.3
43	86	261738.2	2.2	13.4	1.2	1.9	1.8	0.2	1.3	0.7	1097.5	13.4	1085.4	11.9	1061.4	24.1	**1061.4**	**24.1**	103.4
44	15	10397.0	1.1	13.6	1.4	1.7	2.1	0.2	1.5	0.7	996.2	14.3	1006.9	13.5	1030.2	28.9	**1030.2**	**28.9**	96.7
45	209	201916.8	6.8	18.7	1.0	0.4	1.4	0.1	1.0	0.7	380.8	3.7	377.1	4.4	353.9	21.5	**380.8**	**3.7**	107.6
46	58	22599.8	2.7	18.2	1.7	0.5	2.1	0.1	1.3	0.6	402.2	5.1	403.4	7.1	410.4	38.0	**402.2**	**5.1**	98.0
47	24	40149.6	1.6	5.7	1.1	11.7	1.8	0.5	1.4	0.8	2556.0	29.6	2580.3	16.7	2599.5	18.3	**2599.5**	**18.3**	98.3
48	211	152952.1	1.3	10.9	0.9	3.2	1.6	0.3	1.3	0.8	1463.9	17.0	1466.3	12.5	1469.8	17.9	**1469.8**	**17.9**	99.6
49	89	281198.5	3.2	13.0	0.8	2.0	1.7	0.2	1.5	0.9	1127.1	16.0	1122.5	11.8	1113.6	16.0	**1113.6**	**16.0**	101.2
5	196	146727.5	3.5	12.1	0.8	2.4	2.0	0.2	1.8	0.9	1224.7	20.1	1236.5	14.2	1257.1	16.5	**1257.1**	**16.5**	97.4
50	235	109065.2	3.1	12.4	0.7	2.3	1.3	0.2	1.1	0.8	1199.2	12.1	1202.0	9.4	1207.0	14.6	**1207.0**	**14.6**	99.3
53	78	69900.6	3.0	12.8	0.9	2.0	2.0	0.2	1.8	0.9	1119.8	18.2	1129.3	13.4	1147.6	16.9	**1147.6**	**16.9**	97.6
54	65	6770.3	2.4	11.9	5.8	0.8	6.0	0.1	1.3	0.2	444.8	5.5	612.3	27.5	1293.2	113.8	**444.8**	**5.5**	34.4
55	88	68978.6	2.3	12.5	1.3	2.3	2.1	0.2	1.6	0.8	1203.3	17.9	1202.9	14.5	1202.2	24.9	**1202.2**	**24.9**	100.1
56	88	72760.2	1.2	16.6	1.2	0.8	1.9	0.1	1.5	0.8	613.6	8.6	612.2	8.8	606.8	26.5	**613.6**	**8.6**	101.1
57	62	73710.4	0.8	8.4	1.0	6.0	1.7	0.4	1.4	0.8	1989.4	24.0	1969.0	15.1	1947.7	18.3	**1947.7**	**18.3**	102.1
58	60	24024.7	2.0	9.5	2.2	4.2	3.2	0.3	2.4	0.7	1630.2	34.2	1668.5	26.6	1716.9	40.7	**1716.9**	**40.7**	94.9
59	82	96905.7	3.3	13.5	0.9	1.7	2.0	0.2	1.8	0.9	978.1	16.0	998.1	12.6	1042.3	18.7	**1042.3**	**18.7**	93.8
6	120	1367274.8	3.0	13.3	0.9	1.9	1.5	0.2	1.2	0.8	1071.0	11.8	1072.6	9.8	1075.9	17.5	**1075.9**	**17.5**	99.5
60	119	330517.6	4.0	9.4	1.1	4.7	2.0	0.3	1.7	0.8	1789.2	26.5	1769.7	16.9	1746.6	20.0	**1746.6**	**20.0**	102.4
61	85	112309.4	1.7	9.9	0.9	4.2	1.8	0.3	1.6	0.9	1704.1	24.0	1679.3	15.1	1648.6	16.7	**1648.6**	**16.7**	103.4
64	109	34699.1	2.6	12.9	2.5	1.8	2.8	0.2	1.2	0.4	982.3	11.0	1031.2	18.0	1136.4	49.7	**1136.4**	**49.7**	86.4
65	48	17244.0	1.7	16.9	1.6	0.8	2.1	0.1	1.3	0.7	572.5	7.3	572.3	9.0	571.3	33.8	**572.5**	**7.3**	100.2
66	103	75770.6	3.1	11.4	0.9	3.0	1.6	0.2	1.3	0.8	1419.7	16.4	1401.0	11.9	1372.7	17.0	**1372.7**	**17.0**	103.4
67	94	103050.3	3.4	12.4	1.2	2.0	1.7	0.2	1.2	0.7	1089.9	12.1	1131.0	11.8	1210.9	24.2	**1210.9**	**24.2**	90.0
68	496	209476.5	61.4	12.8	1.2	2.0	1.8	0.2	1.4	0.8	1087.7	13.6	1107.0	12.1	1145.2	23.2	**1145.2**	**23.2**	95.0
69	313	1027789.8	5.1	13.5	1.0	1.8	1.5	0.2	1.1	0.8	1032.3	10.4	1037.6	9.5	1048.6	19.4	**1048.6**	**19.4**	98.5
7	296	773049.0	9.6	9.7	0.7	4.0	1.5	0.3	1.3	0.9	1610.8	18.0	1637.1	11.8	1671.0	13.4	**1671.0**	**13.4**	96.4
70	35	42016.7	1.3	9.9	1.3	4.1	2.1	0.3	1.6	0.8	1649.5	23.7	1645.3	16.9	1639.9	23.8	**1639.9**	**23.8**	100.6
71	108	660358.3	3.1	12.1	1.0	2.5	1.6	0.2	1.2	0.8	1284.7	14.4	1275.7	11.7	1260.4	20.2	**1260.4**	**20.2**	101.9

72	91	126565.9	3.3	10.7	0.9	3.4	1.6	0.3	1.3	0.8	1501.7	18.0	1501.6	12.9	1501.5	17.9	**1501.5**	**17.9**	100.0
73	61	43352.6	2.5	13.6	1.3	1.8	1.9	0.2	1.4	0.7	1039.1	13.3	1037.0	12.3	1032.4	26.1	**1032.4**	**26.1**	100.6
74	18	8923.6	1.7	13.6	1.7	1.8	2.3	0.2	1.5	0.7	1053.8	14.4	1045.5	14.7	1028.2	34.4	**1028.2**	**34.4**	102.5
75	101	120550.9	3.6	12.0	1.0	2.5	1.7	0.2	1.3	0.8	1287.5	15.5	1284.9	12.3	1280.7	20.2	**1280.7**	**20.2**	100.5
76	146	124621.6	4.0	14.4	1.1	1.5	1.8	0.2	1.5	0.8	917.2	12.6	916.8	11.2	916.1	22.8	**916.1**	**22.8**	100.1
78	129	734713.1	5.3	8.3	1.0	6.1	1.7	0.4	1.4	0.8	1999.7	24.6	1986.4	15.2	1972.6	17.8	**1972.6**	**17.8**	101.4
79	59	147525.5	1.3	8.5	1.0	5.6	1.7	0.3	1.4	0.8	1920.6	23.5	1918.2	14.7	1915.6	17.2	**1915.6**	**17.2**	100.3
8	215	271231.0	6.7	10.8	0.9	3.3	1.4	0.3	1.1	0.8	1483.4	14.9	1482.7	11.1	1481.7	16.5	**1481.7**	**16.5**	100.1
80	125	103524.7	9.8	13.9	0.8	1.7	1.4	0.2	1.1	0.8	1016.8	10.8	1005.2	9.0	980.2	16.6	**980.2**	**16.6**	103.7
81	56	43779.9	2.8	13.6	1.1	1.8	1.7	0.2	1.3	0.8	1068.4	12.9	1054.0	11.1	1024.1	21.9	**1024.1**	**21.9**	104.3
82	74	37502.0	2.1	10.8	0.8	3.1	1.5	0.2	1.3	0.9	1419.8	16.9	1440.7	11.9	1471.6	14.9	**1471.6**	**14.9**	96.5
83	255	276625.9	2.7	8.3	0.9	6.1	1.6	0.4	1.3	0.8	2010.2	22.0	1988.6	13.6	1966.2	16.0	**1966.2**	**16.0**	102.2
84	10	90982.2	0.9	10.8	1.5	3.4	2.1	0.3	1.4	0.7	1515.1	18.3	1502.7	16.1	1485.2	29.1	**1485.2**	**29.1**	102.0
85	73	72812.3	2.1	13.4	0.9	1.8	1.5	0.2	1.2	0.8	1039.0	11.3	1043.0	9.5	1051.3	17.6	**1051.3**	**17.6**	98.8
86	118	118156.4	2.2	13.5	1.0	1.8	1.6	0.2	1.2	0.8	1055.9	11.9	1051.4	10.4	1042.0	20.3	**1042.0**	**20.3**	101.3
87	74	129812.7	3.5	12.8	1.0	2.2	1.7	0.2	1.4	0.8	1182.4	14.7	1170.8	11.6	1149.4	19.1	**1149.4**	**19.1**	102.9
88	107	373646.1	3.1	12.8	0.8	2.1	1.5	0.2	1.3	0.8	1128.5	13.2	1136.7	10.3	1152.2	15.9	**1152.2**	**15.9**	97.9
9	17	16854.8	3.6	13.7	1.9	1.8	2.3	0.2	1.4	0.6	1048.1	13.8	1036.3	15.2	1011.6	37.7	**1011.6**	**37.7**	103.6
90	43	404382.4	2.4	13.6	1.2	1.8	1.7	0.2	1.2	0.7	1061.8	11.6	1051.4	10.9	1029.8	23.8	**1029.8**	**23.8**	103.1
91	68	50268.3	2.1	16.1	1.2	1.0	1.9	0.1	1.4	0.8	680.9	9.2	679.5	9.2	675.1	25.7	**680.9**	**9.2**	100.9
92	29	136494.3	0.7	10.8	1.0	3.3	1.7	0.3	1.3	0.8	1474.3	17.8	1478.7	13.1	1484.9	19.1	**1484.9**	**19.1**	99.3
93	33	8761.7	1.6	14.0	1.3	1.6	1.8	0.2	1.1	0.6	987.8	10.5	983.0	11.1	972.3	27.4	**972.3**	**27.4**	101.6
94	232	757976.6	0.8	17.1	1.0	0.7	1.6	0.1	1.2	0.8	545.4	6.3	546.7	6.6	552.2	21.1	**545.4**	**6.3**	98.8
95	90	194369.2	1.9	9.4	1.0	4.5	1.5	0.3	1.1	0.8	1711.4	16.7	1725.9	12.3	1743.6	17.9	**1743.6**	**17.9**	98.2
96	134	91559.0	3.4	10.7	0.8	3.5	1.5	0.3	1.3	0.8	1531.3	17.5	1517.4	12.0	1498.1	15.4	**1498.1**	**15.4**	102.2
97	104	226982.6	1.7	13.3	0.9	1.9	1.8	0.2	1.5	0.9	1081.8	15.3	1077.2	11.9	1068.0	18.4	**1068.0**	**18.4**	101.3
98	18	9235.7	2.7	14.2	1.5	1.6	2.0	0.2	1.3	0.7	961.2	11.9	954.0	12.6	937.5	31.6	**937.5**	**31.6**	102.5
99	165	135402.5	3.6	12.8	1.0	2.2	1.6	0.2	1.3	0.8	1195.5	13.8	1179.6	11.4	1150.4	20.6	**1150.4**	**20.6**	103.9
xx	262	206126.3	2.5	13.0	0.7	1.7	1.3	0.2	1.1	0.9	972.0	10.3	1017.6	8.6	1117.3	13.8	**1117.3**	**13.8**	87.0
89	249	253437.4	3.9	11.7	0.9	2.7	1.9	0.2	1.6	0.9	1337.3	19.8	1334.0	14.0	1328.6	18.2	**1328.6**	**18.2**	100.6

9	163	180675.6	1.9	11.5	0.7	2.7	1.5	0.2	1.3	0.9	1294.2	15.1	1317.0	10.9	1354.3	14.0	**1354.3**	**14.0**	95.6
90	95	50153.2	1.2	11.7	0.8	2.7	1.5	0.2	1.3	0.8	1316.4	15.0	1317.2	11.0	1318.5	15.2	**1318.5**	**15.2**	99.8
91	189	276715.6	2.5	10.7	0.8	3.4	1.3	0.3	1.0	0.8	1493.1	13.8	1495.7	10.1	1499.4	14.7	**1499.4**	**14.7**	99.6
92	376	265557.1	2.8	16.9	0.9	0.7	1.5	0.1	1.2	0.8	562.7	6.7	565.3	6.7	576.0	19.8	**562.7**	**6.7**	97.7
93	126	28570.4	2.3	17.9	1.2	0.5	2.0	0.1	1.6	0.8	430.6	6.5	433.2	6.9	446.8	26.4	**430.6**	**6.5**	96.4
94	1225	161548.0	1.2	17.7	0.9	0.6	1.9	0.1	1.6	0.9	471.5	7.4	471.1	7.1	469.0	20.6	**471.5**	**7.4**	100.5
95	328	168385.5	4.6	13.4	1.0	1.8	1.9	0.2	1.6	0.9	1044.3	15.8	1046.3	12.5	1050.7	19.9	**1050.7**	**19.9**	99.4
96	99	69029.7	1.3	17.3	1.2	0.6	1.7	0.1	1.3	0.7	460.0	5.8	470.7	6.6	523.2	25.4	**460.0**	**5.8**	87.9
97	714	948389.0	7.7	9.6	0.9	4.3	1.9	0.3	1.7	0.9	1672.7	24.5	1685.3	15.6	1701.0	16.7	**1701.0**	**16.7**	98.3
98	231	578919.6	4.0	12.6	0.9	2.2	1.7	0.2	1.4	0.8	1171.3	15.5	1175.4	12.1	1183.2	18.8	**1183.2**	**18.8**	99.0
99	43	23042.2	1.6	13.2	1.2	2.0	1.8	0.2	1.4	0.8	1147.6	14.4	1129.1	12.3	1093.6	23.6	**1093.6**	**23.6**	104.9
xx	620	176870.1	5.3	17.7	1.0	0.8	3.0	0.1	2.8	0.9	624.7	16.9	593.3	13.6	475.2	22.7	**624.7**	**16.9**	131.5
xx	9255	3270241.3	0.6	18.2	1.0	0.5	2.0	0.1	1.8	0.9	387.2	6.7	391.1	6.6	414.2	21.9	**387.2**	**6.7**	93.5
xx	6332	746429.0	0.7	18.3	0.9	0.5	1.9	0.1	1.6	0.9	402.7	6.4	401.5	6.2	394.3	20.3	**402.7**	**6.4**	102.1